THE MECHANICAL BEHAVIOUR OF POLYETHYIENE PIPE SYSTEMS

Michael Bradley Barker

This thesis is submitted in accordance with the requirements of Brunel University for the degree of Doctor of Philosophy, by Michael Bradley Barker.

Department of Non-Metallic Materials

April 1982

CONTENTS

ACKNOWLIEDGEMENTS

I would like to thank Professor M.J. Bevis for his encouragement and guidance throughout the course of the project and for the provision of laboratory facilities.

The help, advice and many useful ideas contributed by Dr J. Bowman are gratefully acknowledged and thanks also go to Mr S. Bentley for his technical assistance, to Mrs D. Denby for patiently typing the manuscript and to the Associated Octel Company for the use of their analytical equipment.

Finally I wish to acknowledge the financial support provided by the Science and Engineering Research Council.

SUMMARY

The design of polyethylene (PE) pipelines for applications in the gas, water and chemical process industries has been based on data mainly obtained from stress rupture testing pipes only. In practice, installations are composed of both extruded pipe and injection moulded fittings which are joined by a fusion welding technique and are very often subjected to internal pressures of a fluctuating nature. Several makes of PE pipe systems were therefore obtained and work was undertaken to fully characterise mechanical performance in terms of internal pressure loadings. Butt-welded test specimens comprising pipe lengths and fittings were subjected to both static and fluctuating conditions at 80°C, at pressures resulting in brittle fractures (below the knee on stress rupture curves) and at frequencies not exceeding 7.5 cpm (0.125 Hz). Resulting fracture surfaces were examined to identify sources of crack initiation and mechanisms of failure.

Mechanical behaviour of the PE pipe samples was found to be markedly influenced by the grade of plastics compound, the pipe system dimensions, mould designs and methods of processing. Fatigue loading was the most aggressive test method and significant reductions in lifetimes were observed in fittings or joints between pipes and fittings with only modest increases in the frequency of pressurisation. It was also demonstrated that improved stress rupture behaviour did not necessarily lead to better fatigue performance.

For the square-wave loading profiles used, an idea of the relevant failure mechanisms in any given system was obtained by comparing experimental N_f values with those predicted from cumulative damage principles based on $N_f = \tau_{SR}/t_{max}$.

In all types of system, failure was initiated at a defect residual from processing or jointing. Over 95% of all small diameter pipe fractures originated from

inclusions at or close to the inside wall. They were geometrically and elementally analysed and suggestions made as to their possible origin and means of elimination. For one PE a reasonable correlation was obtained between lifetime under stress rupture or fatigue and the inclusion size as measured in the fracture plane.

LIST OF TABLES

LIST OF FIGURES

CHAPTER 2

CHAPTER 7

NOMENCLATURE

a	Crack length
a_o	Original crack length
A_1	Constant
B, B_1, b	Constants
d	Inside diameter of a pipe; Constant
D	Outside diameter of a pipe; Constant
f	Frequency; Weld factor
h	Pipe wall thickness; Planck's constant
H	Activation energy
ΔH_f	Enthalpy of fusion
$\Delta^{\Theta} H_f$	Enthalpy of fusion for 100% crystalline linear PE
k	Boltzmann's contant
K_c	Stress intensity at the tip of a growing crack
ΔK	Stress intensity range
L	Crack breadth
L_c	Thickness of crystalline lamellae
$\bar{M}w$	Weight average molecular weight
$\bar{M}n$	Number average molecular weight
N	Constant; Number of cycles
N_f	Number of cycles to failure
P	Applied internal pressure
r	Radius
r_i	Inside radius of a pipe
r_o	Outside radius of a pipe
r_m	Mean radius of a pipe
R	Bend radius
S	Stress
t	Time to fracture
t_{cycle}	Time for one complete fatigue cycle
t_{max}	Section of a fatigue cycle at maximum load

T	Absolute temperature
T_m	Crystalline melting temperature
T_m^o	Equilibrium melting temperature of an infinitely thick crystal
Y	Geometrical correction factor
da/dN	Fatigue crack growth rate
da/dt	Crack growth rate
α	Angle around the circumference of a bend
β	Activation volume
ε	Mean deformation
$\Delta\varepsilon$	Strain amplitude
ν	Frequency
σ	Applied stress
$\Delta\sigma$	Stress amplitude
σ_H	Pipe hoop stress
$(\sigma_H)_r$	Pipe hoop stress at a radius r
σ_L	Longitudinal stress in a pipe with closed ends
σ_m	Mean stress level
$\tau_{FATIGUE}$	Fatigue or pseudo stress rupture life
τ_{SR}	Stress rupture life
τ_{TEST}	Total testing time

ABBREVIATIONS

ABS	Acrylonitrile butadiene styrene
DGB	Discontinuous growth band
DSC	Differential scanning calorimetry
EDAX	Energy dispersive analysis by X-rays
FCP	Fatigue crack propagation
GRP	Glass reinforced plastic
HDPE	High density polyethylene
LDPE	Low density polyethylene
MDPE	Medium density polyethylene
MFI	Melt flow index
MWD	Molecular weight distribution
OD	Outside diameter

PB	Polybutene - 1
PE	Polyethylene
PMMA	Polymethyl methacrylate
PP	Polypropylene
pPVC	Plasticised polyvinyl chloride
PVDF	Polyvinylidene fluoride
SDR	Standard dimension ratio
SEM	Scanning electron microscopy (microscope)
uPVC	Unplasticised polyvinyl chloride

CHAPTER 1

INTRODUCTION AND OBJECTIVES

1.1

CHAPTER 1 - INTRODUCTION AND OBJECTIVES

Thermoplastics pipelines are being used increasingly in the chemical, gas and water industries in this country and throughout Europe and North America. The materials which have dominated this trend are unplasticised polyvinyl chloride (uPVC) together with the polyolefins such as polypropylene (PP) and polyethylene (PE) in the high (HDPE) and medium (MDPE) density forms.

To date PE fusion welded systems have been employed successfully by British Gas in parts of their distribution network and some of the British Water Authorities are now showing an interest in certain grades of PE for water mains applications. (This is a market which has previously been dominated by uPVC.) The chemical industries, although not a large tonnage user of PE, usually require such pipe systems for exacting service duties where hazardous chemicals are contained under a variety of operating conditions. It is under such circumstances that the limits of the material and the system can be reached, and where there is the greatest need for reliable data on the behaviour of PE pipelines, to enable engineers to produce designs resulting in fewer instances of premature failure.

The available design data for PE pipe systems are generally in the form of stress rupture curves. The major standards organisations, in their respective publications (BS 4728, ASTM 1598, DIN 16963) have prescribed a test procedure which examines the performance of PE pipe under static internal pressures. Although each standard varies in detail the information obtained from such tests relates pipe hoop stress and times to failure at various temperatures. This enables working stresses for the required lifetime of 50 years to be predicted by extrapolation. Although the use of such tests and related stress rupture data have been generally successful over the last twenty years or so in ensuring satisfactory service performance, failures do occur under conditions which are not covered by the stress rupture test.

Since PE pipelines are usually composed of extruded pipe, injection moulded fittings and fusion joints made between pipe lengths and between pipes and fittings and the whole network can be subjected to fluctuating as well as static internal pressures, the design information based upon stress rupture performance of pipe alone was insufficient to predict the behaviour of complete pipelines under the wide range of duties likely to be experienced in service. Thus systems comprising pipes, fittings and fusion joints were subjected to both static and fluctuating conditions to fully characterise performance in respect of internal pressure loadings.

The project was, in general, intended to improve the understanding of the factors influencing PE pipeline performance with the following specific objectives:-

a. To generate basic design data for PE pipe systems subjected to fluctuating internal pressures.
b. To examine the behaviour of selected butt-welded PE pipe systems under short term rupture, stress rupture and fatigue loadings to identify possible sources of weakness.
c. To compare the performance of butt-welded PE pipe systems from different manufacturers when subjected to stress rupture and fatigue conditions.
d. To examine the use of the internal pressure fatigue test as a means of accelerating failure in pipe systems.
e. To compare the usefulness and ease of applicability of the short term rupture, stress rupture and fatigue tests as means of characterising the mechanical performance of thermoplastics pipelines.
f. To identify the causes of and mechanisms leading to instances of premature fracture in PE pipe systems.

As a result of some sections of the work reported in later chapters, the company who initiated the first investigation into fatigue failures of HDPE pipelines has amended certain parts of its in-house code of practice relating to the design, installation and operation of thermoplastics pipelines, to take account of the fatigue weaknesses observed in some PE systems.

CHAPTER 2

LITERATURE REVIEW

2.1

CHAPTER 2 - LITERATURE REVIEW

2.1 MATERIALS

2.1.1 Properties of Polyethylenes

The properties of PE are based essentially on three molecular parameters described by Timmer (1)* as:

Molecular Weight ($\bar{M}w$ and $\bar{M}n$)
Density (Molecular Branching)
Molecular Weight Distribution (MWD) (1)

The molecular weight is generally regarded as being the weight average molecular weight or $\bar{M}w$. The molecular weight distribution or MWD is the numerical ratio of the average molecular weight ($\bar{M}w$) to the number average molecular weight ($\bar{M}n$).

Variations in the parameters listed above will produce polyethylenes of use in a number of applications and it is possible to "fine tune" specific molecular properties to satisfy the most demanding situations within the general limits of the material.

2.1.2 Materials Selection

A set of criteria considered essential for plastics pipes has been defined for gas distribution purposes (1). They are considered to be generally applicable to thermoplastics pipe networks under most conditions. These guidelines are as follows:-

Long Term Strength
Ageing Resistance
Impact Resistance
Chemical Resistance
Temperature Resistance
Impermeability
Pipe Attributes - Ability to Heat Fuse for Joining.
Coil for Ease of Handling.
Squeeze-off for Pressure Control (Gas Only).

* Numbersin brackets (1) denote references detailed at the end of Chapter 7.

In the final selection however, a compromise must be sought between processing requirements, mechanical properties and ease of jointing for each pipe system application.

The most practical solution to the problem of identifying the optimum material should be obtained if the following design sequence proposed by Price and Gray (2) is followed.

a. Establish the required end use performance for the pipe system.
b. Express the required performance in terms of yield stress, modulus and fracture toughness.
c. Establish product and installation constraints in terms of extrusion, moulding, fabrication and welding.
d. Design material in terms of density, molecular weight and molecular weight distribution.

2.1.3 Types of Polyethylene

Generally PE is arbitrarily classified into three types based on density:-

Low Density PE	910 - 935 kg m^{-3}
Medium Density PE	926 - 940 kg m^{-3}
High Density PE	940 - 965 kg m^{-3}

LDPE is commonly manufactured in autoclaves or tubular reactors in which ethylene monomer is polymerised with oxygen (or other free radicals) as an initiator. Pressures during the reaction range from 103 to 308 MPa resulting in polymer chains which have a high degree of side branching.

MDPE can be manufactured by using a high or low pressure process, thereby chemically controlling the amount of side chain branching, or alternatively, it can be made by physically blending LDPE and HDPE.

HDPE is produced with the aid of special catalysts such as vanadium and molybdenum oxide, chromium oxide or organometallic compounds. This enables ethylene to be polymerised at pressures less than about 10 MPa. The resulting polymer chains are almost linear having very few side chains..

For pipe system applications such as those of interest in the present work, MDPE and HDPE are the only materials considered. Their properties are of course modified to a certain extent by additives and fillers. Most are mixed into PE during melt compounding. Such additions include antioxidants, UV stabilisers, extenders and pigments (3, 4).

2.2 PROCESSING EFFECTS ON MECHANICAL PROPERTIES OF PIPE SYSTEMS

The processing techniques employed to produce the various pipe system components under investigation were,

a. Extrusion for pipes.
b. Injection moulding for fittings.

Extrusion is a method of continuous manufacture of pipe where a screw plasticates the polymer feedstock within a heated barrel and forces it through a die under uniform pressure. A variety of defects can occur in the extruded sections including gas bubbles, particles of foreign material and flow lines running longitudinally in the pipe commonly called "spider lines". To monitor the presence of such inhomogeneities and to keep close control of the dimensions of the finished product various ultrasonic and calibration devices are used (5,6).

The process alters material properties considerably (7, 8) tending to orient molecular chains in a non-random fashion, thereby imparting a degree of anisotropy to the extruded article. During cooling, differential shrinkage through the pipe wall produces internal stresses which vary from compressive near the skin to tensile at the core, where there is some elongation (9).

Injection moulding also causes the finished product to be anisotropic and non-homogeneous since the polymer chains are oriented by the flow and shearing effects sustained by the melt during the moulding cycle.

The mechanical properties of both extruded pipes and moulded fittings are thus a result of fluctuations in temperature, shear and flow in the polymer melt prior to crystallisation (8, 10 - 18).

Until recently because of residual stresses etc., it was very difficult to realise the necessary dimensional tolerances on larger pipe fittings in a moulding cycle time which could be considered economic. These articles were thus fabricated by means other than injection moulding. However, recent developments have resulted in moulded articles of 100 kg with cross-sections in excess of 50mm (19). Nevertheless, complicated pipeline components, tees and bends for example, require multi-section moulds which give rise to defects such as mould parting lines and internal weld lines which may be instrumental in causing premature failures (20).

2.3 CHARACTERISATION OF THE STRUCTURE OF PROCESSED SEMI-CRYSTALLINE PLASTICS MATERIALS

2.3.1 Overall Structure

(i) Microtomy.

For some semi-crystalline plastics morphology can be conveniently inspected by the examination of thin sections cut from the surface of bulk specimens using a sharp tool (21,22). It is particularly useful in the study of strongly birefringent samples if used in conjunction with a transmitted light microscope set up to view sections between crossed polars.

Thin sections cut from PE butt-welds and examined by the above means have been described by Barber and Atkinson (23). They identified a variety of microstructures in and around such joints resulting from the temperature distribution and the flow of molten material at the weld.

A second microtoming method based on cutting sections from a bulk sample has also proved useful on the macroscopic level at least (22). The surfaces of specimens are cut using a sledge microtome and examined using a microscope in the reflected light mode. Features such as weld bead assymetry, weld misalignment, voids, skin remnants and columnar growth regions are brought out clearly on the surface shown in Figure 2.1 which is a carbon black filled HDPE sample. The patterns of stress whitening are considered to be indicative of different morphologies through the various regions of the specimen (22).

(ii) Light Microscopy.

Two types of light microscopy are normally used for semi-crystalline plastics namely reflected and transmission. Ideally such techniques will separate entities 0.2 μm apart (24). Strongly birefringent plastics are shown to good advantage under conditions of transmitted light viewed between crossed polars whereas reflected light finds particular use for the examination of fracture surfaces. Physical properties of polymers on a microscale, can be examined readily together with quantitative birefringent measurements of both bulk samples and microscopic particles (24, 25).

Filled polymers such as carbon black filled HDPE, as used in water, gas and chemical plant pipe applications, pose difficult problems when examined using transmitted light microscopy, since not only does the carbon in the thin sections absorb most of the light, but the filler or pigment particle dispersion produces a microstructure so fine that only a granular mass of depolarised light is observed. However, bulk changes in HDPE butt-welds have been examined (26, 27) and a variety of microstructural zones were identified which are thought to be regions of different crystallinities and molecular orientation imposed by the flow and shear of the molten plastic as the pipe ends are being joined.

A simple method of revealing a polymer's inner structure is the examination of fracture surfaces. Such an exercise will also provide information about failure mechanisms. The difficulty here is being able to separate those features related to the deformation process and those resulting from inherent microstructure.

2.3.2 Fine Structure

(i) Scanning Electron Microscopy (SEM).

Scanning electron microscopy extends the limit of detailed microstructural studies down to a resolution of 10 nm under ideal conditions (24, 25, 28). Plastics are often coated with a conductive layer to prevent excess static charge building up on the polymer surface which can affect the resulting image adversely. Inner structures can be viewed

after various preparations such as microtoming, etching or even breaking specimens. SEM for fracture surface analysis is particularly useful for composite structures where individual components vary greatly in mechanical behaviour (24).

(ii) Energy Dispersive X-Ray Analysis.

A variety of radiations are emitted from a bulk specimen when it is bombarded with the electron beam of the scanning electron microscope. One type of radiation is X-rays which by means of suitable detectors can be analysed spectrometrically in terms of energies. The energies are characteristic of any elements present and any object of a few microns in size or larger can be readily observed and analysed (28). Most common applications in polymers relate to the analysis of segregates, inclusions and particulate fillers.

2.3.3 Differential Scanning Calorimetry and Crystallinity

In recent years the technique of DSC has been usefully employed to determine variations in melting temperatures and percentage crystallinities as a function of time (29) and also through the wall thicknesses of HDPE pipes (30). Gedde and Jansson (31) have also analysed the thermal oxidation of HDPE pipes using the same technique.

Fatigue crack propagation of several HDPE samples of different molecular weight have been compared by de Charentenay et al (32) who were able to correlate such behaviour with percentage crystallinities as determined by DSC.

Several papers have critically discussed the application of DSC for crystallinity measurements in semi-crystalline plastics particularly PE (33 - 38). Both Hay (33) and Still (38) report on its limitations in terms of inherent problems associated with the technique itself, the apparatus used to obtain thermal responses, difficulties associated with calibration and standardisation procedures and problems related to the polymeric materials in general.

In spite of these limitations, DSC is very useful to examine, for example, effects of thermal history, Figure 2.2, thermal-mechanical history, Figure 2.3 and

batch variations in similarly processed polymers, Figure 2.4, Since the density of a semi-crystalline plastic is related to its crystallinity, the three density groups of PE can be distinguished readily. Filled polymers such as the black HDPE pipe material pose problems in that it must be assumed the density of the filler throughout the polymer matrix is the same. Results can then only be considered comparatively and not in absolute terms. In fact the percentage crystallinity is defined essentially by the method used to measure it (33, 38).

With respect to molecular structure it is possible to obtain information about fold lengths in the polymer crystallites since higher crystallisation temperatures lead to longer fold lengths (39). Heat annealing can give rise to higher melting temperatures and increased crystallinities as measured by DSC (35, 40). It has also been reported recently that the DSC endotherm exhibits a taller, narrower peak for HDPE pipe material which has been held at 80°C for 430 hours when compared with the original plastic taken from the same batch (42). These results were taken to be indicative of an annealing process which produced a more uniform and regular molecular structure of the type discussed by Keller (39) and other workers (35, 40).

The effect of testing at elevated temperatures can therefore induce DSC measured crystallinity changes and since it is well established that mechanical properties of polymers are sensitive to the degree of crystallinity (33) it was no surprise to find that the density, residual internal stress and bursting strength of PE pipes would all be altered after being subjected to a temperature of 80°C (41). Predicting long term behaviour by using accelerated tests at elevated temperatures, although not ideal, is not invalidated as long as these effects can be identified and accounted for in the proposed failure model.

2.4 BUTT WELDING

2.4.1 General Comments

A variety of methods are available for welding together two thermoplastics components including hot-gas welding, hot-tool welding, radio frequency and friction

welding (43).

Hot-tool welding can be accomplished by two methods namely mirror-plate butt-welding and socket fusion welding. Both systems are used for joining thermoplastics pipe networks and a substantial amount of literature relating to the actual techniques involved and their applications in the chemical process and gas industries has been produced (see for example Proceedings of the PRI 4th International Conference on Plastics Pipes - March 1979, papers 4 - 6, 10, 13 and 24 together with references 6, 20, 27, 43, 44). This section will deal only with mirro-plate butt-welding which was the technique used in the experimental programmes.

2.4.2 Microstructure of Butt-Welded Joints

The butt-welding process may induce microstructural changes at the joint due to temperature gradients and shear stresses applied to the polymer (21, 23, 27, 45, 46). Such changes could result in the mechanical behaviour of the joint being at variance with the behaviour of the parent material.

The microstructures in HDPE and MDPE butt-welds made between pipes have been characterised to some extent by the work of Atkinson and his co-workers (23, 26, 47, 48), Menges and Zöhren (45) and by Cowley and Wylde (20, 27). Cowley (27) went on to suggest these various microstructures will exhibit different crystallinities and orientation and consequently varying yield and tensile strengths. Thus it was necessary to determine how these structures affected the subsequent performance of a butt-weld and hence the pipe network as a whole.

2.4.3 Evaluation of Butt-Welded Joint Quality

Although the inspection techniques applied throughout a butt-welding operation for thermoplastics pipe materials are well defined (43), there is no guarantee that any weld will satisfy its duty requirements (49).

Recently, radiographic, ultrasonic and spark testing techniques (43, 44, 50, 51, 52) have been employed to check the integrity and alignment of welds and may be considered complementary. Such procedures will only

provide information about the presence of any inhomogeneities or holes in or around the weld, they cannot determine either short or long term strength.

Another approach to the non-destructive testing of mirror-plate butt-welds has been described by Potente (53). The strain behaviour at the joints was examined by means of Holographic Interferometry which is able to measure residual stresses and strains and slight surface shifts due to loading.

Destructive testing of butt-welded joints is usually carried out by means of tensile testing (21, 26, 43, 44, 55.- 58 for example), stress rupture testing (20, 43, 48, 54), impact testing (44), bend testing (43, 44) and more recently fatigue testing (20). The stress rupture and fatigue tests relate here to butt-welded pipe specimens which are subjected to static and fluctuating internal pressures respectively.

2.5 TESTING AND FAILURE OF PIPE SYSTEMS

2.5.1 Introduction

Pressure pipelines under service conditions may be subjected to both static and fluctuating internal pressures. The PE pipe systems, of interest here, have been used extensively in applications where both forms of loading are present.

It is proposed to review the information available which relates not only to the effect of conditions upon the performance of such systems but also to the theoretical fundamentals of creep and fatigue failure which can be used successfully to predict system lifetimes. The review will also encompass those theories based on fractographic methods which provide models for the mechanisms of failure.

2.5.2 Standards

A list of relevant standards according to which the internal pressure testing of pipe systems was carried out is given in Chapter 3. In general the dimensions and test parameters applied to all pipe systems conformed to at least the minimum requirements of the standards, particularly reference 59. Standardisation has been defined as the simplification of production by the elimination of

the unnecessary variety of patterns and sizes and the consolidation of requirements for quality (60); with this in mind the testing procedures are also standardised.

For plastics pipes the resistance to internal water pressure is used as a quality control test and to predict long term properties. Lack of time and testing capacity requires that accelerated tests are used, the results being subsequently extrapolated to the desired requirements - an expected admissable hoop stress after fifty years under static load is the basic design criterion used in the UK (61, 62).

Test parameter consistency is required for the test results to be of use, particularly temperature, pressure and specimen dimensions (61). Figure 2.5 shows the effect the free length of a thermoplastic pipe can have on the failure times at 20°C. The diagram also indicates the variation induced by unconstrained and constrained ends (61) which can result in biaxial or uniaxial stress systems in a pressurised pipe altering the slopes and positions of stress rupture curves, possibly a reflection of a craze criterion such as proposed by Sternstein and Ongchin (65) for the failure of thermoplastics under this type of stress.

2.5.3 Stresses in Pipes and Fittings Under Internal Pressure

(i) Pipes as Thin-Walled Cylinders.

If a pipe is allowed to expand and extend freely and is subjected to an internal pressure, three mutually perpendicular stresses will be produced as shown in Figure 2.6. Such stresses are generally termed hoop or circumferential, longitudinal or axial and radial stresses (63, 64).

Hearn (63) considers that a criterion for the assumption that a pipe is a thin-walled circular cylinder is if the ratio of the wall thickness to the inside diameter of the pipe is less than 1/20. If such is the case it is possible to assume that the hoop and longitudinal stresses remain constant through the wall thickness and that the radial stress is small enough to be neglected. (In practice its value increases from zero on the outside surface to equal the internal

pressure at the inside surface of the pipe.) In this approach the effects of any end fittings are considered so far removed as to be negligible.

For the above conditions the hoop stress applied to a thin-walled pipe is given by

$$\sigma_H = P \frac{d}{2h} \qquad (2.1)$$

where σ_H is the hoop stress
d is the internal diameter
h is the wall thickness
P is the applied internal pressure.

The longitudinal stress in a pipe wall produced under similar conditions is given by

$$\sigma_L = P \frac{d}{4h} \qquad (2.2)$$

where σ_L is the longitudinal stress. For longitudinal stresses to apply the pipe system must have closed ends. Once again the ends are considered as having no reinforcing effect on the pipe.

From these equations it is evident that:

$$\sigma_H = 2 \sigma_L \qquad (2.3)$$

Another relation for the effect of internal pressure on a thin-walled pipe is known as Barlow's formula. It is considered to be a reasonable description of circumferential stresses in pipes of most thickness ratios and is expressed as

$$\sigma_H = P \frac{D}{2h} \qquad (2.4)$$

where σ_H, P and h are defined as before and D is the outside diameter of the pipe.

The Nadai formula is a further variation on the hoop stress/pipe dimensions relationship and is given by

$$\sigma_H = \frac{P\,(D - h)}{2h} \qquad (2.5)$$

where all symbols have meanings previously defined. It is this relationship which has been applied in the first instance, to all the related experimental data reported in later chapters. The approach concurs with the method of obtaining hoop or comparative stresses in thermoplastics pipes used by most manufacturers and other workers in the field of internal pressure testing.

(ii) Pipes as Thick-Walled Cylinders.

The theoretical treatment of stresses in thin cylinders under internal pressure with free ends assumes that

a. The hoop stress is constant across the cylinder wall, and

b. There exists no pressure gradient across the wall.

Neither assumption is valid for thick-walled pipes or cylinders and Figure 2.7 demonstrates how the hoop stress will vary in all SDR* 11 pipes. It is evident that the hoop stress on the inside surface of the pipe is greater by about 25% than the hoop stress experienced on the external surface. The expression describing this variation is developed from Lamé equations and is given by

$$[\sigma_H]_r = P\left[\frac{r_i^2}{(r_o^2 - r_i^2)}\right]\left[1 + \frac{r_o^2}{r^2}\right] \qquad (2.6)$$

where $[\sigma_H]_r$ is the hoop stress at radius r and r_i and r_o are the inside and outside radii of the pipe respectively.

* SDR - Standard Dimension Ratio
defined as the ratio of the pipe outside diameter (OD) to wall thickness.

An equation such as that above will enable the true hoop stress at any point within a pipe wall to be identified.

(iii) Internal Pressure Stresses in Thin-Walled Fittings.

The stress distribution set up in fittings, such as 90^{o} bends and 90^{o} equal tees, subjected to internal pressures are particularly complex. In the case of PE pipe systems, butt-welded joints and their distance from each other will modify such stresses and there are bending stresses to take into account also. British Standard 806 (66) and "Design of Piping Systems" (67) considers stresses in bends and tee-junctions made from metals. It would appear that similar principles can be applied to thermoplastics fittings.

Figure 2.8 shows the distribution of hoop stresses in thin-walled pipe bends subjected to internal pressure. (The limitations of thin-walled cylinder theory also apply here.)

The hoop stress is given by

$$\sigma_H = \frac{(2R + r\sin\alpha)}{2(R + r\sin\alpha)} \frac{r\,P}{h} \qquad (2.7)$$

or $$\sigma_H \doteq P\,\frac{r}{h}\,\frac{(R + a)}{2a} \quad \text{where } a = r\sin\alpha + R \qquad (2.8)$$

In this case R is the bend radius and r can be either the inside radius of the pipe or the mean radius (r_m) of the pipe. If the internal radius is used this gives a slightly higher value for the hoop stress.

Written in terms of inside diameters the expression becomes

$$\sigma_H = P \frac{d}{2h} \left[\frac{R + a}{2a} \right] \qquad (2.9)$$

which is identical with the formula for the hoop stress applied to thin-walled pipe under internal pressure except for the factor $\left[(R + a)/2a\right]$, which can be considered a stress concentration factor.

At different values of the angle α the hoop stress in the bend due to internal pressure is summarised in Table 2.1 (for convenience this is compared with straight pipe).

TABLE 2.1 Variation of Hoop Stress in a 90^o Bend Subjected to Internal Pressure and Compared with Values Obtained for Straight Pipe.

Angle α	Hoop Stress in 90^o Bend	Hoop Stress in Straight Pipe
0^o	$P \frac{d}{2h}$	$P \frac{d}{2h}$
$+ 90^o$	$P \frac{d}{2h} \left[\frac{2R + r}{2(R + r)} \right]$	$P \frac{d}{2h}$
$- 90^o$	$P \frac{d}{2h} \left[\frac{2R - r}{2(R - r)} \right]$	$P \frac{d}{2h}$

The definitions of the above terms are given in Figure 2.8.

Under similar conditions, with closed ends showing no appreciable effect, the longitudinal stress is identical in bends as in straight pipes, i.e.

$$\sigma_L = P \frac{d}{4h} \qquad (2.10)$$

where σ_L is the longitudinal stress.

With these formulae in mind the thickness of a pipe bend which will give the same lifetime under the same internal pressure can be calculated from

$$\frac{\text{Bend Wall Thickness}}{\text{Equivalent Pipe Wall Thickness}} = \frac{\text{Stress Concentration Factor}}{1} \quad (2.11)$$

Alternatively if the bend wall thickness is the same as that of the equivalent pipe then the lifetime of the bend is reduced by the factor of stress concentration. Also the equations for hoop stresses in a bend predict that maximum stresses will be reached at the line of the bend having the least radius of curvature, and failure ought to initiate somewhere along this line.

With respect to branch connections or equal tees, their presence in a pipe network is inherently a point of structural weakness (67). Severe stress intensification occurs at points of abrupt directional changes and because of sharp variations in cross-section. And, of course, there are the usual defects residual from processing thermoplastics components such as tees, not to mention the effect of adjacent butt-welds.

An involved geometrical shape and the strong influence of secondary effects such as non-directional bending stresses for example, make the analytical investigation of 90° equal tees subjected to internal pressure a particularly difficult process. (British Standard 806 (66) does, however, give equations for combined stresses, hoop stresses and bending stresses for steel tee junctions.)

2.5.4 Short Term Rupture Testing

(i) Testing Method.

Short term rupture testing differs from static and fluctuating internal pressure testing by virtue of the fact that pressure is continuously increased, at a given temperature, until the pipe sample fails. It can be considered as the pipe equivalent of tensile testing carried out on dumb-bell shaped test pieces, and like

tensile testing results are influenced particularly by strain rate and temperature. ASTM D1599-74 (1980) Short-Time Rupture Strength of Plastic Pipe; Tubing and Fittings (68) gives a detailed account of the test procedure which was adopted for such tests in the experiments reported in subsequent chapters.

Literature dealing with this type of pressure test for thermoplastics pipe systems is somewhat limited, possibly due to the fact that it is not easy to determine long term mechanical performance from the data obtained by this method. However, such effects as the ductile failure of PE and measurement of fracture toughness by using short term rupture tests have received attention (71, 72).

Comparisons of this type of short term data with long time properties of various thermoplastics pipes under hydrostatic pressure have also been made by Goldfein (69) and Sansome (70). Such methods can only predict long term failure if the mode of fracture is ductile. It is not at all possible to predict long term brittle failure in this manner.

2.5.5 Stress Rupture Testing of Polyethylene Pipe

(i) Stress Rupture Data and Failure Modes.

The behaviour of polyethylene pipe subjected to a static internal pressure (creep loading) is characterised by a family of stress rupture curves. There is general agreement in Europe that the stress rupture curves for both MDPE and HDPE have the general form shown in Figure 2.9, which indicates the presence of a "knee". Above the knee the material deforms in a gross ductile manner with significant local straining of the material prior to failure, whereas below the knee a brittle crack propagates through the wall with little or no evidence of ductility and strains of usually less than 3% (73,74). At longer times and lower stresses, the mode of failure of HDPE and MDPE pipe is by the propagation of a brittle crack through the wall of the pipe. Experience has shown that such cracks nucleate on the inside wall of a pipe

and propagate through to the outside (74, 75). In general this effect would be expected considering hoop stresses are greatest on the inside wall of a pipe. It may be necessary, however, to modify this reasoning if the pipe materials are not completely free of inhomogeneities (which inevitably they are not). Cracks may then initiate at positions lying away from the inside surface where local stresses may be greater due to the presence of inclusions or voids or other nucleation sites. When pipes do fail by the propagation of a brittle crack, the fracture lies parallel with the pipe extrusion direction forming in response to the largest principal stress in the circumferential or hoop direction (20).

It has been shown that any anisotropy introduced during the production of pipes has a greater influence on the stress rupture performance than on the creep response of the material itself. Uniaxial orientation, for example, can lead to an increased tendency to brittle cracking parallel to the orientation direction (76), in the case of pipes this generally lies in the extrusion direction.

So there is a combination of the largest principle stress and probably some residual orientation in the pipe material, which causes a brittle crack to form parallel to the pipe axis.

These processing effects and the geometry of pipes makes it necessary to determine stress rupture behaviour on the pipe itself. It is not really valid to rely entirely upon uniaxial tensile creep tests.

(ii) Prediction of Stress Rupture Lifetimes.

Two different approaches to calculate the lifetimes of plastics pipes subject to static loads or stresses have been proposed, one based upon the application of fracture mechanics (2, 79) to slow stable crack growth, the other from the theory of activated rate processes developed by Eyring et al (77) and applied to thermoplastics pipes by Barton and Cherry (42, 78). The fracture mechanics approach will be dealt with first.

Gray, Mallinson and Price (79) applied fracture mechanics to the case of slow stable crack growth in HDPE materials and found that the rate of crack growth da/dt could be given by

$$\frac{da}{dt} = BK_c^{\,b} \qquad (2.12)$$

where B and b are material constants and K_c is the stress intensification at the tip of the growing crack, and is given by

$$K_c = Y \sigma \sqrt{\pi a} \qquad (2.13)$$

where Y is a geometrical correction factor
a is the crack length
σ is the applied stress

It was assumed that the PE pipes failed from the inside surface by the propagation of a brittle crack of initial defect size a_o. The crack was also considered to propagate from the defect immediately upon application of a load. With the factors Y, σ and temperature remaining constant (2, 79) then by substituting for K_c in the crack growth rate expression and integrating between the limits of a_o and h (the pipe wall thickness), the lifetime of the pipe under static internal pressure, τ_{SR}, can be expressed as

$$\tau_{SR} = \frac{2}{b-2}\left[a_o^{(1 - b/2)} - h^{(1 - b/2)}\right]\frac{(Y \sigma\sqrt{\pi})^{-b}}{B} \qquad (2.14)$$

If the size of the defect changes such that Y varies significantly, then the change in Y should be allowed for during integration.

If $h \gg a_o$ and b typically greater than 2, the above equation simplifies to

$$\tau_{SR} = \left[\frac{2}{b-2}\ \frac{(Y\sigma\sqrt{\pi})^{-b}}{B}\right] a_o^{(1 - b/2)} \qquad (2.15)$$

where the terms in square brackets are constant for testing at both a given fixed temperature and pipe hoop stress. Assuming then that equation (2.12) is obeyed by the material, the lifetime of the pipe is then dependent upon the initial defect size. It also implies that the initial crack growth dominates the lifetime since smaller cracks grow more slowly than larger ones.

As an example, for an unnotched HDPE pipe material (006-60), Price et al (2, 79) demonstrated that lifetimes could be predicted using the above approach if defect sizes between 10 and 100 μm were assumed. This material obeyed the crack growth rate law.

The same method was applied to another pipe material Rigidex MDPE 002-40 which is much tougher than conventional HDPE, but since it failed to obey equation (2.12), that is the crack propagation rate was not a straightforward function of stress intensity at the crack tip, then the equation used for predicting lifetimes became invalid.

It should be stressed that the model of creep crack propagation in HDPE pipes under constant internal pressure proposed by Price et al (2, 79) does not allow any period spent initiating cracks. The theory assumes that for a particular value of the critical stress intensity factor, there is a corresponding crack speed. However, Bragaw (80) has reported on work with MDPE pipe systems and shown that there is a significant incubation time for a crack to start growing in a slow, stable manner. He therefore casts doubt on the validity of the use of fracture mechanics concepts to determine the failure performance of such ductile materials. Price and Gray (2) answer this by insisting that although no incubation process has been included in their treatment, such an approach does describe the lower bound case of immediate stable crack growth. Also their experimental results agree with predicted values for HDPE pipes, which can be considered as having an insignificant period of crack initiation, that is, the cracks or defects are probably present prior to testing.

Activated rate processes have been used (78) to describe the rate at which activated complexes pass over an energy barrier and assuming a local critical failure strain the time to fracture under static loading can be described by

$$t = \frac{Nh}{kT} \exp\left[\frac{H - \frac{\beta\sigma}{2}}{kT}\right] \qquad (2.16)$$

which leads to

$$\sigma = \frac{2kT}{\beta}\left[\ln N - \ln\frac{kT}{h} + \frac{H}{kT}\right] - \frac{2kT}{\beta}\ln t \qquad (2.17)$$

where N is a constant

σ is the applied stress

H and β are the activation energy and activation volume of the process leading to either ductile or brittle failure

h and k are Planck's and Boltzmann's constants respectively

T is the absolute temperature

Equation (2.17) implies a linear stress-log time to failure relationship with a slope of $2kT/\beta$ or in other terms the equation can be written

$$\sigma = A_1 - B_1 T \ln t \qquad (2.18)$$

sometimes referred to as the "Russian" method for the prediction of stress rupture performance.

Barton and Cherry (42, 78) obtained stress rupture data from Hoechst A.G. for Hostalen GM 5010 pipes and plotted the results in this linear stress-log lifetime fashion. Reasonable curves at testing temperatures of 40, 60 and 80°C were constructed from the data using the activated rate process theory. However, evidence (42, 78) suggests that for HDPE the activation volume β is not

constant and will increase with temperature. (Kubat et al (81) produced results indicating that β also varies with stress.) These effects are contradictory to the proposals by Barton and Cherry (42, 78) since in order that they were able to produce curves to fit the pipe data more closely, a temperature dependent activation volume was required. In fact for GM 5010 HDPE pipes the value of β more than doubled as the test temperature increased from $20^{o}C$ to $80^{o}C$.

In spite of these difficulties Barton and Cherry (42) formulated a general equation describing the brittle rupture time at any temperature for HDPE GM 5010 pipes, which is based on a knowledge of the temperature variation of the activation volume and other terms in the rate process equation, and is expressed as

$$\sigma = 7.10 \times 10^{16}\, T^{-4.30}(1.12 \times 10^{4}\, T^{-1} - 13.5 - \ln t) \qquad (2.19)$$

which at $20^{o}C$ becomes

$$\sigma = 201 - 175 \ln t \qquad (2.20)$$

(iii) Fractography and Failure Mechanisms.
In non-oriented thermoplastics such as HDPE and MDPE the failure mechanism under static loads is dominated by the development of creep cracks (73).

The failure mechanism can be divided into three growth periods.

a. Homogeneous deformation which induces a crack to form.
b. A period of slow stable crack growth.
c. A period of unstable crack growth.

Generally, this formation and growth of creep cracks can be examined from the resultant fracture surfaces which can exhibit a number of features, as shown in Figure 2.10.

Although not always the case, cracks are often observed to initiate at defects within the material. A stable crack growth follows which is considered to be thermally activated (73). The supposed constant conditions during this period cause a circular or elliptical smooth fracture surface to form which can extend across the thickness of the material, depending upon the applied stress.

Higher magnifications reveal that for HDPE a cellular, locally highly drawn surface has formed in the mirror zone and can be seen in Figure 2.11.

(Niklas (82), Gaube (74) and their co-workers have also found, with transparent PE pipes, that the period taken to initiate a crack could account for 90% of the lifetime of the pipe.)

From the fractographic analysis of surfaces of MDPE pipes, slowly spreading cracks and ring-like traces of the crack front can be seen in Figure 2.12 under low power light microscopy (83). Here a creep crack surface distinctly shows elliptical rings, the centre of which lies at the nucleation site. The crack had apparently propagated slowly, the surface being uniformly covered with drawn fibrils as in Figure 2.13. High local ductile drawing occurs at or ahead of the crack tip, which Bragaw (83) suggests results from a craze preceeding the crack.

It is also indicated that the fatigue cracks in HDPE pipes reported by Cowley and Wylde (20) are due to a creep type failure which is evident from the surface being covered with drawn fibrils, upon which, however, are superposed gross rings of a very different nature from sustained load markings. Bragaw (83) suggests that these rings are caused by a discontinuous crack growth.

Hannon (84) reports on the mechanism of crack growth in a variety of HDPE samples under constant stress in a water environment. His findings are that the fracture surface of an HDPE copolymer produced in a water environment at 60°C shows a macroscopically brittle mode of

failure, the crack being preceeded by a void nucleation and growth process with considerable ductile deformation between the voids which results in the formation of fibrils.

To summarise, the brittle fracture of HDPE in a water environment at elevated temperatures ($-60^{o}C$), under plane strain conditions, at stresses well below the yield stress, proceeds by a mechanism of hole nucleation, hole growth and finally followed by the plastic deformation (yielding) of the molecules surrounding the voids.

In pipes under internal pressure, the complex stress system will give the crack growth mechanism a sense of direction and will nucleate at positions of highest stress.

(iv) Effect of Material Properties on Fracture Behaviour.

Creep is able to proceed unaffected by crack propagation although the reverse is not true. Every fault in a pipe requires a different initiating stress to start a crack and a different propagating stress, in many cases caused by the geometry of the crack tip (85). Therefore, as the general stress level increases due to creep under constant internal pressure, more cracks will open up and propagation rates will increase. Only one crack will be in evidence at failure, if there is a fast crack propagation, at slower rates a number of cracks will have initiated and be on their way through the pipe wall, only the fastest will actually cause failure.

Naturally creep and crack propagation can occur at the same time, but since the relationship between the initial stress levels and time to failure for both mechanisms is different, the process leading to failure in the shortest possible time will predominate. In HDPE, the failure process has been shown to change at different stress levels (86 - 88).

With respect to the brittle failures a variety of factors affect the resistance of PE pipes to crack propagation under static internal loads.

Kagan et al (89) have studied the effect of microstructure on the time dependent behaviour of HDPE. They found a clear tendency for the increase in resistance against creep crack formation with an increase in density and size of crystallites and with a reduction in spherulite diameter. Also Gaube et al (74) have reported that an increase in crystallinity will lead to a higher yield strength at lower strain values and also to higher ductile strength. They go on to suggest that the higher the crystallinity and molecular weight the sooner the brittle fracture curve begins on a stress rupture plot.

Kausch (73) judges from these observations that the process of creep crack formation is related to a gradual disentanglement of chains and the ease of void opening in the intercrystalline and/or interspherulitic regions. Both mechanisms being essentially independent of creep deformation.

2.5.6 Fatigue Testing and Fatigue Failure

(i) Introduction.

The process of fatigue failure can be defined by conditions of a repeated or cyclical form of loading where the maximum applied stress is less than would lead to immediate failure (90).

The test methods, as summarised by Andrews (90) involve,

a. A periodically varying stress system having a characteristic stress amplitude $\Delta\sigma$,
b. A corresponding periodic strain amplitude $\Delta\varepsilon$
c. A mean stress level σm
d. A mean deformation εm
e. A frequency ν
f. A characteristic waveform for both stress and strain.
g. Ambient and internal temperatures, which in general will not be precisely identical
h. A given specimen geometry.

For pipe systems the actual tests involve a periodic loading between fixed stress limits, in tension, where normally σm is set at some positive value and the minimum stress is zero or close to it (91, 92, 93).

The object of fatigue testing is generally to develop a so-called S-N curve or Wöhler curve. Such curves relate the maximum or mean applied stress or stress amplitude to the number of cycles it takes to produce failure. This is particularly time consuming and expensive when carried out on pipe systems. Tests are therefore generally conducted at elevated stresses and temperatures to produce failure in reasonable times. A particular drawback, however, is that the use of too high a frequency may lead to a mode of failure called thermal melting and not to failure caused by cumulative damage or crack initiation and propagation.

Fatigue failure by thermal melting is due to the hysteretic energy generated during each loading cycle (94, 95, 96) causing a rise in temperature which lowers yield stresses. Such failures occur usually at high loading frequencies of 10 H_z or more, large stress amplitudes and when the rate of cooling is low. The other two failure modes mentioned above will be discussed in more detail later in this chapter, since they are more relevant to the work presented herein.

The schematic Wöhler curve for a creep sensitive thermoplastic material is shown in Figure 2.14. Stapel (97) describes it in three stages. (It should be noted here that although Stapel is referring to uPVC, which in pipe form does not exhibit a "knee" in its stress rupture curve, his description of the Wöhler curve can, in general, be applied to PE pipe materials since they are creep sensitive.) Stage 1 is considered highly dependent on the applied frequency, such that at lower frequencies the number of cycles leading to failure reduces. Stage 2 has a greater slope and creep tends to exhibit diminishing influence with reduction in stress. The influence of frequency declines steadily at lower stress levels in Stage 3 and is often referred to as the fatigue or endurance limit. Strictly, Stage 3 can only be considered limiting if it is horizontal, implying that as the stress falls below this limit an infinite number of cycles at any frequency can be applied without inducing failure.

Practically, for thermoplastics, Stage 3 is slightly inclined which means that the number of cycles leading to failure increases sharply with only a modest reduction in stress. In spite of this, Stage 3 can still be considered as practically independent of frequency.

(ii) Effect of Fatigue Testing Variables on Fracture Behaviour.

The fatigue properties of pipe systems subjected to internal pressures can be affected by a variety of parameters such as environment, temperature, frequency of pulsation and so on. It is proposed, therefore, to discuss the effect of a relevant selection of such properties on pipe system lifetime.

Since fatigue failure generally includes a creep component (particularly if the waveform is square) any factors which can influence the time to failure caused by static loads ., will also affect time to failure under fatigue conditions. Such variations can be more or less significant depending upon the contribution of creep to the failure process in fatigue.

Pipe and Fitting Quality -

The grade and quality of pipe and fitting materials have been shown to have a significant influence on fatigue performance. Moore et al (18) found that in poorly processed uPVC pipe, identified by the relatively large concentration of polymer granules which had not become homogenised with the remainder of the plastic during processing, exhibited a reduction in time to failure when tested under fatigue loads using D-shaped spacers. To the author's knowledge no work of this nature has been published for PE pipes.

Other investigations with uPVC pipes have been carried out by, for example, van Crombrugge (98), where times to failure for different manufacturers' pipes showed distinct variations, when subjected to identical fatigue conditions of frequency, load and temperature.

The S - N curves obtained by Joseph (91) shows the variations that can be obtained when different manufacturers' pipe materials are used. There is no reason to suppose that such effects will not occur in PE pipes and fittings, but the documentary evidence for this is limited.

Pipe Size -

A number of studies of the influence of pipe diameter and wall thickness on fatigue performance of uPVC have been reported. The findings of these studies are summarised below

a. Larger diameter pipes do not of necessity exhibit lower fracture strength under fatigue at the same maximum hoop stress (18).
b. Pipes of larger wall thickness exhibit lower fracture strength and allow the process of fatigue crack propagation to progress more easily (18).
c. Smaller diameter pipes last longer than larger diameter pipes when subjected to the same maximum hoop stress, all other parameters being equal (99).
d. Tests on pipes with different SDR's indicate that the thin walled pipes sustain fatigue loadings better than thick walled pipes, for the same maximum hoop stress (98).

The conclusions drawn in 'a' by Moore et al (18) and in 'c' by Kirstein (99), although not exactly contradictory, certainly do not reinforce each other's findings. In other words, by increasing the pipe diameter and maintaining the same wall thickness, but subjecting all pipes to the same hoop stress, the lifetime under fatigue may or may not be reduced.

Test Frequency -

As a general rule for semi-crystalline thermoplastics, the lower the frequency of the applied load, the fewer the number of cycles to failure, and the greater the period of test (the number of cycles multiplied by the cycle time) (97, 100, 101, 102).

There is an immediate contradiction of this "general rule" in a paper by McKenna and Penn (102). For conditions of zero-tension sinusoidal fatigue tests they found that the lifetime (time of test) of PE increases with increasing test frequency. For polymethylmethacrylate (PMMA) increasing frequency caused the fatigue lifetime to decrease. Thus PMMA obeys the "general rule" as suggested by Stapel (97) but PE does not, when subjected to the conditions stated above. There would appear to be some process at work in PE which is not yet obvious, but may have something to do with the waveform of the applied load. Also, these results are not produced on pipe

samples and as yet there appears to be no data available for the fatigue properties of PE pipes from the frequency variation point of view.

Depending on the frequency of internal pressure pulses, two types of failure are observed:

a. Fatigue crack initiation and propagation.

b. Fatigue thermal melting.

To obtain fatigue failures in reasonable time, the highest practical level of frequency is normally used. However, as mentioned earlier the accumulation of hysteretic energy produced during each cycle is largely dissipated in the form of heat generating a temperature rise in thermoplastics, especially in the absence of isothermal conditions.

This rise in temperature can be so great as to eventually cause the sample to melt, thereby preventing any load bearing capability (94, 96, 103, 104, 105).

For pipes of uPVC, Stapel (97) discusses the effect of a range of fatigue frequencies from 0.1 to 23.0 cycles per minute (cpm). He reports that Hucks (106) found no significant differences in the performance of the pipes fatigued in the stated frequency range. (The stress levels of these tests by Hucks (106) are not recorded and since the influence of frequency clearly varies with different stress levels (reference 97, Figure 8 and reference 102, Figures 10 and 11), the results must be confirmed by other workers for them to be generally accepted.)

Several other researchers have examined fatigue properties of thermoplastics pipe (91, 93, 107) but in general only at one frequency, so that comparisons cannot be drawn to identify any frequency induced effects on lifetime.

No mention is made in the literature on the effect of fatigue frequency on fitting performance except by Jacobi (108). He subjected injection moulded uPVC tee fittings to two frequencies at several pressures in a range up to about 6 ± 2 atmospheres (0.606 ± 0.202 MPa) and at a temperature of $20^{\circ}C$. He found that the increased

frequency (80 cpm) reduced the lifetime of the tee significantly, compared with a lower frequency of 2 cpm. Jacobi considered such failures to be related to the effects of processing, and went on to say that the results from his work proves the unsuitability of short term tests and long term tests under constant load for industrial plastics articles such as pipe fittings, which are subjected to periodically changing stresses. In such cases he considers that only testing with alternating internal pressure or alternating stresses is useful.

Cowley and Wylde (20) also indicate a definite weakness in 160mm OD tee fitting to pipe butt-welds in HDPE when subjected to fatigue loadings of 0.63 MPa internal pressure, at 50°C, with a frequency of 4 cpm.

Thus, again, the necessity of examining every type of joint and fitting as well as pipe, under fatigue conditions, becomes apparent.

Shape and Loading Profile -

Stapel (97) refers to work by Oberbach and Heese (109) which suggests that square wave loading profiles lead to failure sooner than either sinusoidal or sawtooth types of waveforms. It appears that such differences occur more markedly at high stresses, whereas at lower stresses no significant differences are apparent.

The reason for this appears to be due to the effect of creep deformation which has greater influence at elevated stresses; coupled with this is the reasonable assumption that since a rectilinear waveform imposes a maximum stress for longer compared with a sinusoid or sawtooth, the amount of creep damage per cycle would be greater.

Hertzberg and Manson (94) discuss the effect of loading profile on fatigue crack propagation and propose theories which conflict to some extent with those suggested by Oberbach and Heese (109).

A change in strain rate is brought about by altering the waveform from rectilinear to sinusoidal or triangular, this will affect the material's stiffness

as well as its yield strength, particularly with non-linear viscoelastic polymers such as HDPE. The higher the strain rate, the stiffer the material and the higher its yield stress.

To summarise Hertzberg and Manson's opinion, the effect of loading profile on fatigue behaviour has been examined on a number of polymers where, for example, a square waveform has provided a strongly beneficial effect, no effect and a decidedly deleterious effect (94, 96). Since polymers such as PE, uPVC and so on differ with respect to their viscoelastic response, the different strain rates provided by the three types of waveform mentioned above will have different effects on each material. There is, apparently, no hard and fast rule to enable a prediction of behaviour to be made.

However, because the various loading profiles result in different load-time integrated areas and different loading rates, the effects due to creep deformation and load application, as described by Oberbach and Heese, have to be isolated. Hertzberg and Manson (94) show for a number of thermoplastics (not including PE) that for the same loading rate, crack growth rates were consistently higher in association with the square wave which possesses twice the load-time integrated area (⊓), compared with the negative sawtooth waveform (◺).

For any work specifically related to PE plastic pipes, it is necessary to refer to Lörtsch (92), who found that a sinusoidally varying internal pressure on HDPE pipes increases time to failure if compared with a static load.

From the preceeding discussions it becomes clear that both loading rate and load-time integrated area must be considered when examining fatigue response in PE pipe systems. This will supply only part of the solution, however, since stress levels and frequency will also produce significant effects, for reasons described previously. Fatigue response in PE is thus apparently a result of a complex interaction in a number of variables, which has not been clearly defined in the literature to date.

Static Loads -

A series of interesting tests have been carried out by Hucks (106, 110, 111) whereby the effect of a static load prior to cyclic loads was examined. The reverse case was also considered. One test is described where a uPVC pipe was put under a fatigue load for 90% of the average number of cycles to cause failure, the pipe was then subjected to a static load at the same maximum pressure. No reduction was observed in the static load time to failure at a given stress, for the previously fatigued pipe compared with the life of a pipe subjected to static load only.

The converse also appeared to be true, that there was no reduction in fatigue life after a pipe had been subjected to static load.

(iii) Prediction of Fatigue Lifetimes.

When failure of plastics components by fatigue thermal melting is precluded the lifetimes of such articles subjected to certain fluctuating loads have been successfully predicted by using the concepts of cumulative damage and cycle dependent failure which can be described in terms of fracture mechanics.

The cumulative damage concept of fatigue failure assumes damage accumulates only during the time when the part is subjected to stress, failure occurring when the accumulated damage reaches a critical value (102).

For simple loading profiles, such as a rectilinear waveform, the cumulative damage model is able to predict the number of cycles to failure, N_f, using an expression similar to that of Stapel (97):

$$N_f = \left[\frac{\tau_{SR}}{t_{max}} \right]_{T,\sigma} \qquad (2.21)$$

where τ_{SR} is the stress rupture lifetime and t_{max} is the section of the time cycle under the set maximum load, both at the same stress and temperature. In theory equation (2.21) is frequency independent and no restriction is placed on the length of the period t_{max} spent at maximum stress during each cycle. There is also no

allowance made for recovery of damage, so that it must be assumed that either the recovery or the time off load is negligible.

In cycle dependent fatigue failure the repeated application of stress, rather than the time for which the stress is applied, induces damage and causes a crack to propagate. It implies that a component will fail after a given number of fatigue cycles and the total lifetime to failure decreases proportionately with increasing test frequency. McKenna and Penn (102, 112) have shown that PE subjected to sinusoidal fatigue loading does not fail in a cycle.dependent manner, nor can the previously described cumulative damage concept describe the material's frequency dependence.

The actual rate of crack propagation is in terms of the number of loading cycles, N, and is usually expressed in a form attributed to Paris (113):

$$\frac{da}{dN} = D(\Delta K)^d \qquad (2.22)$$

where D and d are material constants and ΔK is the stress intensity factor range given by

$$\Delta K = K_{max} - K_{min} = Y(\Delta\sigma)\sqrt{\pi a} \qquad (2.23)$$

and Y is again a geometrical correction factor

$\Delta\sigma$ is the gross stress range

a is the crack length.

In this mode of fatigue failure, for plastics, the frequency of loading can have a considerable influence on both "constants" D and d.

Equations (2.22 and 2.23) can be further integrated with respect to N between the limits of initial crack length a_o and the final crack length, which for pipes is the wall thickness h (2, 8, 79). Thus we have

$$N_f = \frac{2}{d-2}\left[a_o^{(1 - d/2)} - h^{(1 - d/2)}\right]\frac{(Y(\Delta\sigma)\sqrt{\pi})^{-d}}{D} \qquad (2.24)$$

This equation assumes that the geometrical correction factor, Y, remains constant between a_o and h. If, however, Y depends strongly upon crack length then the equation for N_f must be evaluated numerically.

When $h \gg a_o$, its contribution to the expression for N_f is very small and the equation can be simplified to

$$N_f = \frac{\text{Constant}}{\Delta\sigma^d} \qquad (2.25)$$

which can prove useful for determining stress level effects on the fatigue crack propagation lives of samples with identical geometries and flaws (114).

(iv) Fractography and Fatigue Failure Mechanisms. The majority of work reported in the literature refers to the fatigue of glassy polymers (73, 94, 96 for example). However, White and Teh (115) have helped to rectify this position and discuss results obtained mainly with LDPE, but also refer to HDPE and plasticised polyvinyl chloride (pPVC). Laghouati et al (32) detail results specifically related to FCP and HDPE and Cowley and Wylde (20) deal with the fracture morphology and mechanisms of fatigue failure in HDPE pipe systems. It is proposed to discuss these papers separately.

White and Teh (115) used a specially constructed fatigue rig at a frequency of 0.24 Hz (15 cpm) on compression moulded parallel sided dumb-bells where the internal stresses had been removed. The HDPE material had an average molecular weight $\bar{M}w$ of approximately 10^5 and a number average molecular weight of approximately 10^4, a density of 960 kg m^{-3} and a melt flow index of 2.5. They indicated that stress whitening was found to occur at the crack tip prior to crack growth. The surface showed a fibrous type of failure where the fibrillation was more extensive and developed to a degree greater than in the other polymers of their investigation. Microfibrils were observed with lengths of the order of nanometers and were found to be comparable to the well developed microfibrils produced by "cold drawing" of HDPE at elevated temperatures. The

fractured fibril remnants were generally less than 3 μm in length.

During large cyclic crack advances it is often the case that fatigue striations are formed particularly under conditions of high tensile strain and during the final stages of fracture. Slow crack growth in HDPE is usually related to a rough fibrous region on the fracture surface. The striations, it is proposed, normally form at the rate of one per cycle, however microstriations are also shown to be present. They are not thought to be caused by a mechanism of crack arrest, rather the microstriations were consistent with their identification as lamellae, either exposed ends or fractured sections which lie parallel to the crack front. Hertzberg and Manson (94), however, consider that the 0.5 μm wide bands found on fracture surfaces in their own studies may represent a cluster of several lamellae or different sections through such crystalline units.

Microstriations were also in evidence in the fibrillated region again approximately parallel to the crack front, although some orientation effects have been observed thought to be caused by modifications to the stress field direction corresponding to stress concentrations associated with fibrils. It is difficult to observe microstriations in the fibrillated regions however.

During rapid crack advance, the material at the head of the crack tip is strained at a much higher rate which subsequently prevents cold drawing and the high degree of fibrillation is lost.

The lines (referred to by White and Teh (115) as river lines) which lie in the direction of crack propagation are determined, it is thought, by interspherulitic paths at slightly different levels. Similarly the generally undulating appearance of the fracture surface when tracing paths in a radial direction from the nucleating spherulite can also be related to the boundaries between the spherulites, though plastic deformation can mask such evidence.

Laghouati et al (32) carried out their fractographic and mechanistic analyses on HDPE of various molecular

weights and crystallinities at 20°C. The specimens were notched prior to testing, σ_{max} was maintained throughout the test and no compressive stress was applied to the sample. They found that the lower molecular weight samples of $\bar{M}w$ = 45000, 70000 and 72000 showed extensive micro-ductility arising from micronecking and cracking of damaged regions (voids) in a continuous propagating mechanism, i.e. no striations. The discontinuous propagating mechanism in the cracking of a high molecular weight sample ($\bar{M}w$ = 200,000) was shown by the presence of several crack arrest lines. In the area preceeding the crack arrest lines microstriations were observed. They suggest that microscopic growth calculated on the basis of one striation space for one cycle is much larger than macroscopic observation and it is proposed that a step-wise mechanism, with the formation of a crack in the process zone behind the crack tip gives a reasonable explanation of the fracture surface as shown in Figure 2.15.

This is somewhat different to the mechanisms proposed by McEvily et al (116) for LDPE, who describe a crack tip blunting model for fatigue striation formation. Figure 2.16 shows that during the stress-off period of the fatigue cycle, elastic contraction of the plastic zone ahead of the crack tip imposes a residual compressive stress on the tip, This resharpens, reduces the material ductility ahead of the crack front and produces a fracture surface of alternating troughs and flat regions, where the two surfaces are mirror images.

Cowley and Wylde (20) separate their study of fatigue fracture surface into discussions relating to crack initiation and crack propagation. They indicate that environmental and/or microstructural effects do not have the most significant effect on the initiation of cracks. They observed failures in a water environment and pipe/pipe welds made at the recommended welding temperatures and suggest that the factors causing failure must operate in the absence of environment. They go on to say that failures in pipes are observed well away from the heat affected zones near butt-welds, where there has been significant microstructural change, but which is not considered as a prerequisite for

crack initiation. In general it appeared that failures occurred from either voids within pipes walls or at pipe/pipe welds where defects caused by pipe wall misalignment and weld mismatch could be seen.

In a second series of tests failures initiated at weld bead discontinuities produced by the effect of internal weld lines in injection moulded fittings. The weld defects act as stress raisers and during cyclic loading cracks are initiated at such points.

The fatigue tests on the HDPE systems were carried out at elevated temperatures 43 - 70°C but at a constant frequency of 4 cpm. The pressure profile was of a ramped square waveform.

Scanning electron microscopy confirmed that whatever the mode of crack initiation, the crack growth took the same form in these pipe systems. All surfaces revealed a banded structure which were concentric and allowed the nucleation site to be located. The general structure of the failure surfaces consisted of light areas with a high degree of fibrillation. White and Teh (115) showed the lighter areas to be caused by stress whitening at the crack tip prior to crack growth.

The mechanism used by Cowley and Wylde to explain these fracture surfaces is similar to that proposed by McEvily et al (116). A reduction of ductility ahead of the crack tip during the stress-off part of the cycle is again assumed and when the stress is applied again the crack propagates through the now less ductile zone and into the more ductile normal material producing dark and light bands. Evidence for this effect is also drawn from the fact that the two fracture surfaces for each failure are indeed mirror images of each other.

The underlying microstructure of the material just below the fracture surfaces is also regarded as having an effect upon its appearance. Evidence is found to suggest that material flow during butt-welding and during extrusion or injection moulding induce a directional preference for the fibrils on the surfaces. The fibrils have been shown to point in the direction of material flow. It can be

regarded, therefore, that the fracture surface features are influenced strongly by the microstructure of the material through which the crack has to pass and conversely fracture surface examination can provide microstructural information.

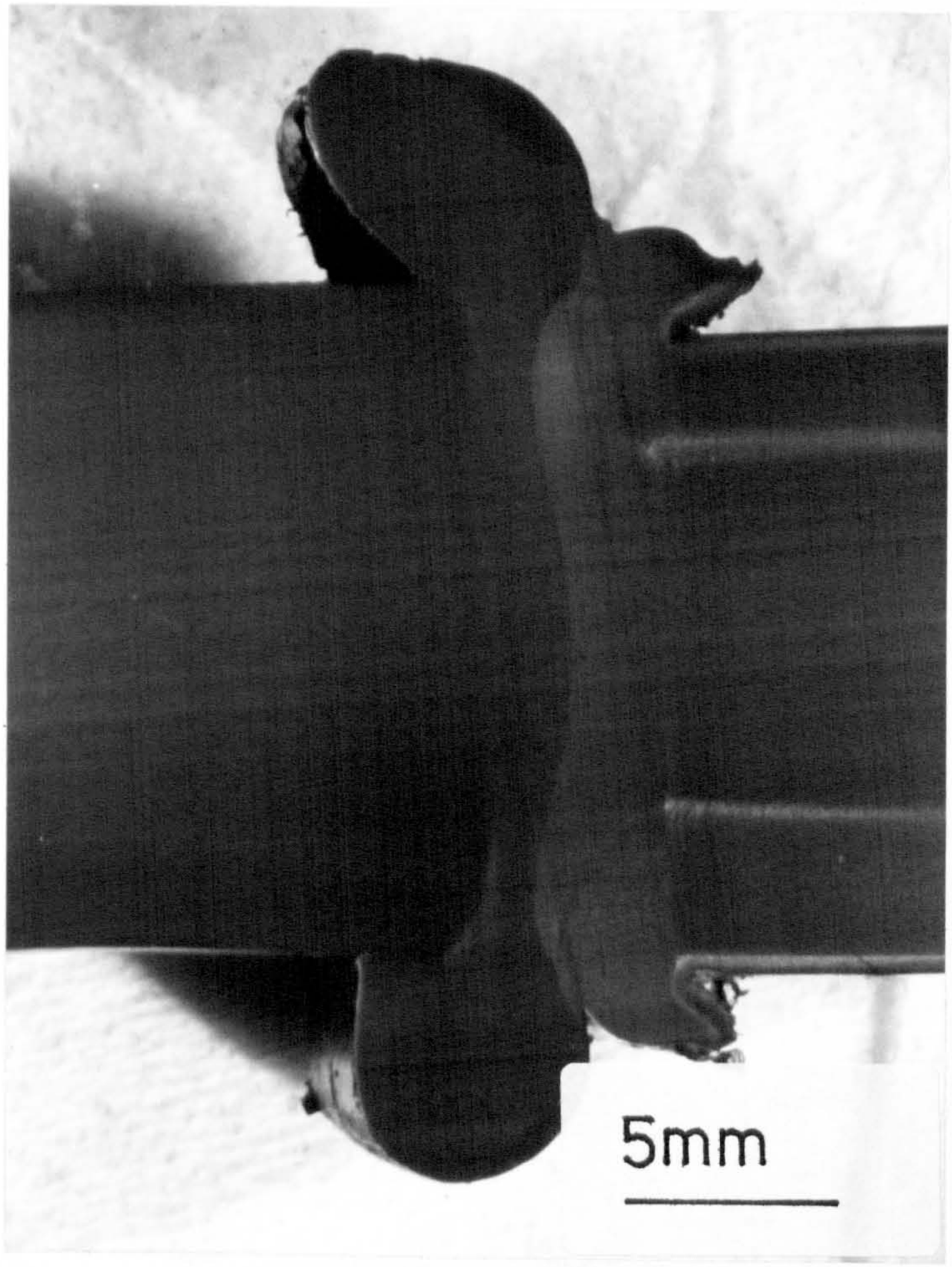

FIGURE 2.1 Morphological variations across an HDPE pipe sample prepared by cutting a thick section from the surface with a sledge microtome.
(After reference 22)

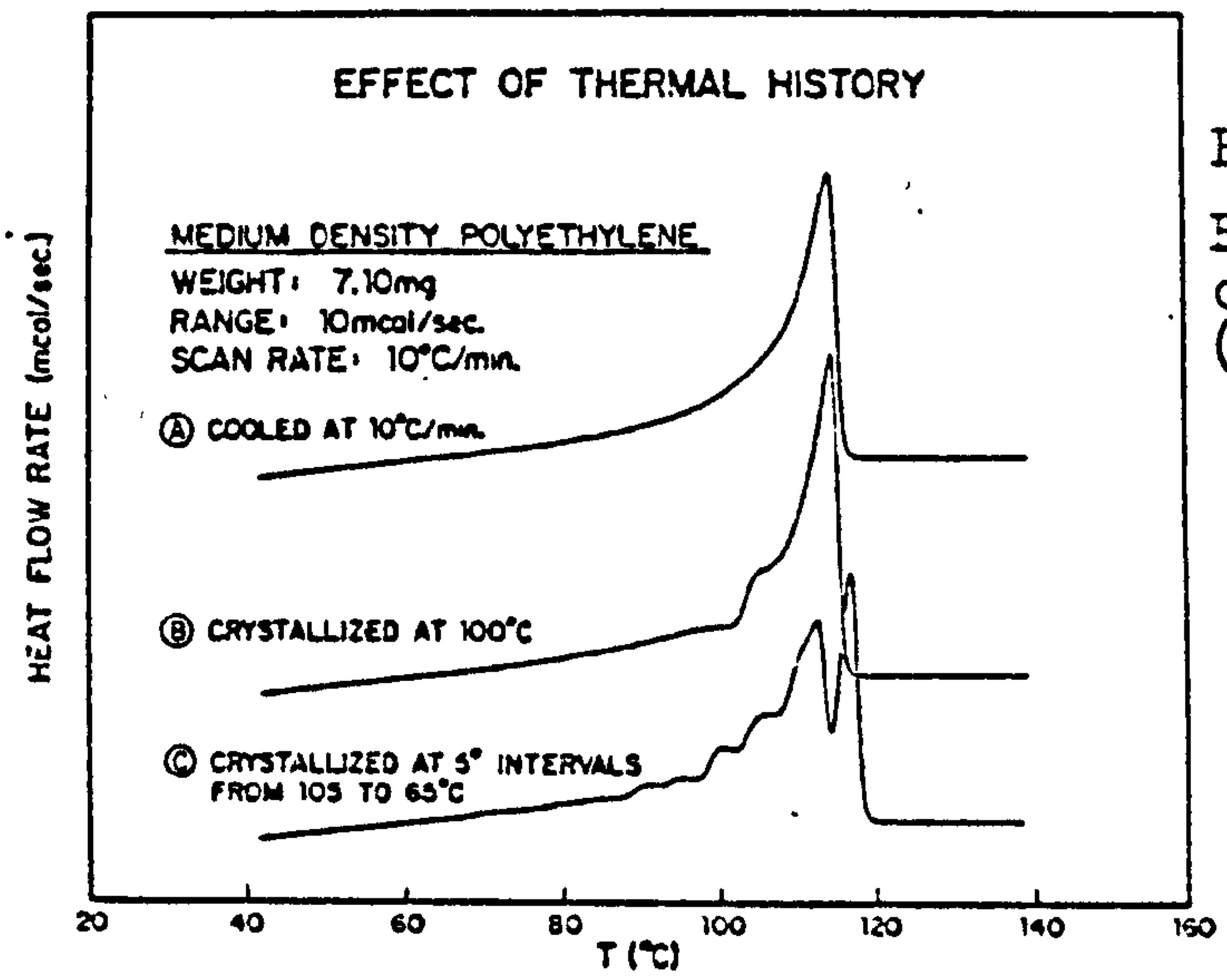

FIGURE 2.2

Effect of thermal history on the DSC endotherm of MDPE. (After reference 36)

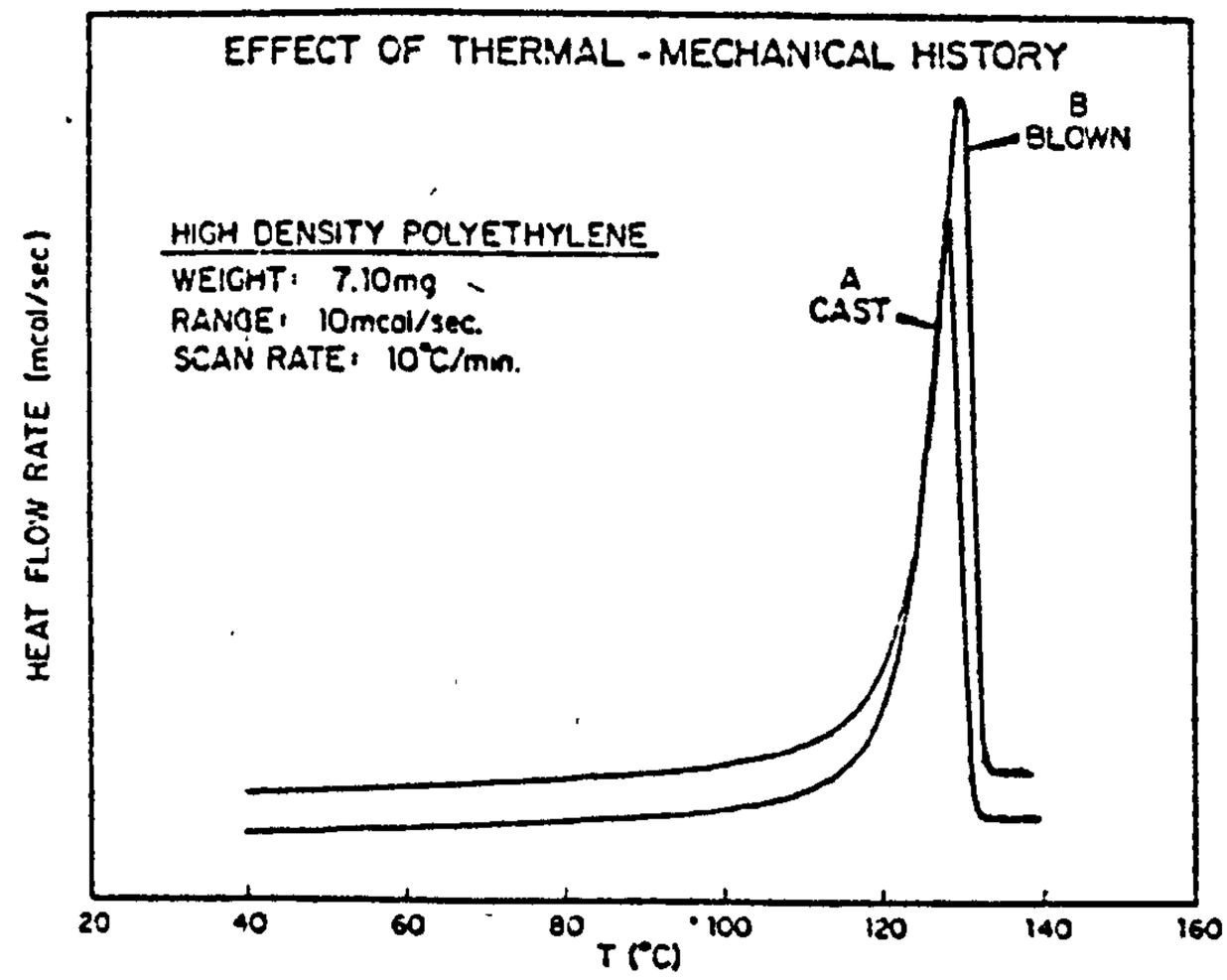

FIGURE 2.3

Effect of thermal-mechanical history on the DSC endotherm of HDPE. (After reference 36)

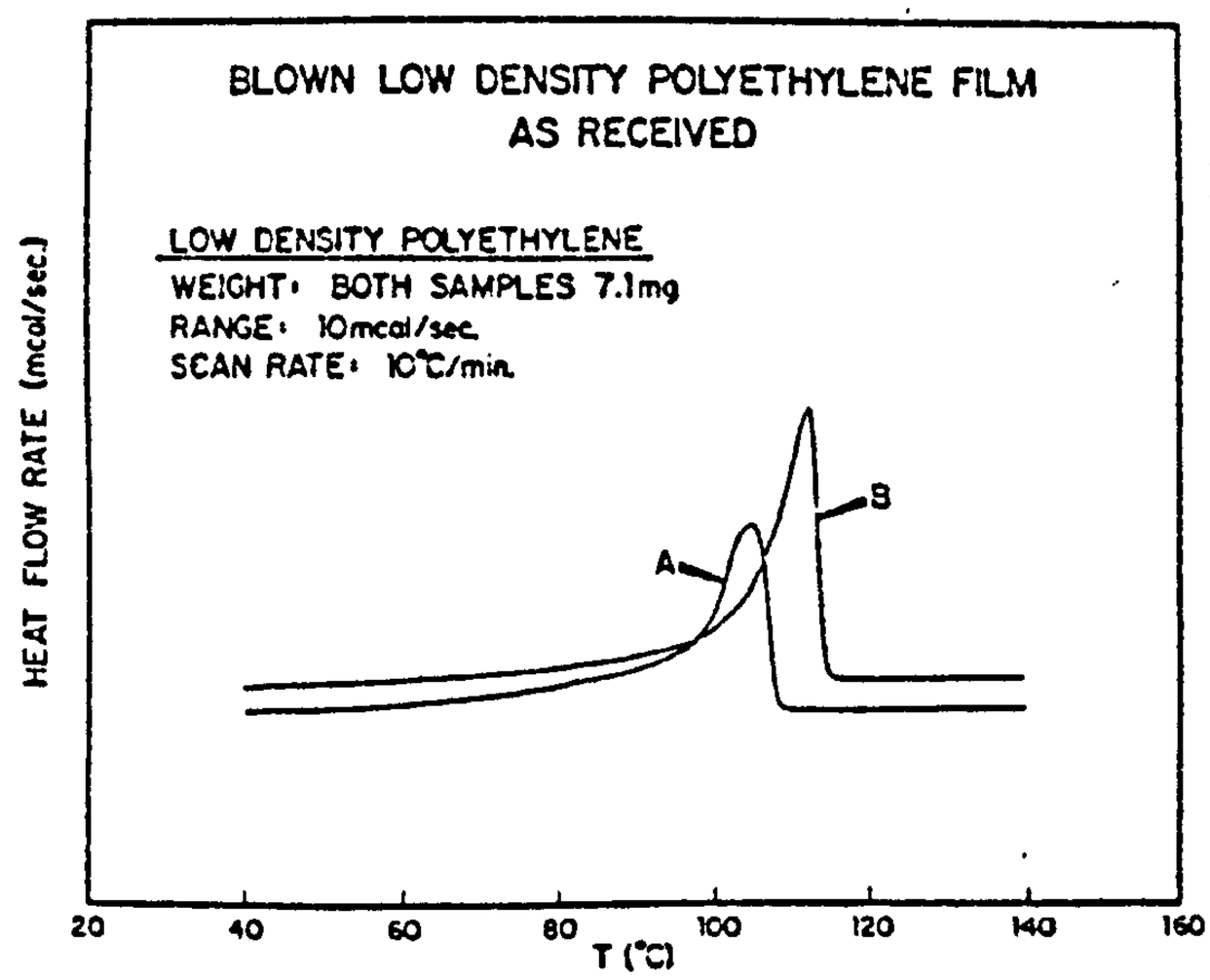

FIGURE 2.4

Effect of different batches of similarly processed LDPE on the DSC endotherm. (After reference 36)

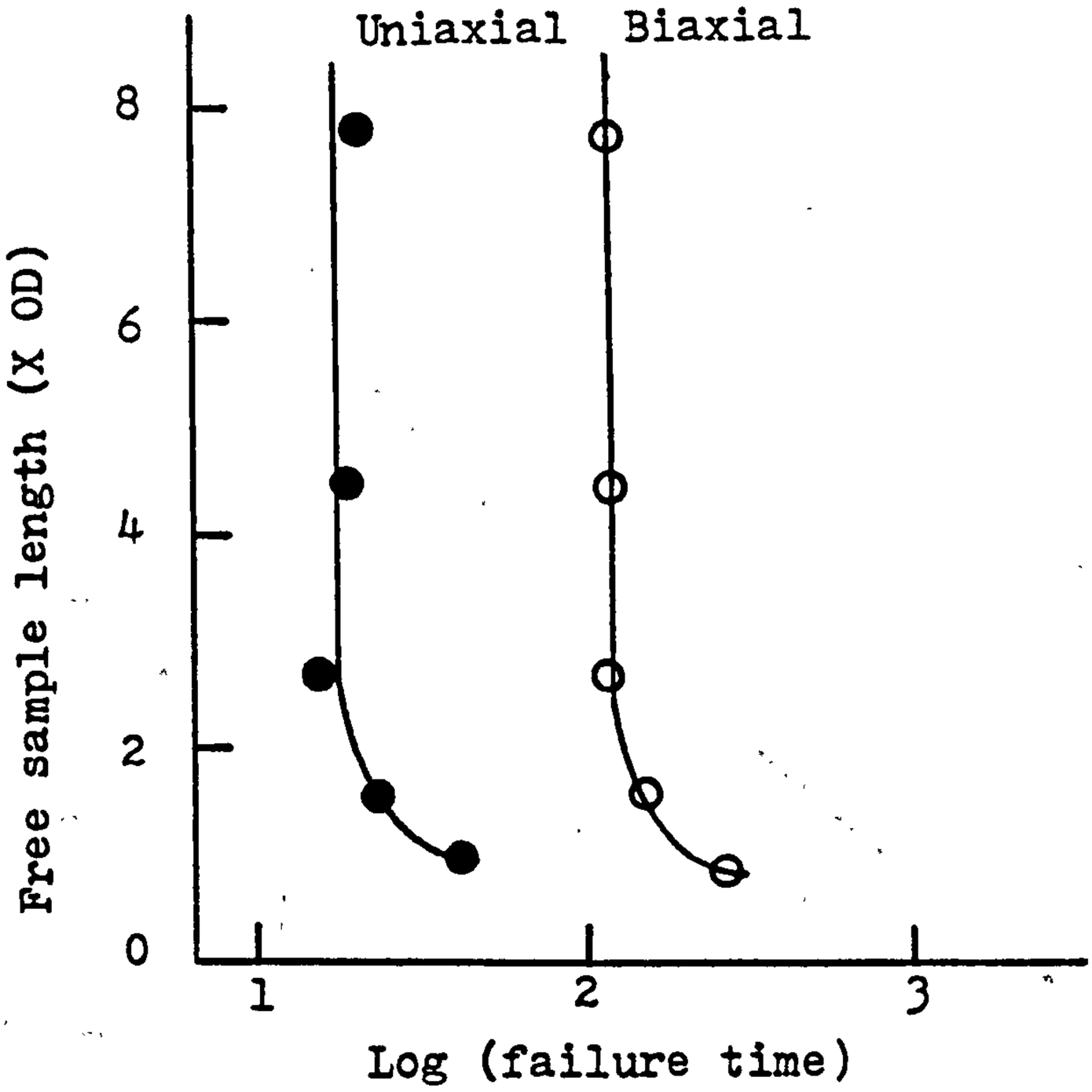

FIGURE 2.5 Dependence of failure time on free sample length of uPVC pipe. expressed in outside diameter units (X OD) for uniaxially and biaxially stressed pipes.
Temperature 20°C; Hoop stress 39.3 MPa
Pipe dimensions:- OD 110mm; Wall 3.3mm
(After reference 61)

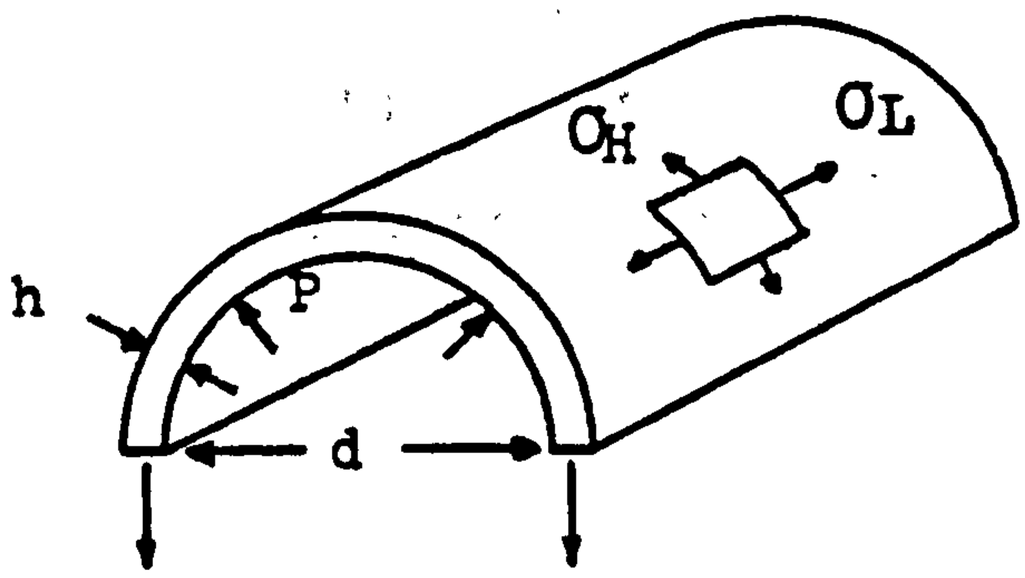

$$\sigma_H = \frac{Pd}{2h}$$

FIGURE 2.6 Half of a thin cylinder subjected to internal pressure showing the hoop and longitudinal stresses acting on any element in the cylinder surface.
(After reference 63)

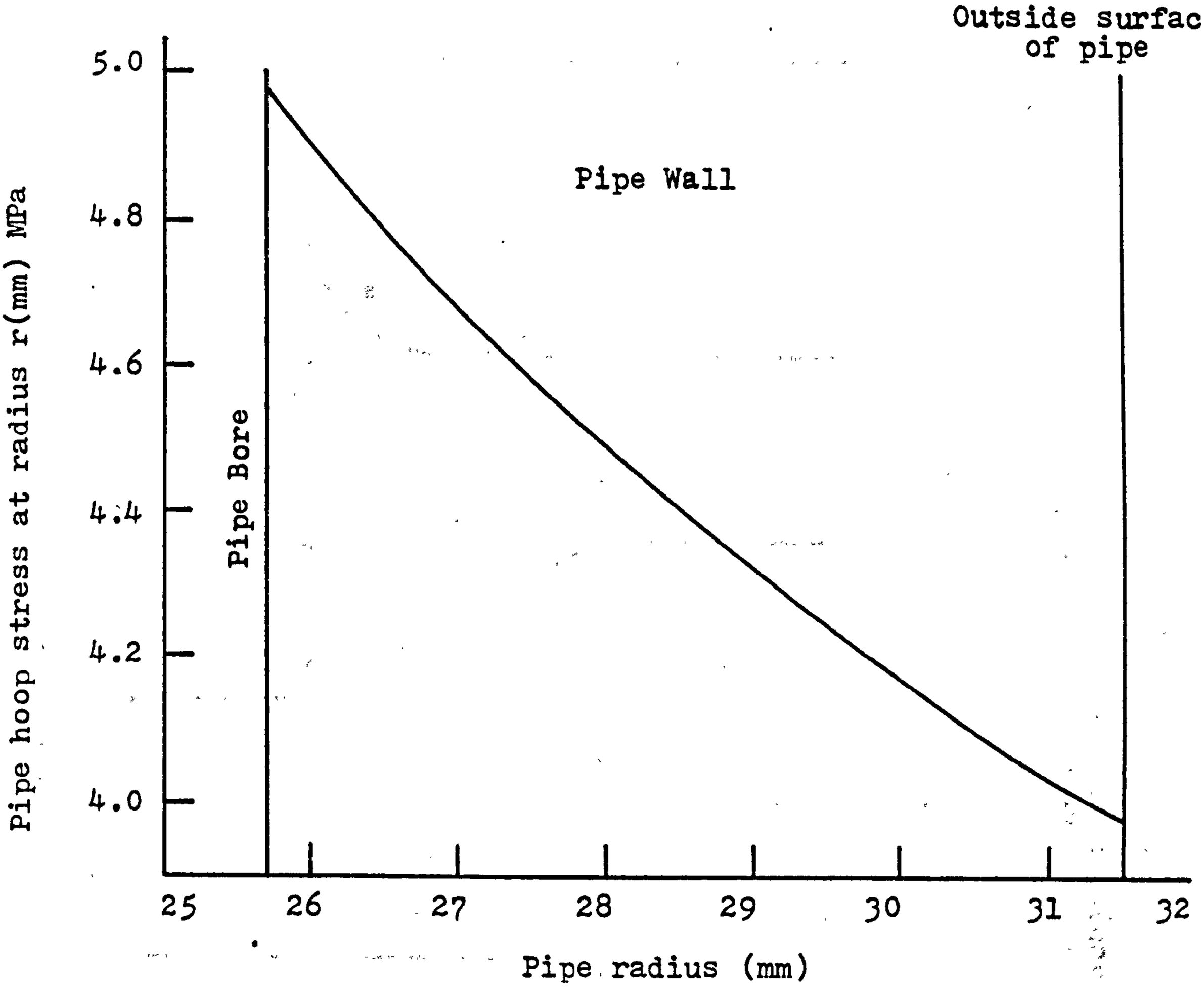

FIGURE 2.7 **Variation of hoop stress through the wall of a 63mm OD SDR 11 pipe using thick-walled cylinder theory.** (For unit internal pressure).

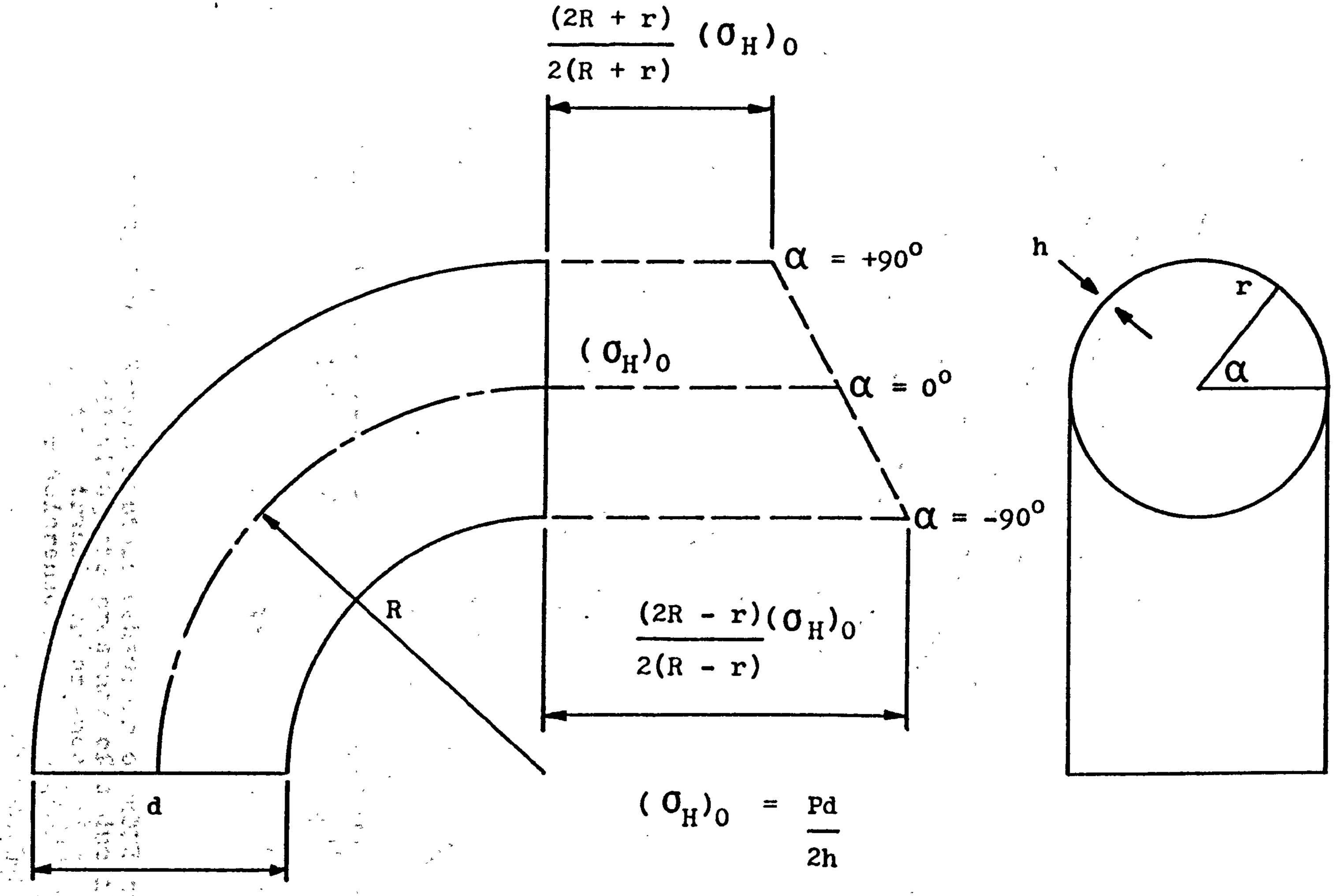

FIGURE 2.8 Distribution of hoop stresses in a thin-walled pipe bend subjected to internal pressure.

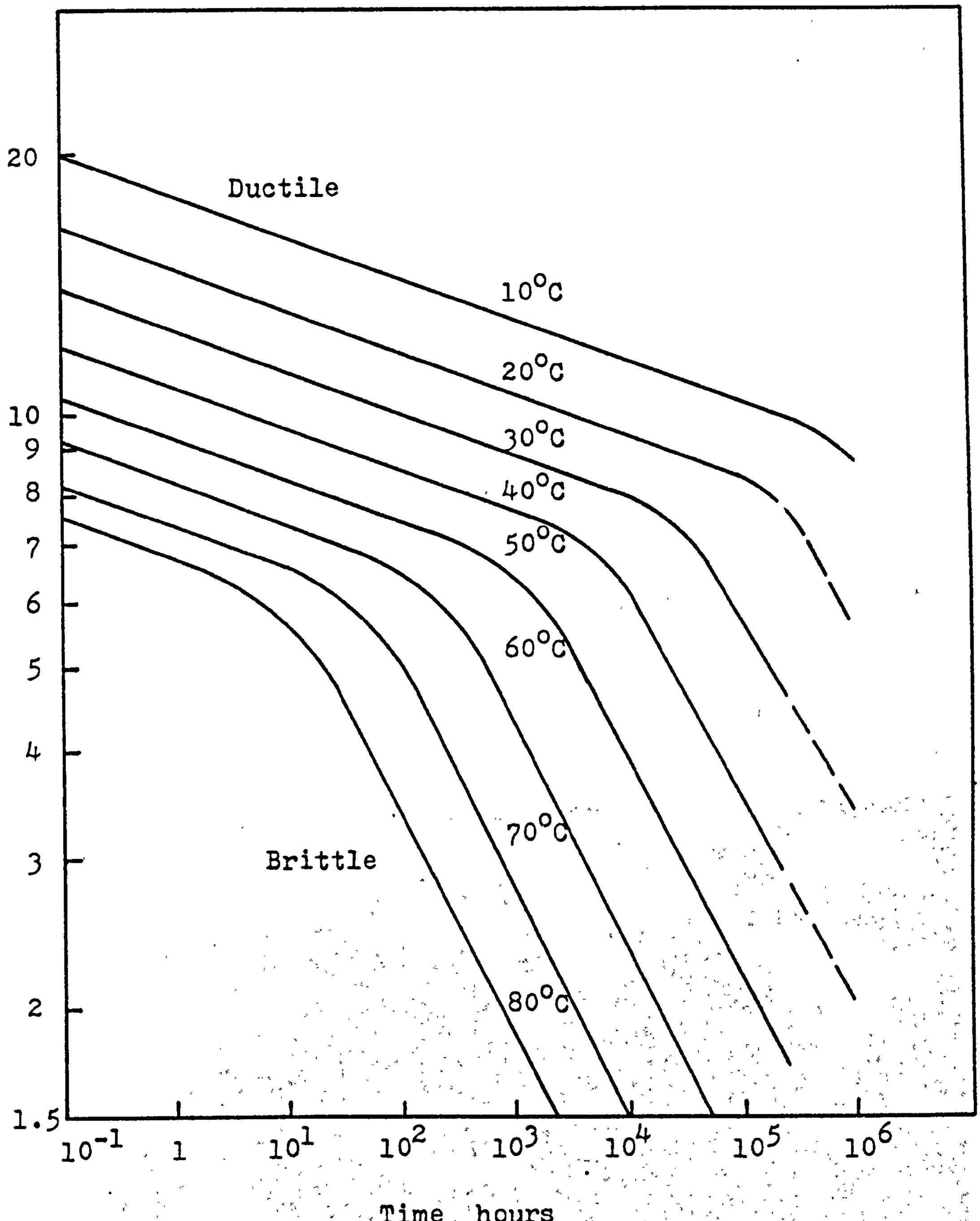

FIGURE 2.9 Stress rupture behaviour of HDPE pipes indicating the presence of a ductile/ brittle transition or knee. (After Reference 6)

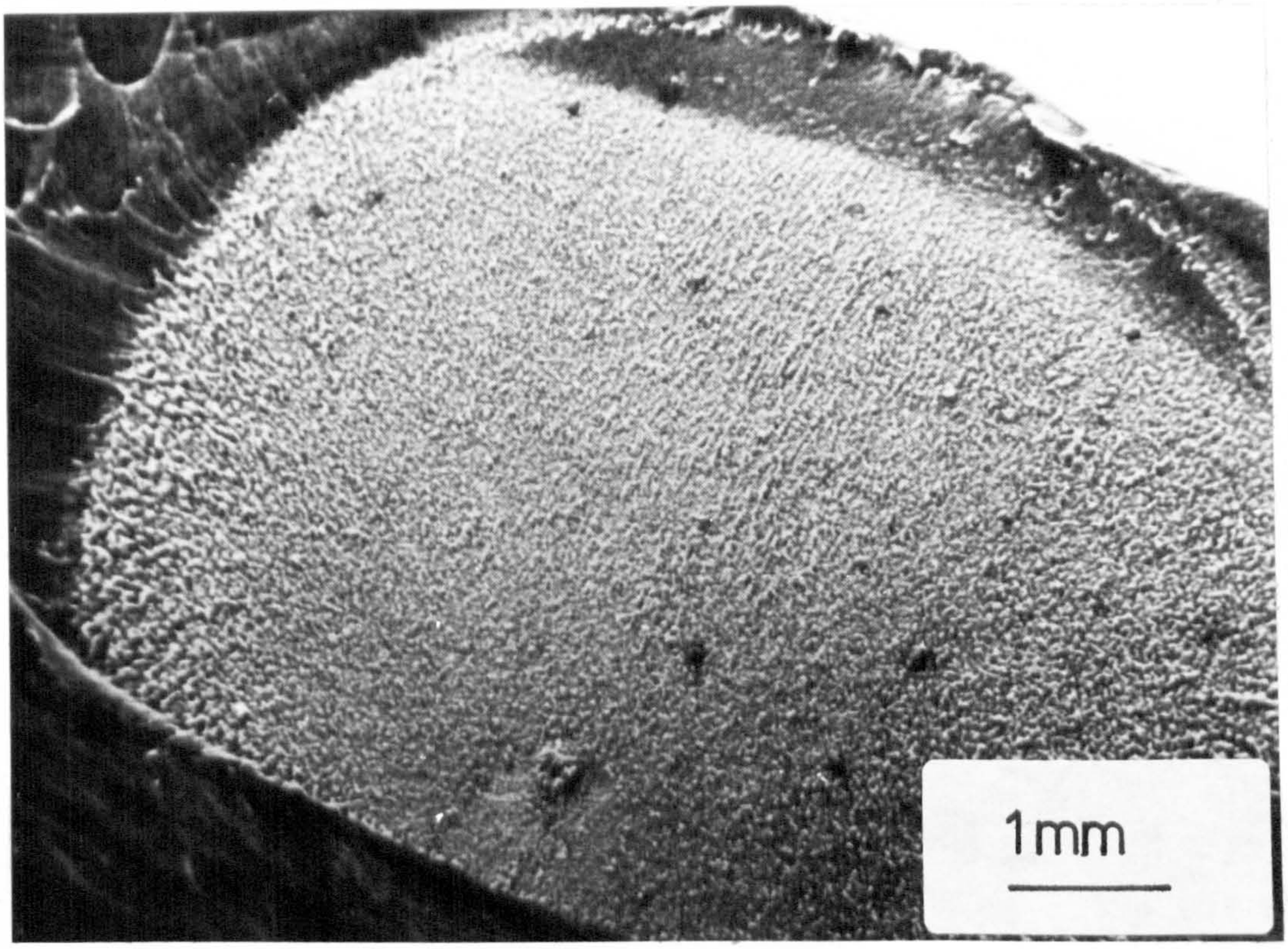

FIGURE 2.10 General fracture surface features of an HDPE brittle pipe failure resulting from static internal pressure.
(After reference 126)

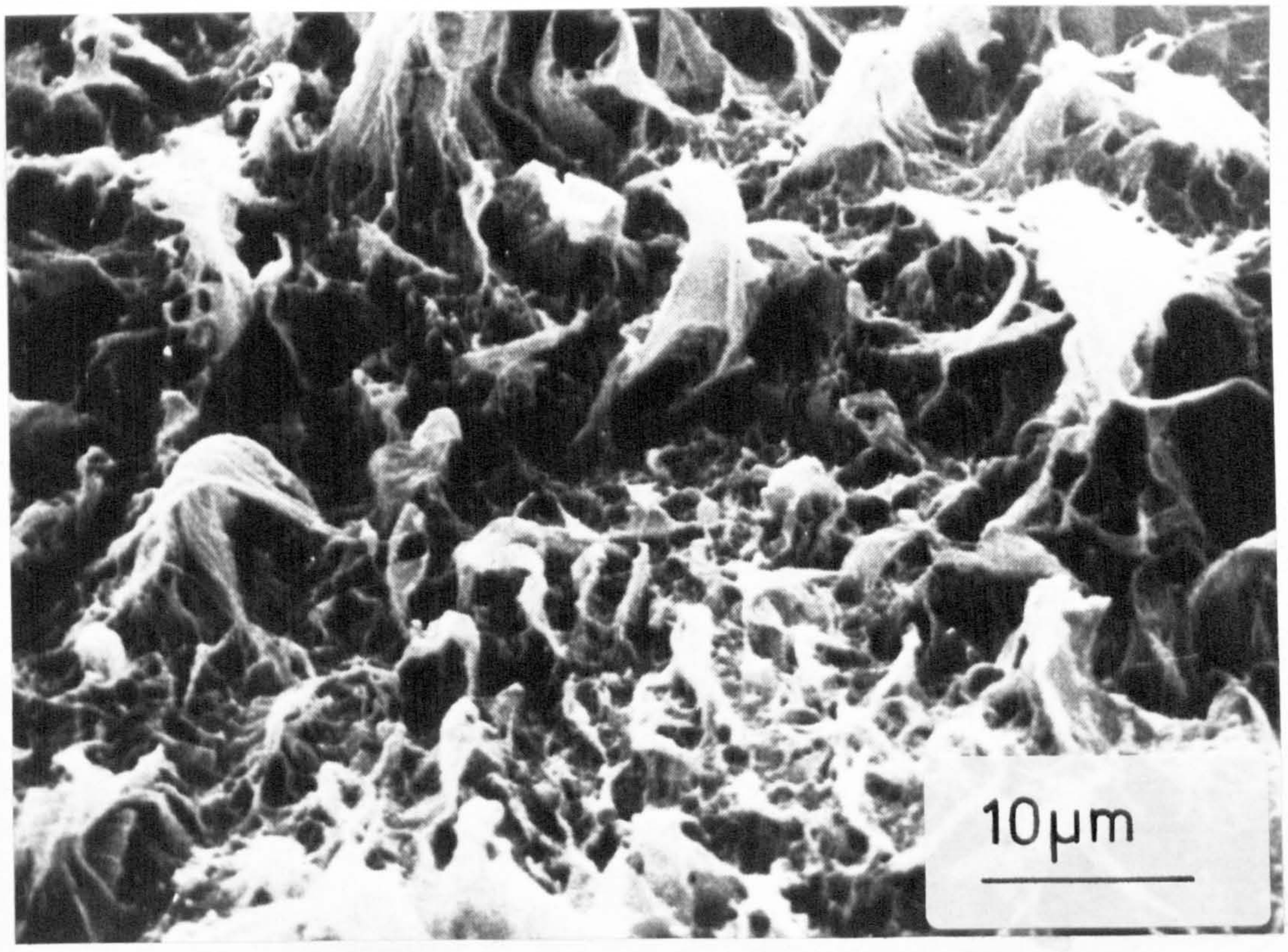

FIGURE 2.11 High magnification fracture surface features of an HDPE brittle pipe failure resulting from static internal pressure.
(After reference 126)

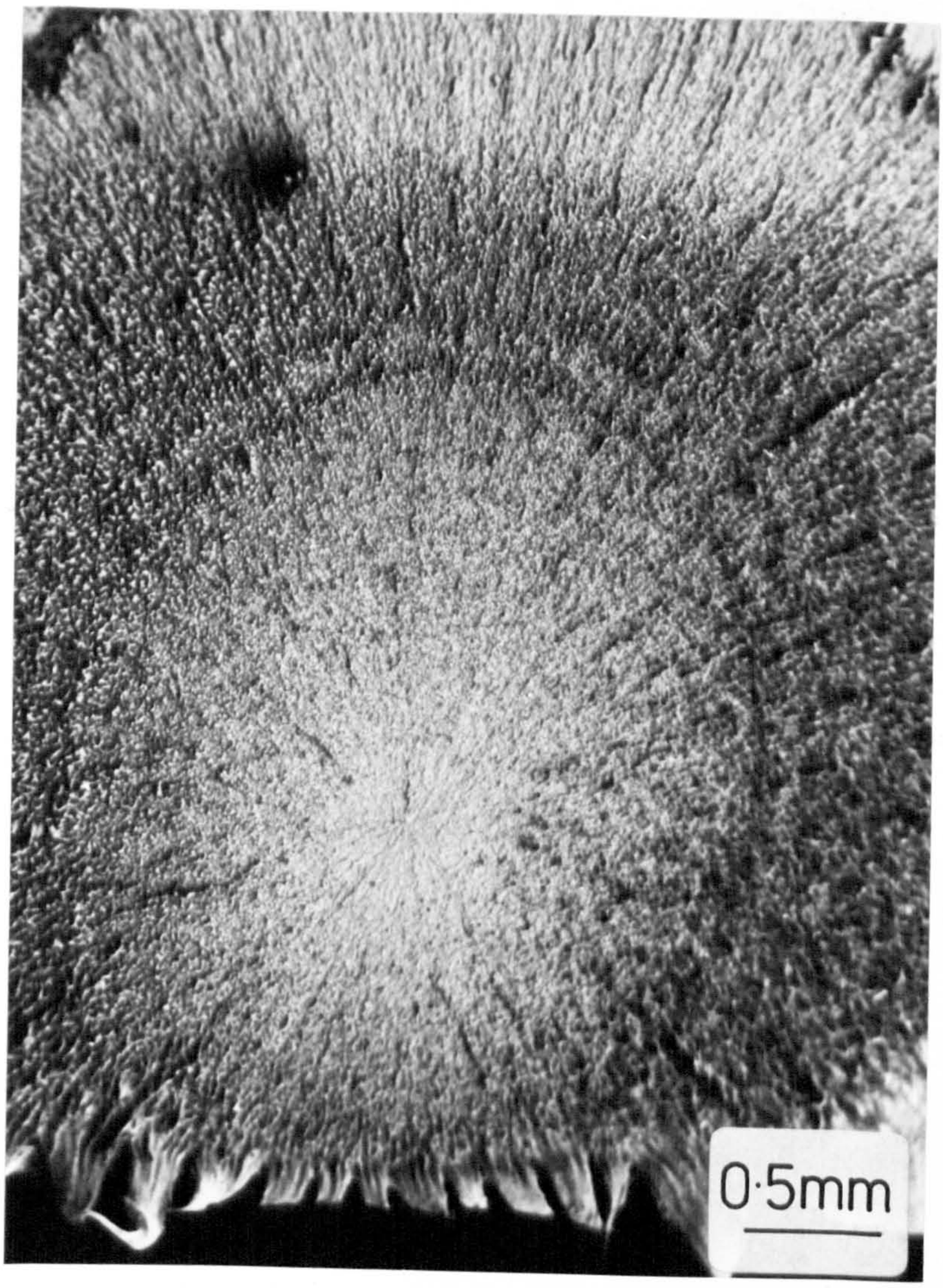

FIGURE 2.12

General fracture surface of an MDPE brittle pipe failure resulting from static internal pressure.

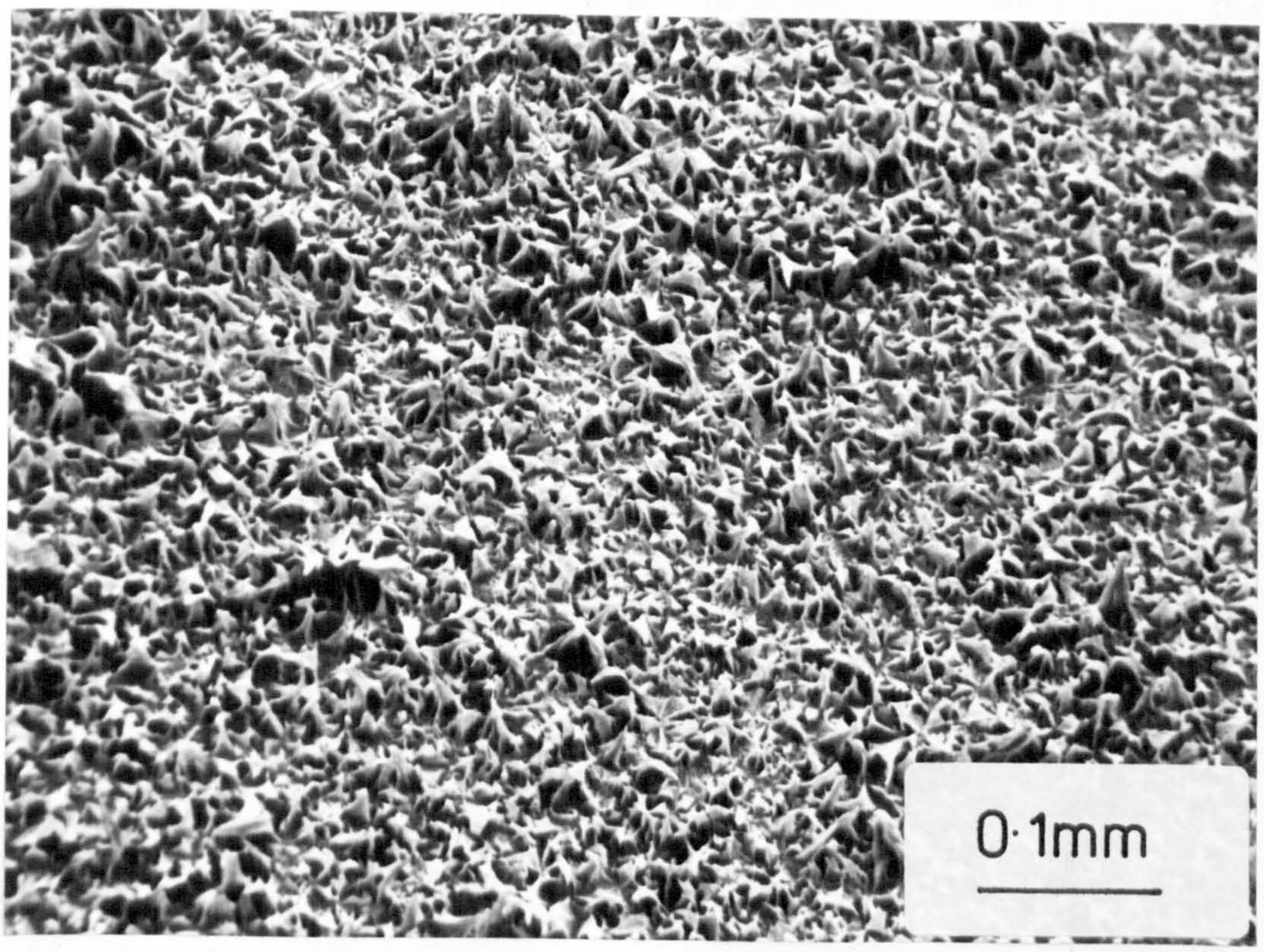

FIGURE 2.13 High magnification fracture surface features of an MDPE brittle pipe failure resulting from static internal pressure.

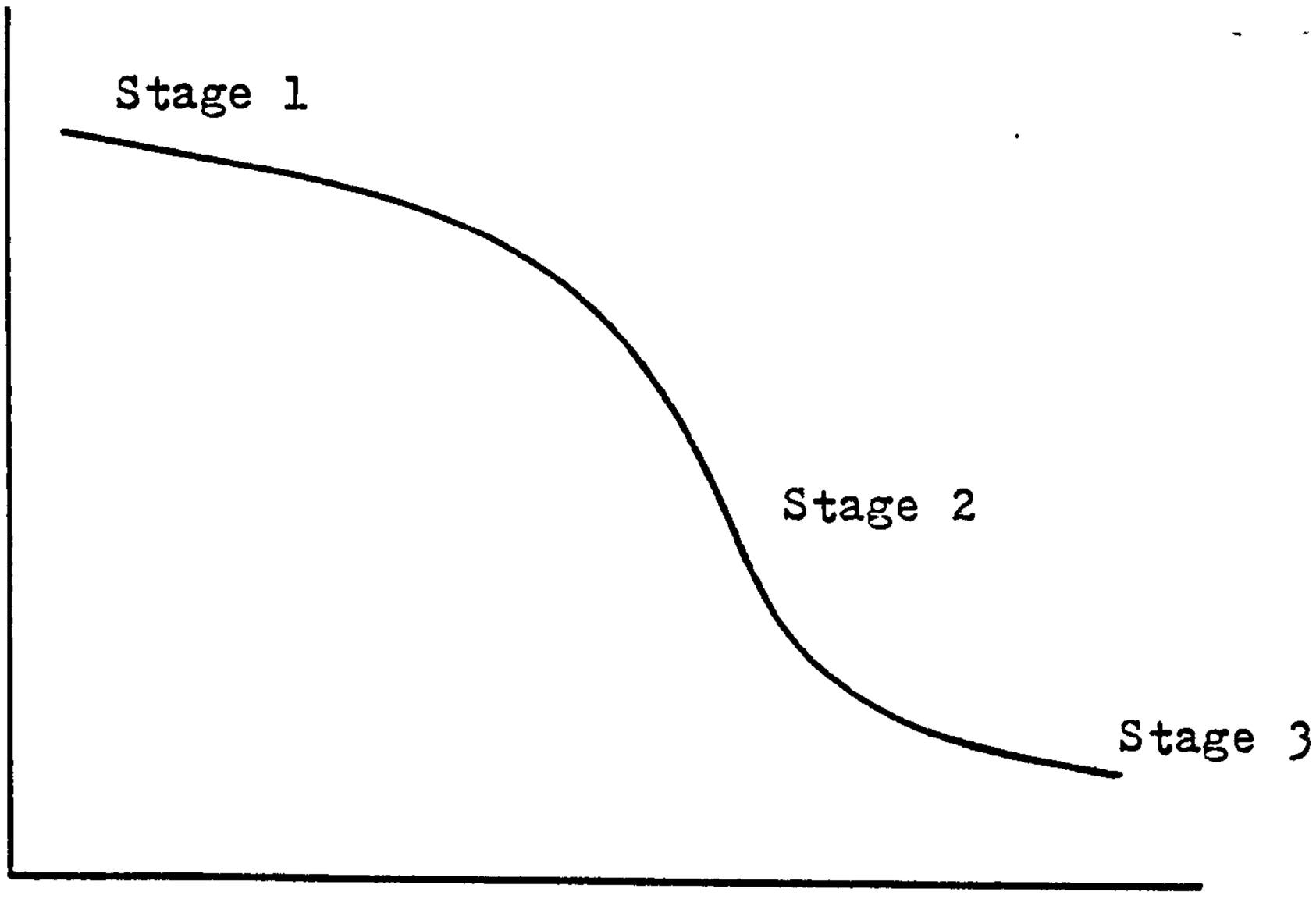

FIGURE 2.14 Schematic Wöhler curve for a creep sensitive thermoplastic.
(After reference 97)

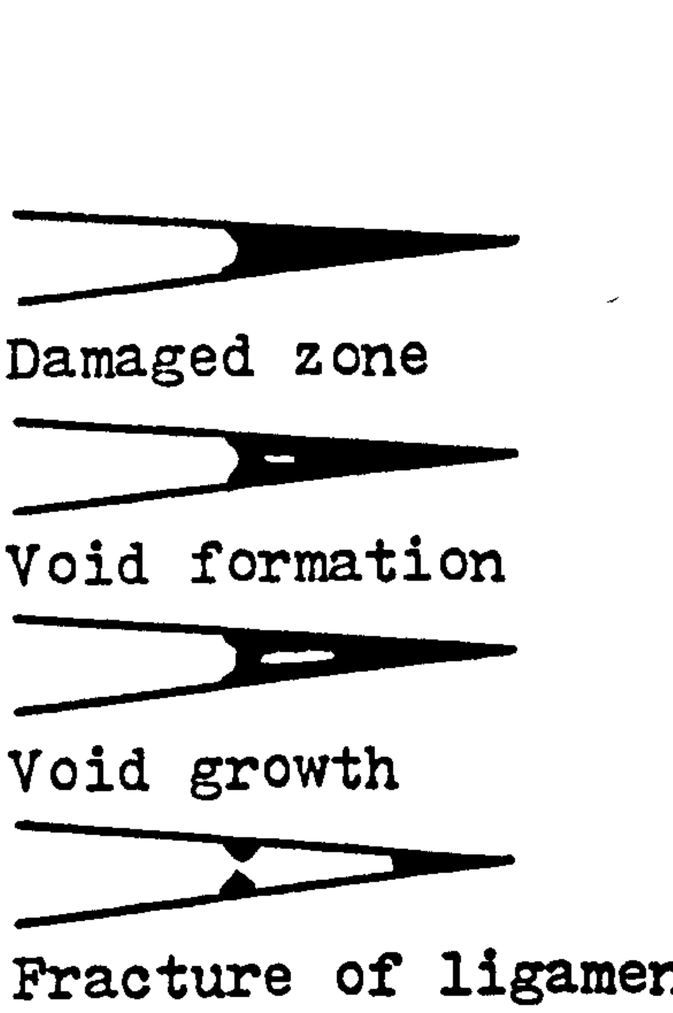

FIGURE 2.15

Mechanism of fatigue crack propagation in a semi-crystalline thermoplastic (HDPE)
(After reference 32)

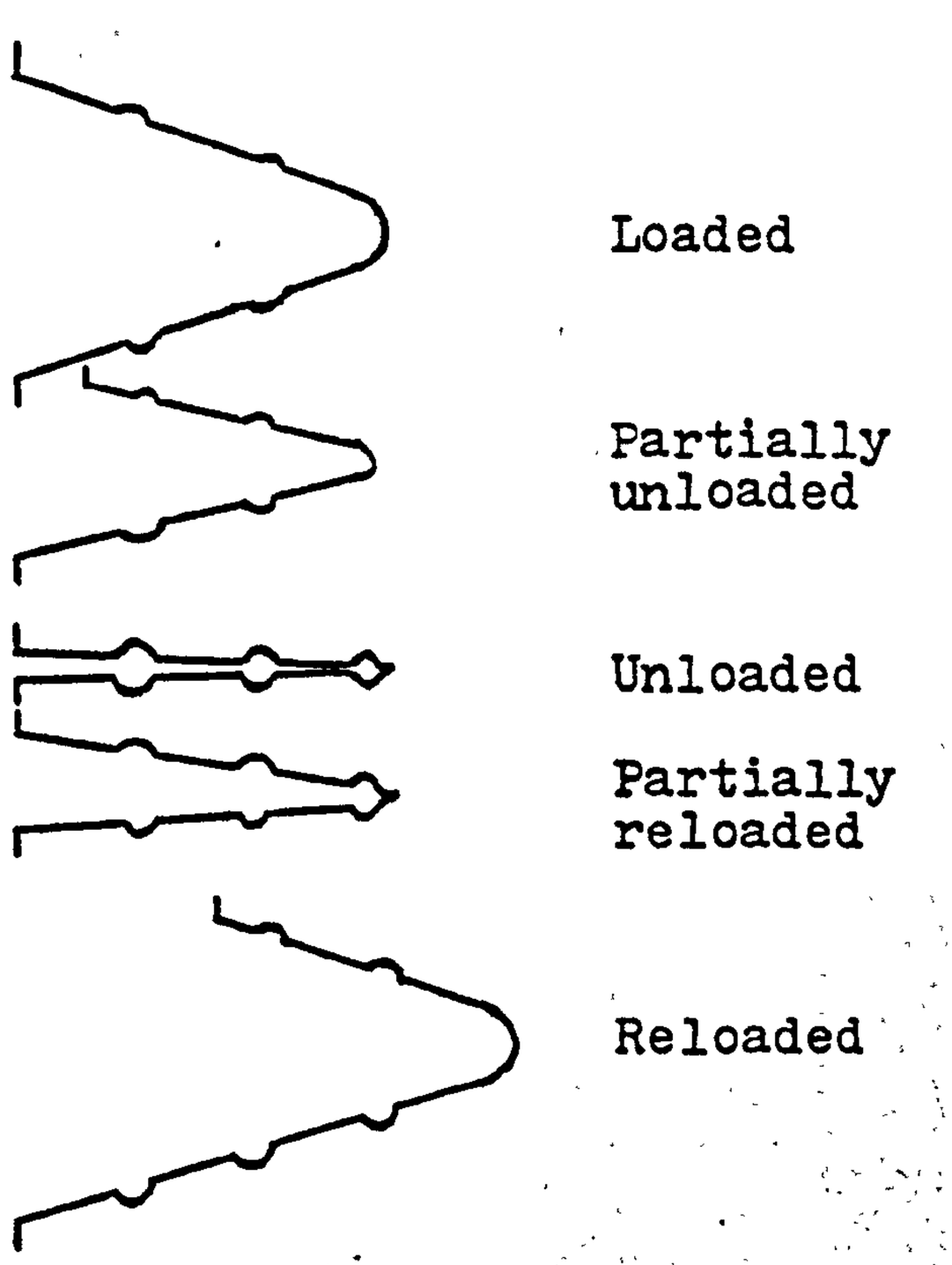

FIGURE 2.16

Mechanism of fatigue crack propagation in a semi-crystalline thermoplastic (uPVC).
(After reference 116)

CHAPTER 3

MATERIALS AND EXPERIMENTAL METHODS

3.1

CHAPTER 3 - MATERIALS AND EXPERIMENTAL METHODS

3.1 INTRODUCTION

3.1.1 Laboratory Development and Experimental Objectives

A laboratory was allocated and equipped for the purpose of internal pressure testing thermoplastics pipe systems with the following objectives in mind.

a. To test thermoplastics pipe systems with a range of outside diameters from 60mm up to 180mm.
b. To test as many systems as possible at any time within the available space.
c. To test the systems under a wide range of pressures and temperatures.
d. To enable a comparison of failure behaviour to be made for the pipe systems in three different modes of internal pressure testing, namely
   Short term rupture (burst) testing.
   Stress rupture (creep or static fatigue) testing.
   Fatigue (intermittent creep or dynamic fatigue) testing.
   These guidelines have led to a flexible, reliable and comparatively inexpensive pressure testing facility.

3.1.2 Experimental Programme - General Description.

All thermoplastics pipe systems were obtained directly from manufacturers in the form of extruded pipe lengths and compatible injection moulded fittings. All were typical of those used in applications such as chemical process, water and gas installations.

The pipes and fittings were all joined using the mirror-plate butt-welding technique with conditions as recommended by the respective manufacturers.

The strength and integrity of such welds were determined by tensile testing a selection of typical joints in a similar fashion to that described by Atkinson (48).

Pipe systems fabricated by the butt-weld technique were subsequently pressure tested by methods noted in the previous section. Such testing provided basic design and mechanical performance data which is invaluable for deciding whether or not a thermoplastics pipeline is suitable for a given service duty.

To examine material properties before and after pressure testing and to identify the effects of testing variables upon the pipe material behaviour, a variety of characterisation techniques were employed. These included microtomy and light microscopy, scanning electron microscopy (SEM) and differential scanning calorimetry (DSC).

To identify the mechanisms of failure, the fracture surfaces of failed specimens were photographed to characterise their "macrostructure" while SEM was used to examine both the fine detail of the fracture surfaces and the shape, size and position of any particle initiating fracture. The elemental composition of such particles was determined using energy dispersive x-ray analysis, such data being invaluable to discover from what source the crack initiating particles had arrived.

By correlating mechanical performance data and fracture surface analyses the effect of processing defects, of one sort or another, on subsequent behaviour would be ascertained, resulting in suggestions for improved processing techniques which if implemented could lead to longer service lives and reduced instances of premature failure.

3.2 MATERIALS AND PHYSICAL PROPERTIES

Small diameter (60 and 63mm outside diameter (OD)) SDR11 pipes extruded from two high density polyethylene (HDPE) and two medium density polyethylene (MDPE) resins were used in the course of the investigations.

The injection moulded fittings, bends, tees and flanges were made from compatible materials to the pipes but may be slightly different because of processing requirements. Test specimens were fabricated only from those pipe and fitting grades recommended to be joined by the manufacturers.

All four resins were thermoplastic non-crosslinked polyethylenes which are most easily characterised by a density and melt flow index (MFI), the latter being commonly used as a guide to the molecular weight. The density and MFI of these materials were determined and in all cases, found to be within the manufacturers specifications.

The performance of selected large diameter (160mm OD and 180mm OD) SDR 11 PE pipe systems from the same manufacturers as for the smaller pipes was also investigated.

The four materials and their commercial designations are presented in Table 3.1.

Relevant physical properties for each of these materials are compared in Table 3.2 and their stress rupture performances are given in Figures 3.1 - 3.4. A comparison of stress rupture performance at 80°C is drawn in Figure 3.5.

All data presented in Table 3.2 and Figures 3.1 to 3.5 are obtained from manufacturers published literature (6, 117 - 119).

3.3 MATERIALS CHARACTERISATION TECHNIQUES

Materials characterisation studies, particularly related to the examination of microstructure began in the early stages of the project and were initially of an exploratory nature. At the time the mechanical testing programme had not identified potential weaknesses in the pipe systems and therefore specific areas upon which to concentrate the microstructural examination.

The spherulitic structure in the HDPE and MDPE pipe materials was found to be particularly fine and since the polymers were mixed with significant quantities of pigments or fillers, the characterisation of microstructure, by the combined techniques of thin section microtomy and light microscopy, was a particularly difficult task.

It was therefore decided that such an approach would be used only when other techniques failed to provide the required information.

As a consequence only coarse surface preparation methods were, in general, used to highlight morphological variations through pipe or fitting walls.

Thermal analysis in the form of differential scanning calorimetry (DSC) was used to obtain some measure of the materials' peak melting temperatures and crystallinities, and also to identify any variations in these parameters which might be induced by internal pressure testing at elevated temperatures, and so alter mechanical performance.

TABLE 3.1 - Materials of Test and Their Respective Commercial Designations

MATERIAL	ABBREVIATION	COMMERCIAL DESIGNATION	MANUFACTURER
High Density Polyethylene Type 1	HDPE 1	HOSTALEN GM5010	HOECHST
High Density Polyethylene Type 2	HDPE 2	HOSTALEN GM5010 T2	HOECHST
Medium Density Polyethylene Type 1	MDPE 1	ALDYL 'A' (ALATHON RESIN)	DU PONT
Medium Density Polyethylene Type 2	MDPE 2	RIGIDEX 002-40 R919	BP CHEMICALS

TABLE 3.2 - Comparison of Selected Physical Properties for the Pipe Systems' Materials

PROPERTY	UNIT	HDPE 1	HDPE 2	MDPE 1	MDPE 2
DENSITY	$kg\ m^{-3}$	954	954	937	940
MELT FLOW INDEX.	$g\ 10\ min^{-1}$	0.3	0.4	1.1 (Pipe material)	0.2
YIELD STRESS	MPa	24	21	19.3 (Pipe material)	19
ELONGATION AT BREAK	%	800	800	>500	300
ELASTIC MODULUS	MPa			662 (Pipe material)	
IMPACT STRENGTH	Jm^{-1} notch				930
CRYSTALLITE MELTING RANGE	^{o}C	127 - 131	127 - 131		
VICAT SOFTENING POINT	^{o}C			121 (Pipe material)	118
COEFFICIENT OF LINEAR EXPANSION	K^{-1}	2×10^{-4}	2×10^{-4}	1.62×10^{-4} (Pipe material)	1.5×10^{-4}
THERMAL CONDUCTIVITY	$Wm^{-1}\ K^{-1}$	0.43	0.43		0.25

Notes
1) All values reported are obtained from manufacturers published literature
2) The test methods for determining material properties are in accordance with relevant British, American or German Standards. However, wherever possible all data is directly comparable. For example, the strain rates for all tensile tests were reported to be 125mm min^{-1}.
3) Unless otherwise stated all properties relate the pipe base resin (with additives and pigments.
4) Further information relating to methods of test can be found in manufacturers published literature ([6, 117 - 119])

Finally, other methods such as tensile testing and melt flow index determination were employed to confirm manufacturers' or other experimental data or to follow material changes produced as a consequence of testing.

3.3.1 Microtomy and Light Microscopy

(i) Thin Sections.

For highly birefringent semi-crystalline plastics a convenient method of making an accurate microstructural analysis is by the use of microtomy coupled with microscopy (120).

In the experimental method a sledge microtome of the type shown in Figure 3.6 was used for preparing the thin sections. The specimens were held rigidly and the blade operated with the minimum of vibration. Sections were cut to a thickness of less than 10 μm, but usually to between 4 and 6 μm. This generally allowed enough light to pass through to enable the microstructure of the section to be viewed. All sections were transferred to clean microscopy slides, immersed in a setting oil and protected with glass cover-slips. They were subsequently viewed by means of a Reichert "Zetopan" microscope, with camera attachment, set up for transmission polarised light microscopy with the polariser and analyser crossed. The light source could be varied in intensity and was of the reflective type.

Since any section taken from a position perpendicular to an extruded pipe axis through its wall can be considered to have essentially the same microstructure as any other position in that plane, or indeed in any parallel plane along the pipe length, it is possible to identify the pipe microstructure from a relatively small number of samples. This is not the case with an injection moulded article since the polymer melt is subjected to various shear stresses and temperature changes throughout the mould cavity. The finished article contains a variety of localised microstructural features which can have a great effect upon the overall appearance and mechanical performance of the moulding. It was for this reason that a general microstructural examination of the

pipe system fittings was not undertaken and only those areas which demonstrated obvious weaknesses were investigated, if this was possible.

In spite of the difficulties encountered obtaining useful microstructural data, it was however possible to examine the dispersion of pigments and fillers and also to determine, to some extent at least, the direction of polymer flow in a given section.

Fillers and pigments tend to congregate along flow lines and thus are an indication of the polymer melt behaviour.

When sections were required for examination of flow or orientation they were microtomed parallel to the flow direction.

Butt-weld or internal weld interfaces were shown to reasonable effect even in the heavily pigmented materials along with any associated heat affected zones.

(ii) Planed Surfaces.

A very straightforward means of examining variations of morphology through the walls of extruded pipes and injection moulded fittings consists simply of planing bulk specimen surfaces with a steel blade. Sledge microtomy is the most convenient method of such surface preparation and requires that the cutting edge be relatively blunt but to be used with a minimum of vibration.

An example of a surface prepared in this way is shown in Figure 3.7 and indicates that the interaction between the blade edge and sample material produces stress whitening of varying intensity. It is believed by Hunter and Bevis (22) that such variations reflect the changing microstructure across the wall of a pipe or fitting made from pigmented PE.

Welded areas and heat affected zones were also shown to good effect by this method.

If thick layers of about 40 μm are removed from the sample surface with a relatively blunt blade the stress whitening is shown most clearly as in Figure 3.8. Only 10 μm were removed to produce the surface presented in Figure 3.7.

3.3.2 Melt Flow Index Determination

The melt flow indices of both extruded and injection moulded components of all systems were determined in accordance with ASTM D 1238 procedure A-MFI condition E (121) The equipment used was a Davenport Melt Indexer Model III.

In all cases care was taken to ensure that MFI determinations were made on material taken from the same relative positions.

The MFI of a thermoplastic is usually the measured gravimetric flow rate of the sample melt expressed in units of grams per ten minutes (g 10 min^{-1}) through an orifice of diameter 2.095mm at a defined pressure and temperature. It is generally regarded as being a measure of the molecular weight ($\bar{M}w$), with the low index being indicative of high molecular weight.

The feedstock was produced by granulating the bulk pipe or fitting material.

The temperature was set at 190°C $\pm$ 0.3°C and the applied load kept constant at 2160g.

Two methods were used to determine the indices. The first involved weighing the amount of material extruded through the standard die in a given time. The second involved measuring the time taken for the dead weight piston to fall 2mm during a melt flow test.

No less than five individual determinations were made for each material component.

3.3.3 Differential Scanning Calorimetry

The crystallinity and peak melting temperature of a polymer can be obtained by using the technique of Differential Scanning Calorimetry (DSC). Significant variations in the materials thermal properties can occur through the thickness of pipes or at different positions within injection moulded fittings. Thus, samples were removed from pipe systems consistently from the same relative position and at the same distance from the inside surface of all pipes with identical wall thicknesses. With respect to failed specimens material was removed adjacent (within 5mm) to the fracture surface.

The analyses were carried out on a Perkin-Elmer DSC-2 differential scanning calorimeter according to ASTM D 3417-75 (122). Melting points were determined at the peak value and crystallinity measured in terms of the areas beneath the melting endotherms as illustrated in Figure 3.9.

The instrument was calibrated with indium, whose melting point of 429K is close to the melting temperatures of the polyethylenes under investigation. Accurate heats of fusion were assured by obtaining a horizontal base line, over a temperature range of about 500K, while both the reference and sample pans were empty.

The heating rate was set to 10 $Kmin^{-1}$ at a sensitivity of 5 mcal s^{-1} for sample weights of approximately 5 mg.

The unit employs an average temperature circuit to measure and control the temperature of the reference and sample holder which conforms to a pre-determined profile. This temperature is plotted on one axis of an X-Y recorder and simultaneously a monitor compares the temperature difference between the sample and reference holders, supplying energy to each so that their temperatures remain equal. When a sample undergoes a thermal transition a signal proportional to the power difference which is required to maintain identical temperatures, is plotted on the second axis of the recorder. The area under the curve is a direct measure of the enthalpy of fusion (ΔH_f) which is considered linearly proportional to the crystallinity in the sample.

As a measure of the accuracy of the instrument a quantitative comparison was made by running the endothermic peak for indium. The value of ΔH_f for indium is well documented at 28.4 kJ kg^{-1} (36) and an average of five experimental determinations on the DSC-2 was in close agreement with this figure.

The percentage crystallinity was calculated from

$$\% \text{ Crystallinity} = \frac{\Delta H_f}{\Delta H^{\ominus}_f} \times 100$$

where ΔH_f was the enthalpy of fusion of the sample, and where $\Delta H^{\ominus}_f$ was the enthalpy of fusion for a 100% crystalline linear PE. The value of $\Delta H^{\ominus}_f$ was taken from Brennan (36) at 286 kJ kg^{-1}.

In all pipe materials examined pigment was present. The crystallinity values obtained are therefore underestimates as no attempt was made to determine the pigment content to provide for a more accurate crystallinity result. It was also assumed that the pigment dispersion was constant throughout the materials. The results must therefore be considered comparatively and are in no way absolute.

3.3.4 Tensile Testing

Tensile tests were used as a means of assessing the short term performance of the pipe materials and as a measure of the strength of butt-welds. They were not employed to determine long term mechanical behaviour of a pipe since such extrapolations have not yet been proved to be valid.

Tensile test samples were cut from pipes and butt-welded pipes parallel to the pipe axis, on a milling machine in accordance with the overall dimensions described by ASTM D 638 type 1 (123). Typical welded and unwelded samples are shown in Figure 3.10.

For welded samples, specimens were cut so that the weld joint lay in the middle of the guage length.

On a number of welded test specimens the effect of removing the weld bead by machine was also examined.

The testing was carried out on an Instron tensile testing machine at an ambient temperature of 23°C. The cross head speed was set at 0.85mm s^{-1} (2 in min^{-1}) giving a strain rate of 1.44×10^{-2} s^{-1}.

In each case the dimensions of tensile samples were measured prior to testing with thicknesses being determined by the pipe walls.

Engineering stresses and strains were subsequently calculated from load/extension curves.

For the butt-welded samples it was possible to use a short term weld factor as a measure of the quality of a butt-joint, where

$$\text{Weld factor (f)} = \frac{\text{Tensile strength of a butt-weld}}{\text{Tensile strength of the parent material}}$$

3.4 PIPE SYSTEMS

Emphasis was given to testing pipeline systems which included extruded and moulded parts that were processed from essentially the same material and which would be used in commercial practice.

The range of pipe systems tested is summarised in Table 3.3. Figures 3.11 and 3.12 illustrate schematically the overall designs of each system and the corresponding dimensions are given in Table 3.4.

The systems' dimensions conform to, at least, the minimum requirements of the following American, British and German Standards,

ASTM	D 2610-73	BS 4728
	2611-73	4962
	3261-73	4991
	1599	1973
	1598	3796
	2104-73a	1972
	2143-69	
DIN	16963	

These standards cover pipe system dimensions for static fatigue testing and short time rupture testing for thermoplastics and cyclic internal pressure testing for thermosetting plastic pipe systems.

Similar dimensions have been used for the cyclic internal pressure testing (fatigue) of the thermoplastics examined during this investigation.

3.5 MIRROR-PLATE BUTT-WELDING OF PIPE SYSTEMS

3.5.1 Butt-Welding Method

Butt-welded joints are produced by heating two mating surfaces with a hot tool and by forcing both surfaces together under pressure.

For best results welding machines are used. The component faces having been aligned and machined to ensure that they are parallel and flat are cleaned with a degreasing agent such as acetone and then heated to a

TABLE 3.3 - Pipe Systems and Test Methods Used During the Internal Pressure Testing Programme

MATERIAL DESIGNATION	PIPE OUTSIDE DIAMETER mm	PIPE STANDARD DIMENSION RATIO	FITTINGS TESTED (INJECTION MOULDED)	FITTINGS BATCH DESIGNATION	MODE OF TESTING
HDPE 1	63	11	90° EQUAL TEES	A	SHORT TERM RUPTURE + STRESS RUPTURE + FATIGUE
			90° BENDS	A	
HDPE 1	160	11	90° EQUAL TEES	A	FATIGUE
			90° BENDS	A	
			STUB FLANGES		
HDPE 2	63	11	90° EQUAL TEES	B	SHORT TERM RUPTURE + STRESS RUPTURE + FATIGUE
			90° BENDS	B	
MDPE 1	60	11	90° EQUAL TEES	A	SHORT TERM RUPTURE + STRESS RUPTURE + FATIGUE
			90° BENDS	A	
MDPE 2	63	11	NONE		STRESS RUPTURE + FATIGUE
MDPE 2	180	17 (All fittings SDR 11 but machined to fit SDR 17 pipes at welds.)	90° EQUAL TEES	A	STRESS RUPTURE + FATIGUE
			STUB FLANGES	A	

TABLE 3.4 - Pipe Systems' Dimensions

MATERIAL DESIGNATION	PIPE OUTSIDE DIAMETER mm	SDR	SYSTEM	DIMENSIONS
HDPE 1 (Threaded Ends)	63	11	PIPE (P)	A = 10D
			PIPE WELDED TO PIPE (P/P)	A = 10D B = C = 5D
			90° BEND (B)	D = E = 265mm
			90° EQUAL TEE (T)	F = G = 265mm
HDPE 1 (Flanged Ends)	160	11	PIPE	A = 1m + 2fl
			PIPE WELDED TO PIPE	A = B + C B = 1m+fl C=1D + fl
			90° BEND	D = 1m+fl E=1D + fl
			90° EQUAL TEE	F = 1D+fl G=1m + fl
HDPE 2 (Threaded Ends)	63	11	PIPE	A = 10D
			PIPE WELDED TO PIPE	A = 10D B = C = 5D
			90° BEND	D = E = 265mm
			90° EQUAL TEE	F = G = 265mm
MDPE 1 (Threaded Ends)	60	11	PIPE	A = 10D
			PIPE WELDED TO PIPE	A = 10D B = C = 5D
			90° BEND	D = E = 150mm
			90° EQUAL TEE	F = G = 150mm
MDPE 2 (Threaded Ends)	63	11	PIPE	A = 10D
MDPE 2 (Flanged Ends)	180	17 (Fittings SDR 11)	PIPE	A = 1m + 2fl
			PIPE WELDED TO PIPE	A = B + C B = 1m+fl C=1D + fl
			90° EQUAL TEE	F = 1D+fl G=1m + fl

Note D - pipe outside diameter
mm - millimetre
m - metre
fl - flange length, along pipe direction

temperature at which the polymer is fluid enough to flow and intermix across the joint. This is effected by planing both surfaces in contact with a thermostatically controlled heating element. Both parts are then brought together under pressure. Some of the molten plastic exudes from the joint face to form a weld bead.

The temperature of welding is quite critical since it needs to be high enough to allow for adequate flow and mixing, which should result in a joint strength comparable to the parent material strength, but not too high so that the plastic degrades. This would result in a weaker weld. Other factors such as weld pressure, heat soak time, etc, all can affect the strength and integrity of a weld and should be closely controlled.

3.5.2 Equipment and Modifications.

The equipment used during this investigation for effecting butt-welded joints in PE pipe systems comprised a "Wavingas" Mark II butt-welding machine manufactured by Haxey Engineering Limited together with a hot-plate as shown in Figure 3.13. The machine is of the type which applies pressure directly along the central pipe axis.

The hot-plate is thermostatically controlled with a power rating of 1250 watts and covered on both faces with PTFE impregnated glass cloth which prevents the molten material adhering to the hot-plate and thus damaging the plasticised surfaces.

The temperature of the hot-plate was checked using a Digitron contact digital thermometer. Once the temperature had been set, it did not vary appreciably with time but was not consistent around the hot plate surface.

Table 3.5 shows the temperature differences obtained along four lines at right angles to each other radiating from the approximate centre of the tool.

The pressures used during the welding process were ascertained by the use of an Instron load cell mounted horizontally in the welding machine which enabled a calibration of the integral pressure guage to be made.

TABLE 3.5 - Temperature Distribution Around the Hot-Plate Used for Butt-Welding Pipe Systems.

ANGLE	TEMPERATURE RANGE °C	NUMBER OF READINGS
0°	203 - 204	17
90°	202 - 203	17
180°	201 - 202	17
270°	211 - 212	17
Weight average temperature - 205°C		

Notes (1) Required temperature set at 205°C (used for HDPE 1 + 2).

(2) The angle is related to the hot-plate handle pointing vertically downwards.

(3) All results relate to one side of the hot-plate only but tests indicated a similar temperature distribution on the opposite face.

After reference 124.

The machine was used for joining pipes and pipeline fittings such as tees, bends and flanges in the range of outside diameters 60mm to 180mm. This was only possible by utilising re-rounding clamps and specially designed modifications including 3-and 4-jaw chucks.

The re-rounding clamps are held in the machine one side of which moves along tie bars, the other side held stationary. A fluid operated ram system activates the moveable half of the pipe clamps, the direction of which can be chosen by a two-way selector switch. The rams are pressurised using a nitrogen gas cylinder, foot-pump or compressed air system to the inlet port. This enables component faces to be brought together or separated as required.

3.5.3 Procedural Conditions

The welding conditions adopted were those recommended by the manufacturers of the different pipe systems. For convenience and ease of comparison these have been drawn schematically in Figures 3.14 - 3.17 in terms of force or pressure against time.

All steps during the welding process and the specific conditions are tabulated for each material and size in Table 3.6.

In general it is a three step process, weld bead formation, heat soak and weld formation. The values for the force in Figures 3.14 - 3.17 were derived from calibrating the welding machine using the Instron load cell and the actual pressure obtained from a measure of the force and the cross-sectional area of the pipe being welded.

It is useful to note that the schematic representations of the welding profiles for all systems are to the same force scale and therefore reflect the marked differences in recommended welding procedures for the different grades of pipe material.

In all cases care was taken to ensure that misalignment, either lateral or axial, was kept to a minimum (under 0.5mm for lateral mismatch and a minimum included angle of 179^{o}). The modifications to and accurate calibration of the welding machine also facilitated optimisation

TABLE 3.6 - Butt-Welding Conditions Used For All Materials.

WELDING VARIABLE	HDPE 1 + 2 MDPE 2 63mm OD WALL THICKNESS 5.8mm SDR 11	HDPE 1 160mm OD WALL THICKNESS 14.6mm SDR 11	MDPE 1 60mm OD WALL THICKNESS 5.5mm SDR 11	MDPE 2 180 mm OD WALL THICKNESS 10.6mm SDR 17
HOT PLATE TEMPERATURE (^{o}C)	205 $\pm$ 5	205 $\pm$ 5	205 $\pm$ 10	200 $\pm$ 8
INITIAL HEATING PRESSURE (MPa)	0.07	0.06	0.40	0.14
INITIAL HEATING TIME	UNTIL 1mm BEAD HAS FORMED	UNTIL 2mm BEAD HAS FORMED	UNTIL 1mm BEAD HAS FORMED	UNTIL 2mm BEAD HAS FORMED
HEAT SOAK PRESSURE (MPa)	0	0	0	0
HEAT SOAK TIME (s)	40 - 70	120 - 170	15 - 20	60 - 90
CHANGEOVER TIME (s)	4 - 8	7 - 15	4 - 8	7 - 15
WELDING PRESSURE (MPa)	0.14	0.12	0.80	0.14
COOLING TIME UNDER PRESSURE (mins)	5	10	5	10
COOLING TIME OUT OF MACHINE (mins)	10	10	10	10

Note All values were obtained from manufacturers published literature and used during the test programme to fabricate pipe systems.

and reproducibility of the welding conditions.

More detailed information relating to the actual welding procedure can be found in manufacturers literature or in the EEUA Handbook No. 35 p.31 (43).

3.5.4 Evaluation of Joint Quality

All butt-welds were inspected visually to check that they complied with the specific requirements of manufacturers literature. The general inspection procedure has been outlined in Chapter 2 and is presented more fully in reference 43.

Apart from the destructive tensile testing described in Section 3.3.4 and the burst, stress rupture and fatigue testing described later on in this chapter, no other forms of weld quality evaluation were undertaken.

3.6 INTERNAL PRESSURE TESTING

3.6.1 Equipment

Descriptions of the equipment used for internal pressure testing of the thermoplastics pipe systems is given below. Specific differences in apparatus is detailed under the appropriate test method section.

(i) Testing Tanks.

Four glass-reinforced plastic testing tanks supplied by Hepworth Industrial Plastics Limited were employed. Two tanks had the dimensions 1.8 x 1.2 x 1.2m and were fabricated in 160g GRP with two channel reinforcing iron bands. The tanks were used continuously to contain ordinary tap water at a temperature of 80°C to obtain stress rupture and fatigue test results. The capacity of these tanks amounted to 2700 litres and were used to simultaneously test a maximum of fifteen of the smaller diameter systems (60 and 63mm), examples of which are shown in Figure 3.11.

Two other tanks had dimensions 1.8 x 0.9 x 0.9m and were able to hold 1450 litres. Ten of the smaller diameter pipe systems were tested at one time in these tanks.

Obviously a smaller number of the 160 and 180mm OD. systems were tested in the tanks at any one time. A typical example of a 160mm OD. specimen based on a

90^{o} equal tee is shown in Figure 3.12 .

Only two of these specimens were conveniently pressure tested in the smaller tank whereas up to six straight pipe systems of the same diameter (Figure 3.12a and b) were pressurised in the large tanks.

The sides of all tanks were lagged with approximately 10cm of fibre insulation or with a similar thickness of expanded polystyrene. The tank bases were supported and also insulated by Tico rubberised anti-vibration pads. PE and PP heat retaining spheres were floated on the test fluid to prevent excess evaporation during elevated temperature testing.

(ii) Fluid Circulation and Temperature Control.

Thermostatically controlled heater/circulators manufactured by Grant Instruments and Churchill Fluid Heat were used to afford good fluid temperature control and at the same time circulate fluid around the test tanks to avoid any localised hot-spots. The circulators controlled temperature in the range $-10^{o}C$ to $90^{o}C$ and kept the set temperature to within $\pm$ $0.5^{o}C$ even at the highest temperature of $80^{o}C$.

A reference thermometer was used to calibrate temperatures in all test tanks to provide consistency of measurement.

(The tap water in the Uxbridge area where all pressure tests were carried out was fairly hard containing significant amounts of lime (calcium carbonate ') which tended to coat the exposed surfaces of the pipe systems manifesting itself as a fine whitish film. A similar effect was observed on the fracture surfaces.)

(iii) End Closures.

Two of the variety of available forms of end closing for the pipe systems were adopted and are illustrated in Figure 3.18, with a more detailed description in Table 3.7.

The screw cap fittings were only used on the 60 and 63mm OD pipe systems and are particularly easy to handle when fitting to the pipe system. It was the only form of end closing used for short term rupture testing. It does not, however, allow stub flanges and related welds to be tested.

TABLE 3.7 - End Closing Systems.

60mm SDR 11 MDPE 1)		Threaded ends
63mm SDR 11 HDPE 1 + 2)		Threaded ends
63mm SDR 11 MDPE 2)		Threaded ends
System Comprises	(a)	Pipe thread, metric left hand, pitch of 2mm and depth 1.25mm. End squared, 1mm lead in and 24mm of thread.
	(b)	Plug, manufactured from poly-propylene, and seal ensured by rubber "O" rings. Orifices are provided on certain plugs to admit pressure and failure sensor probe. Plug length, 50mm.
	(c)	Retaining cap, manufactured from either 70/30 brass or aluminium.
160mm SDR 11 HDPE 1)		Flanged ends
180mm SDR 17 MDPE 2)		Flanged ends
System Comprises	(A)	Injection moulded flange mirror-plate butt-welded to the pipe system. Flange is as supplied by the manufacturer of the pipe.
	(B)	Backing plate, manufactured from mild steel and coated with nylon to reduce corrosion. Figure 3.18 shows in plan view only half the plate. A natural rubber gasket, placed between the flange and the backing plate, ensures a water tight seal.
	(C)	Retaining rings, manufactured from mild steel and coated with nylon. 3/8" nuts and bolts bind retaining ring and backing plate.

The advantages of using a split-ring bolted flange are; firstly its relative cheapness, secondly systems containing stub flanges can be readily tested and thirdly, the pipe ends do not have to be threaded. To prevent corrosion the steel end plates and split-rings were coated with nylon. This type of flanged end fitting was found to be unsuitable for use in short term rupture testing since at pressures in excess of 3.5 MPa (>500 psi) the plates began to buckle breaking the seal.

All internal pressure tests were conducted on specimens which were freely supported with uncontrained ends because of the difficulty ensuring that, at the elevated temperatures used, no end loads would be imposed on a pipe system with constrained ends.

3.6.2 Short Term Rupture Testing

Short term rupture (burst) tests were carried out in accordance with ASTM 1599-69 (68). The rate of pressure rise was adjusted to give failure within 60 to 90 seconds of the start of the test.

The test rig used to effect this form of internal pressure test is shown in the lower half of Figure 3.19. It has a maximum pressure limit of approximately 17 MPa (2500 psi).

During the test the specimen is pressurised hydraulically.

Only one pipe system was tested at a time, failure being observed when the specimen undergoes catastrophic failure.

Data was obtained over a range of temperatures and only on the smaller diameter pipe systems (60 and 63mm OD). The short term rupture strength was calculated from the maximum pressure the system sustained prior to failure.

3.6.3 Stress Rupture Testing

Stress rupture tests were carried out in accordance with ASTM D1598-76 (59) by pressurising water filled systems with either compressed air or by employing a nitrogen cylinder with a regulator to provide a pressure to one side of a transfer barrier type hydraulic accumulator. The other side of which contained water which pressurised the test specimens.

A three-way solenoid valve was placed between the pressurising mechanism and the pipe systems which were immersed in the test tank filled with tap water at the desired temperature.

The observation of a failure was facilitated by an electrical current detection technique which activated the three-way solenoid valve and terminated the test by relieving the pressure in the failed pipe system.

A schematic presentation of the testing system for the generation of stress rupture data is shown in Figure 3.20a.

3.6.4 Fatigue Testing

(i) Low Pressure [$\leqslant$ 1.10 MPa($\leqslant$160 psi)] Fatigue Tests. Low pressure fatigue tests on small and large diameter pipe systems were conducted at frequencies between 0.86 and 7.5 cpm using a ramped square wave form of loading with a fixed period off load of six seconds. Compressed air top loading the water filled systems was used to provide the desired internal pressure up to a maximum of 1.10 MPa (160 psi). The samples were, as for stress rupture testing, immersed in a water bath at the set temperature. A three-way solenoid valve, controlled by an electronic timer directed the compressed air to and from the systems under test; when failure occurred in a pipe sample the failure detection device activated the stop valve to isolate the system from the pressurising medium (see Figure 3.20b). At the next "time off" in the cycle, the three-way solenoid valve vented any excess pressure remaining in the pipe system. The failure detection device enabled fracture to be detected within one cycle of a crack breaking through a pipe system wall.

For all the low pressure fatigue tests, the internal pressure was cycled between the set maximum and zero gauge pressure giving a stress ratio R (σ min/ σ max) of zero or at least close to it. The rate of pressure build up was constant for all frequencies of testing at any one set maximum pressure. For example, the rate of pressure build up for a maximum of 1 MPa was approximately 1 MPa s^{-1}.

The total time under load for a given specimen was computed using the time when the pressure of the fluid within the system had attained 95% of the set value.

(ii) High Pressure [>1.10 MPa (>160 psi)]
Fatigue Tests.

The hydraulic pulse/burst test rig for high pressure fatigue testing is schematically illustrated in the upper half of Figure 3.19.

The system enabled tests to be carried out in a temperature range 5°C to 80°C and to simultaneously test up to six small diameter pipe systems. Frequencies (assuming a time off load of six seconds) could again be varied between 0.86 and 7.5 cpm. Maximum internal pressures were up to 5 MPa (700 psi).

The high pressures involved enabled failure to be detected by catastrophic pressure loss.

3.6.5 Failure Detection System

The upper half of Figure 3.20a shows a schematic representation of the failure detection device. Figure 3.21 portrays the control modules in a racking system.

The principle of operation relies on the fact that a pipe test specimen is filled with an electrically conductive fluid, which in this instance was tap water, with the pipe system itself being immersed in a bath of similar fluid. Electrodes were inserted internally and externally to the pipe system. The external electrode being connected to a positive bias voltage derived from the amplifier power supply, thus sustaining a potential between both electrodes.

When a crack propagates through the wall of the pipe system an electric current (of the order of microamps) flows between the external and internal electrodes. This signal current turns on the amplifier which is biased off with a small negative voltage. (The sensitivity of the device can be altered by changing the negative bias voltage.) When the output from the amplifier becomes positive, the current driver is turned on which then operates a relay. This relay was fitted with a sufficient number of contacts to operate whatever control or indicating devices were required for the pressure testing.

For the purposes of the present work the relay, when activated because of failure, stopped a timer, isolated the failed system from the compressed air and vented any

excess pressure remaining. Visually, failure was indicated by a red warning light on the appropriate control module.

3.6.6 Pressure/Time Testing Profiles.

Test pressures were monitored by means of glycerine filled pressure gauges placed in the pressurising line before the pipe systems or by using a Pye Ether linear displacement transducer which drove a chart recorder, and showed the pressure profile applied to a specific test specimen.

(i) Short Term Rupture Test.

Typical pressure/time profiles for pipe systems subjected to rupture testing at two different temperatures are given in Figure 3.22.

The test specimens were 63mm OD HDPE 1 and failure was controlled in both cases to occur between 60 and 90 seconds.

(ii) Stress Rupture Test.

The set pressure applied to pipe systems during the course of stress rupture tests was found to vary by less than 2%.,

(iii) Fatigue Test.

Selected pressure profiles for low and high frequency fatigue tests on small diameter pipe systems are shown in Figures 3.23 and 3.24.

The test frequencies and pressures were all chosen to simulate conditions likely to be encountered by thermoplastics pipelines and to avoid the possibility of temperature increase as a result of hysteretic heating.

As mentioned previously, time under load was calculated using the time when the pressure of the fluid within the system had attained 95% of the set value.

The number of cycles to failure were obtained by dividing the time to failure by the cycle time or in the case of the higher pressure tests by reading from a cycle counter.

3.6.7 Ageing Tests

Since all pipe systems were subjected to the effects of both internal pressure and elevated temperatures, control experiments were carried out to determine the effect of the elevated temperature of the water bath

environment alone on the properties of the pipe system materials.

This involved cutting samples from pipes and immersing them in the same tank environment as the specimens used in pressure testing.

Property changes were subsequently investigated using DSC.

3.7 FRACTURE SURFACE ANALYSIS

All pipe systems which failed in a brittle manner were cut to isolate and reveal the fracture surface or surfaces.

The objectives were to maintain a complete record of all fractures produced during testing, to enable measurements and analyses of surface features to be effected and to use such data to identify fracture mechanisms.

3.7.1 Light Microscopy of Fracture Surfaces

The surfaces were photographed using a Pentax camera with bellows attachment. Low angle illumination was employed to obtain sufficient contrast on the essentially flat specimens.

The ratio L/h was determined on each fracture where h is the pipe wall thickness and L is the maximum extent of the brittle fracture along the pipe direction as shown in Figure 3.25.

3.7.2 Scanning Electron Microscopy

After being photographed using light microscopy specimens were subsequently coated using gold or gold/palladium in a Polaron E5000 SEM coating unit. Care was taken to avoid local heating.

The fracture surfaces were examined by scanning electron microscopy (SEM) on a Cambridge Instruments Stereoscan Mark 2a and on a Cambridge Instruments Stereoscan 600.

In general, the accelerating voltage for the beam was set at 20 or 25 kV. It was necessary, however, for this to be lowered for micrographs taken at magnifications in excess of 1000x.

Three features of the fracture surfaces, in particular, were examined by SEM. Firstly, the shape, size and position (with respect to the inside wall of the pipe or pipe system) of any particle apparently initiating a fracture were ascertained. Secondly, the elemental composition of such particles was determined using energy dispersive x-ray analysis. Thirdly, details of the fracture surface remote from the initiation site were examined. The presence of possible surface striations from step-wise movement of the crack, the level of local microductility and any evidence of voiding and other inhomogeneities were investigated.

3.7.3 Energy Dispersive X-Ray Analysis

To determine the elemental composition of fracture surface inclusions or other substances present, a Cambridge Instruments Stereoscan 600 was used in conjunction with a Link System X-ray analyser. The beam voltage was set at 25 kV with a count time of 100 seconds. The count rate was adjusted, if possible, to be similar for each sample.

The technique, generally referred to as energy dispersive analysis by x-rays (EDAX) is limited to detecting the presence of those elements whose atomic number is above that of oxygen.

The data was normally obtained in terms of an x-ray spectrum, however other methods of presentation such as the photographic line scans and dot pictures were also utilised.

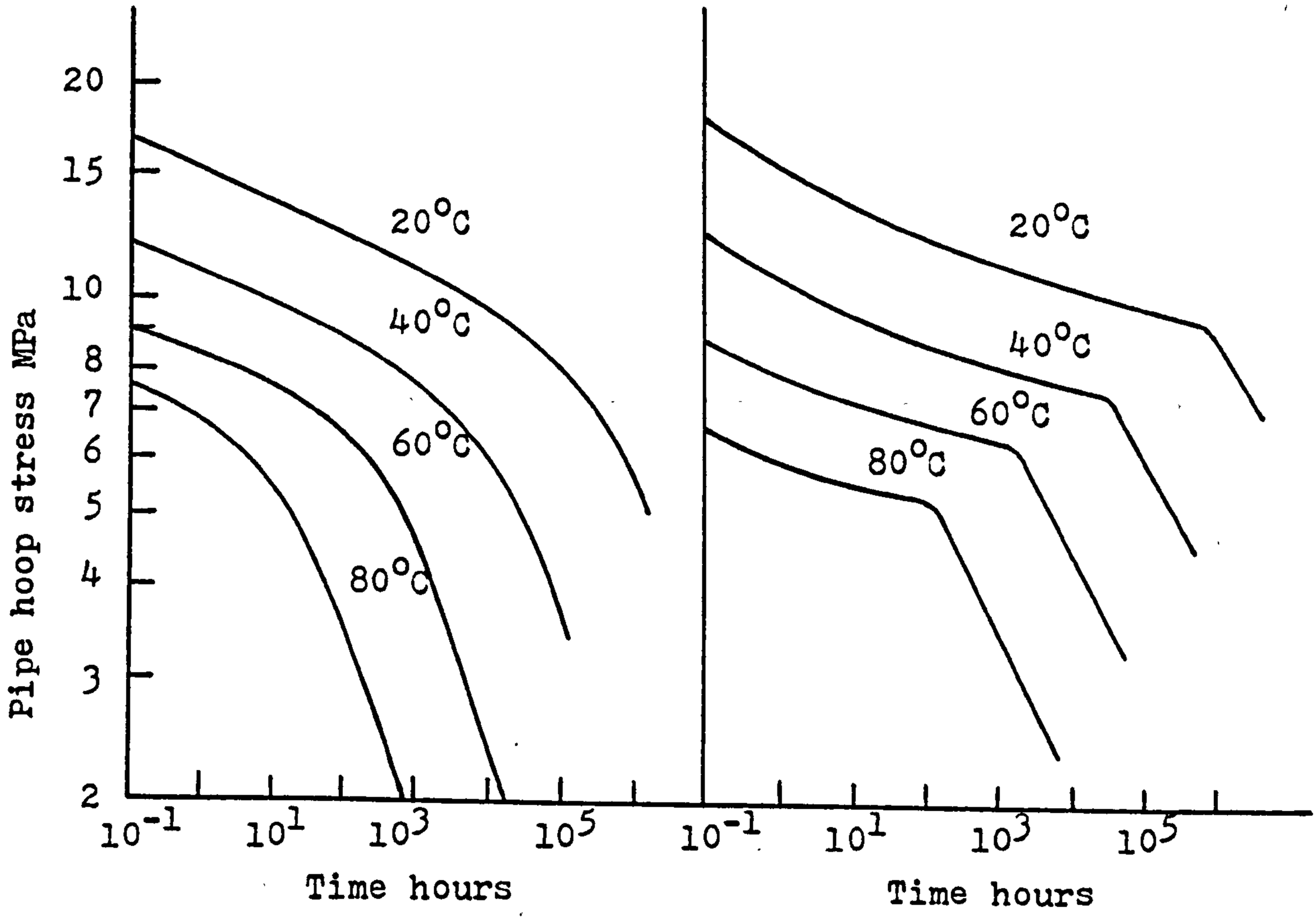

FIGURE 3.1 - HDPE 1

FIGURE 3.2 - HDPE 2

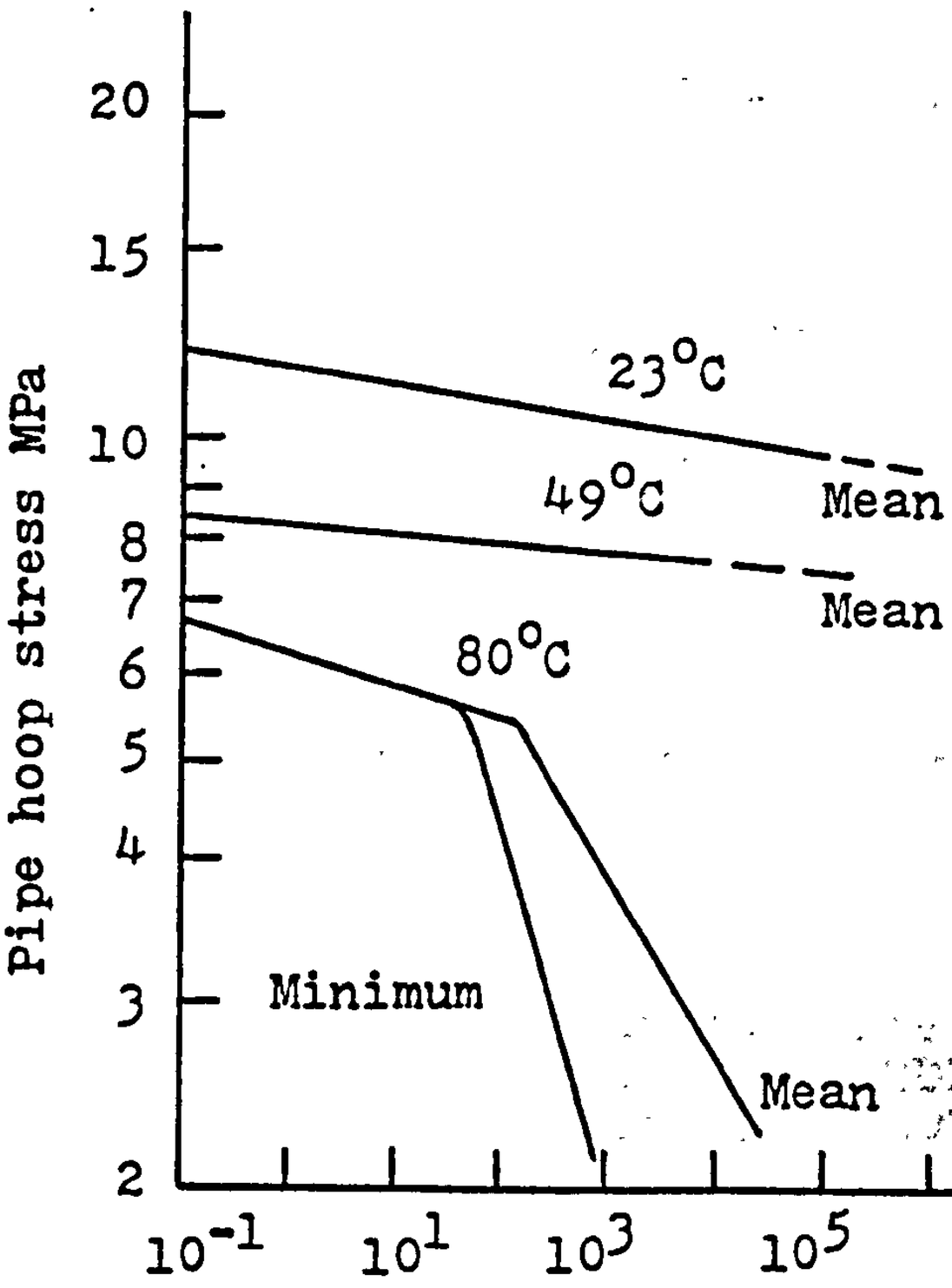

FIGURE 3.3 - MDPE 1

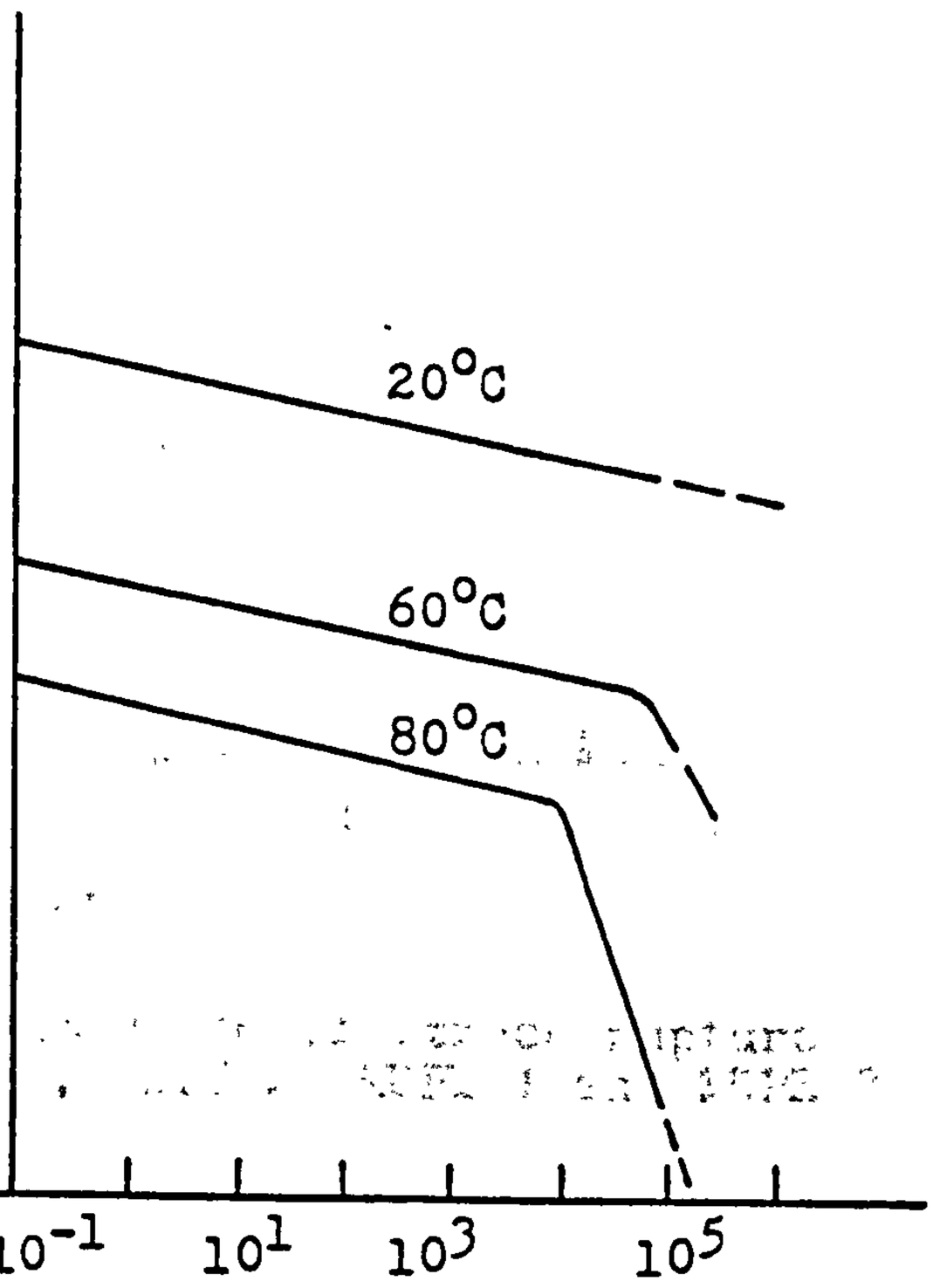

FIGURE 3.4 - MDPE 2

FIGURE 3.1 - 3.4 Stress rupture data for PE pipes

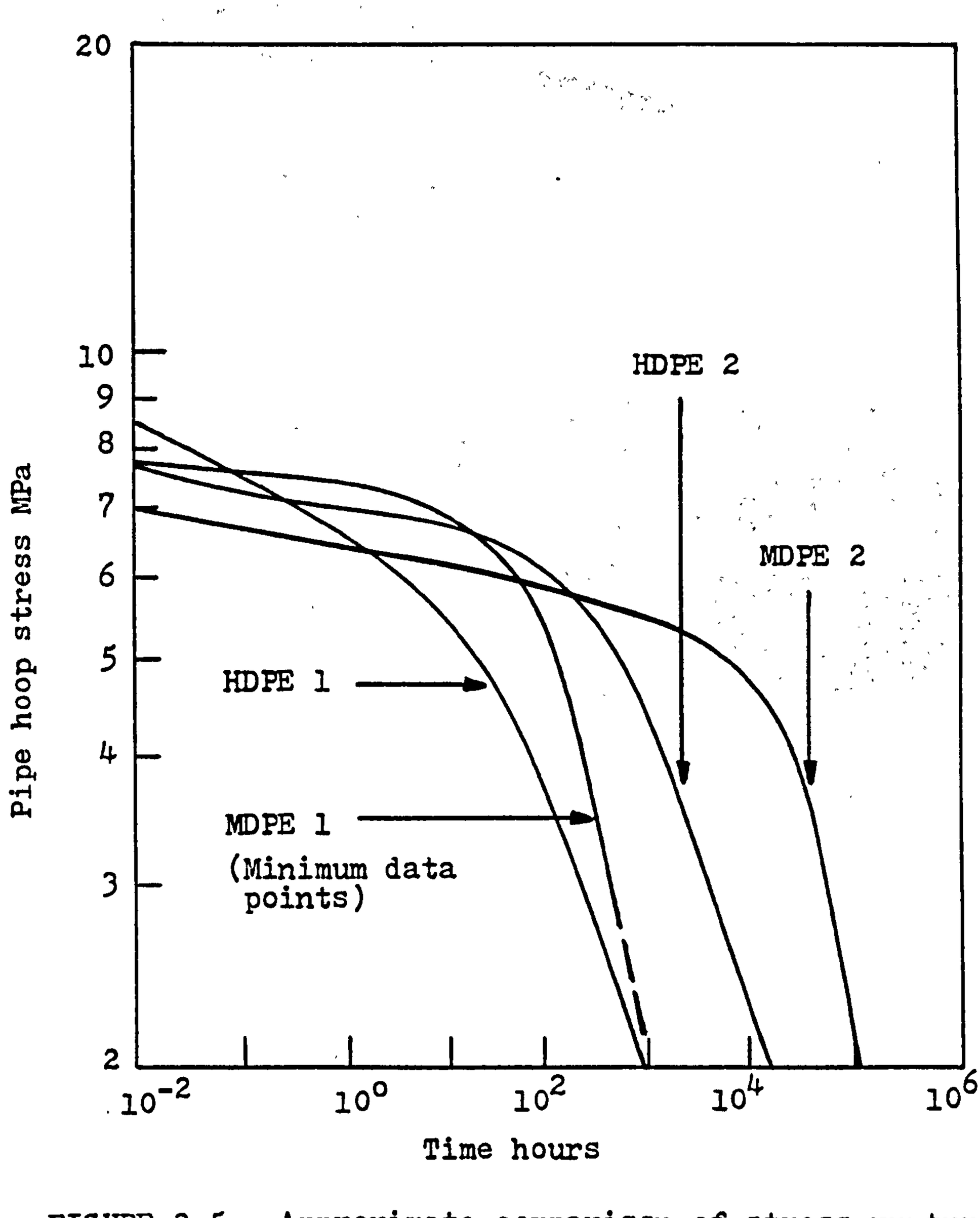

FIGURE 3.5 Approximate comparison of stress rupture data for HDPE 1, HDPE 2, MDPE 1 and MDPE 2 pipes at 80°C.

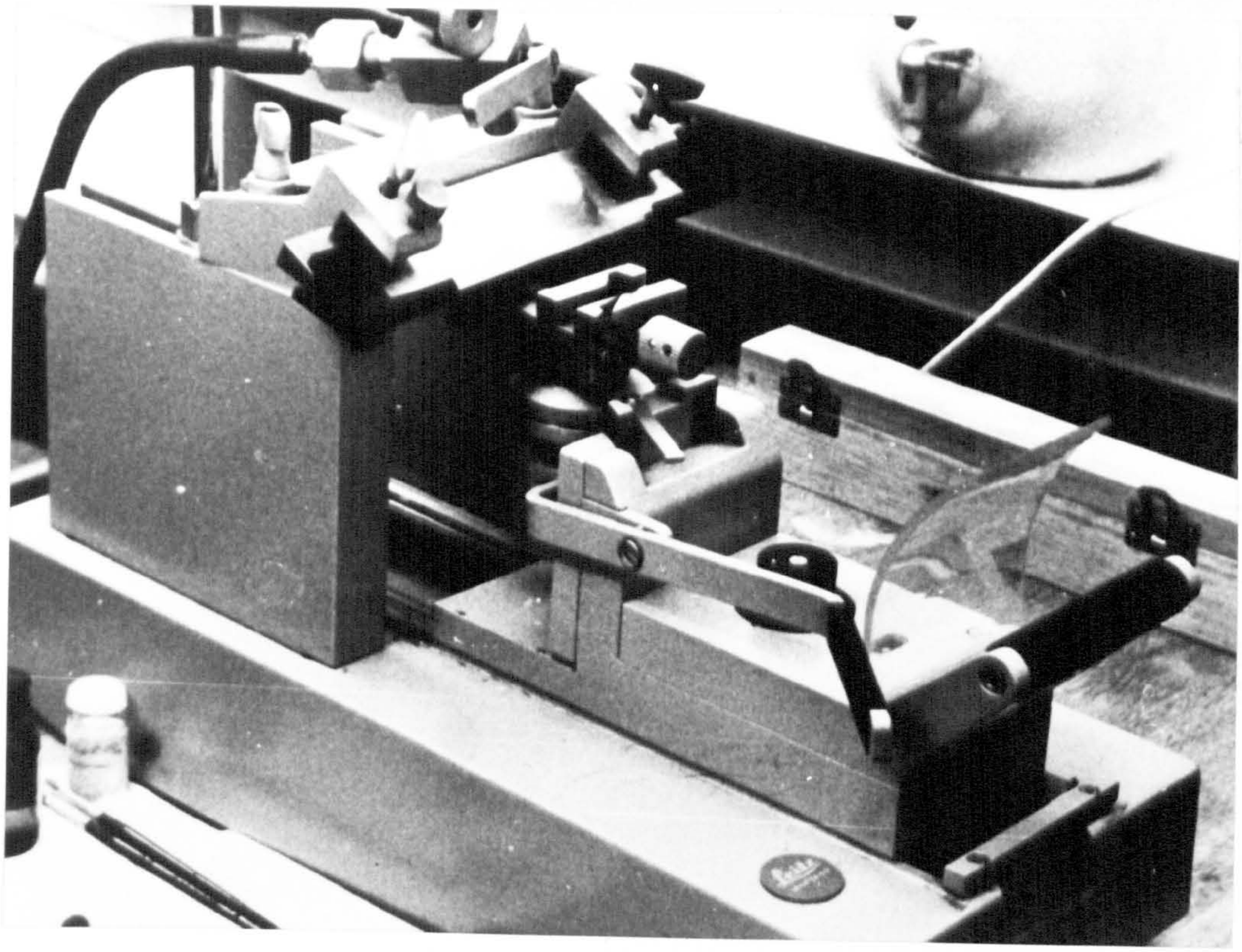

FIGURE 3.6 Typical sledge microtome.

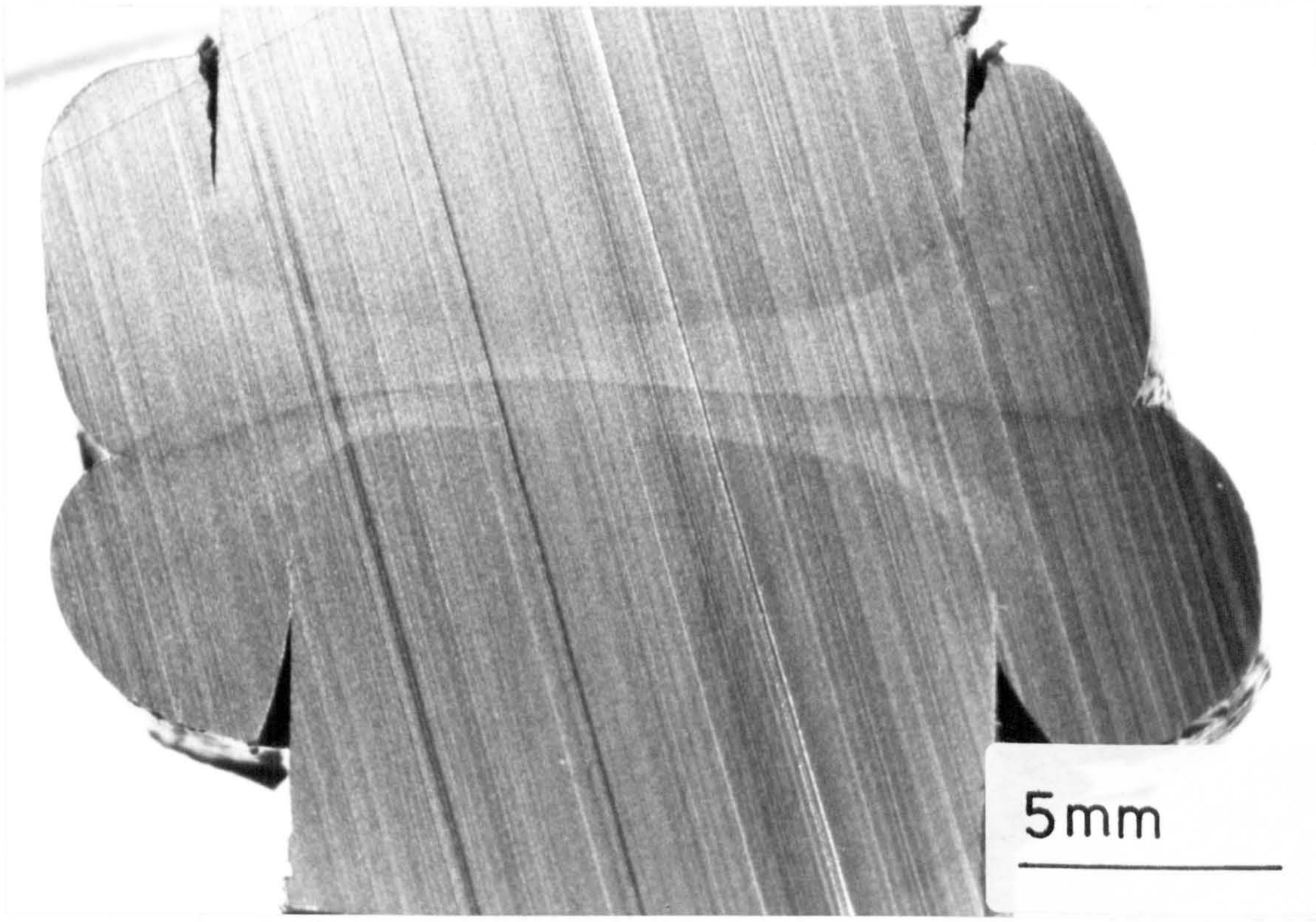

FIGURE 3.7 Surface of an HDPE butt-weld produced by removing a thin section of less than 10 μm.

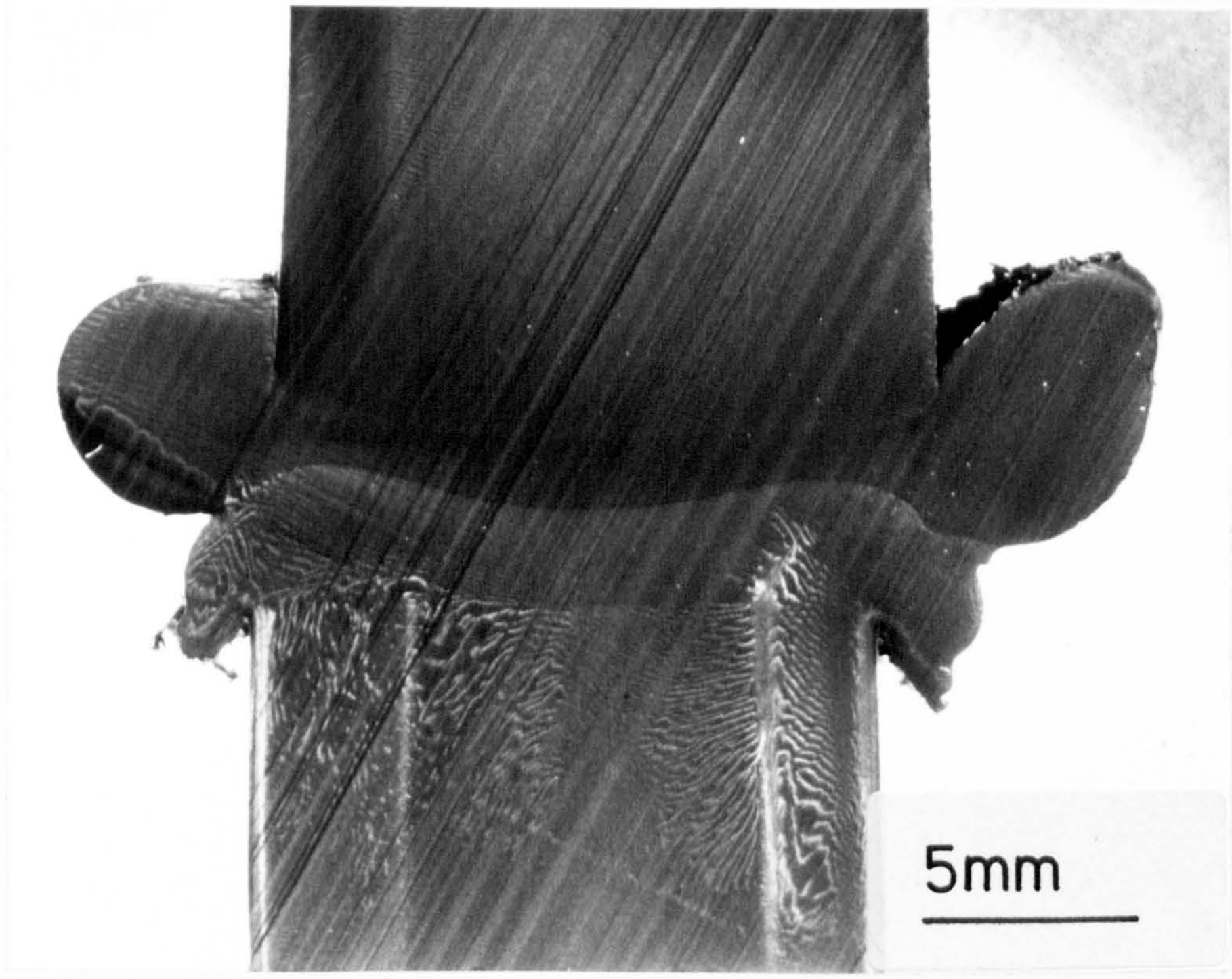

FIGURE 3.8 Surface of an HDPE butt-weld produced by removing a thick section of nearly 40 μm.

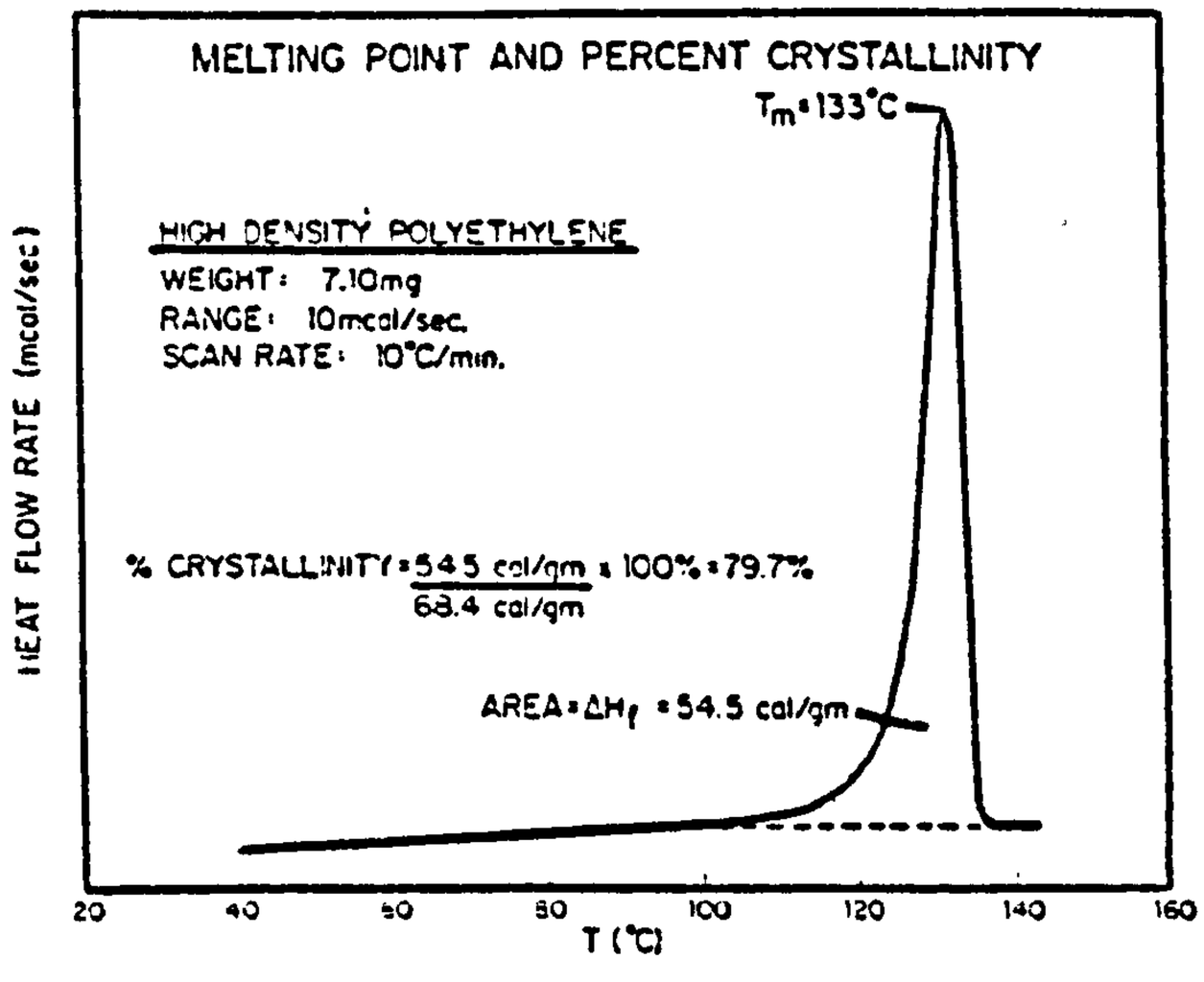

FIGURE 3.9 Typical DSC endotherm for virgin HDPE.
(After reference 36)

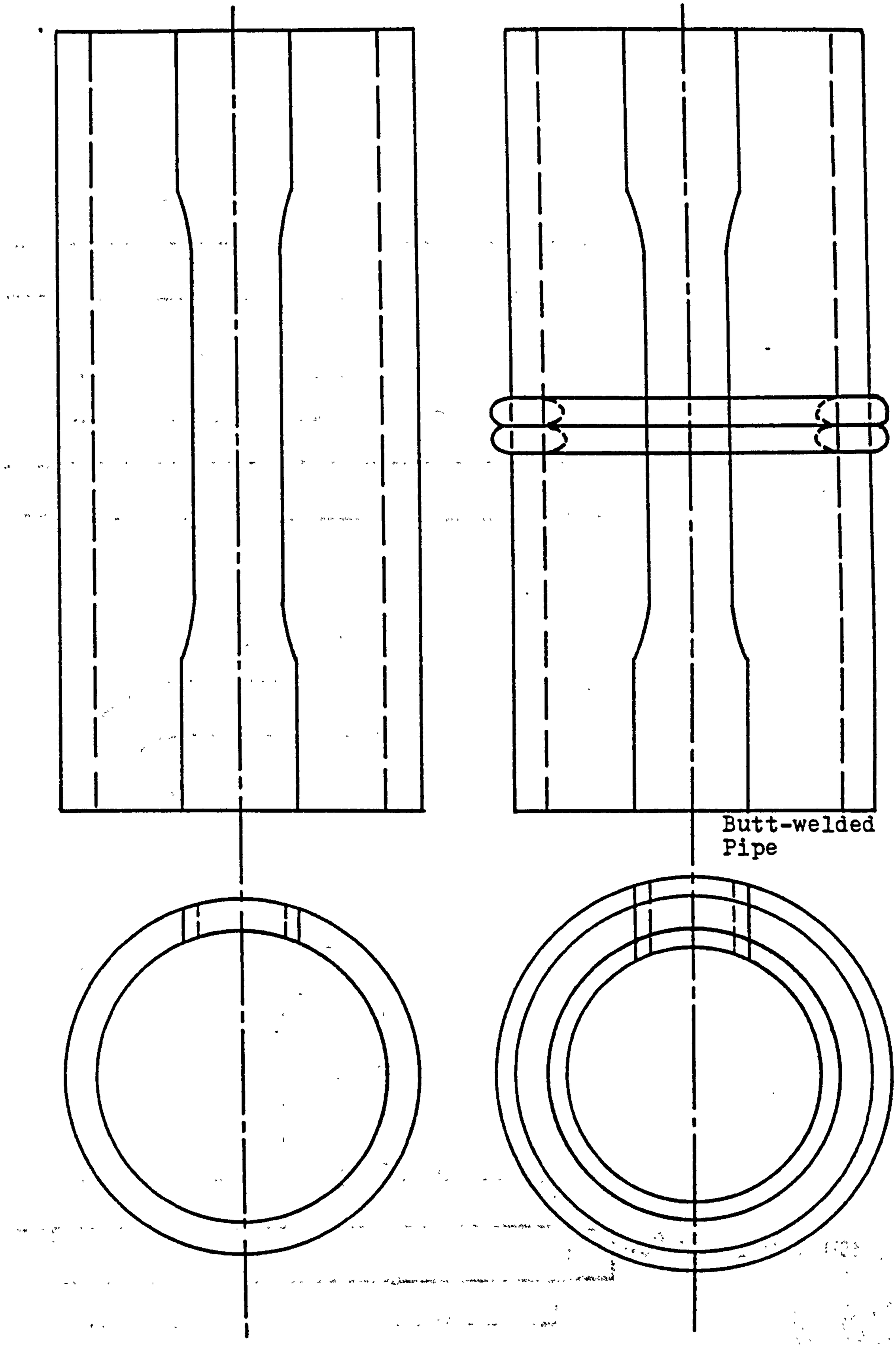

FIGURE 3.10 Orientation of tensile test specimens taken from pipes and butt-welded pipes

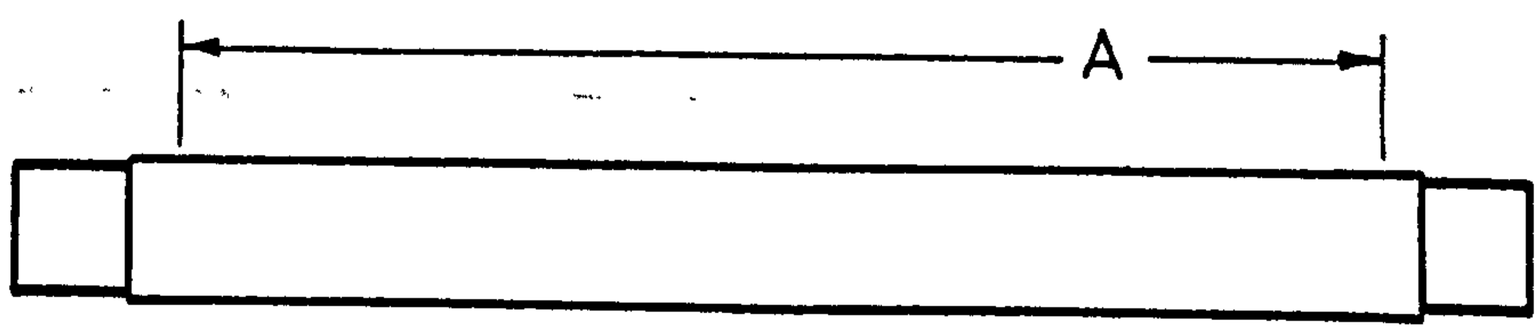

Pipe (P)

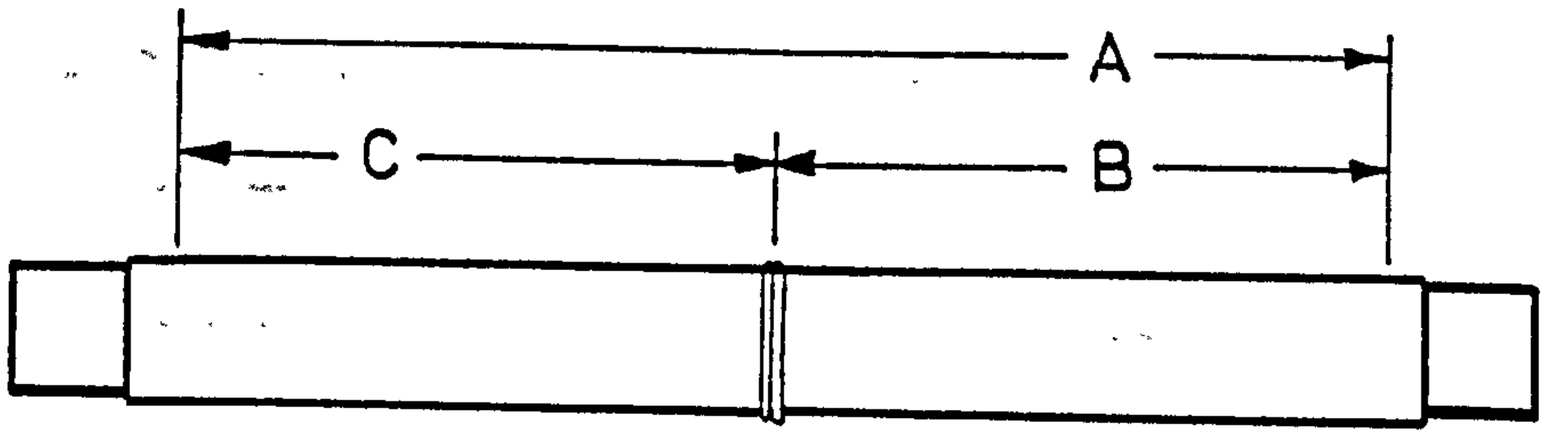

Pipe welded to pipe (P/P)

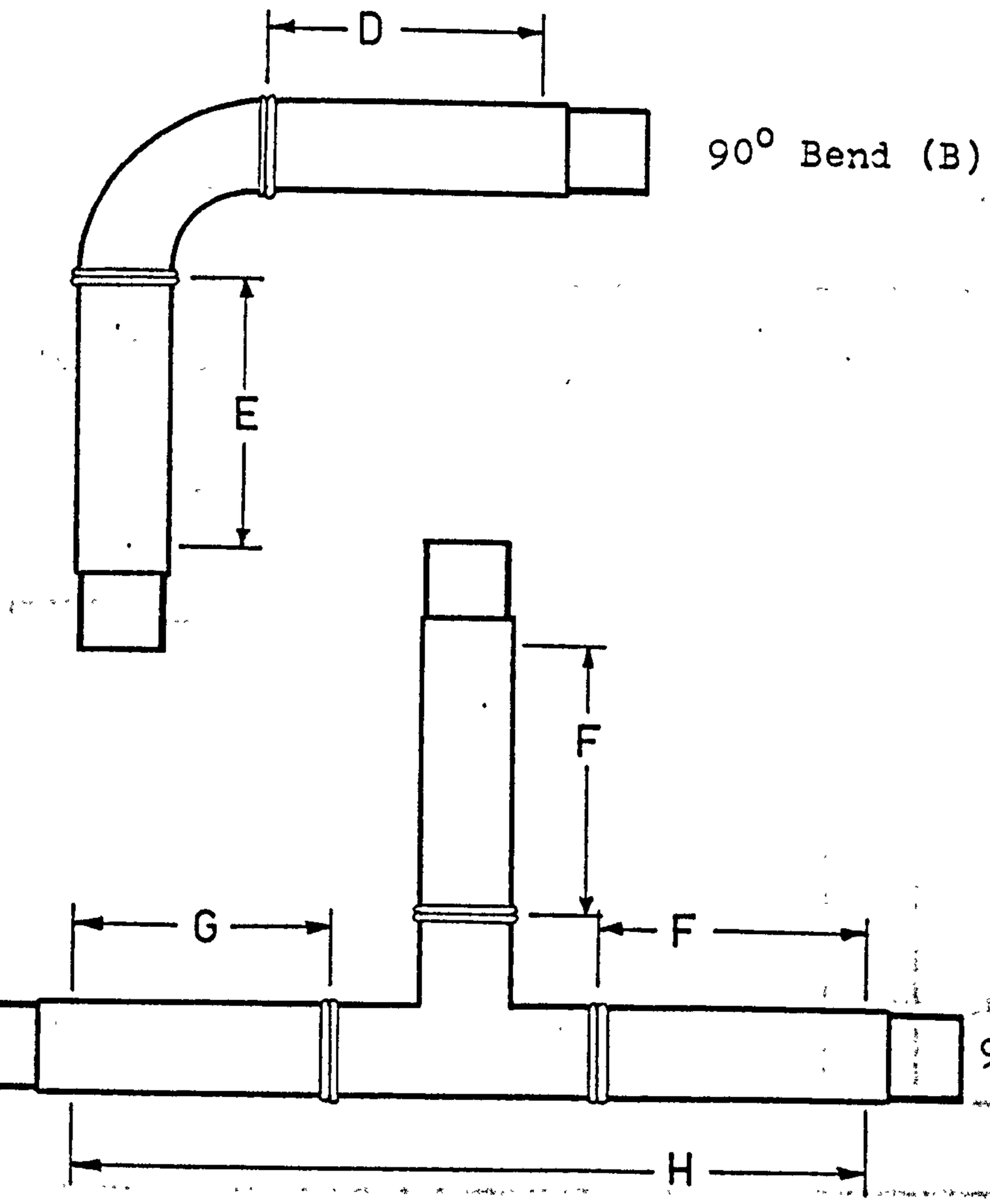

90^{o} Bend (B)

90^{o} Equal Tee (T)

FIGURE 3.11 Configurations of the 60 and 63mm OD SDR 11 PE pipe systems.
(Dimensions are given in Table 3.4)

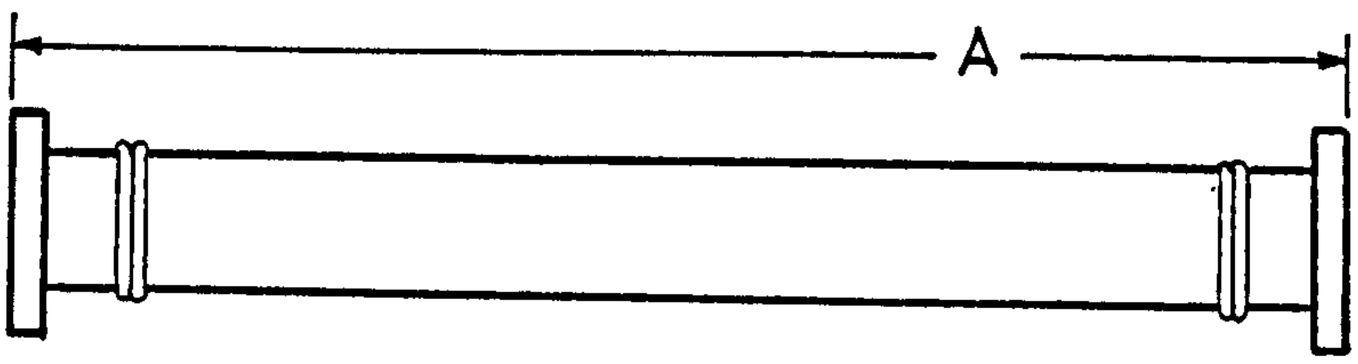

Pipe (P)

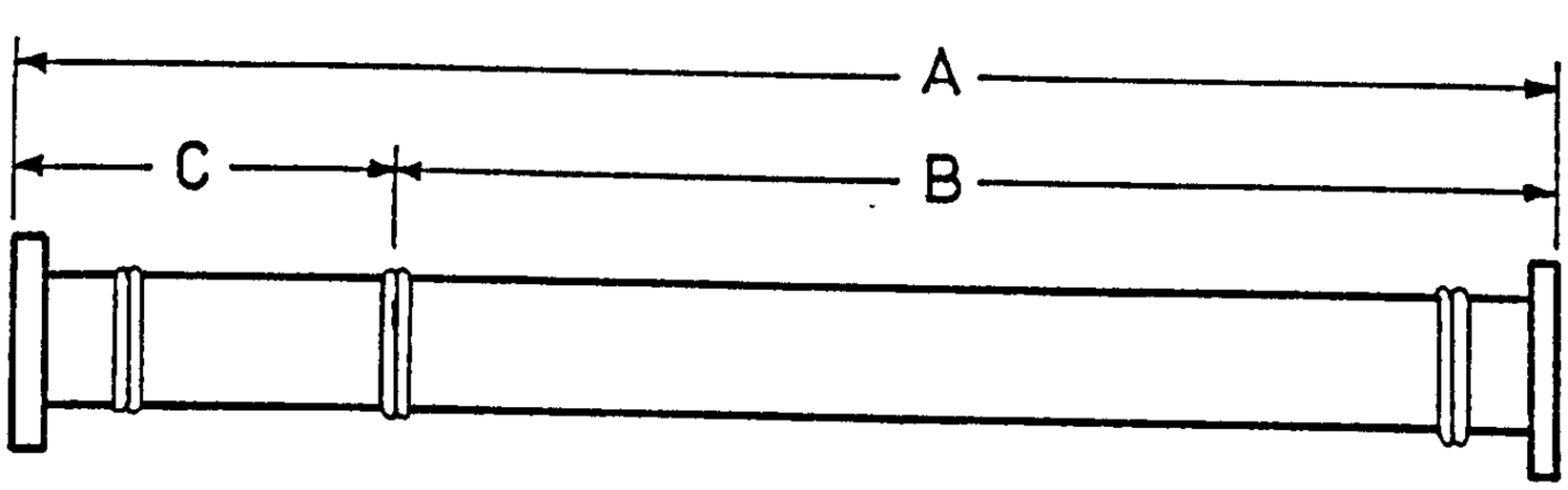

Pipe welded to pipe (P/P)

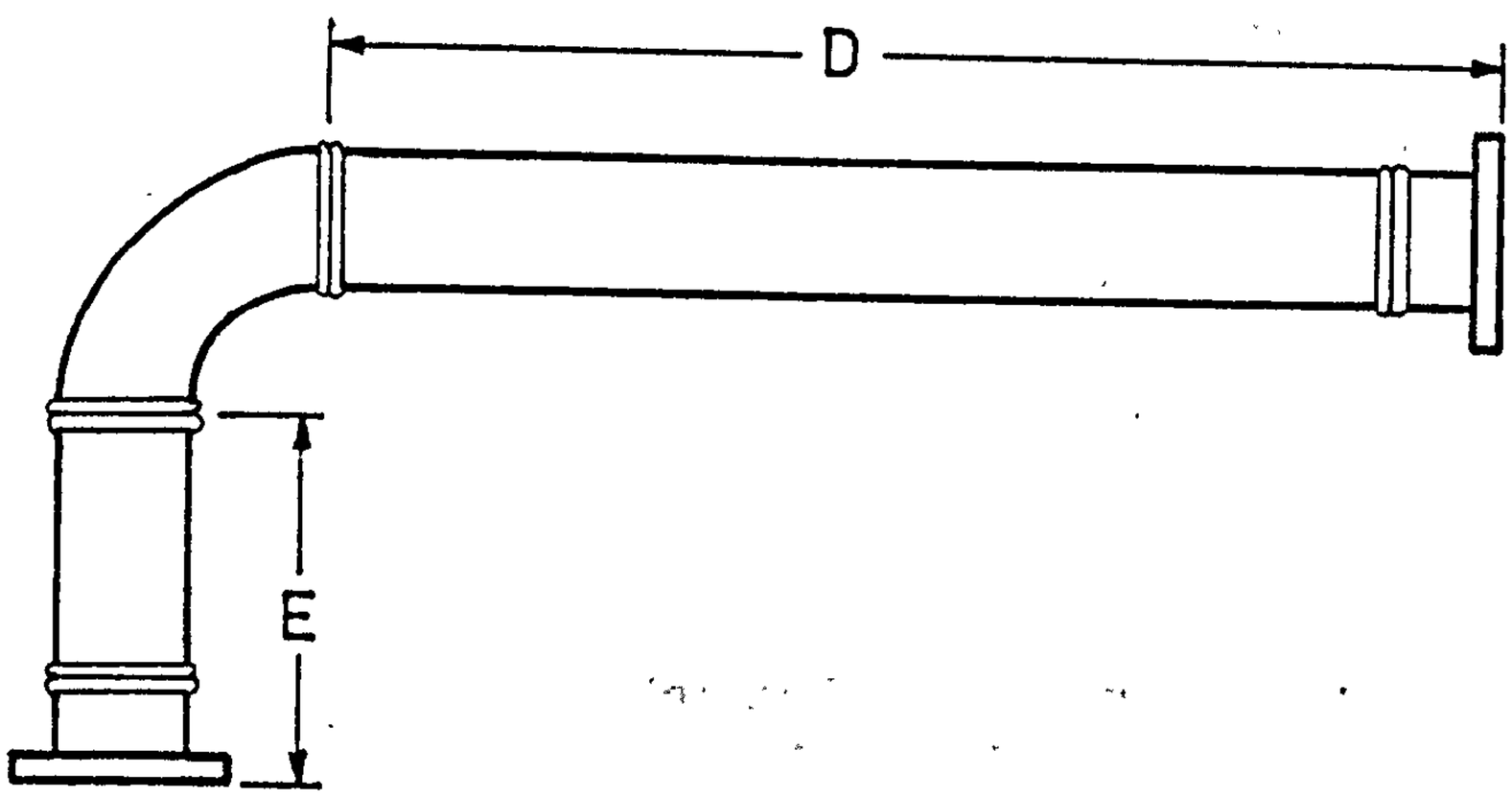

90° Bend (B)

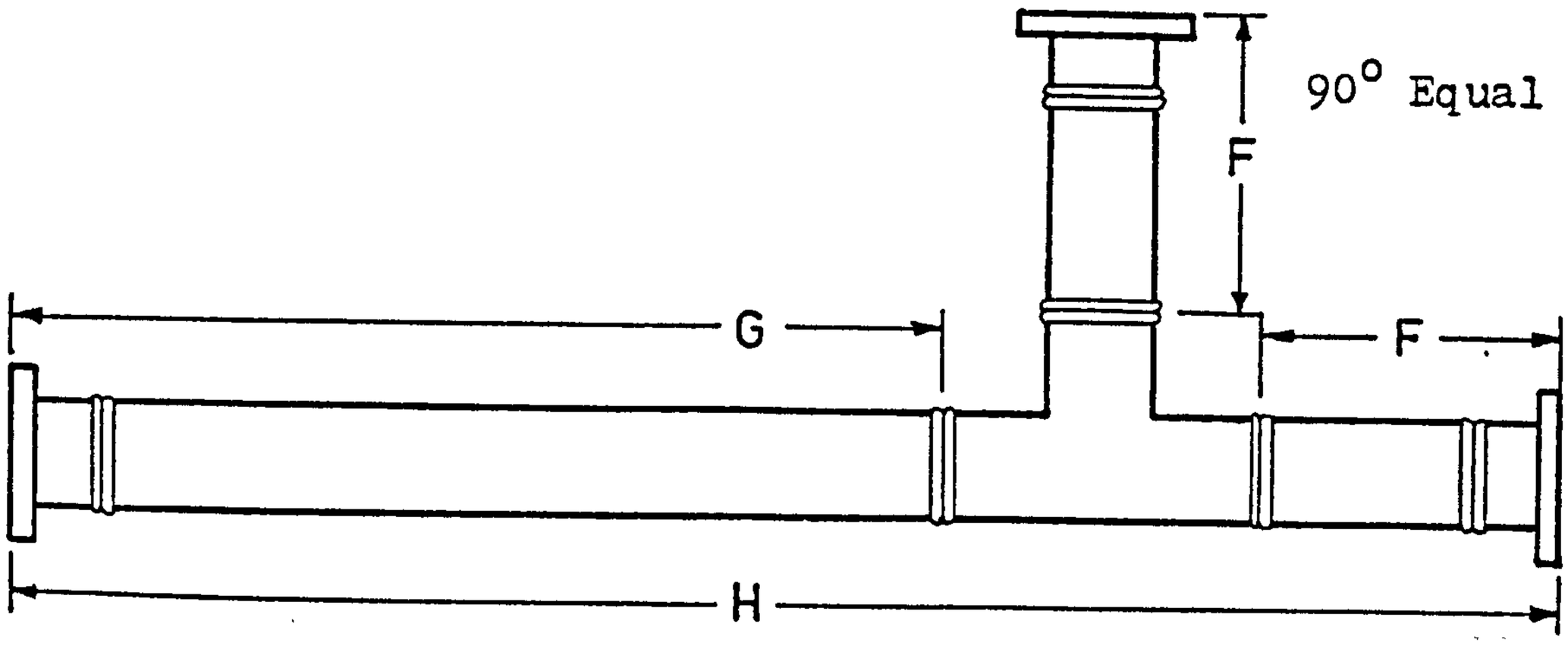

90° Equal Tee (T)

FIGURE 3.12 Configurations of the 160mm OD SDR 11 and 180mm OD SDR 17 pipe systems.
(Dimensions are given in Table 3.4)

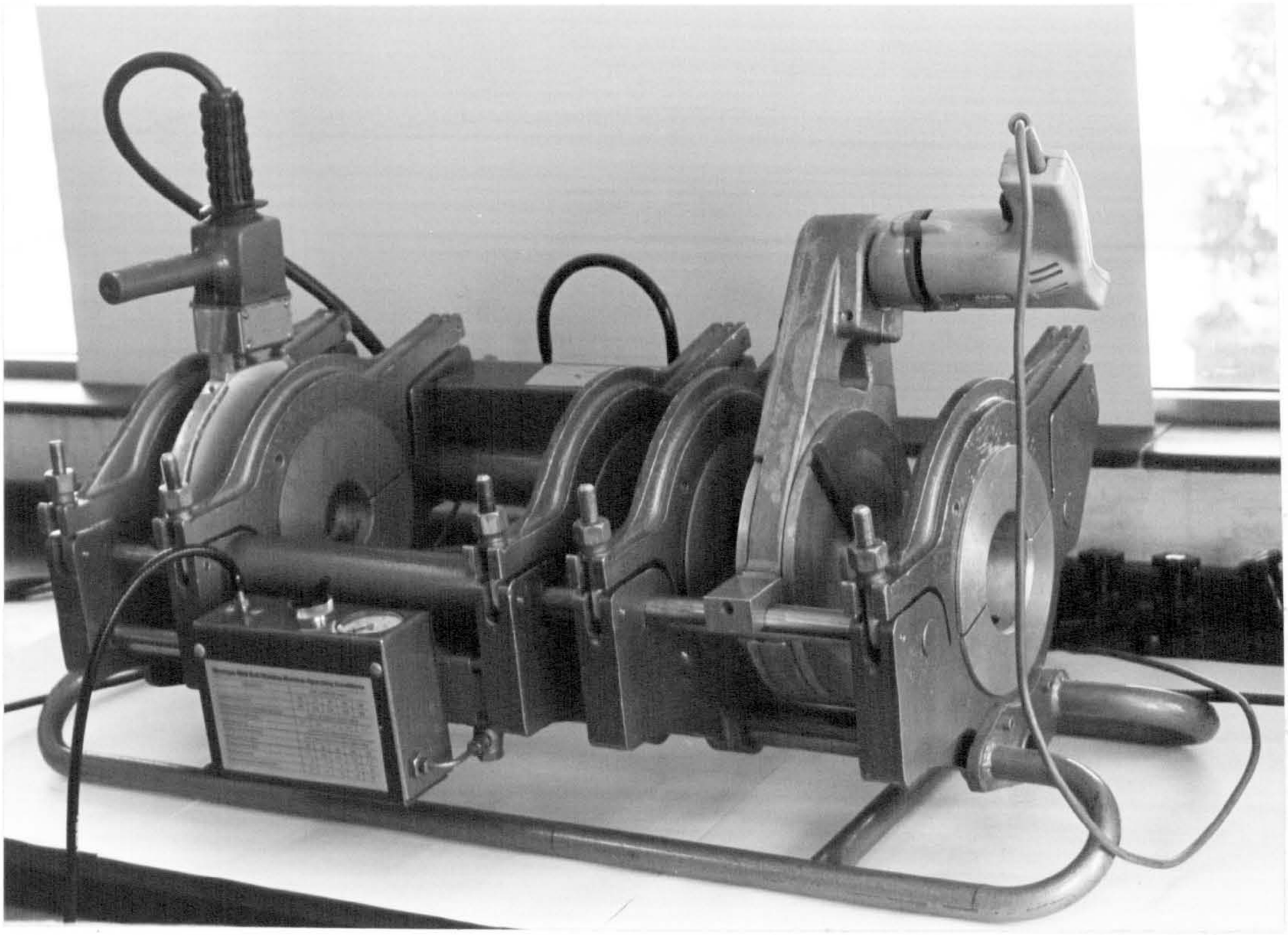

FIGURE 3.13 Haxey Mark II mirror-plate butt-welding machine for thermoplastics pipe systems.

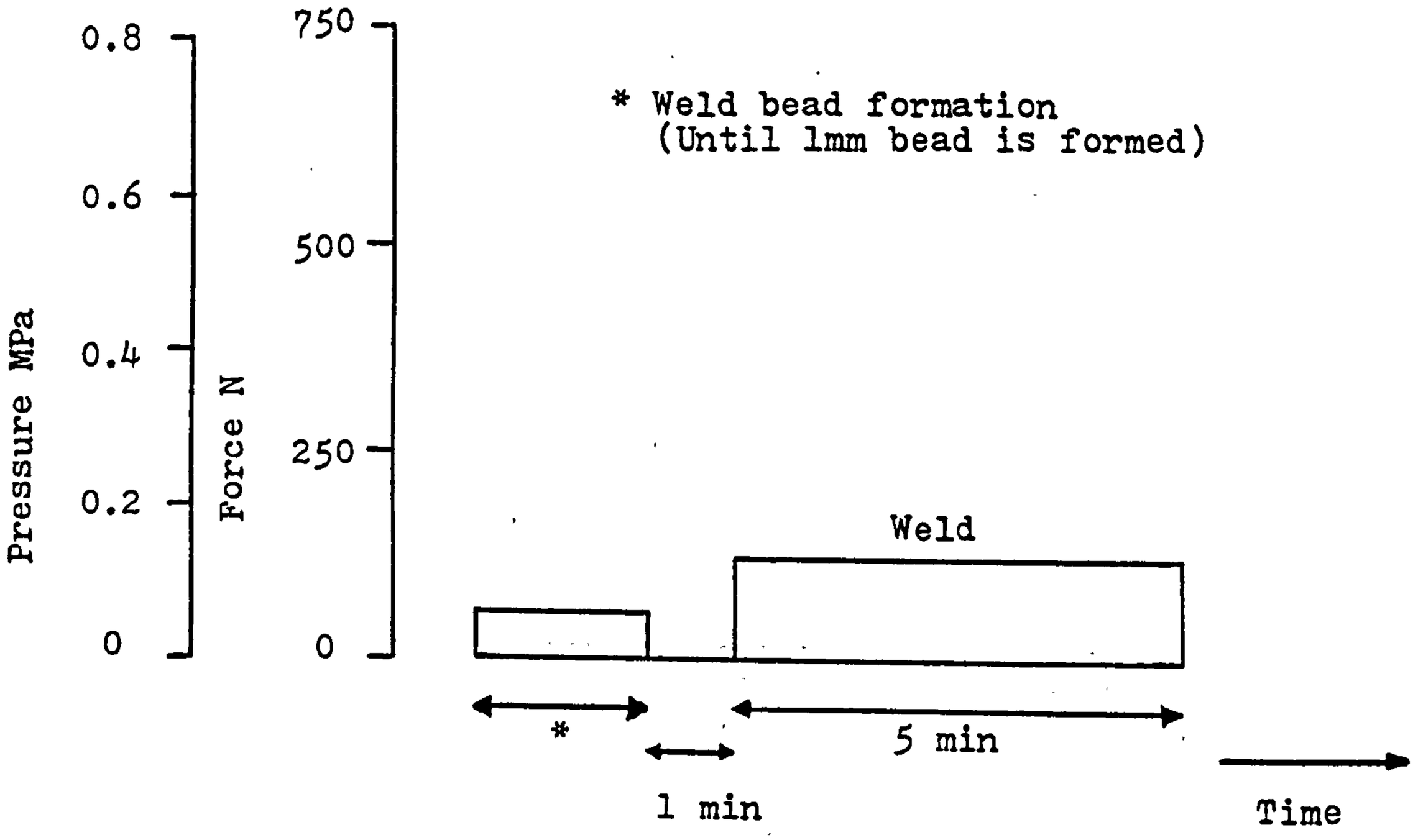

FIGURE 3.14 Schematic representation of the butt-welding pressure/time profile for HDPE 1, HDPE 2 and MDPE 2 63mm OD SDR 11 pipe systems.

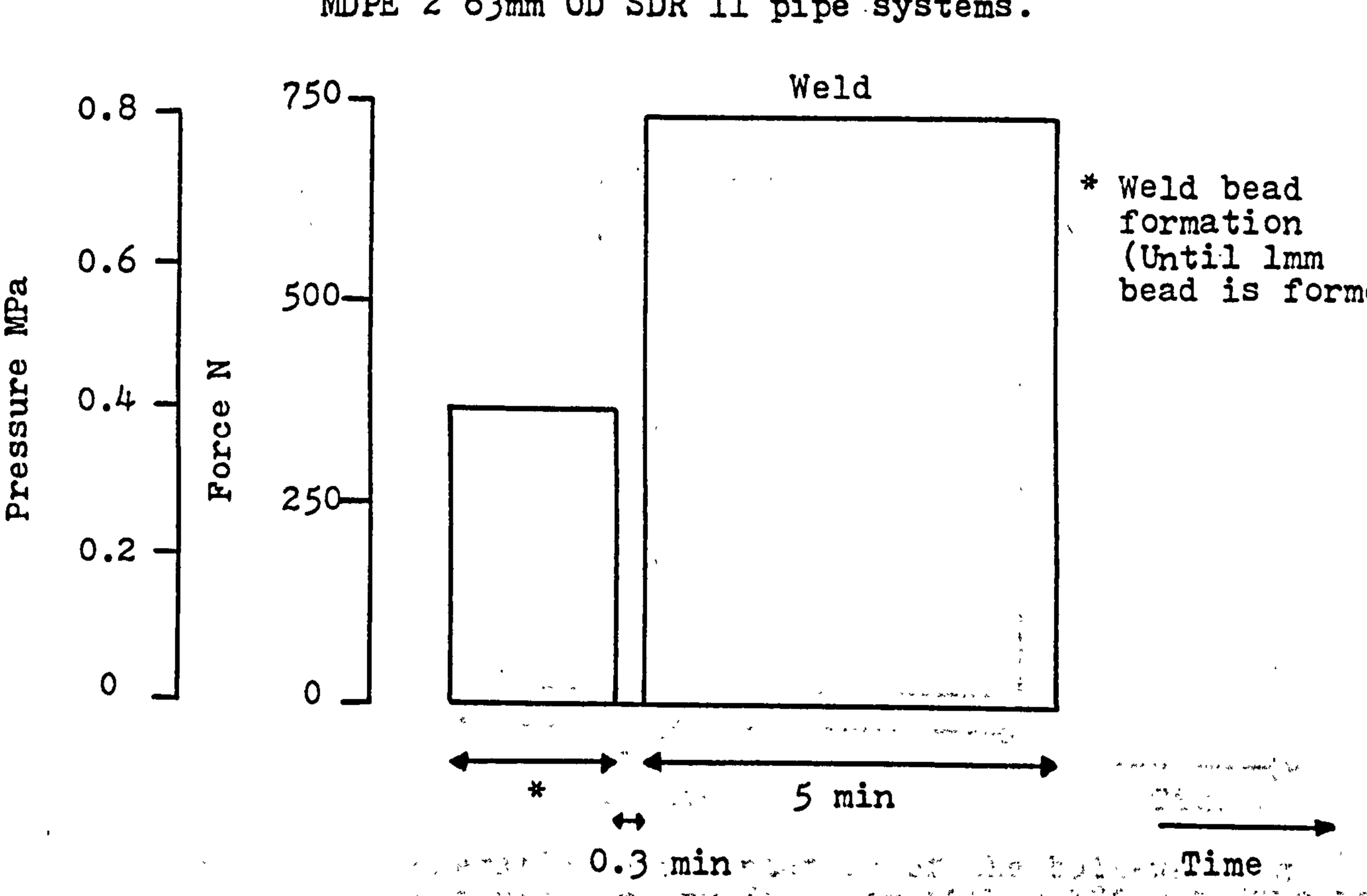

FIGURE 3.15 Schematic representation of the butt-welding pressure/time profile for MDPE 1 60mm OD SDR 11 pipe systems.

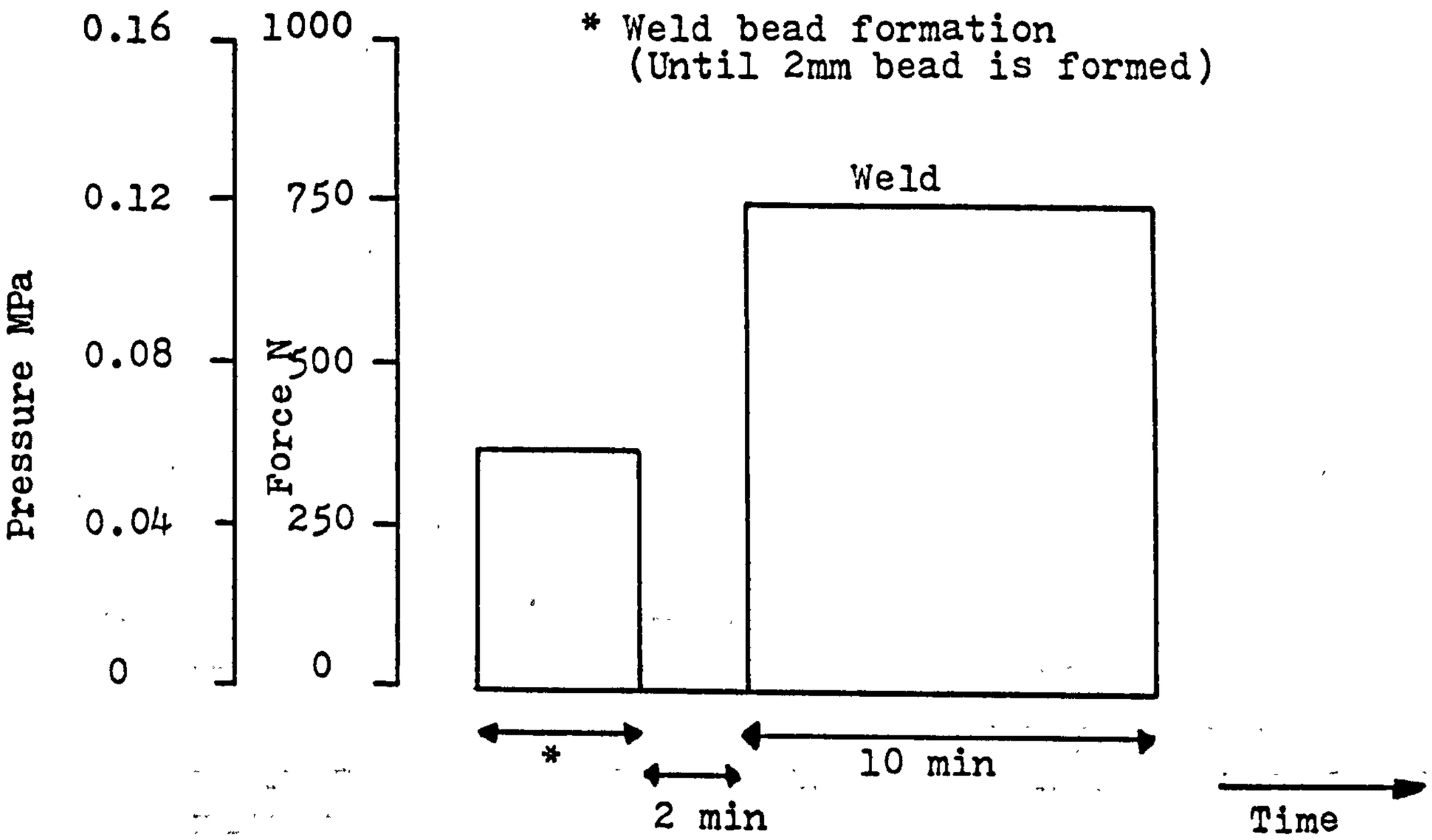

FIGURE 3.16 Schematic representation of the butt-welding pressure/time profile for HDPE 1 160mm OD SDR 11 pipe systems.

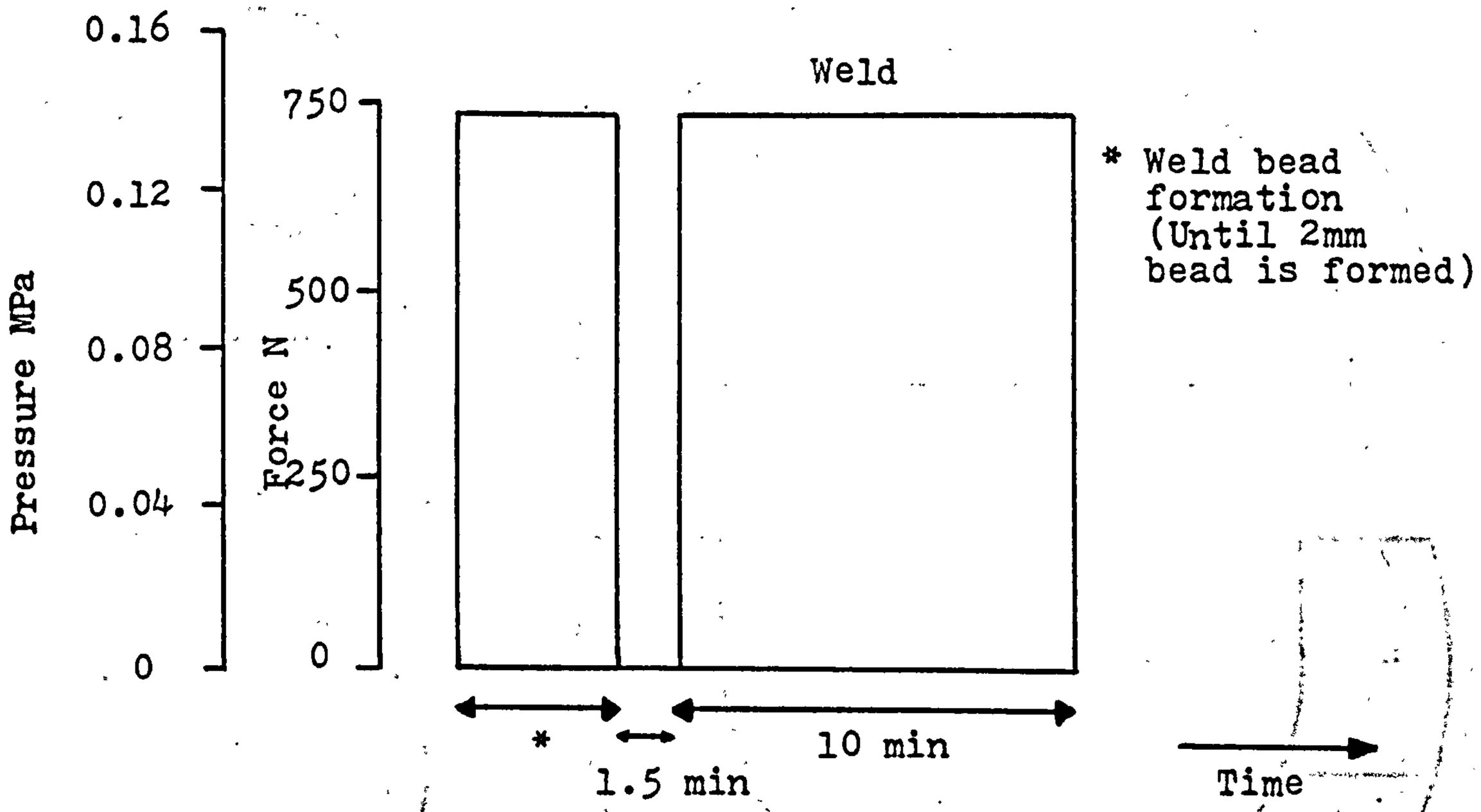

Figure 3.17 Schematic representation of the butt-welding pressure/time profile for MDPE 2 180mm OD SDR 17 pipe systems.

Threaded Ends

Flanged Ends

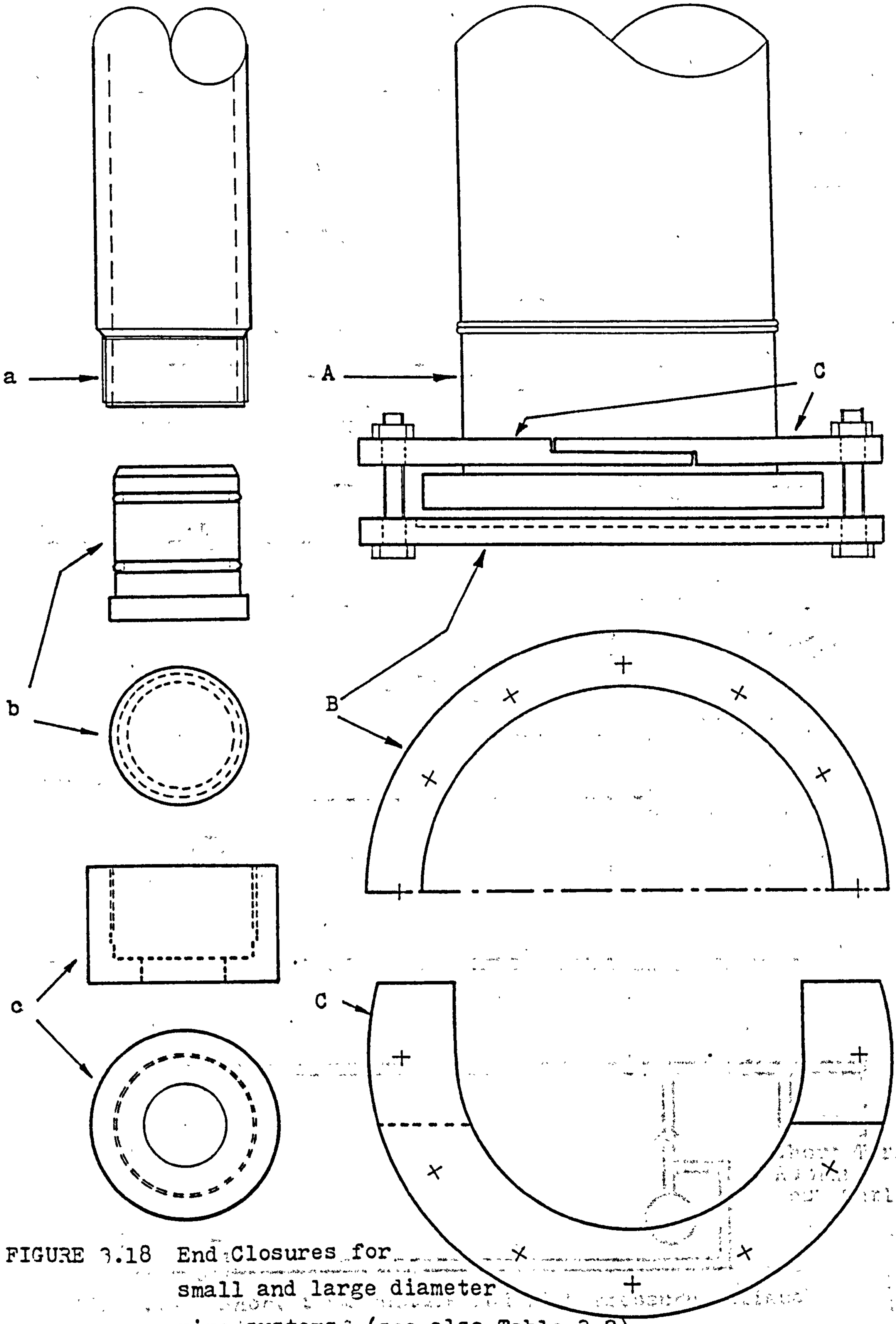

FIGURE 3.18 End Closures for small and large diameter pipe systems. (see also Table 3.7)

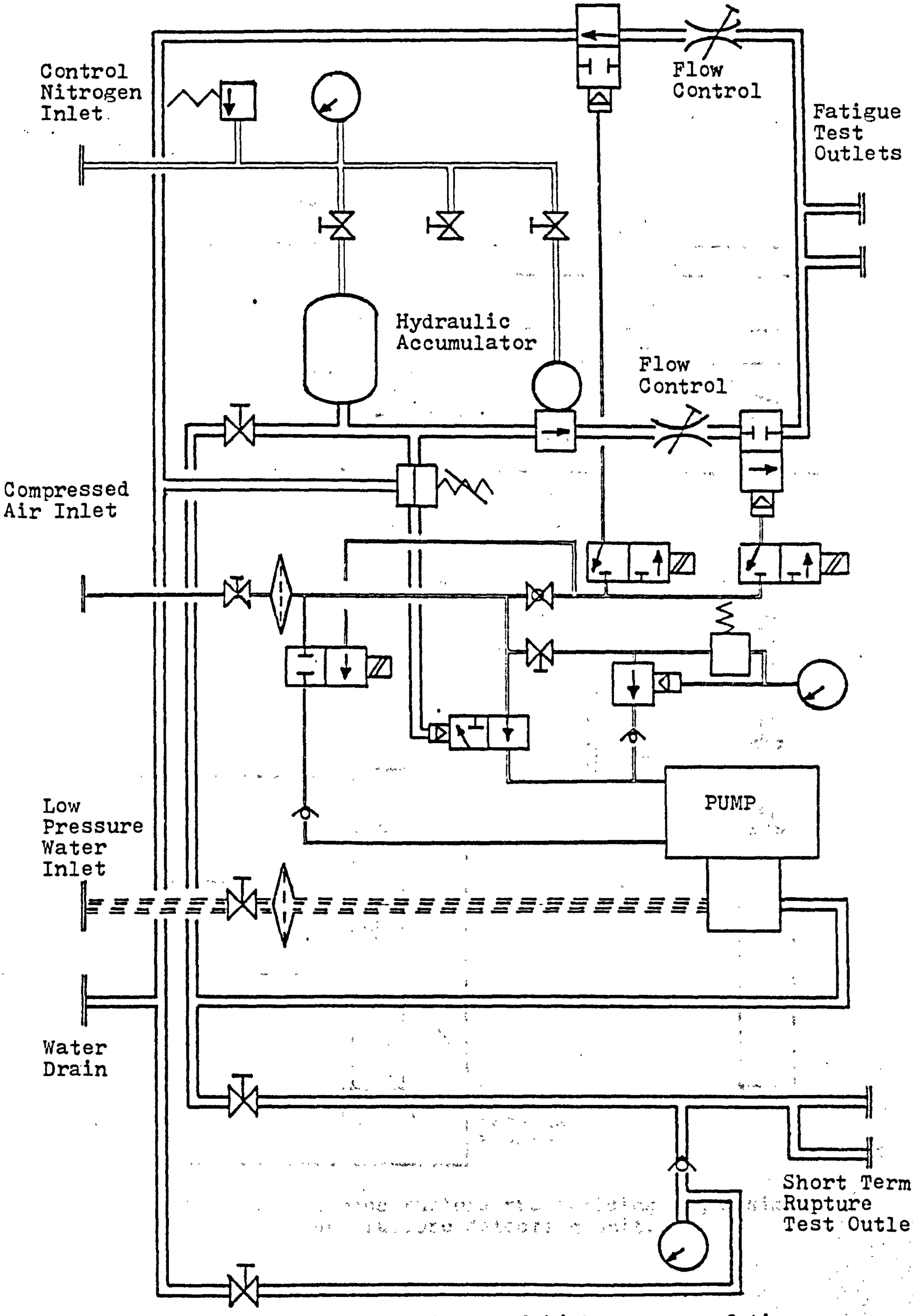

FIGURE 3.19 Short term rupture and high pressure fatigue rig design.

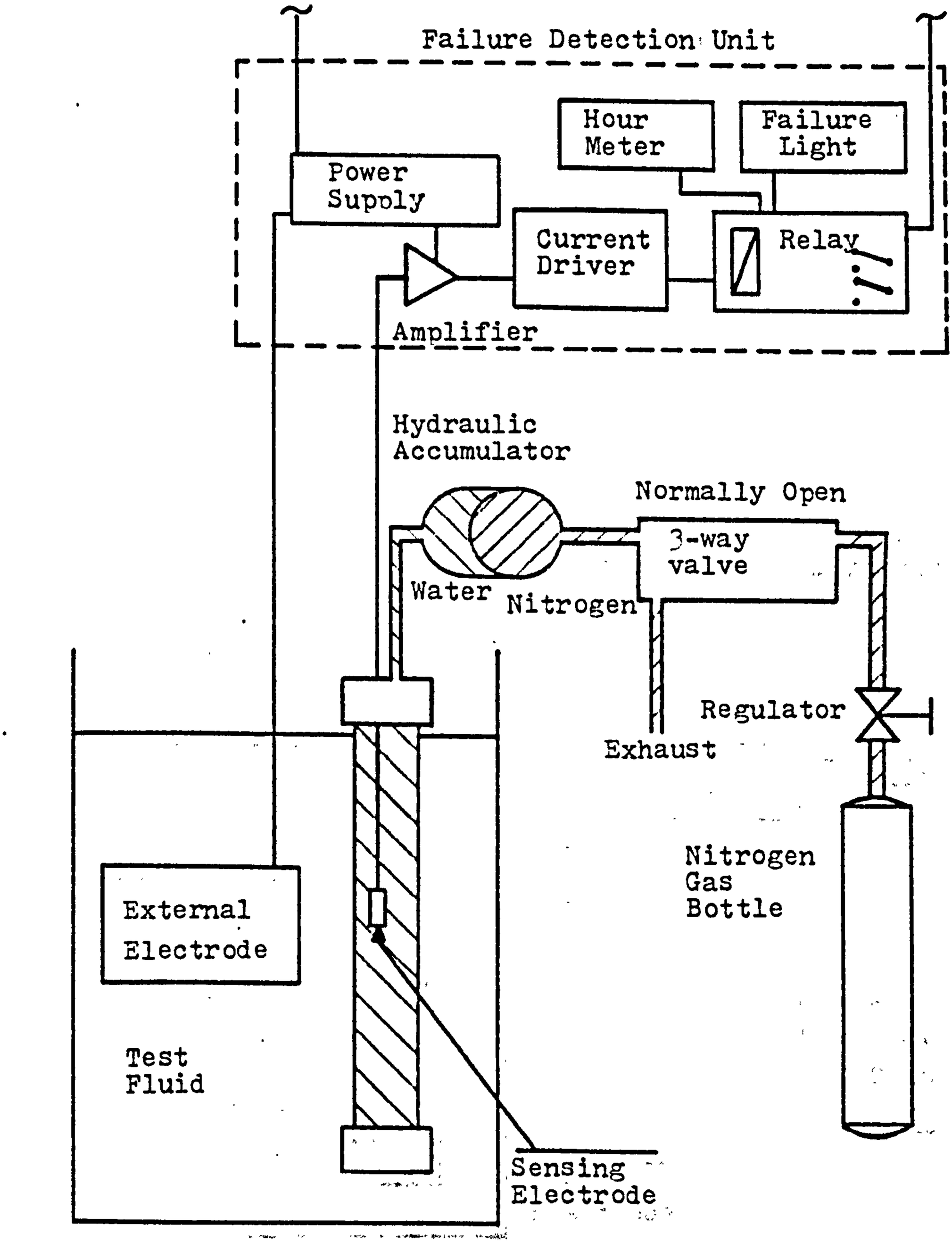

FIGURE 3.20a Stress rupture pressurising rig design and failure detection unit.

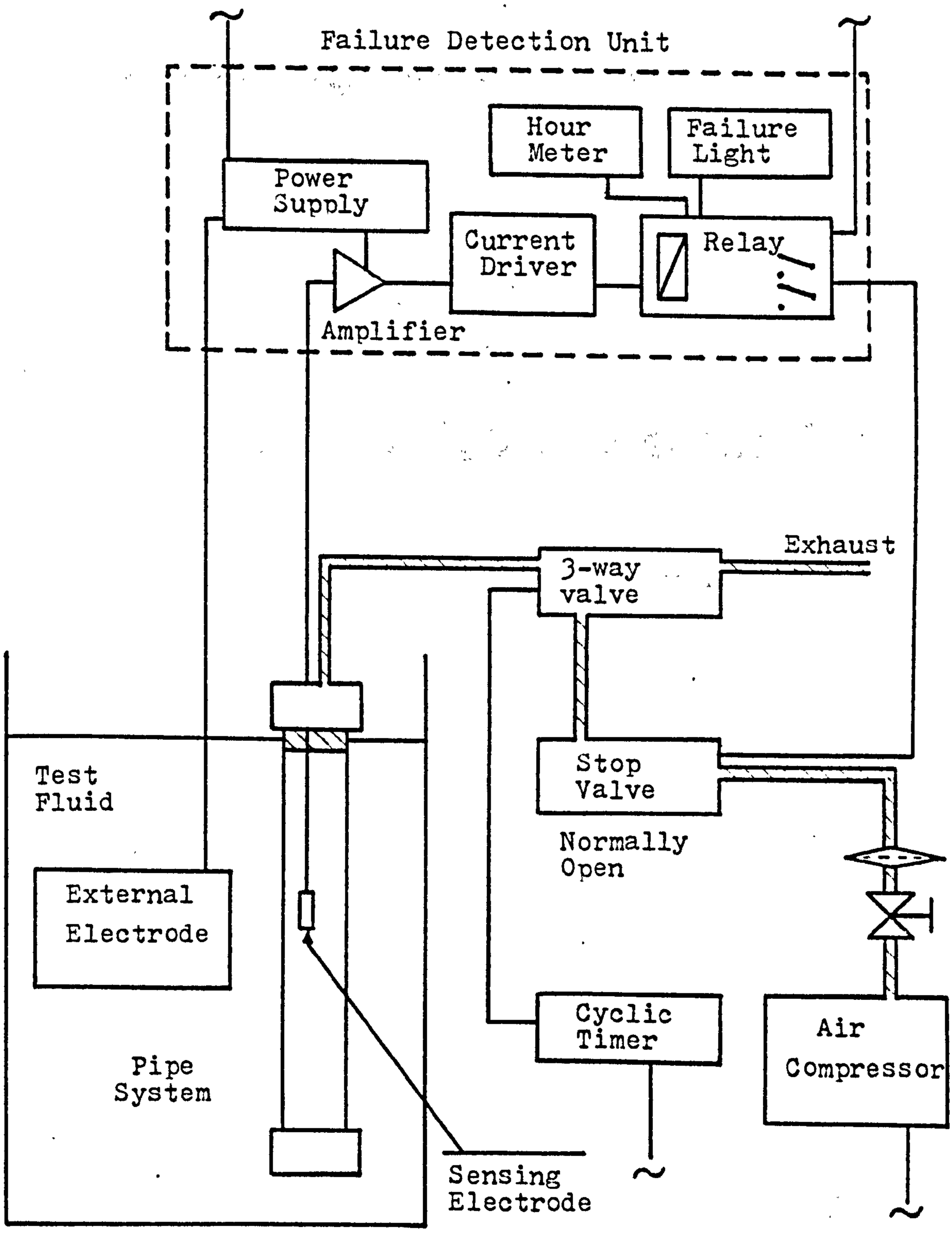

FIGURE 3.20b Fatigue pressurising rig design and failure detection circuit.

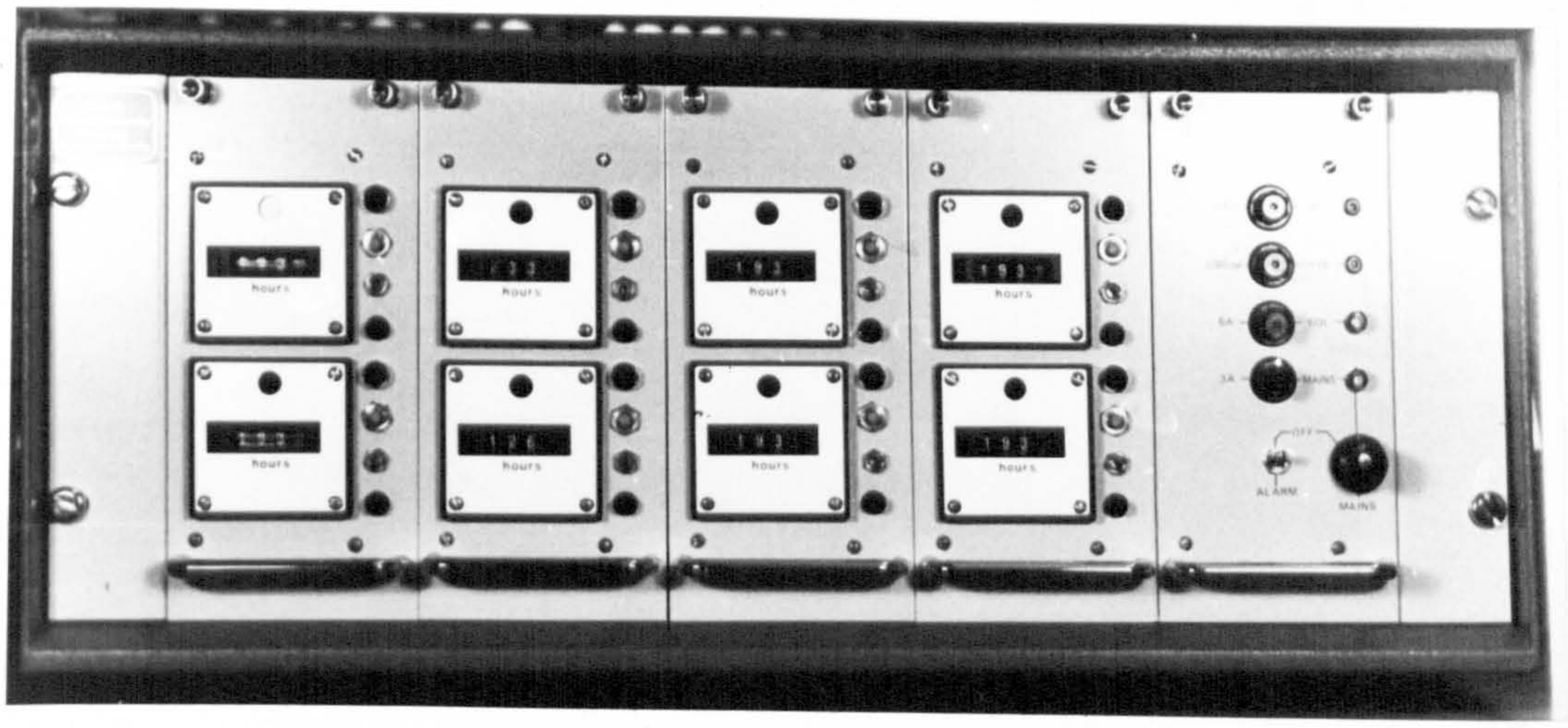

FIGURE 3.21 Failure detection unit for thermoplastics pipe systems.

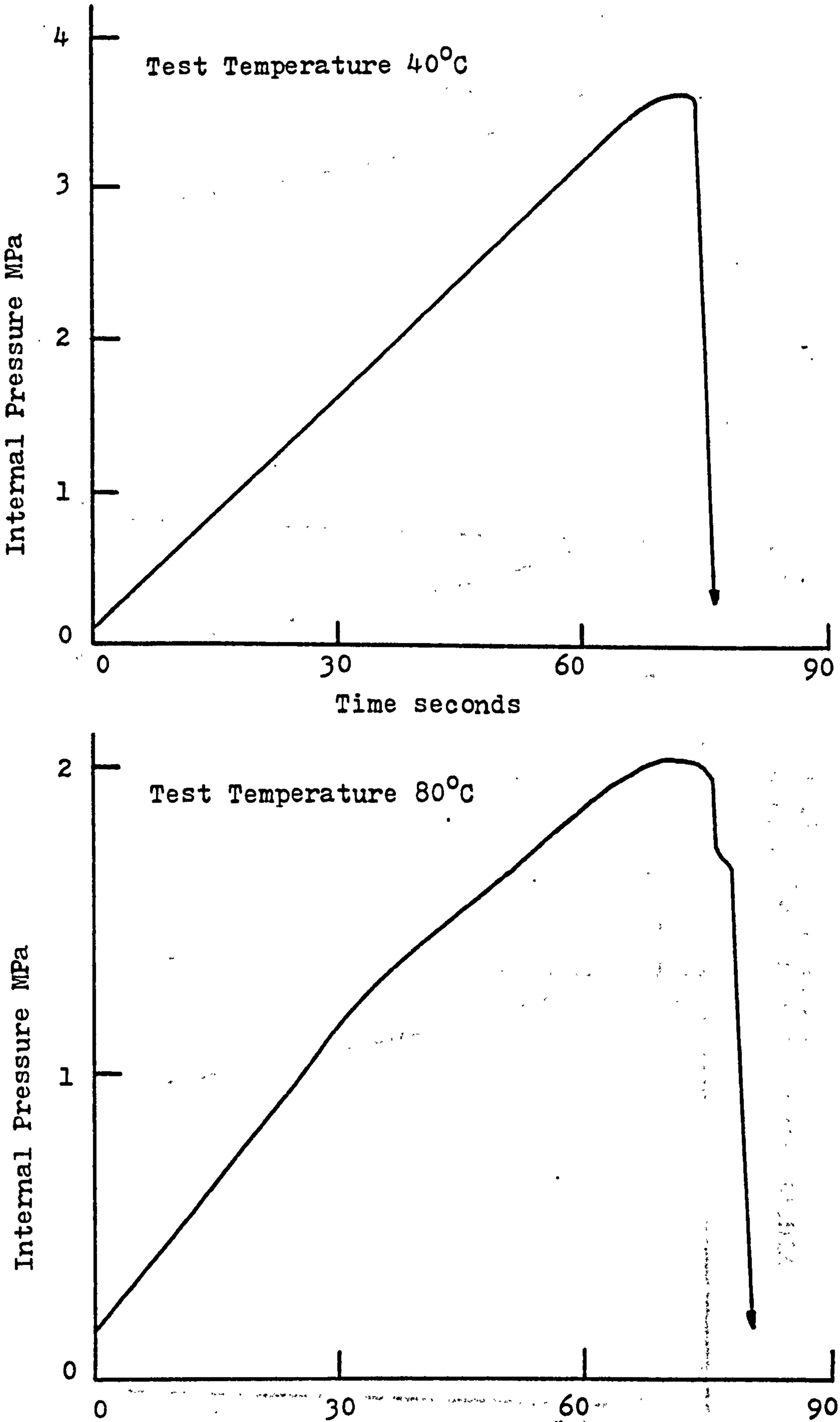

FIGURE 3.22 Two examples of short term rupture test pressure/time-profiles.
(HDPE 1 63mm OD SDR 11 pipes)

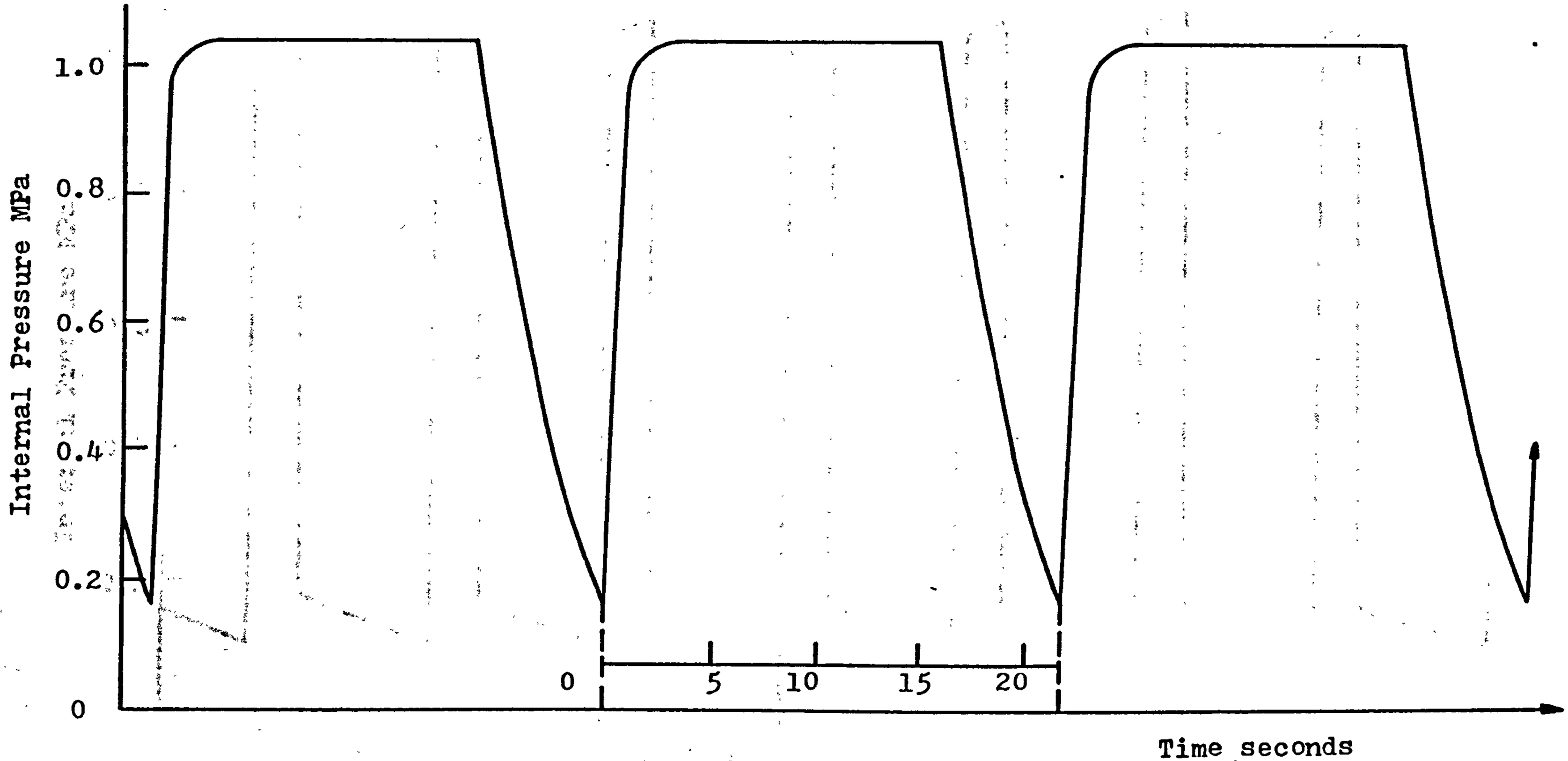

FIGURE 3.23 Low frequency (2.7 cpm) fatigue test pressure/time profile at 80°C.

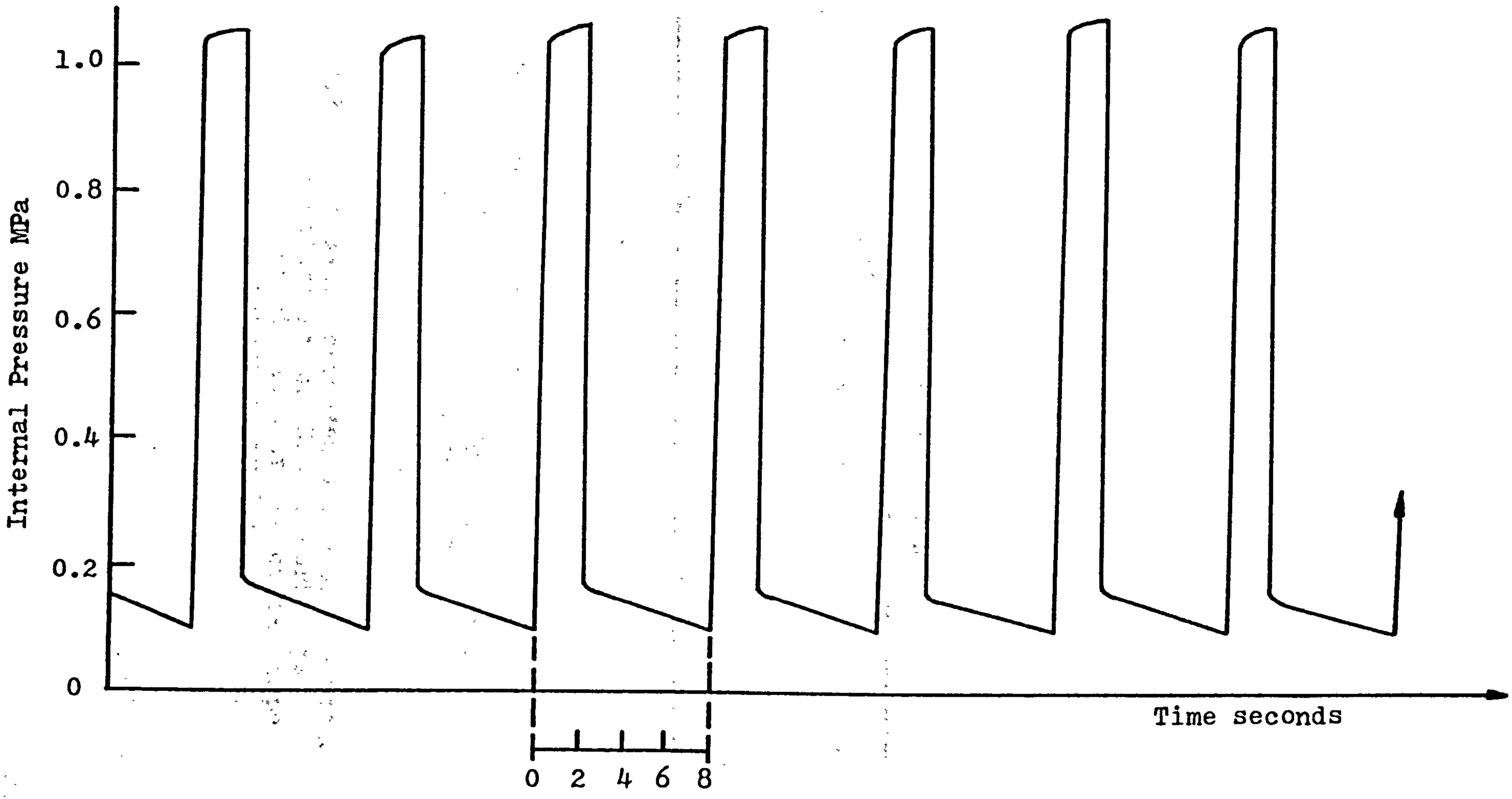

FIGURE 3.24 High frequency (7.5 cpm) fatigue test pressure/time profile at 80°C.

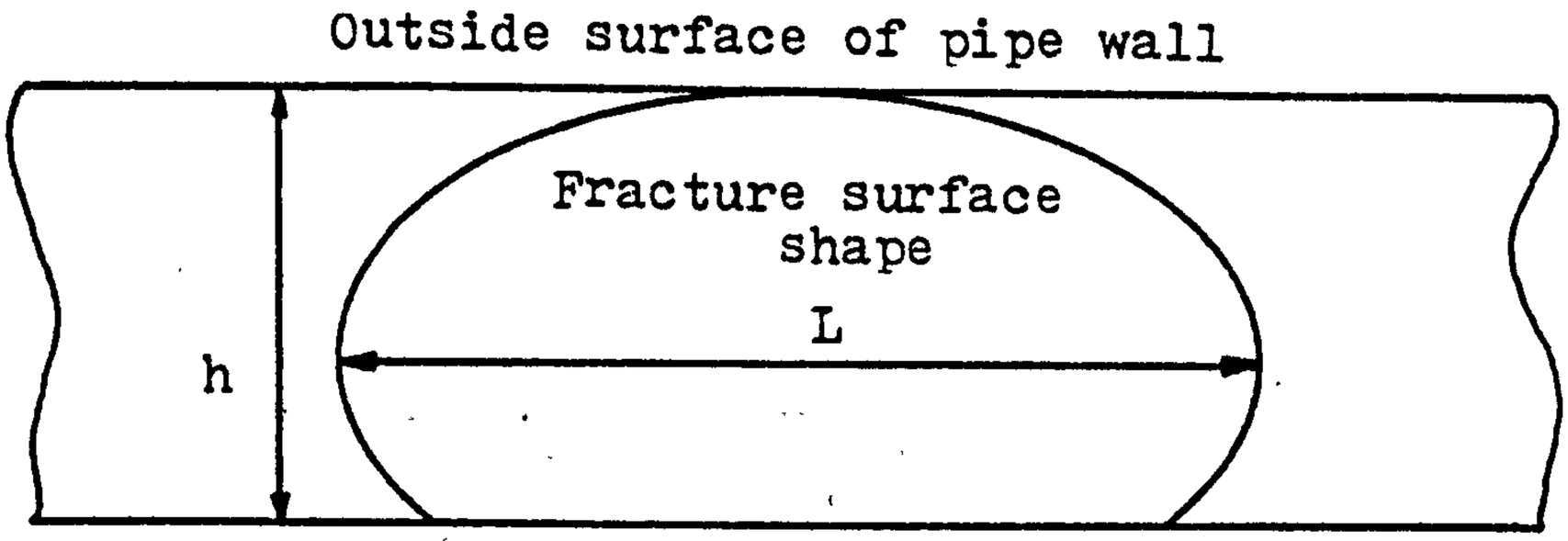

h = wall thickness

L = maximum width of fracture surface parallel to the pipe axis

FIGURE 3.25 Schematic representation of a brittle fracture in an HDPE or MDPE pipe. The aspect ratio of the crack shape is characterised by L/h.

CHAPTER 4 - RESULTS

SMALL DIAMETER PIPE AND WELDED PIPE SYSTEMS
(60mm and 63mm OD/SDR 11)

4.1 RESULTS - PRESENTATION AND ANALYSIS

The research programme concentrated mainly upon obtaining data from HDPE 1 and 2 pipe systems. Such information was used as a reference with which other materials and system designs could be usefully compared.

In detail the results can be divided into three main areas:-

a. Small diameter (60 and 63mm OD) SDR 11 pipes extruded from two HDPE and two MDPE resins were tested mainly at 80°C (plus lower temperatures for the short term rupture tests) under various forms of internal pressure loadings. In fatigue tests pressure was cycled between a set maximum and zero gauge pressure using a ramped "square wave" loading with frequencies in the range 0.8 to 7.5 cpm (0.014 to 0.125 H_z). The strength and lifetimes of the pipes were recorded for the various internal pressures and loading profiles employed.
Selected pipe systems containing a butt-welded joint were also subjected to the above test programme using the same batches of pipe.

b. The fracture surfaces of failed pipe and welded pipe systems were examined in detail. Photographs of all surfaces were taken to characterise macro-structure while scanning electron microscopy was used to examine both the fine detail of fracture surfaces and any particles initiating such fractures. Energy dispersive x-ray analysis was utilised to characterise the elemental nature of these initiating particles.

c. Crystallinities and melting point variations induced by pressure testing the pipe materials at elevated temperatures, for selected failed pipes, were investigated, using differential scanning calorimetry. Controlled ageing tests were also carried out where samples of pipe material were immersed in a water bath and held at the elevated temperatures used during pressure testing. No external stresses were appled to these samples.

To describe the performance of the plastics pipes subjected to constant and fluctuating internal pressures three approaches were adopted.

First, the concept of time under maximum load was utilised. For stress rupture testing this is simply τ_{SR}, while for fatigue the corresponding parameter is $\tau_{FATIGUE}$, given by

$$\tau_{FATIGUE} = \sum_{N=1}^{N=N_f} (t_{max})_N \qquad (4.1)$$

where t_{max} is the time during each loading cycle when the internal pressure is greater than 95% of the set maximum value and N_f is the number of cycles to failure. $\tau_{FATIGUE}$ may be termed the pseudo stress rupture life-time and is a concept previously utilised to allow comparisons to be made between stress rupture and fatigue data (94). If $\tau_{SR} = \tau_{FATIGUE}$ at all frequencies, then for those testing conditions the plastics pipes exhibit no substantial weakness under fatigue. If, however, $\tau_{SR} \gg \tau_{FATIGUE}$, the reverse is true.

Secondly, pipe performance was defined by the total testing time τ_{TEST}. Clearly for stress rupture testing, $\tau_{SR} = \tau_{TEST}$. For fatigue,

$$\tau_{TEST} = \sum_{N=1}^{N=N_f} (t_{cycle})_N \qquad (4.2)$$

where t_{cycle} is the time required for one complete loading cycle. Since t_{max} must be less than t_{cycle}, then $\tau_{TEST} > \tau_{FATIGUE}$, for fatigue loading.

In practice, it is τ_{TEST} that is normally recorded for service failures rather than $\tau_{FATIGUE}$, although the latter presents a more fundamental description of pipe performance.

Thirdly, the behaviour of plastics pipes under fatigue loading was determined by recording the number of cycles to failure. This approach necessarily precluded the meaningful presentation of any stress rupture data. Under these conditions as the frequency varies only the time under maximum load per cycle, t_{max}, alters. The rate of pressurisation and time off load are kept constant by using a trapezoidal shaped fatigue loading profile.

To simplify data analysis, the mean values for τ_{SR}, $\tau_{FATIGUE}$, τ_{TEST} (when applicable) and N_f are recorded in tabulated and graphical presentations. The distribution of lifetimes was assumed normal and the sample standard deviation calculated and inserted to indicate the spread in the values of lifetimes. It is understood that for much larger sample numbers the distribution of stress rupture lifetimes for HDPE pipes has been shown to be logarithmic - normal (74).

The mean and standard deviation approach to presenting internal pressure test results is also applied to pipe systems containing injection moulded fittings and were appropriate to the large diameter pipe results.

4.2 MECHANICAL PERFORMANCE OF PIPE AND WELDED PIPE SYSTEMS

4.2.1 Tensile and Short Term Rupture Tests

Tensile tests were used to determine the quality of the pipe material and butt-welds with and without weld beads. Typical stress/strain curves are plotted in Figures 4.1 and 4.12. Mean values of stresses and strains and their standard deviations along with short term weld factors are detailed in Table 4.1.

The welding conditions used throughout the mechanical testing programme were as recommended by individual manufacturers and the results of Table 4.1 indicate that in the short term at least these conditions are correct and also validate weld quality.

Table 4.2 identifies the short term rupture strengths (maximum sustained hoop stress) of pipes and welded pipe systems produced from materials HDPE 1 and 2 and MDPE 1 at various temperatures. Figures 4.13 and 4.14 show the variation of maximum hoop stress as a function of temperature for pipes and welded pipe systems fabricated from HDPE 1 and 2 respectively.

Figure 4.15 indicates, for HDPE 1 SDR 11 63mm OD pipes, the effect of increasing test specimen length upon the maximum sustainable hoop stress obtained during the short term rupture test. The curve shows the need for consistency in pipe lengths used during this test since short term mechanical properties can be affected to a significant degree by such dimensional variations.

For all materials at all the temperatures examined, failures were of a ductile nature with the site of rupture in the welded pipe specimens lying remotely from the mirror-plate butt-welds. The short term rupture strengths were also apparently insensitive to the presence of a butt-weld in any of the materials investigated.

TABLE 4.1 - Tensile Test Results at 20°C.

MATERIAL	OD (mm)	SDR	PARENT MATERIAL		WELDED SPECIMEN			WELDED SPECIMEN WITH BEAD MACHINED OFF		
			YIELD STRESS (MPa)	MEAN STRAIN AT FAILURE (%)	YIELD STRESS (MPa)	STRAIN AT FAILURE (%)	SHORT TERM WELD FACTOR	YIELD STRESS (MPa)	STRAIN AT FAILURE (%)	SHORT TERM WELD FACTOR
HDPE 1	63	11	22.88 ±0.83	>365 (No failures)	22.48 ±0.37	289 ±18	0.93	22.35 ±0.21	192 ±99	0.98
HDPE 2	63	11	20.96 ±0.36	>365 (No failures)	22.03 ±0.39	339 ±18	1.05	21.98 ±0.31	203 ±31	1.04
MDPE 1*	60	11	19.71 ±0.18	>500 (No failures)	20.09 ±0.47	263 ±27	1.02	19.92 ±0.11	>500 (No failures)	1.03
MDPE 2*	63	11	19.02 ±0.42	>500 (No failures)	20.06 ±0.18	238 ±41	1.05	19.11 ±0.74	>500 (No failures)	1.00

Notes * 1) Carried out on a T.J. Lloyd Tensile Testing Machine.
2) At least five samples were tested at any one condition.

TABLE 4.2 Short Term Rupture Strengths of Pipe and Welded Pipe Systems (60 and 63mm OD/SDR 11)

MATERIAL	SYSTEM	20°C MAXIMUM HOOP STRESS MPa	40°C MAXIMUM HOOP STRESS MPa	60°C MAXIMUM HOOP STRESS MPa	80°C MAXIMUM HOOP STRESS MPa
HDPE 1	PIPE	25.67 ± 0.05	20.76 ± 0.25	13.95 ± 0.30	9.66 ± 0.39
	WELDED PIPE	27.02 ± 0.15	19.62 ± 0.20	13.70 ± 0.49	10.21 ± 0.49
HDPE 2	PIPE	26.97 ± 0.49	20.66 ± 0.39	15.48 ± 0.30	9.81 ± 0.64
	WELDED PIPE	26.38 ± 0.20	19.97 ± 0.44	14.99 ± 0.64	10.21 ± 0.30
MDPE 1	PIPE	24.60 ± 1.03	-	-	-

Notes 1) At least three specimens of each material and system type were tested at each condition.

2) All failures were ductile and occurred in the pipe sections. No butt-weld failures were observed.

A typical short term rupture test failure (ductile) is shown in Figure 4.16. (Pressure profiles for such tests were given in Chapter 3.)

A further series of tests were carried out to compare tensile and short term rupture testing directly on HDPE 1 pipe material.

The tensile tests were conducted such that the yield stress of the material was attained between 60 and 90 seconds so that conditions previously employed in the short term rupture test were approximately duplicated.

In spite of the fact that the tensile test is uniaxial in nature whereas the rupture test is biaxial, reasonable correlation was obtained between the maximum hoop stresses attained by rupture test specimens and the yield stresses observed in HDPE 1 at 20 $\pm$ 1°C. For five tensile bars the average yield stress was found to be 22.88 $\pm$0.83 MPa and the maximum hoop stress for five pipes was 26.67 $\pm$ 0.05 MPa.

This indicates that tensile tests can be used to predict short term rupture test properties, with fairly close agreement, much more cheaply in terms of material costs.

4.2.2 Stress Rupture and Fatigue Tests

(i) Position and Description of Brittle Failure Sites.

Figure 4.17 is a schematic representation of pipe and welded pipes indicating the typical sites of brittle failure observed during the stress rupture and fatigue testing programme. For ease of reference the pipe system is designated P and the welded sample referred to by P/P. The failure at a butt-weld in the welded pipe system is then termed site P/P2.

Site P1 (and P/P1) - Fractures at these positions are cracks approximately five millimetres long lying parallel to the pipe extrusion direction. Due to their small size a fracture of this sort is particularly difficult to observe on the pipe surface. So Figure 4.18 shows schematically the fracture orientation and its appearance within the pipe wall.

Site P/P2 Type 1 (HDPE 1 and 2) - A crack lying parallel to the pipe extrusion direction which runs across the butt-weld. Again such a failure is almost impossible to observe since the actual point of failure is often hidden beneath the weld bead. Figure 4.19 sketches this longitudinal butt-weld failure.

Site P/P2 Type 2 (HDPE 1 and MDPE 1) - A butt-weld failure in these materials can initiate at the notch formed between the inside surface of the pipe and the weld bead (or occasionally at the notch formed between the beads at the weld interface). The crack does not then propagate across the weld parallel to the pipe extrusion direction but rather opens up at or near the weld interface in a circumferential direction. Figure 4.19 depicts this type of fracture schematically.

HDPE 1 divided its butt-weld failures (which were in the minority compared with straight pipe fractures) between sites P/P2 types 1 and 2 roughly equally, whereas the type 2 failure mode was the only form observed in MDPE 1.

(No MDPE 2 butt-welded systems were tested during the experimental period.)

On a practical note, as mentioned in the experimental techniques section the method of crack detection was so sensitive as to be able to detect a fracture almost immediately it had broken through the pipe wall. This necessarily resulted in a particularly small fracture which was identified on the pipe surface by the position of a fine spray of water produced when the pipe specimen was re-pressurised outside the testing tank.

(ii) Pipe System Results. (60 and 63mm OD/SDR 11) For all four types of small diameter PE pipes the influence of frequency of loading on performance is demonstrated in Figures 4.20 and 4.21. The variation of time under maximum load (τ_{SR} and $\tau_{FATIGUE}$ depending on the type of test) with increasing frequency is presented in Figure 4.20. The stress rupture lifetime is included on the zero frequency axis. All pipe failures for the data in

Figure 4.20 were brittle, occurred at a distance greater than one pipe diameter from the end closures, and lay parallel to the pipe extrusion direction. Increasing the frequency of loading by reducing t_{max} in all cases reduced $\tau_{FATIGUE}$ below τ_{SR}. However, only for HDPE 2 was $\tau_{FATIGUE}$ reduced substantially to indicate a potential fatigue weakness.

For a pipe which does not exhibit a marked fatigue weakness, testing under fatigue prolongs the time to test substantially, a result of the time off load. If, however, the pipe is weak under fatigue then the value of τ_{TEST} can be reduced to below that of τ_{SR}, depending upon the time spent unloaded. This latter case was observed for HDPE 2 pipes.

Figure 4.21 indicates that as frequency was increased, the number of cycles to failure for HDPE 1 and MDPE 1 increased markedly. This behaviour is expected from results presented in Figure 4.20, where $\tau_{FATIGUE}$ is of the same order as τ_{SR}, so that by reducing t_{max} (that is increasing the fatigue frequency) N_f must be increased. The same relationship was not confirmed for HDPE 2 or MDPE 2 pipes since only one fatigue test was undertaken due to the protracted testing time.

Figure 4.22 compares the pseudo stress rupture curves for HDPE 1 material at various frequencies. The fact that only two data points per curve are available indicates that care should be exercised when interpreting these results. However, a general trend is apparent that is with increasing frequency of loading the pseudo stress rupture plots move to the left (lifetimes are reduced). Included in the figure is the manufacturer's stress rupture curve for HDPE 1 straight pipe.

(iii) Welded Pipe System Results (60 and 63mm OD/SDR 11).

A limited number of stress rupture and fatigue tests were conducted on welded pipe systems (P/P) fabricated from HDPE 1 and 2 and MDPE 1 materials with the

following results;

Material	Number of P/P Samples Tested Under All Conditions	Number of P/P Type 1 Failures	Number of P/P Type 2 Failures
HDPE 1	18	2	2
HDPE 2	2	0	0
MDPE 1	4	0	4

τ_{SR} and $\tau_{FATIGUE}$ values for HDPE 1 and MDPE 1 welded pipes are presented in Figure 4.23, also included are the curves generated for stress rupture and fatigue testing straight pipe, as presented in Figure 4.20. In spite of using optimum welding conditions for HDPE 1 and MDPE 1, the butt-welded joint made between two pipe sections was found to be a source of fracture when subjected to either static or fluctuating internal pressure, with MDPE 1 exhibiting a pronounced reduction in measured lifetimes.

4.3 STRUCTURAL AND FRACTURE SURFACE ANALYSIS

4.3.1 Microtomy

Typical microstructures observed in the PE materials used during the course of this research programme are given in Figures 4.24 to 4.27. All were obtained from thin sections taken from pipes or welded pipes using a sledge or glass knife microtome and viewed between crossed polars by means of transmitted light. The very fine spherulitic structure coupled with the presence of significant amounts of pigments in all materials reduced the quality of the structural information available and only relatively large scale variations, such as those observed at butt-welds could be viewed with clarity. Examples of the features observed at butt-welds are shown in Figure 4.28.

Examples of the appearance of surfaces obtained when a bulk specimen is prepared using a sledge microtome fitted with a relatively blunt steel blade are given in Figures 4.29 and 4.30. The position and extent of the stress whitening are considered to reflect morphological variations through a pipe wall which can be indicative of poor mechanical performance.

4.3.2 Macroscopic Features of Fracture Surfaces

(i) Pipe Systems.

Figures 4.31 and 4.32 portray the fracture surface appearances of pipes which have failed due to the application of static and fluctuating internal pressures. They illustrate the overall features common to and characteristic of both loading modes and the different PE pipe materials.

The imposed mode of loading can be seen to have a significant effect upon the general appearance of the fracture surface. Fatigue failures indicated that the fracture tended to propagate preferentially along the pipe axis as shown in Figure 4.32. The influence of the loading frequency on the shape of the surface features is illustrated in Figure 4.33 where L is the maximum distance the crack propagated along a pipe of wall thickness h (see Figure 3.25). The ratio of L/h increased with increasing frequency for all systems.

This method of characterising the brittle fracture surface obtained in straight pipes would be particularly useful in a failure analysis. It is possible to differentiate between static and fatigue loads and it would also be possible, in the latter case, to provide an estimate of the loading frequency.

Comparison of the micrographs in Figures 4.31 and 4.32 also clearly shows that the fracture surface shape is not semi-circular but rather more elliptical in appearance with the crack front being essentially pinned on the inside wall of the pipes, while at the same time, under fatigue, the crack can grow along the pipe axis. For this size of pipe with wall thicknesses of about 5mm the final progress of the fracture just before it breaks through the pipe wall, a distance of about 1mm, is usually characterised by gross yielding and macroductility or at least a distinct change in the mode of fracture.

Fatigue striations are generally considered to be a characteristic of fluctuating loads, however low magnification stereo light microscopy of HDPE 1 and MDPE 1 pipe fracture surfaces revealed no such markings. There was clear evidence for the large scale striations often referred to as "discontinuous growth bands" (94) on the fracture surfaces of HDPE 2 and MDPE 2 pipes. It is interesting to note that the discontinuous growth bands (DGB's) can be seen on HDPE 2 pipes subjected to both stress rupture and fatigue conditions, Figure 4.31; the use of the term "fatigue striations" would be inaccurate, therefore, when describing the stress rupture fractures. For all pipe materials but only on certain fracture surfaces, Figure 4.34, there was evidence of the extrusion process used for pipe manufacture. Lines running parallel with the extrusion direction were discernible for both stress rupture and fatigue testing. In addition multi-plane crack propagation was in evidence on certain surfaces leaving lines or steps emanating in a radial direction from the source of fracture, that is lying perpendicular to the crack front.

The site of fracture initiation appeared to be material and loading mode specific. In HDPE 1 and 2 pipes, under both types of pressure test and in MDPE 2 under fatigue loading only, failure initiated at or near the inside wall of the pipe, Figures 4.31 and 4.32. The few exceptions to this rule occurred when the pipe fracture was initiated by large or fibrous inclusions lying towards the centre of the pipe wall.

For MDPE 1 the evidence indicated that failure was more likely to occur from a site towards the middle of the pipe wall, again see Figures 4.31 and 4.32.

(ii) Welded Pipe Systems.

Of those butt-welded pipe materials tested, failures at joints were observed in HDPE 1 and MDPE 1 only.

Examples of the longitudinal weld failures observed in HDPE 1 are shown in Figure 4.35. Whether tested under stress rupture or fatigue conditions there was a general lack of DGB's on HDPE 1 crack surfaces. The weld interfaces and heat affected zones were well defined, however, along with, in some cases, evidence of the extrusion flow lines.

(Note:- HDPE 2 shows distinct DGB's on the very limited number of butt-weld failures obtained from static and fatigue loaded tests, but all these occurred at pipe/fitting welds.)

In most cases fracture initiation was associated with the notch formed between the bead and the internal wall of the pipe.

Little structural information could be elicited from the appearance of fractures of a circumferential nature as can be seen from Figure 4.36. Fractures of this sort are generally indicative of poor mixing of the molten material at a weld interface.

4.3.3 Microscopic Features of Fracture Surfaces

Fracture surfaces from all pipe systems stress rupture and fatigue tested have been examined in some detail.

A variety of fracture modes have been observed at higher magnifications but in general only two predominate. Figures 4.37 and 4.38 indicate clearly the typicalfracture surfaces observed on pipes subjected to static and fatigue loads respectively. These micrographs were obtained using SEM and clearly show the initiation of fracture and the variation in micro-ductility across the surface. The presence of considerable local drawing and ductility was apparently insensitive to the form of loading. Such fractures have been termed "quasi-brittle" by Flueler et al (127) and are indicative of slow stable crack growth. The large number of strands or fibrils of material (usually highly oriented) result from the formation of a craze which necessarily involves large amounts of plastic yielding whereas truly brittle cracking does not. Hence the term "quasi-brittle". The holes or voids which are surrounded by the yielded fibrils exhibit diameters usually in the range 5 - 20 μm although this becomes more difficult to estimate as the craze grows since fibrillation increases and tends to hide underlying features. Towards the outer surface of the pipe the mode of fracture alters and in some cases gross yielding and macroductility is observed, Figure 4.39.

(On a very few samples the fracture surfaces have exhibited flat, irregular features with no ductility or drawing observable up to 2000x magnification. These regions begin at the initiation site and continue right across the pipe wall. Normally such features would result from fast crack growth. As yet there is no obvious pattern to the occurrence of such fractures and they are considered exceptions to the normally observed failure modes.)

Evidence for fine straitions (not DGB's) due to the step-by-step propagation of the fracture in both loading modes was also sought.

Figures 4.37 and 4.38 indicate clearly that the presence of fine striations was not obvious. In fact none were found on any material whether stress rupture or fatigue tested. This included SEM examination up to magnifications of 3000x.. Only in the last progress of the crack did anything resembling fine striations appear, Figure 4.40.

For those materials which exhibited distinct DGB's, HDPE 2 and MDPE 2, their typical fracture surfaces are shown in Figure 4.41. Again the variation in micro-ductility is apparent particularly at DGB's.

4.3.4 Elemental and Geometrical Analysis of Crack Initiation Sites

(i) HDPE 1.

Examination by SEM of the fracture surfaces of stress rupture and fatigue tested HDPE 1 pipes revealed over 95% of failures initiated from observable particles. Examples of such crack initiators are shown in Figure 4.42. No failures were found to begin at macrovoids such as those observed in the larger diameter pipes to be discussed in a later chapter.

The particles were geometrically characterised by measuring their maximum dimension parallel to the fracture plane. The size distribution of the particles is plotted on a histogram chart in Figure 4.43. It is evident that the majority of particles initiating failure lie in the range 50 μm to 350 μm. The position of these particles lay predominantly within 200 μm of the inside wall of the pipe, Figure 4.44. The distances measured for Figure 4.44 relate to the approximate centre of area of each particle as projected onto the fracture plane.

To determine the elemental composition of these crack initiators energy dispersive x-ray analysis was employed. For each fracture surface examined an x-ray spectrum was obtained for the site of initiation and in a position remote from this area. The peaks due to palladium and gold are from the alloy used to coat some of the non-conducting plastic specimens.

Three main types of particle were encountered namely metallic, calcium rich and those particles for which the energy dispersive technique was unable to detect any elements except the Au and Pd of the coating alloy. This implies that the elements composing these latter particles will have atomic numbers less than sixteen (that is, elements such as oxygen, nitrogen and more particularly carbon will not be observed). It would be necessary to use wavelength dispersive x-ray analyses to detect such elements.

Typical spectra of the three particle types are presented in Figures 4.45 to 4.47.

A fourth type of initiating particle of a distinctly fibrous nature was also observed but only rarely. Only two specimens in nearly thirty HDPE 1 pipe failures were found. Figure 4.48 indicates that there is a strong chlorine peak in its x-ray spectrum which possibly suggests the fibre is paper, since chlorinated bleaching agents are used to whiten certain papers. Figure 4.49 is a more detailed view of this fibrous initiating particle.

The geometry of the initiating particles is apparently related to elemental composition, with the more angular examples lying in the "no elements detected" category whilst calcium rich initiators tend to be fragmented groups of small crystalline polyhedrons. Metallic particles are found in various shapes and sizes but tend to be stainless steel.

The elemental distribution of all the HDPE 1 particles is drawn up in Figure 4.50. Calcium and iron are found to predominate.

(ii) HDPE 2

Identical analyses were carried out for failures obtained in HDPE 2 pipes. Particle size distribution is presented in Figure 4.51. Their position with respect to the inside wall of the pipe is detailed in Figure 4.52 and shows that as for HDPE 1 most particles lay very close to the inside pipe wall. The particles were either metallic or contained mainly calcium. Evidence for this is provided in Figures 4.53 and 4.54.

Elemental distribution is given in Figure 4.55.

(iii) MDPE 1

A greater proportion of initiating particles in MDPE 1 were found towards the centre of the pipe wall and were generally larger than those found closer to the inside surface of the pipes.

The majority of particles were titanium rich possibly indicative of a titanium based additive used during processing.

The results of particle size distribution, particle position, elemental compositions and distributions are summarised in Figures 4.56 to 4.60.

(iv) MDPE 2

Although particles were found to initiate cracks in pipes in this material, a detailed analysis of their geometry could not be made due to the relatively small number of available specimens. Results are therefore recorded in Figures 4.56 and 4.58 alongside those obtained for MDPE L. Elemental compositions and particle micrographs are shown in Figures 4.61 and 4.62.

4.4 DIFFERENTIAL SCANNING CALORIMETRY (DSC)

DSC thermograms were employed to identify the effect of elevated temperature testing on the structure of the material comprising the pipe. Two series of tests were undertaken; in the first the samples were obtained as defined in Section 3.3.3 from the failed pipe while in the second series virgin samples of the same pipe were simply left in the water bath for various times (see Section 3.6.7). In the latter tests the material was not subjected to any stress other than body stresses. The peak melting point, Figure 4.63, and DSC nominal crystallinity, Figure 4.64, of both types of sample for HDPE 1 and 2 were recorded and are plotted as a function of testing time. Testing time, for fatigue loaded pipe samples, includes the times when pressure was not applied and is not therefore equivalent to the pseudo stress rupture lifetime $\tau_{FATIGUE}$ (see equation 4.1).

From Figures 4.63 and 4.64 both peak melting temperature and crystallinity increase with testing time for 80^{o}C testing temperatures. In addition it appears that the imposition of a stress further accelerates the changes in these material properties. Both structural parameters appear to stabilise after certain ageing times for both HDPE 1 and 2 and in all DSC thermograms obtained only one peak in the melting curve was observed.

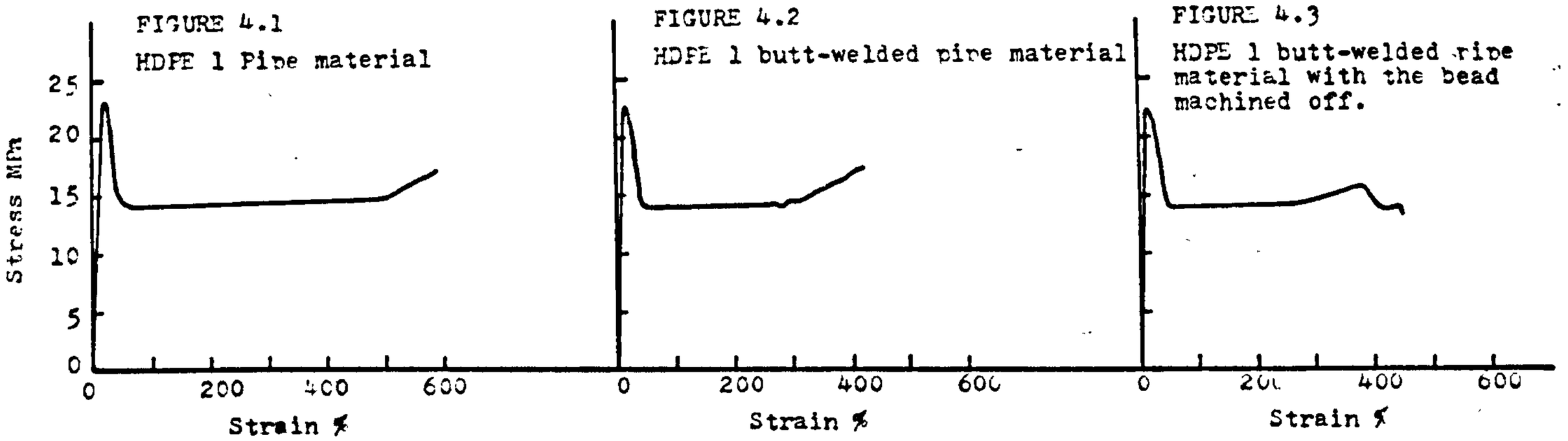

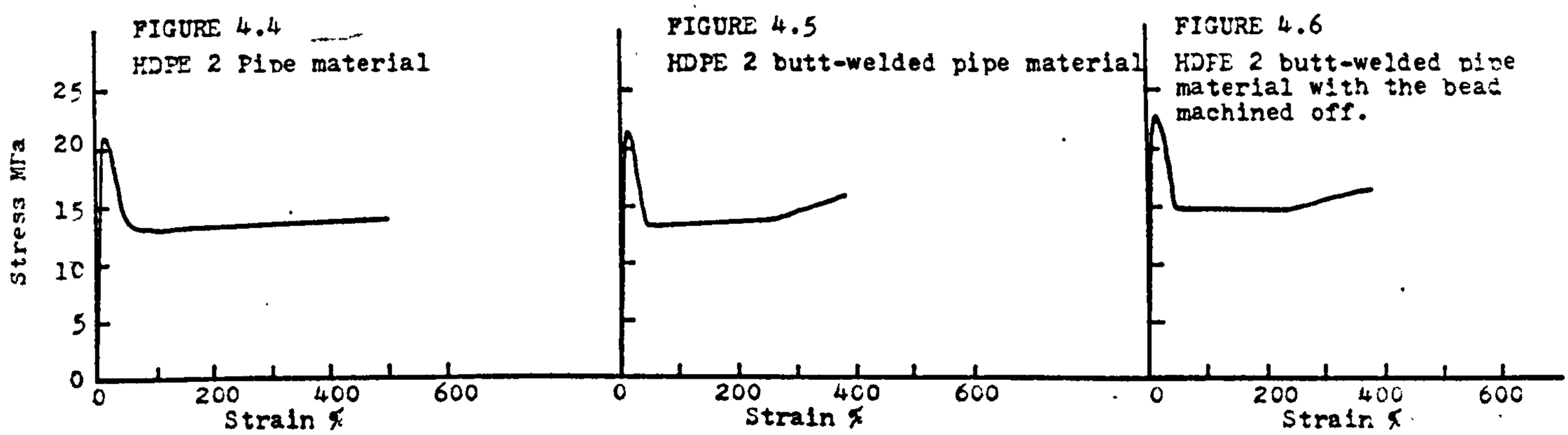

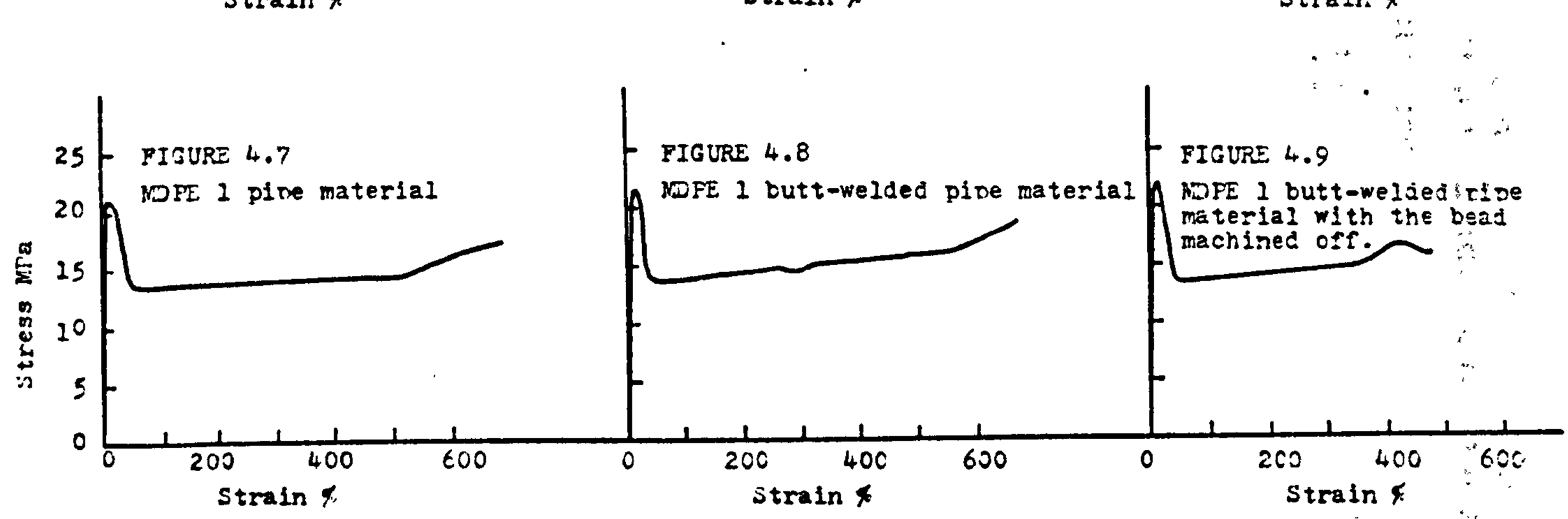

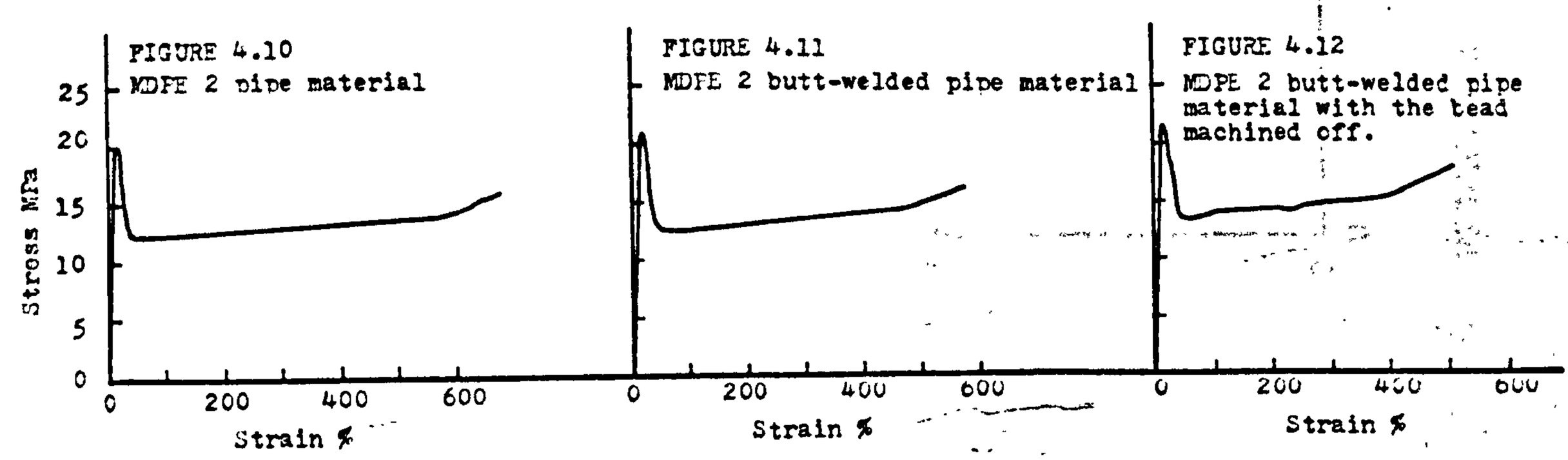

FIGURES 4.1 - 4.12 Typical tensile stress/strain curves for all four PE pipe materials.

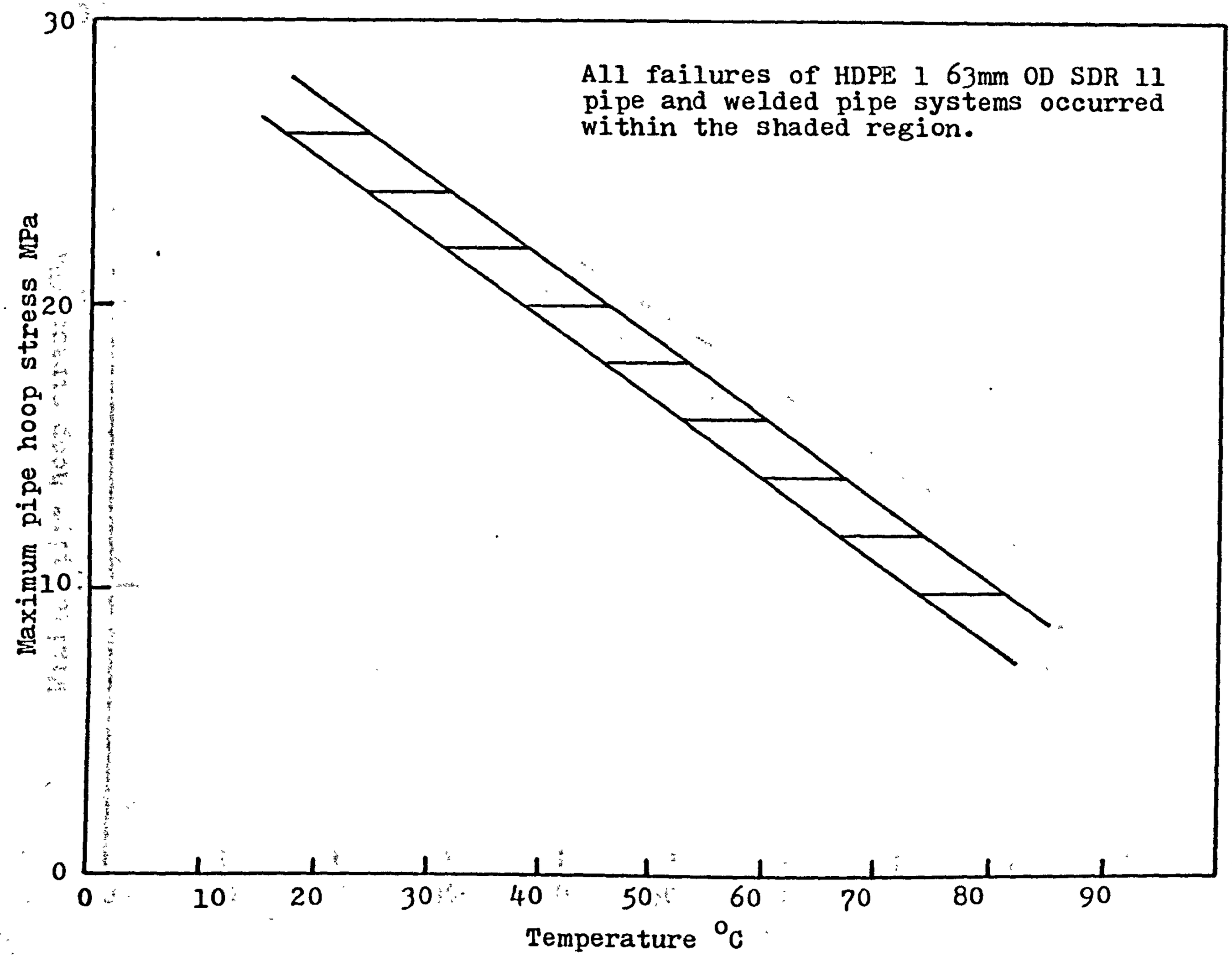

FIGURE 4.13 Short term rupture results for HDPE 1 pipe and welded pipe systems. (All failures were of a ductile nature.)

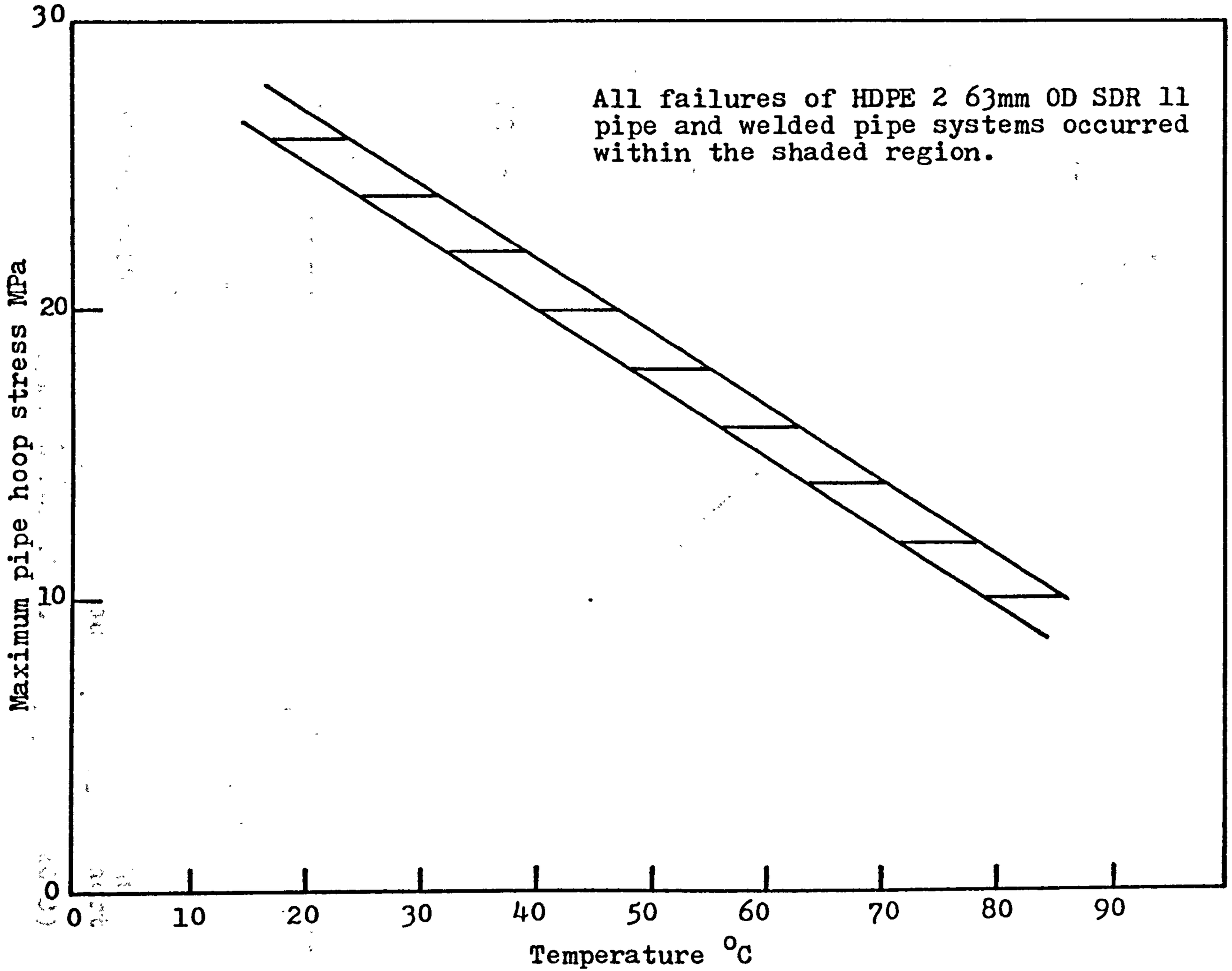

FIGURE 4.14 Short term rupture results for HDPE 2 pipe and welded pipe systems. (All failures were of a ductile nature.)

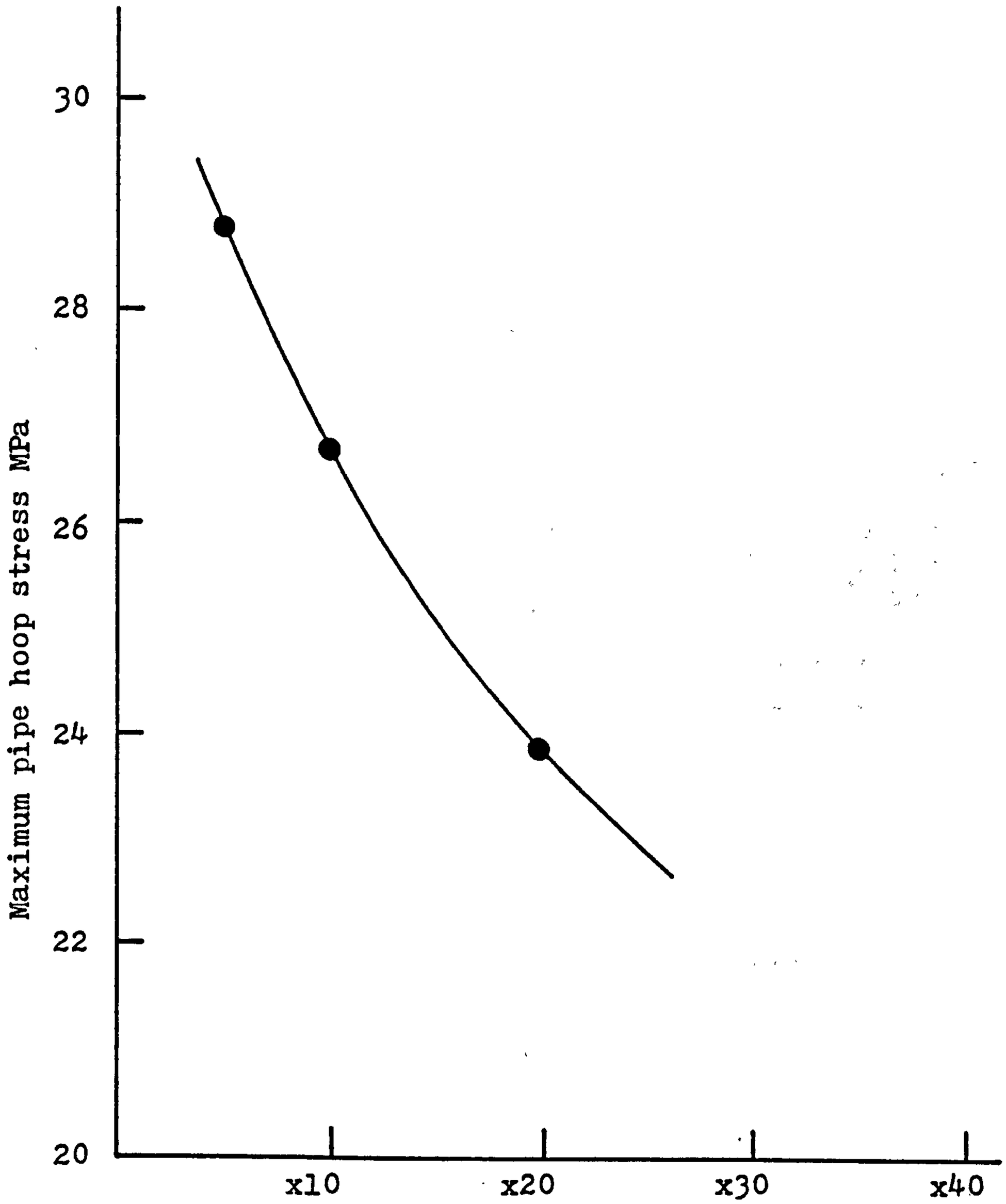

FIGURE 4.15 Effect of pipe sample length on the maximum pressure sustained by a short term rupture test specimen.
(63mm OD SDR 11 HDPE 1 pipes at 20°C)

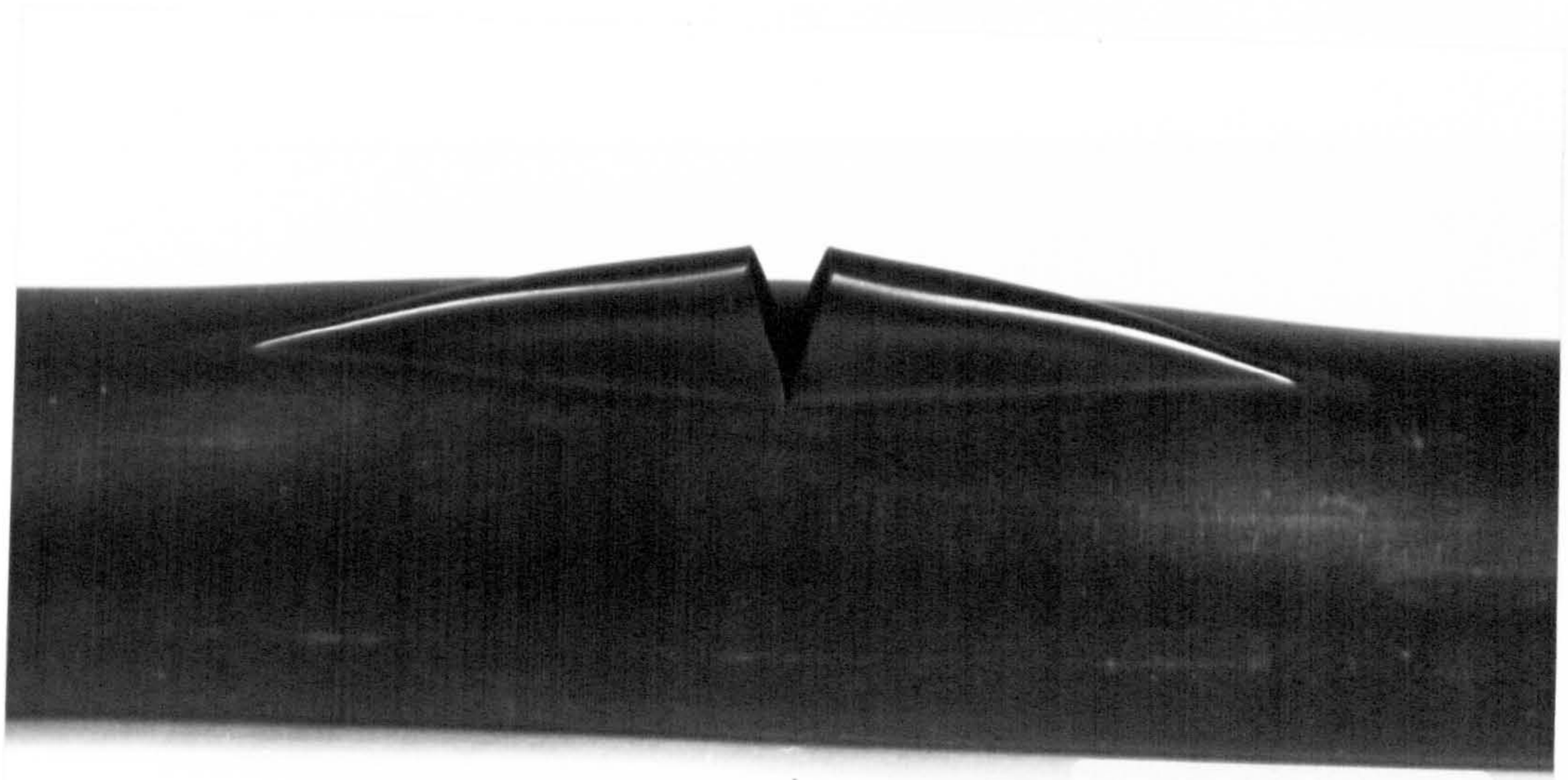

FIGURE 4.16 Ductile failure in an HDPE 1 pipe.

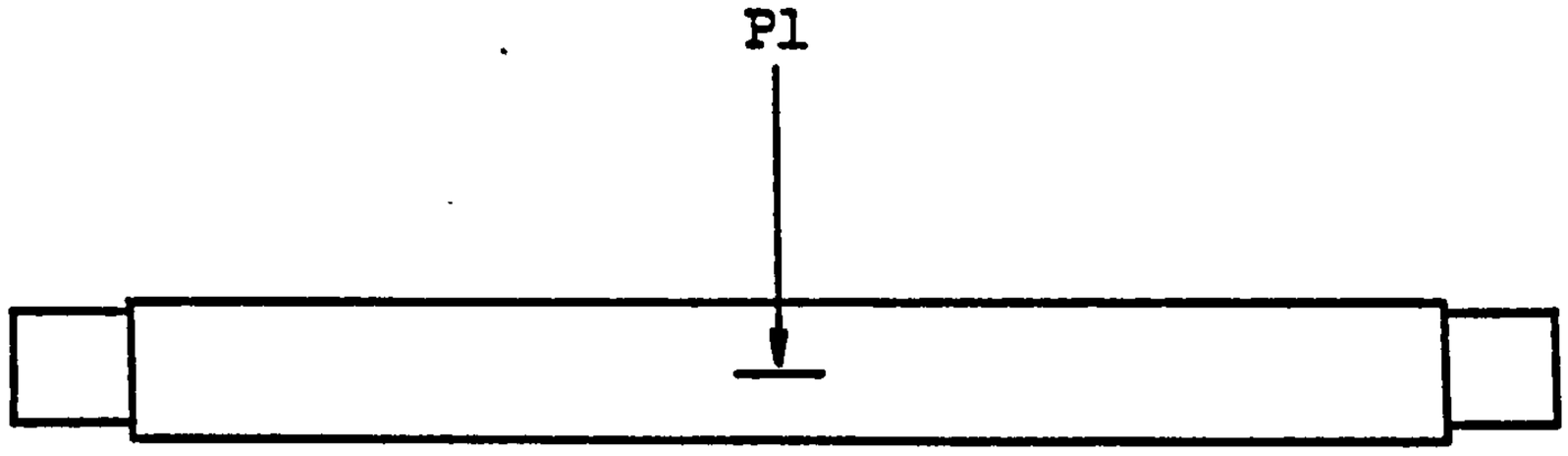

FIGURE 4.17a Schematic representation of observed brittle fracture sites in 60 and 63mm OD SDR 11 PE pipes.

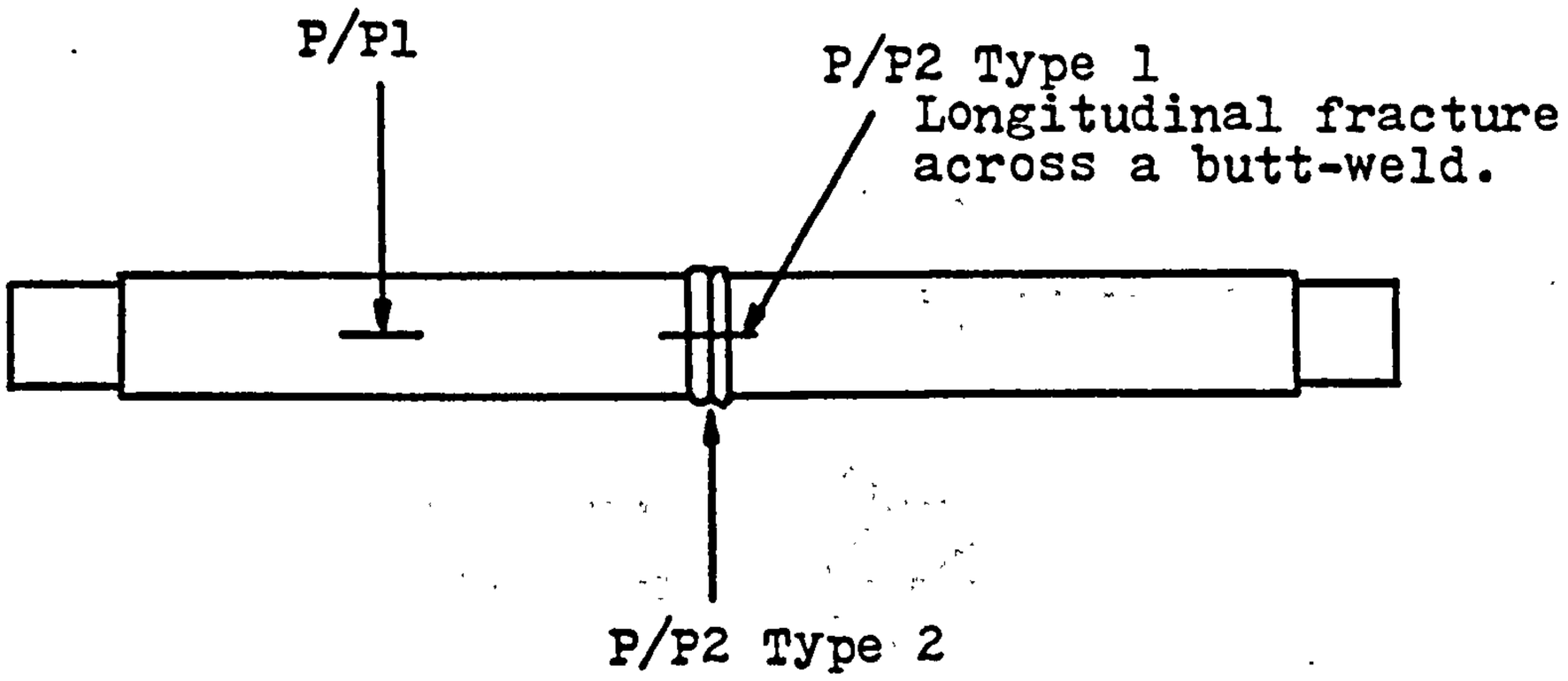

FIGURE 4.17b Schematic representation of observed brittle fracture sites in 60 and 63mm OD SDR 11 butt-welded PE pipes.

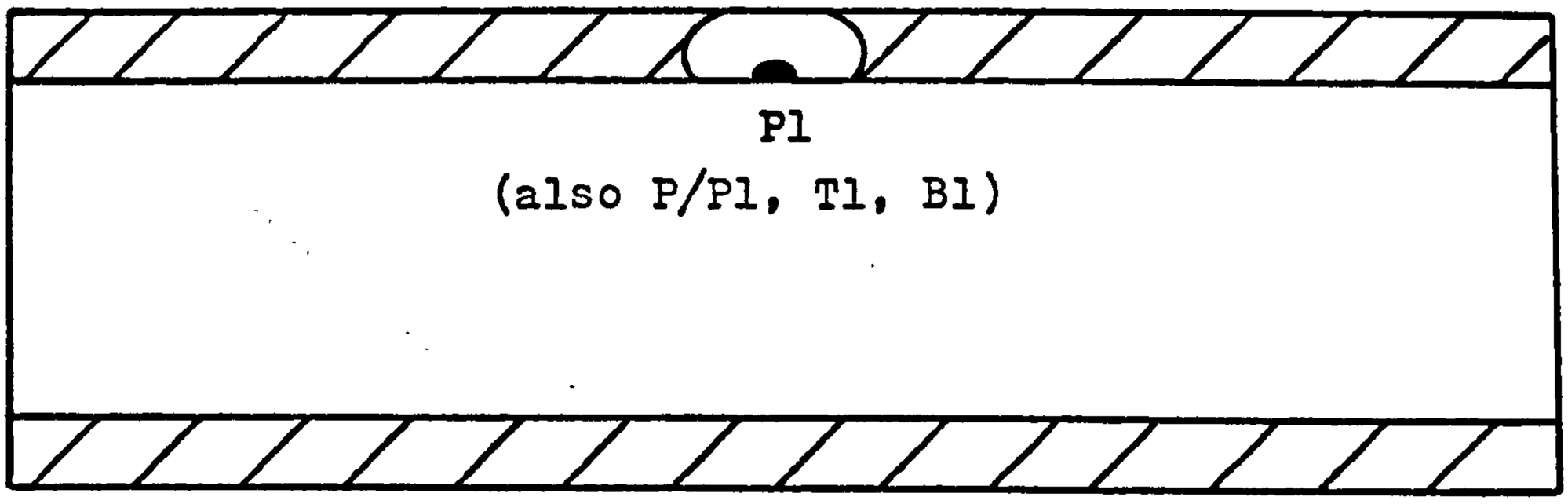

FIGURE 4.18 Schematic representation of observed brittle fractures in 60 and 63mm OD SDR 11 PE pipes.

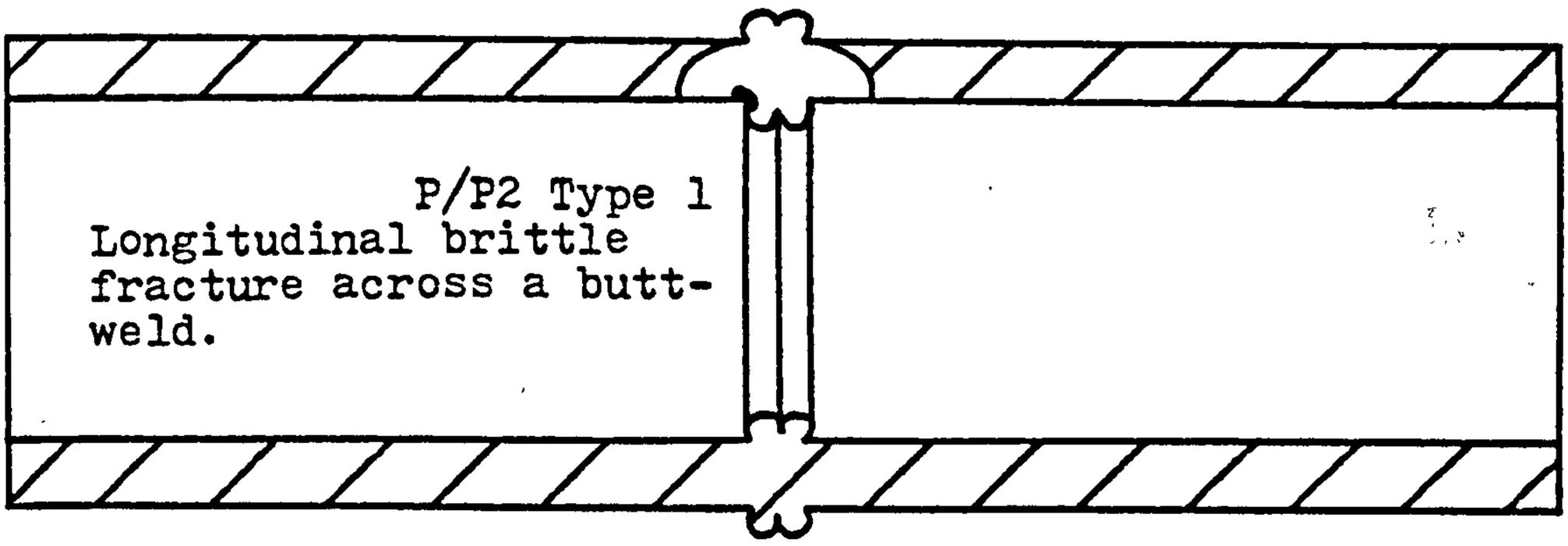

P/P2 Type 2

Circumferential separation at or near a butt-weld.

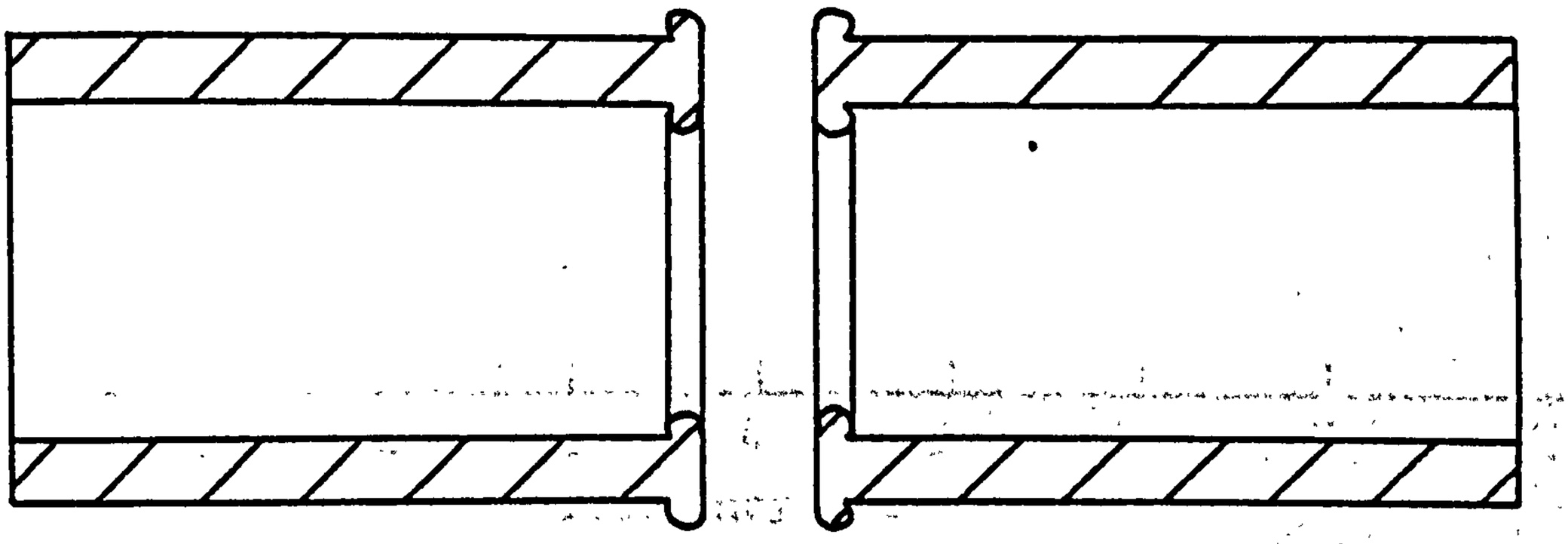

FIGURE 4.19 Schematic representation of observed brittle fractures in 60 and 63mm OD SDR 11 butt-welded PE pipes.

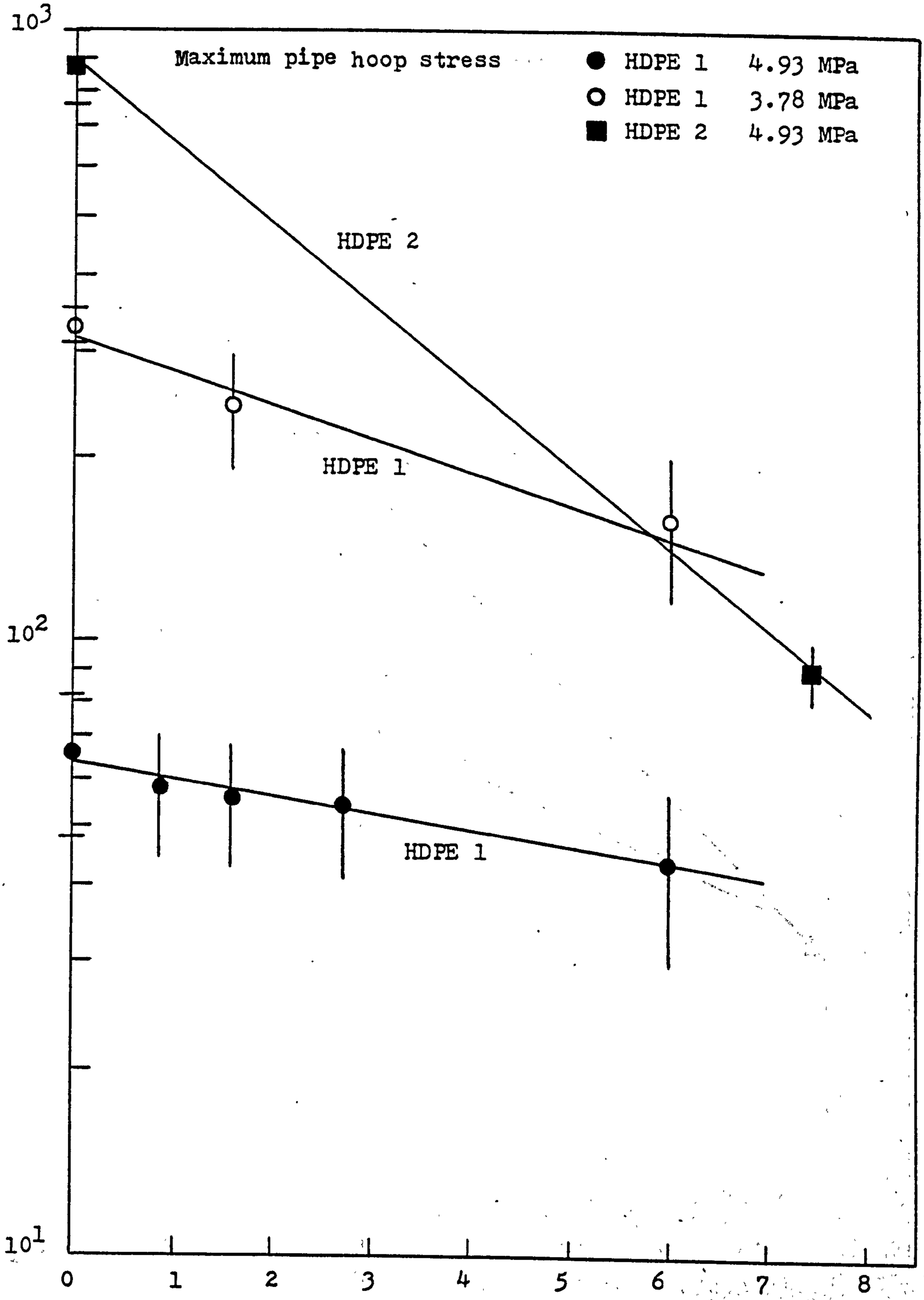

FIGURE 4.20a Variation of τ_{SR} and $\tau_{FATIGUE}$ with frequency for 63mm OD SDR 11 HDPE 1 and 2 pipes at 80°C.

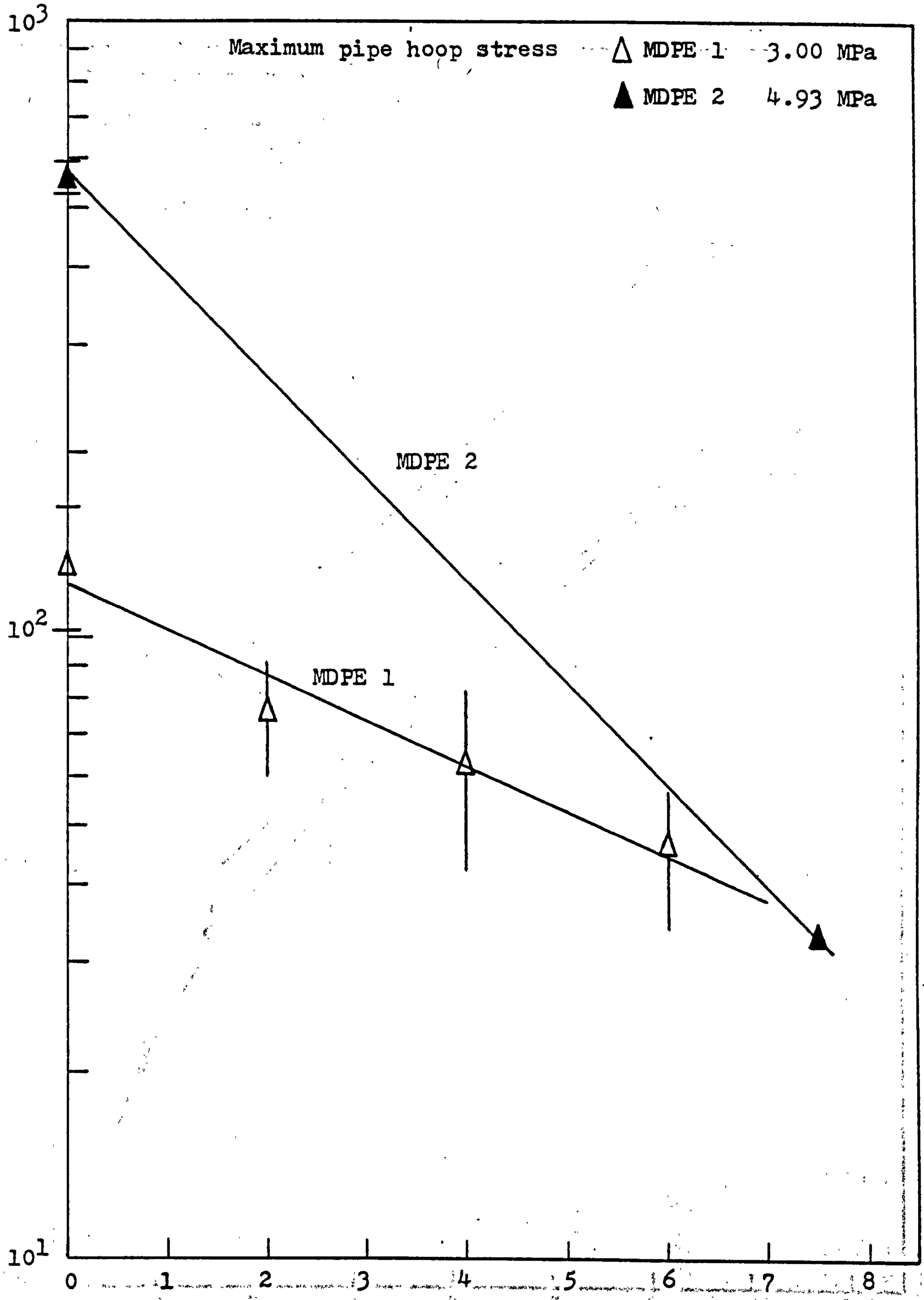

FIGURE 4.20b Variation of τ_{SR} and $\tau_{FATIGUE}$ with frequency for 60mm OD SDR 11 MDPE 1 and 63mm OD SDR 11 MDPE 2 pipes at 80°C.

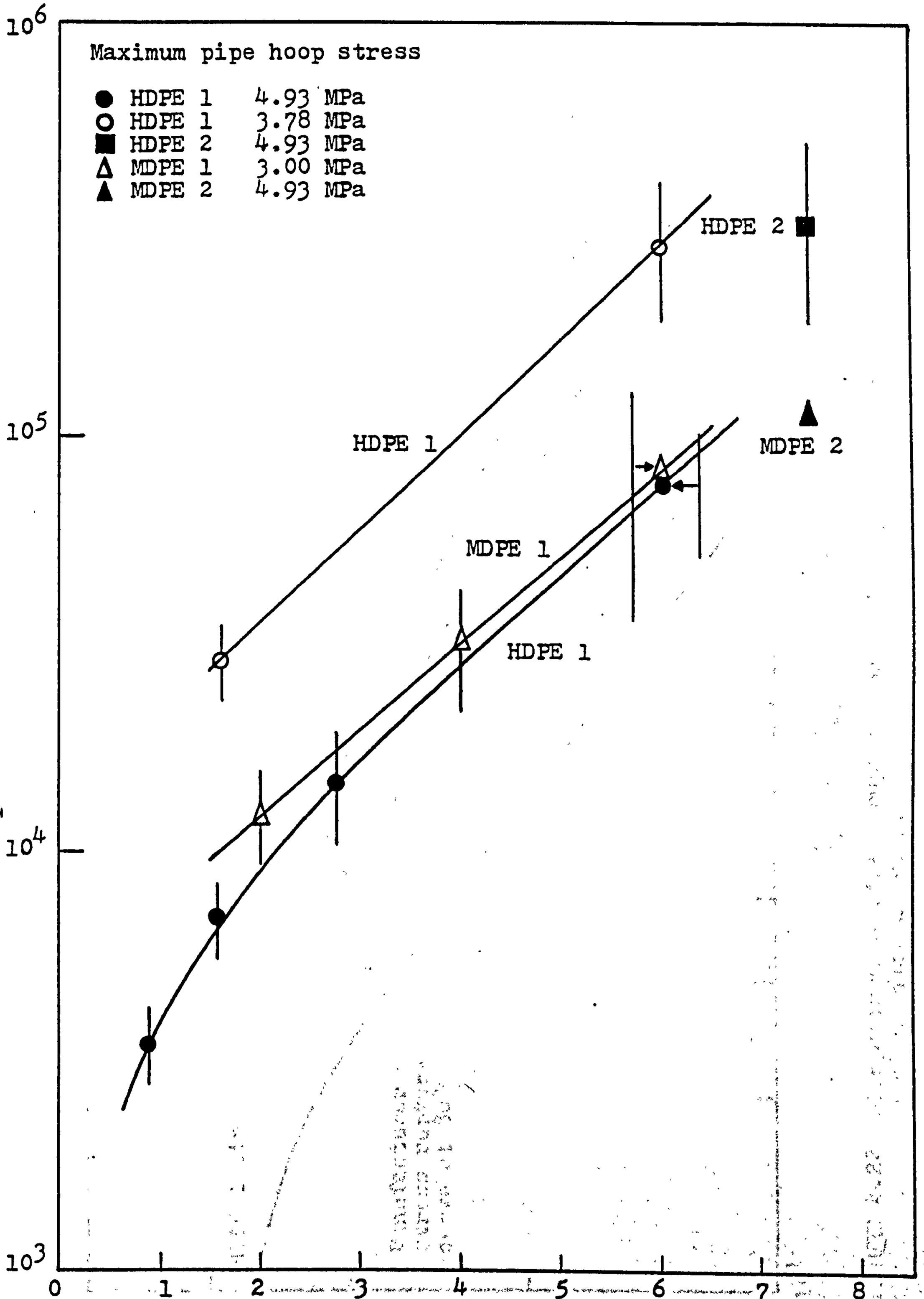

FIGURE 4.21 Variation of N_f with frequency for 60 and 63mm OD SDR 11 pipes at 80°C.

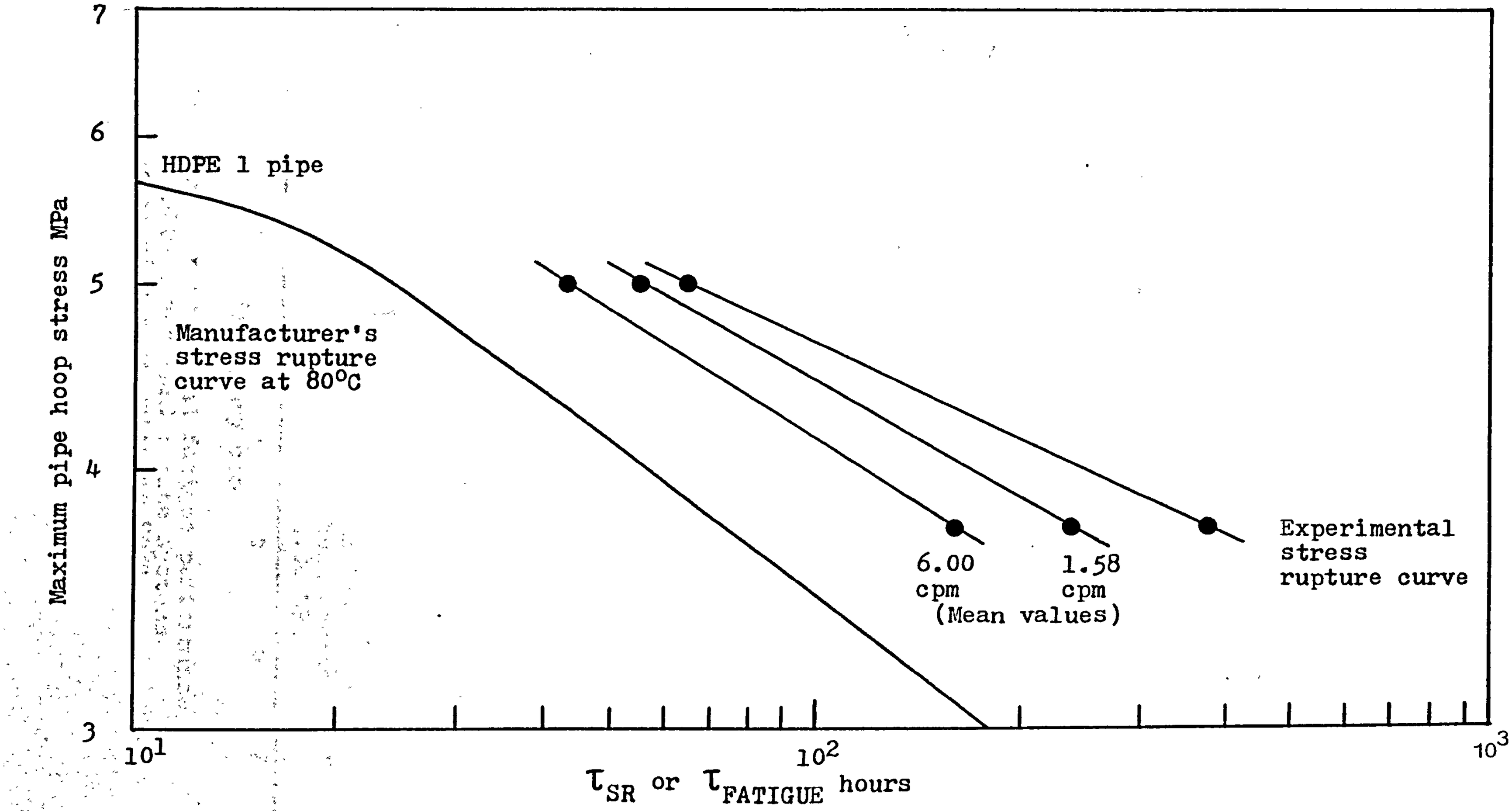

FIGURE 4.22 Comparison of stress rupture and fatigue performance of HDPE 1 pipes at 80°C.

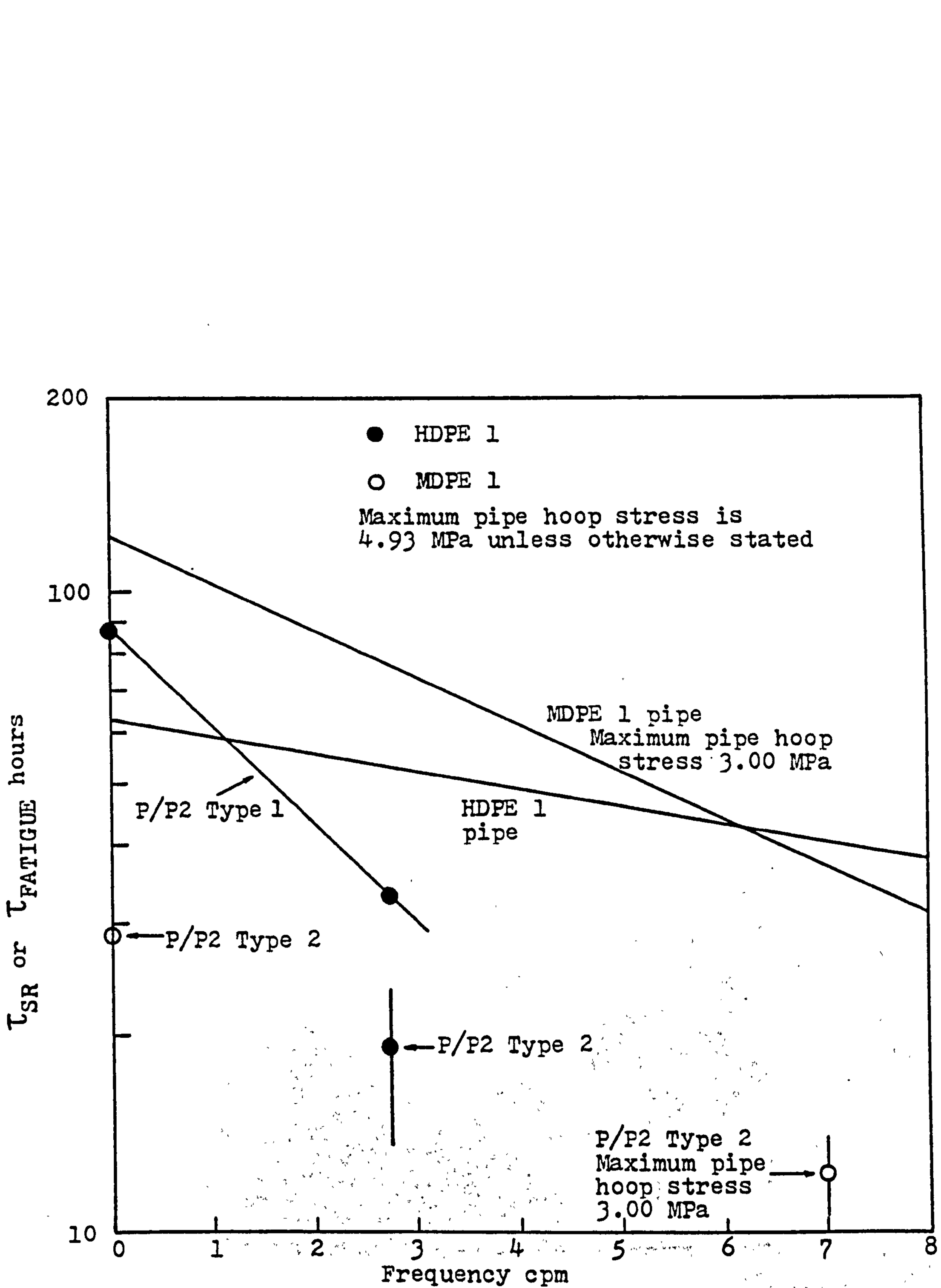

FIGURE 4.23 Stress rupture and fatigue performance of HDPE 1 and MDPE 1 pipe systems containing butt-welds at 80°C.

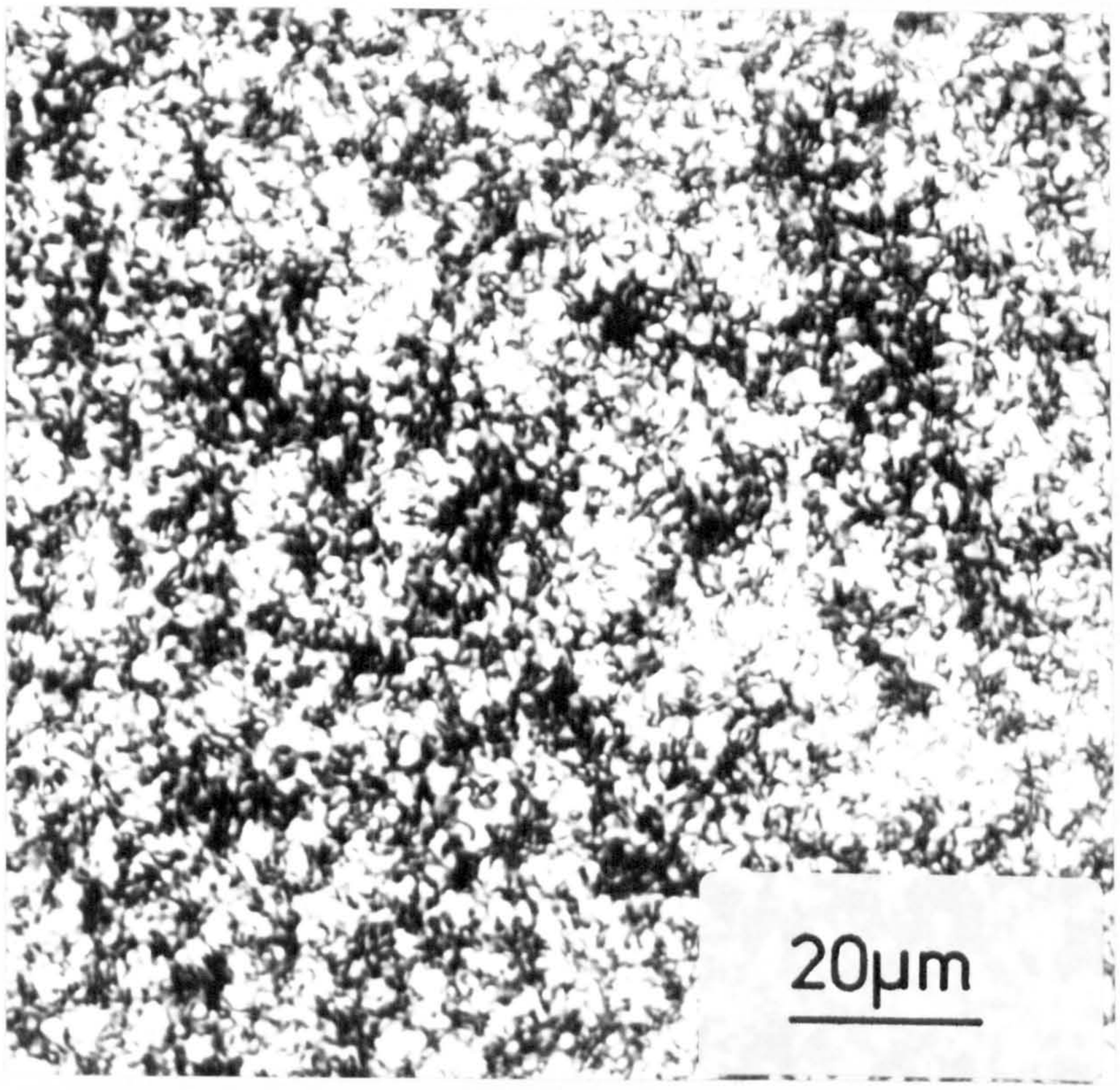

FIGURE 4.24 Thin section microstructure of the middle of an HDPE 1 pipe wall (63mm OD SDR 11).

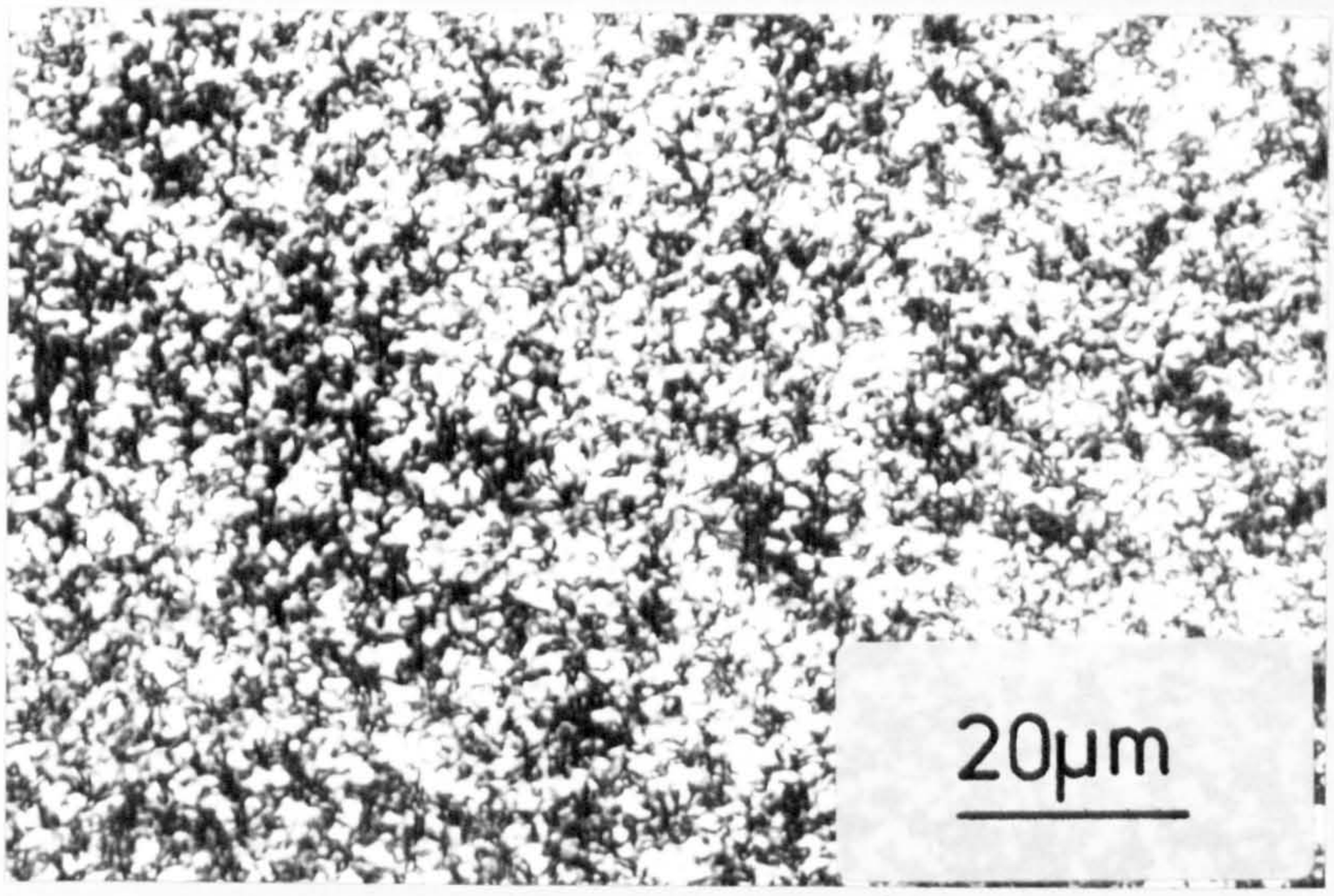

FIGURE 4.25 Thin section microstructure of the middle of an HDPE 2 pipe wall (63mm OD SDR 11).

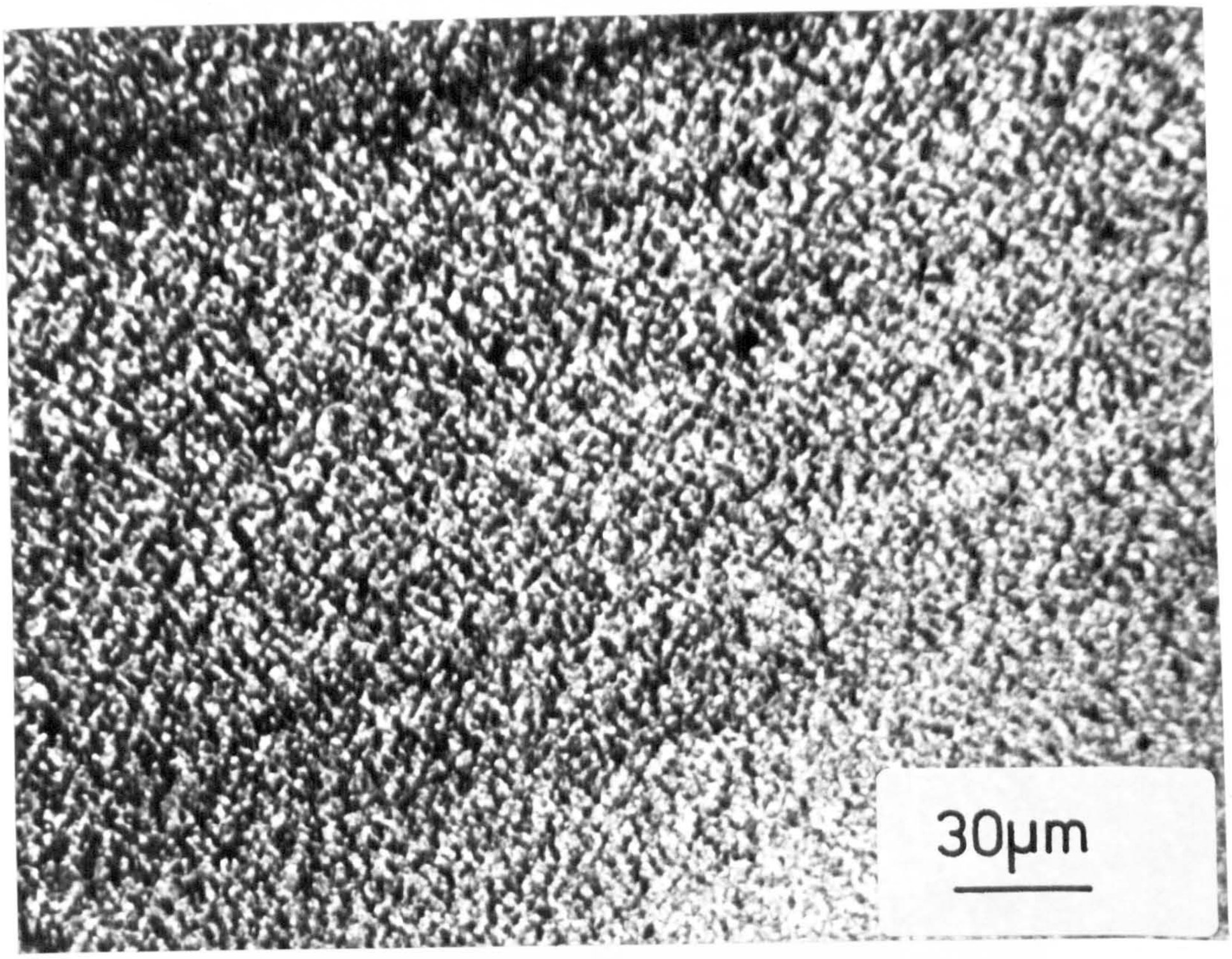

FIGURE 4.26 Thin section microstructure of the middle of an MDPE 1 pipe wall (60mm OD SDR 11).

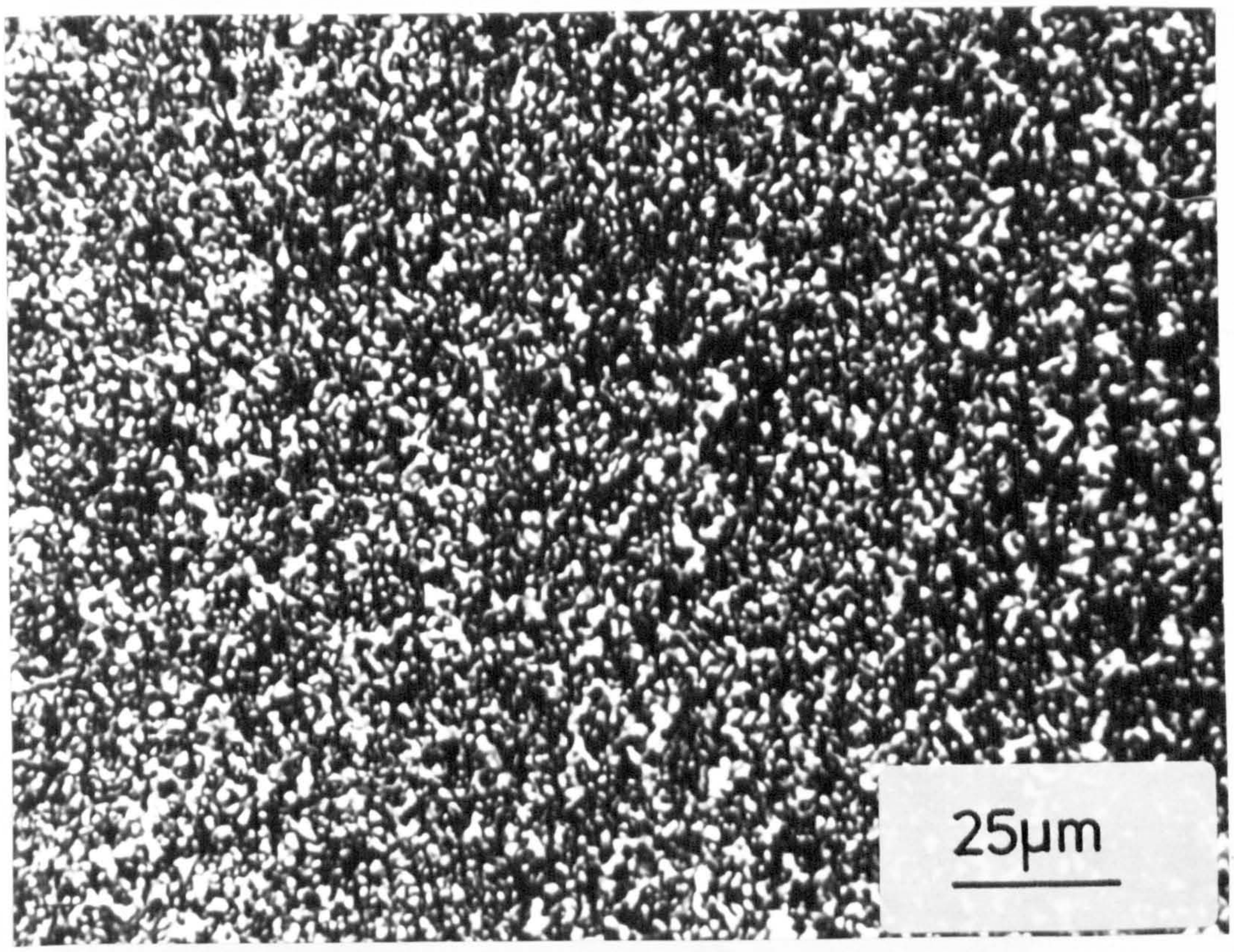

FIGURE 4.27 Thin section microstructure of the middle of an MDPE 2 pipe wall (63mm OD SDR 11).

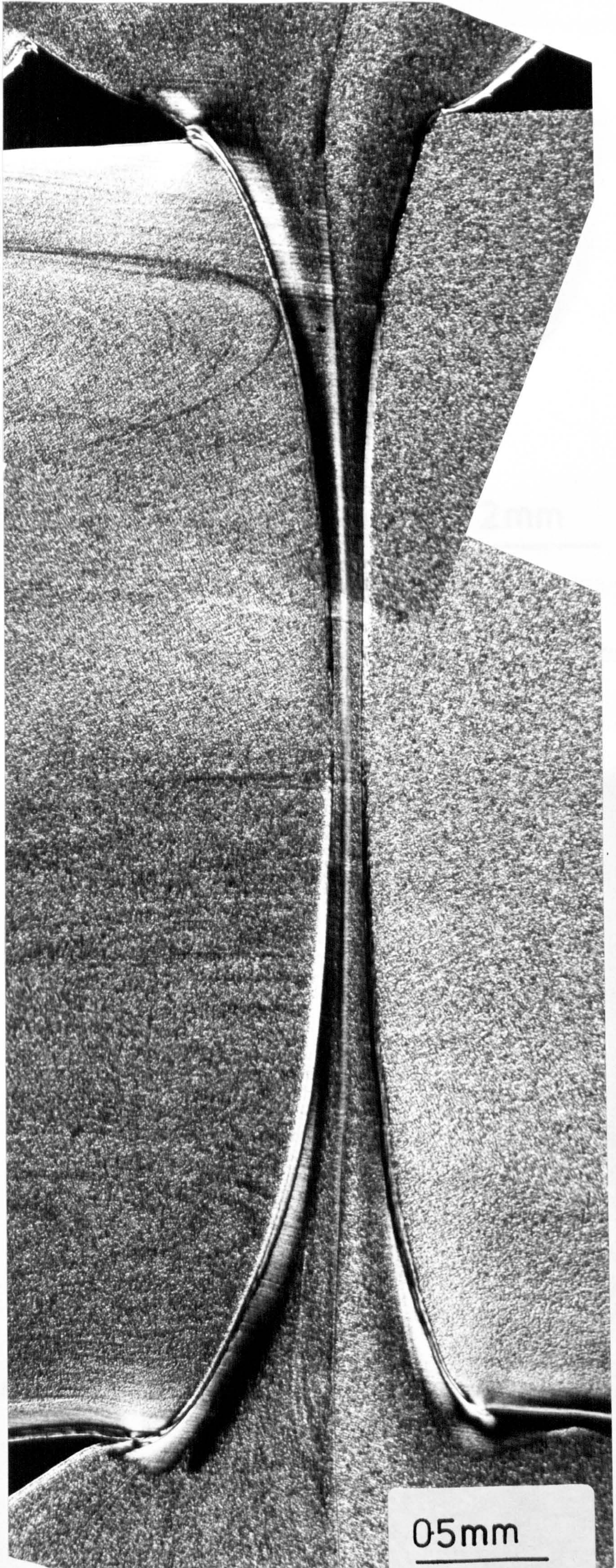

FIGURE 4.28

Microstructure of an MDPE 1 pipe to pipe butt-weld as viewed by transmitted light between crossed polars.

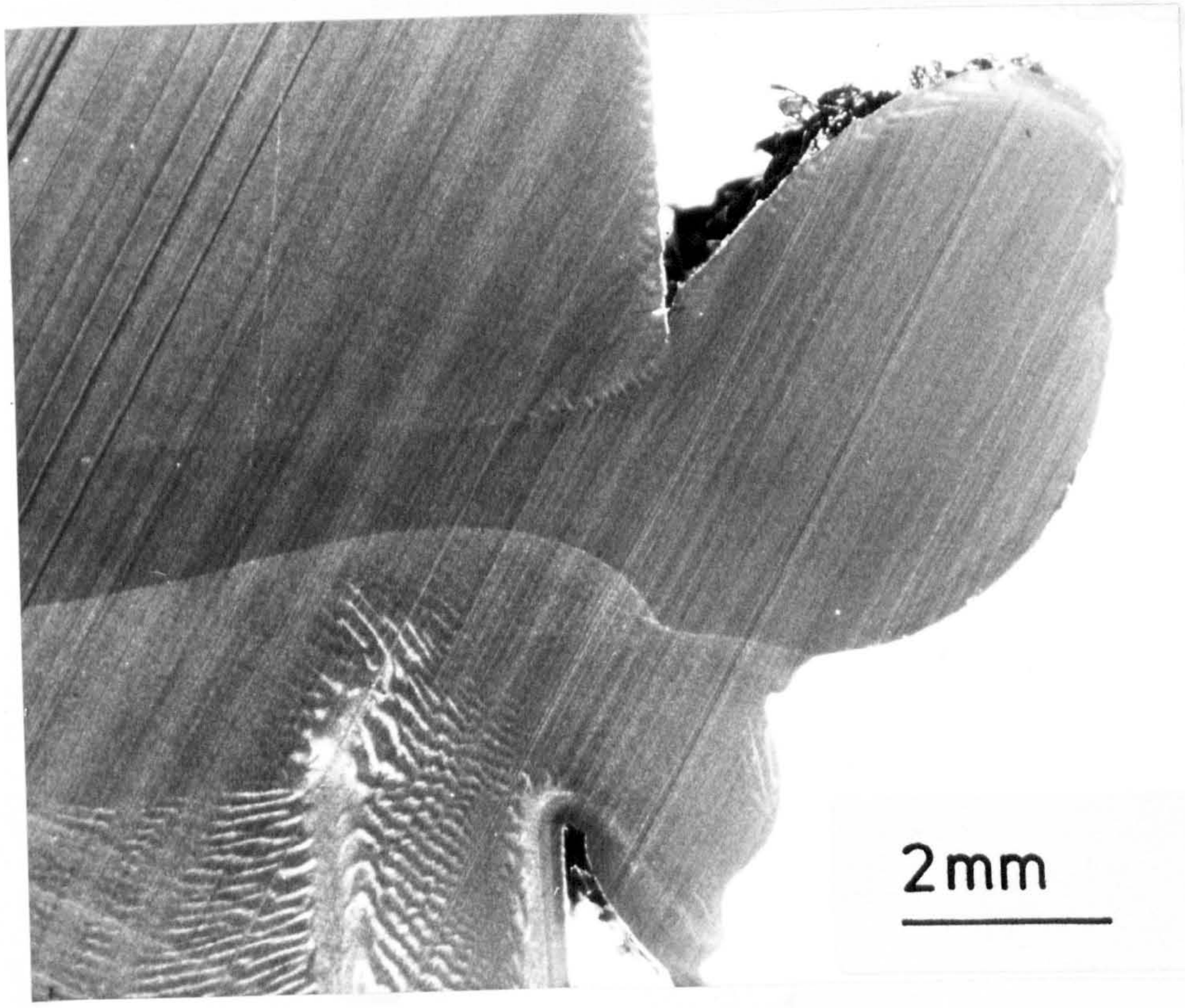

FIGURE 4.29 Surface of an HDPE 1 butt-weld prepared using a sledge microtome.

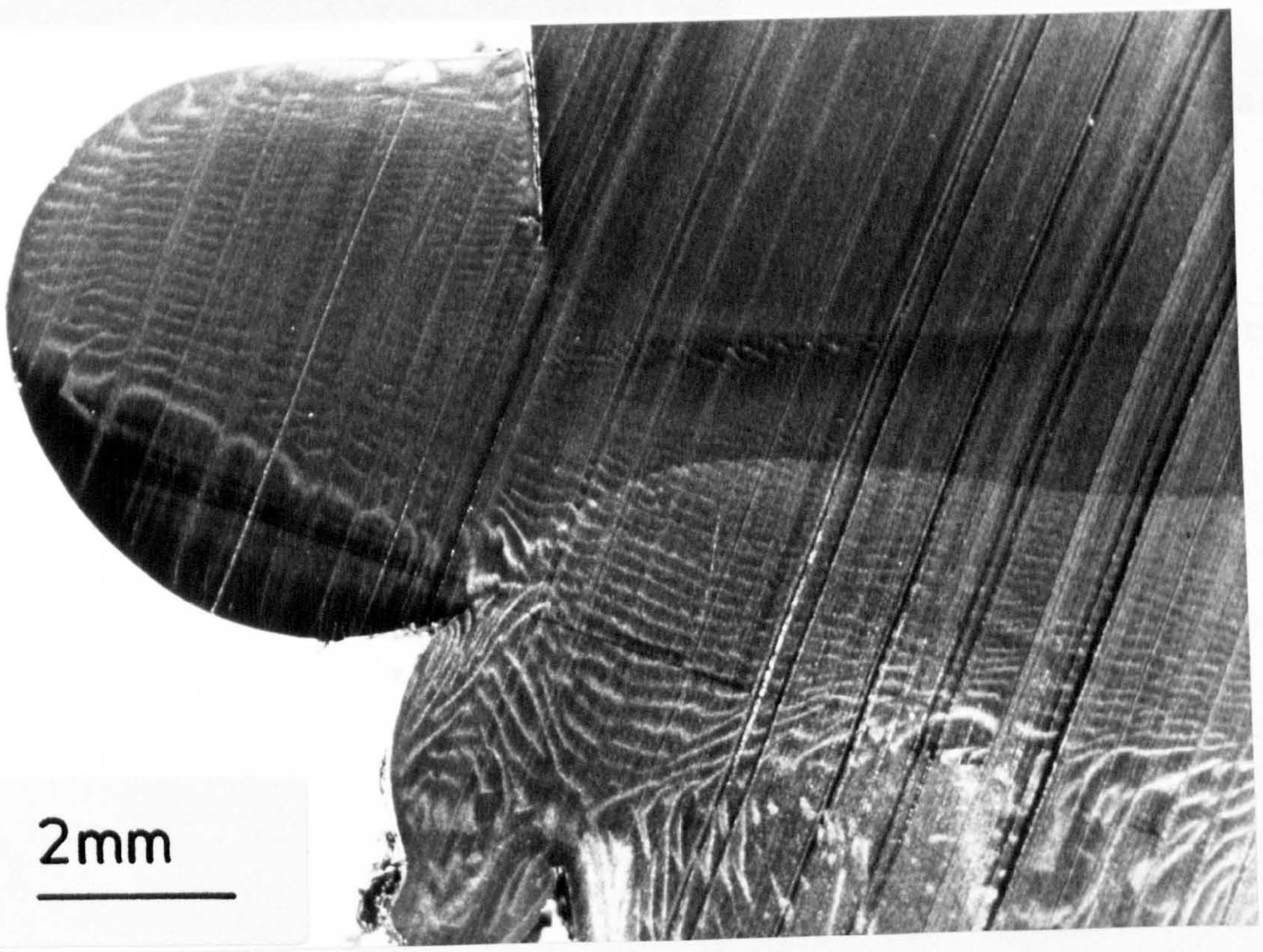

FIGURE 4.30 Surface of an HDPE 1 butt-weld prepared using a sledge microtome.

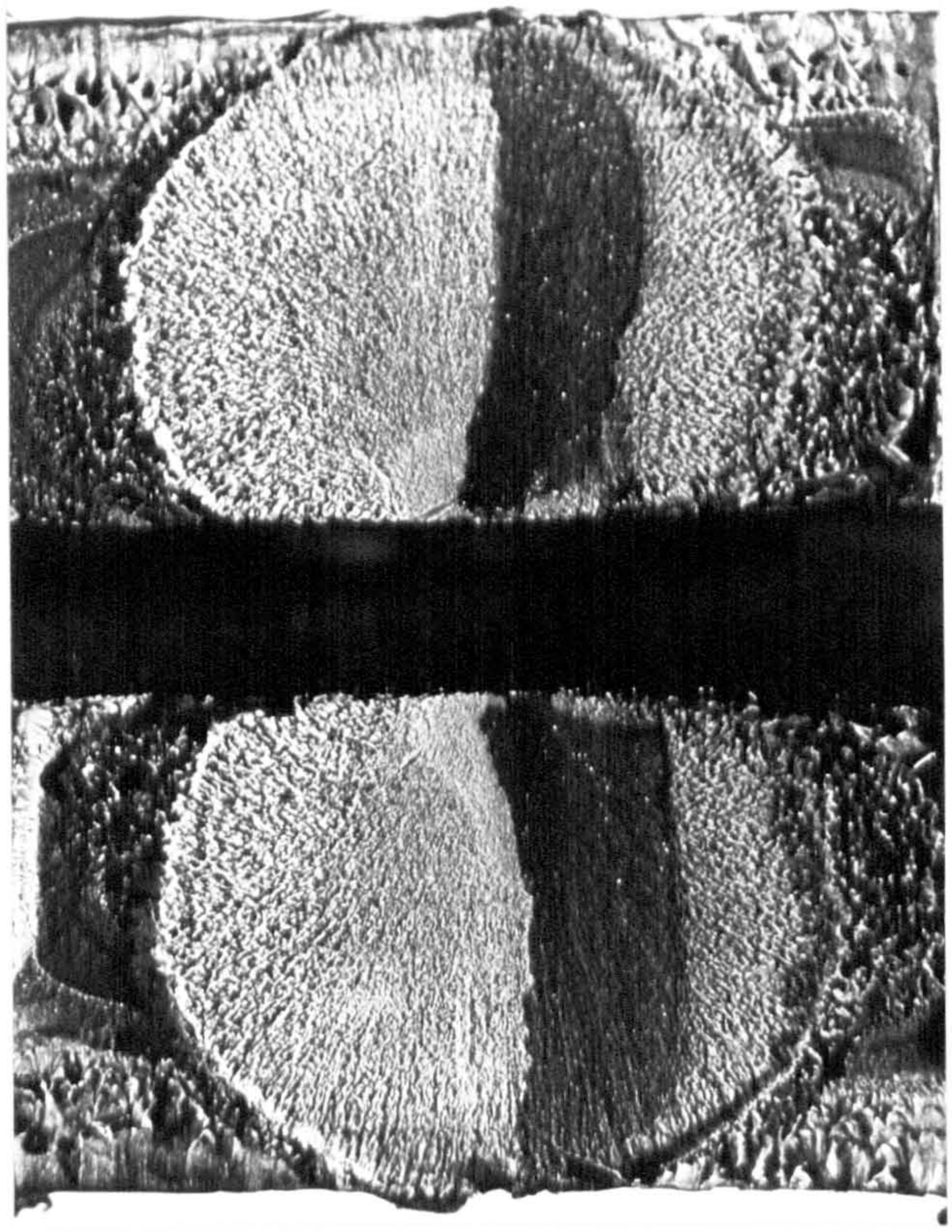

FIGURE 4.31a

Brittle fracture surface of an HDPE 1 pipe subjected to a static internal pressure (stress rupture).
80°C
4.93 MPa pipe hoop stress
63mm OD SDR 11 pipe

2mm

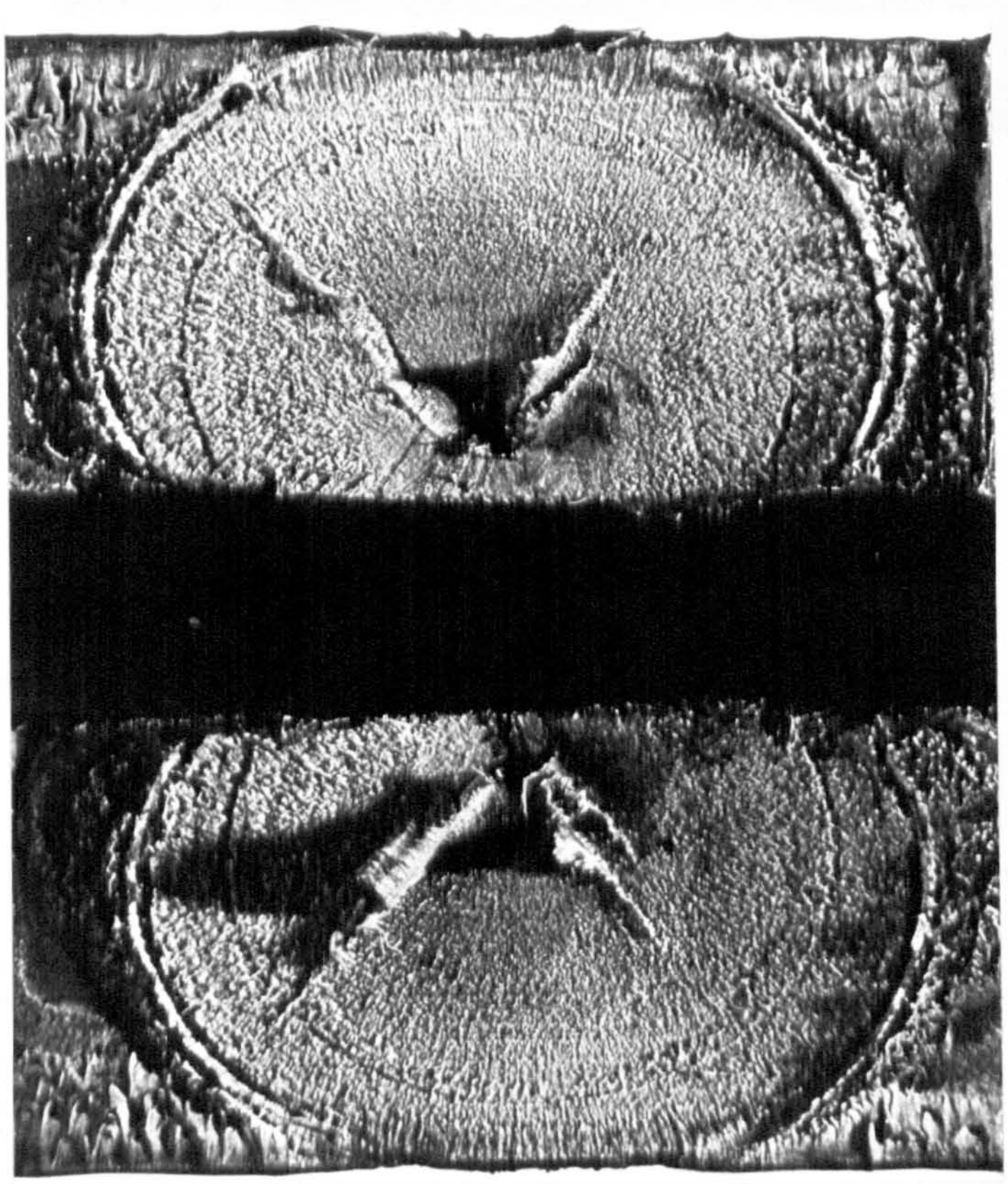

FIGURE 4.31b

Brittle fracture surface of an HDPE 2 pipe subjected to static internal pressure (stress rupture).
80°C
4.93 MPa pipe hoop stress
63mm OD SDR 11 pipe

2mm

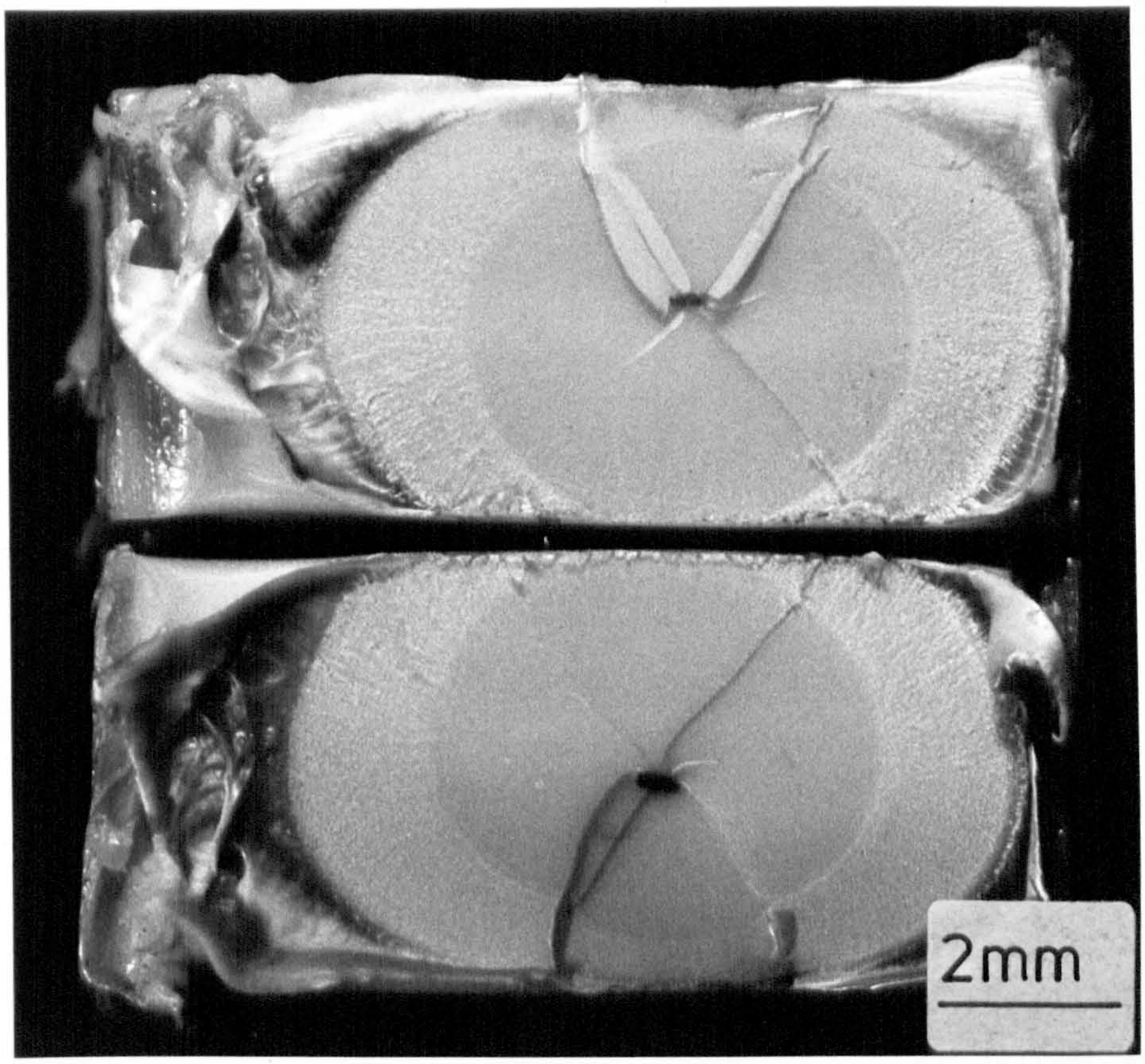

FIGURE 4.31c Brittle fracture surface of an MDPE 1 pipe subjected to a static internal pressure (stress rupture).
80°C
4.93 MPa pipe hoop stress
60mm OD SDR 11 pipe

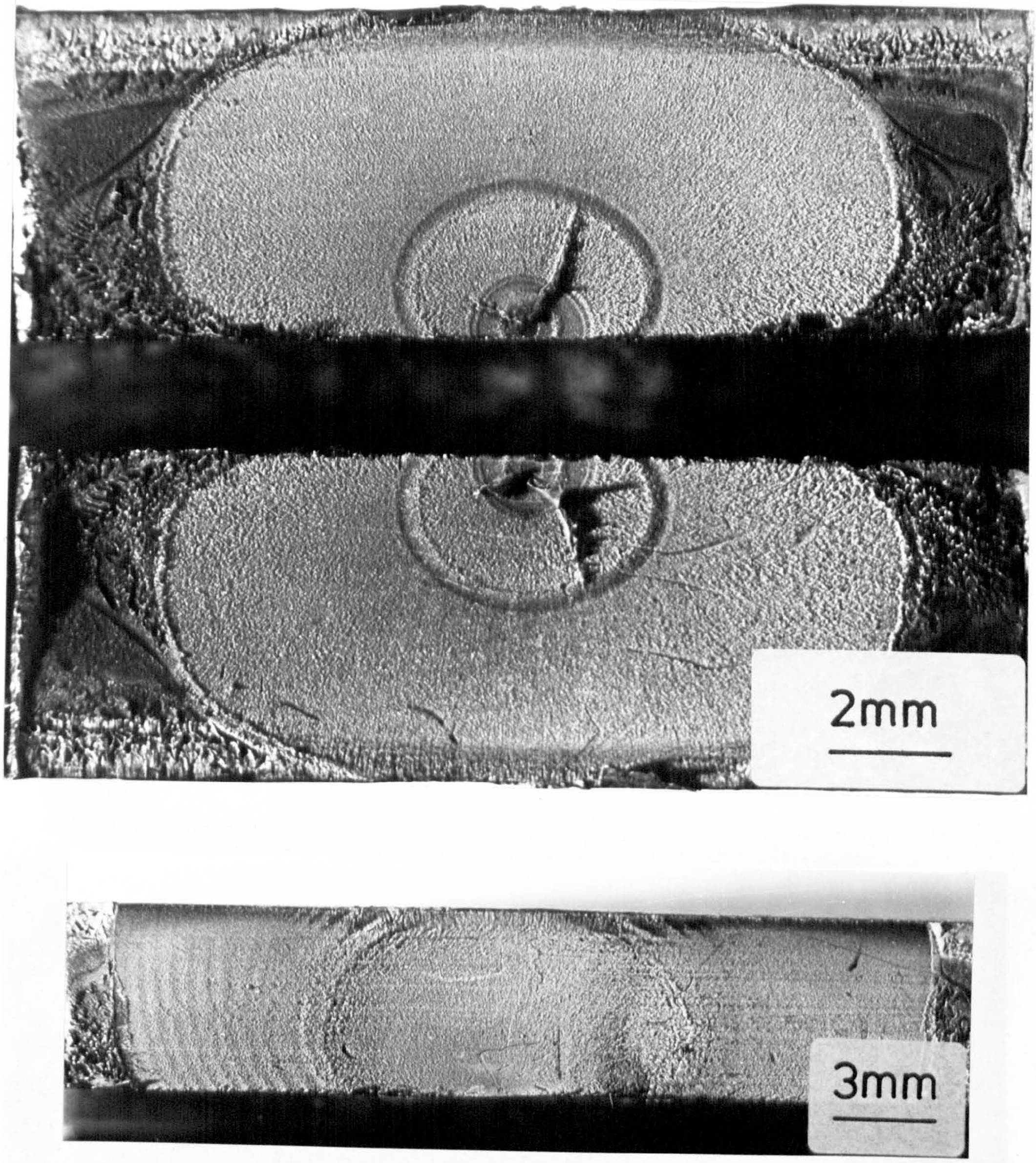

FIGURE 4.32a Examples of brittle fractures in HDPE 1 pipes subjected to fluctuating internal pressure of varying frequencies in the range 0.85 to 6 cpm.
80°C
4.93 MPa maximum pipe hoop stress
63mm OD SDR 11

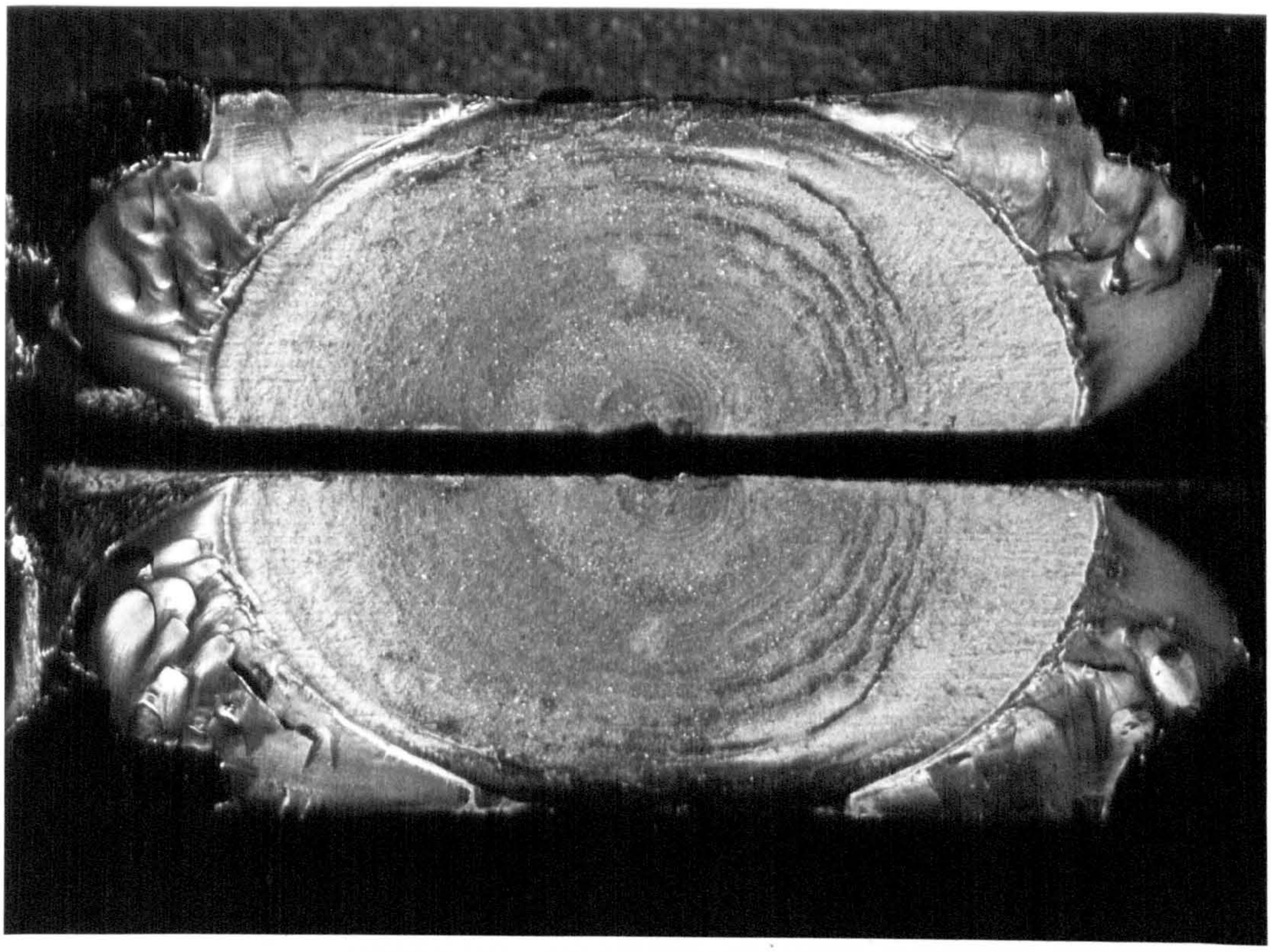

5mm

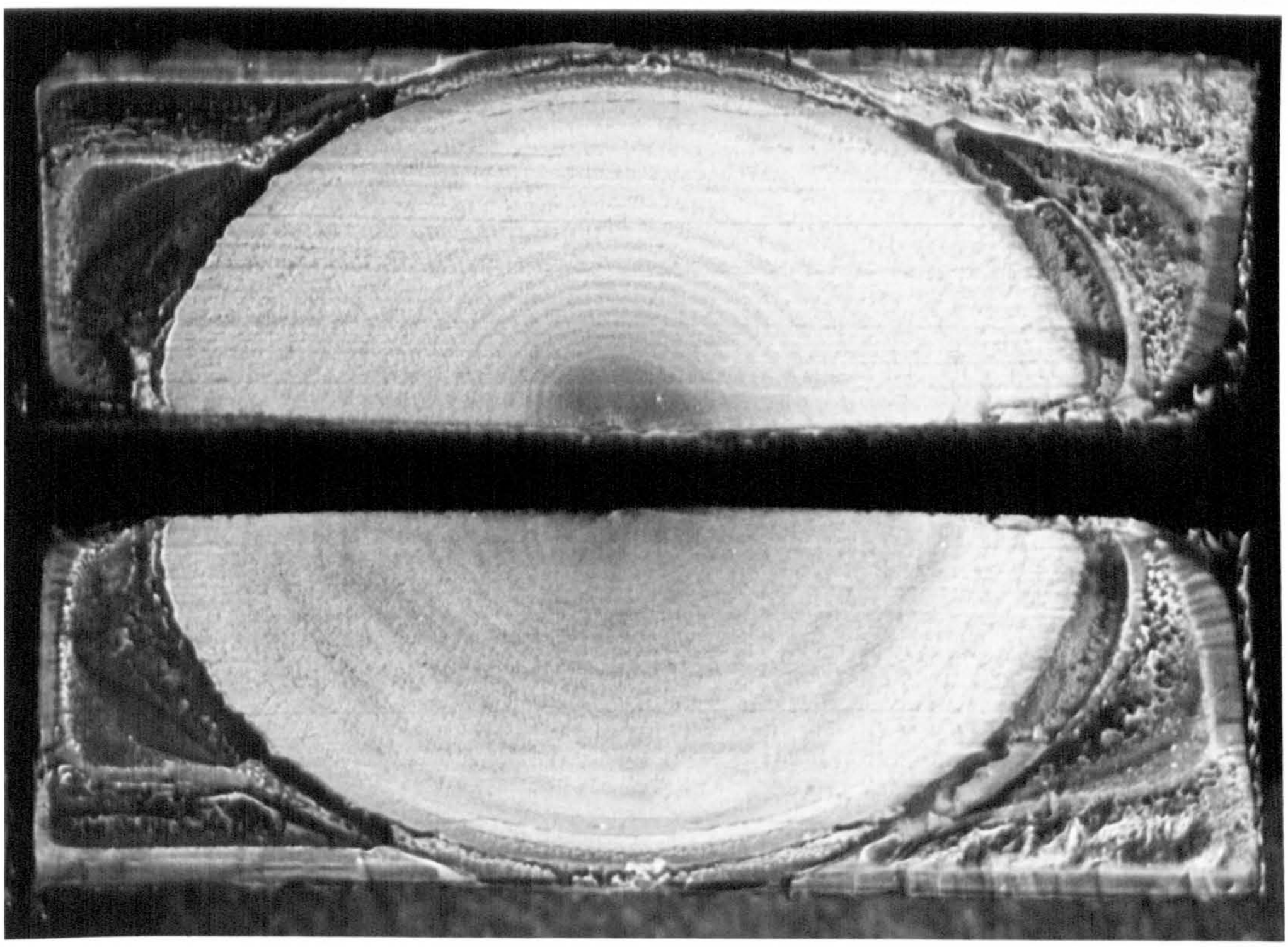

FIGURE 4.32b Examples of brittle fractures in HDPE 2 pipe subjected to fluctuating internal pressures at one frequency of 6 cpm.
80°C
4.93 MPa maximum pipe hoop stress
63mm OD SDR 11

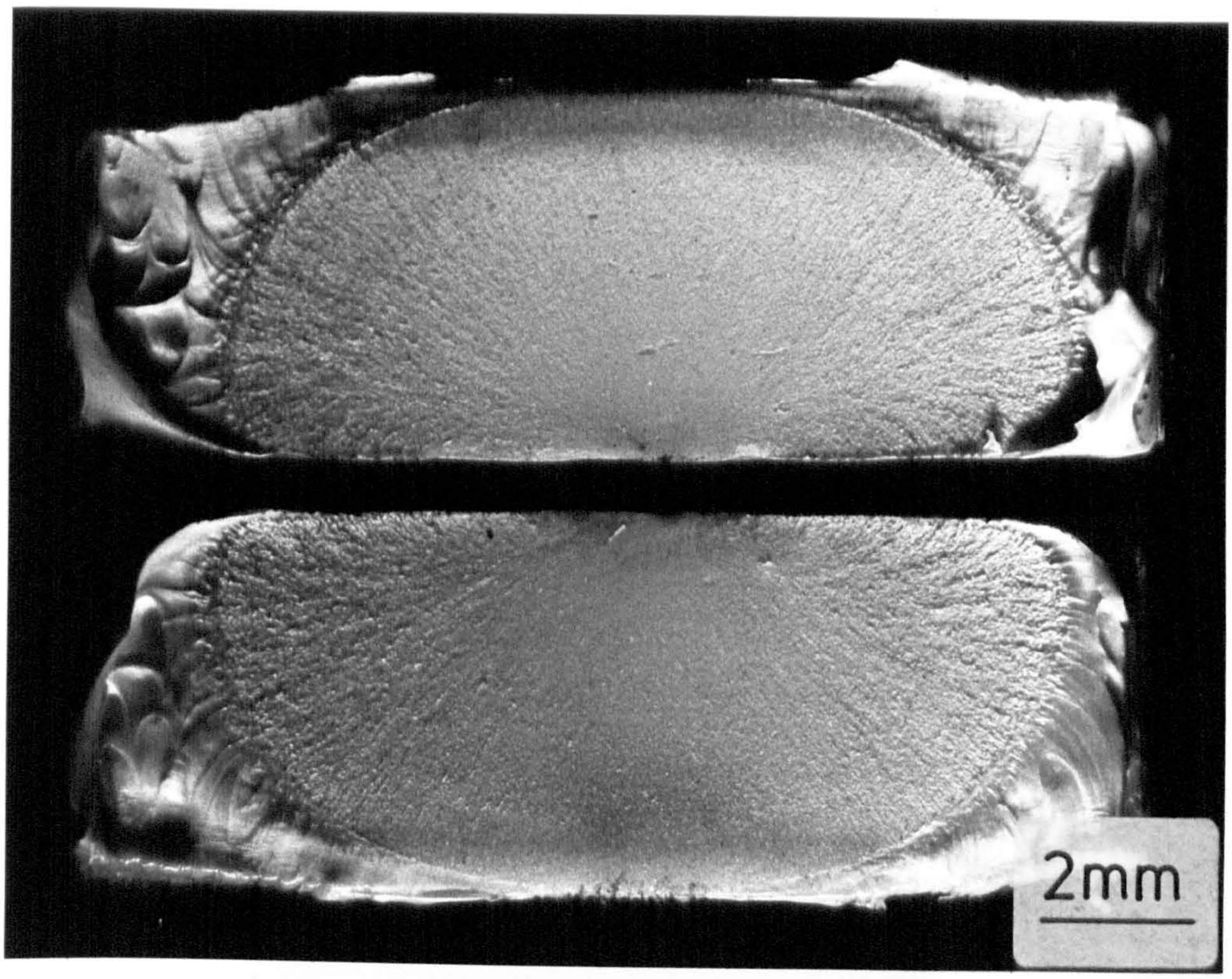

FIGURE 4.32c Examples of brittle fractures in MDPE 1 pipes subjected to fluctuating internal pressure at frequencies in the range 0.85 to 6 cpm.
80°C
3.00 MPa maximum pipe hoop stress
60mm OD SDR 11

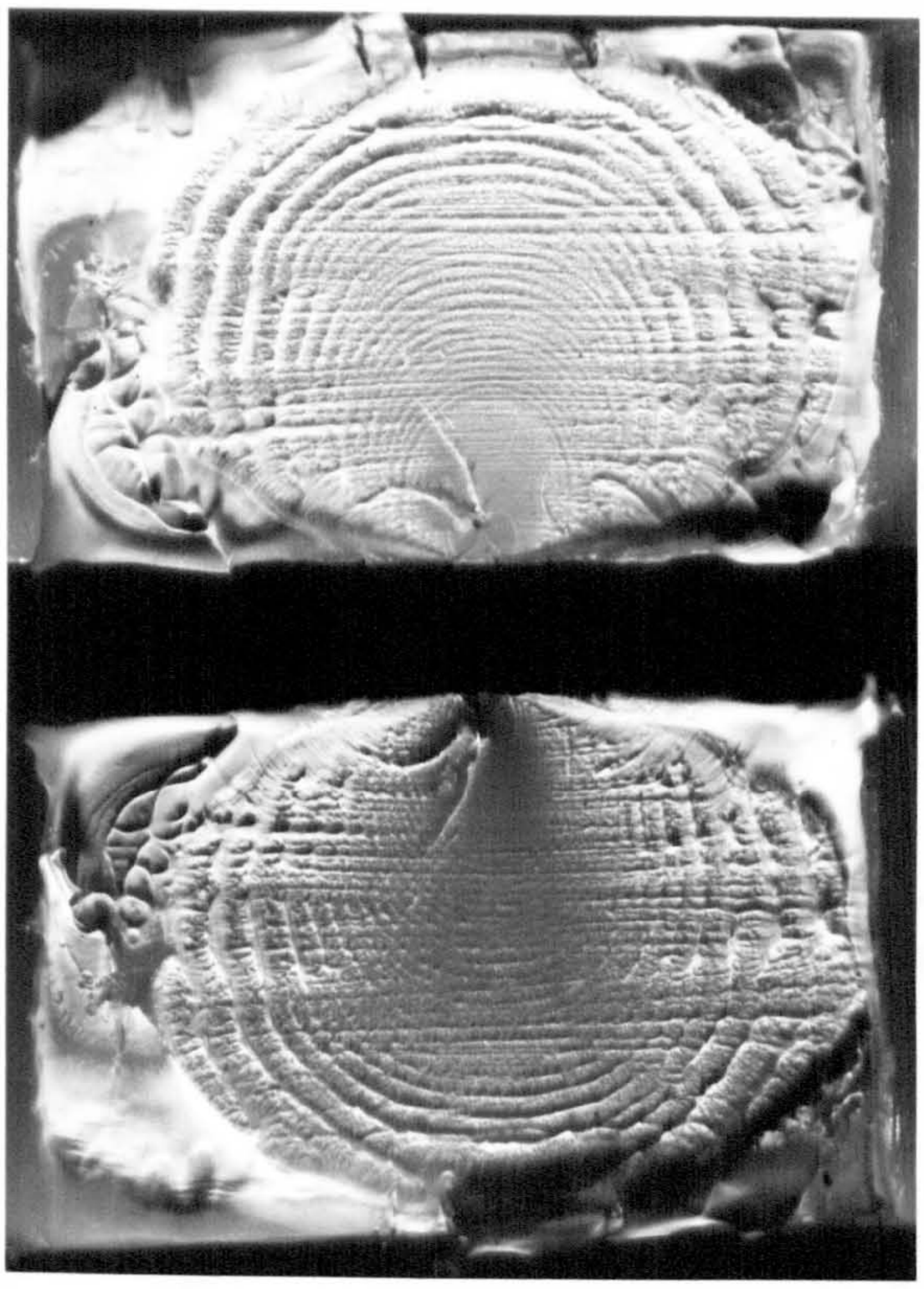

2mm

FIGURE 4.32d Examples of brittle fractures in MDPE 2 pipes subjected to fluctuating internal pressure at a frequency of 7.5 cpm.
80°C
4.93 MPa maximum pipe hoop stress
63mm OD SDR 11

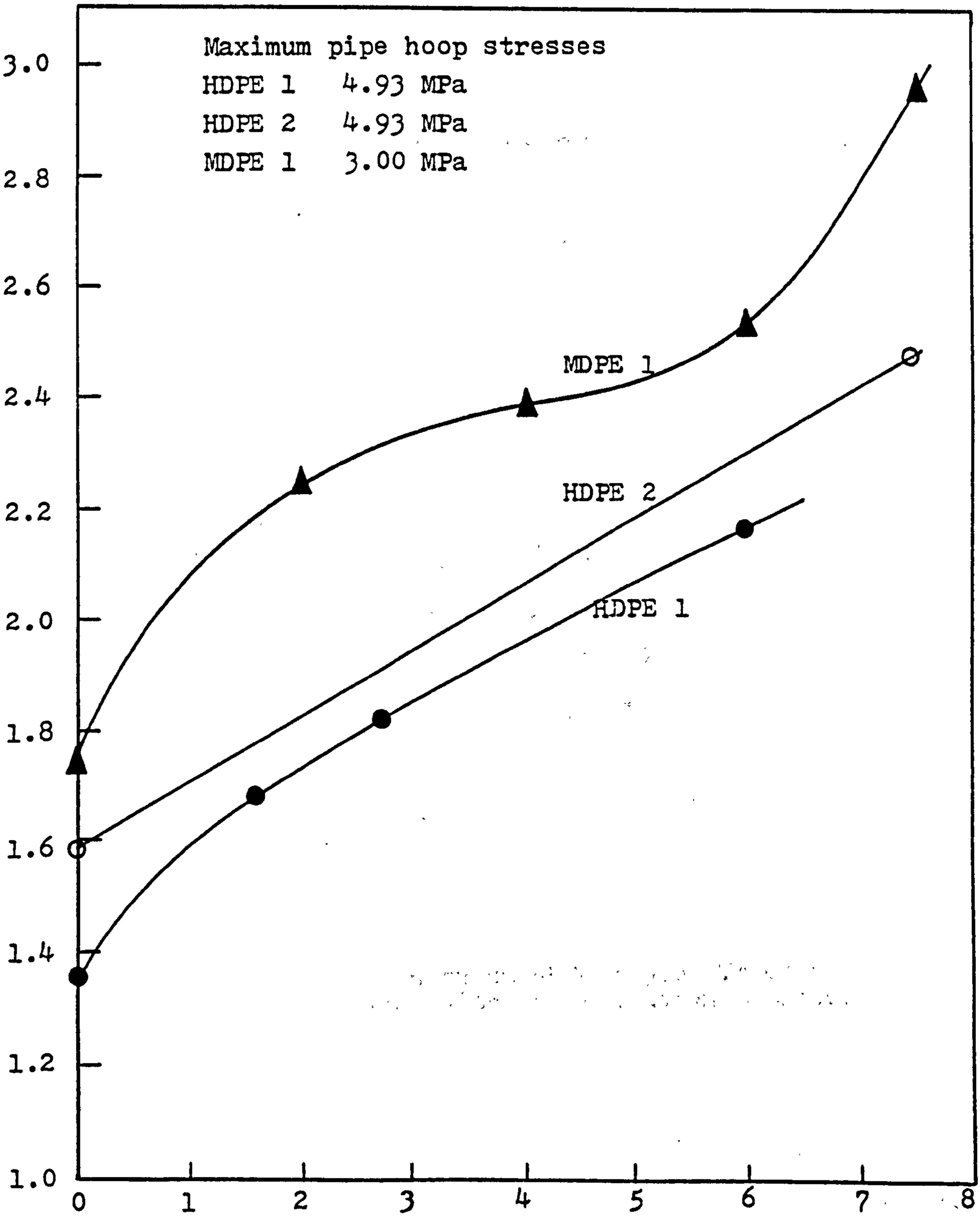

FIGURE 4.33 Variation of L/h with frequency for 60 and 63mm OD SDR 11 pipes at 80°C.

FIGURE 4.34 Flow lines on an HDPE 1 pipe fracture associated with the extrusion process.

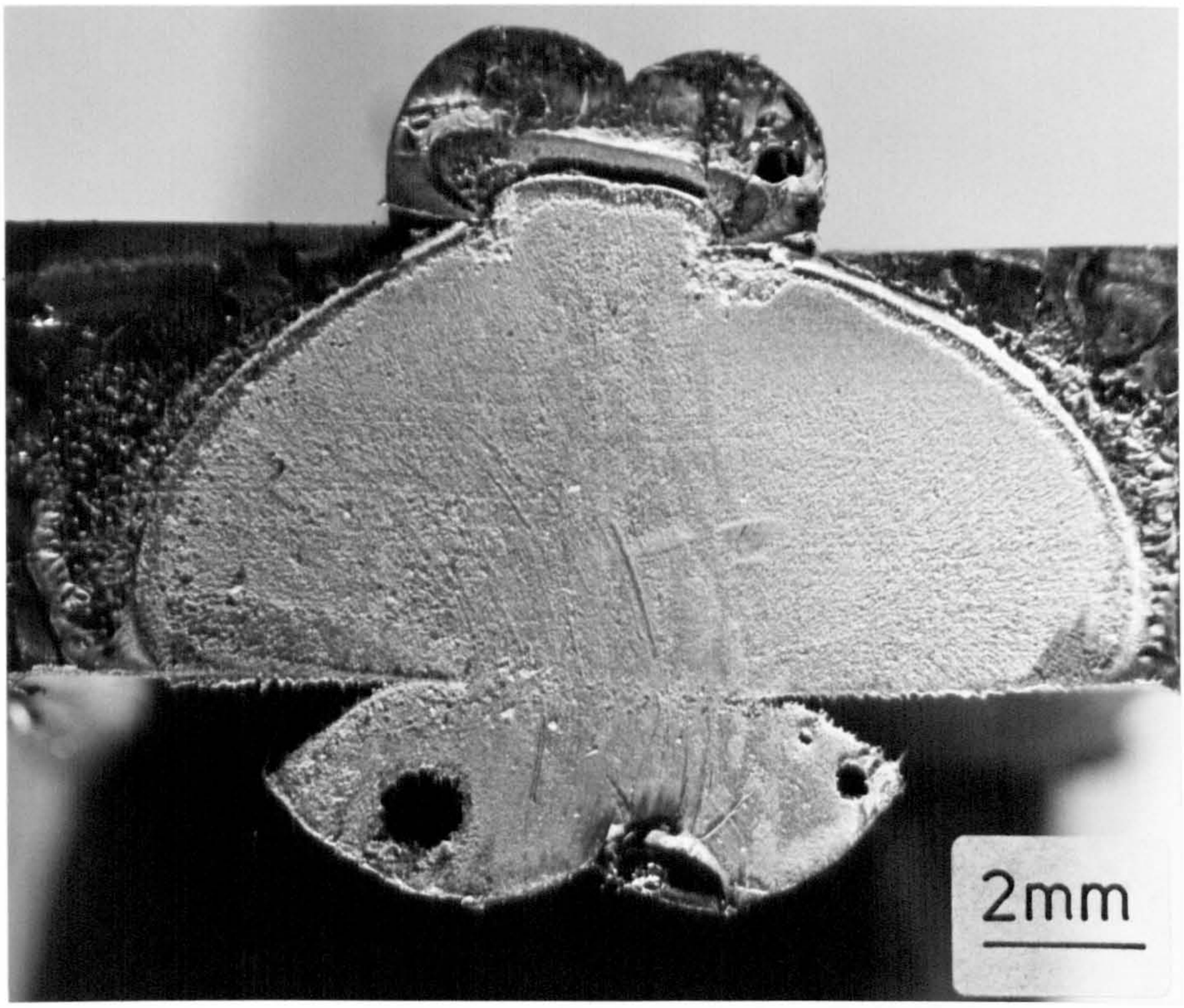

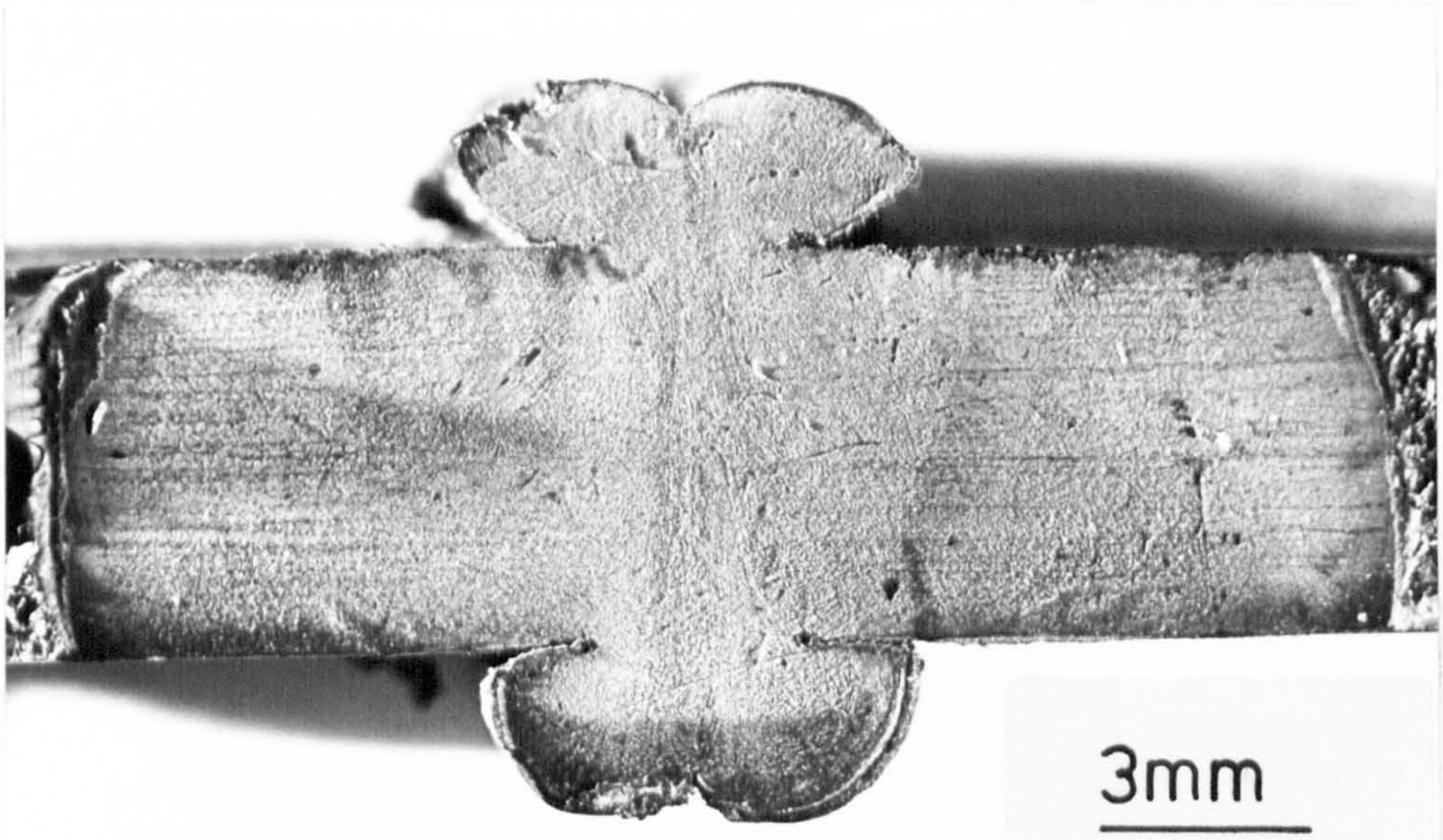

FIGURE 4.35 Examples of pipe to pipe (P/P Type 1) butt-weld fractures in HDPE 1 pipe systems.

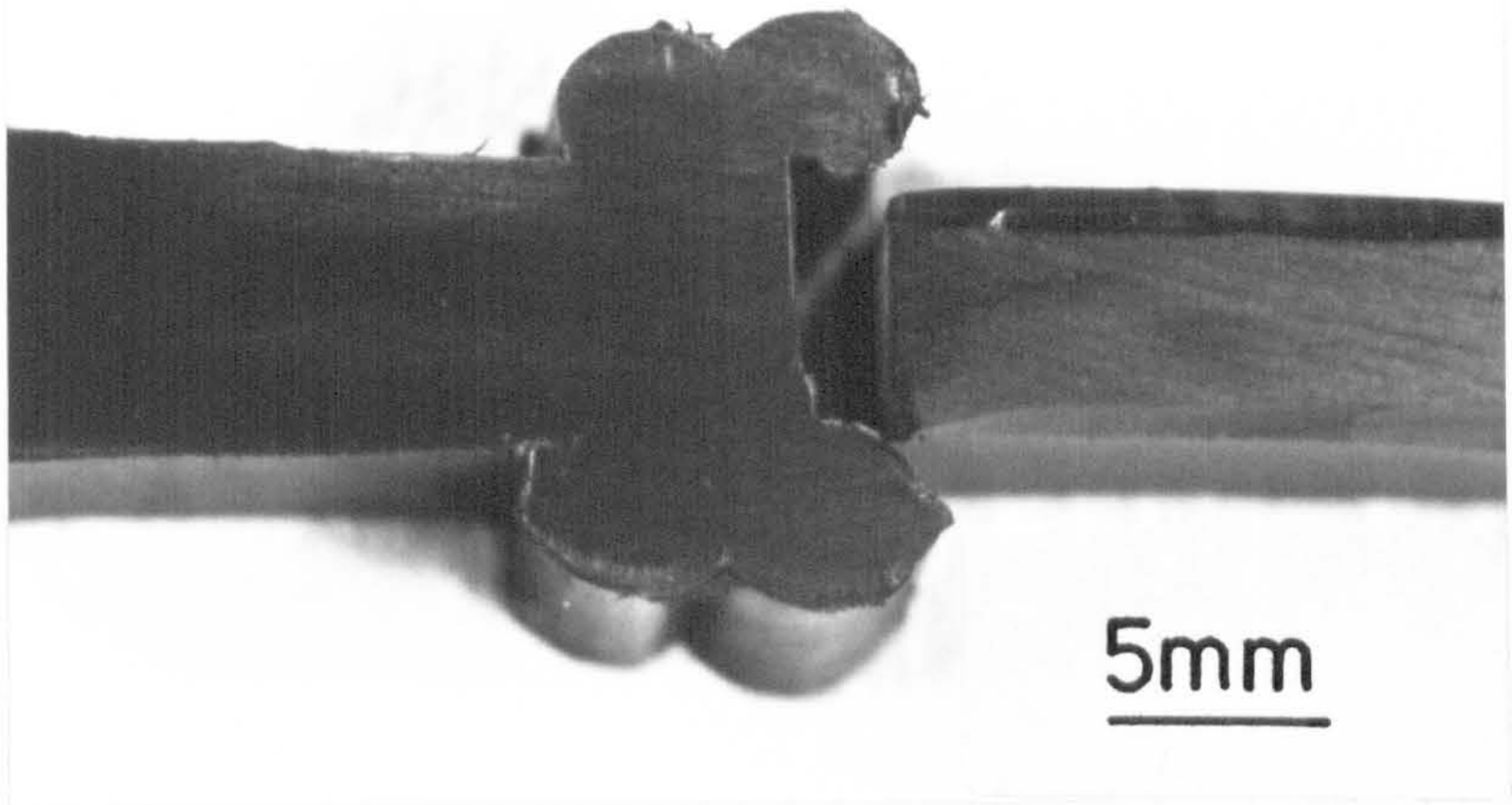

FIGURE 4.36a Circumferential butt-weld fracture (P/P Type 2) in an HDPE 1 pipe system. The path of the fracture is associated with the line drawn between the notches formed by the beads and the pipe surfaces. (Only P/P Type 2 butt-weld fractures were observed in MDPE 1 welded pipe systems.)

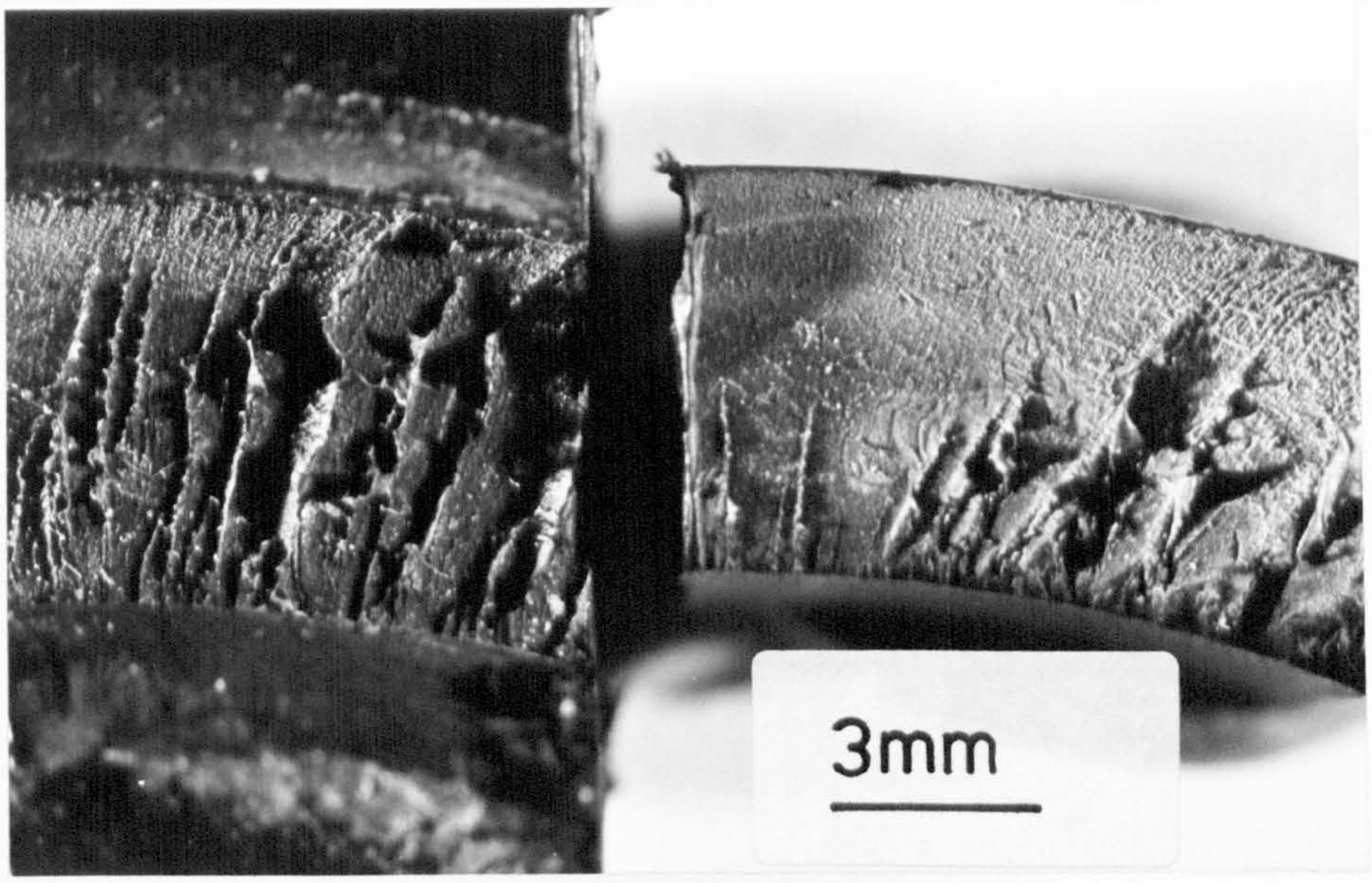

FIGURE 4.36b Fracture surface of a circumferential butt-weld failure (P/P Type 2) in an HDPE 1 pipe system.

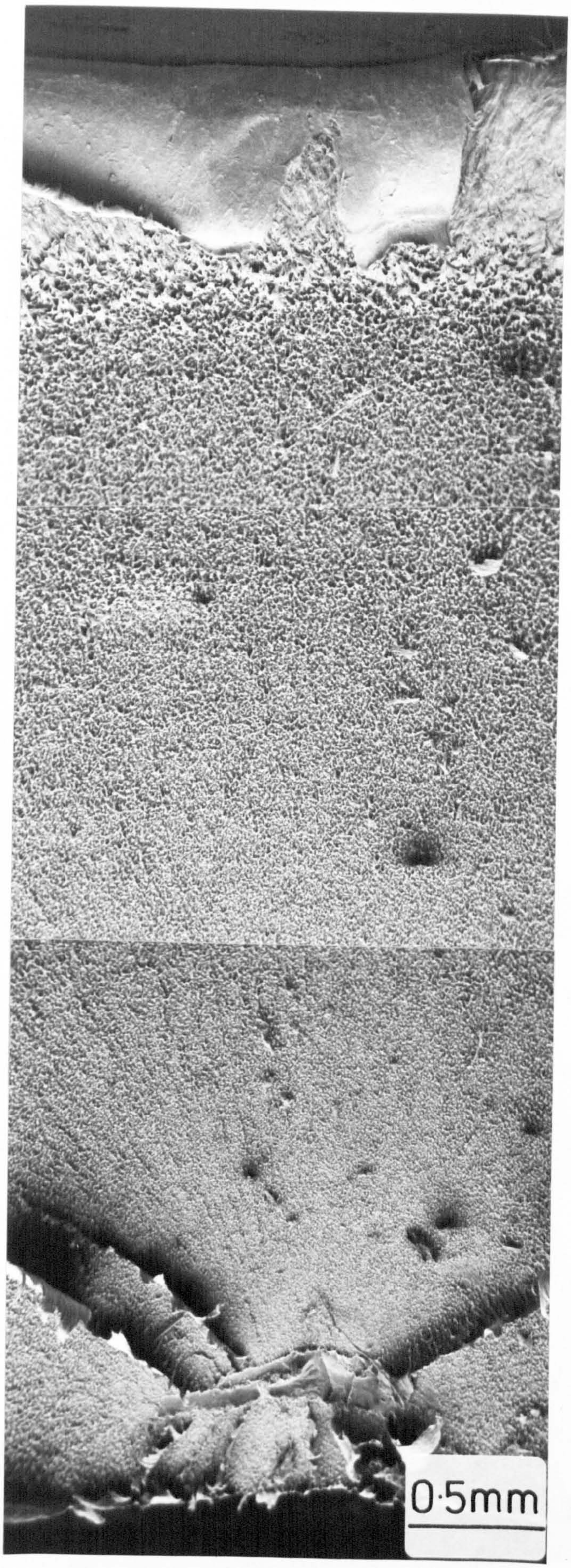

FIGURE 4.37a

High magnification micrograph of a typical HDPE 1 pipe fracture surface obtained under stress rupture conditions.
80°C
4.93 MPa pipe hoop stress

Pipe Bore

FIGURE 4.37b

High magnification micrograph of a typical HDPE 2 pipe fracture surface obtained under stress rupture conditions.
80°C
4.93 MPa pipe hoop stress
The crack initiation particle is clearly seen towards the middle of the pipe wall.

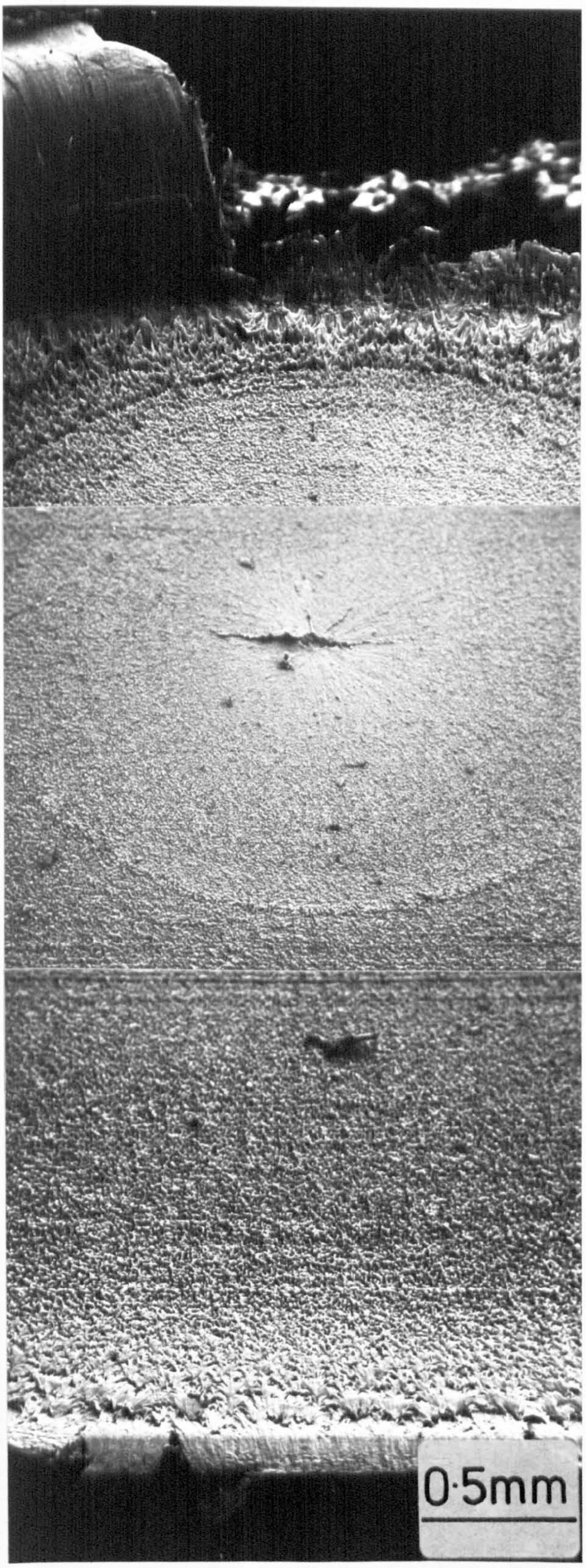

Pipe Bore

FIGURE 4.37c

High magnification micrograph of a typical MDPE 1 pipe fracture surface obtained under stress rupture conditions.
80°C
3.00 MPa pipe hoop stress
The crack initiation particle is clearly seen towards the middle of the pipe wall.

Pipe bore

FIGURE 4.38a

High magnification micrograph of a typical HDPE 1 pipe fracture surface obtained under fatigue conditions.
80°C
4.93 MPa maximum pipe hoop stress
0.85 cpm

Pipe Bore

FIGURE 4.38b

High magnification micrograph of a typical MDPE 1 pipe fracture surface obtained under fatigue conditions.
80°C
3.00 MPa maximum pipe hoop stress
7.5 cpm

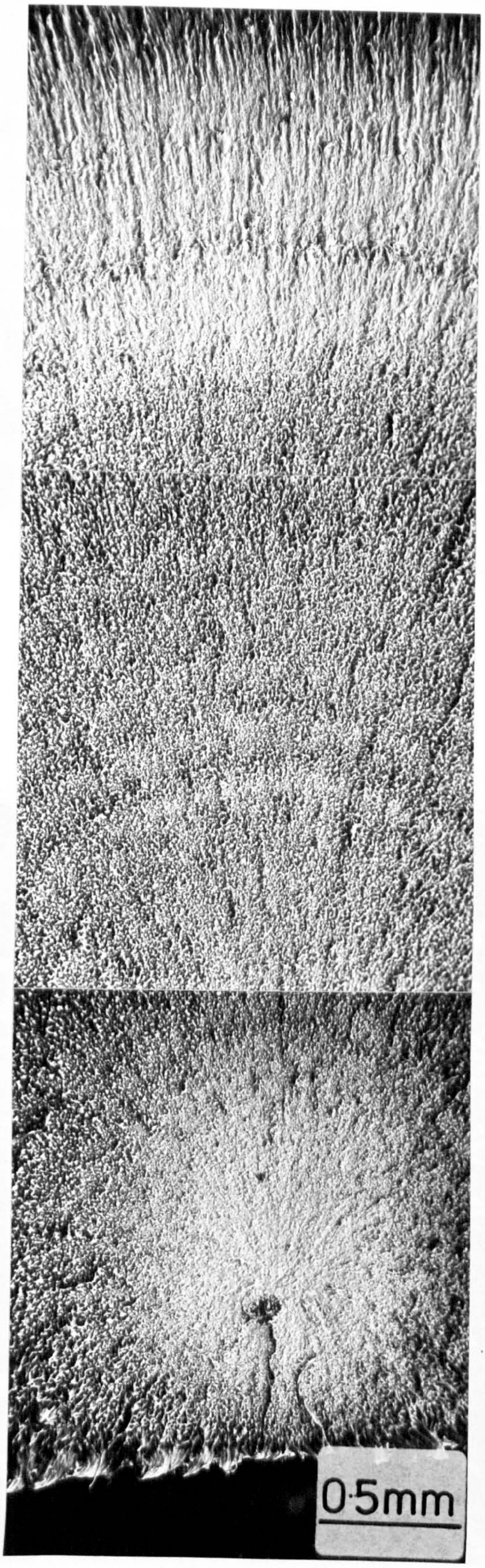

Pipe Bore

FIGURE 4.39 Tearing and macroductility in the final progress of an HDPE pipe fatigue fracture.

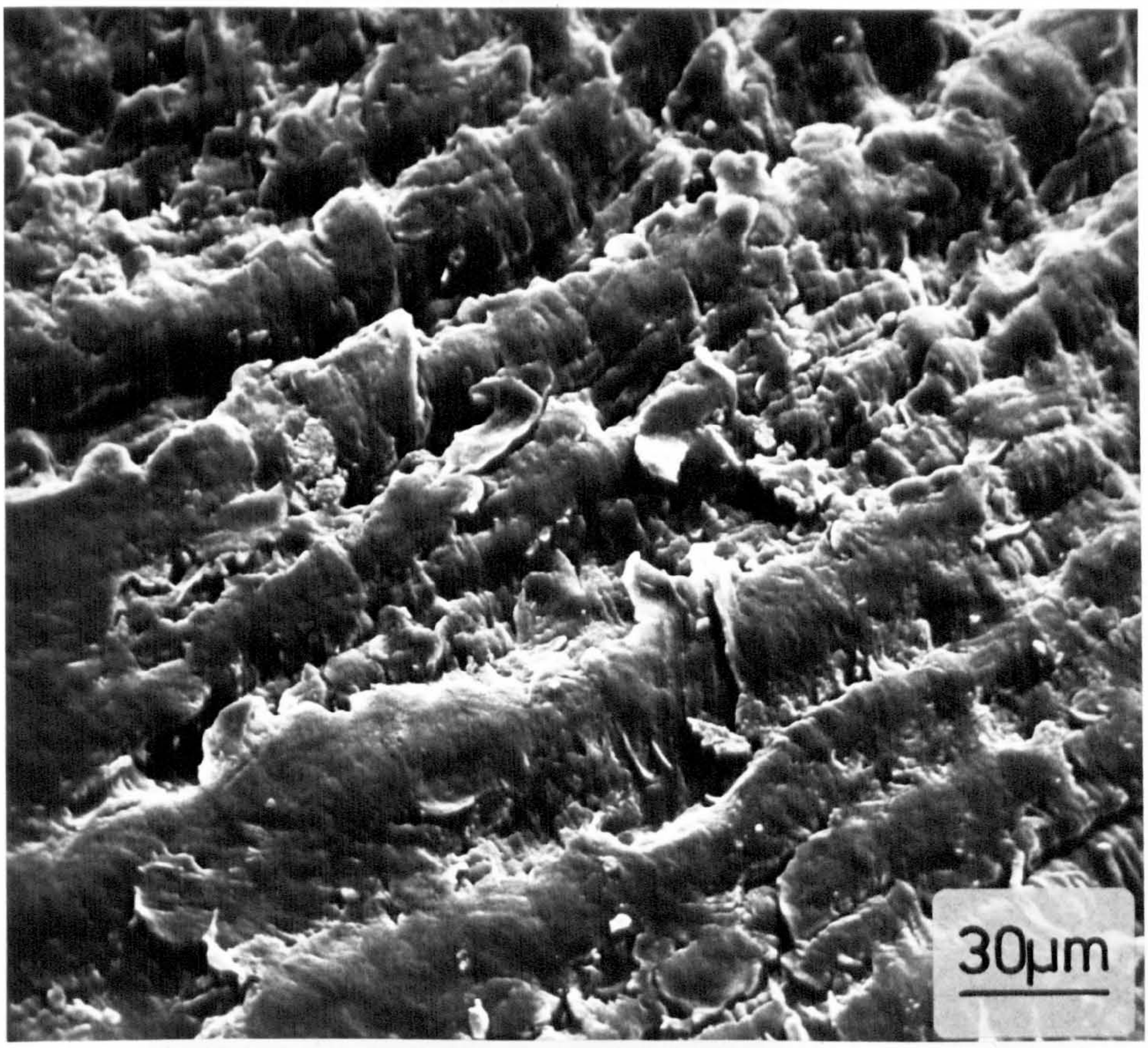

FIGURE 4.40 Fatigue striations in the final progress of an HDPE pipe fatigue fracture.

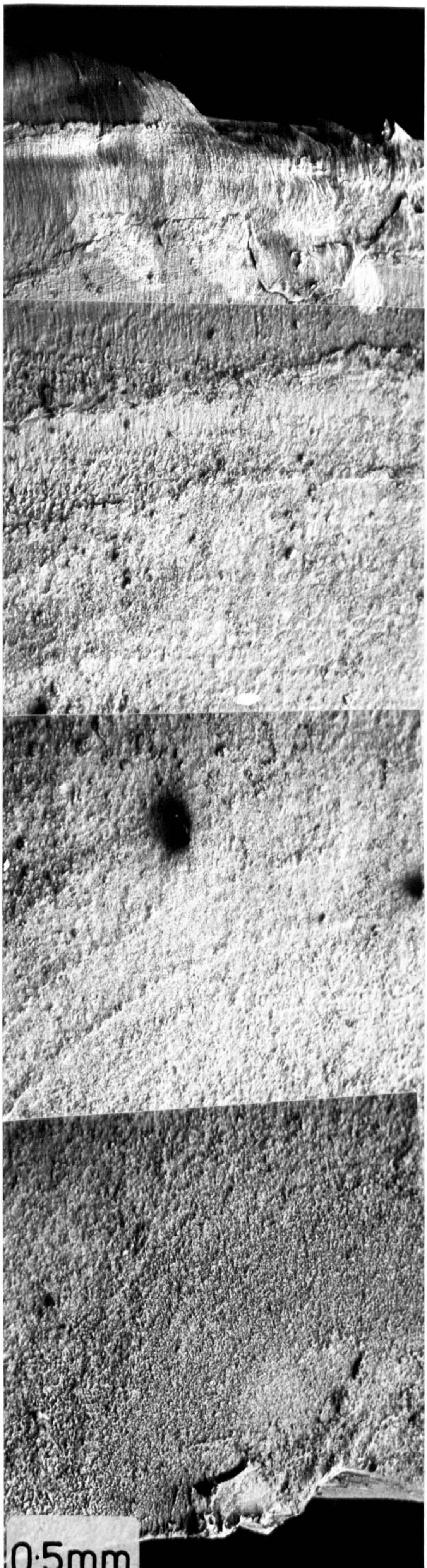

FIGURE 4.41

High magnification micrograph of a typical HDPE 2 pipe fracture obtained under fatigue conditions.
80°C
4.93 MPa maximum pipe hoop stress
7.5 cpm
Discontinuous growth bands are clearly in evidence.

Pipe Bore

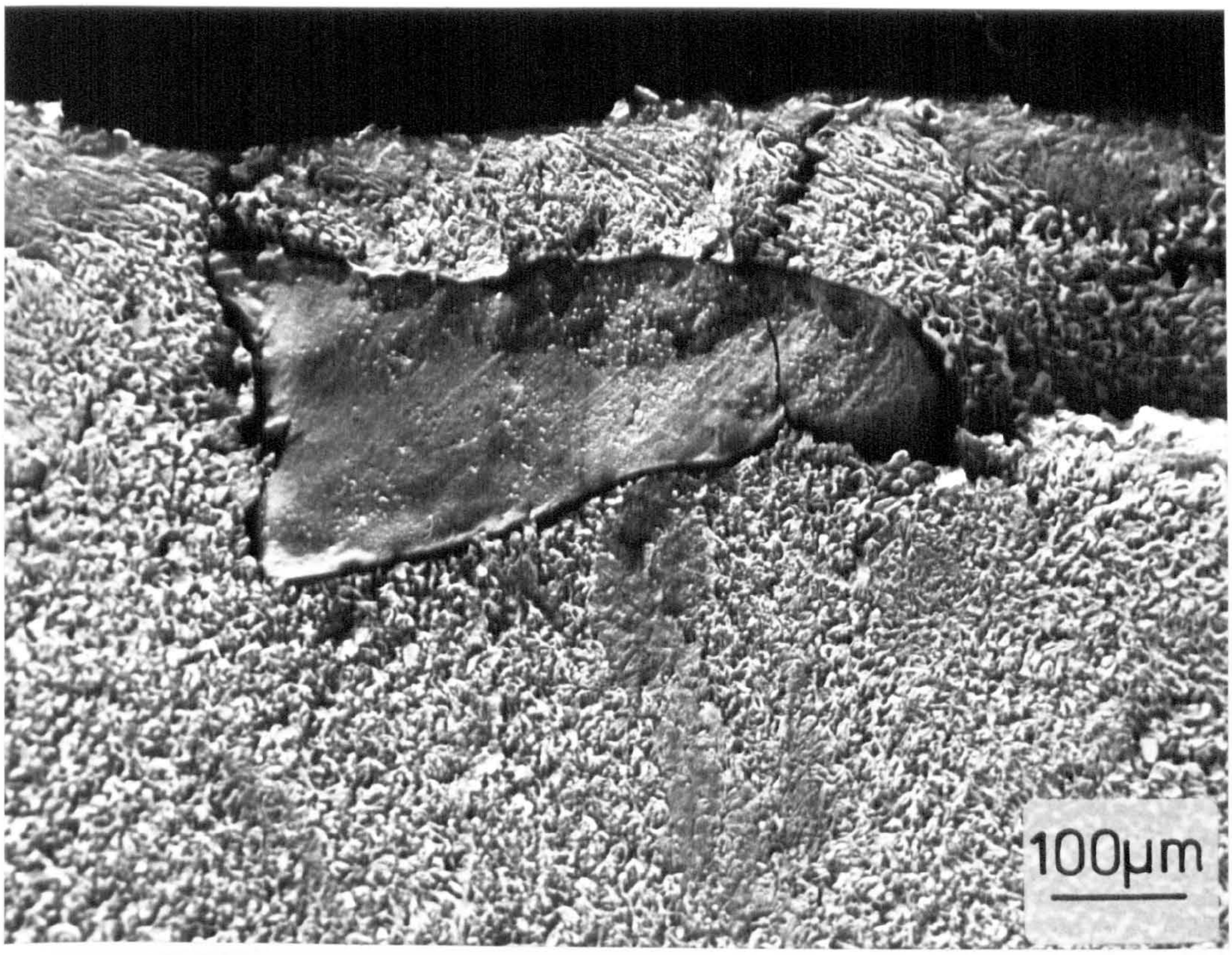

Main constituents - Fe, Cr, Ni (stainless steel)
(see Figure 4.45)

FIGURE 4.42a Examples of metallic crack initiating particles in HDPE 1 pipes.

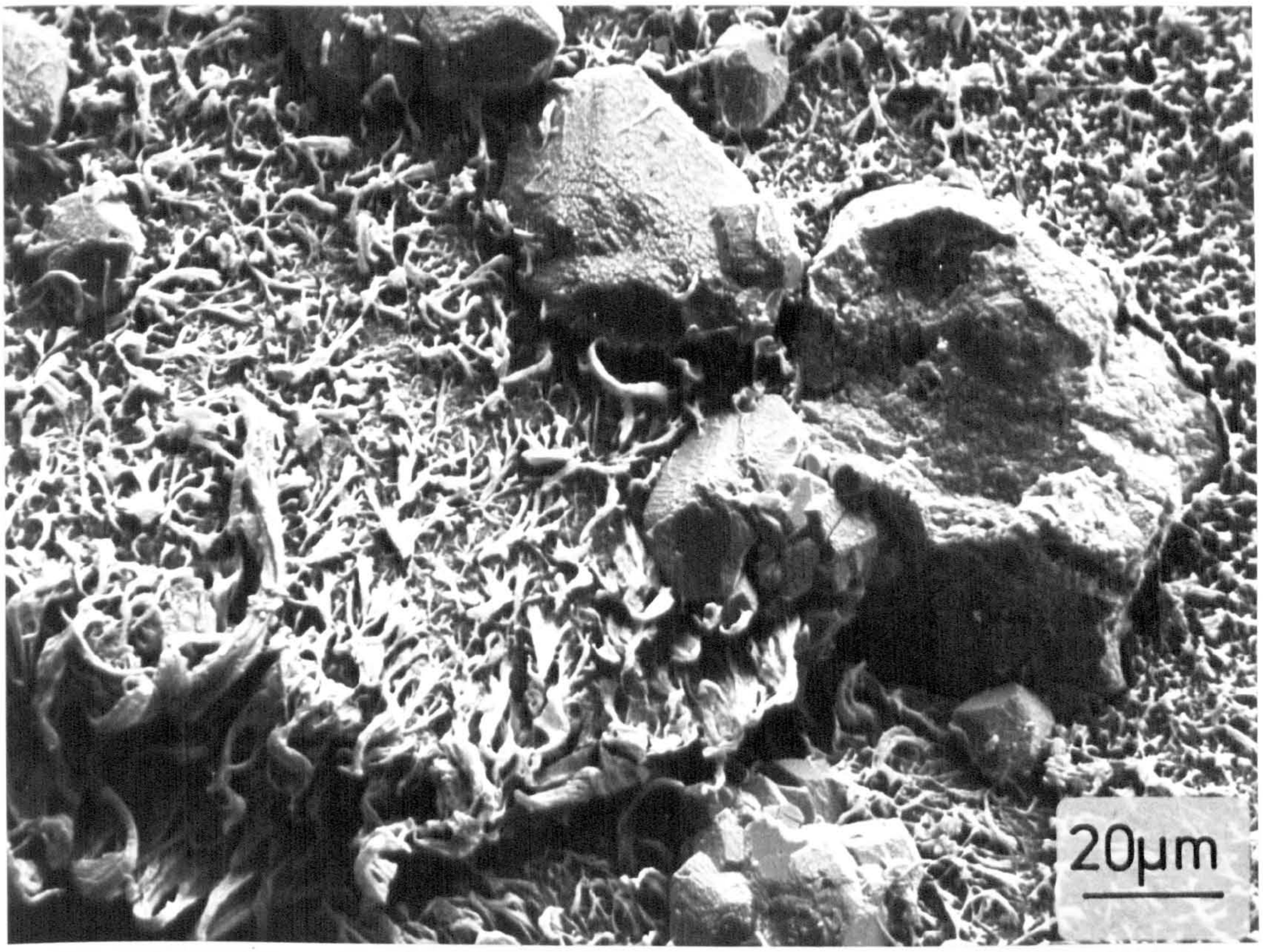

FIGURE 4.42b Example of a calcium rich crack initiating particle in an HDPE 1 pipe. (See Figure 4.46)

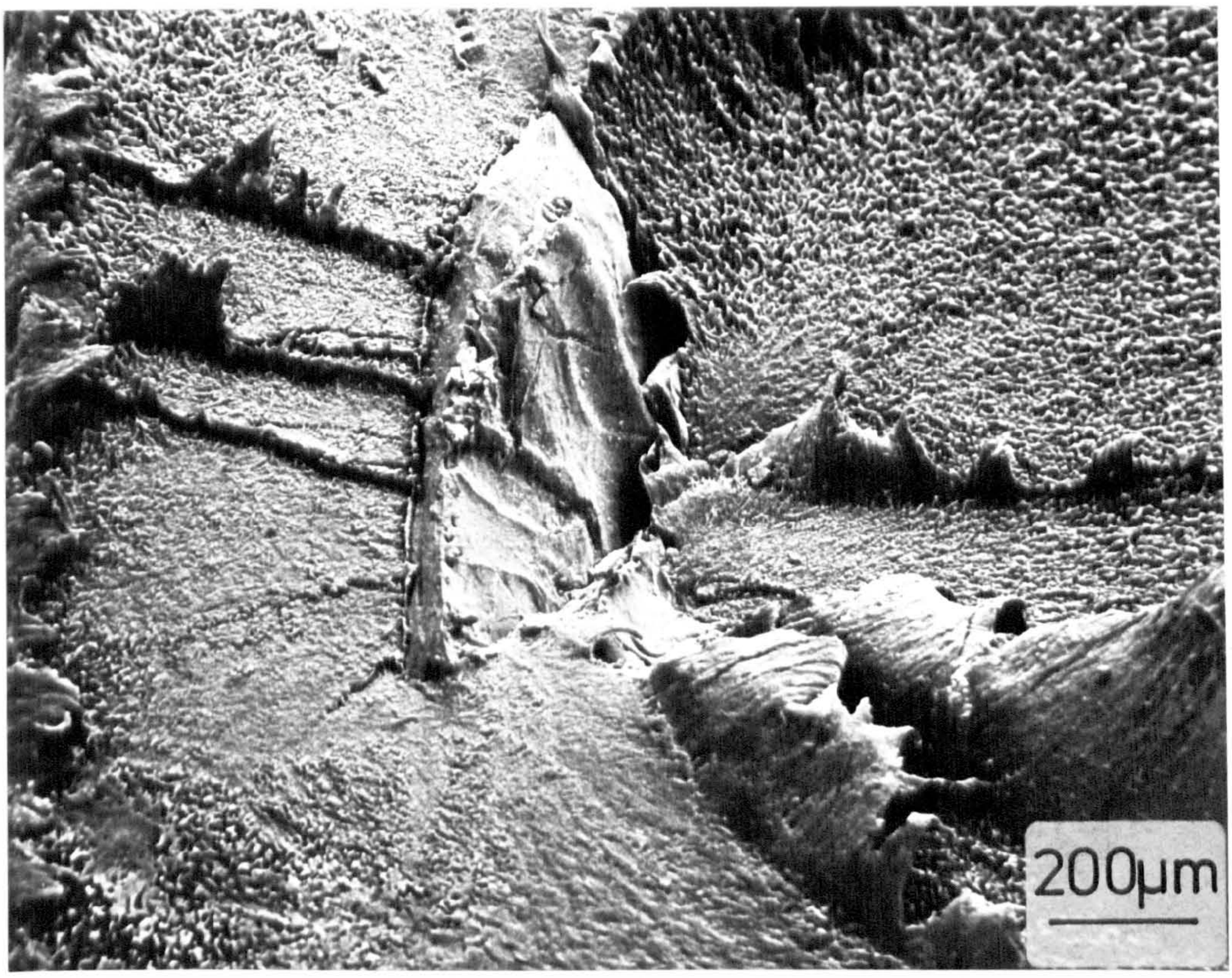

(See Figure 4.47)

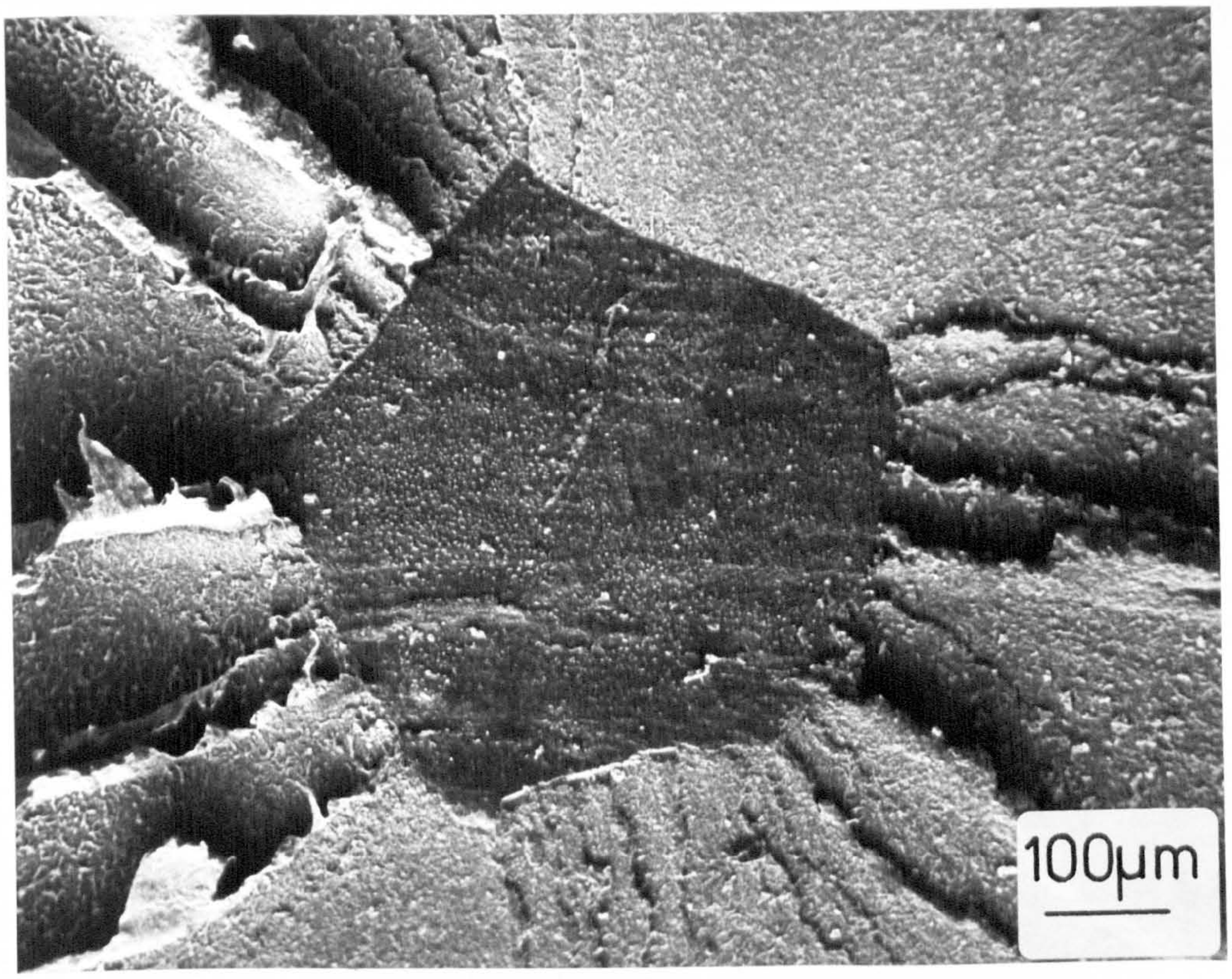

FIGURE 4.42c Examples of crack initiating particles in HDPE 1 pipes. No elements were detected using the EDAX technique.

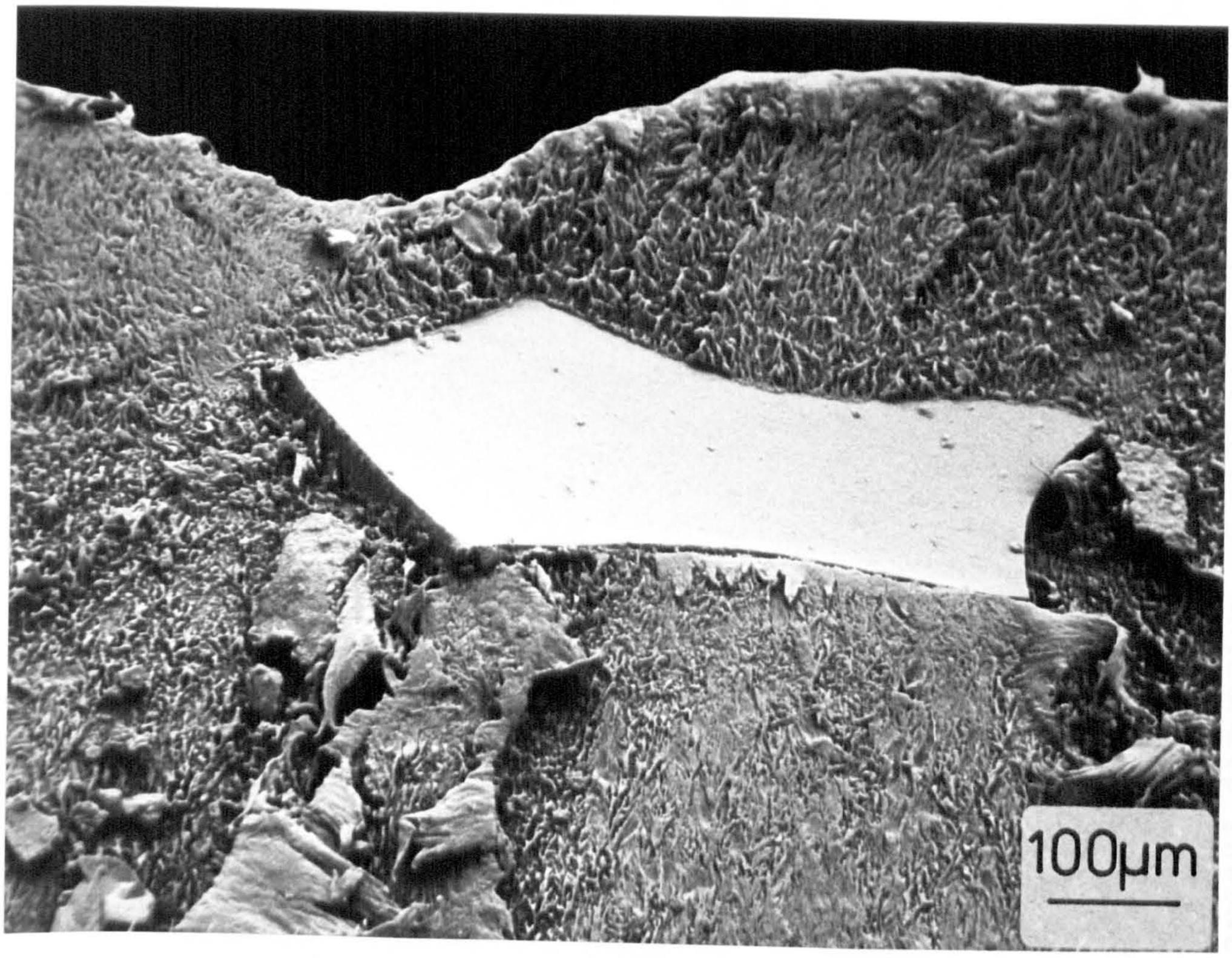

FIGURE 4.42c Example of a crack initiating particle in an HDPE 1 pipe. No elements were detected using the EDAX technique.

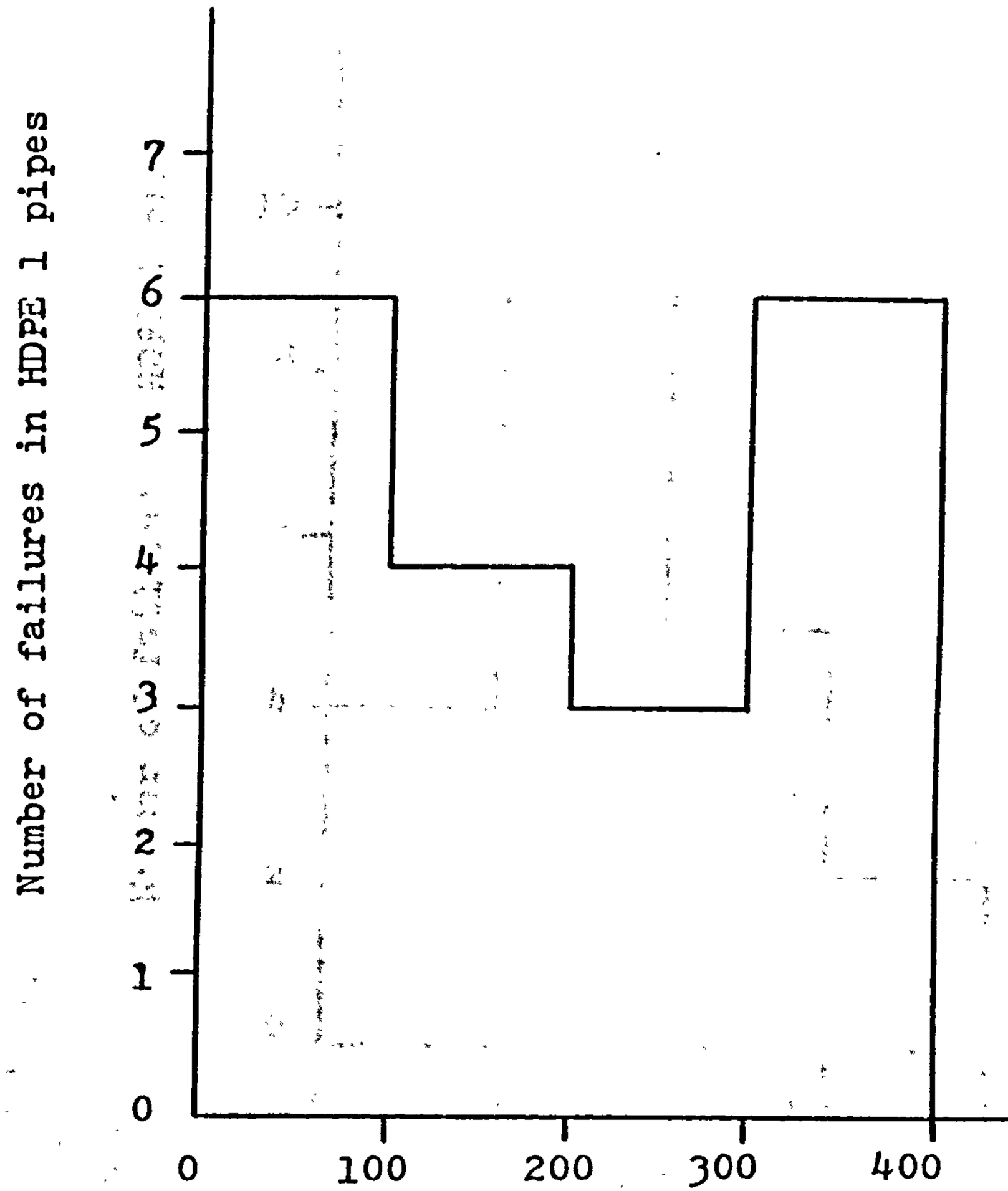

Size Range μm	HDPE 1 Inclusion Sizes μm	Number of Failures
0 - 100	70, 83, 68, 94, 33, 76	6
101 - 200	150, 123, 106, 135	4
201 - 300	213, 207, 210	3
301 - 400	305, 378, 328, 338, 306, 346	6
401 - 500		0
501 - 600	515, 600	2
601 - 700	635, 615	2
701 - 800		0
801 - 900		0
901 - 1000		0
>1001	1030, >5000	2

FIGURE 4.43 Histogram of inclusion sizes at fracture initiation sites in HDPE 1 pipe systems (Failures P1, P/P1, B1, T1).

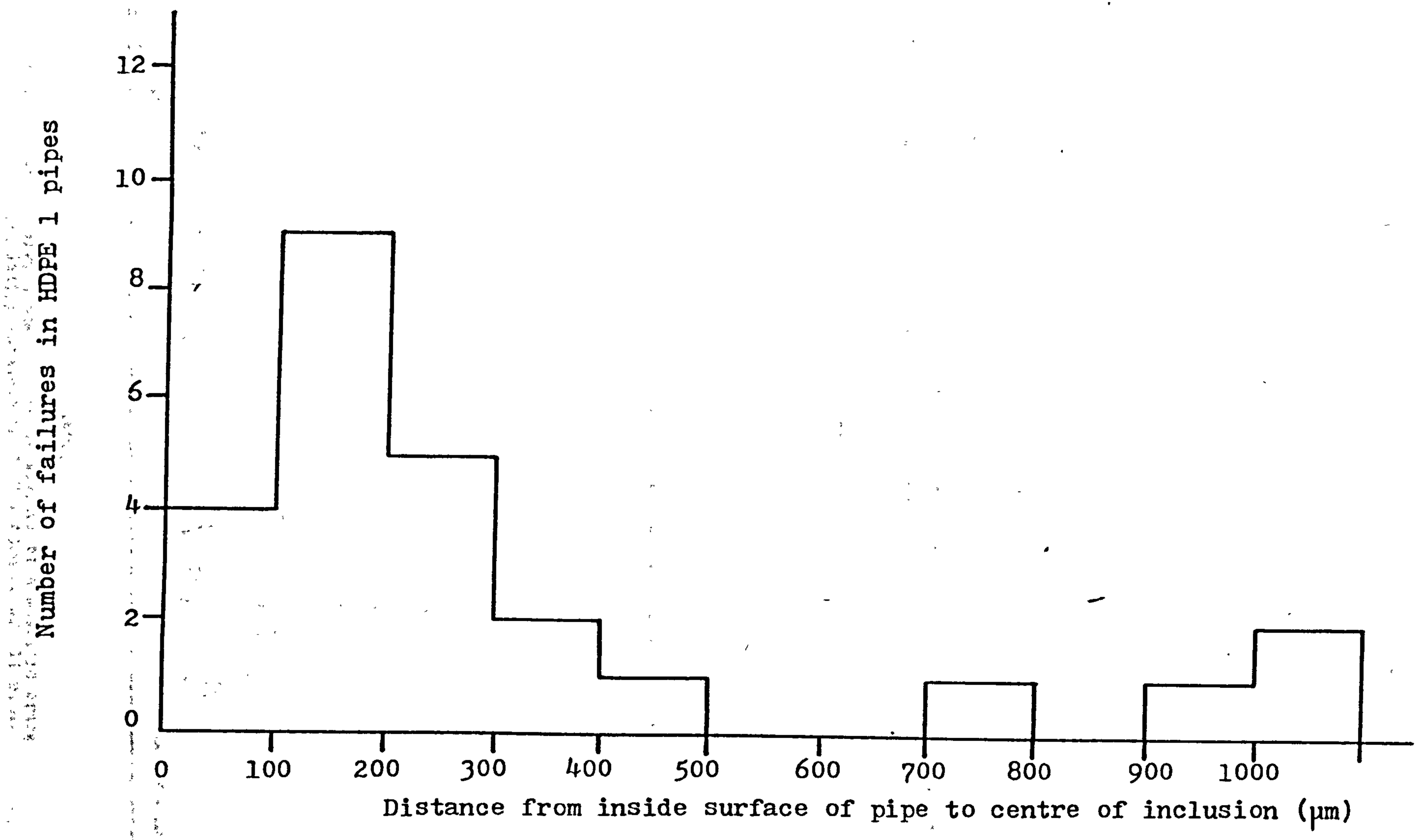

FIGURE 4.44 Histogram of distances from the pipe inside wall of inclusions leading to fracture in HDPE 1 pipes.

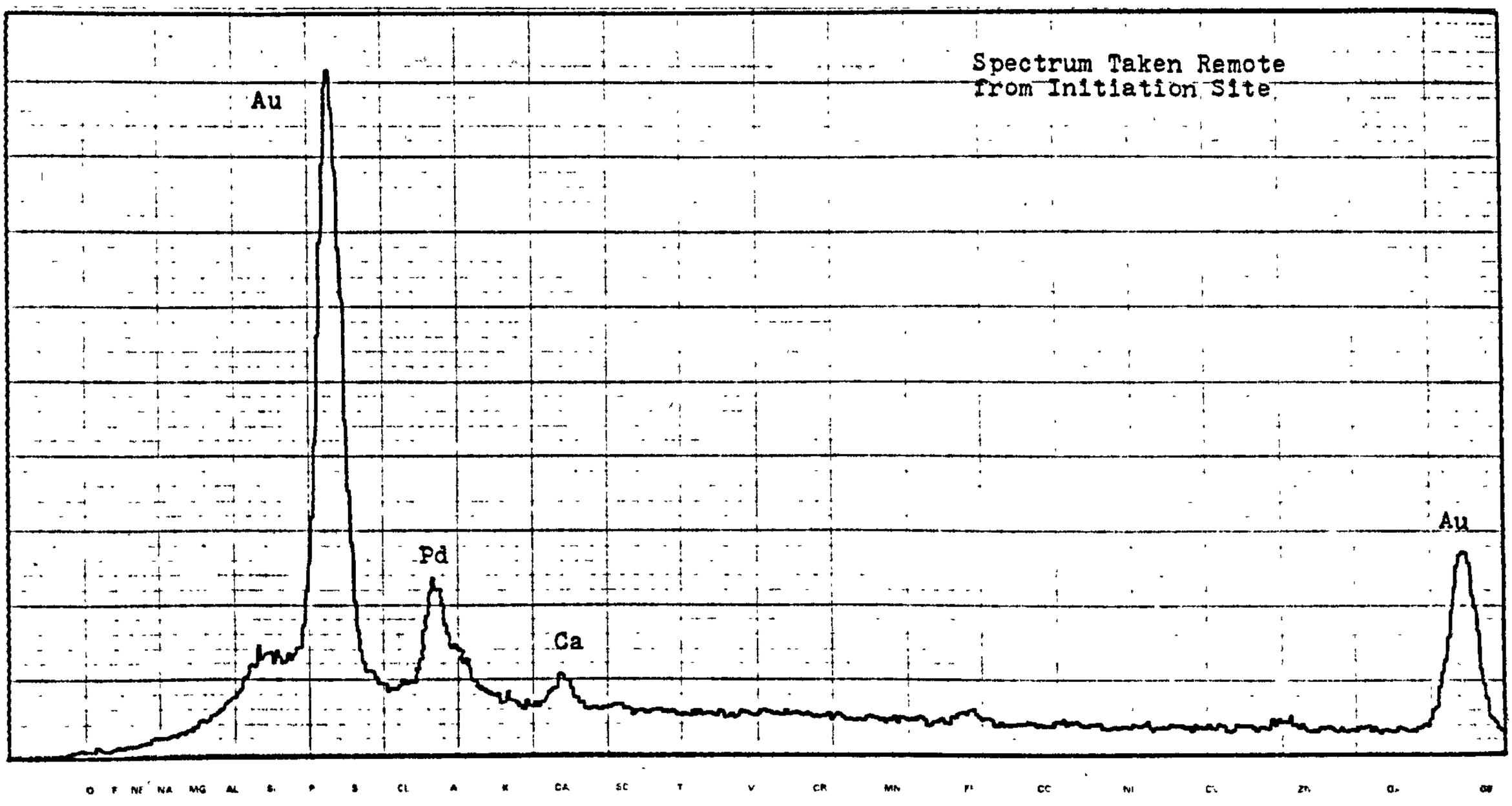

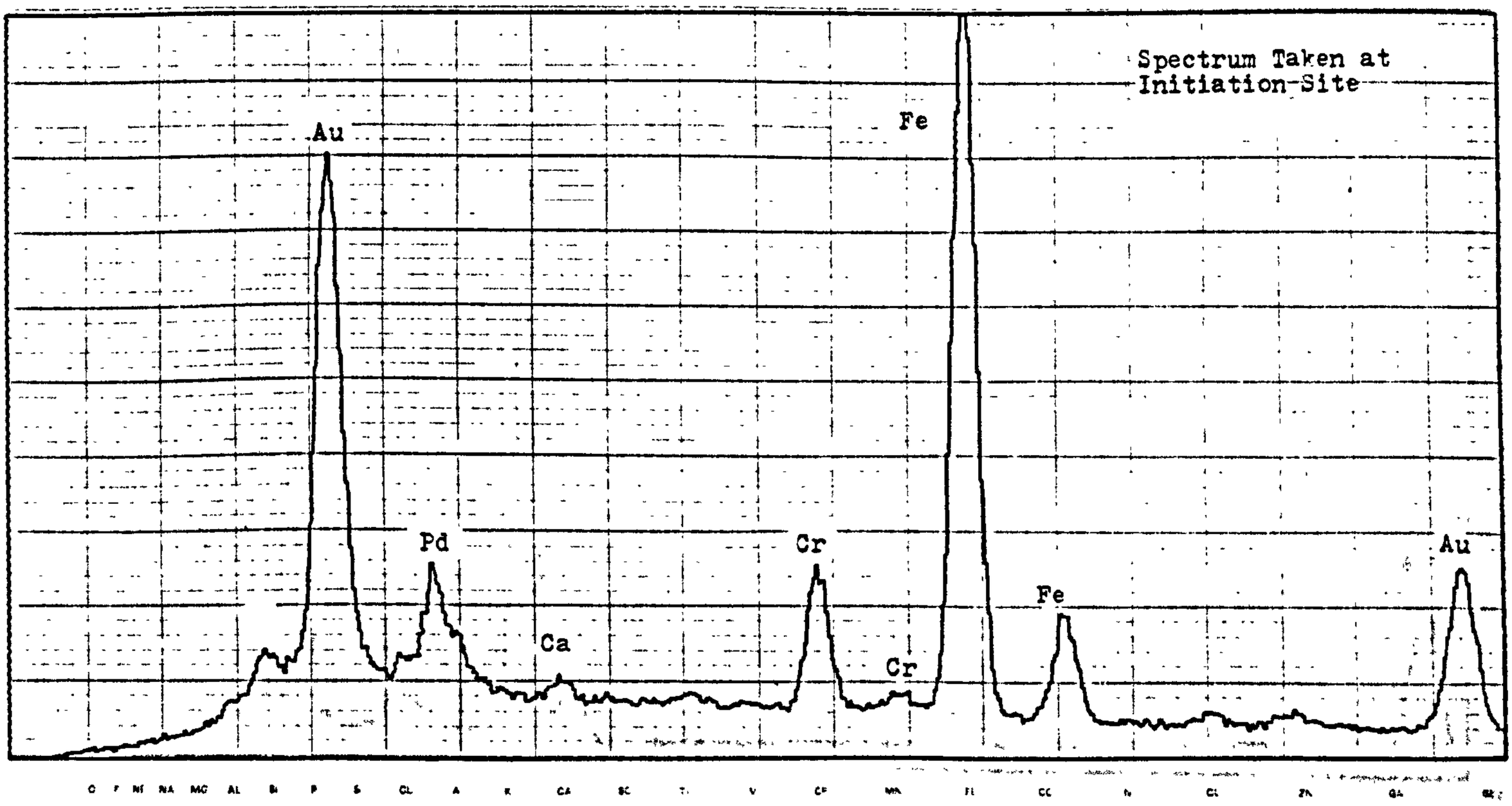

FIGURE 4.45 Energy dispersive x-ray spectra of a metallic crack initiating particle in HDPE 1.63mm OD SDR 11 pipe.

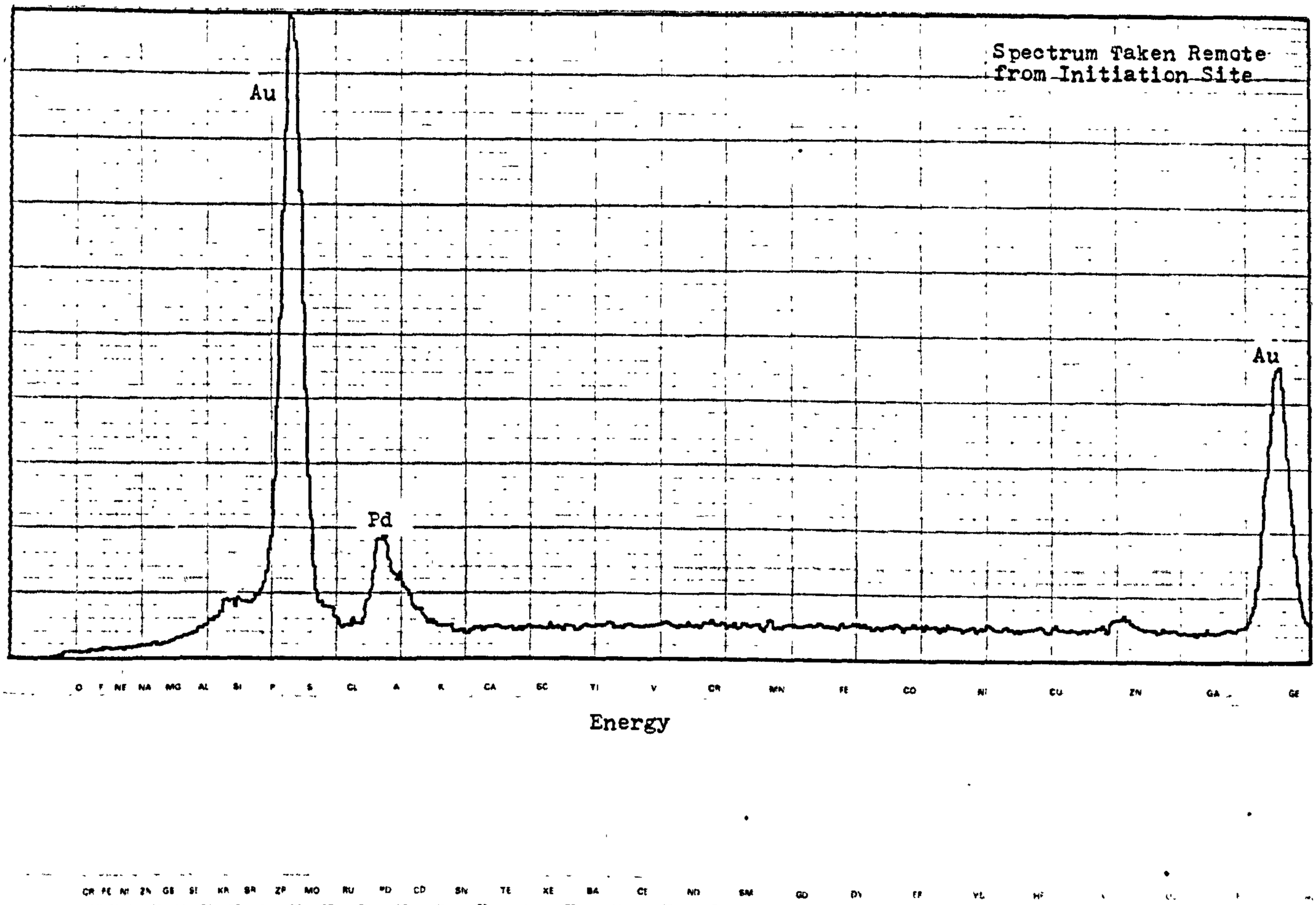

FIGURE 4.46 Energy dispersive x-ray spectra of a calcium rich crack initiating particle in HDPE 1 63mm OD SDR 11 pipe.

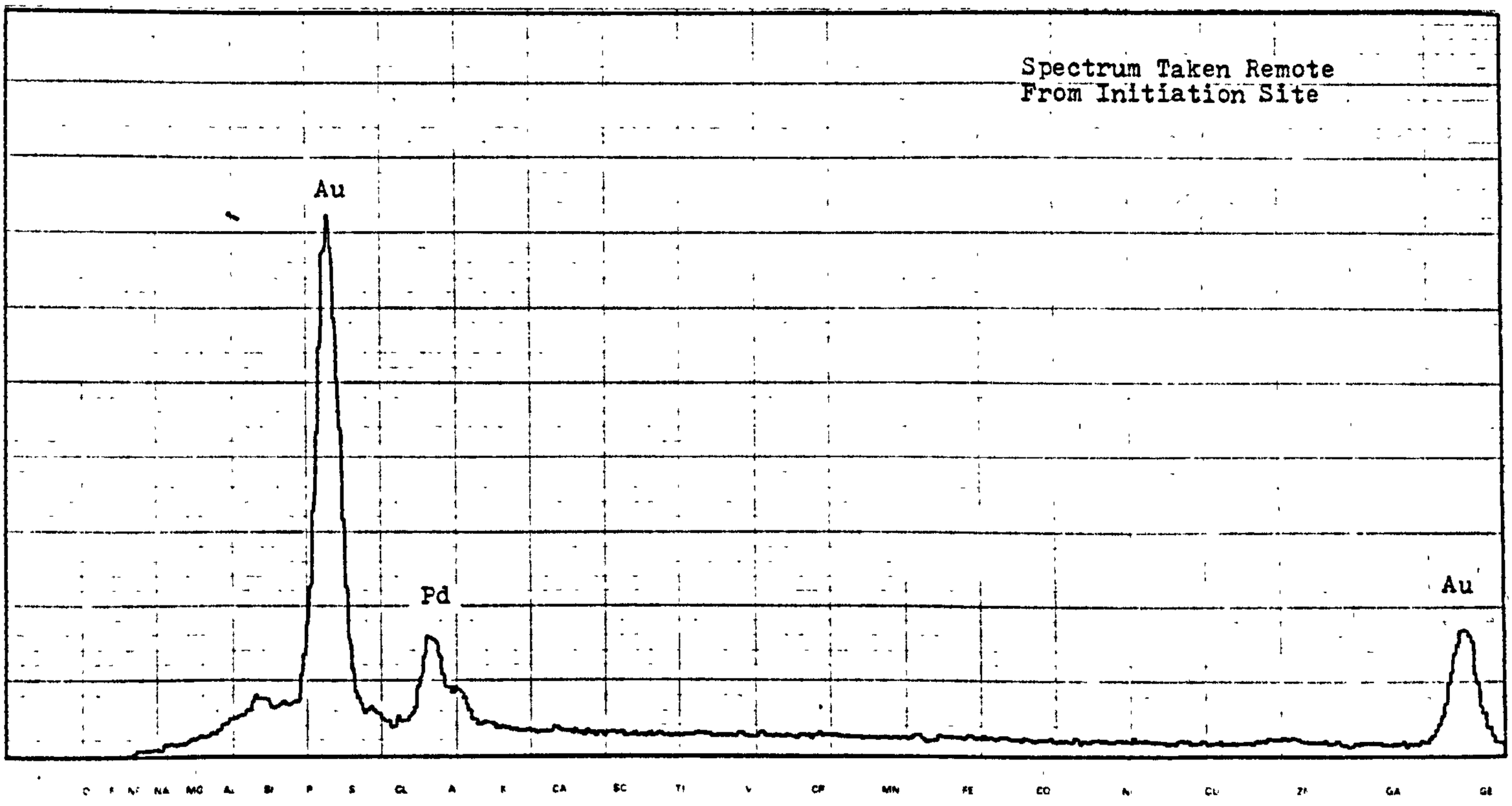

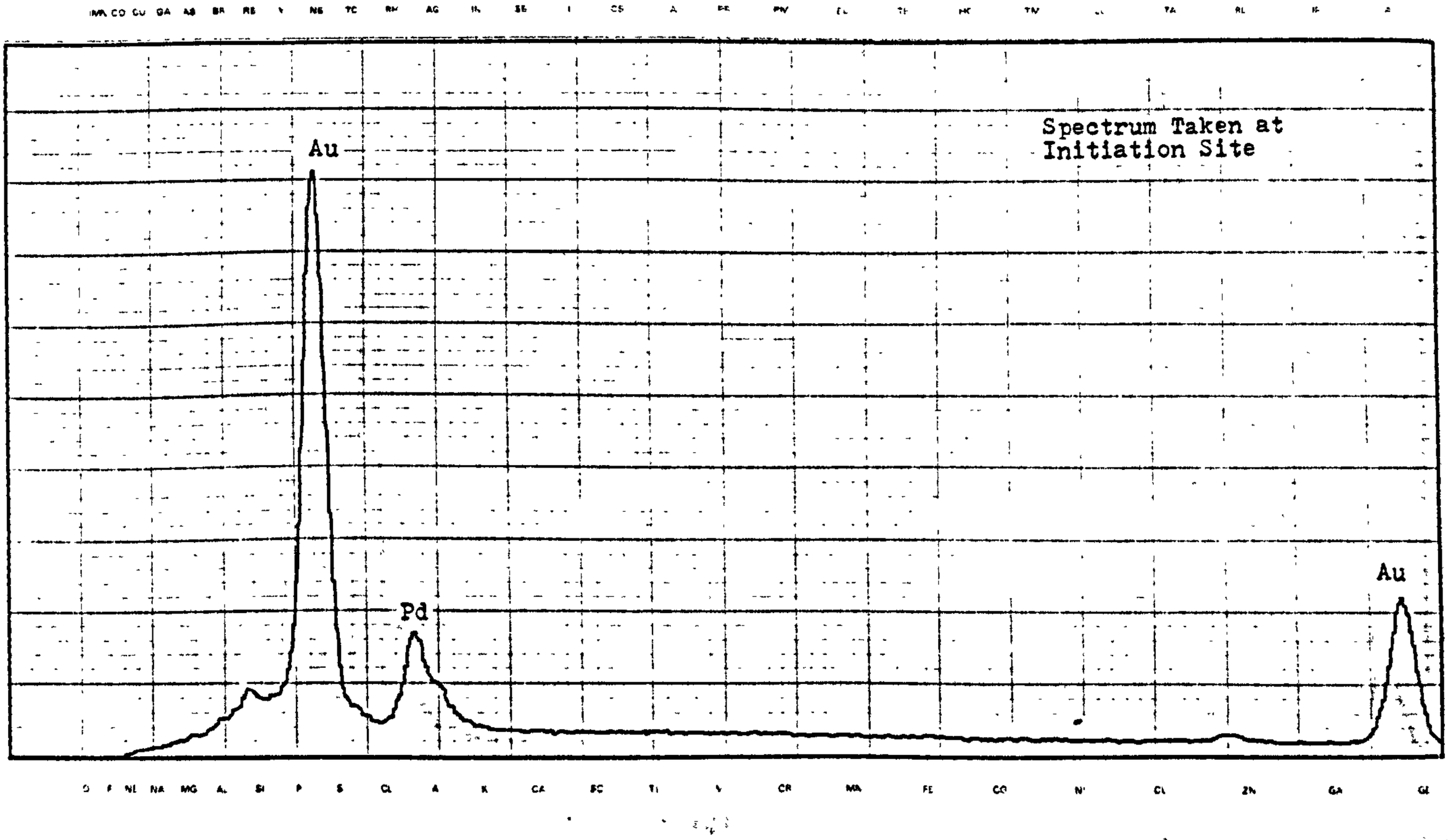

FIGURE 4.47 Energy dispersive x-ray spectra of a crack initiating particle in an HDPE 1 63mm OD SDR 11 pipe. No elements were detected apart from the gold/palladium alloy used to coat the surface of non-conducting specimens.

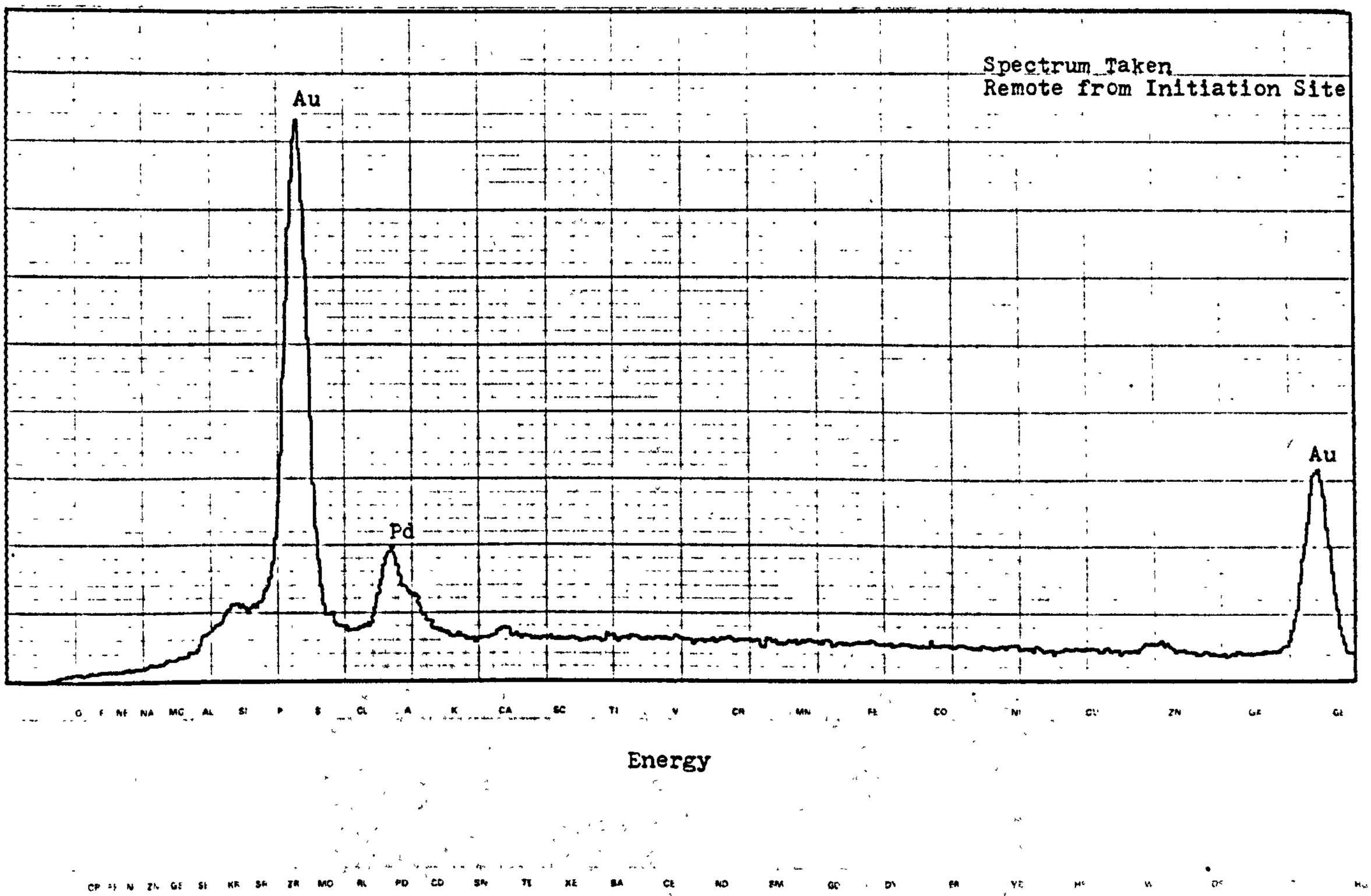

FIGURE 4.48 Energy dispersive x-ray spectra of a fibrous crack initiating particle in HDPE 1 63mm OD SDR 11 pipe.

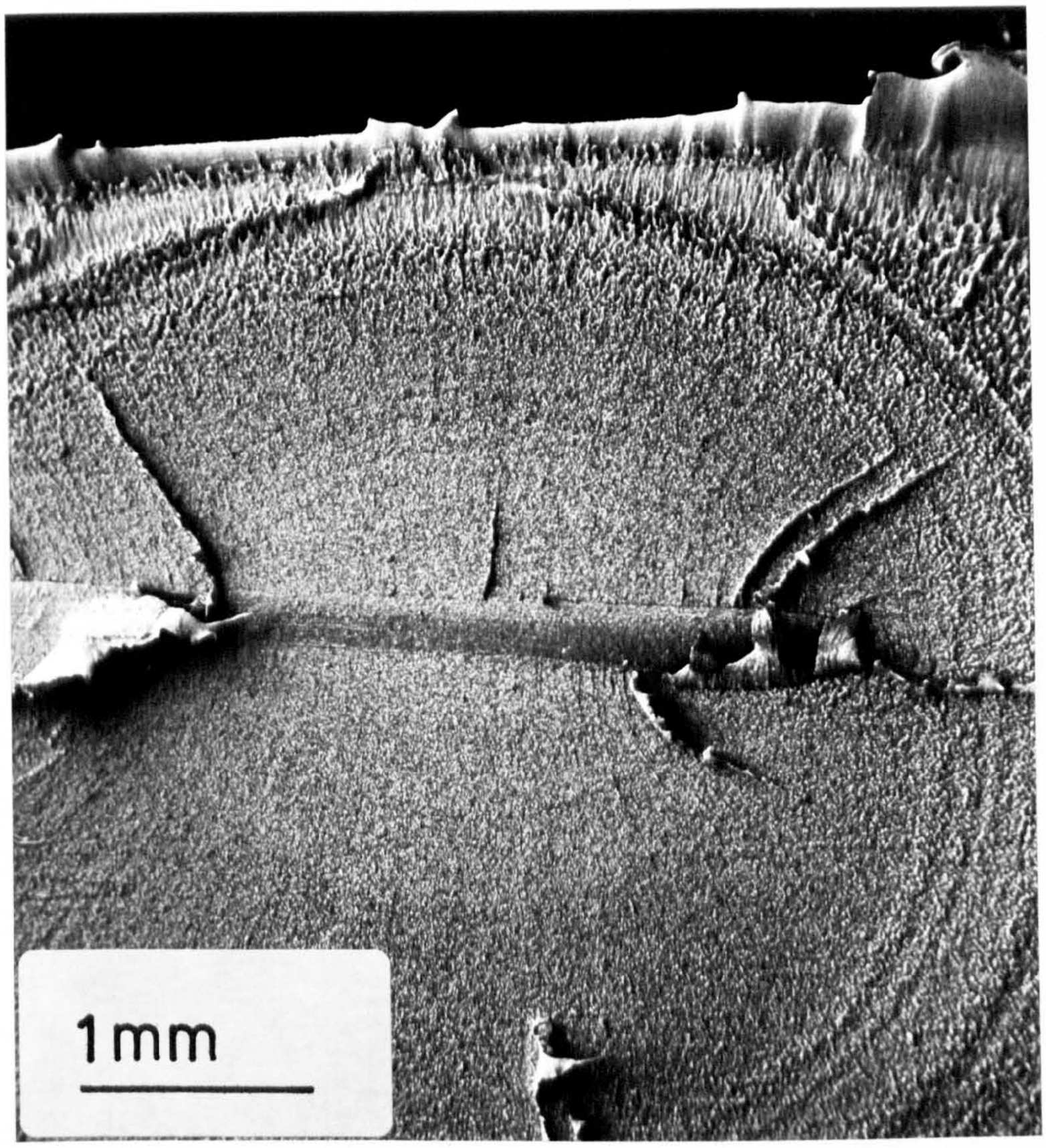

Main constituent - Cl

FIGURE 4.49 Fibrous crack initiating particle in an HDPE 1 pipe.
(See Figure 4.48)

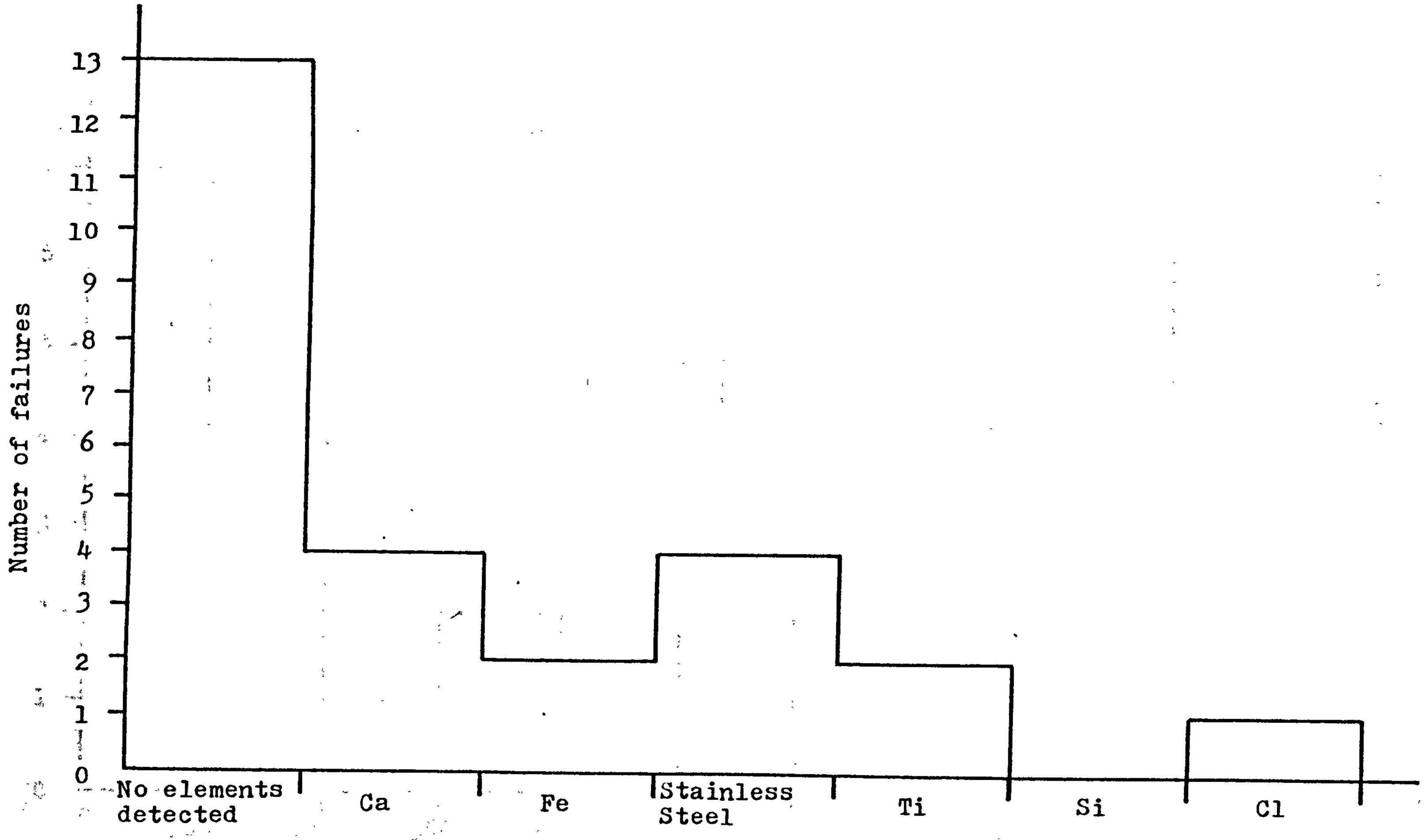

FIGURE 4.50 Main constituents of inclusions leading to fractures in HDPE 1 63mm OD SDR 11 pipes.

Size Range μm	HDPE 2 Inclusion Size μm	Number of Failures
0 - 100	44, 43, 40, 43, 62, 85, 68	7
101 - 200	112, 120, 120, 132	4
201 - 300	240	1
301 - 400	303, 303	2
401 - 500		0
501 - 600	524, 506	2

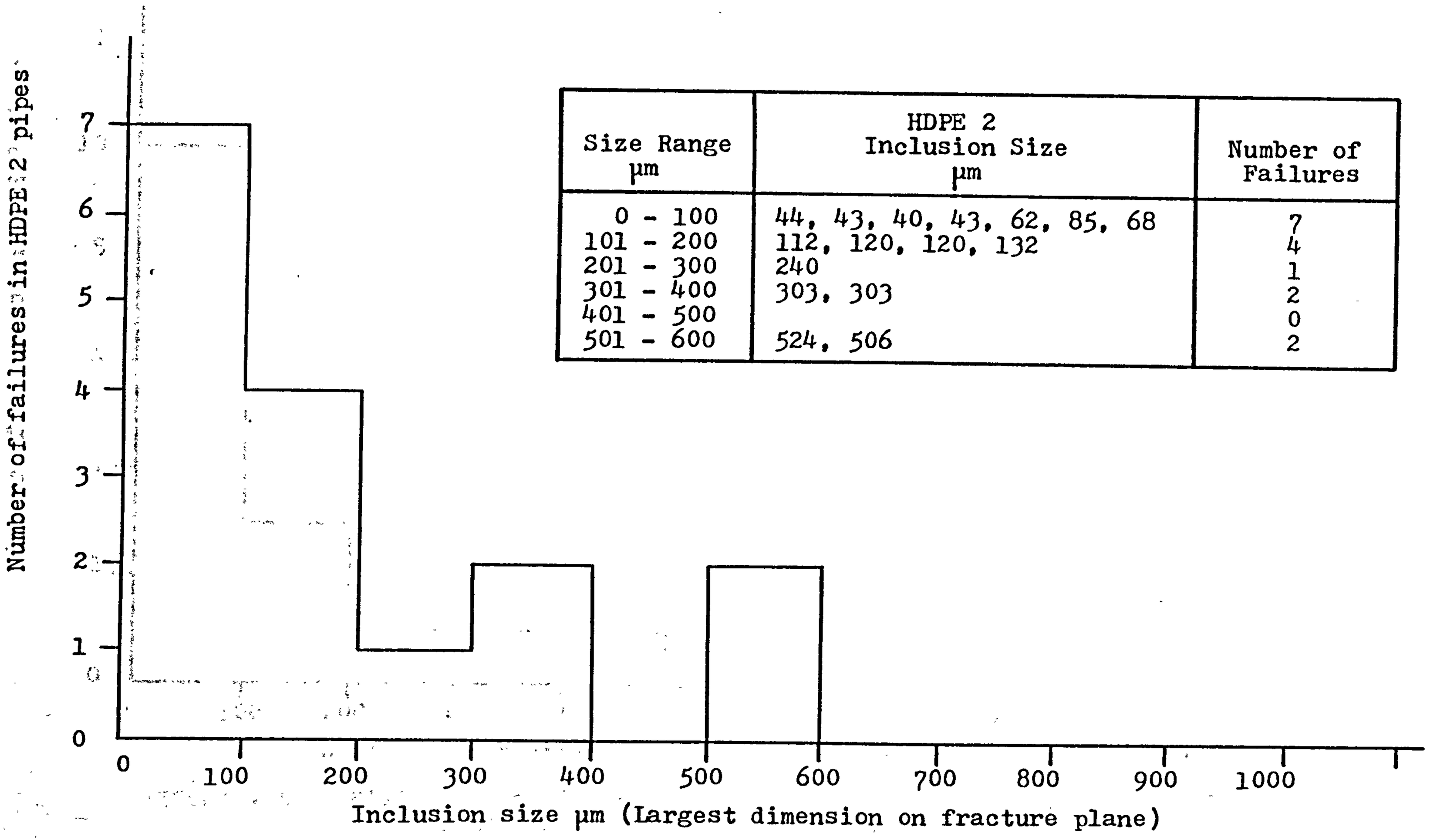

FIGURE 4.51 Histogram of inclusion sizes at fracture initiation sites in HDPE 2 pipe systems. (Failures P1, P/P1, B1, T1)

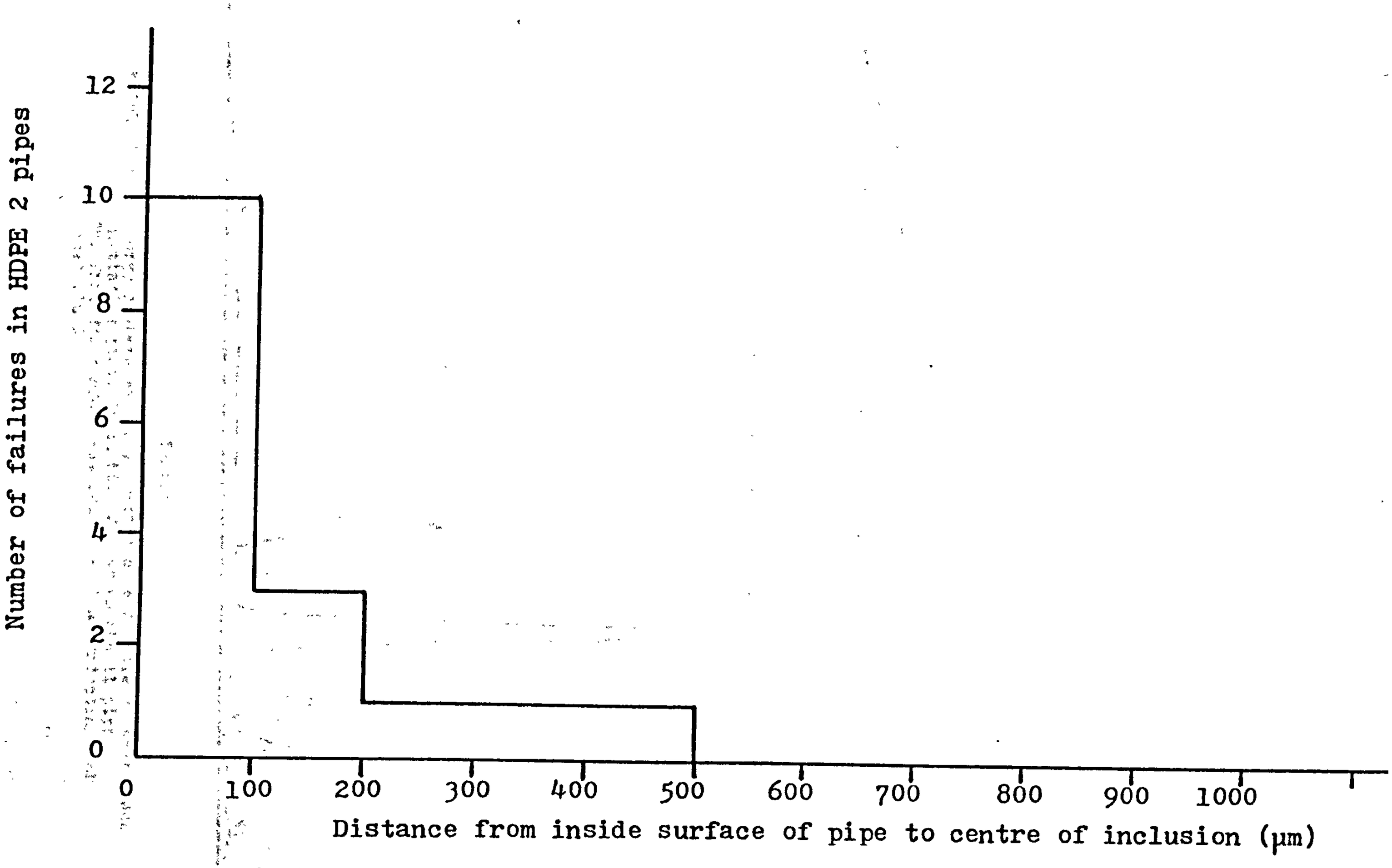

FIGURE 4.52 Histogram of distances from the pipe inside wall of inclusions leading to fracture in HDPE 2 pipes.

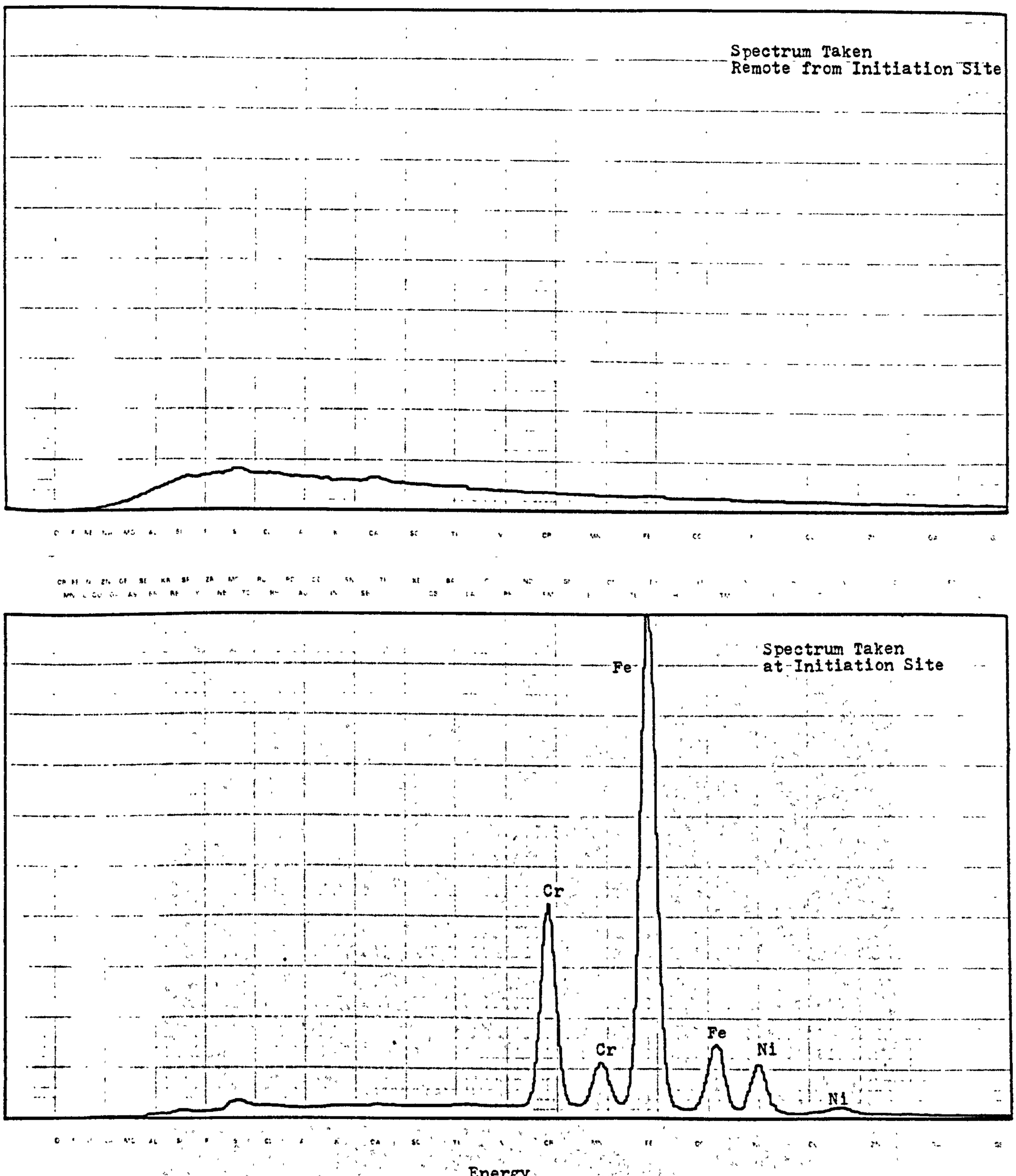

FIGURE 4.53 Energy dispersive x-ray spectra of a stainless steel crack initiating particle in HDPE 2 63mm OD SDR 11 pipe.
The fracture surface was coated with a conducting hydrocarbon based fluid.

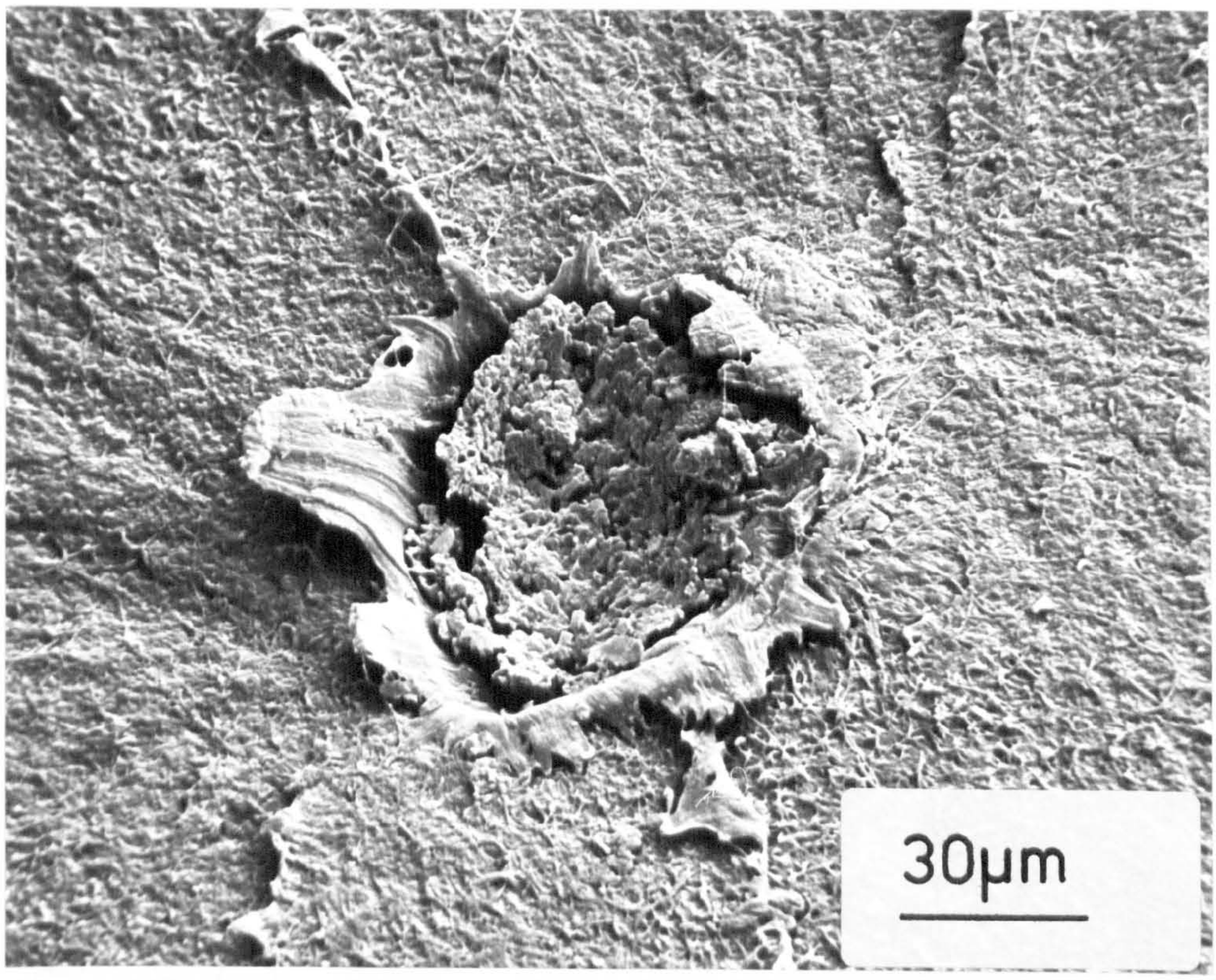

Main constituents - Fe, Cr, Ni, (304 stainless steel)
(see Figure 4.53)

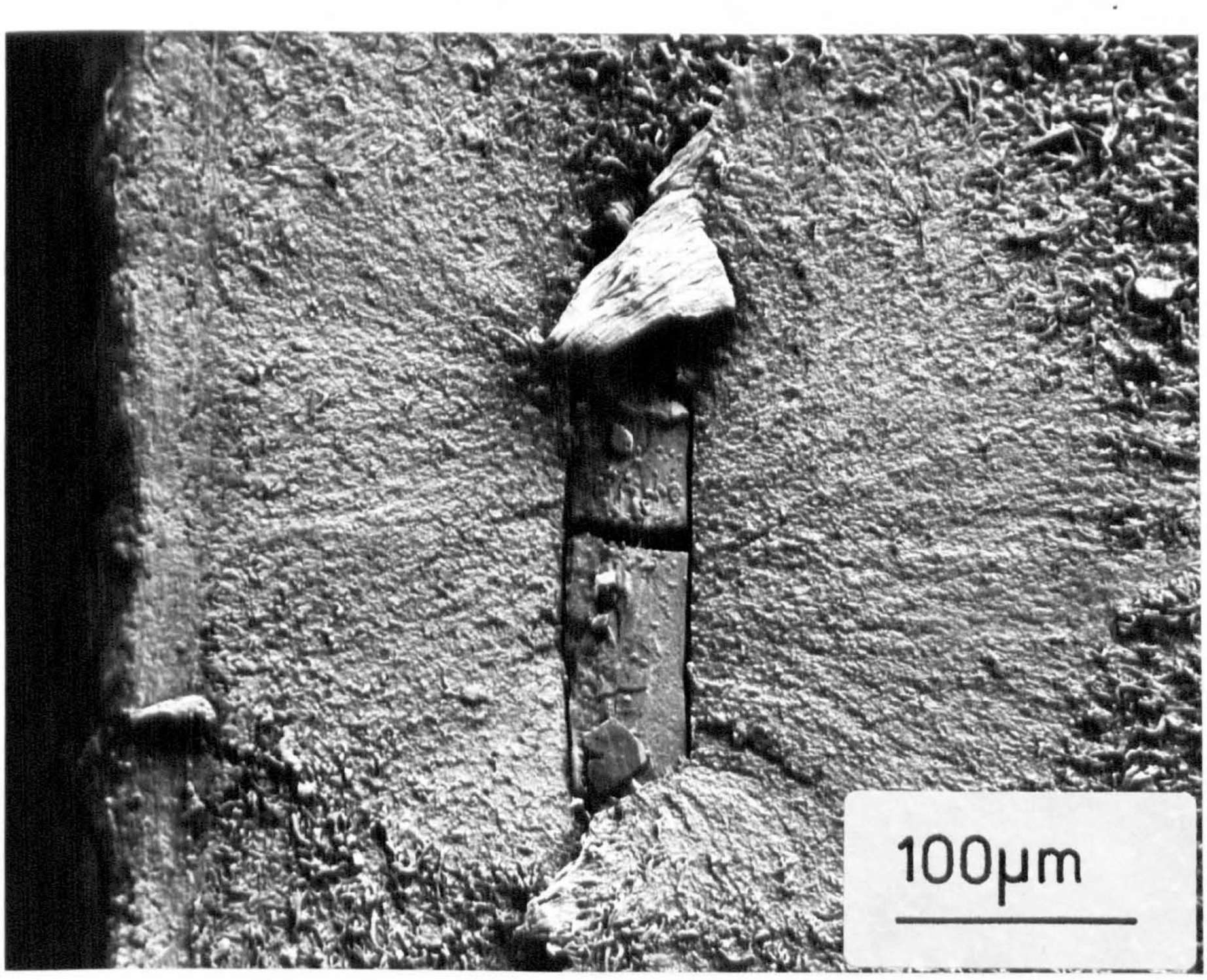

Main constituents - Fe, Cr, Ni, Mo (316 stainless steel)

FIGURE 4.53a Examples of metallic crack initiating particles in HDPE 2 pipes.

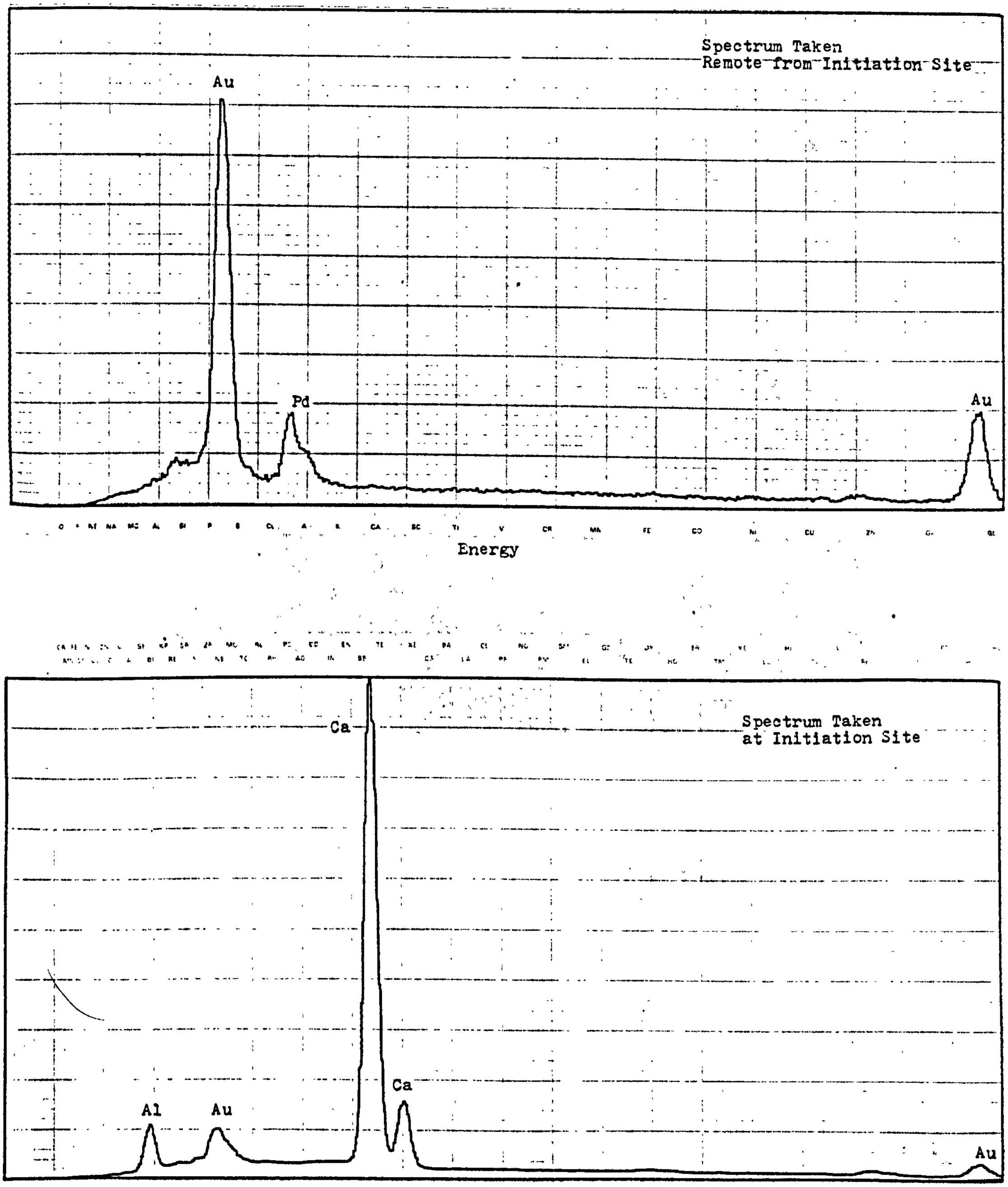

FIGURE 4.54 Energy dispersive x-ray spectra of a calcium rich crack initiating particle in HDPE 2 63mm OD SDR 11 pipe.

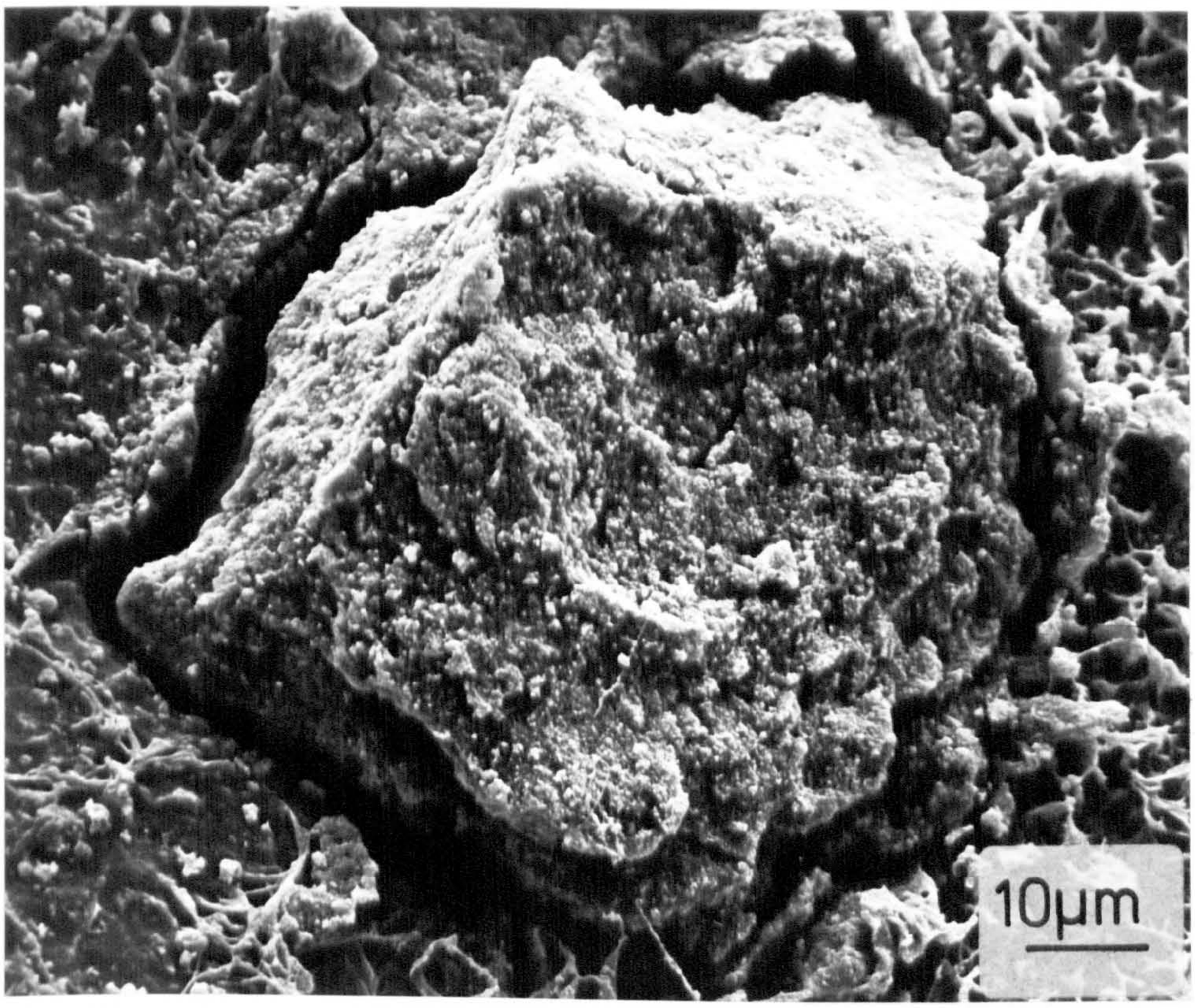

FIGURE 4.54a Example of a calcium rich crack initiating particle in an HDPE 2 pipe.
(See Figure 4.54)

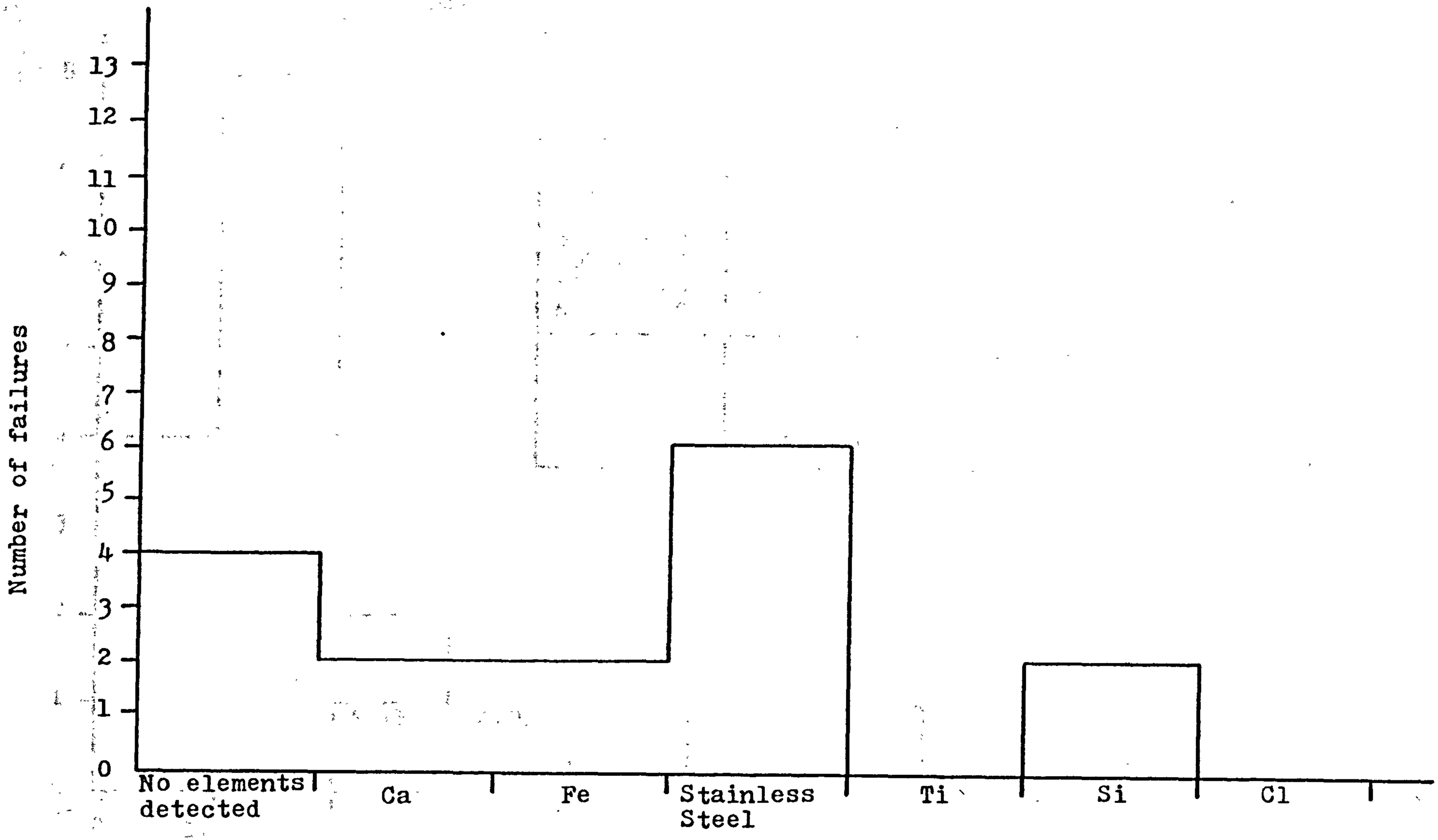

FIGURE 4.55 Main constituents of inclusions leading to fractures in HDPE 2 63mm OD SDR 11 pipes.

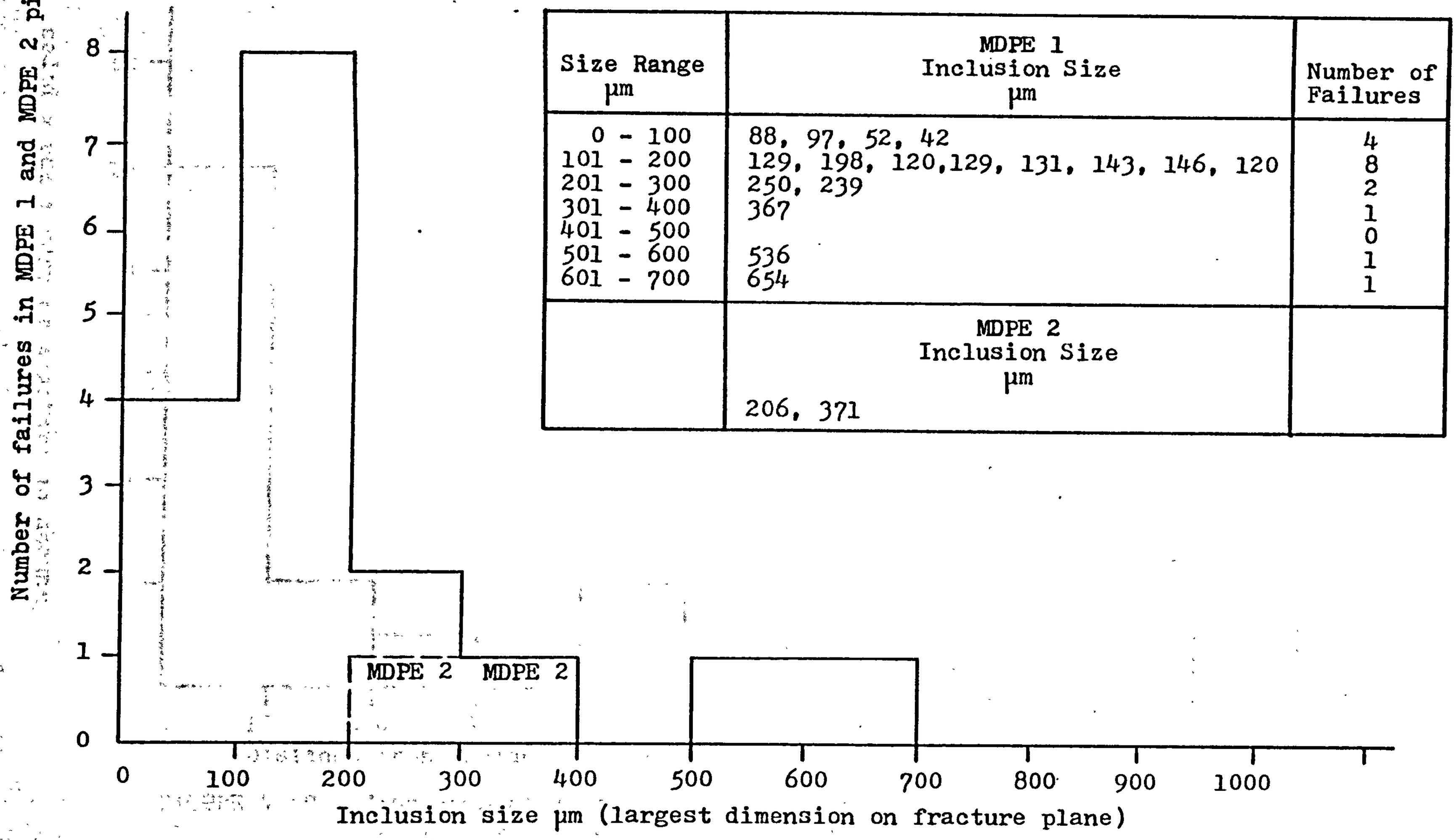

Size Range μm	MDPE 1 Inclusion Size μm	Number of Failures
0 - 100	88, 97, 52, 42	4
101 - 200	129, 198, 120,129, 131, 143, 146, 120	8
201 - 300	250, 239	2
301 - 400	367	1
401 - 500		0
501 - 600	536	1
601 - 700	654	1
	MDPE 2 Inclusion Size μm	
	206, 371	

FIGURE 4.56 Histogram of inclusion sizes at fracture initiation sites in MDPE 1 and MDPE 2 pipe systems. (Failures P1, P/P1, B1, T1)

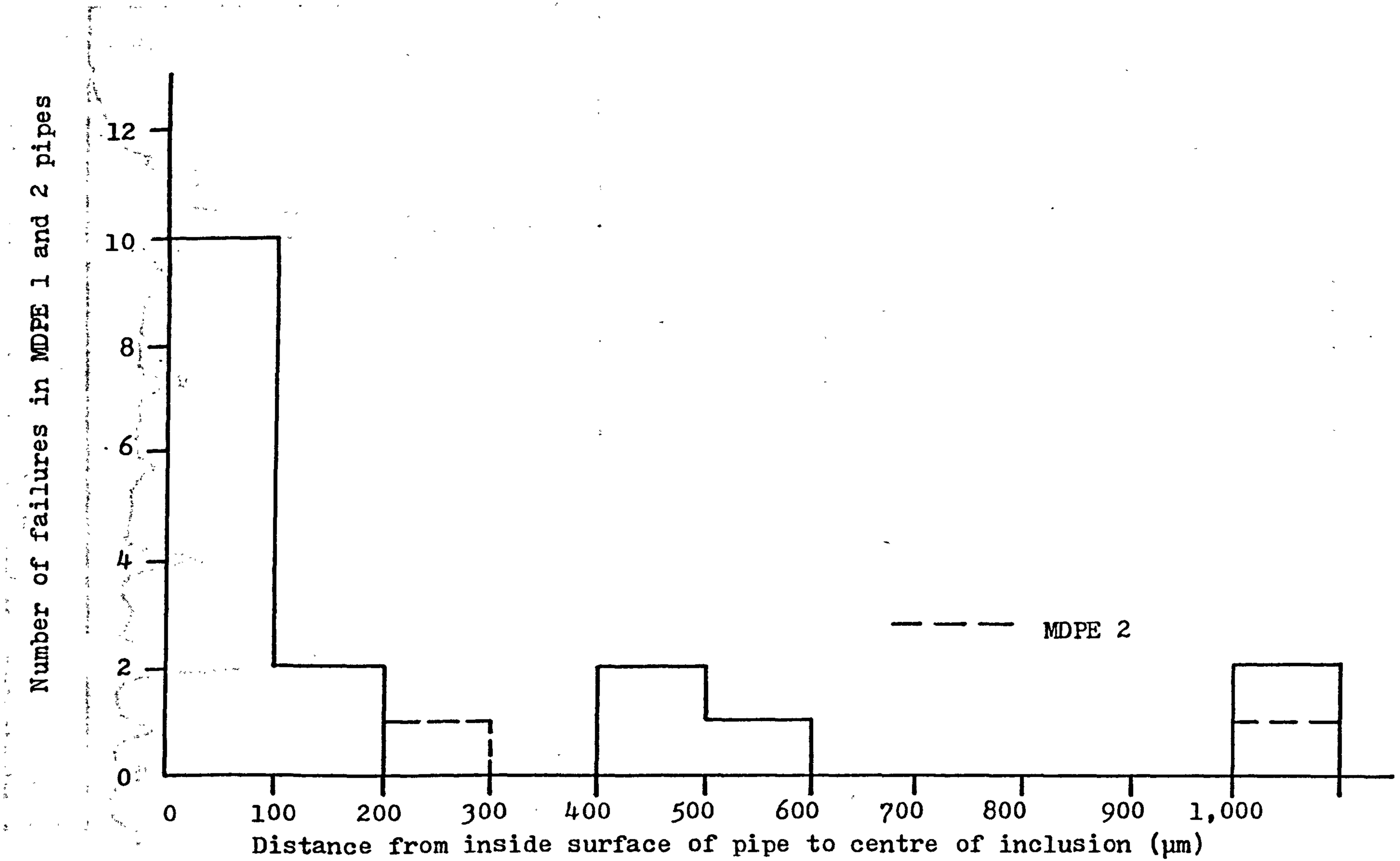

FIGURE 4.57 Histogram of distances from the pipe inside wall of inclusions leading to fracture in MDPE 1 and MDPE 2 pipes.

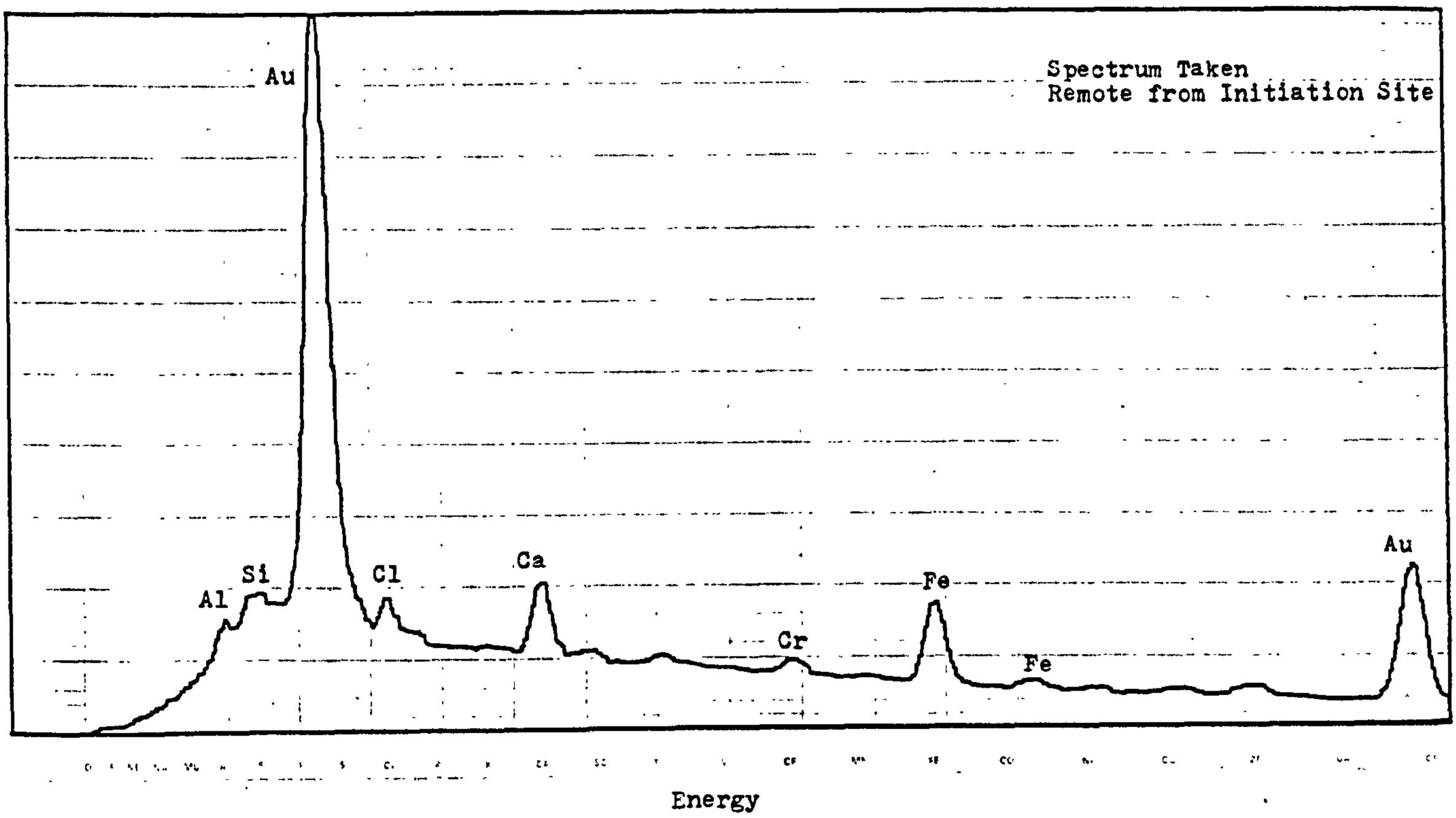

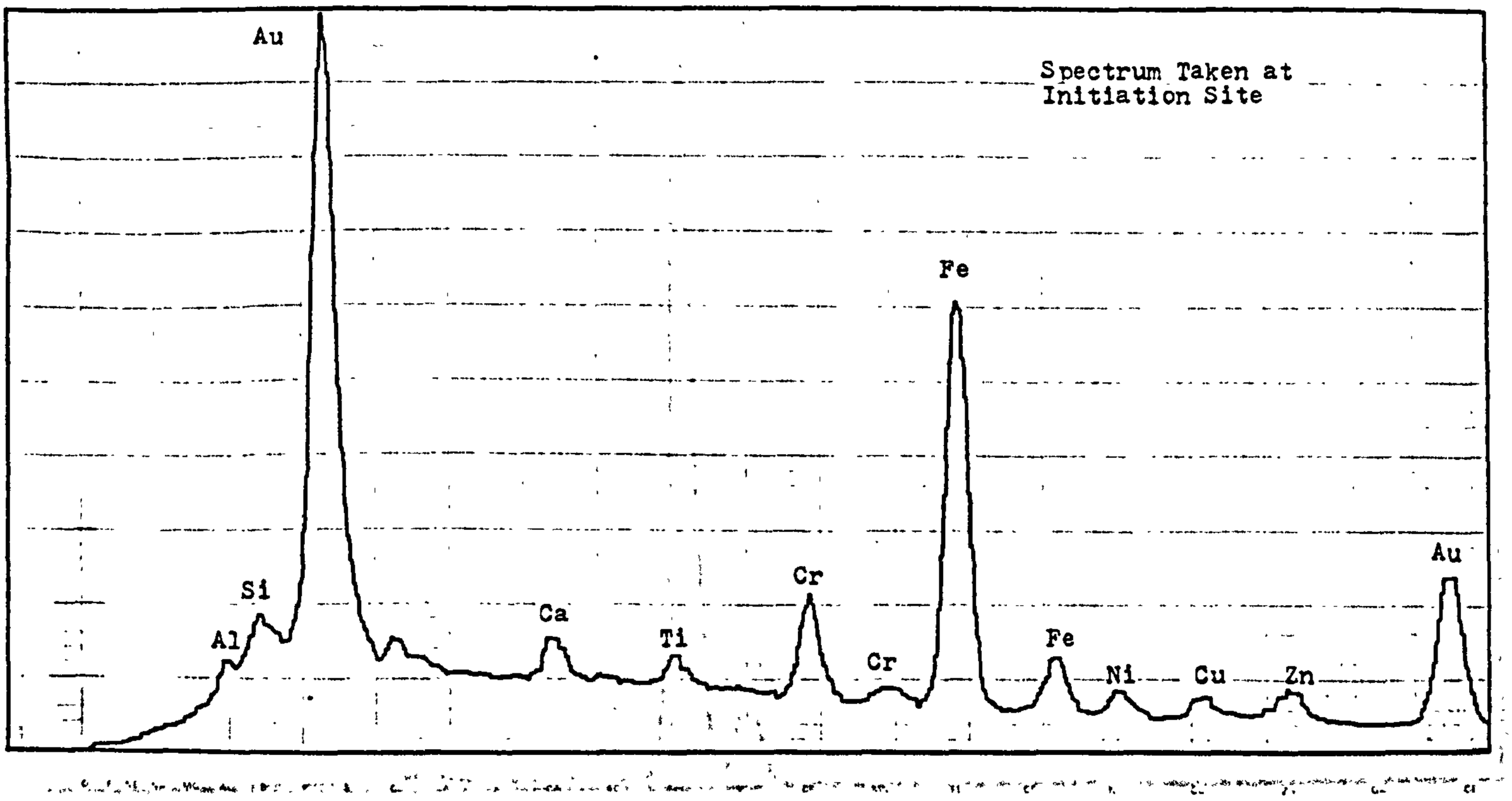

FIGURE 4.58a Energy dispersive x-ray spectra of a mainly stainless steel crack initiating particle in MDPE 1 60mm OD SDR 11 pipe. Only gold was used to coat the sample in this case.

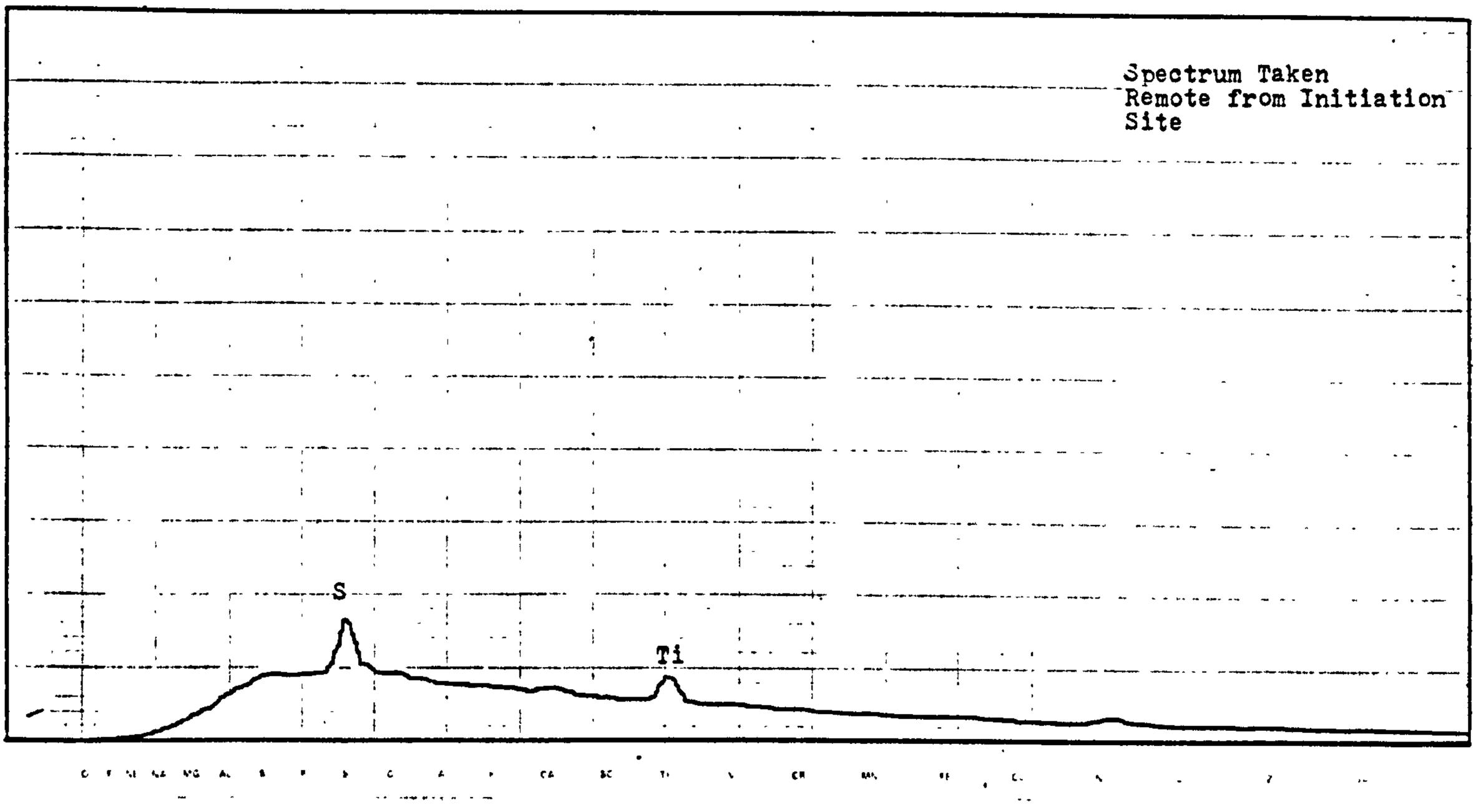

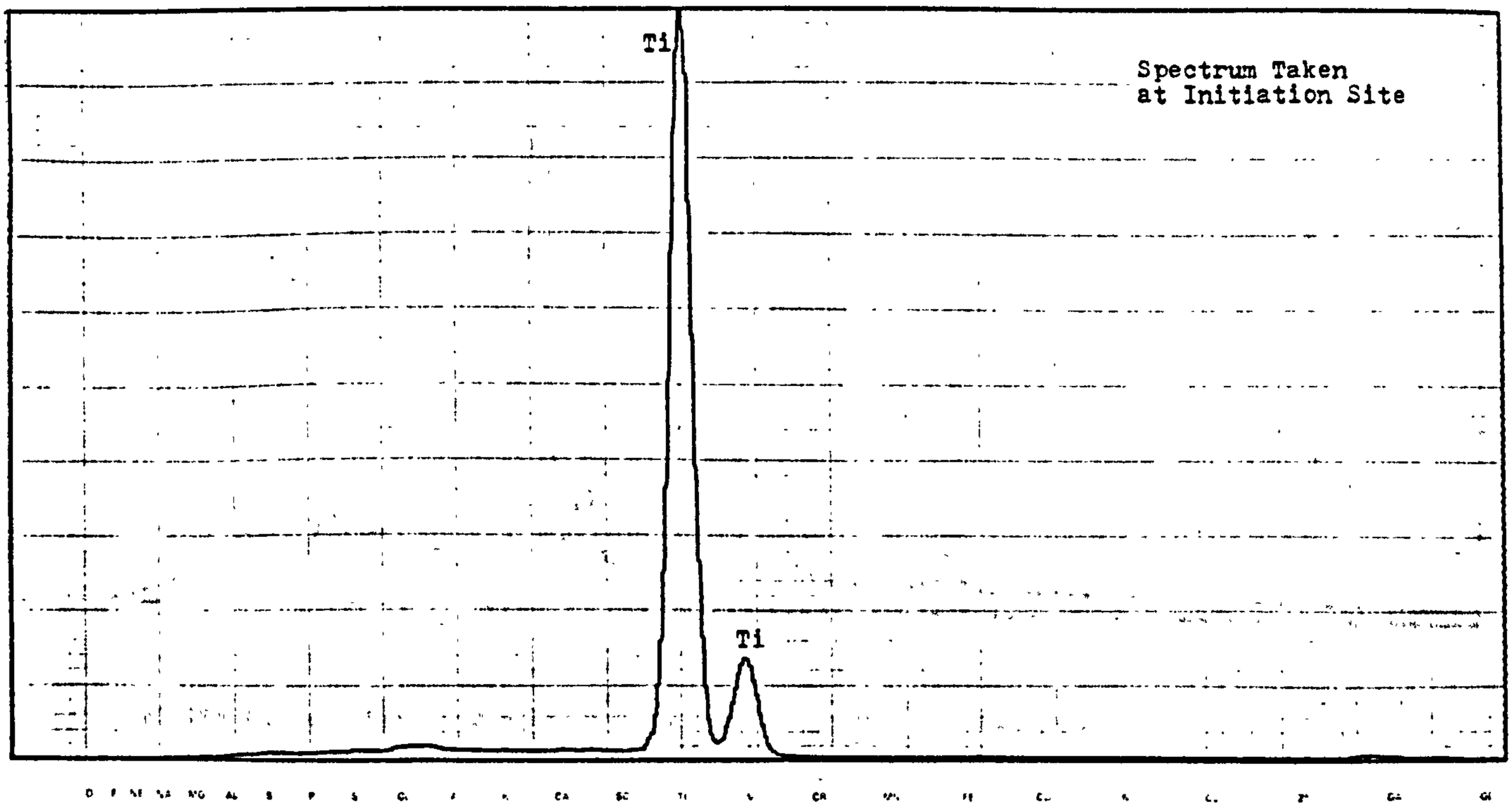

FIGURE 4.58b Energy dispersive x-ray spectra of a titanium crack initiating particle in MDPE 1 60mm OD SDR 11 pipe. The fracture surface was coated with a conducting hydrocarbon based fluid.

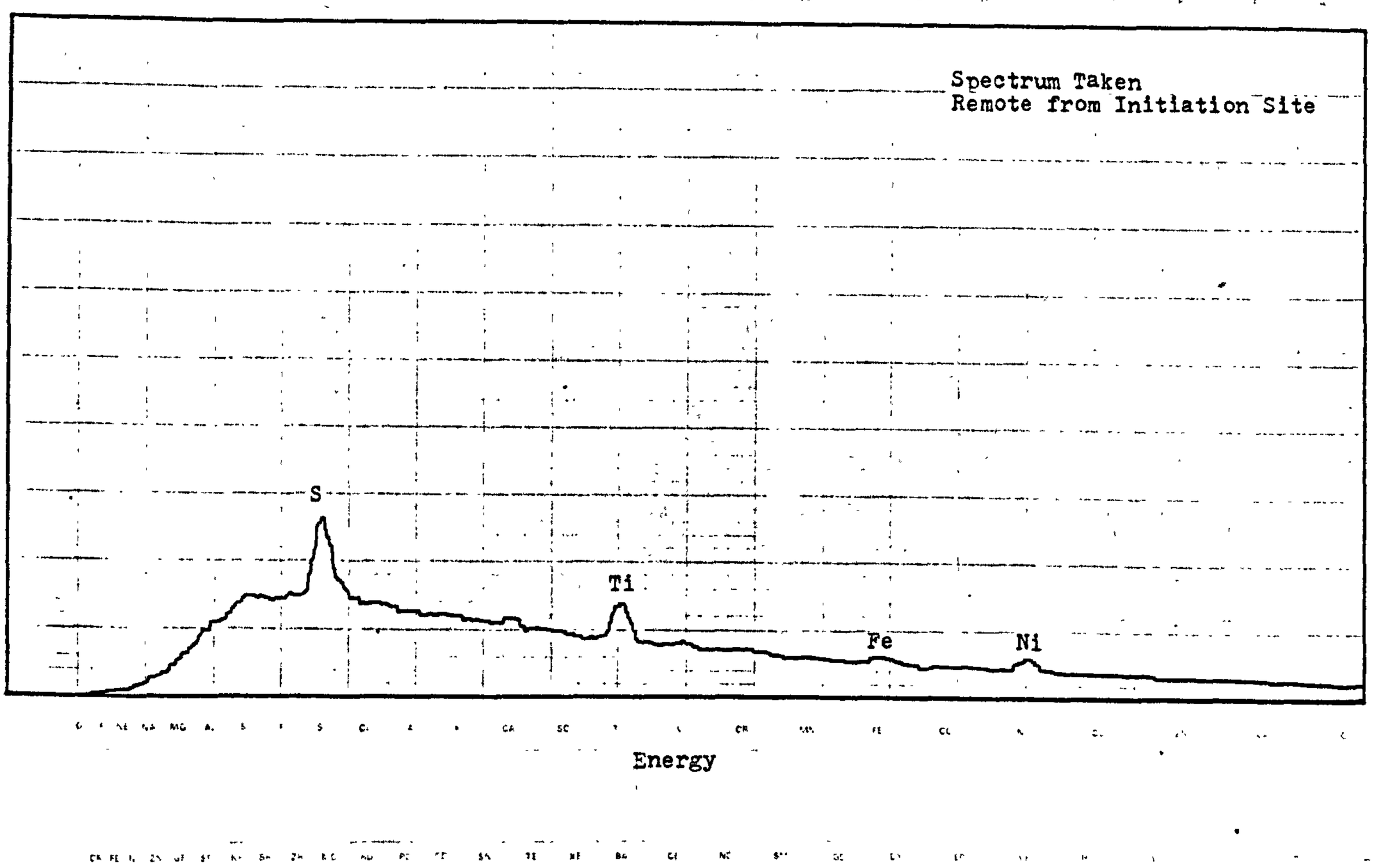

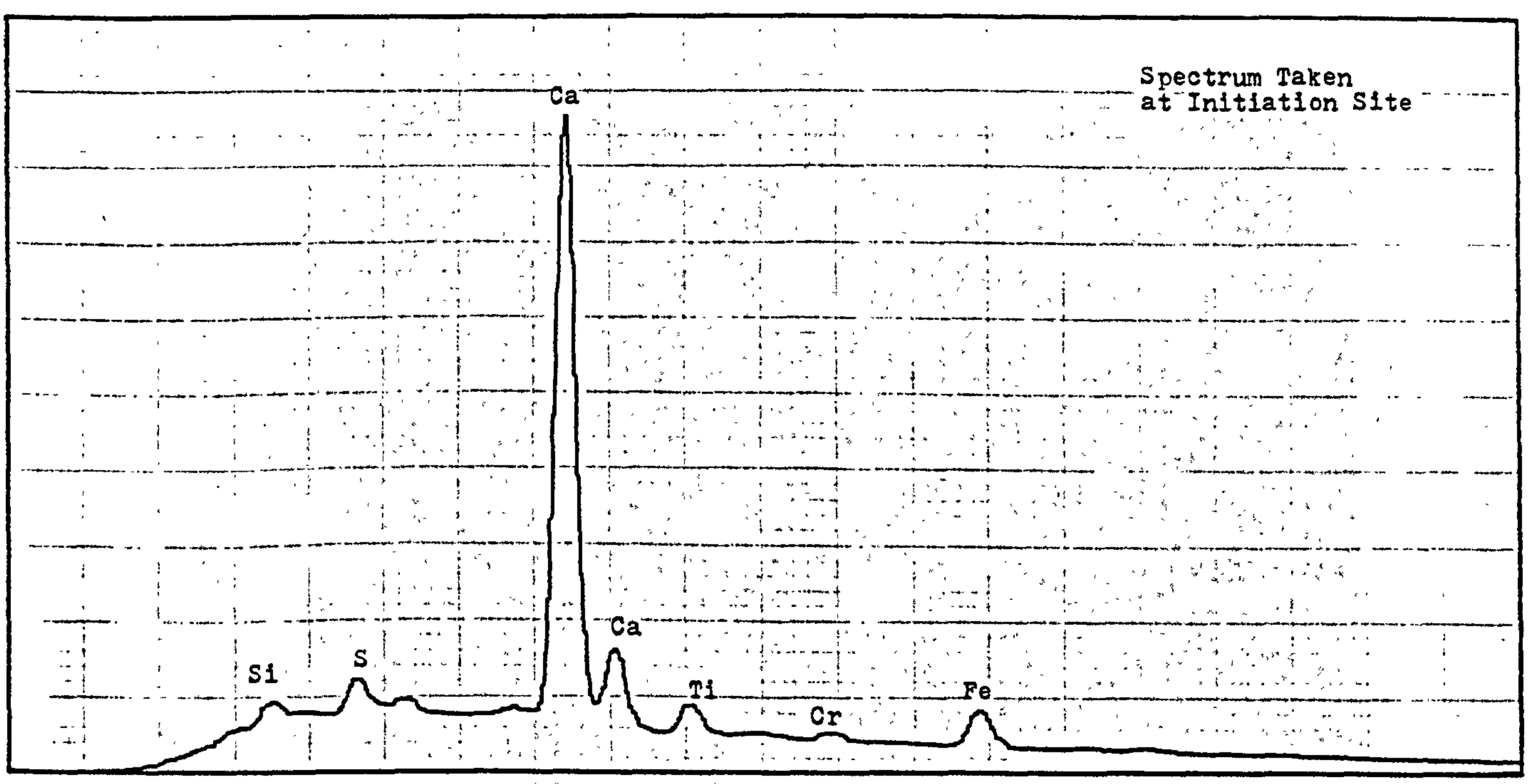

FIGURE 4.58c Energy dispersive x-ray spectra of a calcium rich crack initiation particle in MDPE 1 60mm OD SDR 11 pipe.

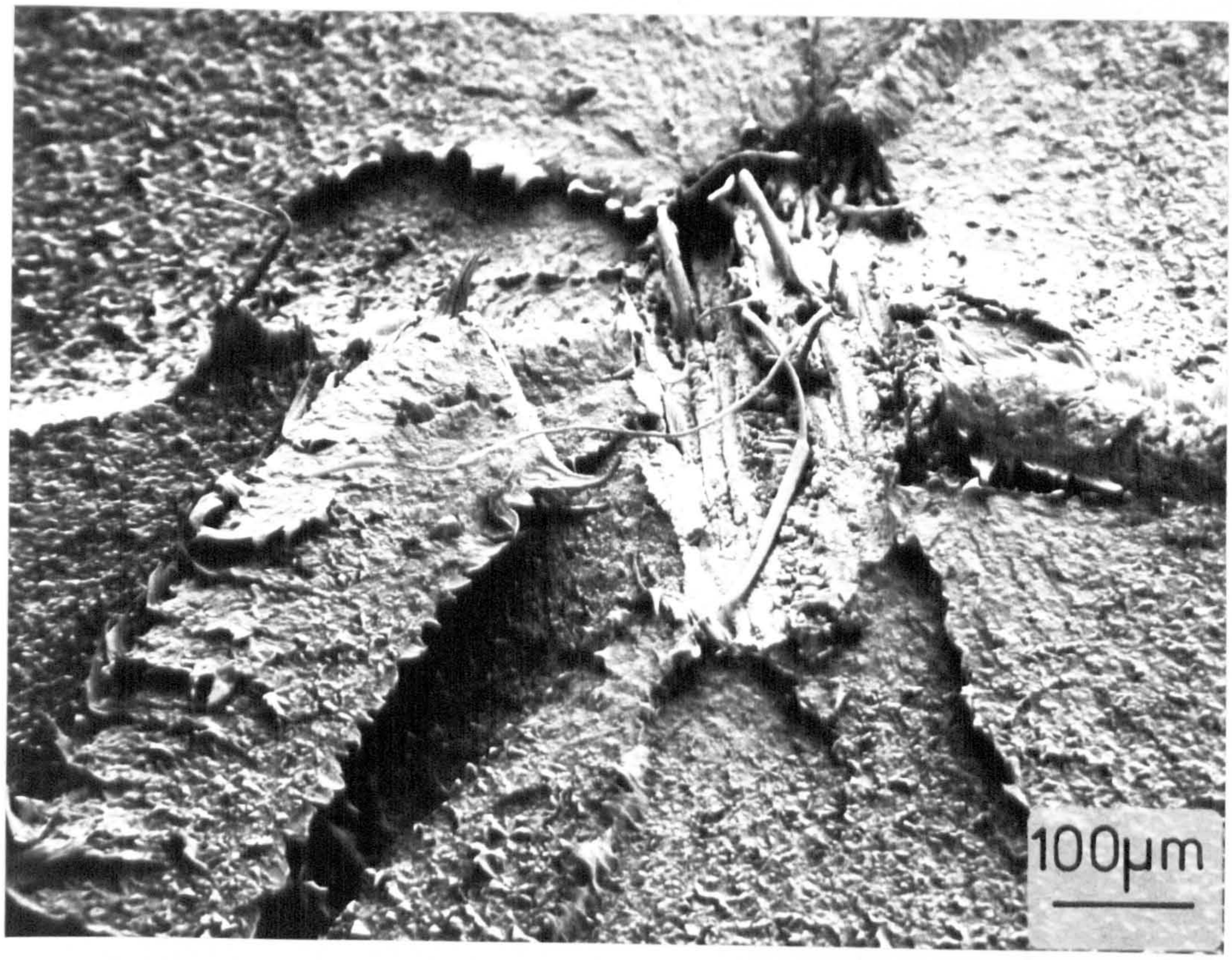

FIGURE 4.59a Crack initiating particle in an MDPE 1 pipe. No elements were detected using the EDAX technique.

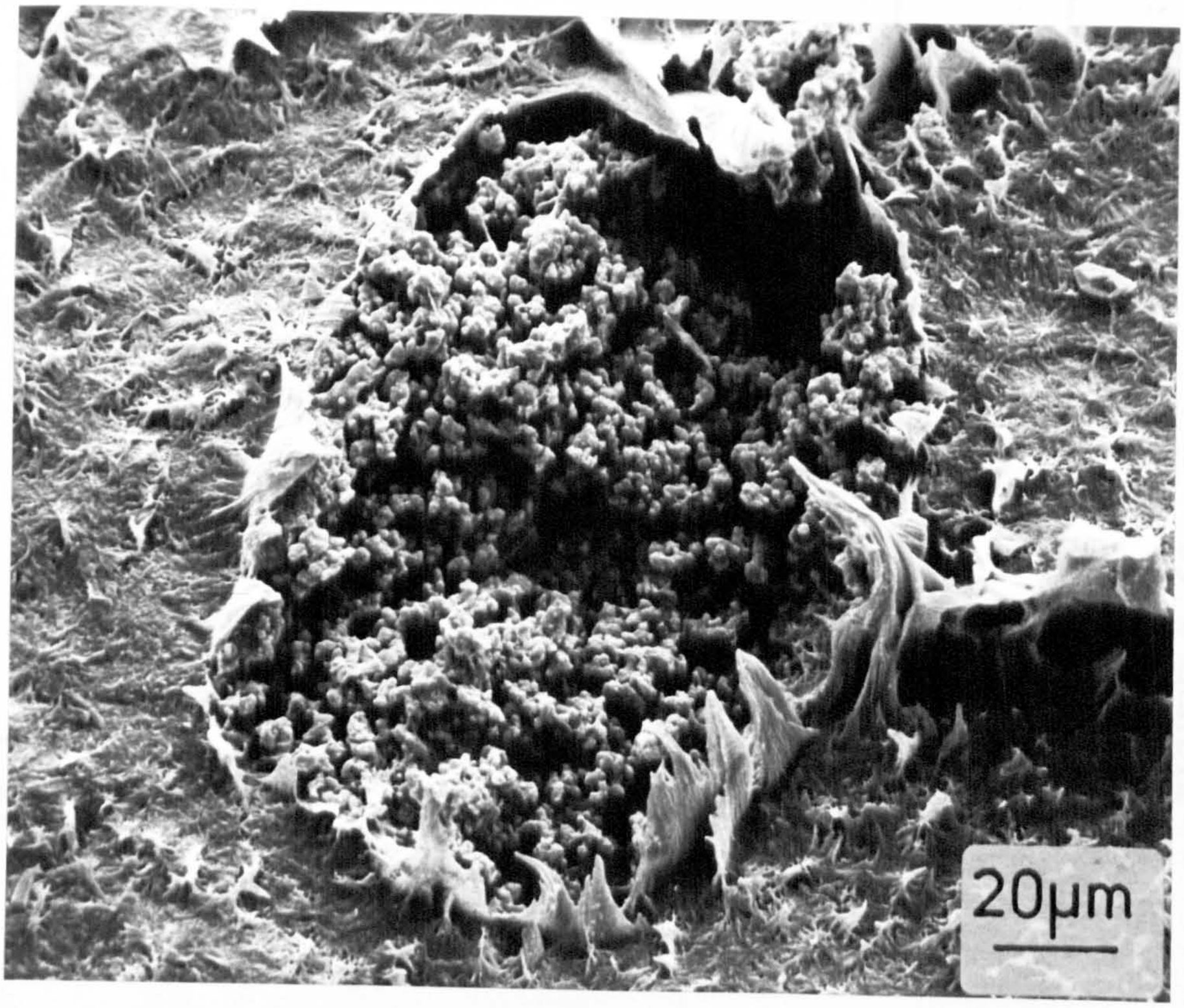

FIGURE 4.59b Example of a titanium rich crack initiating particle in an MDPE 1 pipe. (See Figure 4.58)

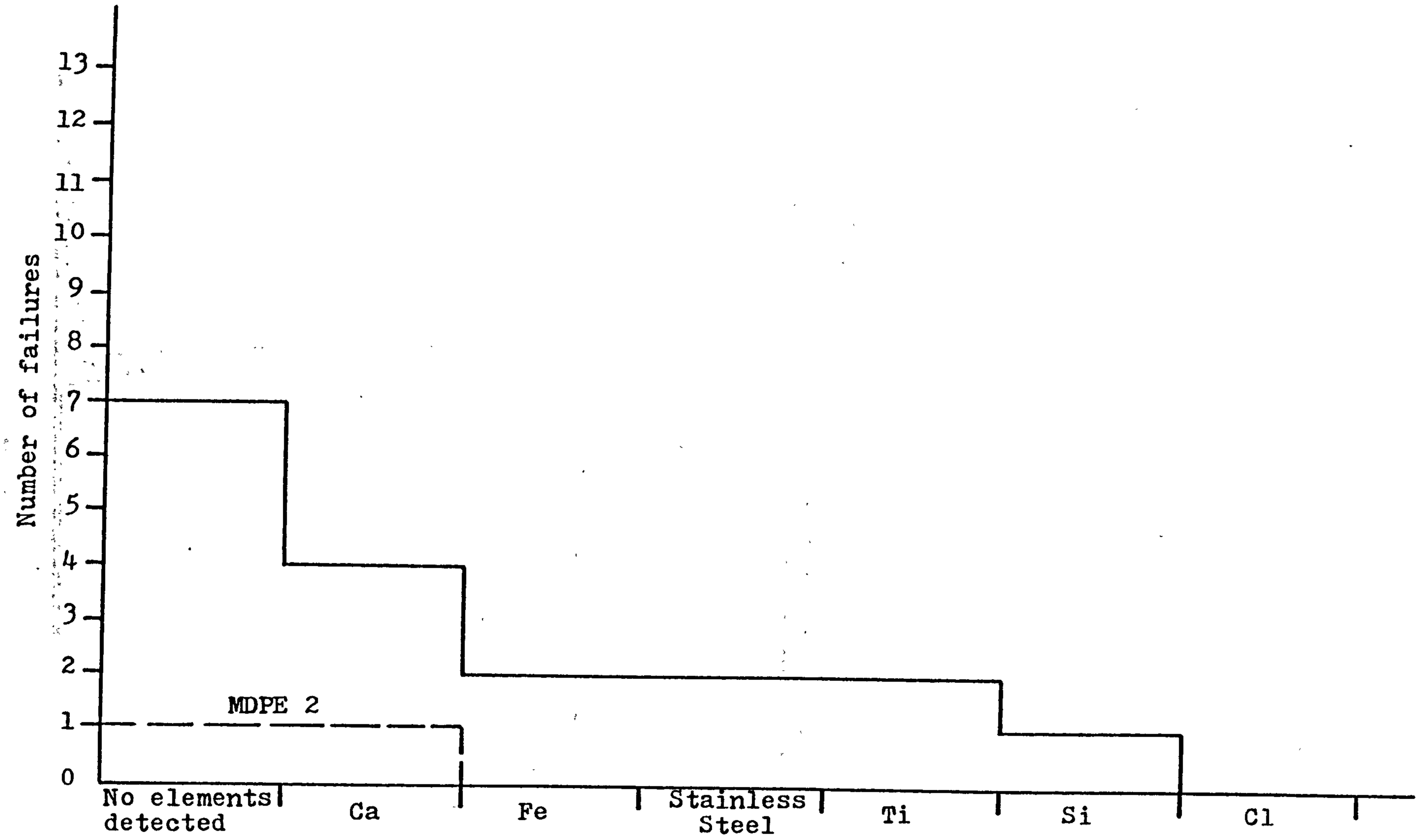

FIGURE 4.60 Main constituents of inclusions leading to fractures in MDPE 1 60mm OD SDR 11 pipes and MDPE 2 63mm OD SDR 11 pipes.

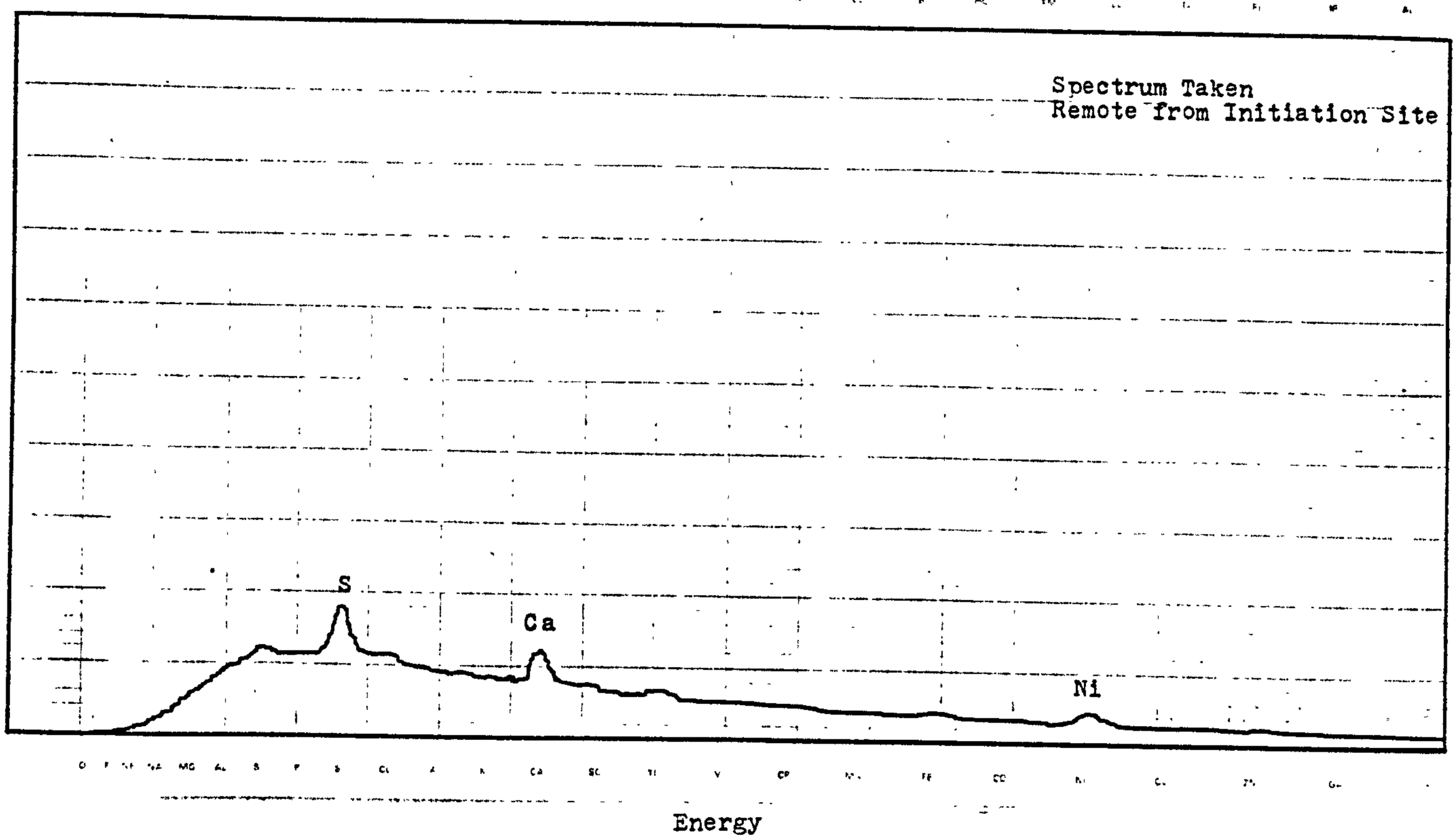

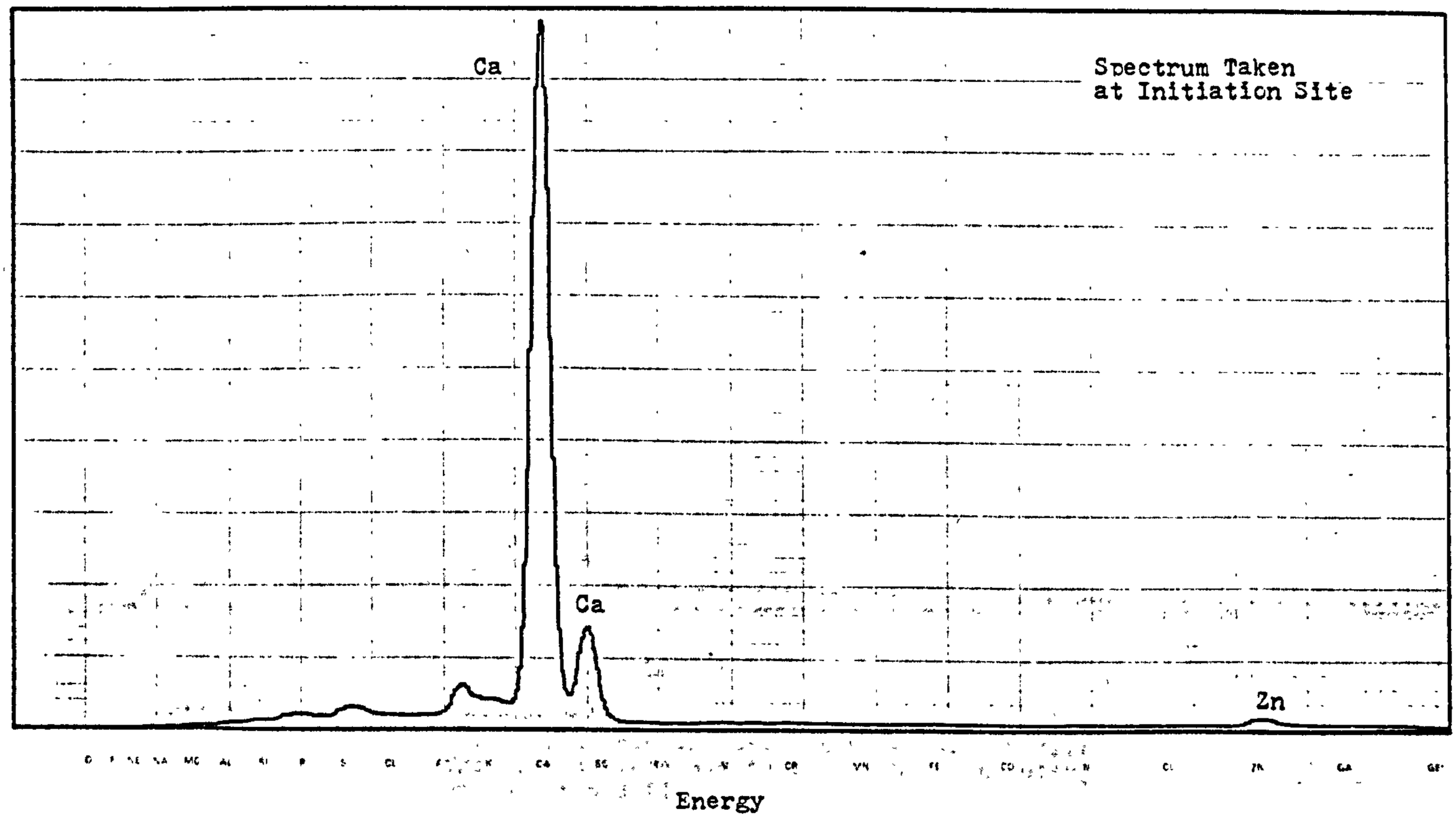

FIGURE 4.61a Energy dispersive x-ray spectra of a calcium rich crack initiation particle in MDPE 2 63mm OD SDR 11 pipe.. The fracture surface was coated with a conducting hydrocarbon based fluid.

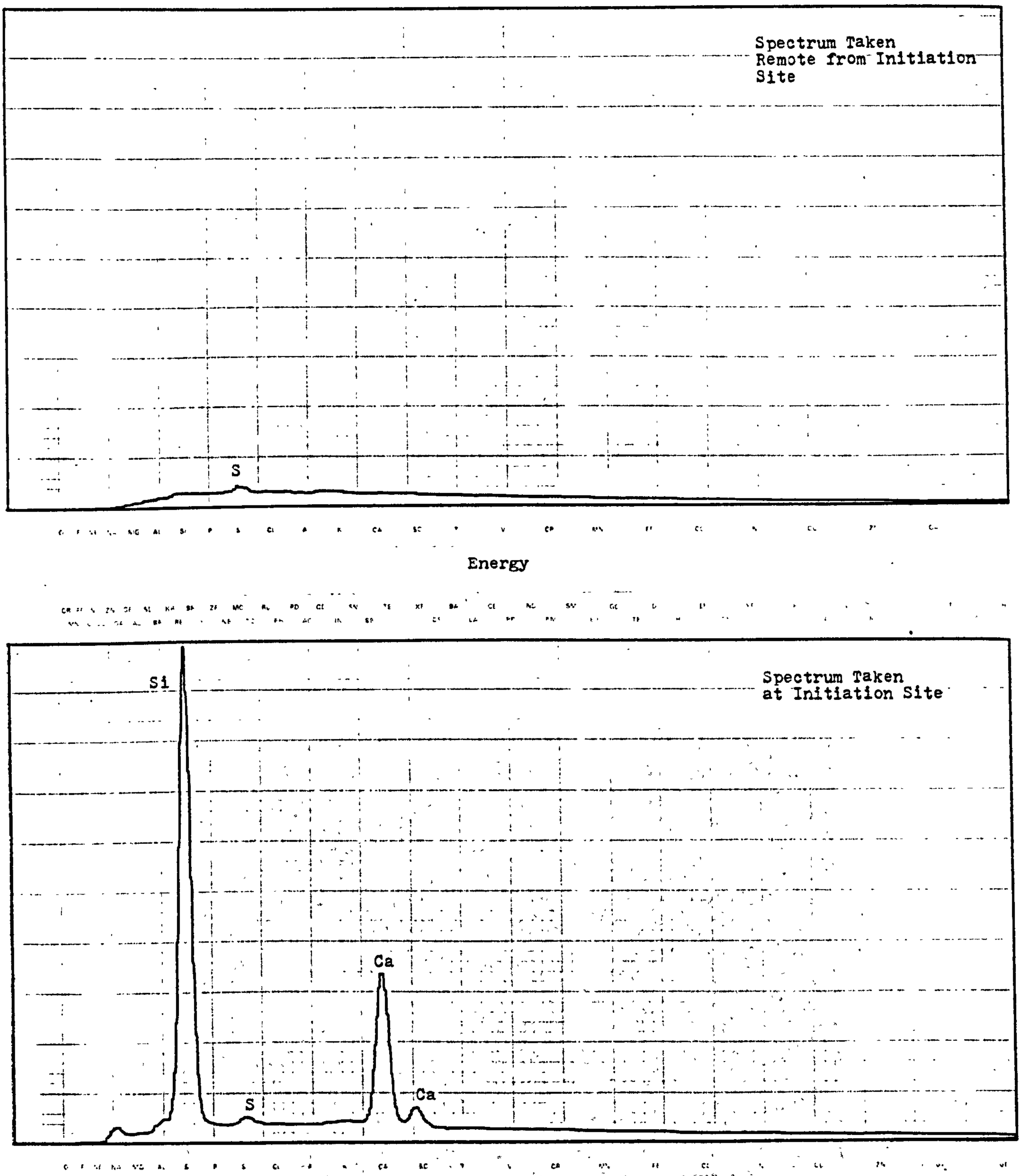

FIGURE 4.61b Energy dispersive x-ray spectra of a silicon rich crack initiating particle in MDPE 2 63mm OD SDR 11 pipe. The fracture surface was coated with a conducting hydrocarbon based fluid.

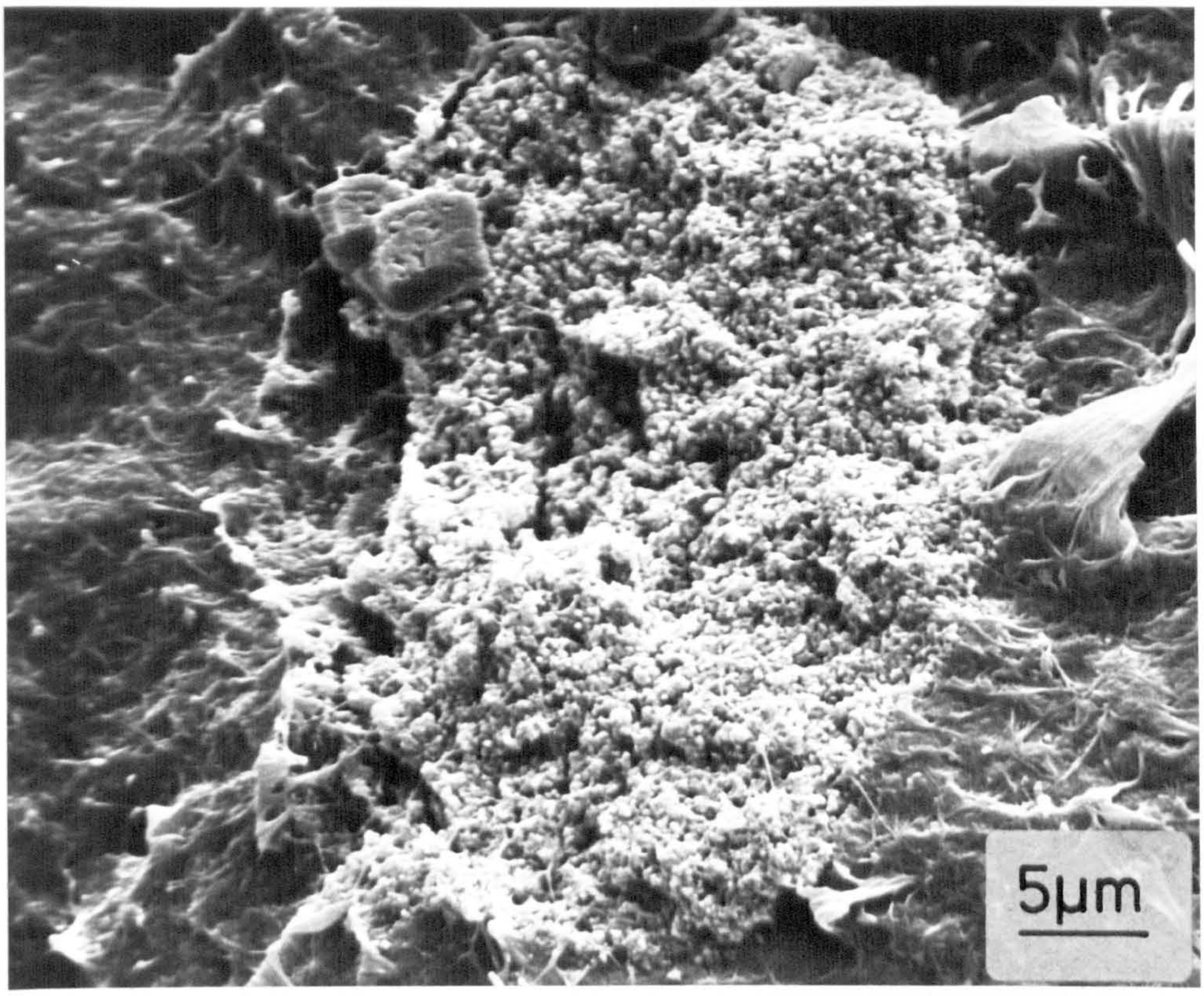

FIGURE 4.62a Calcium rich crack initiating particle in an MDPE 2 pipe. (See Figure 4.61)

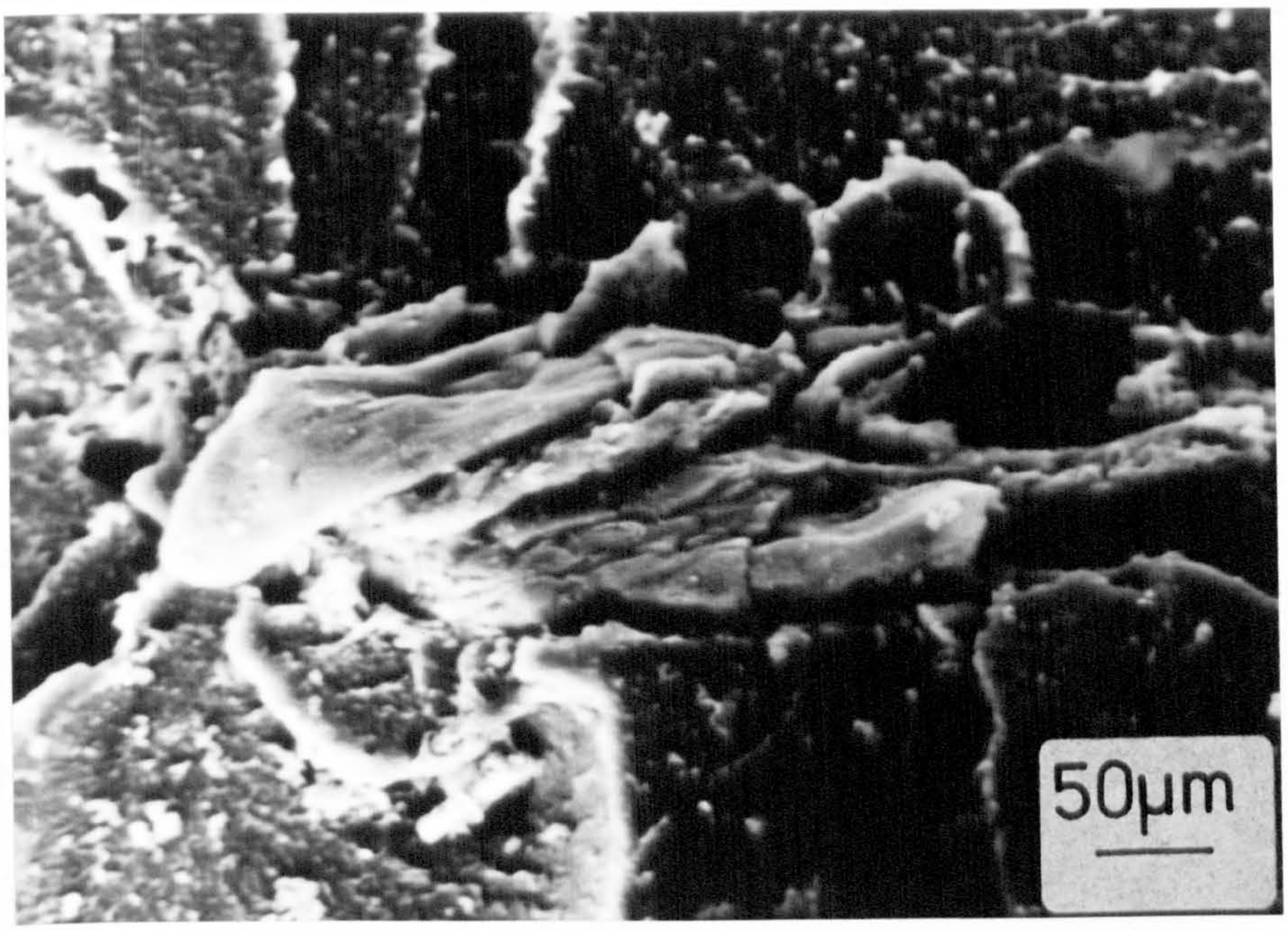

FIGURE 4.62b Silicon rich crack initiating particle in an MDPE 2 pipe.

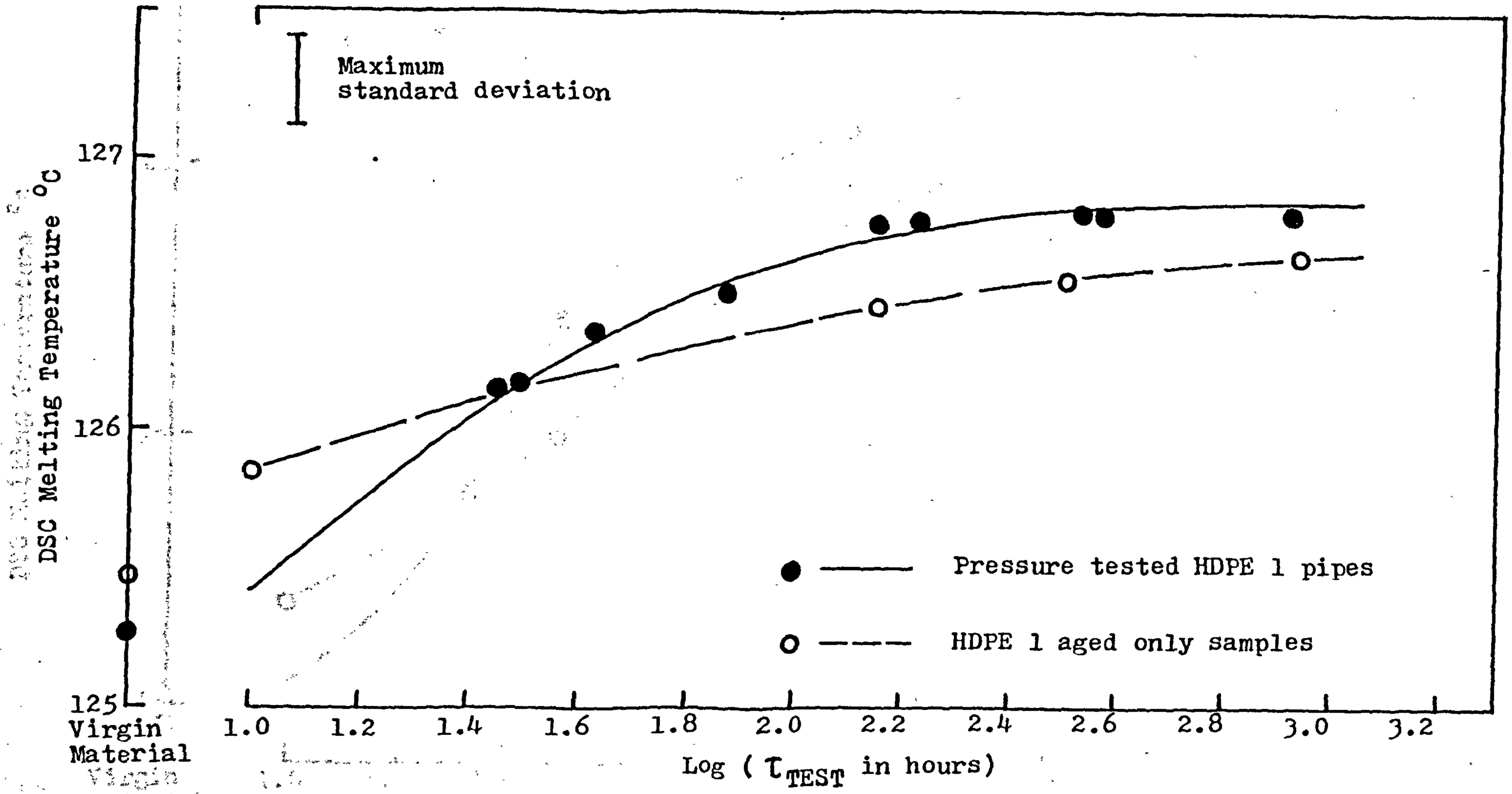

FIGURE 4.63a Variation of DSC measured crystalline melting temperature with time in water at 80°C.

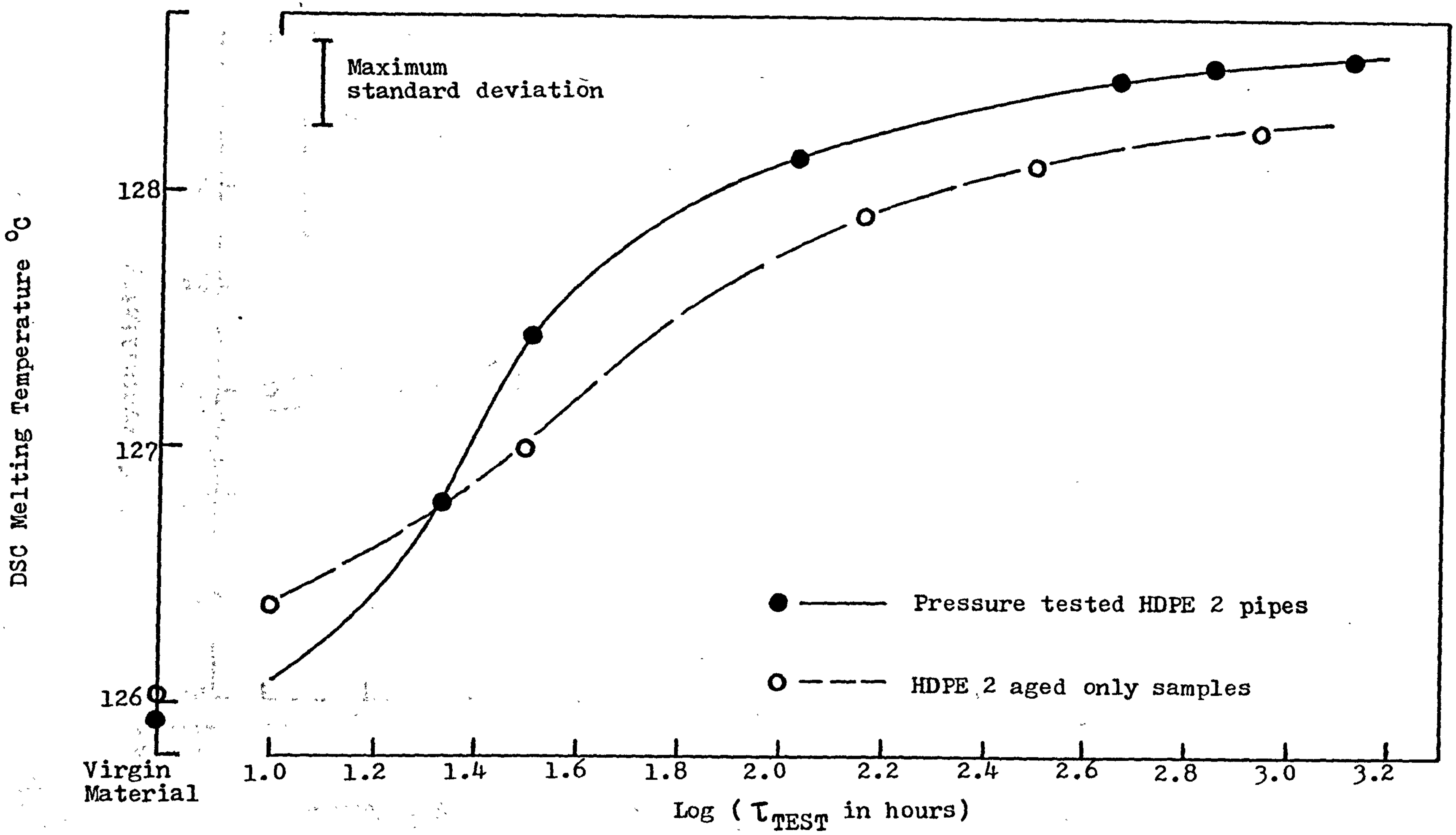

FIGURE 4.63b Variation of DSC measured crystalline melting temperature with time in water at 80°C.

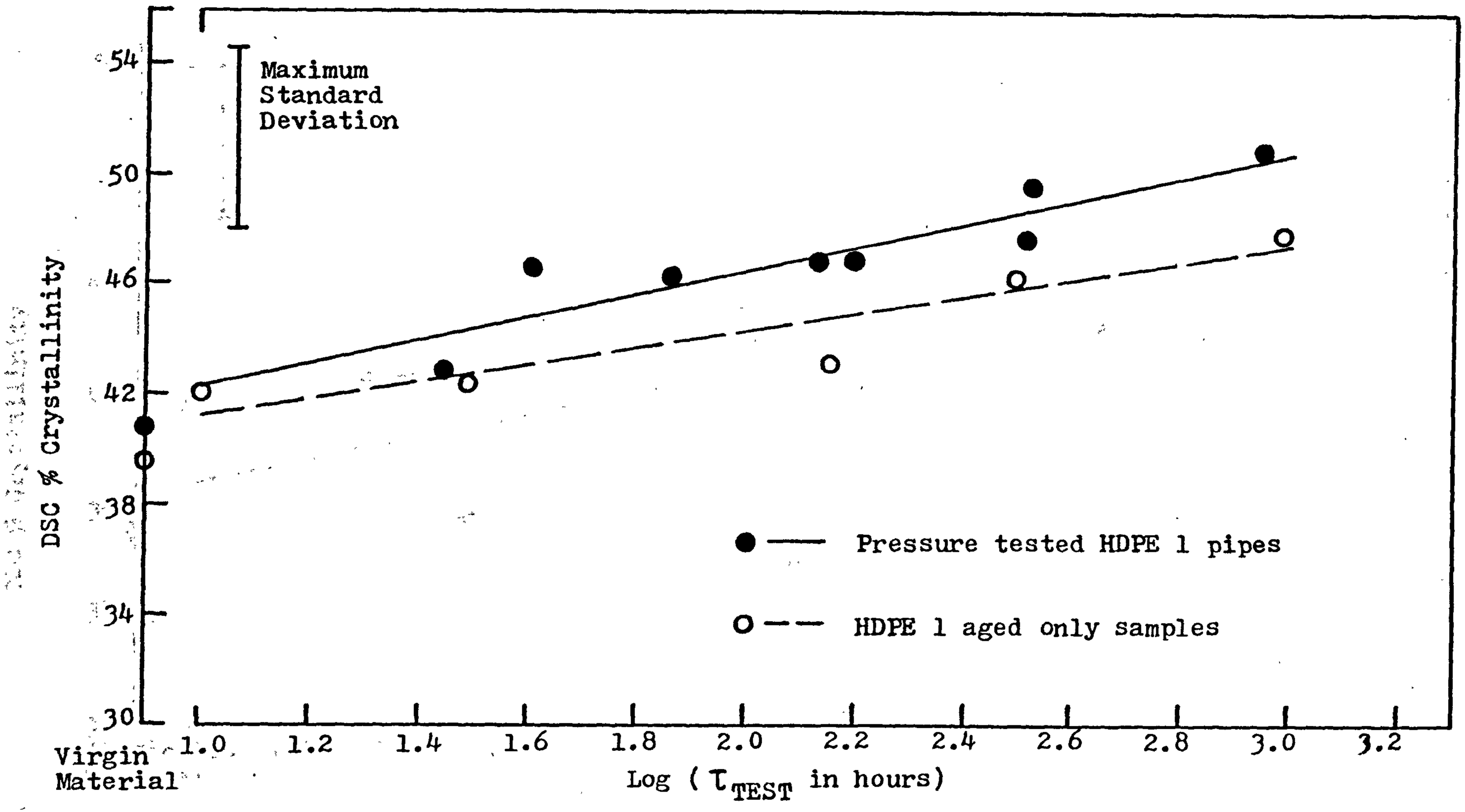

FIGURE 4.64a Variation of DSC measured crystallinity with time in water at 80°C.

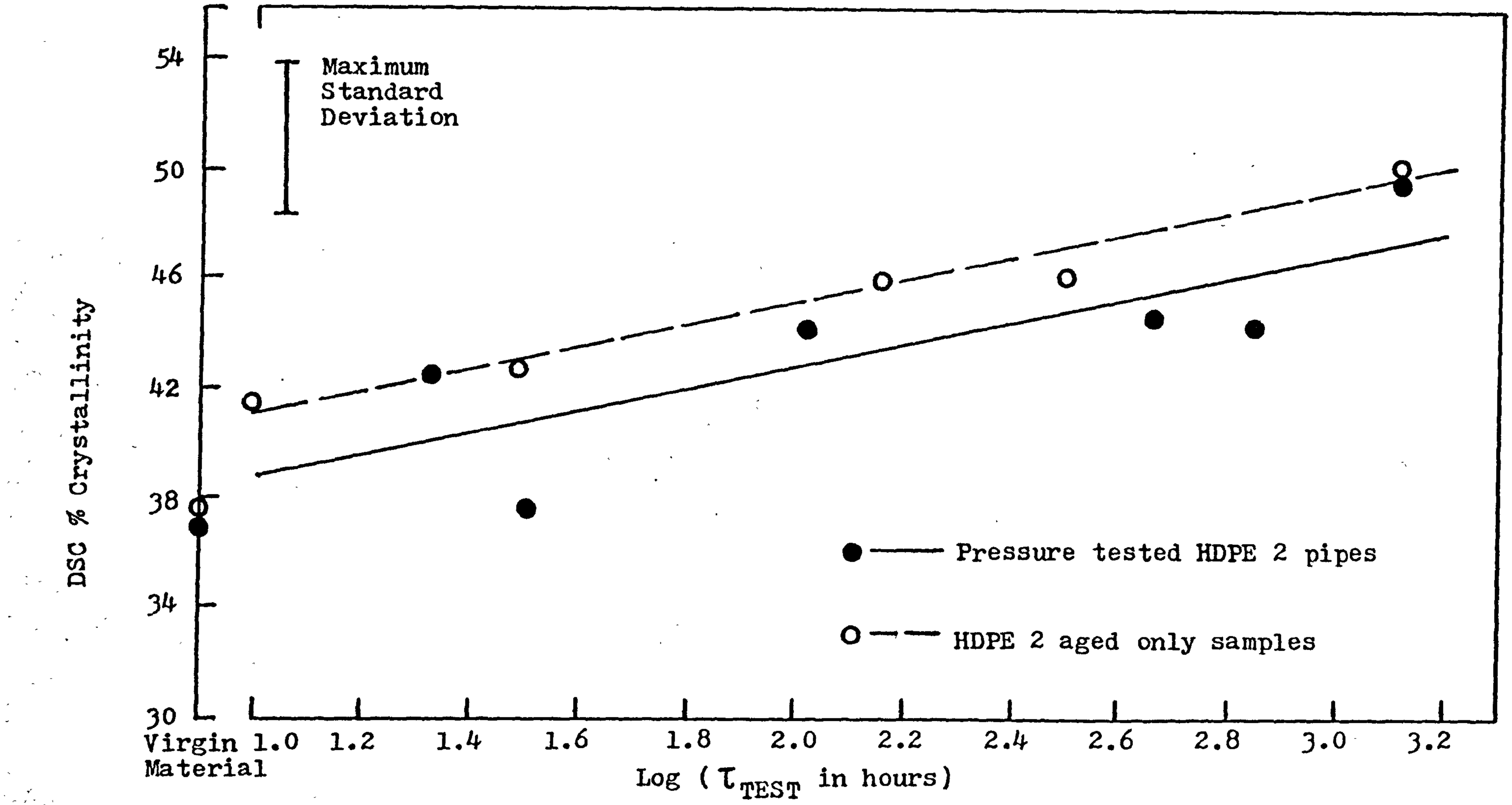

FIGURE 4.64b Variation of DSC measured crystallinity with time in water at 80°C.

CHAPTER 5 - RESULTS

SMALL DIAMETER PIPE SYSTEMS

CONTAINING INJECTION MOULDED FITTINGS

(60 and 63mm OD/SDR 11)

5.1 MECHANICAL PERFORMANCE OF PIPE SYSTEMS CONTAINING INJECTION MOULDED FITTINGS

5.1.1 Introduction

Since thermoplastics pipe networks are generally composed of extruded pipe and injection moulded fittings, such as tees, bends and stub flanges, it must be the case that the service lifetime of the pipe system depends upon the integrity of fittings and/or welds joining fittings and pipe and cannot be determined solely upon the strength of the extruded pipe.

Stress rupture testing of fittings is again the most widely adopted method of identifying the allowable design stress for a given operating temperature and desired lifetime and of assuring quality of the manufactured product. However, fittings can also be subjected to fluctuating internal pressures in day-to-day use so that it is particularly necessary to determine their behaviour under such loading conditions.

Pipe systems containing selected injection moulded fittings were tested by the same methods employed to investigate pipe and welded pipe performance, that is, by means of short term rupture, stress rupture and fatigue experiments.

The data obtained from this work will be compared closely with equivalent pipe and welded pipe material performance to highlight and contrast any observed behavioural differences between the two types of pipe network components. Manufacturers' stress rupture data will also be compared with the results where appropriate.

5.1.2 Position and Description of Failure Sites

Schematic diagrams of the principal 60 and 63mm SDR 11 pipe systems containing fittings are illustrated in Figure 5.1 together with potential sites of failure. A similar notation for failure site position is used for fitting systems as for pipe and welded pipe. That is for a specimen containing 90^{o} equal tees, failure sites are designated T1, T2 and so on. For 90^{o} bends the symbols B1, B2 etc. are used to define position of failure.

Short term rupture tests in a temperature range 20°C - 80°C resulted in ductile failures in pipe sections only. No joint or fitting failures were generated. The type of failure was identical to that in the pipe or welded pipe; it was of a ductile form exhibiting the same gross yielding and tearing in a circumferential direction.

For 90° equal tee systems subjected to stress rupture or fatigue the following brittle failures were observed, the appearances of which through the pipe or fitting wall are illustrated in Figure 5.2.

Site T1 - A crack in a pipe section about 5mm long, parallel to the pipe extrusion direction in any one of the branch arms of the tee specimen.

Site T2 Type 1 - A crack similar to T1, occurring across a butt-weld which joins any arm of the tee with a pipe section. The crack is parallel to the pipe extrusion direction and is generally associated with a defect in the weld bead produced by mould parting lines remaining on the fitting surface after manufacture or internal weld lines, an example of which is shown in Figure 5.3.

Site T2 Type 2 - A circumferential weld failure usually originating at the notch formed between the weld bead and the internal surface of the pipe or at the weld interface notch again at the inside surface of the pipe. The crack was found to propagate along a line drawn between the notches mentioned above from the inside to the outside wall of the system. Complete weld separation at the interface has also been observed although only in a very few cases.

Site T3 - A crack, which appears about 5mm long when observed on the external surface of the tee fitting itself. Its position lies at the transition between the branch pipes of the tee lying in the mirror plane containing both branch pipe axes.

Site T4 - A crack, 5mm long, lying on an internal weld which is located opposite the single branch arm and in the body of the fitting. The fracture lay parallel to the principal pipe axis. Failure T3 and T4 were generally found to be co-planar or very nearly so.

The appearances of brittle fractures in 90° bend systems are illustrated in Figure 5.4 and are described as follows.

Site B1 - A crack in a pipe section about 5mm long parallel to the pipe extrusion direction.

Site B2 Type 1 - A crack similar to B1, occurring across a butt-weld which joins either end of the fitting to a pipe length. The crack is parallel to the pipe extrusion direction and is generally associated with a defect in the weld bead produced by mould parting lines remaining on the fitting after manufacture or internal weld lines. The butt-weld defects in bends look identical with those in tees (see Figure 5.3).

Site B2 Type 2 - A circumferential weld failure usually originating at the notch formed between the weld bead and the internal surface of the pipe or at the weld interface notch again at the inside surface of the pipe. The crack was found to propagate along a line drawn between the notches mentioned above from the inside to the outside wall of the system.

Complete weld separation at the interface was not observed in any instance.

Site B3 - A crack, 5mm long, occurring in the body of the fitting usually associated with an internal weld line.

Due to the sensitivity of the failure detection device the fractures occurring at butt-welds were hidden beneath the lip of the weld bead making exact identification of the failure site a difficult task. On a number of occasions therefore the failed specimen was subjected to further pressure causing the crack to propagate and enable its position to be determined.

The circumferential butt-weld failures described in the pipe results chapter were only very occasionally observed in HDPE 1 and 2 based fitting systems and are not considered a significant mode of failure. Butt-welds made between MDPE 1 pipe and fittings fractured only in this manner.

The failure site in the various systems tested was found to be dependent upon the mode of testing, the type of fitting and material of fabrication. Table 5.1 summarises the influence of loading mode, pipe system construction and pipe system material on actual failure sites for selected 60 and 63mm SDR 11 systems.

TABLE 5.1 - The Influence of Loading Mode, Material and Construction of Pipe Systems on Actual Failure Sites for Selected 60 and 63mm OD/SDR 11 Specimens.

LOADING MODE	PIPE SYSTEMS					
	HDPE 1 PIPE + BATCH A 90° EQUAL TEES	HDPE 1 PIPE + BATCH A 90° BENDS	HDPE 2 PIPE + BATCH B 90° EQUAL TEES	HDPE 2 PIPE + BATCH B 90° BENDS	MDPE 1 PIPE + 90° EQUAL TEES	MDPE 1 PIPE + 90° BENDS
SHORT TERM RUPTURE (20 - 80°C)	T1 (Ductile)	B1 (Ductile)	T1 (Ductile)	B1 (Ductile)		
STRESS RUPTURE (80°)	T1 * T2 (type 1) T2 (type 2) T4	B2 (type 1)	T4 (limited results)	B1 * B2 (type 1) B3	T2 (type 2)	B2 (type 2)
FATIGUE (80°C)	T1 T2 (type 1) T3 *	B2 (type 1)	T3	B1 B2 (type 1)*	T2 (type 2)	B2 (type 2)

Notes 1) The failure sites marked * are those which predominate under the given conditions.
2) The failure sites can be identified in Figures 5.1, 5.2 and 5.4.
3) Except where otherwise stated all failures are of a brittle nature.

5.1.3 Short Term Rupture Tests

Selective short term rupture tests were carried out on HDPE 1 and 2 based fitting systems. (Batch A bends and tees were butt-welded to HDPE 1 pipe while Batch B fittings were joined to HDPE 2 pipe as described in Table 5.3)

The investigation included tests at temperatures lying within the range 20°C to 80°C. None of the butt-welds or fittings failed. Rupture invariably occurred within a pipe section in a ductile manner at a pressure equivalent to that recorded for comparable pipe specimens. An example of a typical ductile failure in an HDPE tee system is shown in Figure 5.5.

Table 5.2 details the results for the HDPE 1 and 2 based fitting systems and are very similar to the data obtained for pipes and welded pipes.

Again the results presented here indicate the good short term quality of butt-welds since no weaknesses were found under any of the test conditions.

5.1.4 Stress Rupture and Fatigue Testing

(i) HDPE 1 Pipe + Batch A 90° Equal Tees (63mm OD/SDR 11)

Table 5.1 demonstrates that the predominant mode of failure for the batch A 90° equal tee systems in a stress rupture test at 80°C (353K) and 1.00 MPa internal pressure was the brittle crack in the pipe section (see Figure 5.1, site T1) with the measured lifetime exceeding the manufacturer's specification for the pipe under the same conditions. Thus no real value for the stress rupture performance could be obtained using HDPE 1 pipe. (In a small number of subsequent tests, HDPE 2 pipe was welded to batch A tees. With the greatly improved stress rupture performance of the pipe the site of failure shifted to the body of the batch A tee in position T4. Actual stress rupture lifetimes for the tees were then obtained and lay between 400 and 500 hours.)

When tested under fatigue conditions at a temperature of 80°C (353K) and pressurised to 1.00 MPa, the site of failure was altered from T1 to, predominantly, site T3, that is, in the body of the tee at the branch arm tran-

TABLE 5.2 - Results of Short Term Rupture Tests on HDPE 1 and 2 Pipe Based Fitting Systems.

TEST TEMPERATURE K (°C)	MEAN MAXIMUM PIPE HOOP STRESS MPa			
	HDPE 1 PIPE + BATCH A 90° EQUAL TEES	HDPE 1 PIPE + BATCH A 90° BENDS	HDPE 2 PIPE + BATCH B 90° EQUAL TEES	HDPE 2 PIPE + BATCH B 90° BENDS
293 (20)	27.23 ± 0.24	26.91 ± 1.05	27.17 ± 0.25	27.81 ± 0.56
313 (40)	20.26 ± 1.12	70.00 ± 0.20	19.89 ± 0.30	20.14 ± 0.89
333 (60)	14.15 ± 0.35	15.05 ± 0.41	14.61 ± 0.47	15.82 ± 0.73
353 (80)	9.93 ± 0.29	9.15 ± 1.35	10.04 ± 0.02	10.15 ± 0.36

Notes 1) At least three specimens were tested at any one condition.
2) The scatter is given in terms of the standard deviation.

section (see Figure 5.2). There were occasional failures observed at site T2 associated with weld bead defects, although the total number of such failures accounted for less than 1% of the tee body fractures when the fatigue frequency was $\geqslant$2 cpm. If systems failed at site T2, the pseudo stress rupture life was on average less than that observed for the pipe. Thus, in summarising, it is evident that

a. Under static load conditions HDPE 1 pipe fails first.
b. Under fluctuating pressures of low frequency ($<$2 cpm) failure occurs at either site T1, T2 or T3 without exhibiting any preference.
c. Under fatigue conditions at frequencies $\geqslant$2 cpm failure invariably occurs in the body of the batch A tee at site T3.

As indicated above, to characterise fully the fatigue performance of pipe systems containing batch A 90^{o} equal tees, the effect of pulse frequency was investigated. Figure 5.6 illustrates the marked effect frequency of internal pressure loading has upon the pseudo stress rupture life ($\tau_{FATIGUE}$) of these tees. Included in this diagram is the data for HDPE 1 pipe failures to highlight the differences in performance of pipe and pipeline systems that incorporate injection moulded 90^{o} equal tees. For example at a frequency of 6 cpm the tee fails at approximately 15% of the pseudo stress rupture life or about 12% of the measured stress rupture life ($\sim$60 hours) representing a dramatic reduction in system lifetime.

The data in Figure 5.6 are replotted in Figure 5.7 to demonstrate the influence of frequency on the number of cycles to failure N_f. The positive slope of the tee results indicate that the failure process is not cycle dependent and hence not a pure fatigue type fracture. It is assumed therefore that some effects due to creep had taken place.

Figure 5.8 plots the performance of the tees and HDPE 1 on a graph of the manufacturer's stress rupture data for HDPE 1 pipe. This again shows with remarkable clarity how a moderate increase in frequency can substantially reduce the $\tau_{FATIGUE}$ value for an injection moulded tee.

Although the information presented in this section relates to one design of a 90° equal tee, an earlier design of identical size was also tested. The main difference between the two types of fitting was related to the position at which the mould used to manufacture the fitting was filled. The earlier tee mould was filled from a single point gate, whereas the batch A tee was ring gated from one of the tee arms.

Results from this series of tests showed that failure invariably occurred at site T3 with a reduction in pseudo stress rupture lifetime, compared with HDPE 1 pipe, greater than that observed for batch A tees. For example, at a frequency of 6 cpm with an internal pressure of 1 MPa (as before) and a test temperature of 80°C the $\tau_{FATIGUE}$ value of the earlier design of tee was only 2% of the equivalent $\tau_{FATIGUE}$ value for HDPE 1 pipe. This is an 11% reduction on the already poor performance of the batch A tees under identical test conditions.

(ii) HDPE 2 Pipe + Batch B 90° Equal Tees
(63mm OD/SDR 11)

Having demonstrated a frequency effect upon one type of injection moulded tee fitting it was proposed to examine a second system based on HDPE 2 pipe and batch B 90° equal tees, in a similar manner, to broaden the scope of the investigation. It was further decided to produce data on the influence of fatigue loading on the pseudo stress rupture lifetimes of tees which could be readily compared with manufacturers' supplied pipe stress rupture data and thus provide information upon which to base the design of pipe systems intended for use in fatigue conditions. This implied obtaining information not only at various frequencies but also at a variety of internal pressures which subsequently led to the generation of S-N or Wöhler curves.

Stress rupture testing of unconstrained HDPE 2 pipe systems containing 90° equal tees (batch B) at 80°C and 1 MPa internal pressure showed that the measured lifetimes of both systems exceeded the material manufacturer's specification. However, as with the HDPE 1 based specimens, the lifetimes (τ_{SR}) of the different systems were not equal. The measured lifetime of the injection moulded batch B tee system (~450 hours) was approximately one half of the measured stress rupture life of the pipe (~900 hours). The lifetime for the batch B tee was thus about the same as that for the batch A tee. Failure in the fitting, under stress rupture conditions was again of a brittle sort lying at site T4 in the body of the moulding on an internal weld line. The mean measured lifetime of tee systems at 80°C and 1 MPa internal pressure (corresponding to a pipe hoop stress of 4.93MPa) is given in Figure 5.9 together with the measured value for the HDPE 2 pipe systems and the material manufacturer's stress rupture curve (A). It is clear that both of the systems under stress rupture loading exceed the manufacturer's specification but that the incorporation of the injection moulded fitting lowers the system performance even though the thickness of the tee at the position of failure is about 50% greater than that of the pipe.

The imposition of a fluctuating internal pressure on the batch B tee system again resulted in a marked decrease in lifetime when considered in terms of $\tau_{FATIGUE}$. Thus the behaviour observed in the batch A tees was not unique. The failure site was always at position T3 and in fact no failures were observed at butt-welds between the batch B tees and HDPE 2 pipes at any of the test frequencies. The observation of a marked reduction in system lifetime is based on tests carried out with six different internal pressures and the results for one frequency of test (7.5 cpm) are represented by curve B in Figure 5.9.

The effect of reducing frequency from 7.50 to 4.29 and 1.57 cpm on the pseudo stress rupture life can be seen in Figure 5.10. A reduction in frequency clearly leads to an improvement in the $\tau_{FATIGUE}$ value so that

it approaches the performance specified by the manufacturer.

The data in Figure 5.10 can be alternatively presented in Figure 5.11 as the number of cycles to failure as a function of the peak test pressure. The curves shown in Figure 5.11 relate again to three test frequencies and are nearly coincident at the higher internal pressures and corresponding hoop stresses, indicating that the frequency has little effect on the number of cycles to failure. This effect is presented more clearly in Figure 5.12 which for an internal pressure of 1 MPa and a temperature of 80°C the plot of N_f against frequency is a line approximately parallel to the horizontal axis. This indicates typical cycle dependent behaviour, at least in the range of conditions described here.

At the lower peak internal pressures the curves of hoop stress against cycles to failure diverge so that they differ by at least a factor of five, again shown more clearly in Figure 5.12 as an obvious increase in N_f with increasing frequency. This behaviour is similar to that observed in the batch A tees under similar conditions (see Figure 5.7).

Extending the range of test hoop stresses to above 5.5 MPa (above the knee of the manufacturers stress rupture curve) and below a 3.0 MPa hoop stress revealed changes in the relationship between pseudo stress rupture life and the actual stress rupture life for batch B tee fitting performance. Above 5.5 MPa hoop stress, the site of failure altered yet again from T3 to T1. All failures at these higher fatigue pressures resulted in ductile failures within the pipe sections of the equal tee systems. None of the weaknesses shown in the tees at lower stresses were revealed and close inspection of the tees after high pressure fatigue testing did not show any obvious signs of fatigue damage. The pseudo stress rupture lives of tees tested above the knee were found to increase compared with lifetimes obtained at the same frequencies but at stresses lying below the ductile/brittle transition of the stress rupture curve. Obviously entirely different failure mechanisms are at work in these cases.

The existence of a fatigue limit for the batch B tees is indicated by the low pressure fatigue test results presented in Figures 5.9 to 5.11. Further long term testing would be required to extend these curves to a point where an approximate limit could be measured. It appears, however, that higher frequency tests will approach a horizontal asymptote at a higher hoop stress compared with the lower frequency results.

(iii) Combined Stress Rupture and Fatigue Tests.

Since pipelines may be subject to both static and fatigue loadings while in service, it was decided to determine the relative contributions made by both modes of loading to the lifetimes of systems containing batch B 90° equal tees (welded to HDPE 2 63mm OD SDR 11 pipe).

In the first instance specimens were subjected to fatigue loads at a maximum internal pressure of 1 MPa, 80°C and 7.5 cpm (2 seconds on load followed by 6 seconds at atmospheric pressure) for 90% of the previously determined fatigue lifetime of the batch B 90° equal tees, failing at site T3. That is 90% $\tau_{FATIGUE}$ where, as defined in Chapter 4,

$$\tau_{FATIGUE} = \sum_{N=1}^{N=N_f} (t_{max})_N \qquad (5.1)$$

with the same meanings for all symbols.

The fitting systems were then subjected to static loads at the same temperature and pressure and the times to failure recorded. These were observed to exceed the manufacturer's specified stress rupture lifetime, τ_{SR}, and indicates that the mechanism or defect leading to failure under fatigue loading at site T3 is much less active when a static load is applied.

The procedure went one step further and included a second fatigue period so that the following loading history was obtained,

(1) the systems were subjected to an initial fatigue period of a length defined by a set percentage of $\tau_{FATIGUE}$, followed by,

(2) a fixed period of static internal pressure, and finally

(3) subjected to a second fatigue period, under the same conditions as the first, until the specimen fractured.

These three-part experiments were structured as shown below:-

PERIOD 1 FATIGUE	PERIOD 2 STRESS RUPTURE	PERIOD 3 FATIGUE
~50% $\tau_{FATIGUE}$ (1.51 hrs)	~25% τ_{SR} (250 hrs)	Until Failure
~90% $\tau_{FATIGUE}$ (2.72 hrs)	~25% τ_{SR} (250 hrs)	Until Failure
~90% $\tau_{FATIGUE}$ (2.72 hrs)	~0.25% τ_{SR} (2.5 hrs)	Until Failure

Note:- τ_{SR} is the lifetime of the HDPE 2 pipe under static load.

The fatigue frequency was set at 7.5 cpm and all test periods were held under conditions of 80°C and 1 MPa maximum internal pressure.

All results are presented in Table 5.3. Of particular interest is the apparent beneficial effect of the stress rupture period which causes the total fatigue lifetime to more than double in some cases. In any event the application of a static load subsequent to a fluctuating internal pressure always increased the fatigue life of the tees failing at site T3.

On the other hand, the application of a fatigue load prior to stress rupture loading seemed to have no beneficial or deleterious effect on systems' stress rupture lives and even after 90% of the expected $\tau_{FATIGUE}$ value, fracture was not observed at the usual site of T3 but rather shifted under the static load to site T1.

(iv) MDPE 1 Pipe + 90° Equal Tees (60mm OD/SDR 11)

Due to the fact that only a limited number of tee systems were available, the performance of individual butt-welds in the specimens was monitored along with pipe and fitting behaviour. Thus if failure occurred at a joint the specimen was re-welded and put back on test until the next failure. This process was carried out as rapidly as possible to preclude the occurrence of any major material alterations.

TABLE 5.3 - Results of the Combined Stress Rupture and Fatigue Tests
HDPE 2 Pipe + Batch B 90° Equal Tees (63mm OD/SDR 11)

TEST STRUCTURE			RESULTS	
PERIOD 1 FATIGUE	PERIOD 2 STRESS RUPTURE	PERIOD 3 FATIGUE	$\frac{\tau_{SR}}{\bar{\tau}_{SR\ Pipe(P1)}}$	$\frac{(\tau_{FATIGUE})_{TOTAL}}{\bar{\tau}_{FATIGUE\ (T3)}}$
$\bar{\tau}_{FATIGUE}^{90\%}$ (2.68 Hours)	UNTIL FAILURE AT SITE T1 (There were no T3 failures)	———	$\geqslant 1$	———
$\bar{\tau}_{FATIGUE}^{50\%}$ (1.51 Hours)	$\bar{\tau}_{SR}^{25\%}$ (251.8 Hours)	UNTIL FAILURE AT SITE T3	———	2.36
$\bar{\tau}_{FATIGUE}^{90\%}$ (2.72 Hours)	$\bar{\tau}_{SR}^{25\%}$ (251.8 Hours)	UNTIL FAILURE AT SITE T3	———	2.06
$\bar{\tau}_{FATIGUE}^{90\%}$ (2.72 Hours)	$\bar{\tau}_{SR}^{2.5\%}$ (2.5 Hours)	UNTIL FAILURE AT SITE T3	———	1.38

Notes
1) The $(\tau_{FATIGUE})$ total is the sum of the fatigue periods 1 and 3.
2) The $\bar{\tau}_{SR}$ and $\bar{\tau}_{FATIGUE}$ used are the mean values obtained under the same conditions during straightforward stress rupture and fatigue tests carried out earlier in the test programme. ($\bar{\tau}_{SR}$ pipe is 898 hours and $\bar{\tau}_{FATIGUE}$ for site T3 is 3.02 hours.)
3) Results are mean values obtained from at least two specimens per condition.

Stress rupture and fatigue tests, all at 80°C, were completed using a range of internal pressures designed to cause failure in a brittle manner.

In all cases of failure, whether under stress rupture or fatigue conditions, the position of fracture lay at site T2 and was of type 2, that is a partial circumferential separation of the weld between the injection moulded fitting and a pipe section close to but not at the interface. In this respect the performance of the MDPE 1 90° equal tees differed markedly from the HDPE 1 and 2 systems. Furthermore, it once again appears that fatigue is a more aggressive type of internal pressure test when compared with stress rupture. Lifetimes were generally considerably reduced under fatigue. In any event both stress rupture and fatigue tests demonstrated the weakness of a butt-weld made between an injection moulded fitting and a pipe section in this size and material.

All results are presented in Table 5.4 and are again quoted in terms of the stress rupture (τ_{SR}) and pseudo stress rupture lives ($\tau_{FATIGUE}$). For comparison the stress rupture and pseudo stress rupture lives measured for pipe are also included.

(v) HDPE 1 Pipe + Batch A 90° Bends
(63mm OD/SDR 11)

The stress rupture tests on the HDPE 1 pipe + batch A 90° bends at 80°C (353K) and 1 MPa internal pressure gave rise to one sort of failure only, corresponding to site B2 type 1 and in all examples the associated lifetime τ_{SR} exceeded the manufacturer's specification for the pipe stress rupture life, although did not exceed the actual measured stress rupture lives.

In fatigue testing, again at 80°C and a maximum internal pressure of 1 MPa, the imposition of an intermittent load resulted in a trend decreasing pipe system lifetime with increasing frequency. The results are consistent with those obtained for the batch A 90° equal tee systems (and with batch B tee data) in demonstrating that the incorporation of an injection moulded fitting is a source of weakness if the system is to be subjected to fatigue. The position of failure which was always at

TABLE 5.4 - Results of MDPE 1 Pipe + 90° Equal Tees (60mm OD/SDR 11)

PIPE HOOP STRESS MPa (Internal Pressure psi)	STRESS RUPTURE		FATIGUE (7.5 cpm)		
	τ_{SR} T2 Type 2 (Hours)	$\frac{\tau_{SR}\ (T2\ Type\ 2)}{\bar{\tau}_{SR}\ Pipe\ (P1)}$	Nf (Cycles)	$\tau_{FATIGUE}$ T2 Type 2 (Hours)	$\frac{\tau_{FATIGUE}\ (T2\ Type\ 2)}{\bar{\tau}_{SR}\ Pipe\ (P1)}$
3.04 (90)	18.7 (Reweld)	0.14	25560	7.10	0.05
	74.4	0.55	26325	7.31	0.05
	75.5	0.56	33660	9.35	0.07
			36720	10.20	0.08
			41445	11.51	0.09
4.05 (120)	18.8	0.14 *			
	20.2	0.15 *			
	55.3	0.42 *			
4.93 (146)	9.2	0.07	3015	0.84	0.006
	9.4	0.07	4410	1.23	0.009
	14.0	0.11	6255	1.74	0.01
	14.5	0.11			

Notes 1) The results marked with * are obtained by using an extrapolated value for τ_{SR} pipe at 120 psi.

2) $\bar{\tau}_{SR}$ Pipe (P1)(90 psi) = 134.0 hrs $\bar{\tau}_{SR}$ Pipe (P1)(120 psi) = 137.3 hrs (extrapolated)
$\bar{\tau}_{SR}$ Pipe (P1)(146 psi) = 131.3 hrs

3) All tests were carried out at 80°C.

the butt-joint was generally associated with weld bead inhomogeneities induced by the presence of mould parting lines and/or internal weld lines. With a frequency in excess of 2 cpm the pseudo stress rupture life of the 90° bend system was reduced below that of the actual stress rupture life for the bend systems and the specific position of the resulting failure, whether associated with internal weld line defects of surface mould line defects, appeared to have little influence on general trends. The effect of frequency of loading on the batch A 90° bend systems performance is illustrated in Figure 5.13. HDPE 1 pipe data is also presented for comparison.

Under both stress rupture and fatigue conditions all batch A bend systems failed at site B2 type 1.

(vi) HDPE 2 Pipe + Batch B 90° Bends
(63mm OD/SDR 11)

Stress rupture and fatigue tests were carried out on 63mm SDR 11 HDPE 2 pipe + batch B 90° bends at 80°C (353K) and with a maximum internal pressure of 1 MPa. In fatigue one frequency of 7.5 cpm was applied.

Stress rupture was evidently less aggressive on the bend systems in that three out of the five specimens tested produced a failure in the pipe section at site B1. It is interesting to note that one of the non-pipe failures occurred at site B3, that is, in the body of the bend and actually lying on an internal weld line. The other non-pipe fracture was found at site B2 type 1 at a fitting/pipe butt-weld. Neither of these last two failures showed a reduction in τ_{SR} compared with the pipe.

Fatigue loading, however, produced a significant difference in the position of failures in the bend systems, in that out of ten results only three specimens fractured in a pipe section. The remainder all failed at site B2 (type 1) after greatly reduced lifetimes compared with the mean stress rupture life of the pipe as measured during the test programme. It was not possible to examine the influence of frequency of the bend performance.

Results are presented in Table 5.5 along with equivalent results for HDPE 2 pipe.

TABLE 5.5 - Results of HDPE 2 Pipe + Batch B 90° Bends (63mm OD/SDR 11)
Pipe Section Fractures (B1) are Not Included.

STRESS RUPTURE		FATIGUE (7.5 cpm)		
τ_{SR} B2 Type 1, B3 (Hours)	$\frac{\tau_{SR}(B2\ Type\ 1,\ B3)}{\bar{\tau}_{SR}\ Pipe\ (P1)}$	Nf (Cycles)	$\tau_{FATIGUE}$ B2 Type 1 (Hours)	$\frac{\tau_{FATIGUE}\ (B2\ Type\ 1)}{\bar{\tau}_{SR}\ Pipe\ (P1)}$
1127 (B2 Type 1)	1.26	188865	52.46	0.06
1542 (B3)	1.72	205830	57.18	0.06
		224280	62.30	0.07
		258615	71.84	0.08
		316170	87.83	0.1
		344700	95.75	0.1
		583515	162.09	0.2

Notes 1) $\bar{\tau}_{SR}$ pipe (P1) for HDPE 2 is 898 hours.
2) The maximum pipe hoop stress was set to 4.93 MPa (146 psi internal pressure).
3) All tests were carried out at 80°C.

Although these findings indicate a fatigue weakness in the pipe/fitting butt-weld for the HDPE 2 pipe + batch B 90° bends, the measured $\tau_{FATIGUE}$ values are at least a factor of five greater than equivalent results obtained with HDPE 1 pipe + batch A 90° bends.

(vii) MDPE 1 Pipe + 90° Bends (60mm OD/SDR 11)

Stress rupture and fatigue tests were also conducted on MDPE 1 pipe + 90° bends at 80°C (353K) and 0.6 MPa (90 psi) maximum internal pressure. The fatigue frequency was, as usual, set to 7.5 cpm.

Once again the performance of the MDPE 1 systems containing an injection moulded fitting (in this case a 90° band) was below that expected for the pipe under similar conditions. All fractures were at site B2 (Type 2) whether subjected to fatigue or static loads. Fatigue induced system failure with $\tau_{FATIGUE}$ values substantially reduced compared with the τ_{SR} values of the bend systems, and both sets of figures are much lower than the τ_{SR} results for pipe alone.

Table 5.6 illustrates these results particularly clearly.

5.2 FRACTURE SURFACE ANALYSIS

5.2.1 Introduction

Strictly speaking only one of the failures occurring in the fitting systems demonstrated a distinct pattern of mechanical behaviour. This was T3 which predominated in the brittle fracture of HDPE 1 and 2 pipe systems containing 90° equal tees. For this reason the main effort in the fractographic study of the fittings was concentrated upon obtaining detailed correlations between T3 fracture surface macro- and micromorphology and the previously imposed mechanical history.

It is intended therefore to discuss in the first instance, the appearance of fractures and fracture surfaces observed in all fitting systems fabricated from each material and then consider in more detail fracture analysis results of the T3 failures in HDPE 1 and 2 as mentioned above.

TABLE 5.6 - Results of MDPE 1 Pipe + 90° Bends (60mm OD/SDR 11)

STRESS RUPTURE		FATIGUE (7.5 cpm)		
τ_{SR} B2 Type 2 (Hours)	$\frac{\tau_{SR}\text{ (B2 Type 2)}}{\bar{\tau}_{SR}\text{ Pipe (P1)}}$	Nf Cycles	$\tau_{FATIGUE}$ B2 Type 2	$\frac{\tau_{FATIGUE}\text{ (B2 Type 2)}}{\bar{\tau}_{SR}\text{ Pipe (P1)}}$
47.4	0.35	27720	7.70	0.06
66.6	0.50	32535	9.04	0.07
103.1	0.77	38565	10.71	0.08
		55620	15.45	0.11
		64620	17.95	0.13

Notes 1) The $\bar{\tau}_{SR}$ value for pipe (P1) is 134.4 hours at 80°C with a pipe hoop stress of 3.04 MPa (90 psi internal pressure).

2) All tests were conducted under the conditions of (1).

Table 5.1 indicates those brittle fracture surfaces to be desribed in the course of this section.

(Detailed descriptions of the failure sites are presented in section 5.1.2.)

Fractures which appeared in the pipe sections making up the fitting systems were discussed in Chapter 4 and will not be dealt with here.

5.2.2 General Fracture Analysis of Pipe Systems Containing Injection Moulded Fittings

(i) Type 1 Butt-Weld Failures (HDPE 1 and 2).

Typical examples of type 1 butt-weld failures in fitting systems fabricated from HDPE 1 and 2 are shown in Figure 5.14 and labelled with their respective test conditions. Since the two materials are very similar with respect to certain physical properties, it is reasonable to expect their fracture surfaces, produced under the same conditions, would show little variation. However, not only do the pipe/tee and pipe/bend butt-welds appear almost identical but the stress rupture and fatigue fractures also exhibit very similar features. Only very occasionally do beach marks due to the discontinuous growth of the fracture appear on any of these surfaces.

Other important features include the difference in the bead size on the fitting side of the weld compared with the well formed pipe bead. This, as mentioned previously, is caused by moulding defects within the fitting such as internal weld lines which affect the formation of the weld sprue during the butt-welding process.

The progress of the brittle fracture tends to enhance underlying structural features and shows clearly the heat affected zones, including the weld interface and also differences associated with the fact that pipes are extruded and the fittings moulded.

It was generally difficult to locate the exact position of crack initiation although on certain surfaces concentric markings allowed an estimate to be made. It appeared that failures usually started at the notch made between the weld bead and the fitting's internal surface at the point where the weld bead had not formed correctly

due to the moulding defects discussed earlier.

Study of these fracture surfaces by means of scanning electron microscopy revealed very similar features to those obtained on pipes. There are regions of highly drawn fibrils which disappear at the weld interface. The amount of localised drawing varies and particularly so when banded structures are observed on the fracture surfaces, see Figure 5.15. At this level no differences between the fittings and pipe fracture surface morphology are apparent.

(ii) Type 2 Butt-Weld Failures (HDPE 1 and MDPE 1) Examples of the circumferential type butt-weld failures, more commonly observed in MDPE 1 welded systems, are presented in Figure 5.16. The photographs show side views which clearly indicate the path of fracture and views normal to the actual fracture surfaces which provide evidence for the fact that such failures are very brittle.

In some instances the circumferential separation has occurred at the weld interface and is almost certainly a result of poor polymer mixing in this region during the jointing process.

The type 1 and type 2 butt-weld failures in the HDPE 1 based tee systems were equally possible under static load conditions whereas in fatigue tests only type 1 fractures were observed. The circumferential failures were absent in the tests conducted on bend systems. (It is useful to note that type 2 butt-weld failures did not occur at all in the HDPE 2 based fitting systems in either loading mode.)

(iii) T3 Tee Fitting Failures (Batches A and B) This type of fracture is associated with fatigue loading conditions only.

This applies to both batch A and batch B 90° equal tees.

Photographs of the general features of such fractures are shown in Figure 5.17. At the point of failure which is the same for both batches of tees, the wall thickness is approximately twice that of the equivalent SDR 11 pipe.

The failure initiation site has been indicated by scanning electron microscopy to be associated with damage induced by the retraction of the mould core (Figure 5.18). Marked changes in microstructure through the thickness of the moulded tees (both batch A and B) are reflected in the fracture surface morphologies shown in Figure 5.19, and in some cases fatigue markings are evident.

Fracture surface morphology also varies as a function of both frequency and test pressure. The results of this work will be presented later in this chapter however.

(iv) T4 Tee Fitting Failures (Batches A and B)

This type of failure occurred solely under conditions of static load and not only do fracture surfaces from both materials exhibit similar features, but they also failed after approximately the same period, that is about 400 to 500 hours at 80°C and 1 MPa internal pressure.

For the batch B 90° tees it is useful to note that allowing for the extra wall thickness the actual stress rupture life was approximately one-half of that expected on the basis of HDPE 2 pipe stress rupture data.

On the other hand, for batch A tees, again allowing for the extra wall thickness, their stress rupture lives were about six times that of the HDPE 1 pipe. Thus only when batch A tees were welded to HDPE 2 pipe could the actual stress rupture performance of the fittings be measured.

In all cases the stress rupture failures in the body of the tees occurred in that part of the wall opposite to the branch arm and lying on a line positioned by discontinuities in the butt-welds which are indicative of the position of a major internal weld line.

Figure 5.20 presents a typical T4 fitting failure. As may be expected there are no apparent DGB's and the aspect ratio of the fracture surface (the maximum length of the crack in the longitudinal direction divided by the wall thickness exhibits good agreement with values obtained for HDPE 1 pipe stress rupture fractures.

(v) B3 Bend Fitting Failures (Batch B Only)

To date only one B3 failure in the body of a batch B bend has been observed. The fracture was again lying directly on a line in the fitting joining discontinuities in the welds and is associated with a major internal weld line. However, the fracture surface was badly marked when it was broken out of the bend and any significant features were masked by the poor quality of the surface. It is mentioned here for completeness, however, and to indicate that under conditions of static load only (not fatigue) a body failure can occur in an injection moulded bend. The time of failure was nearly 500 hours in excess of the measured average HDPE 2 pipe stress rupture life of about 900 hours.

Such fractures will obviously be quite rare since in general the pipe joined to the bend (whether HDPE 1 or 2) will fail before the fitting.

5.2.3 Detailed Analysis of T3 Fracture Surfaces

(i) HDPE 1 Pipe + Batch A 90° Equal Tee Systems.

The batch A 90° equal tees were used in that part of the mechanical testing programme which dealt specifically with the effect of frequency upon the performance of systems contining injection moulded fittings. Thus Figure 5.21 shows the marked changes in fracture surface morphology which occur as a function of test frequency. All these failures were obtained at 80°C with a maximum internal pressure of 1 MPa.

There is clear evidence of the effect the underlying microstructure has upon the fracture surface features. The site of initiation is also seen to good effect on these macrographs and complement the SEM micrographs of the initiation site presented in Figure 5.19.

Patterns of what appear to be fatigue markings are observed emanating from a centre which is not at the initiation site and are probably caused by polymer melt flow in this corner of the moulding.

Towards the edge of the specimens lie regions of very rough material which are possibly related to the skin on the inside walls of the mouldings. There is not a very clear pattern emerging from these surfaces which could, macroscopically be related to the test frequency. There is some indication however, that at higher frequencies the surface becomes slightly rougher and the fatigue markings become less pronounced probably due to a masking effect.

As usual on a high magnification SEM micrograph, as shown in Figure 5.22, there is little difference to be observed between the tees and pipes. Once again, the DGB's are indicative of variations in localised ductility with the fibrils becoming more or less obvious depending upon position of observation.

Only the high magnification micrographs of the fracture initiation sites are of particular use.

Since the surfaces are particularly complicated with a variety of effects combining to produce the observed features, it is difficult to explain the exact nature of the failure mechanisms at work. The most important result elicited from this information is that yet again the pipeline components are failing from defects produced during processing.

(ii) HDPE 2 Pipe + Batch B 90^{o} Equal Tee Systems

The site of fracture for batch B 90^{o} equal tees is common not only at all the test frequencies (which is the same as for batch A tees) but at all the applied internal pressures within the range 1.10 MPa and 0.5 MPa.

The overall features of the fracture surfaces indicated a brittle type of fatigue fracture and again the underlying microstructure of the fitting, the frequency of test and, for the batch B tees, the maximum internal pressures all influenced the fine detail of the surfaces.

Figure 5.23 shows the effect of frequency, at one pressure on the batch B tee surfaces and Figure 5.24 demonstrates the influence internal pressure, at one frequency, can have.

The variations in surface morphology for the batch B tees appear to be more obvious compared with batch A. There is a distinct decrease in surface roughness when the pressure is reduced at constant temperature and frequency. Also at the higher frequencies, at constant pressure and temperature, the surface becomes more ductile.

Fatigue markings are also observed along with a roughening of features towards the inside edges of the tee. Polymer melt flow lines can be seen producing complex interacting patterns in these regions of the fittings.

This form of data is invaluable for failure analysis, since by examining the features of a fracture surface, the conditions which led to the rupture can be approximated. Thus by knowing the cause, a remedy can be proposed.

Scanning electron microscopy again revealed the site of fracture initiation. It is the same defect as observed on batch A tees, associated with the extraction of the mould core.

The defect can be observed easily in un-tested tees in the branch arm of the fitting close to the intersection with the through pipe.

Although high magnification examination of the surface features was carried out, results were similar to those obtained for batch A tees and thus need not be repeated here.

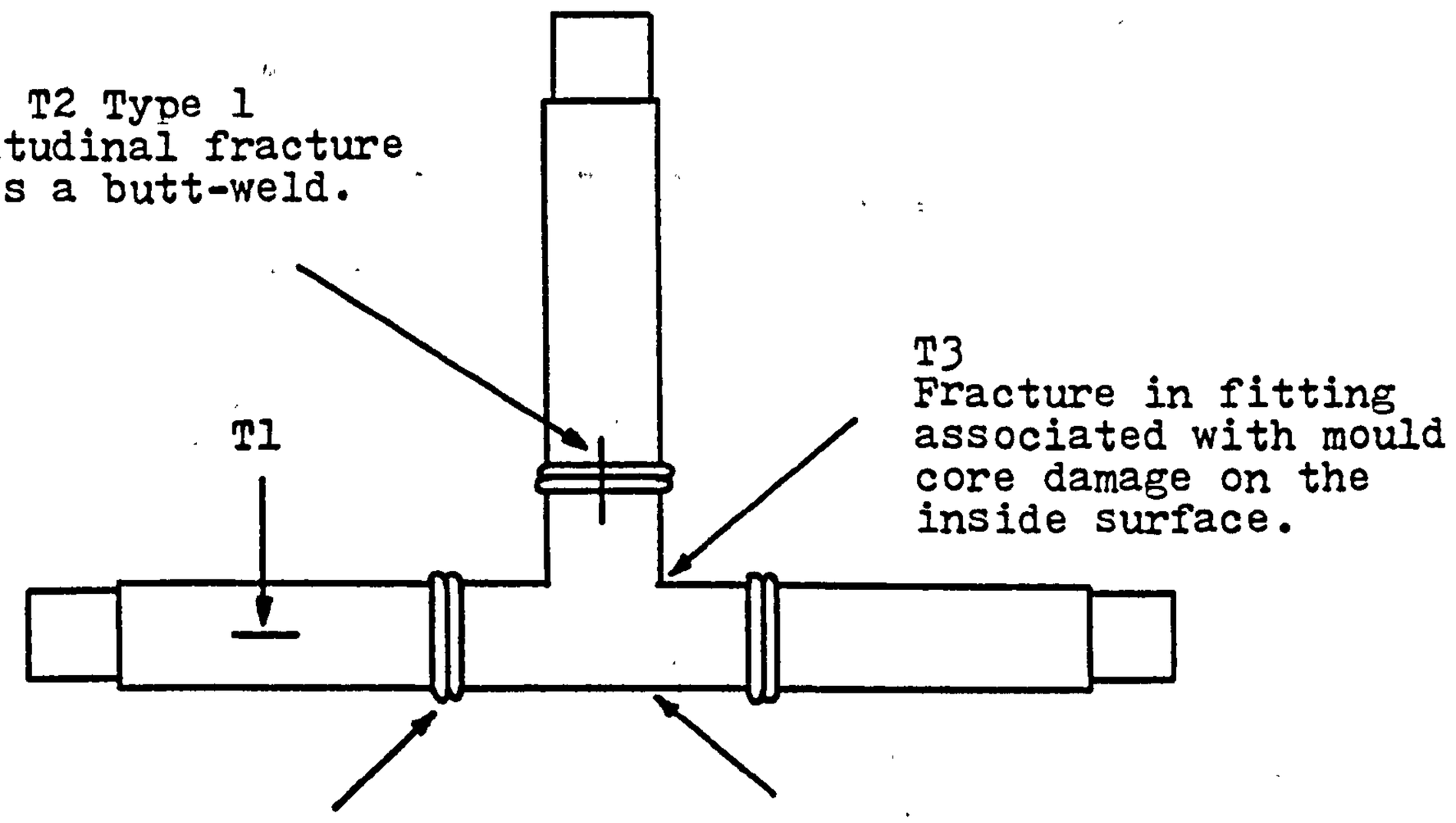

FIGURE 5.1a Schematic representation of observed brittle fracture sites in systems containing 90° equal tees.

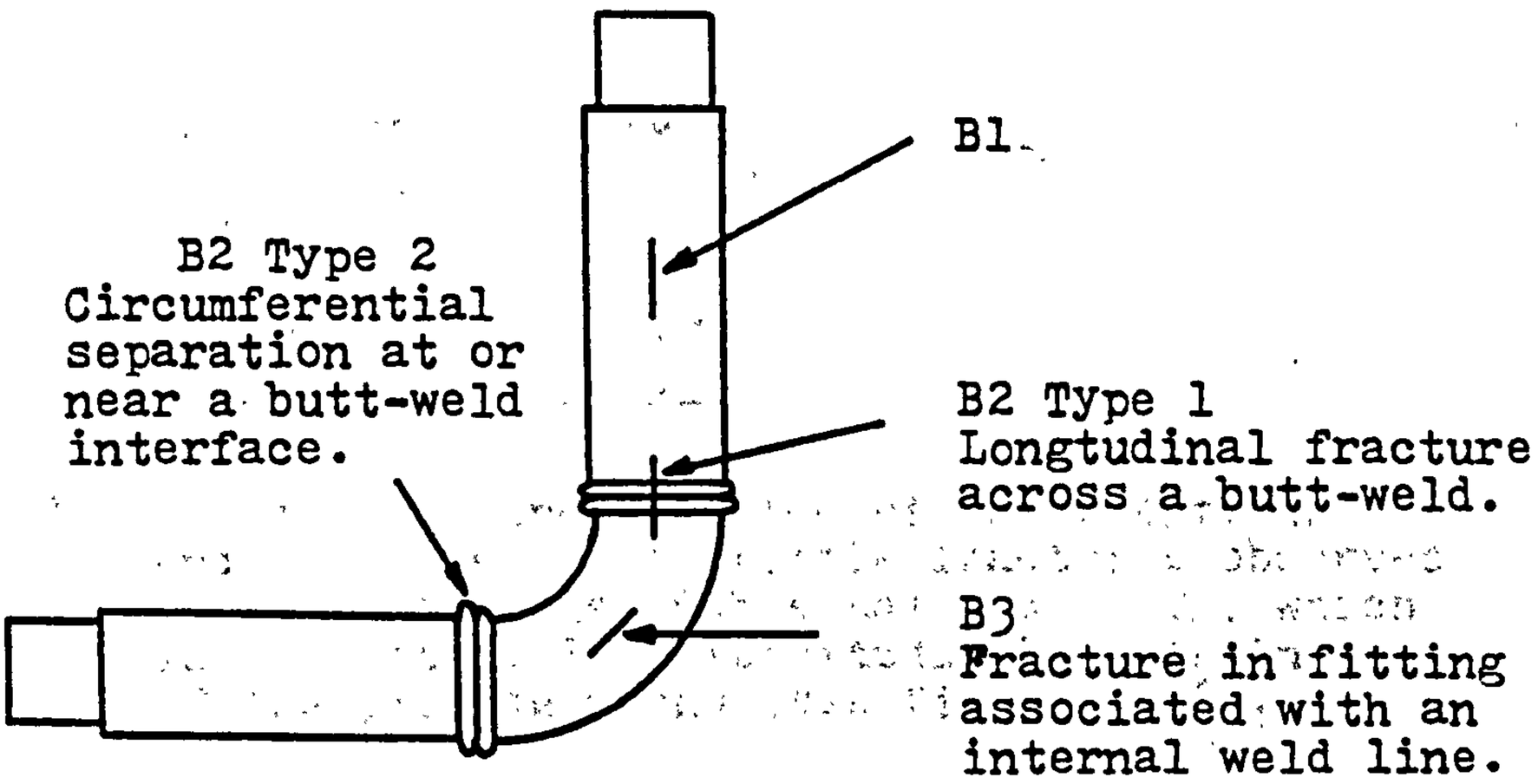

FIGURE 5.1b Schematic representation of observed brittle fracture sites in systems containing 90° bends.

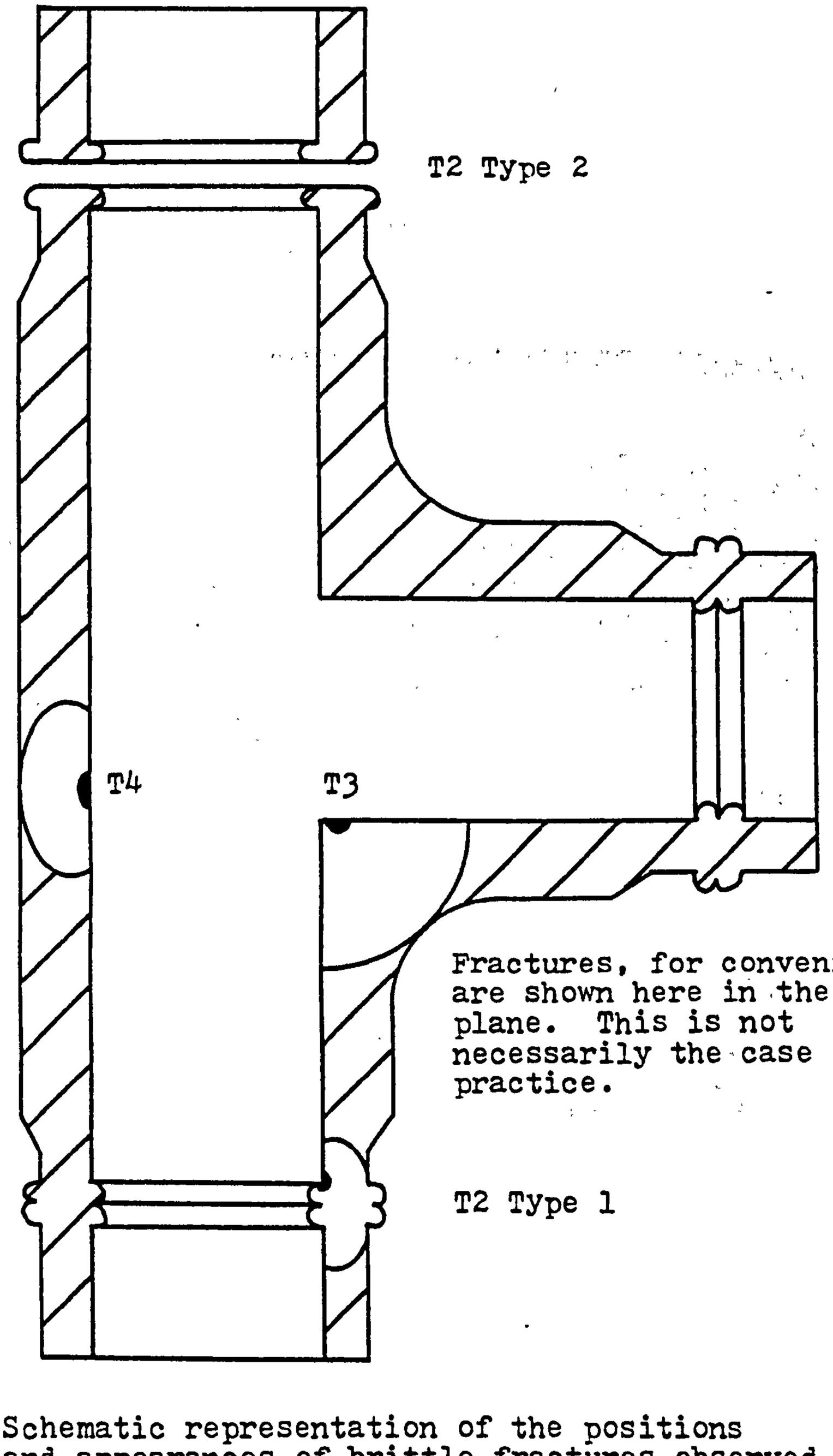

FIGURE 5.2 Schematic representation of the positions and appearances of brittle fractures observed in small diameter 90° equal tees. T1, which is not shown, is a longitudinal crack in any of the pipe sections (see Figure 4.18).

▁▂▁ Denotes an initiation site.

FIGURE 5.3 Weld bead discontinuities in butt-welds made between extruded pipe and a 90° equal tee. The internal weld line along the spine of the fitting can also be seen joining the two discontinuities in the welds.

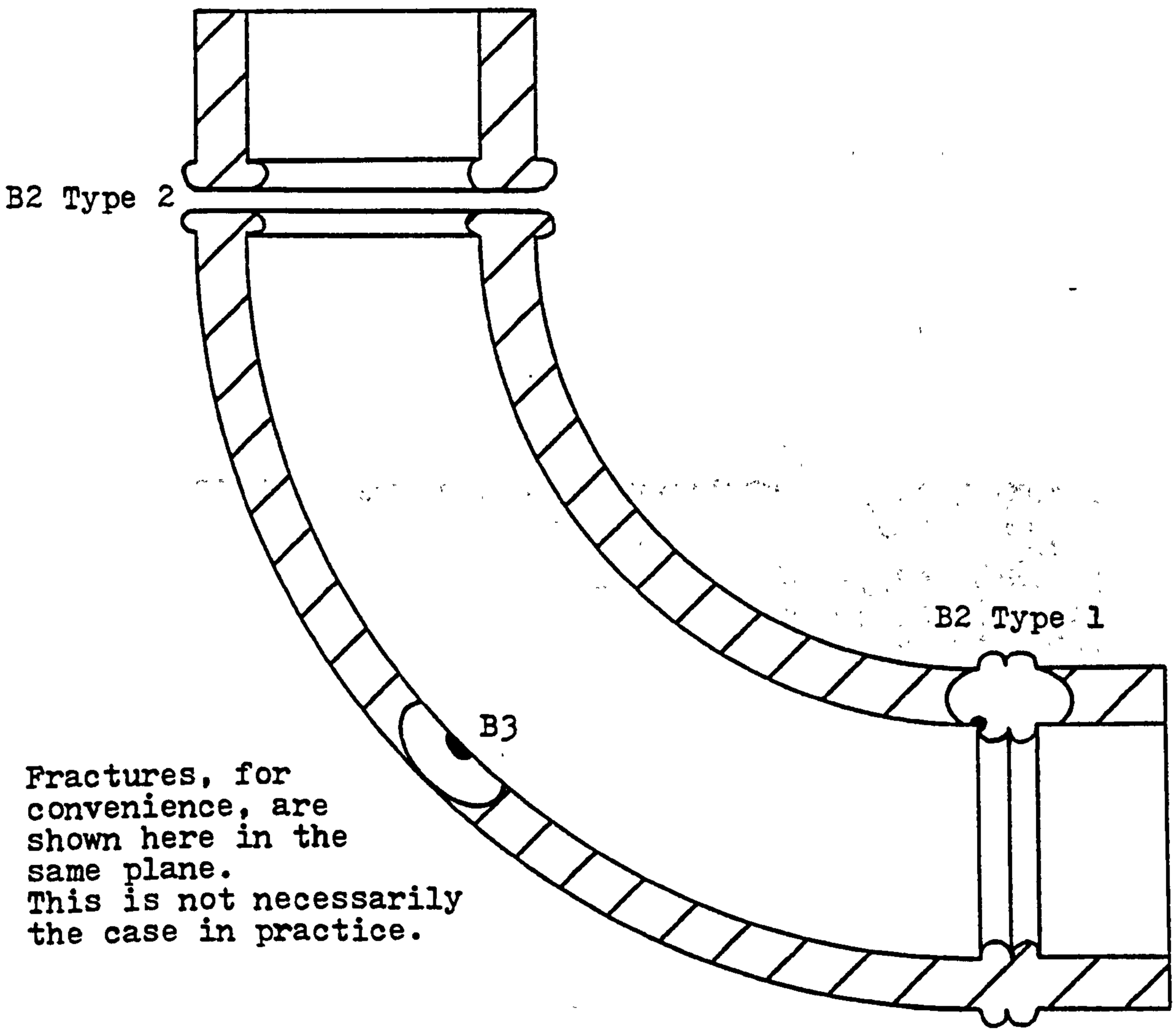

FIGURE 5.4 Schematic representation of the positions and appearances of brittle fractures observed in small diameter 90° bends. B1, which is not shown, is a longitudinal brittle crack in either of the pipe sections (see Figure 4.18).

Denotes an initiation site.

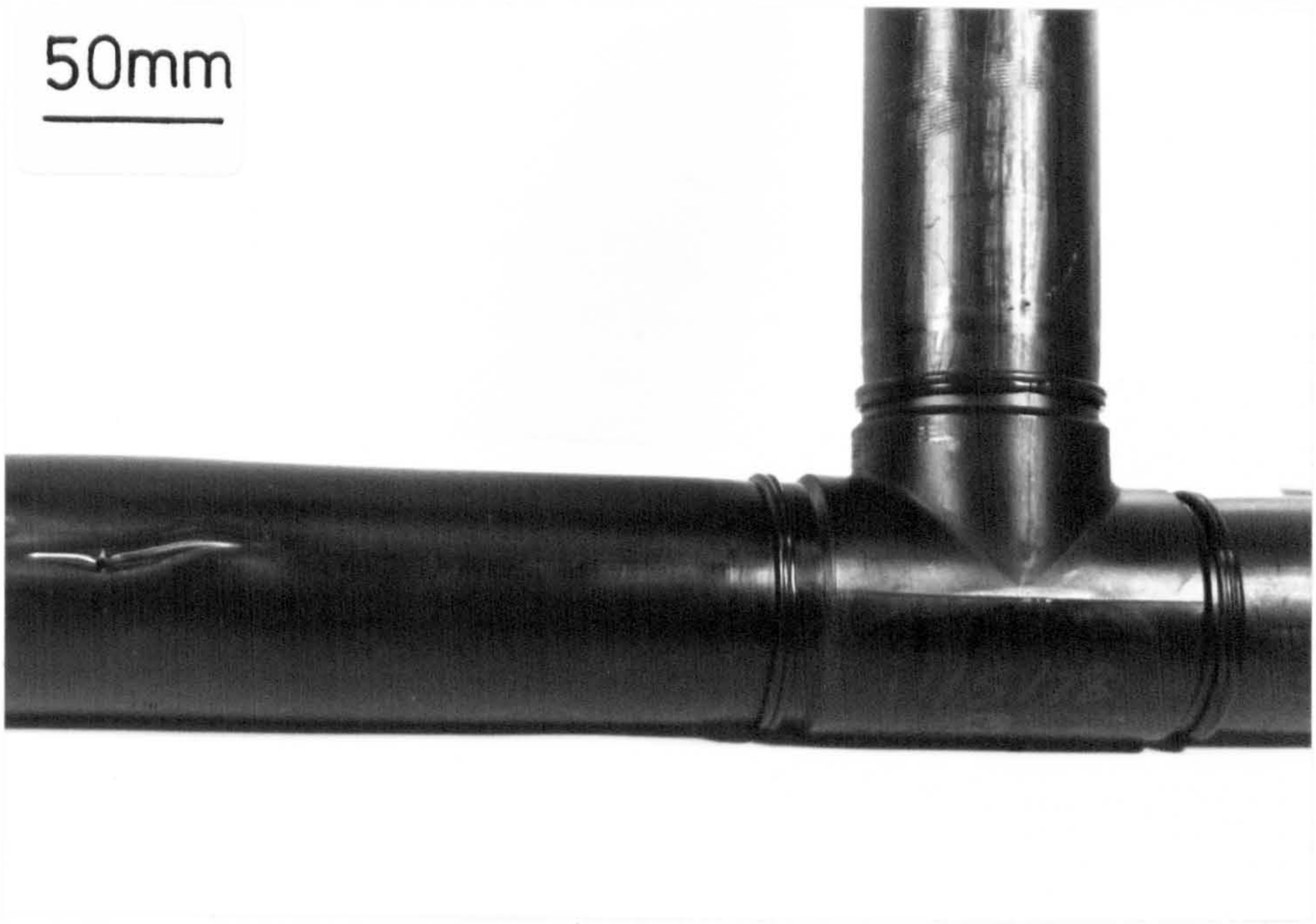

FIGURE 5.5 Short term rupture failure in a pipe system containing a 90° equal tee.

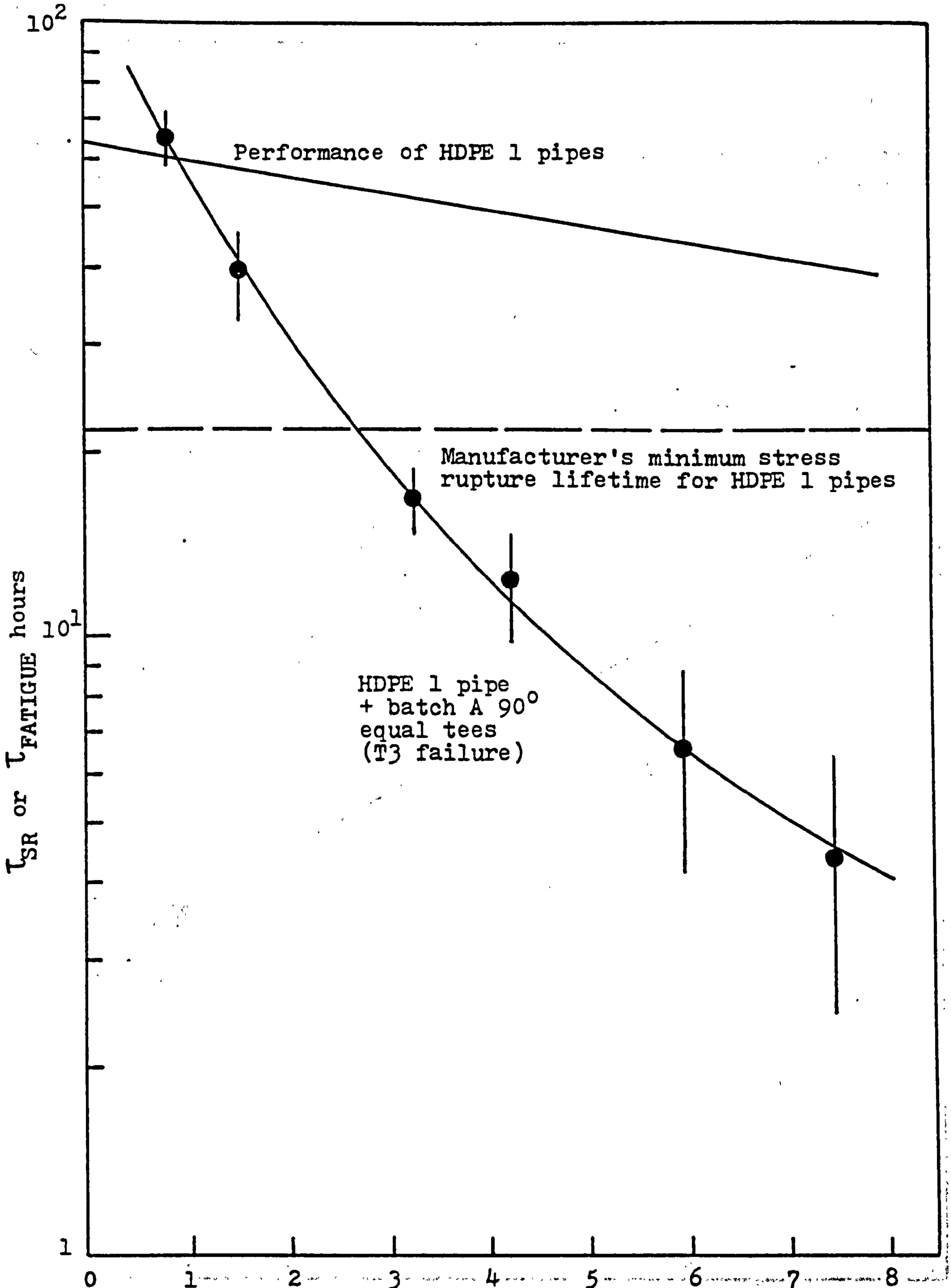

FIGURE 5.6 Fatigue performance of batch A 90° equal tees (T3 failure) compared with fatigue and stress rupture data for HDPE 1 pipes at 80°C.

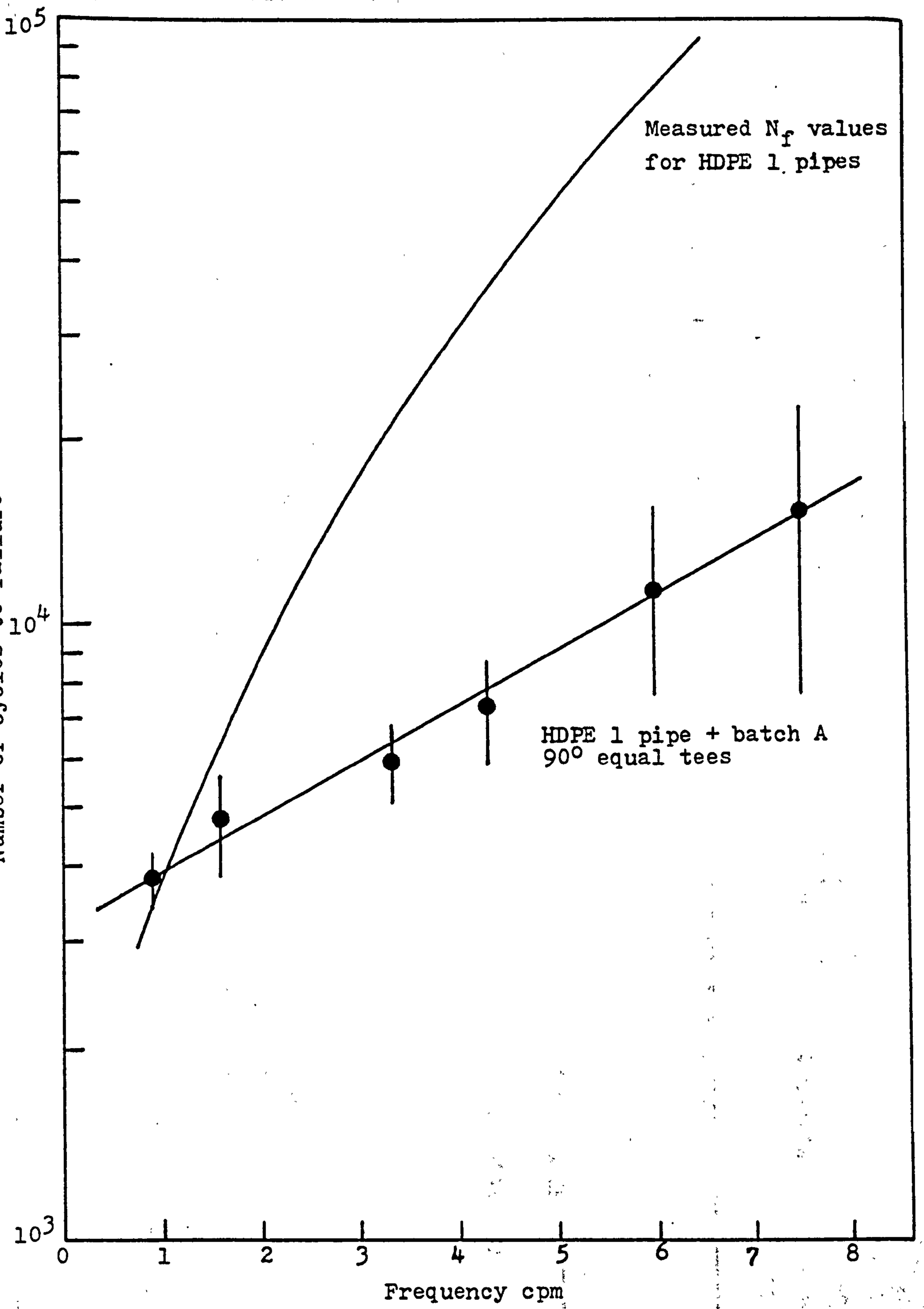

FIGURE 5.7 Variation of Nf with frequency for HDPE 1 pipe + batch A 90° equal tees at 80°C and 4.93 MPa maximum pipe hoop stress.

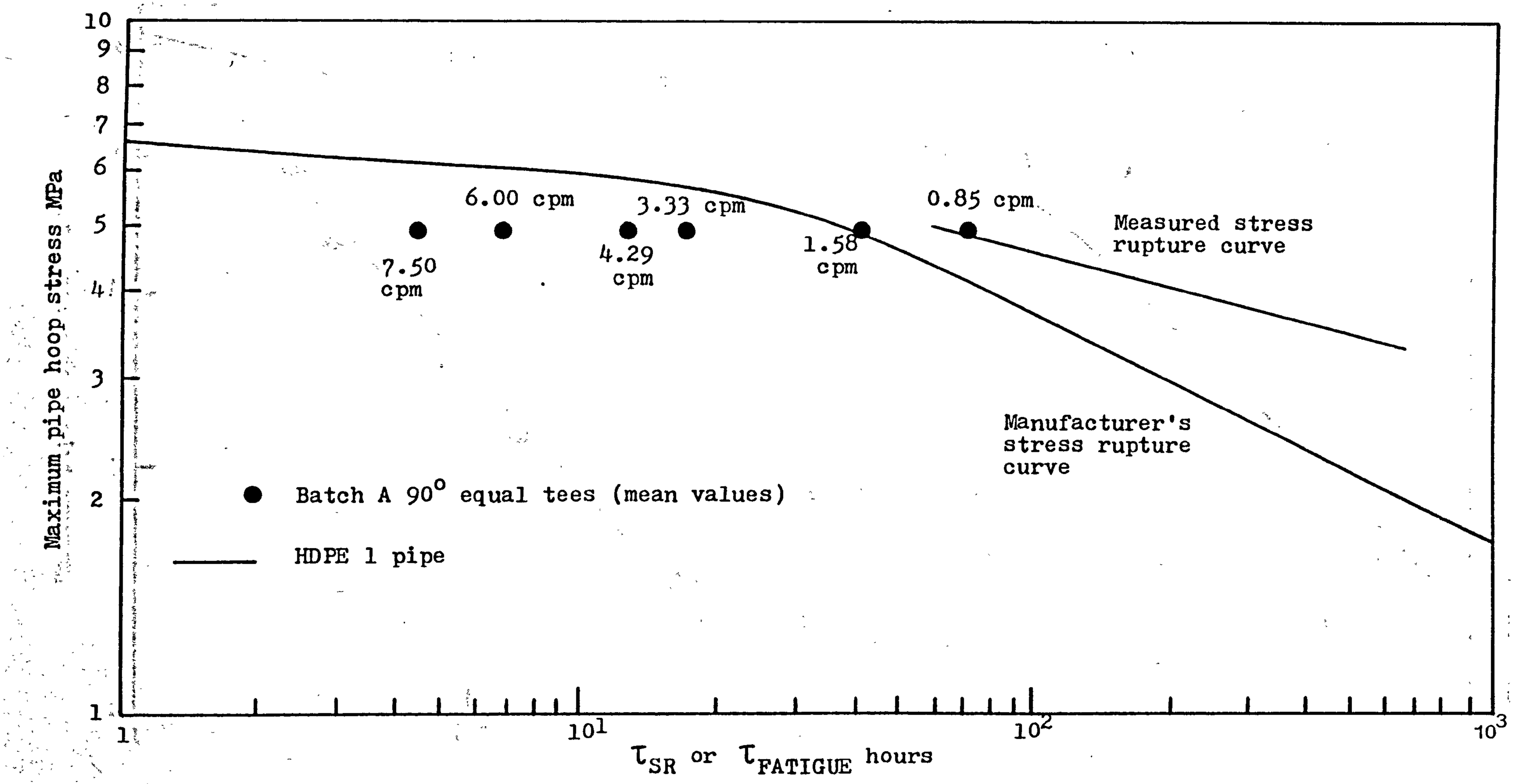

FIGURE 5.8 Fatigue performance of batch A 90° equal tees at different frequencies compared with measured and manufacturer's pipe stress rupture data at 80°C.

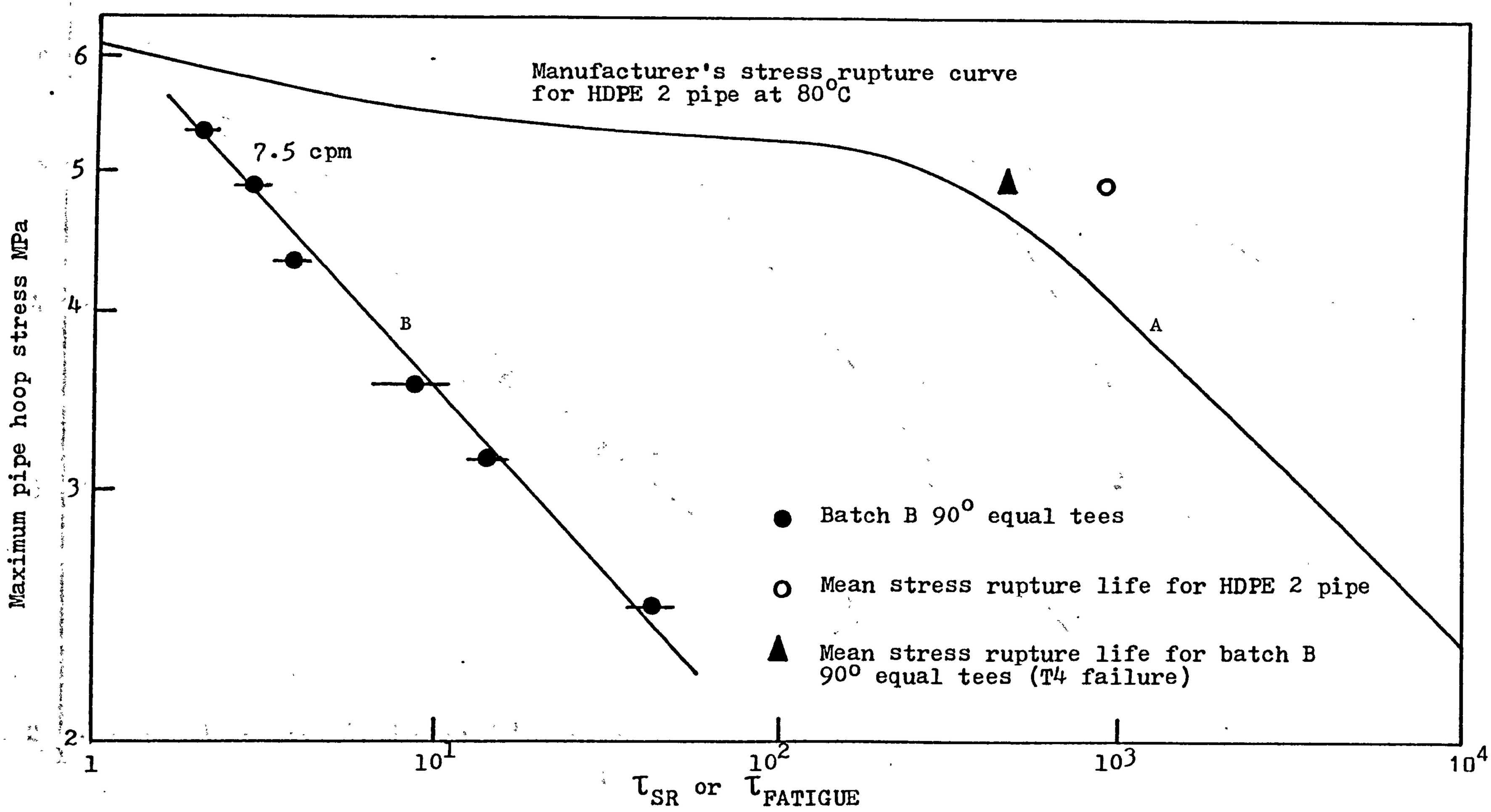

FIGURE 5.9 Comparison of stress rupture and fatigue performance of batch B 90° equal tees and HDPE 2 pipe at 80°C.

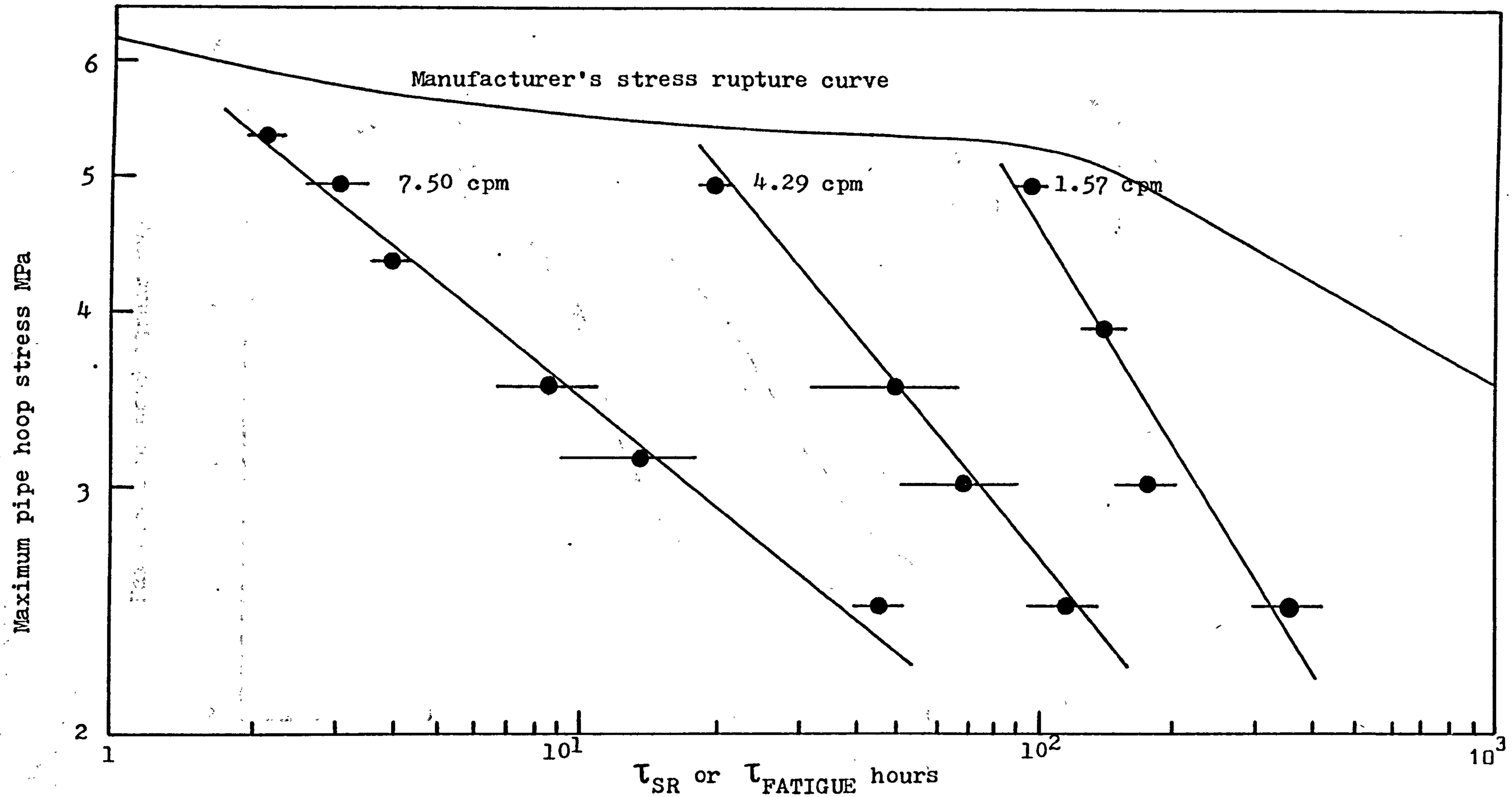

FIGURE 5.10 The performance of batch B 90° equal tees at various pipe hoop stresses and three frequencies. Pipe - 63mm OD SDR 11 HDPE 2.

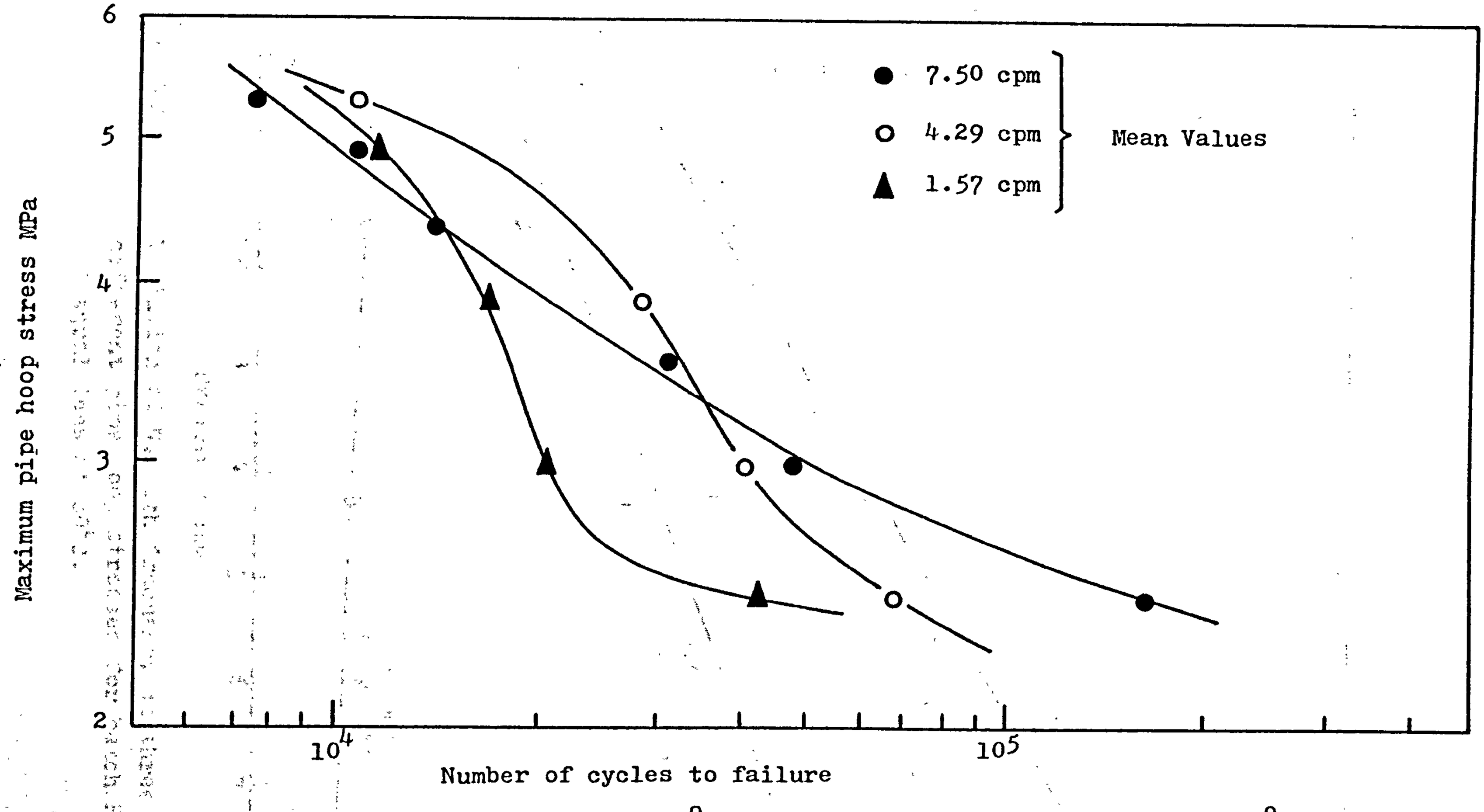

FIGURE 5.11 S-N curves for batch B 90° equal tees at three frequencies and 80°C.

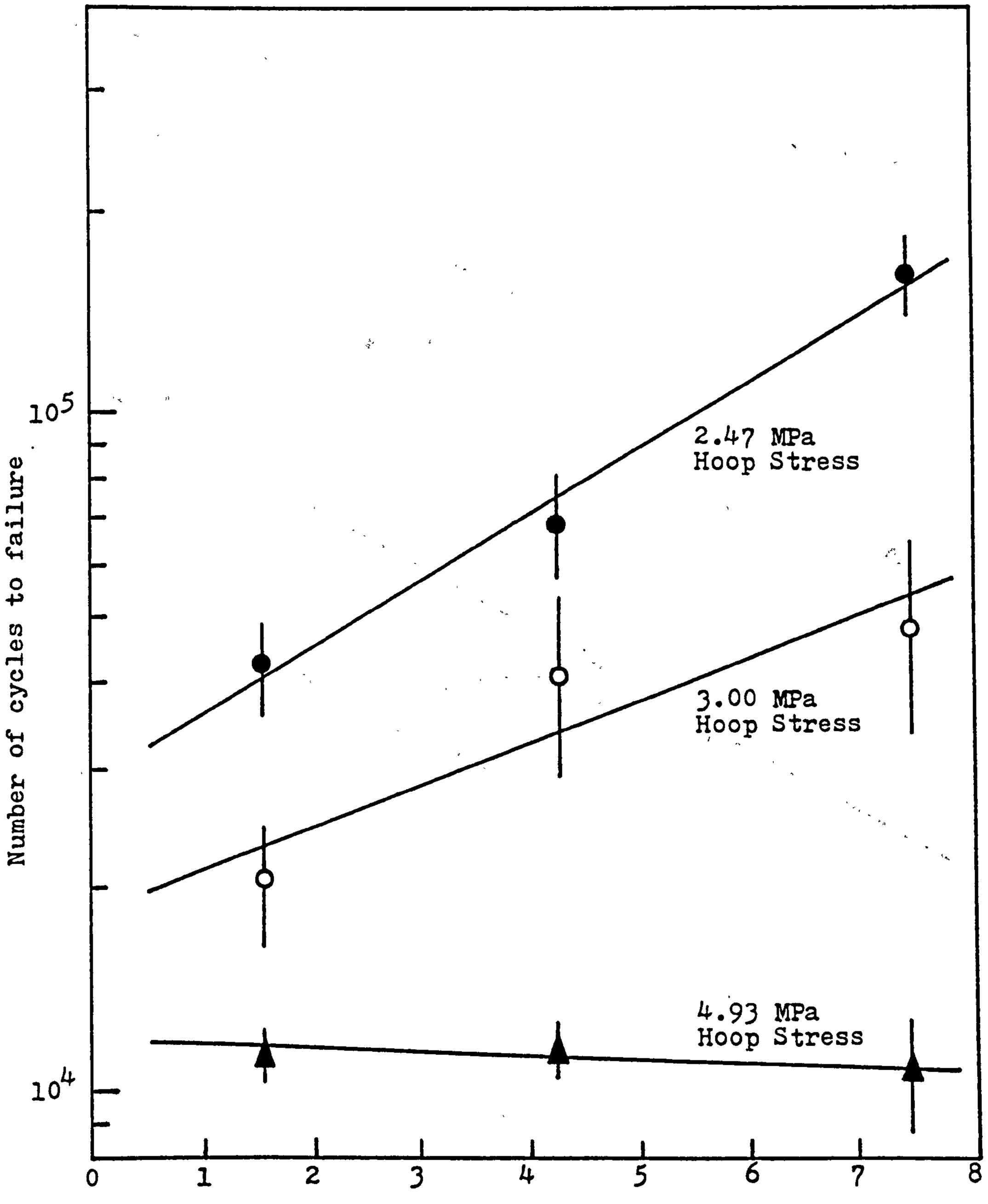

FIGURE 5.12 Variation of N_f with frequency at three different pipe hoop stresses for batch B 90^o equal tees at 80^oC.

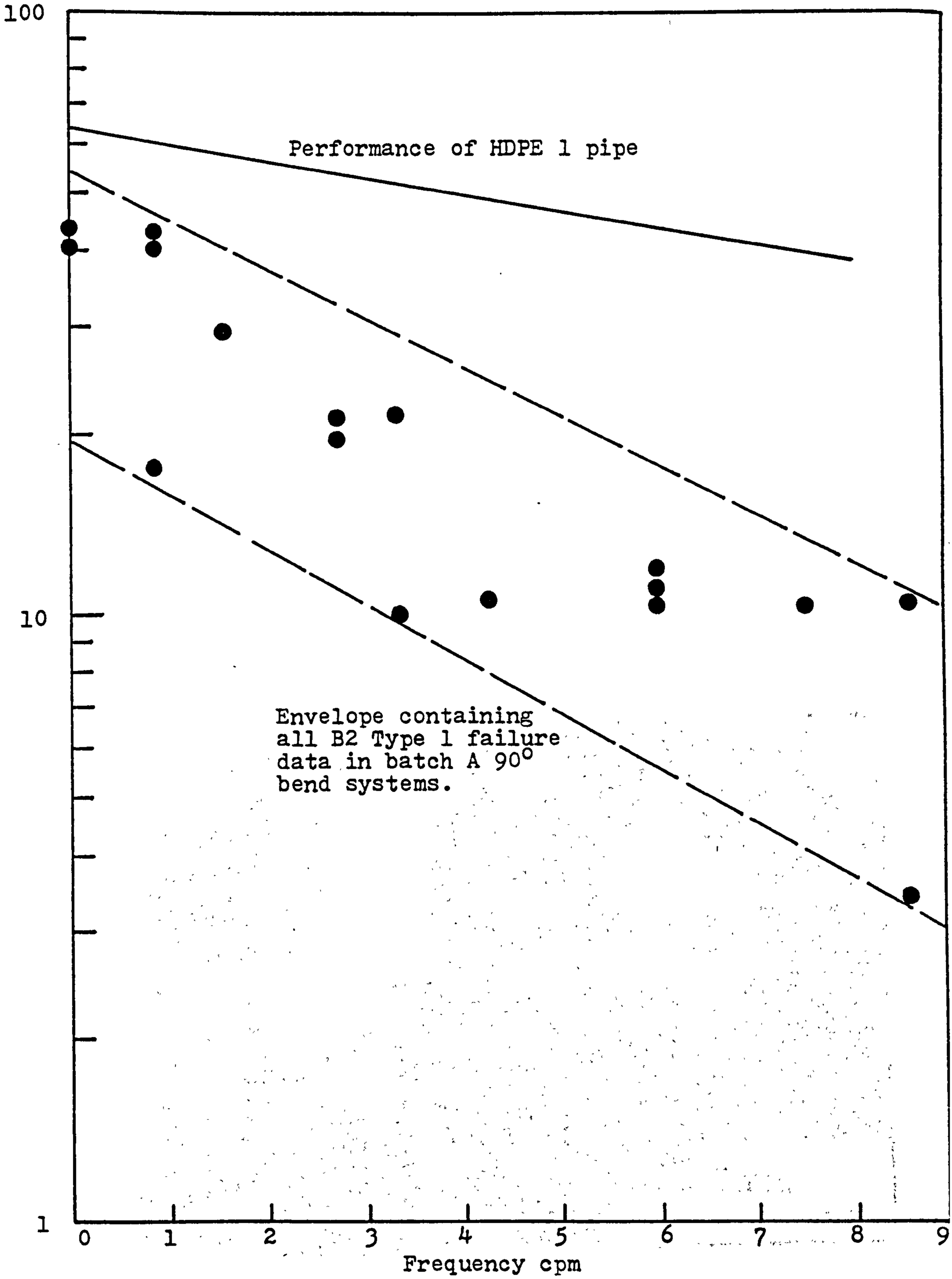

FIGURE 5.13 Performance of batch A 90° bends failing at site B2 Type 1 subjected to static and fatigue loads at 80°C and 4.93 MPa maximum pipe hoop stress.

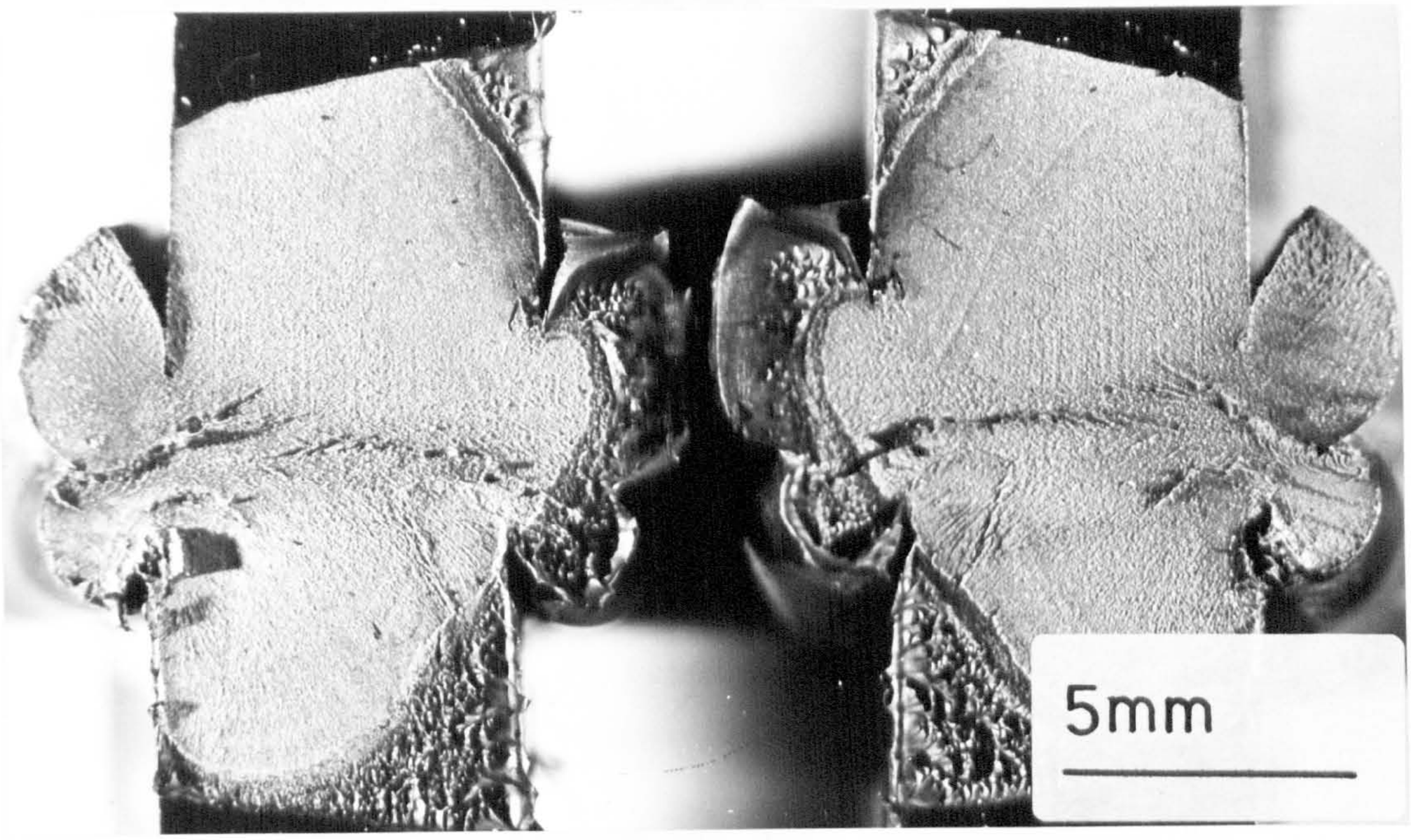

FIGURE 5.14a Example of a B2 type 1 fatigue fracture in HDPE 1 pipe + batch B 90° bend systems. 80°C
4.93 MPa maximum pipe hoop stress
7.5 cpm

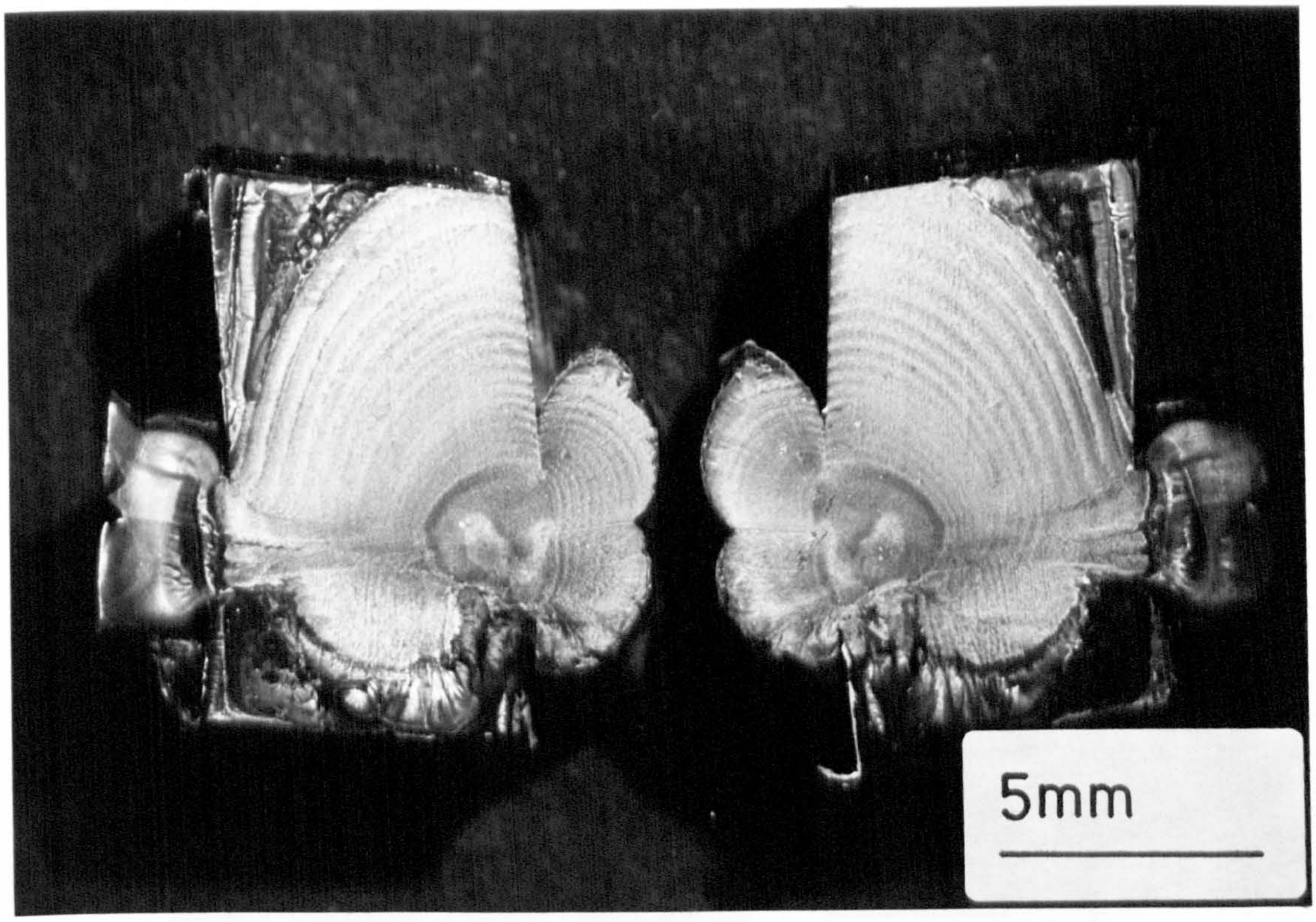

FIGURE 5.14b Example of a B2 type 1 fatigue fracture in HDPE 2 pipe + batch B 90° bend systems showing distinct discontinuous growth bands. 80°C; 4.93 MPa maximum pipe hoop stress; 7.5 cpm.

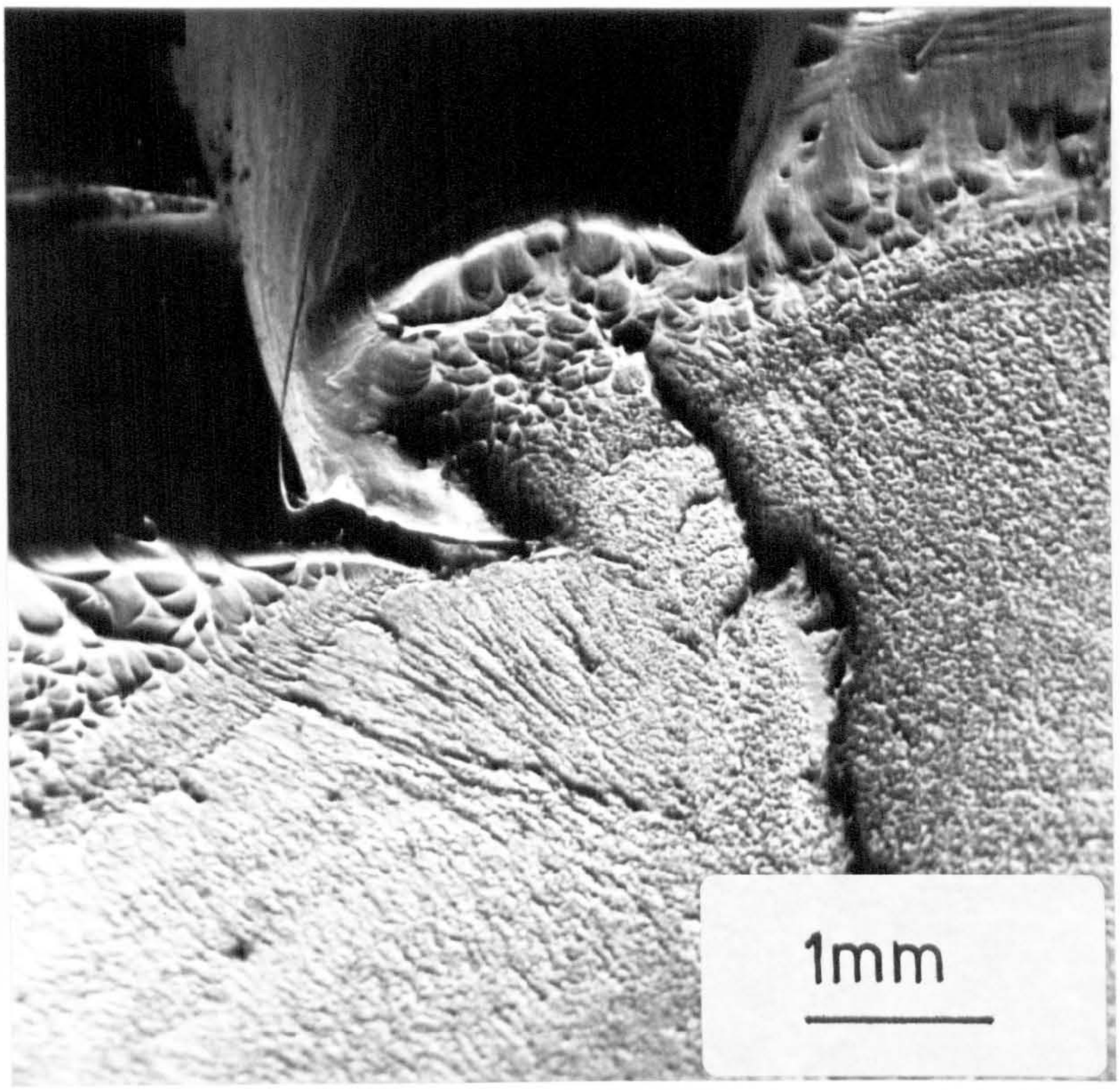

FIGURE 5.15a Scanning electron micrograph of a butt-weld fracture at the weld bead in HDPE 1 showing variations in local ductility.

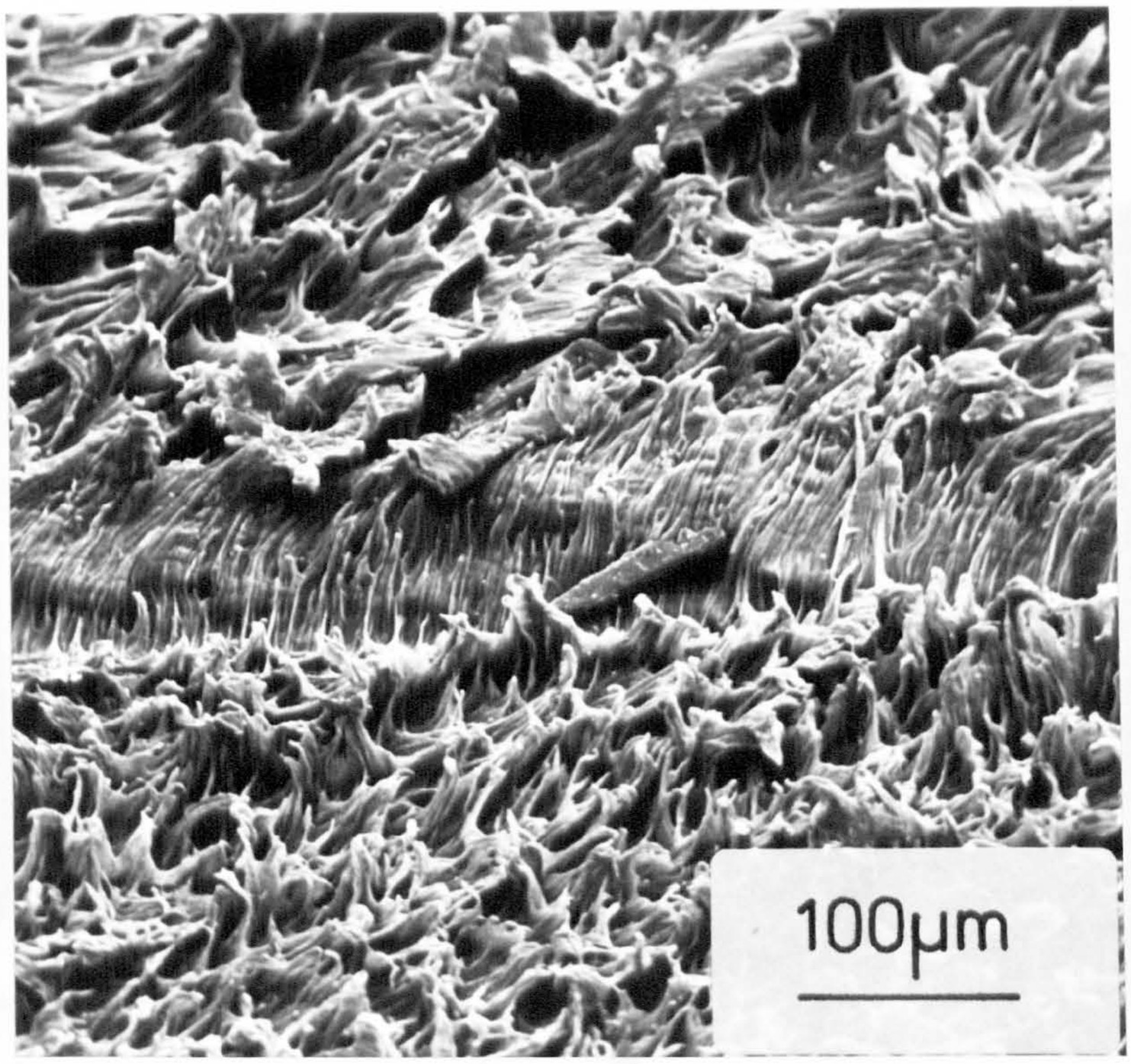

FIGURE 5.15b Scanning electron micrograph of a butt-weld fracture showing the weld interface and local variations in ductility.

FIGURE 5.16a Circumferential butt-weld failure (T2 type 2) in an HDPE 1 pipe + batch A 90° equal tee system. (This mode of failure was the only type of butt-weld fracture observed in MDPE 1 bend or tee systems.)

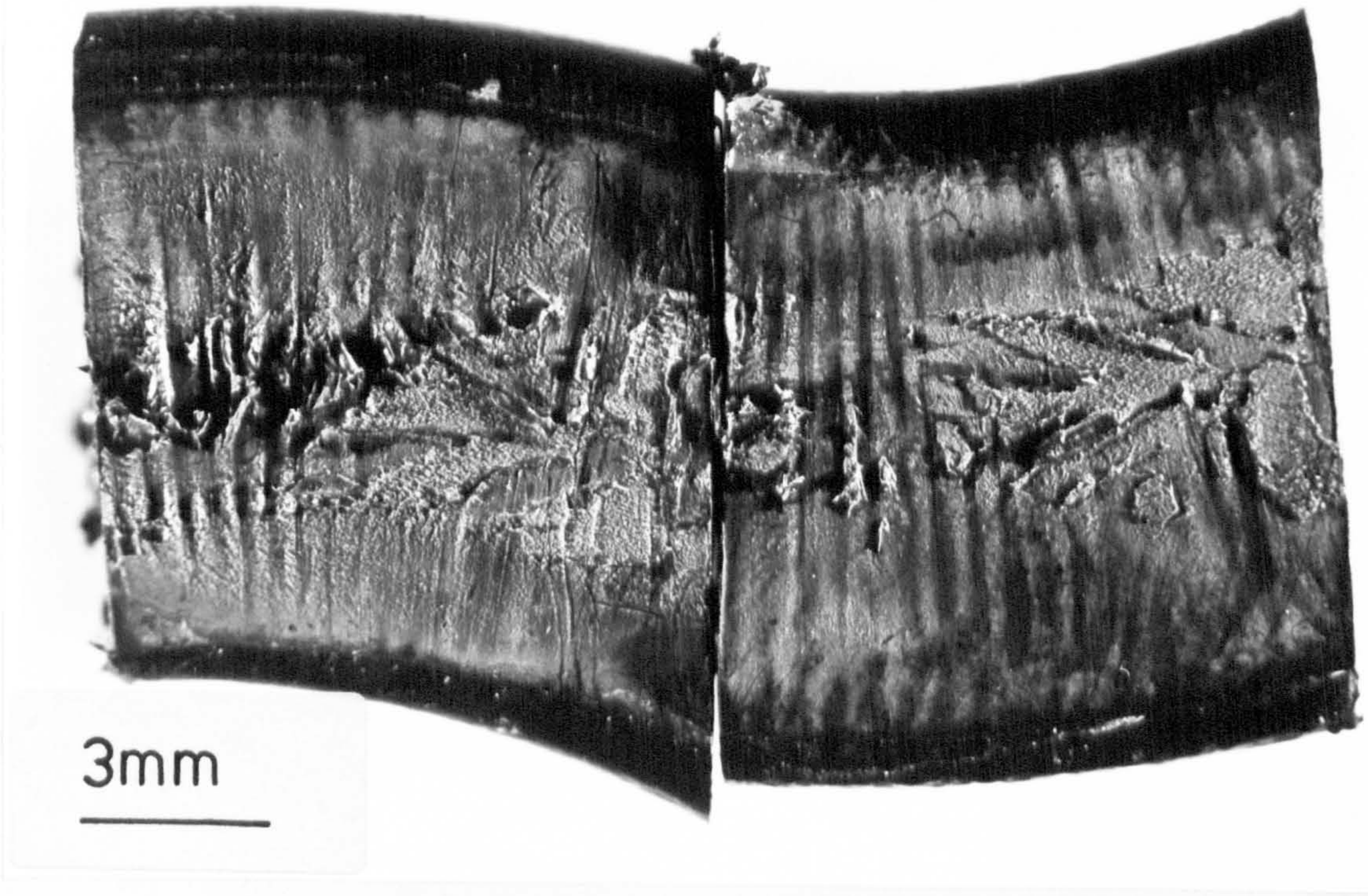

FIGURE 5.16b Fracture surface of a T2 type 2 butt-weld interface failure in an HDPE 1 pipe + batch A 90° equal tee system.

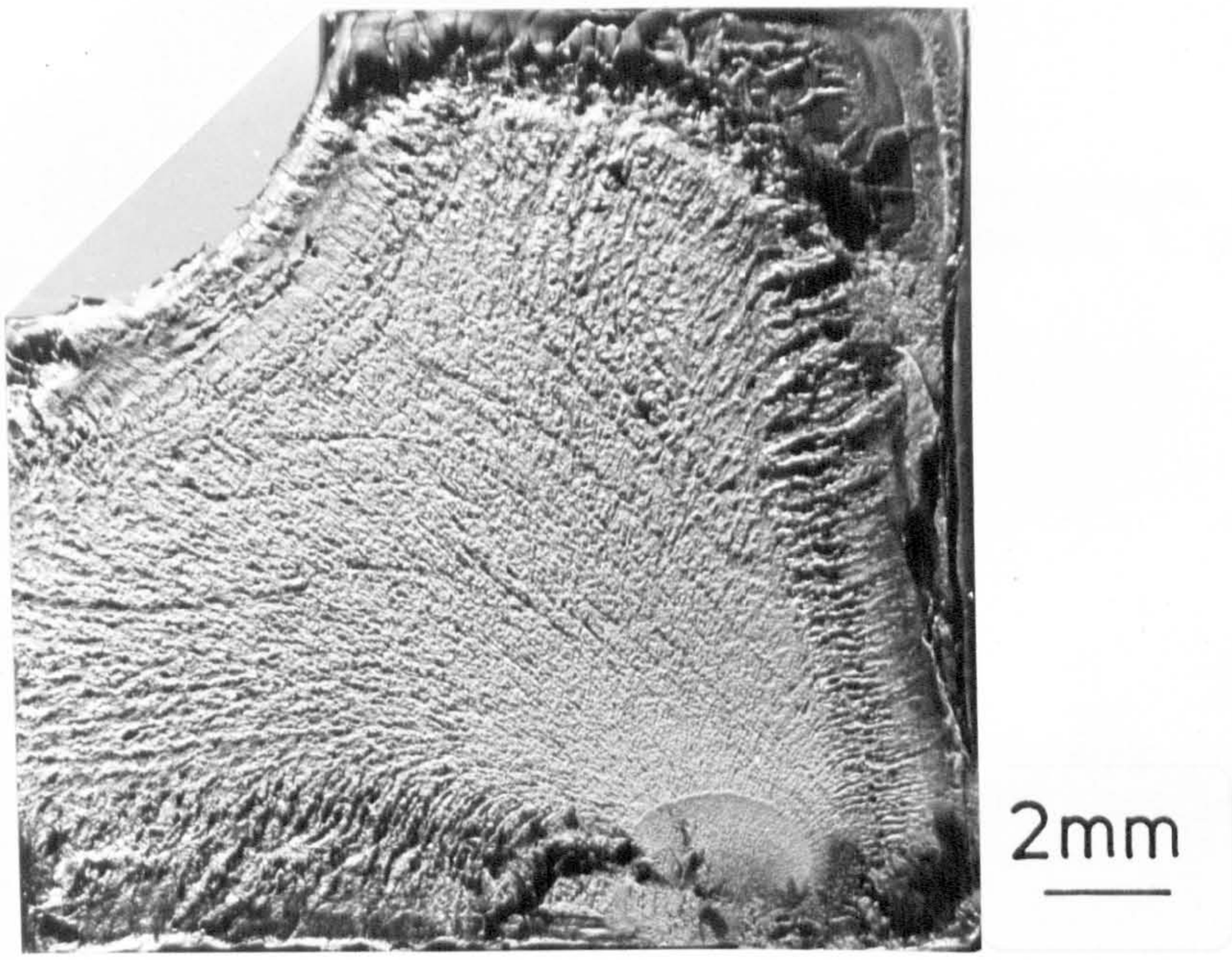

FIGURE 5.17a General features of a T3 fracture surface in an HDPE batch A 90° equal tee.

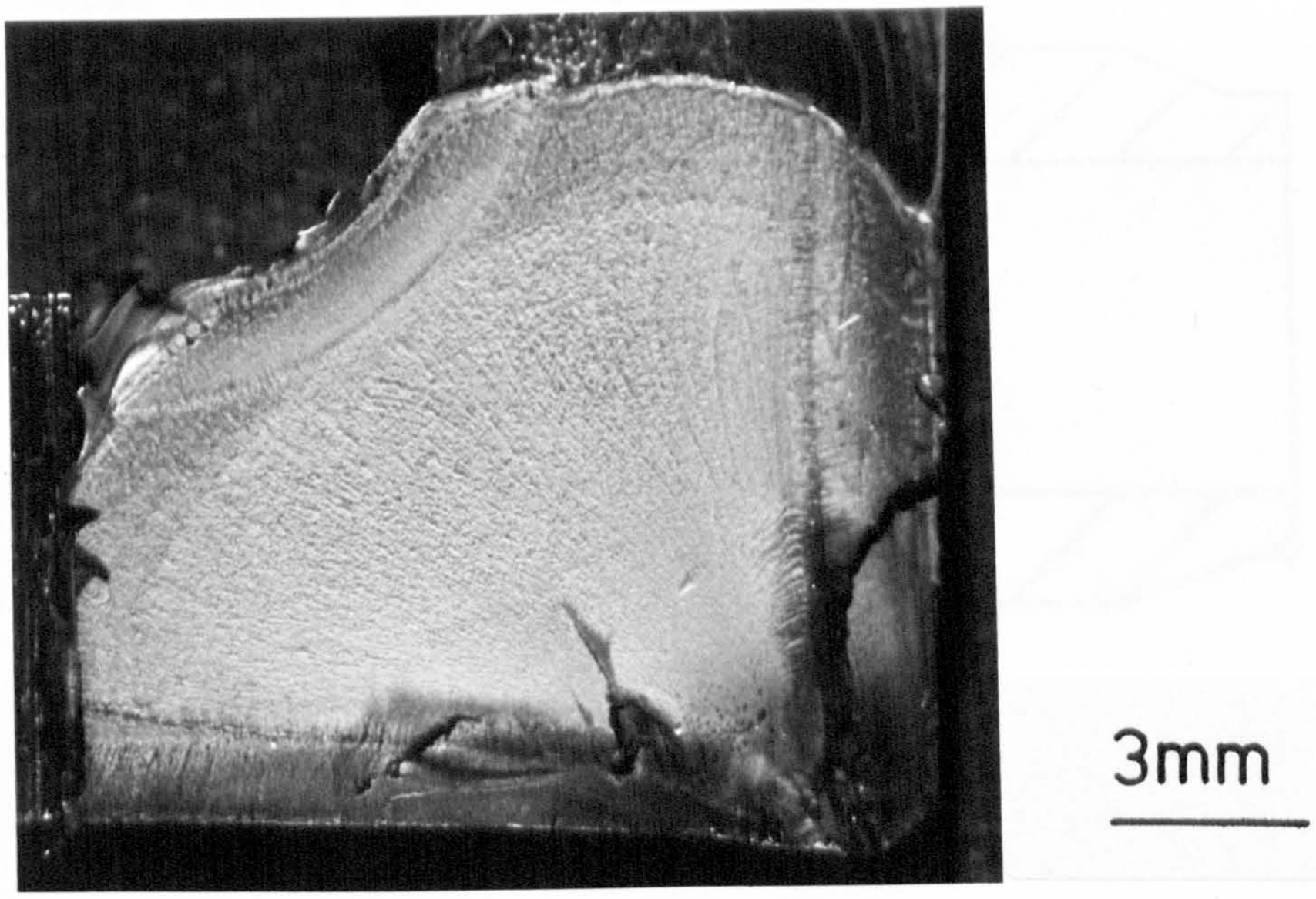

FIGURE 5.17b General features of a T3 fracture surface in an HDPE batch B 90° equal tee.

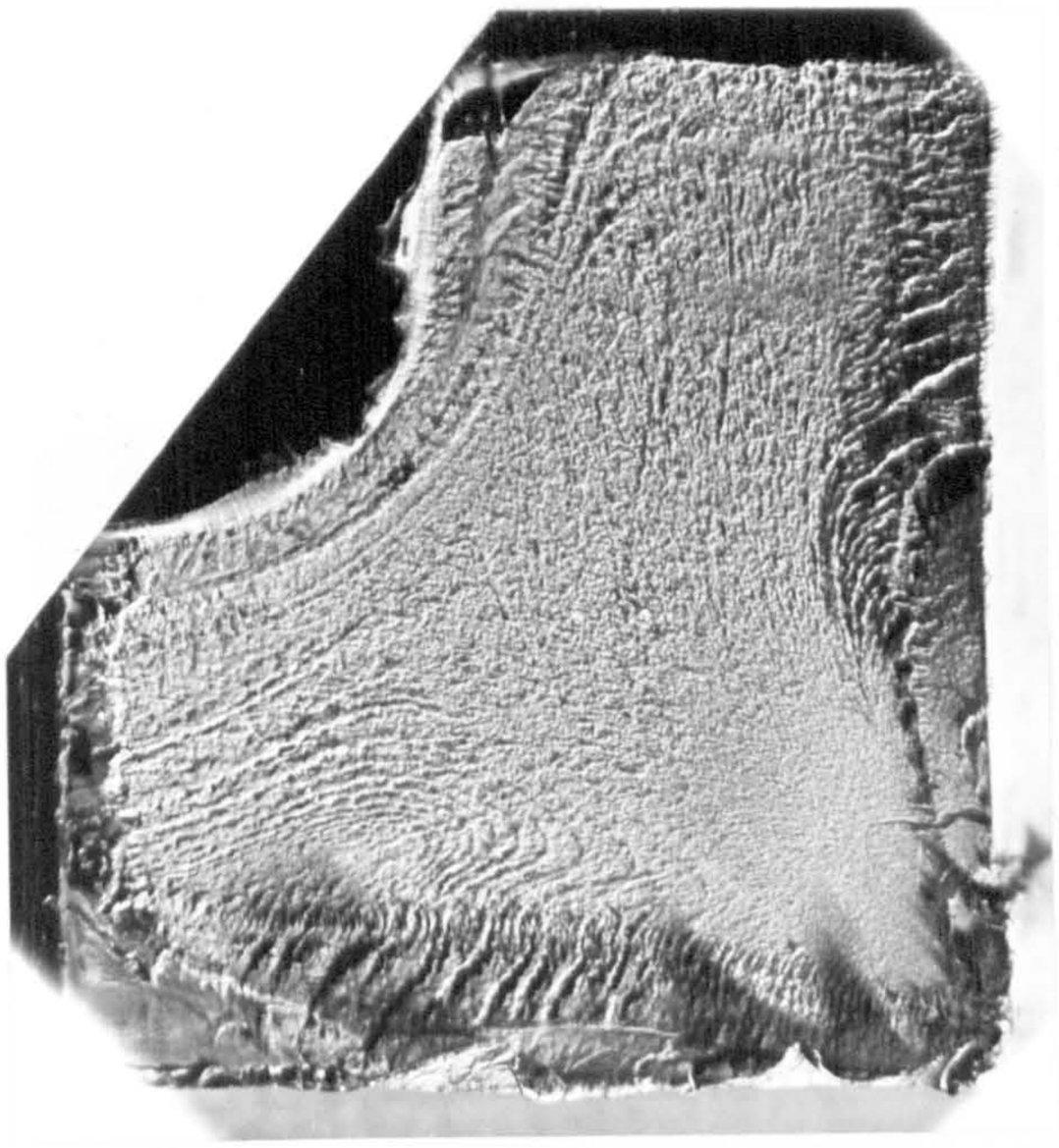

FIGURE 5.18a

Typical T3 fracture surface in an HDPE Batch A 90° equal tee.

3mm

← T3 crack initiation site (mould core damage).

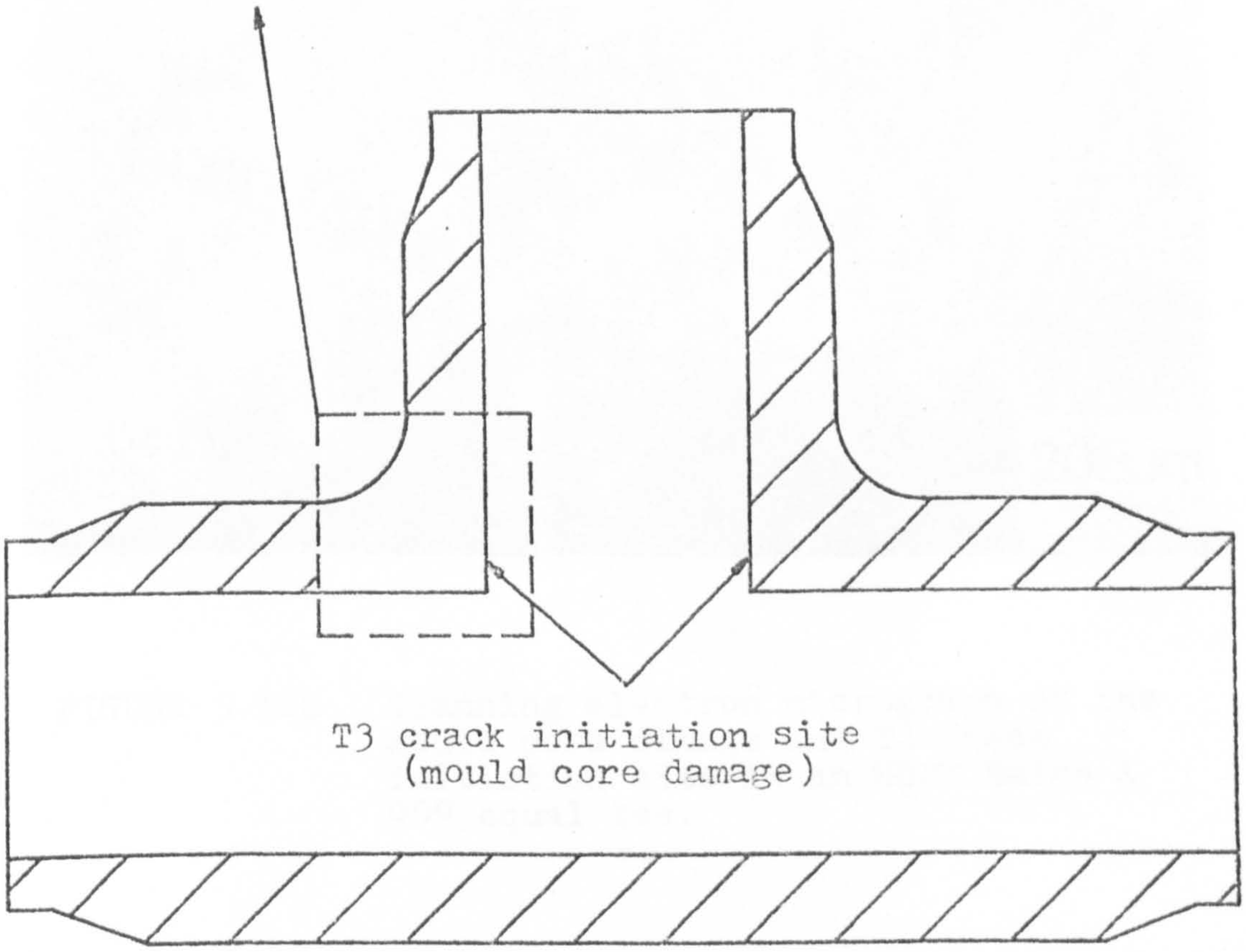

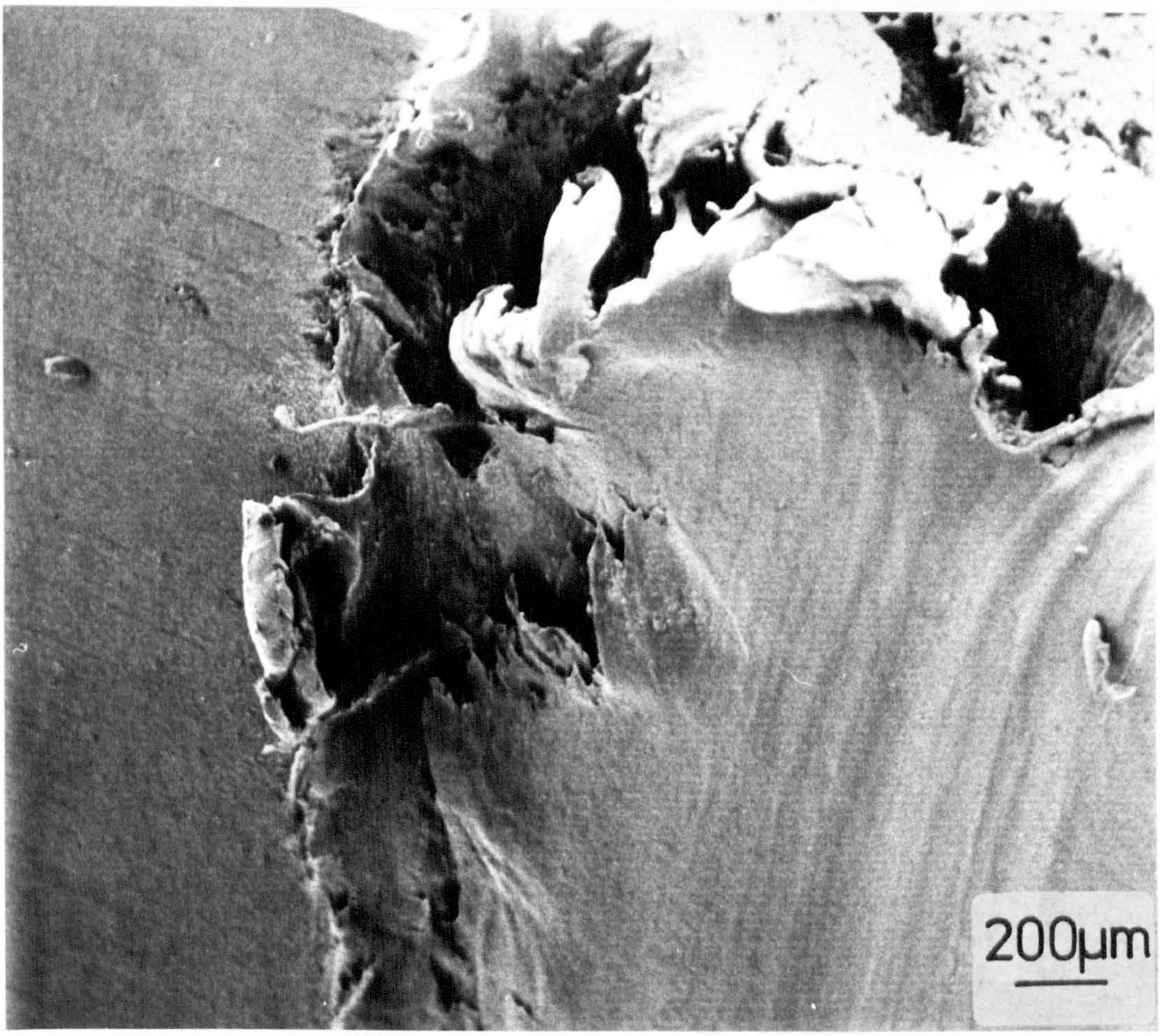

FIGURE 5.18b Scanning electron micrograph of the mould core damage and T3 crack initiation site in an HDPE Batch A 90° equal tee.

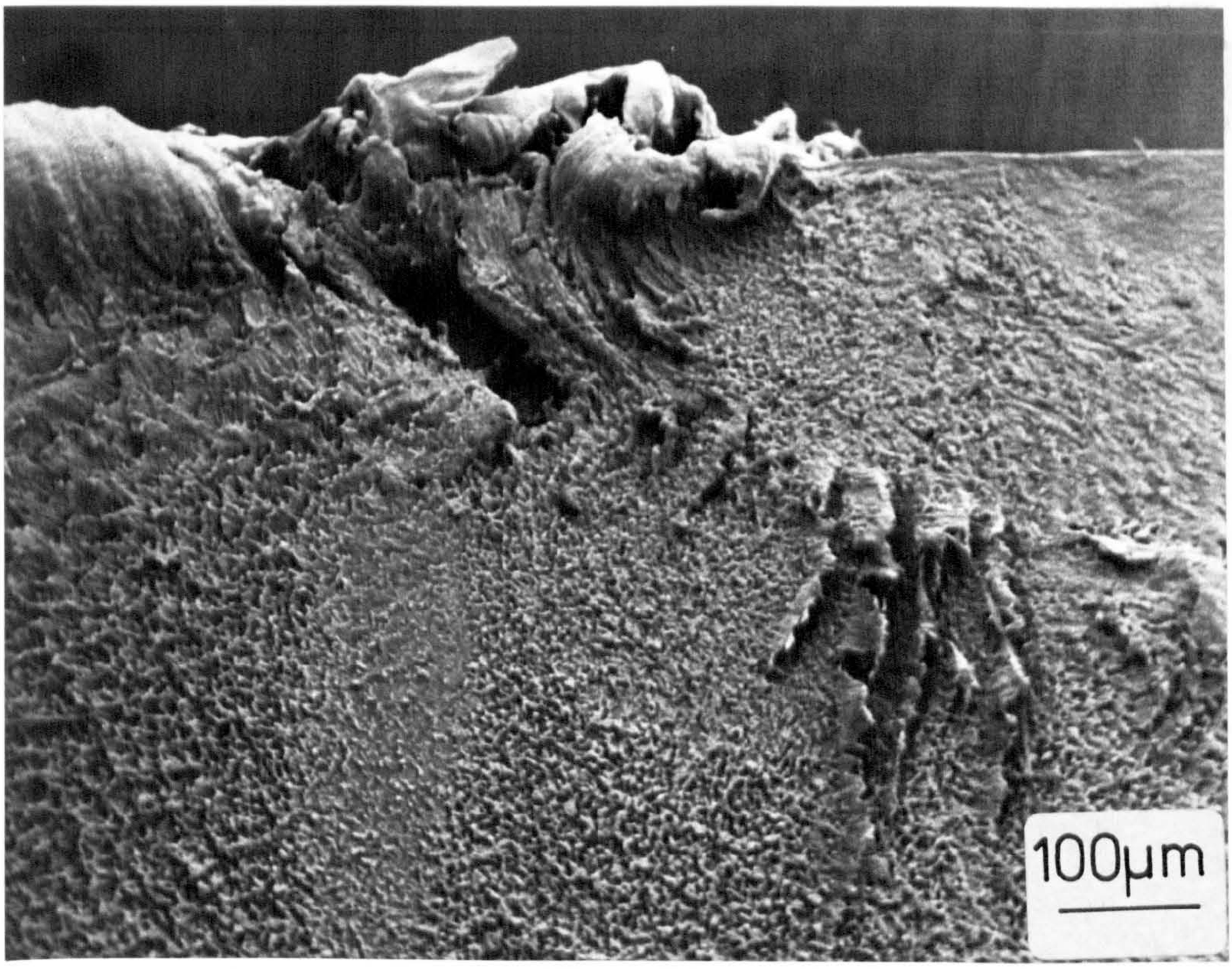

(c)

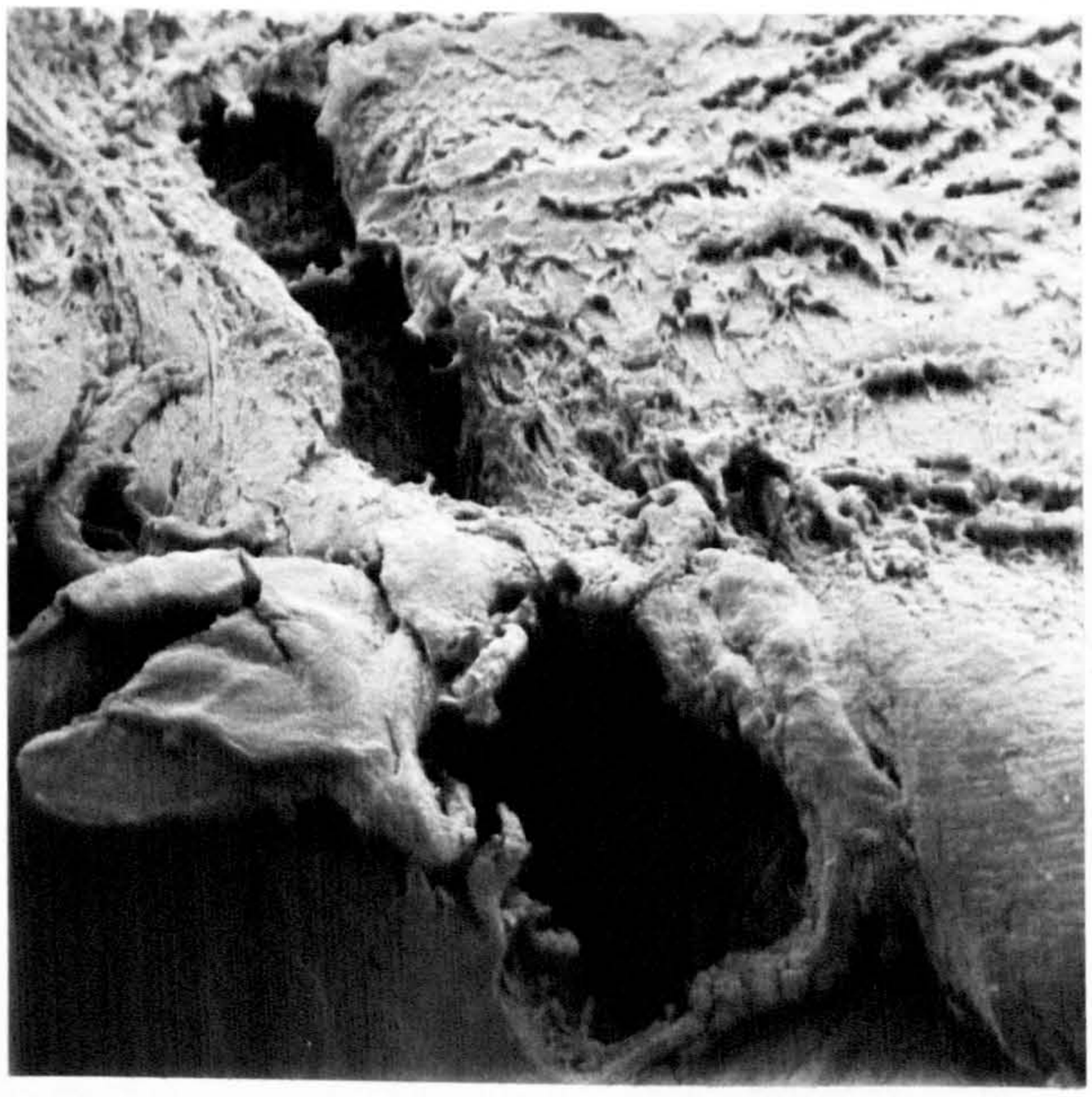

(d)

FIGURE 5.18(c + d) Scanning electron micrographs of mould core damage observed on 63mm OD SDR 11 HDPE Batch A and B 90° equal tees. T3 fracture initiation was invariably associated with these regions.

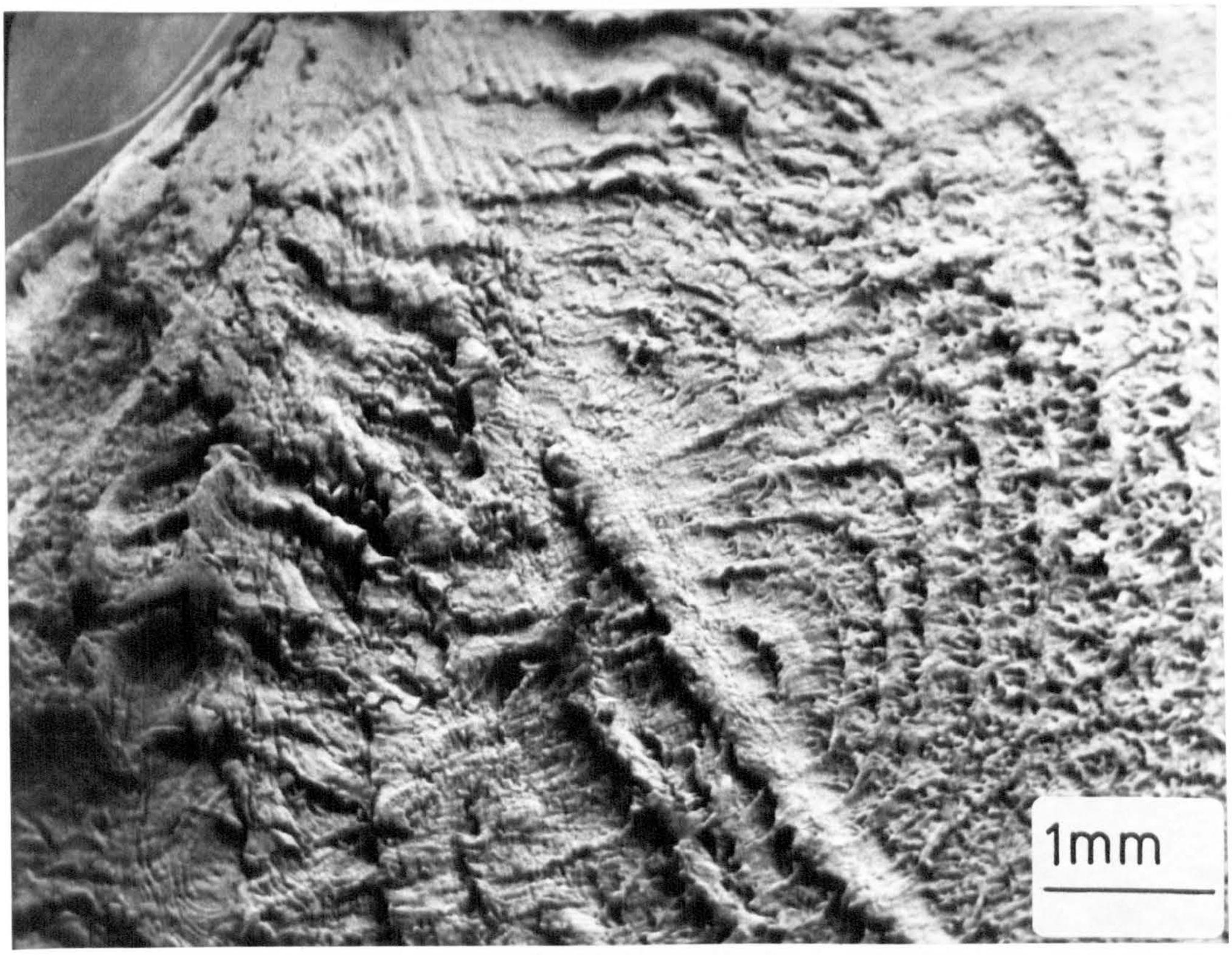

FIGURE 5.19 Scanning electron micrograph of variations in fracture surface morphology on a T3 fracture.

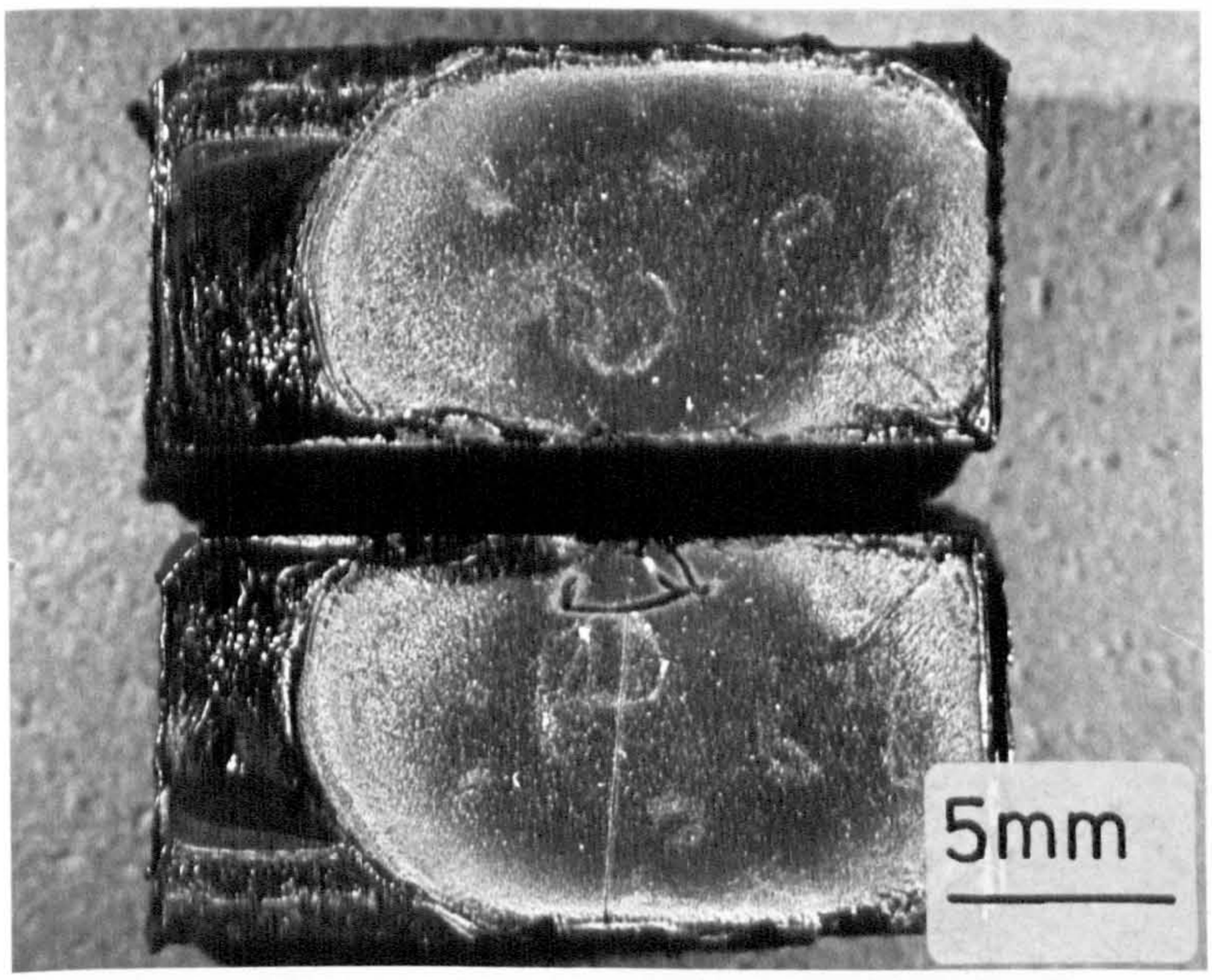

FIGURE 5.20 Typical T4 fracture surface in an HDPE Batch A 90° equal tee which is associated with an internal weld along the spine of the fitting.

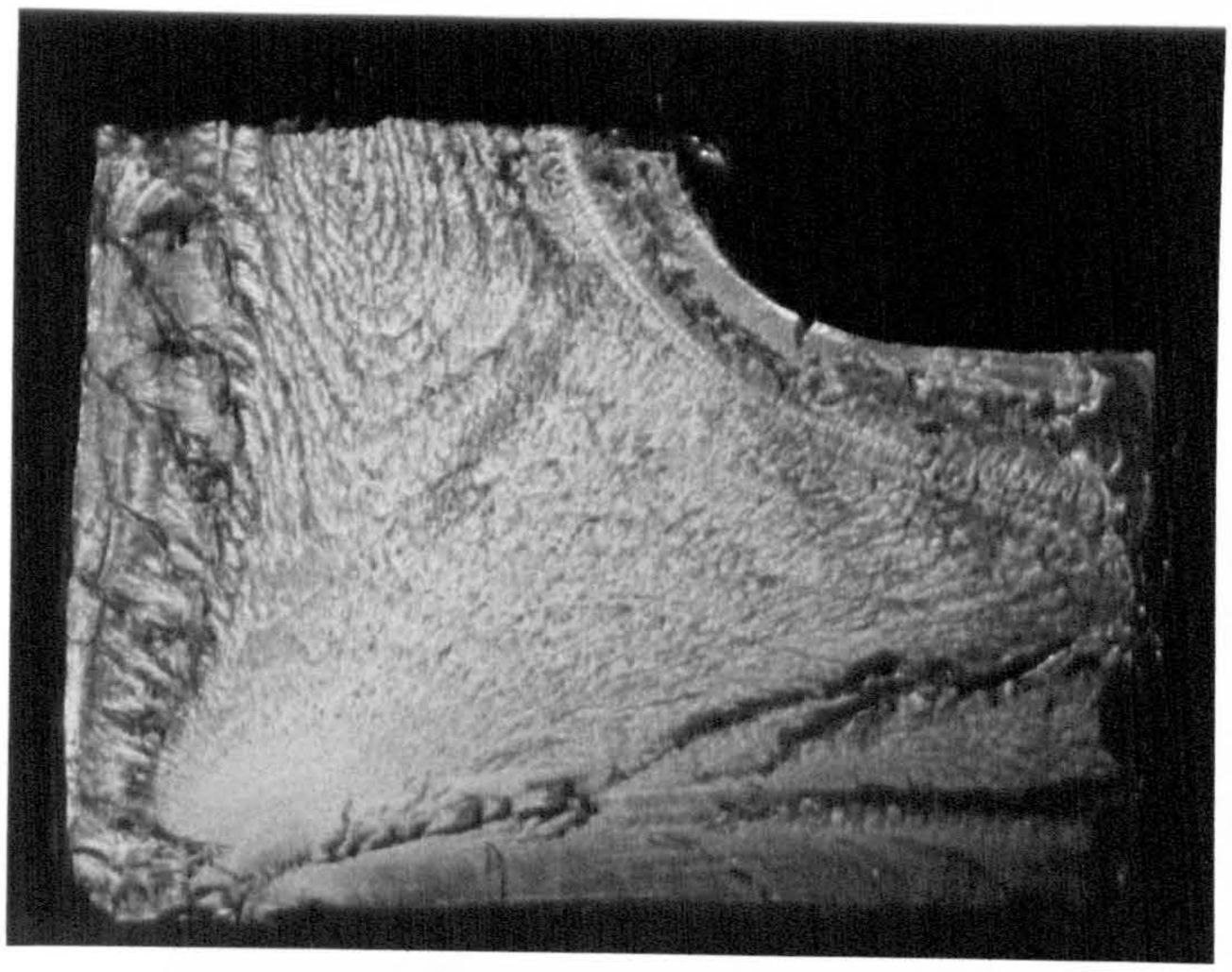

FIGURE 5.21a

HDPE Batch A T3 fatigue fracture surface.
80°C
4.93 MPa pipe hoop stress
8.57 cpm

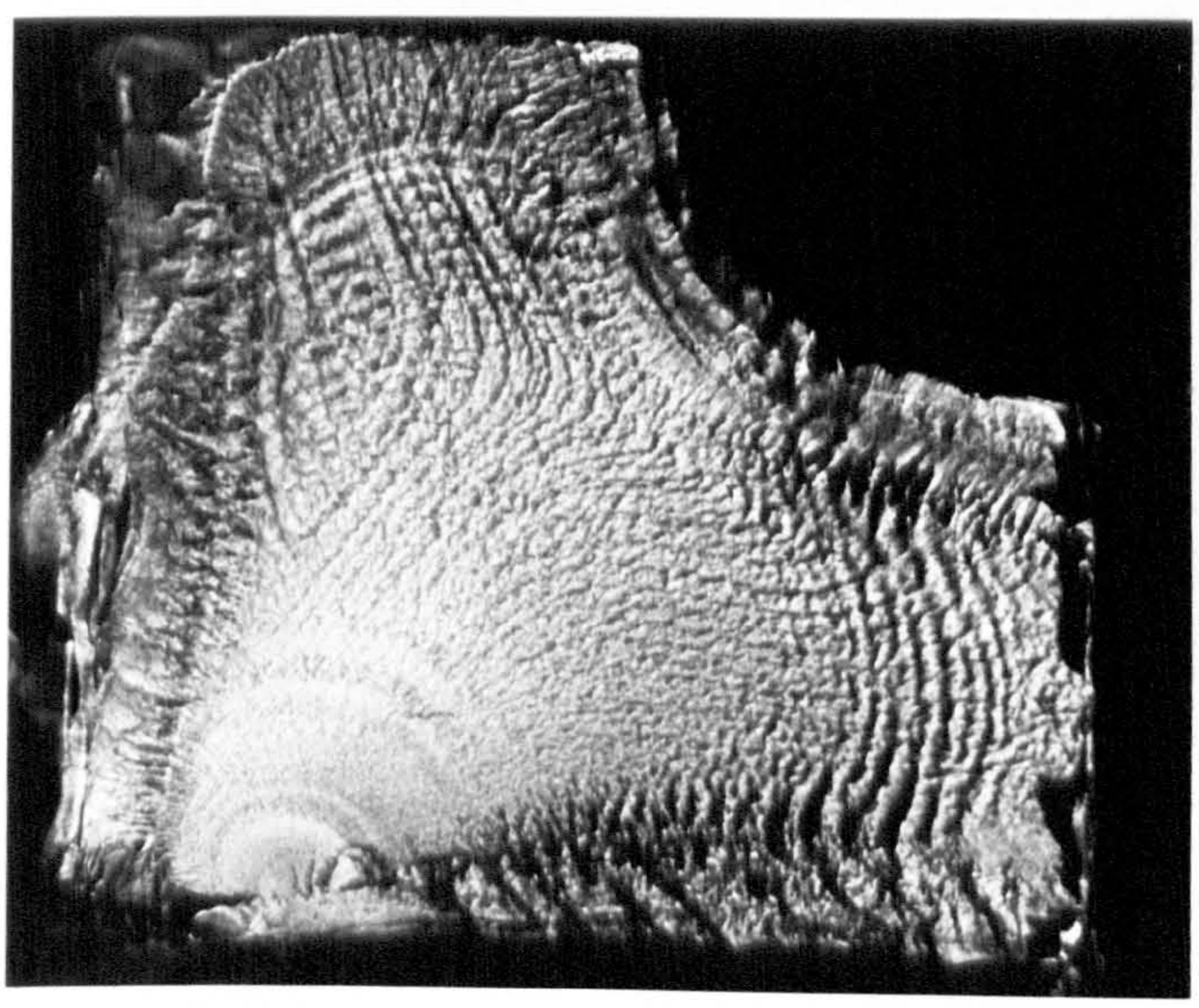

FIGURE 5.21b

HDPE Batch A T3 fatigue fracture surface.
80°C
4.93 MPa pipe hoop stress
2.72 cpm

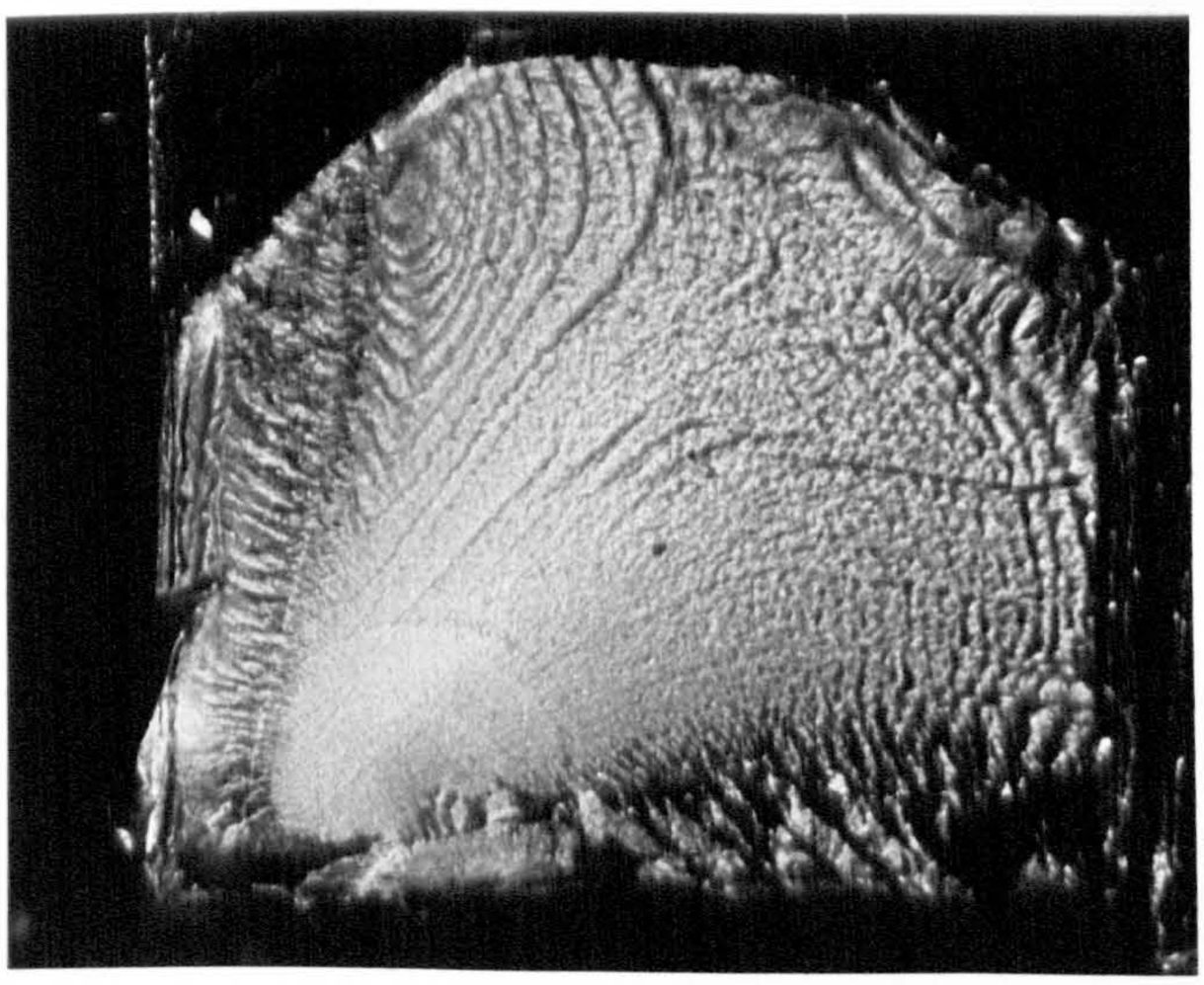

FIGURE 5.21c

HDPE Batch A T3 fatigue fracture surface.
80°C
4.93 MPa pipe hoop stress
1.57 cpm

FIGURE 5.21 HDPE Batch A T3 fracture surface variations with frequency at the same pressure. (Stresses quoted are maximum values.)

3mm

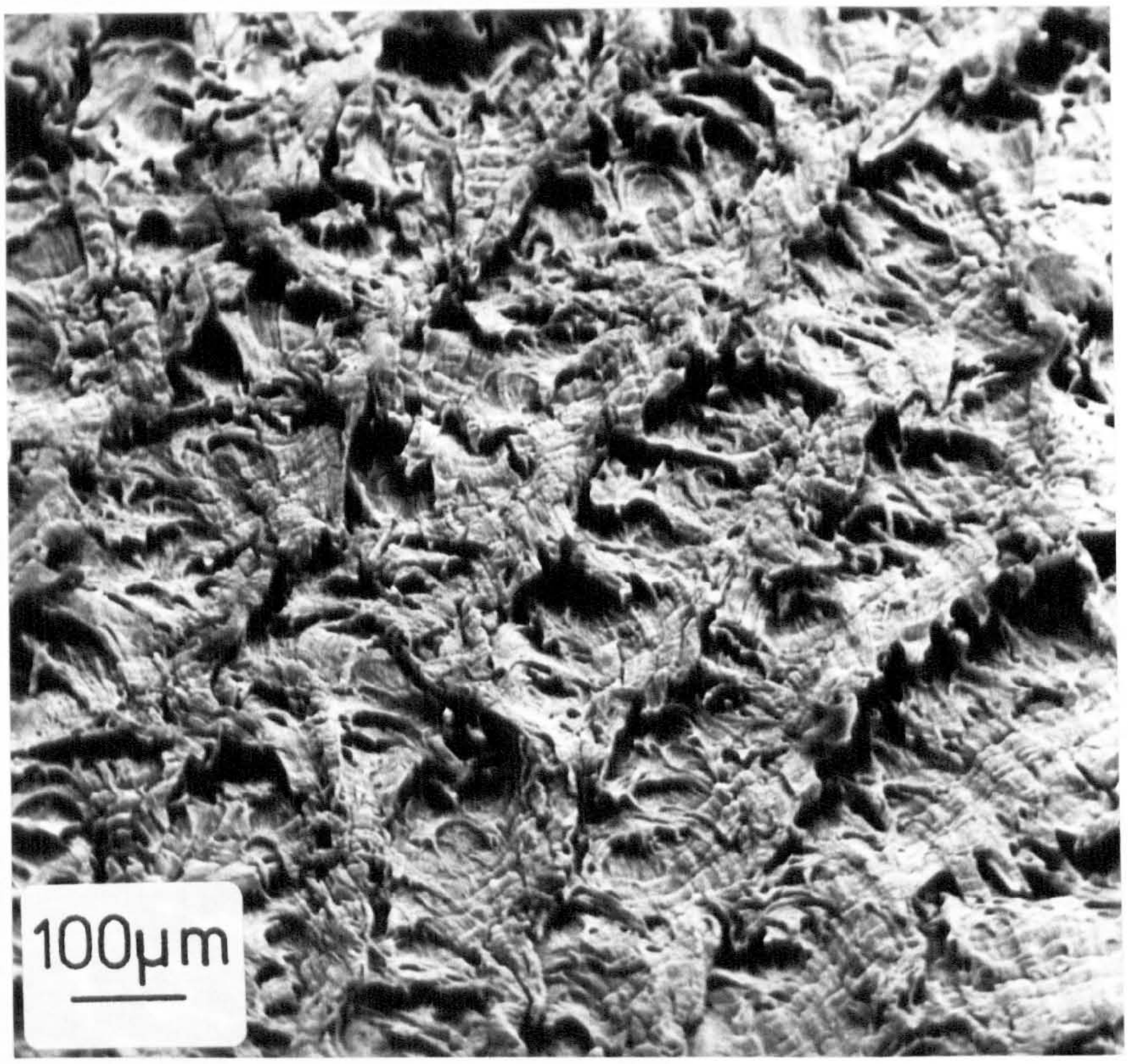

FIGURE 5.22 Scanning electron micrograph of a T3 fracture surface showing bands of varying ductility.

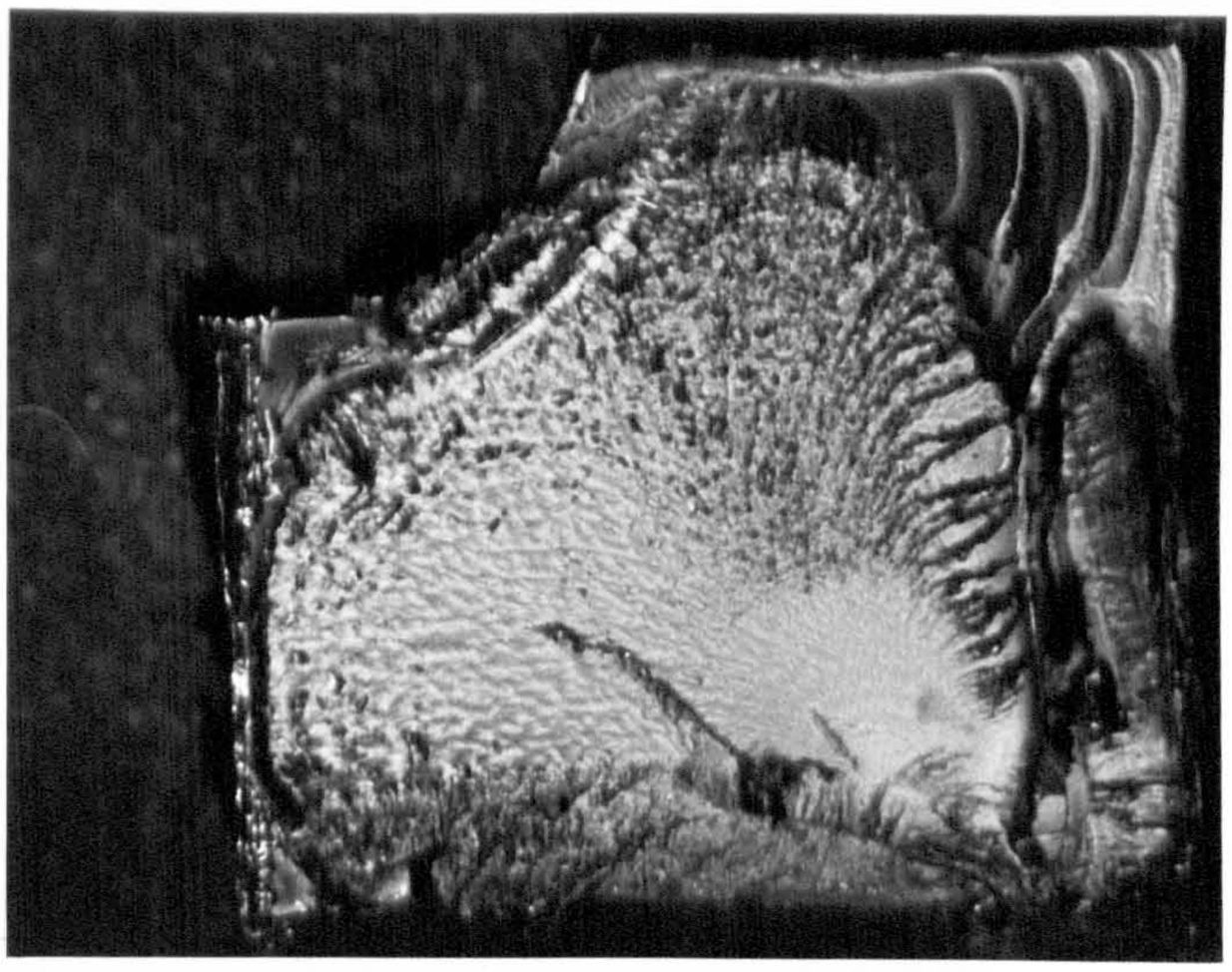

FIGURE 5.23a

HDPE Batch B T3 fatigue fracture surface.
80°C
4.93 MPa pipe hoop stress
7.5 cpm

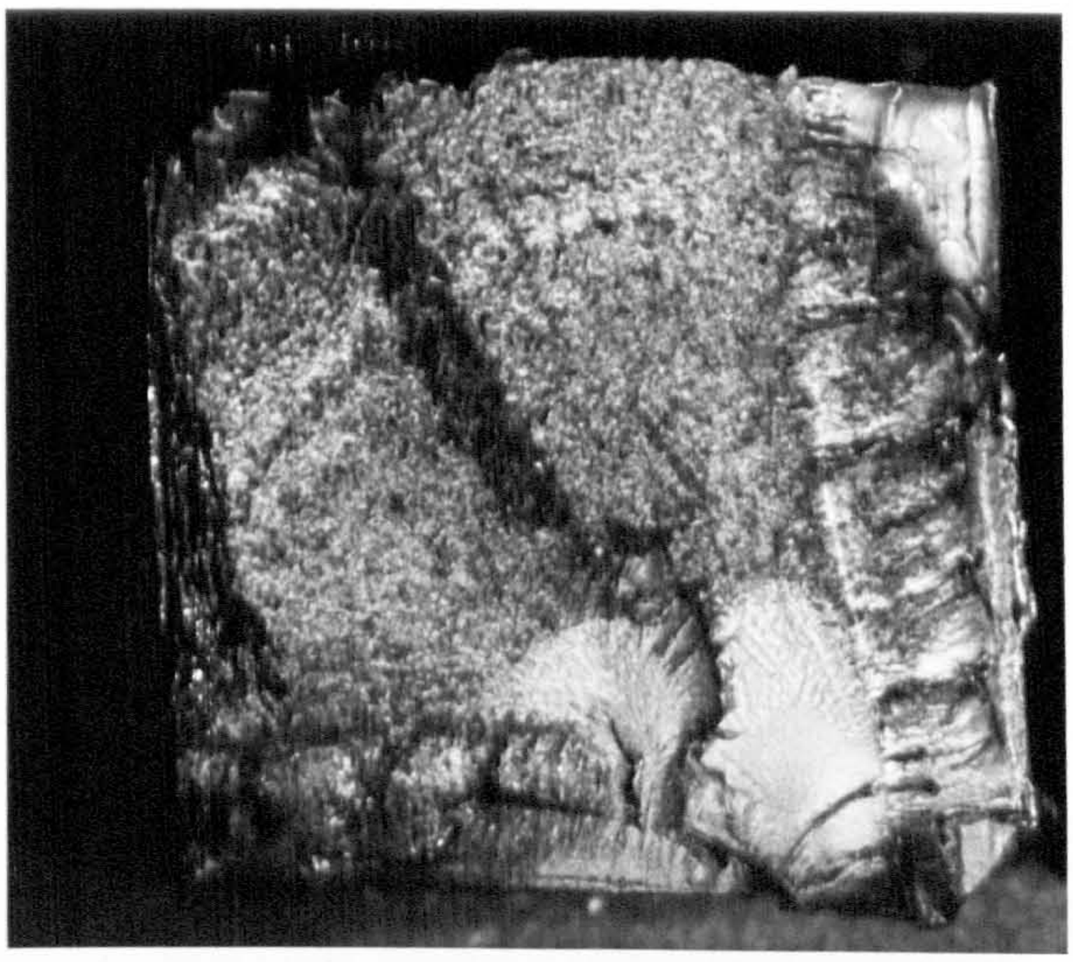

FIGURE 5.23b

HDPE Batch B T3 fatigue fracture surface.
80°C
4.93 MPa pipe hoop stress
4.29 cpm

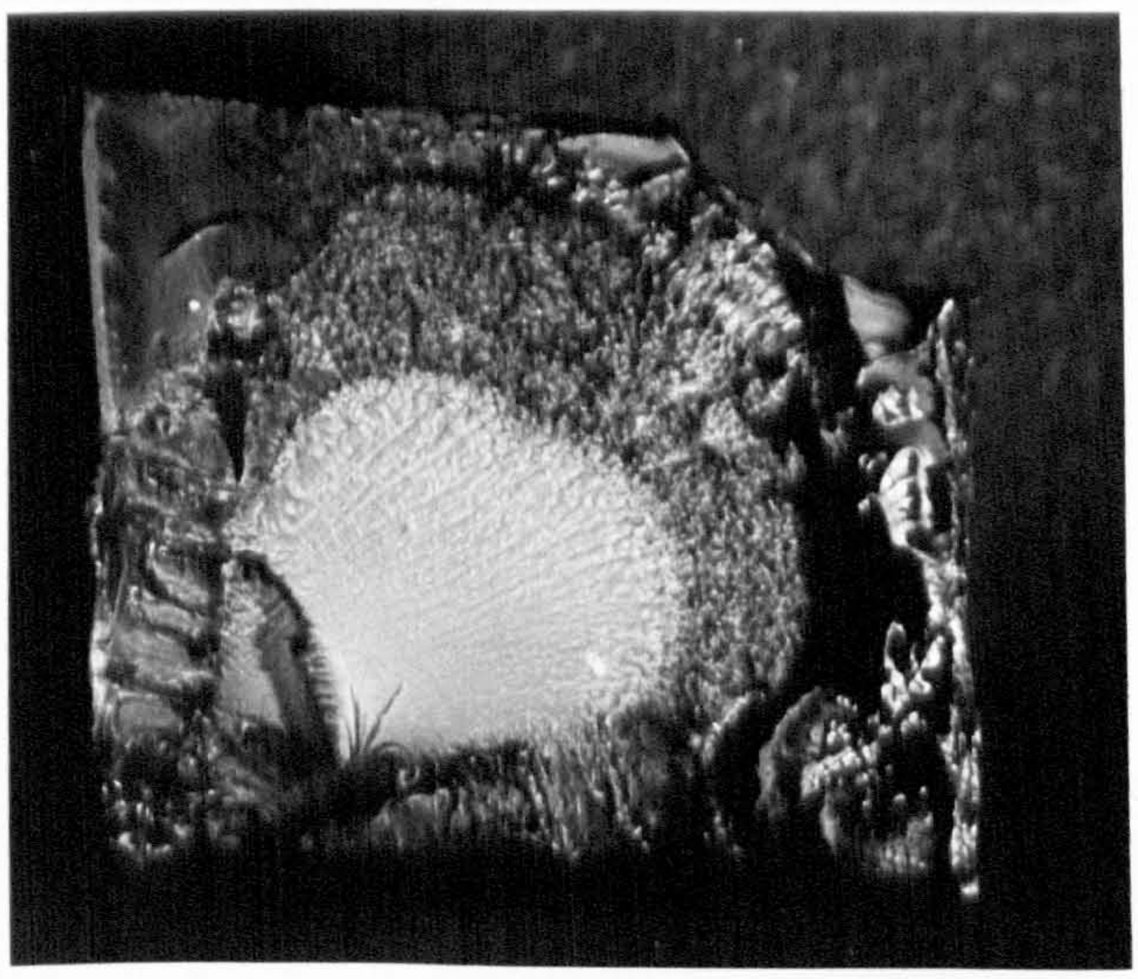

FIGURE 5.23c

HDPE Batch B T3 fatigue fracture surface.
80°C
4.93 MPa pipe hoop stress
1.57 cpm

FIGURE 5.23 HDPE Batch B T3 fracture surface variations with frequency at the same pressure. (Stresses quoted are maximum values.)

3mm

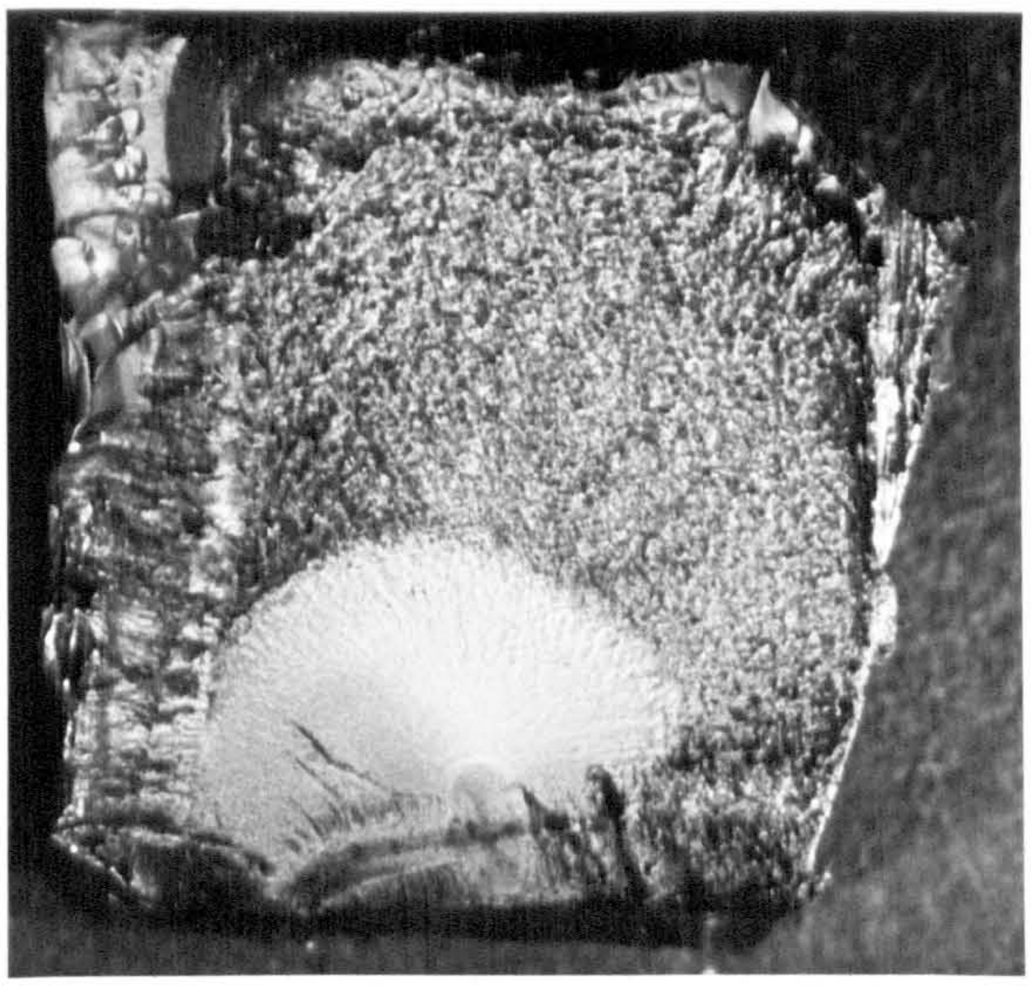

FIGURE 5.24a

HDPE Batch B T3 fatigue fracture surface.
80°C
4.93 MPa pipe hoop stress
4.29 cpm

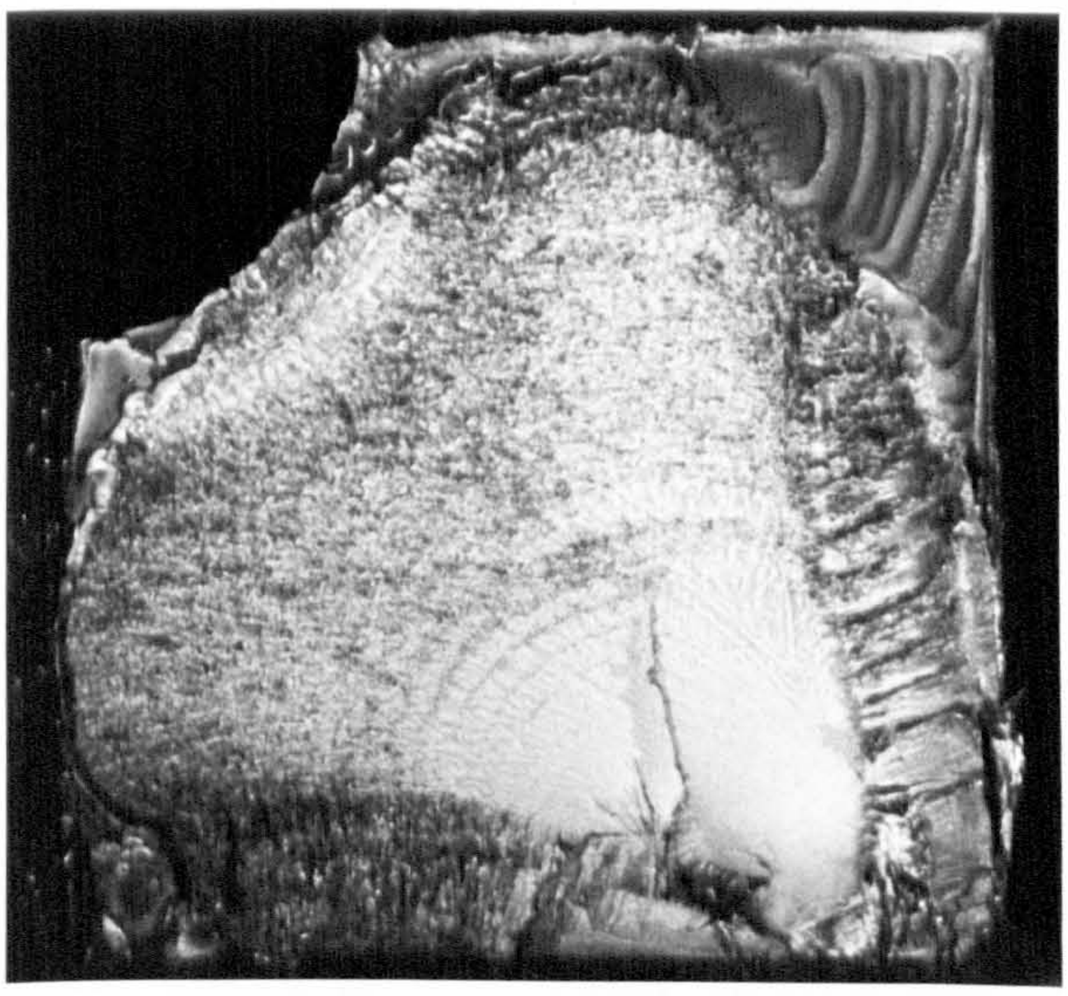

FIGURE 5.24b

HDPE Batch B T3 fatigue fracture surface.
80°C
3.88 MPa pipe hoop stress
4.29 cpm

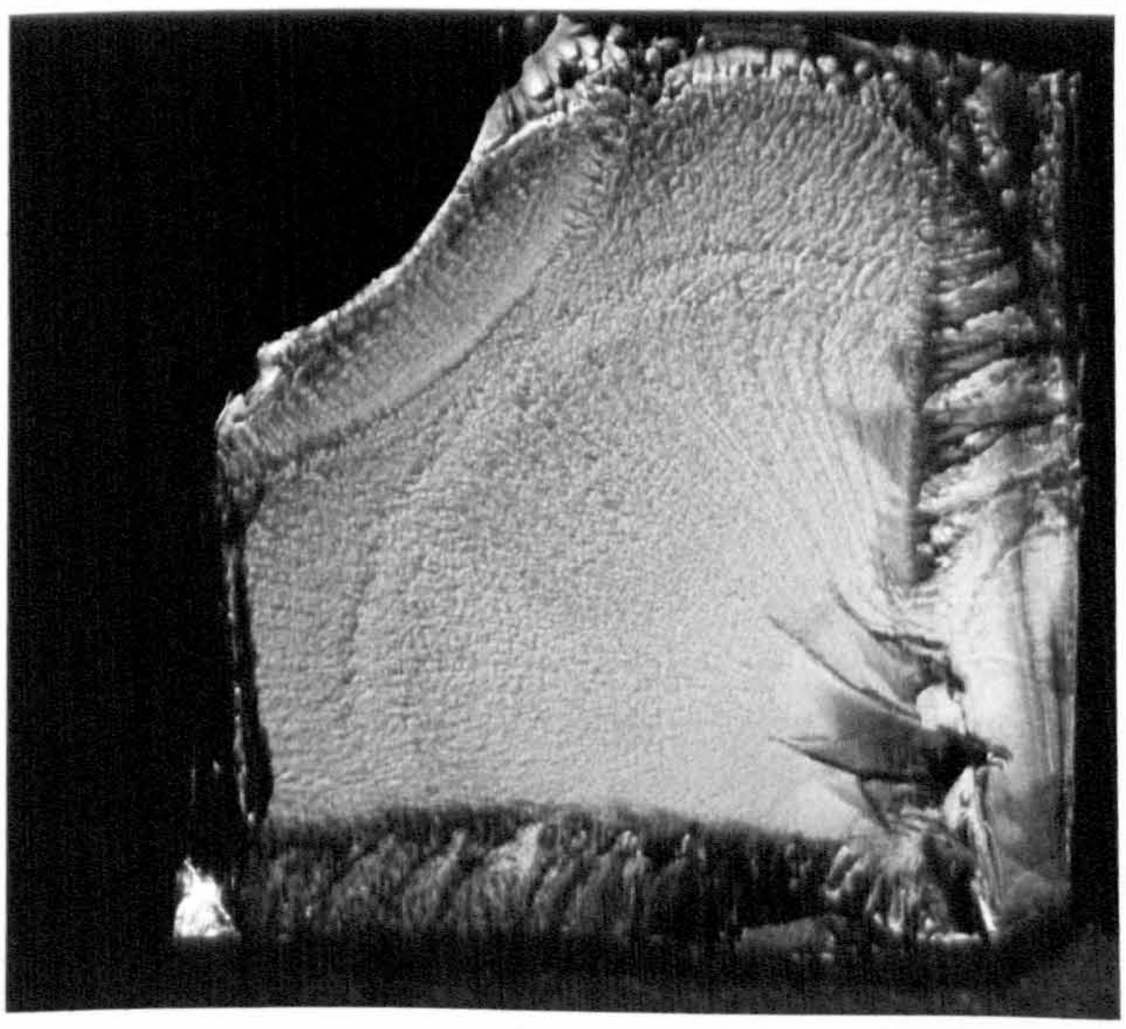

FIGURE 5.24c

HDPE Batch B T3 fatigue fracture surface.
80°C
3.00 MPa pipe hoop stress
4.29 cpm

FIGURE 5.24 HDPE Batch B T3 fracture surface variations with pressure at the same frequency. (Stresses quoted are maximum values.)

3mm

CHAPTER 6 - RESULTS

LARGE DIAMETER PIPE SYSTEMS

(160mm OD/SDR 11 HDPE and 180mm OD/SDR 17 MDPE)

6.1 INTRODUCTION

The cost and size of the larger diameter pipe systems precluded a complete frequency response study as in the case of the smaller diameter systems, nevertheless it was intended to obtain data relating to any obvious mechanical performance weaknesses which would expand the trends observed in the smaller diameter systems and lead to some possible generalisations in behaviour which could be of use to the design engineer.

6.2 160mm OD SDR 11 HDPE 1 Based Pipe Systems

6.2.1 Mechanical Performance and Failure Sites

160mm OD HDPE 1 SDR 11 pipe systems produced from the same pipe and fitting material as used in the 63mm OD HDPE 1 SDR 11 pipes and the batch A fittings, were tested only under fatigue at a fixed loading frequency of 6 cpm (0.1 Hz), a maximum internal pressure of 1 MPa and at a temperature of 80°C.

Behaviour was similar to that of the smaller diameter pipe systems in that a significant reduction in lifetime was obtained. Results are detailed in Figure 6.1. The bold lines show, for the purposes of comparison, the behaviour of the HDPE 1 63mm OD SDR 11 pipe
at the same temperature of 80°C and maximum internal pressure of 1 MPa.

Using the same notation to describe failure sites as that used for the 63mm OD SDR 11 HDPE 1 systems the following brittle fractures were observed:-

Pipe and Welded Pipe Systems
P1, P/P1, P/P2 Type 1

90° Equal Tee Systems
T1, T2 Type 1, T4 (No T3 failures were observed)

90° Bend Systems
B1, B2 Type 1 (No B3 failures were observed)

Five pipe failures were recorded, four of which initiated from macrovoids in the pipe wall. (No small diameter pipes failed from inhomogeneities such as these during the course of the test programme.) These voids

constituted a considerable weakness in the 160mm systems subjected to fatigue. The voids had a maximum dimension in excess of 2mm and the pseudo stress rupture lifetimes ($\tau_{FATIGUE}$) of pipes failing from such defects were between 3 and 6 hours with a mean lifetime of 4.6 hours. The fifth failure of the large diameter SDR 11 HDPE 1 pipe was from a small particle lying close to the inside surface, similar in size to that observed in the smaller pipe sizes. The pseudo stress rupture life for this failure was in excess of 50 hours, a similar lifetime to the 63mm SDR 11 HDPE 1 pipes for identical testing conditions.

One failure was also recorded in a pipe-to-pipe butt-weld (P/P2 Type 1) with a $\tau_{FATIGUE}$ value of 12 hours. It was a butt-weld fracture lying parallel to the pipe extrusion direction across the weld.

Other significant weaknesses occurred at discontinuities present at those welds made between pipe and injection moulded fittings, 90^{o} equal tees, 90^{o} bends and stub flanges. Flow lines in the 90^{o} tee fittings, shown to good effect in Figure 6.2, also constituted a site (T4) of premature failure.

The external appearances of typical examples of these observed failure sites are shown in Figure 6.3. In all cases the orientation of the fractures lay approximately parallel to the pipe extrusion direction.

Comparison of the limited 160mm OD fatigue data with the 63mm HDPE 1 results presented in Figure 6.1 demonstrates that under the same conditions of fatigue test the larger diameter pipe is more likely to fail prematurely. The main source of weakness in the systems was the existence of large voids in the extruded pipe sections, but in all cases a major stress concentration was responsible for failure, particularly in the form of notches formed in the weld beads joining the extruded and moulded parts.

It is also interesting to note that the T4 failure site in the body of the tee fitting which was induced only by static loads in the smaller diameter pipe, was here caused by fluctuating internal pressures. There was no instance of a T3 failure which was the predominant

fatigue weakness in the 63mm HDPE 1 and 2 based tee systems. Closer inspection after failure revealed that no T3 failure had even initiated in the 160mm fittings.

6.2.2 Morphology and Fracture Surface Analysis

(i) Morphology.

Emphasis was given to the characterisation of morphological variations of the 160mm SDR 11 HDPE injection moulded fittings which exhibited pronounced changes in shape in the vicinity of butt-welds as a result of the welding process, further examples of which are shown in Figure 6.4.

These stress concentrations are potential sites of premature failure and were also observed in the 63mm HDPE systems although they were absent in the 60mm MDPE 1 pipe-to-fitting welds.

The method adopted for the morphological characterisation was to examine, with a light microscope, the surface of a bulk specimen prepared by planing with a sledge microtome fitted with a relatively blunt steel blade. Stress whitening of varying intensity was thus produced as the blade cut through the surface and such effects are considered indicative of changing microstructural properties through the thickness of the article. Figure 6.5 shows an example of the type of surface produced by this method of preparation. In addition to the characteristic skin, two additional bands can be clearly seen, the presence of which will always be associated with a poorly developed weld bead, also clearly visible. The absence of these parallel bands would be closely allied with good weld bead formation.

(ii) Fracture Surface Analysis.

Four out of the five recorded fatigue failures in the pipe sections of the systems tested are shown in Figure 6.6. These low magnification micrographs indicate that the single frequency fatigue test at 6.00 cpm produced surface features of similar proportions to those obtained in the HDPE 1 pipes, tested under similar conditions. This is more clearly seen in Figure 6.7 which indicates the fracture surface aspect ratios L/h

(the longest dimension of the fracture surface in a direction parallel to the pipe axis divided by the pipe wall thickness) for the 160mm pipes overlaid upon the curves generated by the 63mm OD SDR 11 HDPE 1 pipes. There is close agreement at the given frequency of 6.00 cpm.

It is very obvious that the primary cause of failure was the presence of large voids, resulting in a dramatic reduction in measured lifetimes.

Fatigue markings DGB's are readily seen on the surfaces although the onset of the bands appears to be associated with the intersection of the growing crack with the pipe surface.

There is also evidence to suggest that the propagation of the crack is affected by the underlying microstructure such as flow lines introduced during the manufacture of the pipes.

Figure 6.8 shows typical low magnification micrographs of the other types of fractures observed in the 160mm pipe systems.

Scanning electron micrographs (Figure 6.9) exhibit even more clearly the features of the 160mm fractures particularly with respect to variations in local ductility which is evidenced by changes in the length of the drawn fibrils. Fatigue markings are also shown to particularly good effect. Once again, however, there is little difference at these magnifications between the small and large diameter pipe fractures.

6.3 180mm OD SDR 17 MDPE 2 BASED PIPE SYSTEMS

Three systems of this type, comprising an injection moulded 90° equal tee, three extruded pipe sections and three stub flanges were fabricated and subjected to fatigue testing.

Two specimens were investigated under conditions of 80°C, a test pressure of 0.61 MPa and at a frequency of 6 cpm (4 seconds on load followed by 6 seconds at atmospheric pressure).

A third sample was tested under conditions of 80°C, 0.58 MPa at a frequency of 7.5 cpm (5 seconds on load and 3 seconds off load).

The object of such experiments was to identify any major fatigue weaknesses in the systems either in the pipe, butt-welds or fittings and correlate the results with those obtained for systems fabricated from entirely different materials and of entirely different designs.

At the time of writing the freedom to publish the specific results of the work carried out on the 180mm OD SDR 17 MDPE 2 pipe systems has not been granted since the company manufacturing the pipeline components have asked that the data remain confidential.

It can be said, however, that failures at site T3 in the body of the tee fittings have been observed. This proves that such fractures are not specific to one design and size of tee as thought possible after the data on the small diameter tee systems had been generated.

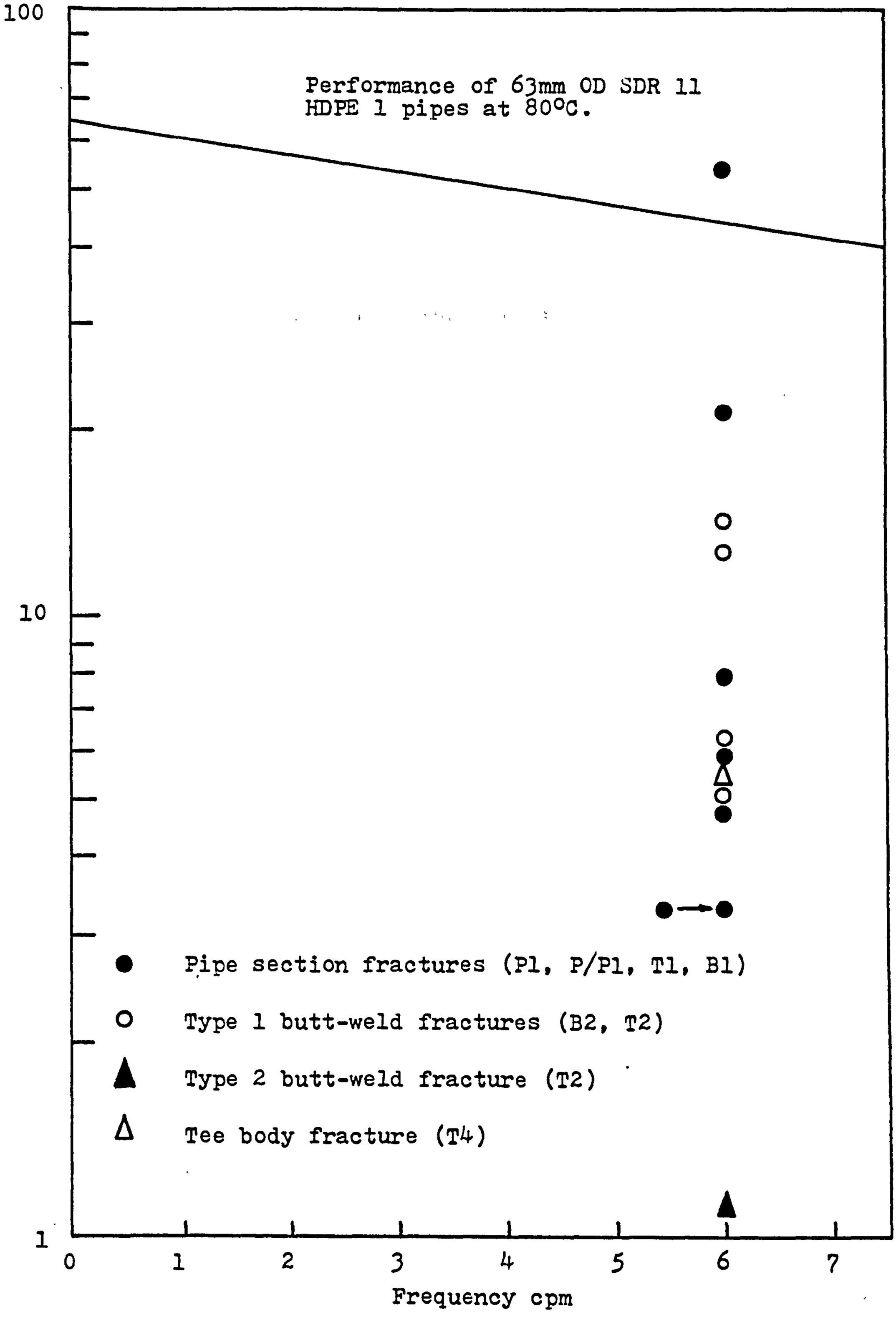

FIGURE 6.1 Performance of 160mm OD SDR 11 pipe systems at 80°C and 4.93 MPa maximum pipe hoop stress.

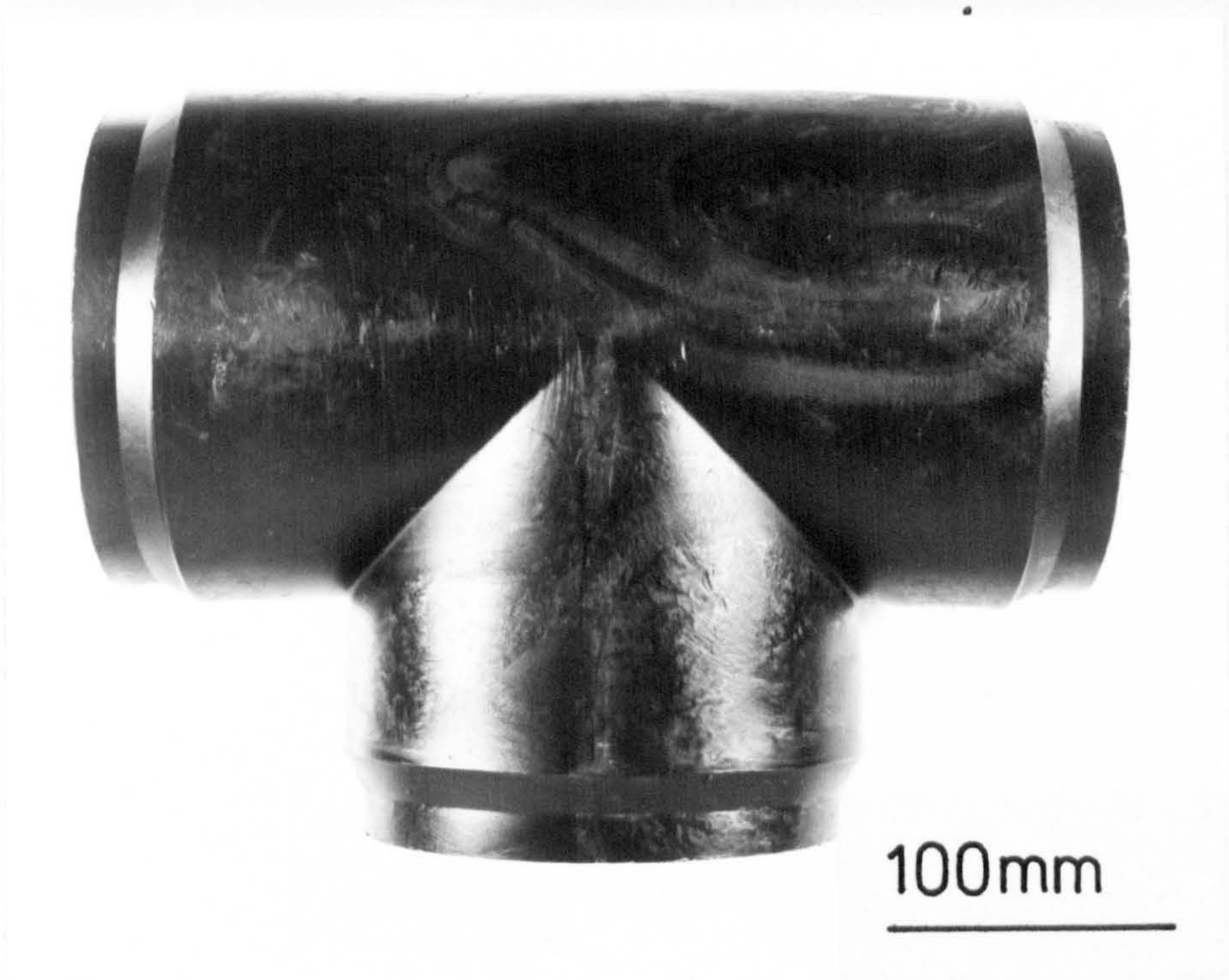

FIGURE 6.2 Close up view of flow lines in an injection moulded 160mm OD SDR 11 HDPE tee.

FIGURE 6.3a Example of the external appearance of a brittle fracture at a butt-weld between an injection moulded tee and extruded pipe (T2 type 1).

FIGURE 6.3b Example of the external appearance of a brittle fracture at a butt-weld between an injection moulded tee and extruded pipe (T2 type 1).

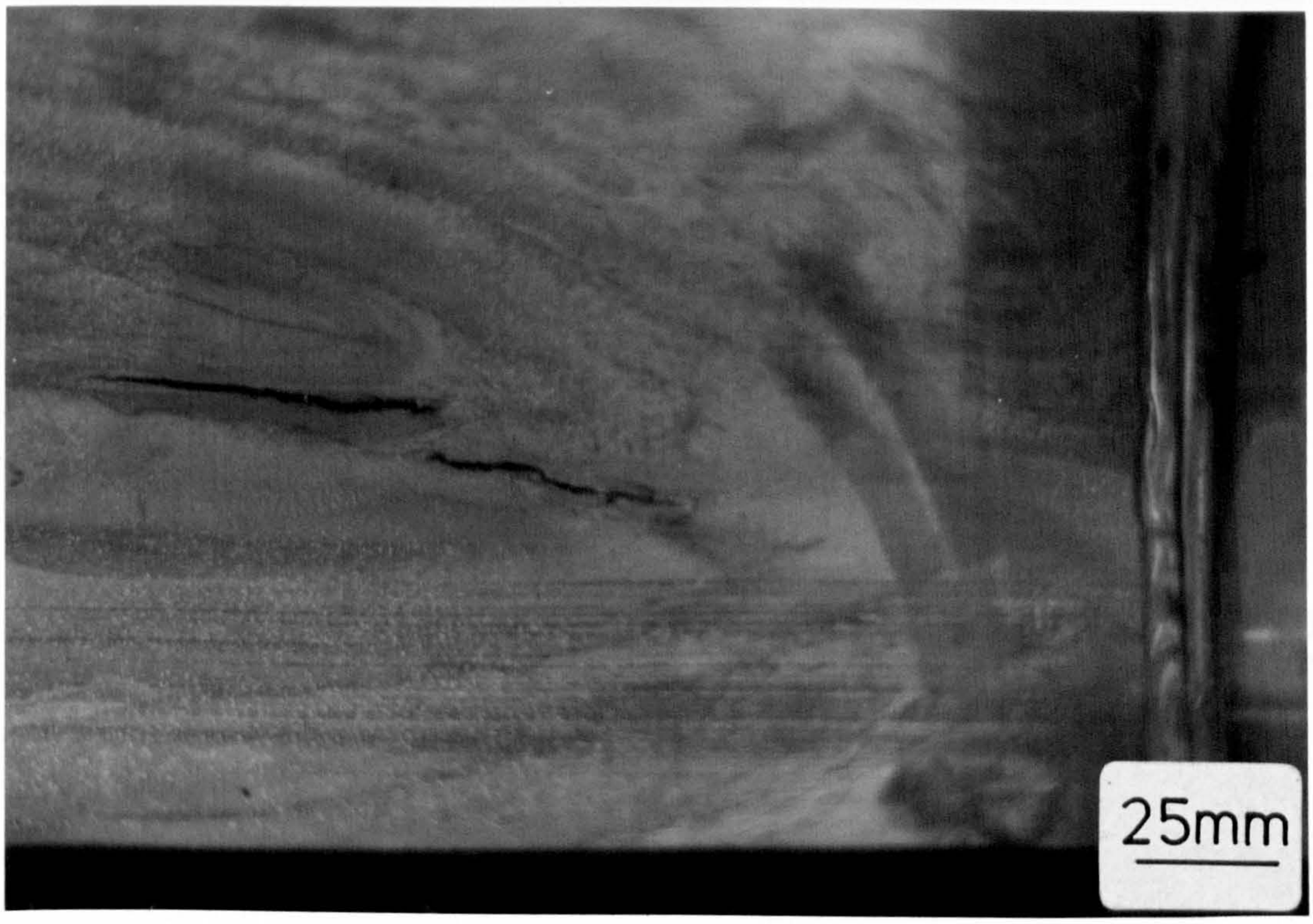

FIGURE 6.3c Example of the external appearance of a brittle fracture through the wall of an injection moulded tee (T4).

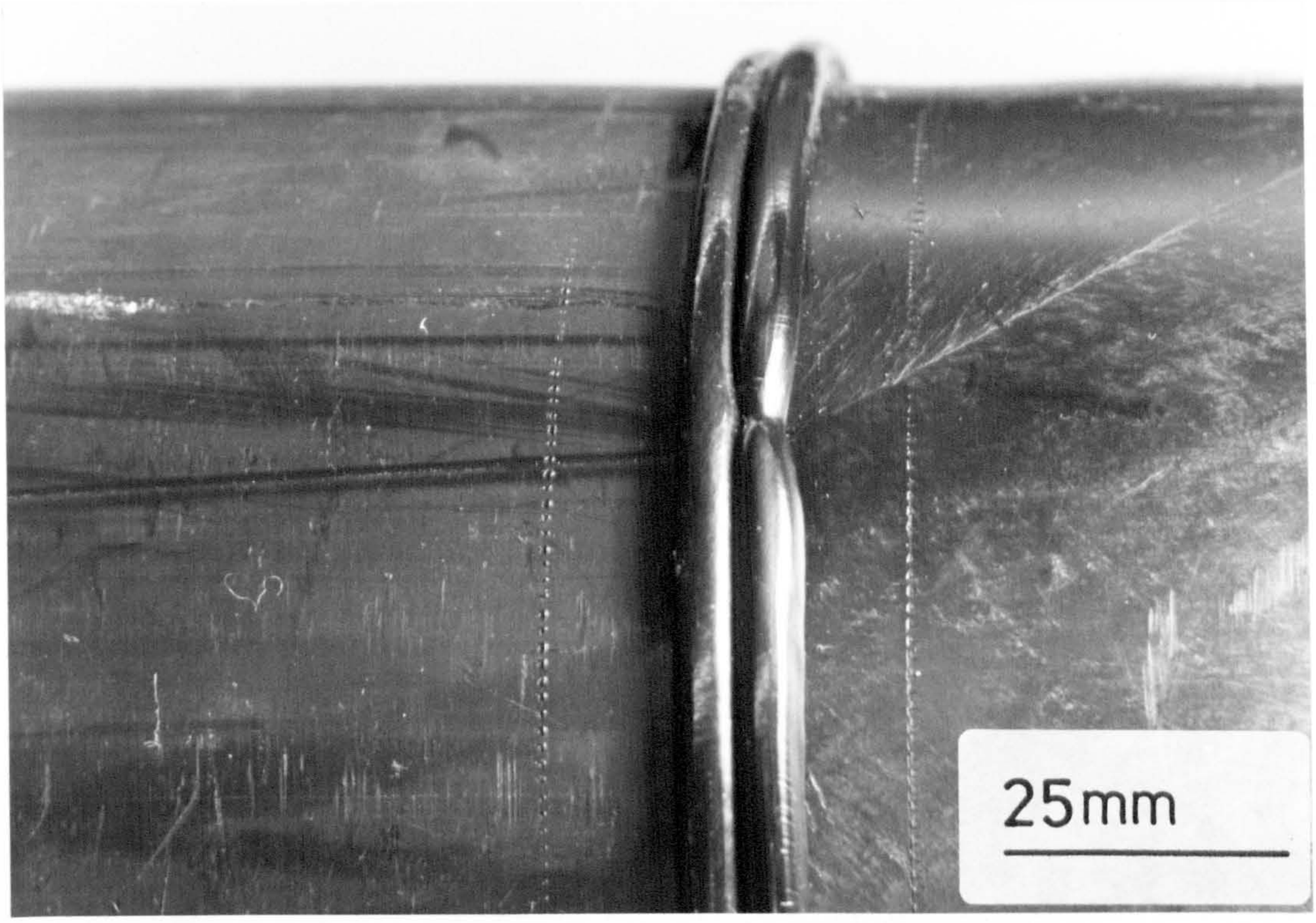

FIGURE 6.4a Weld bead discontinuity between an injection moulded bend and extruded pipe. An internal weld line in the fitting is also shown to good effect.

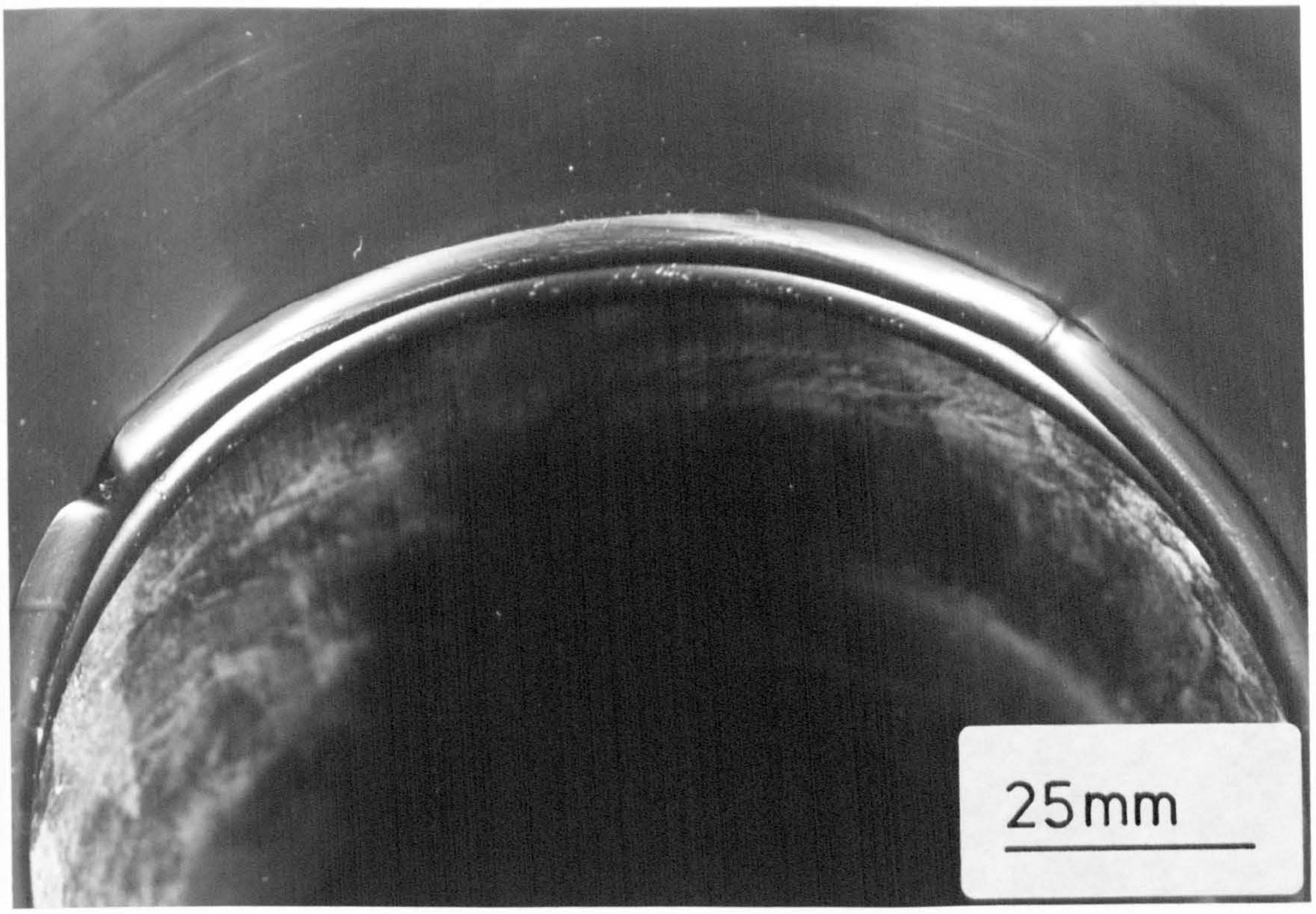

FIGURE 6.4b Weld bead discontinuities between an injection moulded stub flange and extruded pipe.

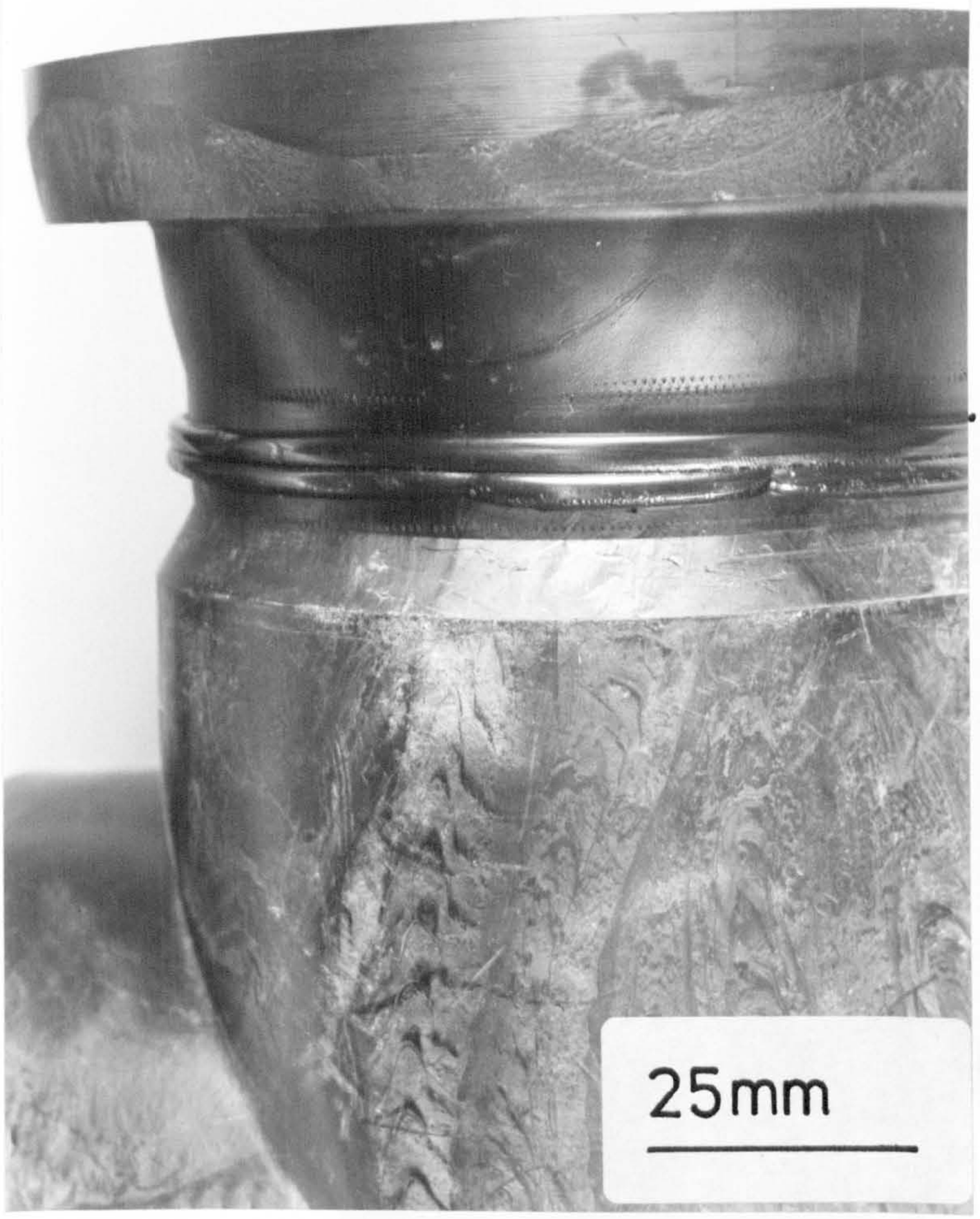

FIGURE 6.4c

Weld bead discontinuities between an injection moulded stub flange and tee.

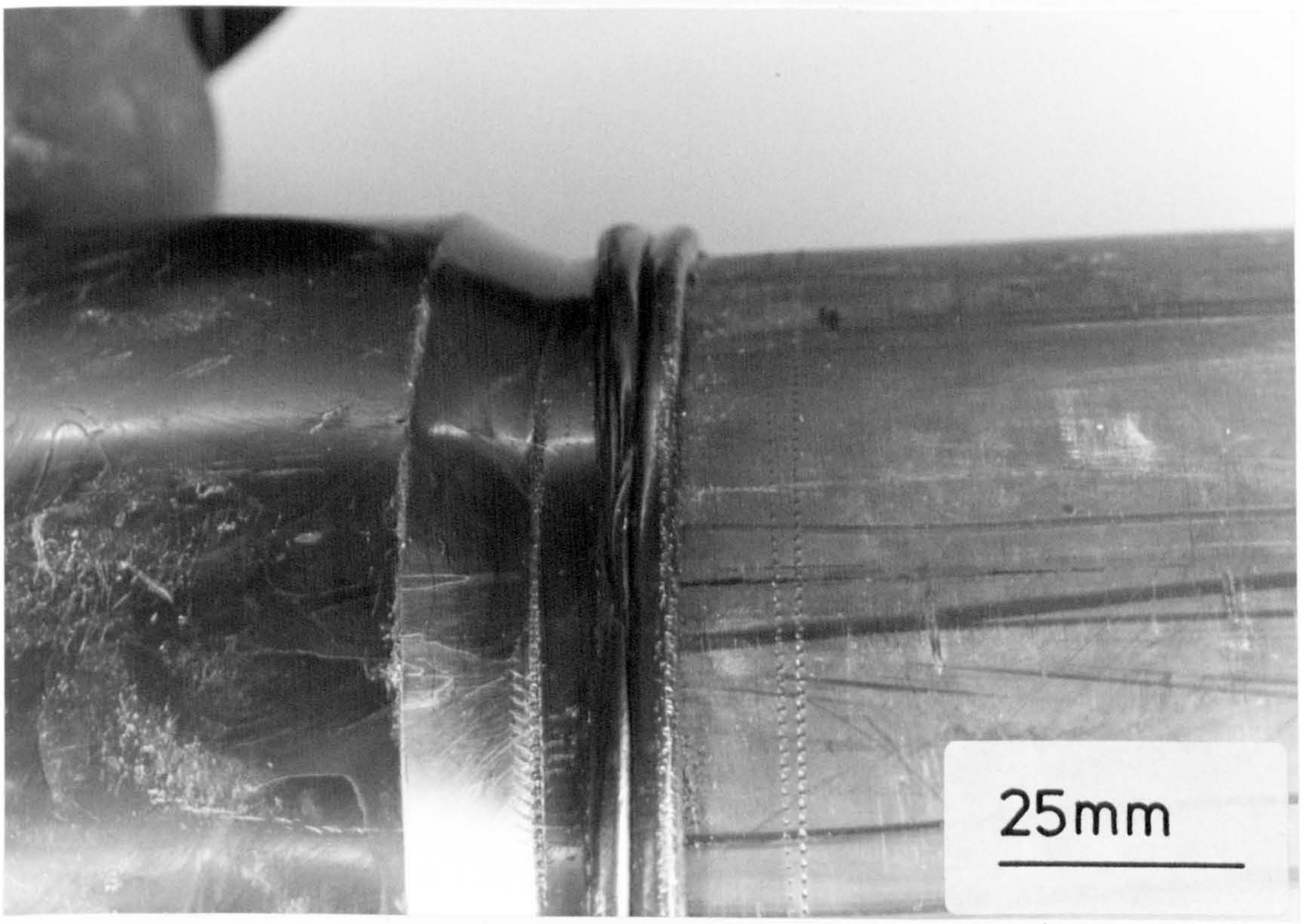

FIGURE 6.4d Weld bead discontinuity between an injection moulded tee and extruded pipe.

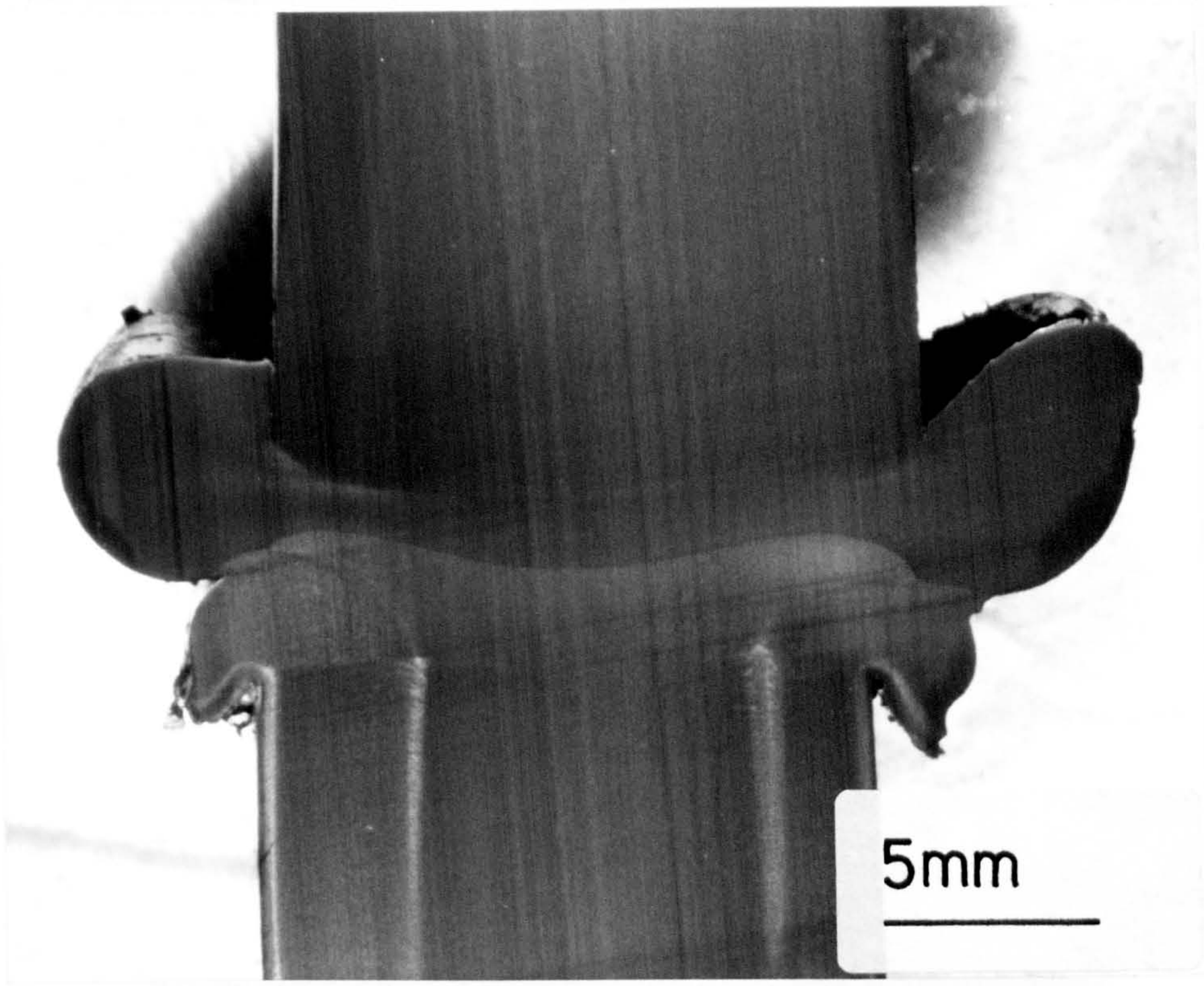

FIGURE 6.5 Surface of an HDPE butt-welded specimen prepared by sledge microtomy showing weld bead assymetry.

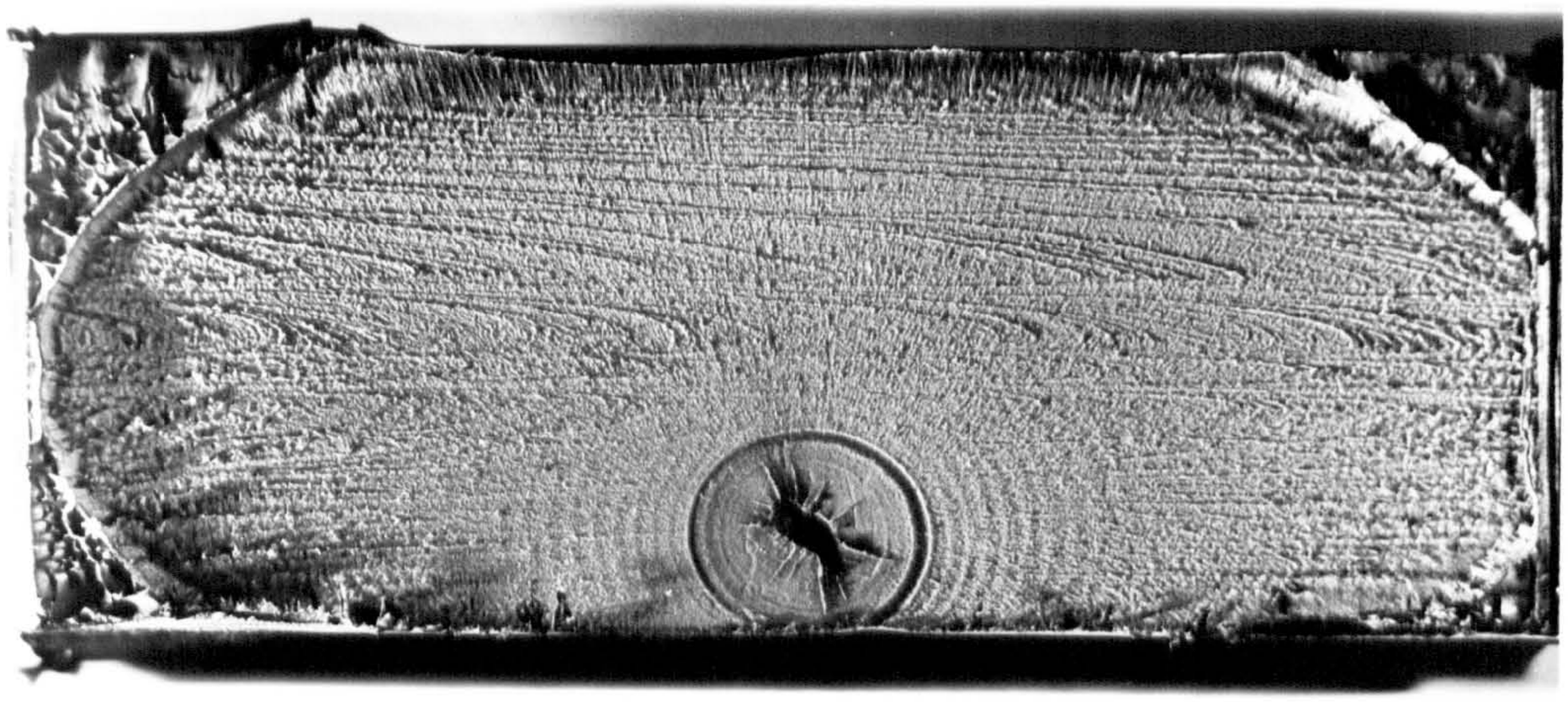

(a)

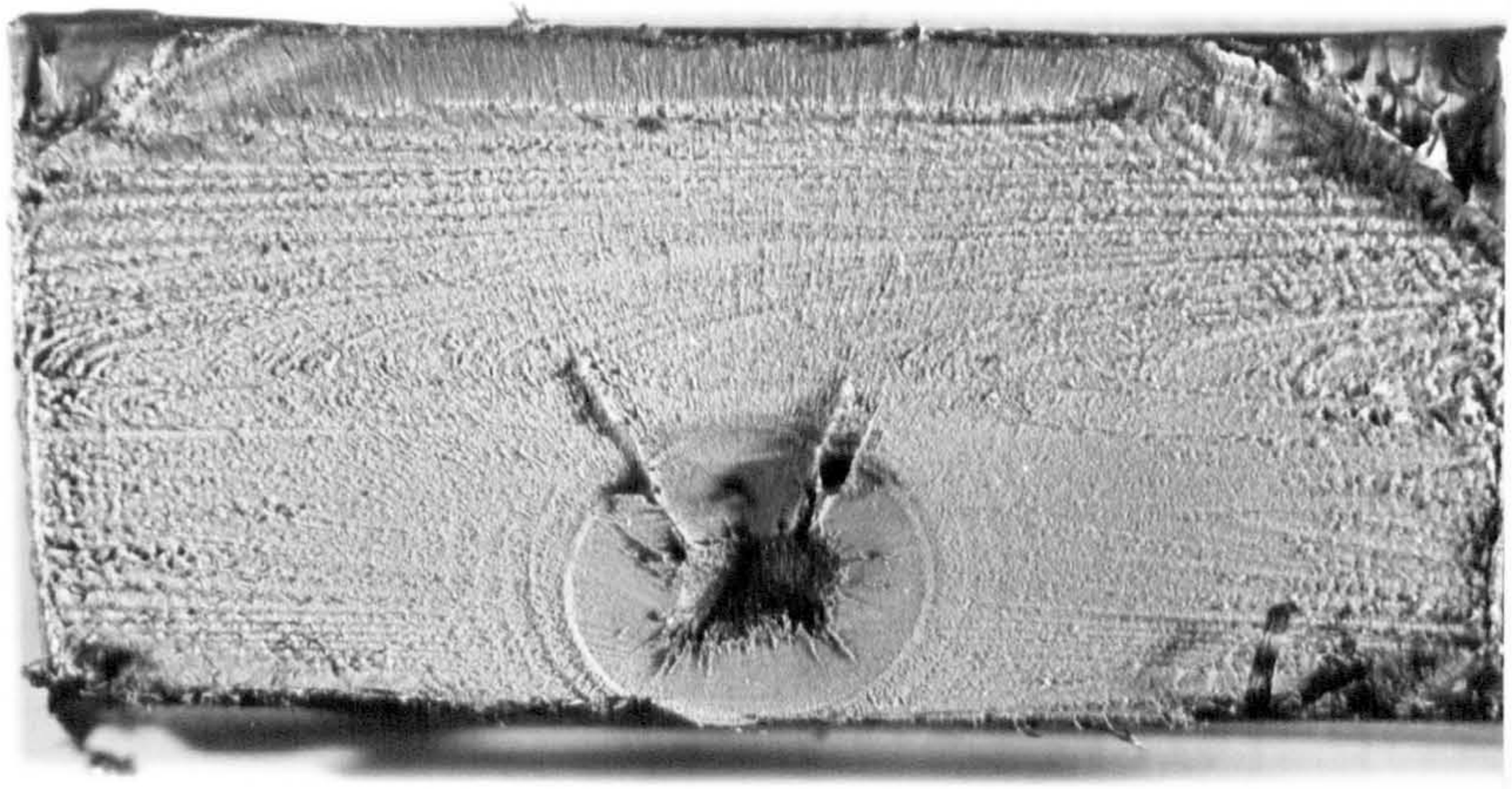

(b)

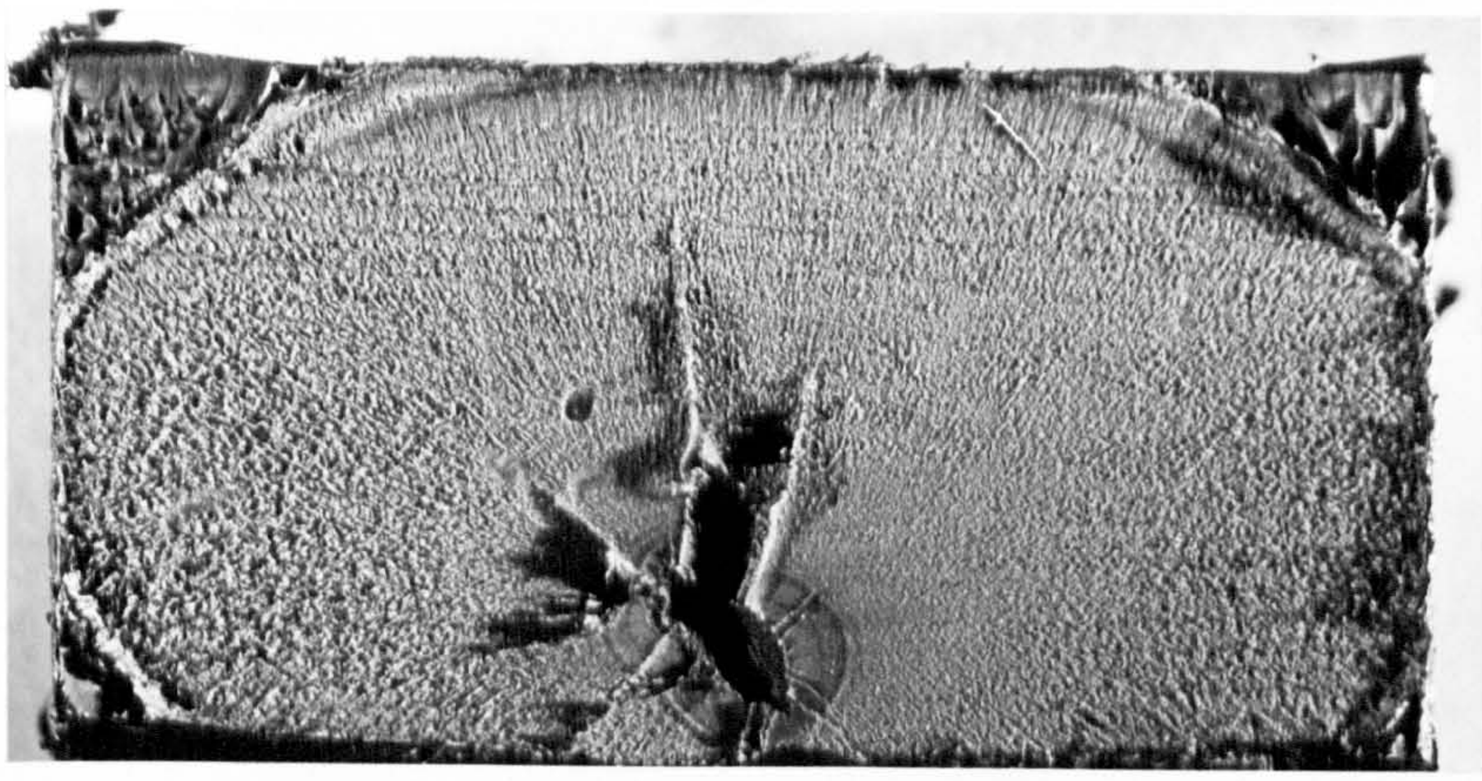

(c)

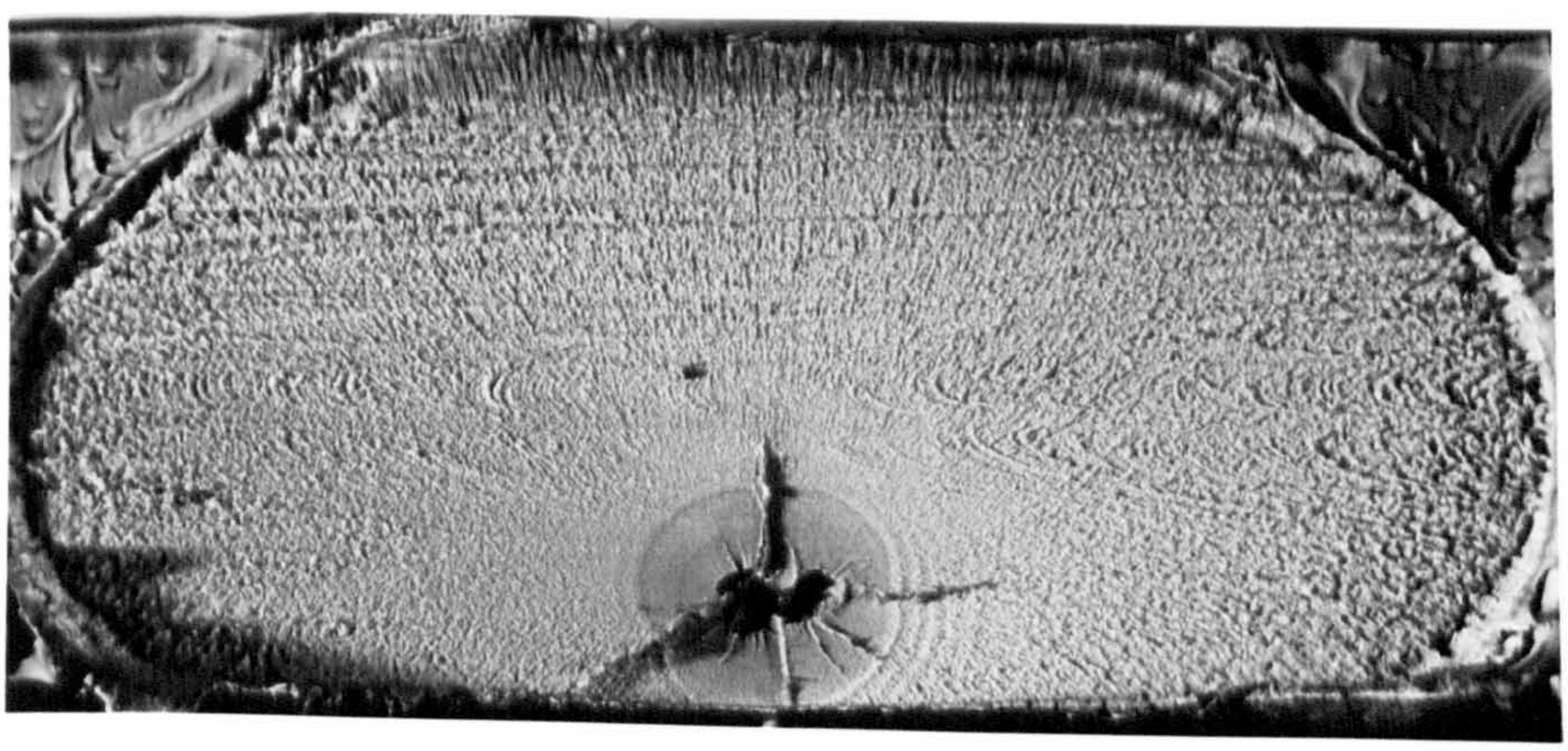

(d)

FIGURE 6.6(a - d) Fracture surfaces of HDPE 1 pipes showing cracks initiating at voids.

5mm

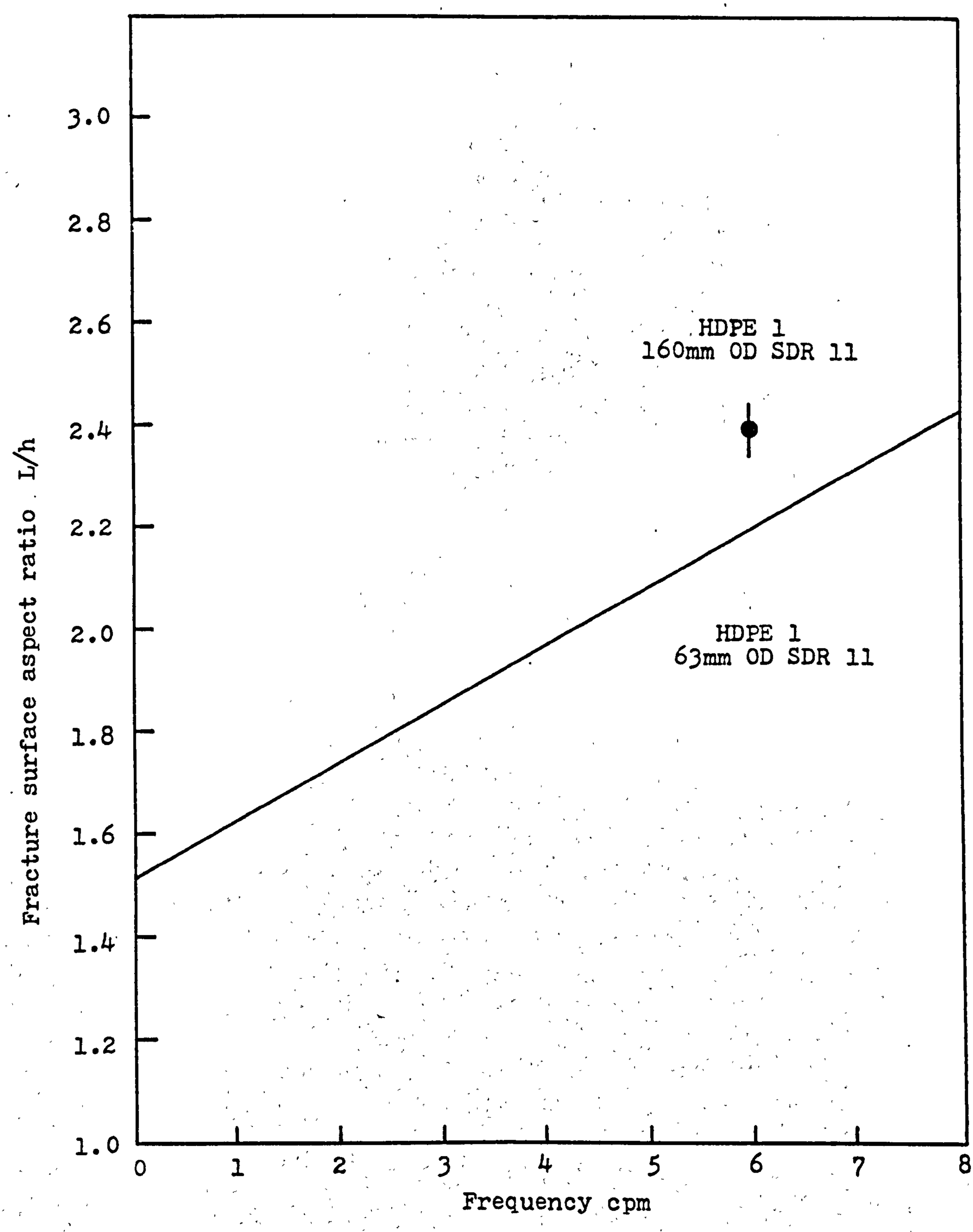

FIGURE 6.7 Comparison of fracture surface aspect ratios, L/h, for HDPE 1 63mm and 160mm OD SDR 11 brittle pipe fractures at 80°C and 4.93 MPa maximum pipe hoop stress.

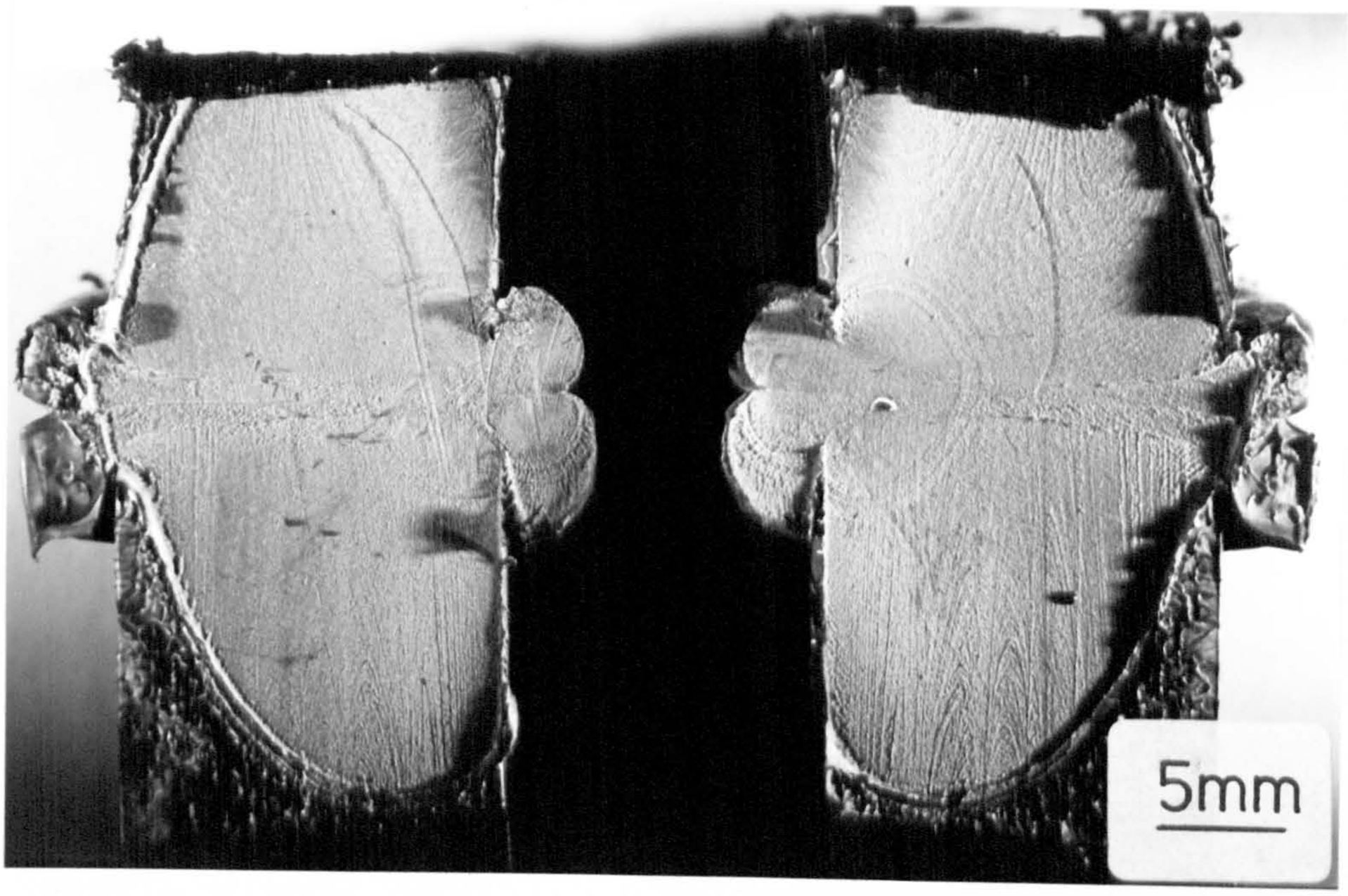

FIGURE 6.8a B2 type 1 fracture surface in HDPE 1 pipe.

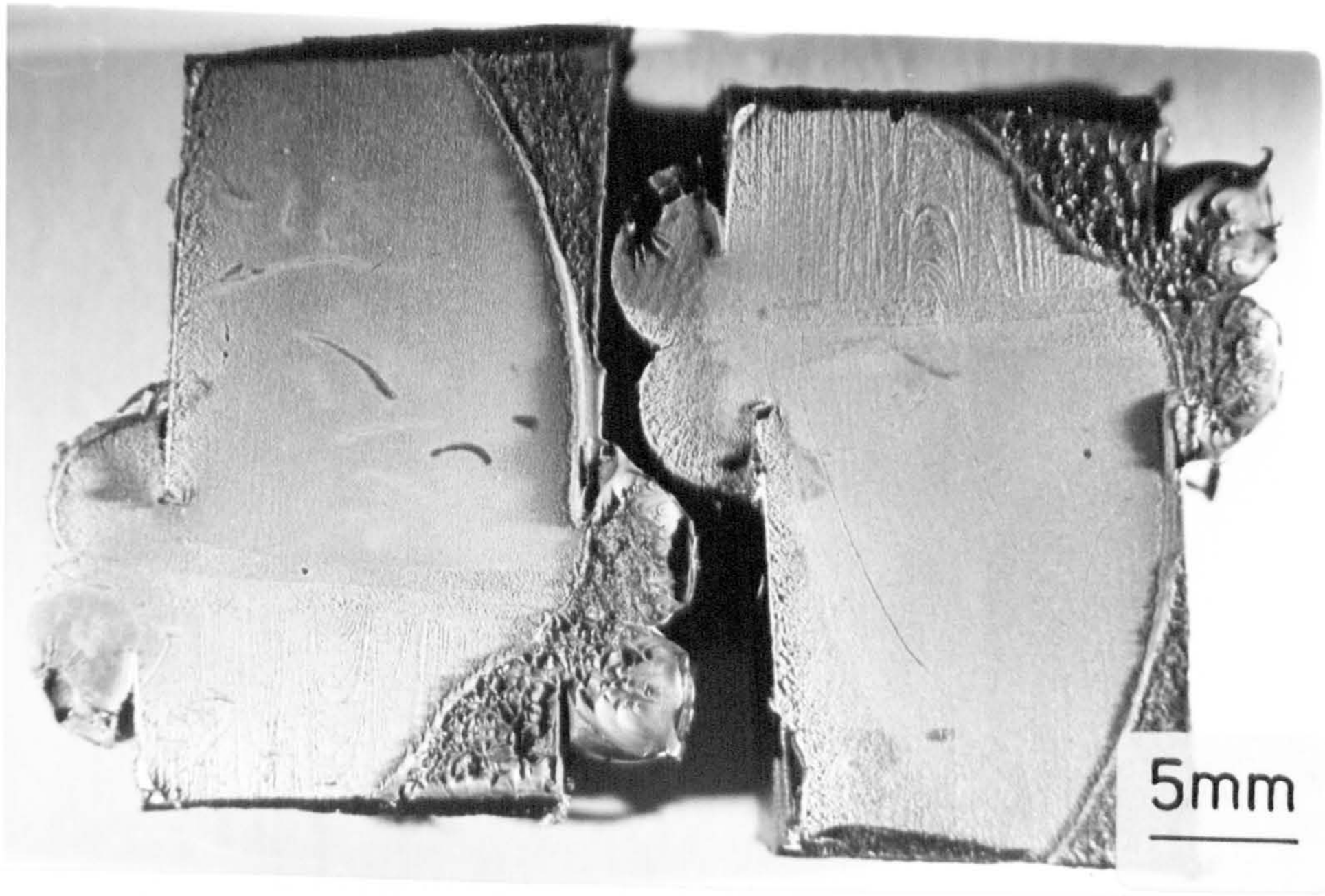

FIGURE 6.8b T2 type 1 fracture surface in HDPE 1 pipe.

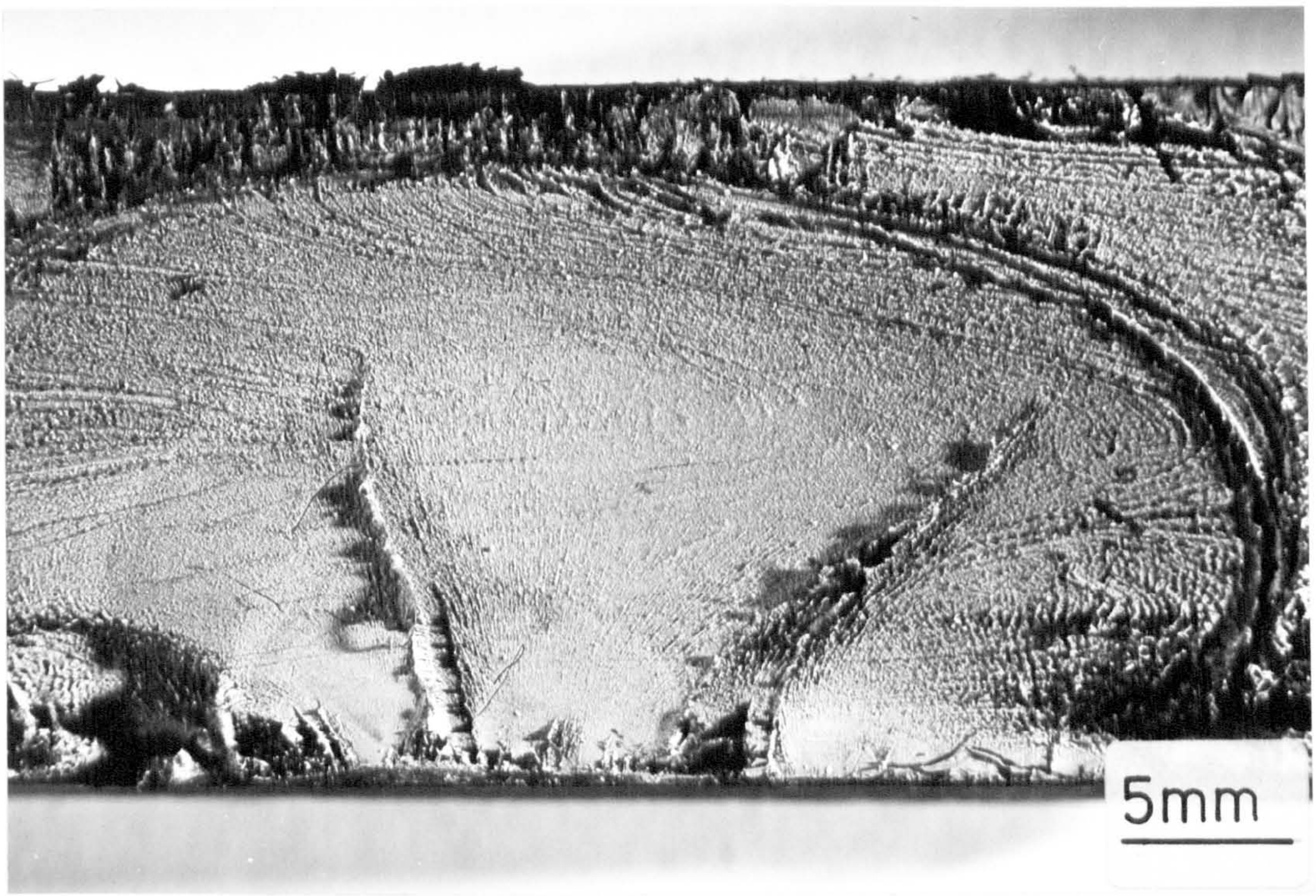

FIGURE 6.8c T4 fracture surface in HDPE 1 pipe.

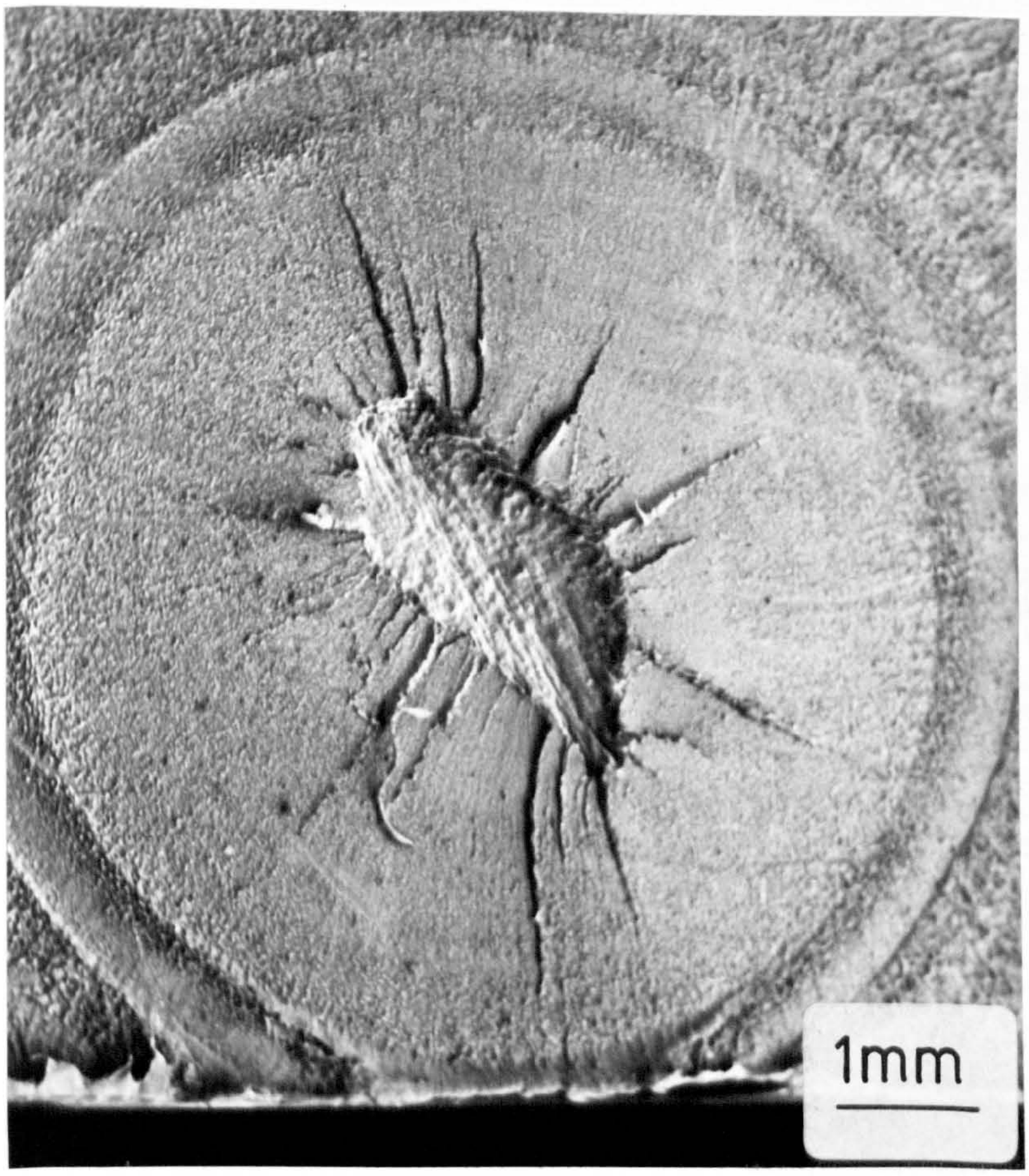

FIGURE 6.9a

Scanning electron micrograph of a void initiating fracture in an HDPE 1 pipe.

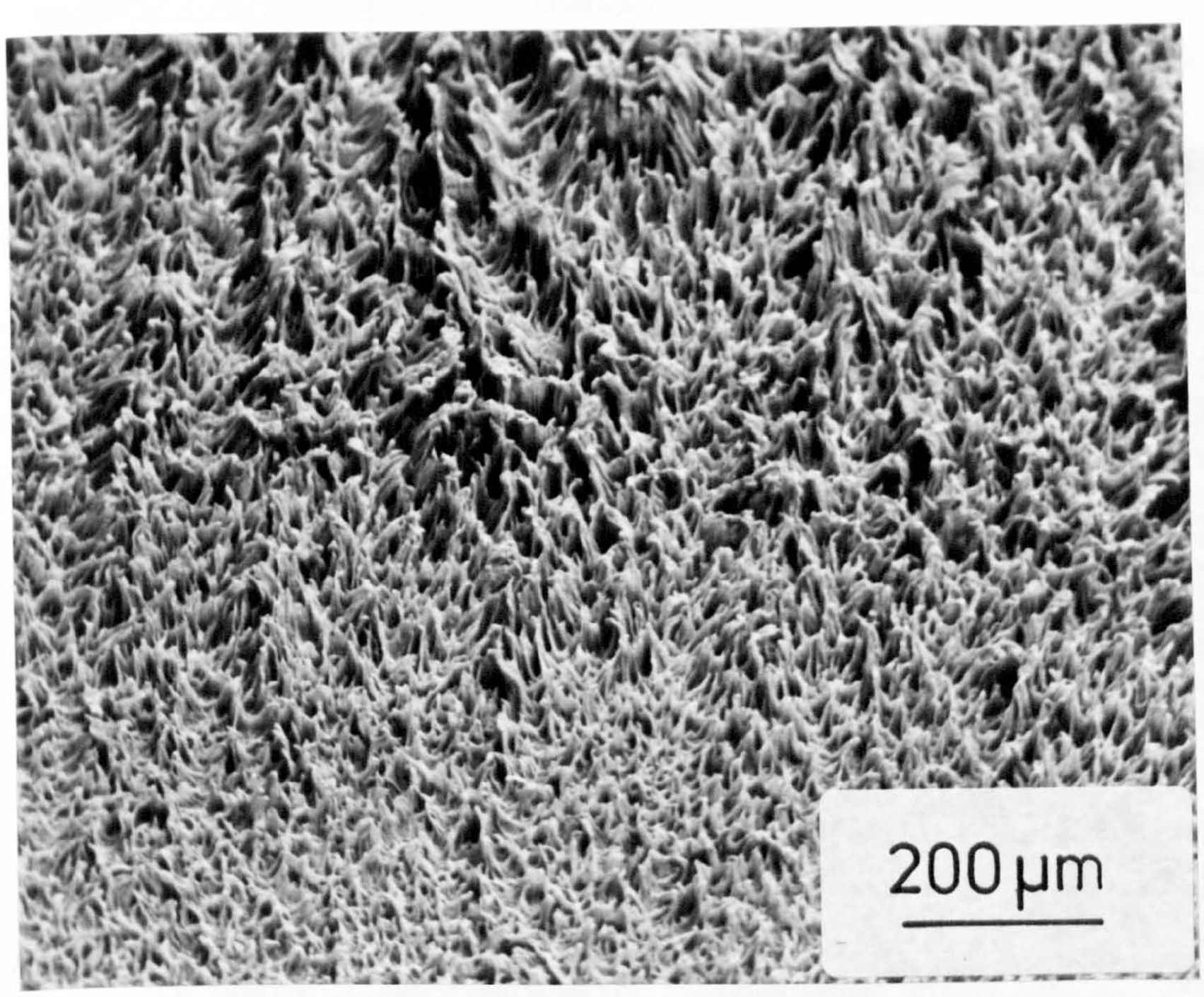

FIGURE 6.9b Scanning electron micrograph of an HDPE 1 brittle pipe fracture indicating variations in fibril length and local ductility.

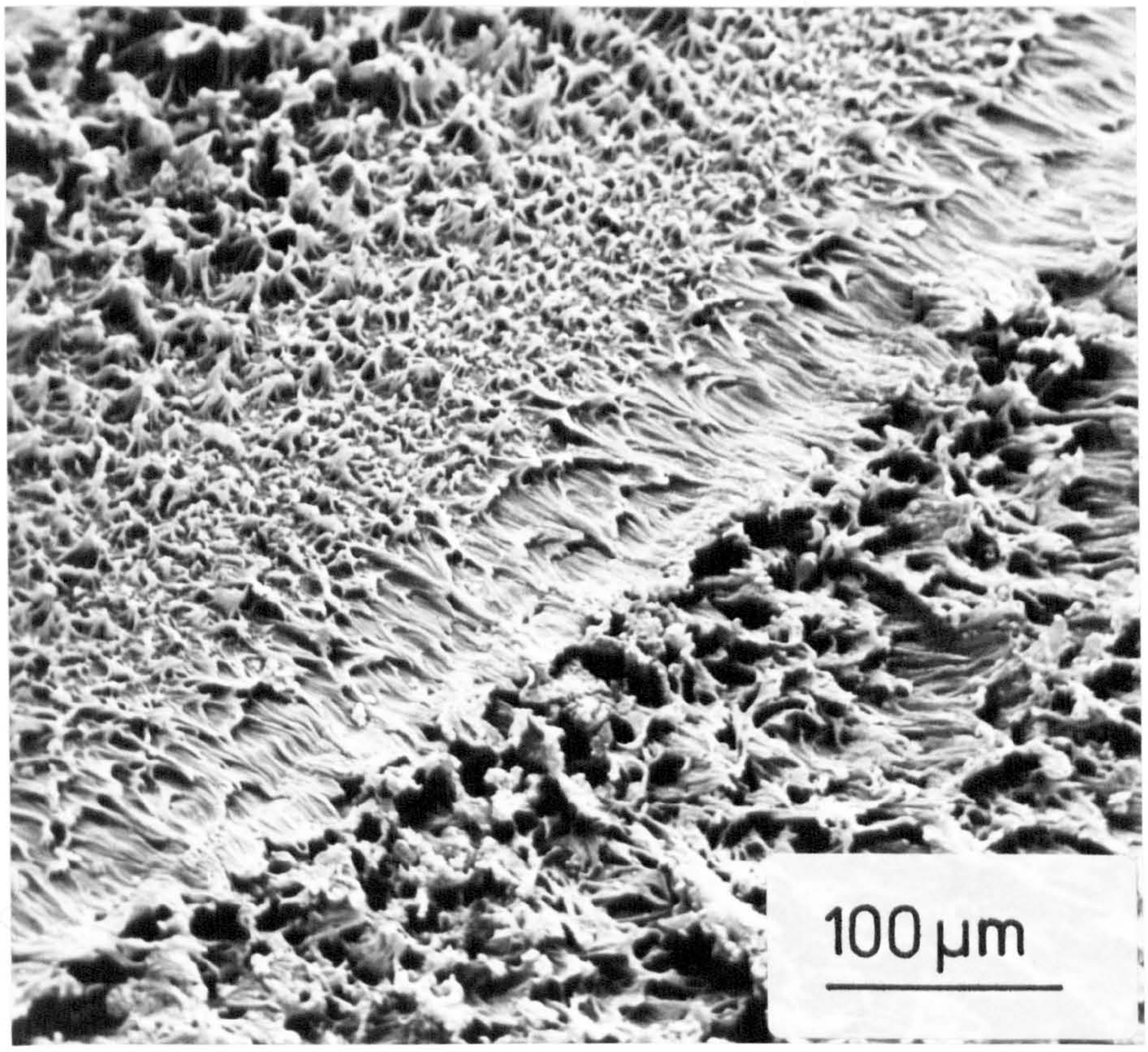

FIGURE 6.9c Scanning electron micrograph of an HDPE 1 brittle pipe fracture indicating variations in local ductility at a discontinuous growth band.

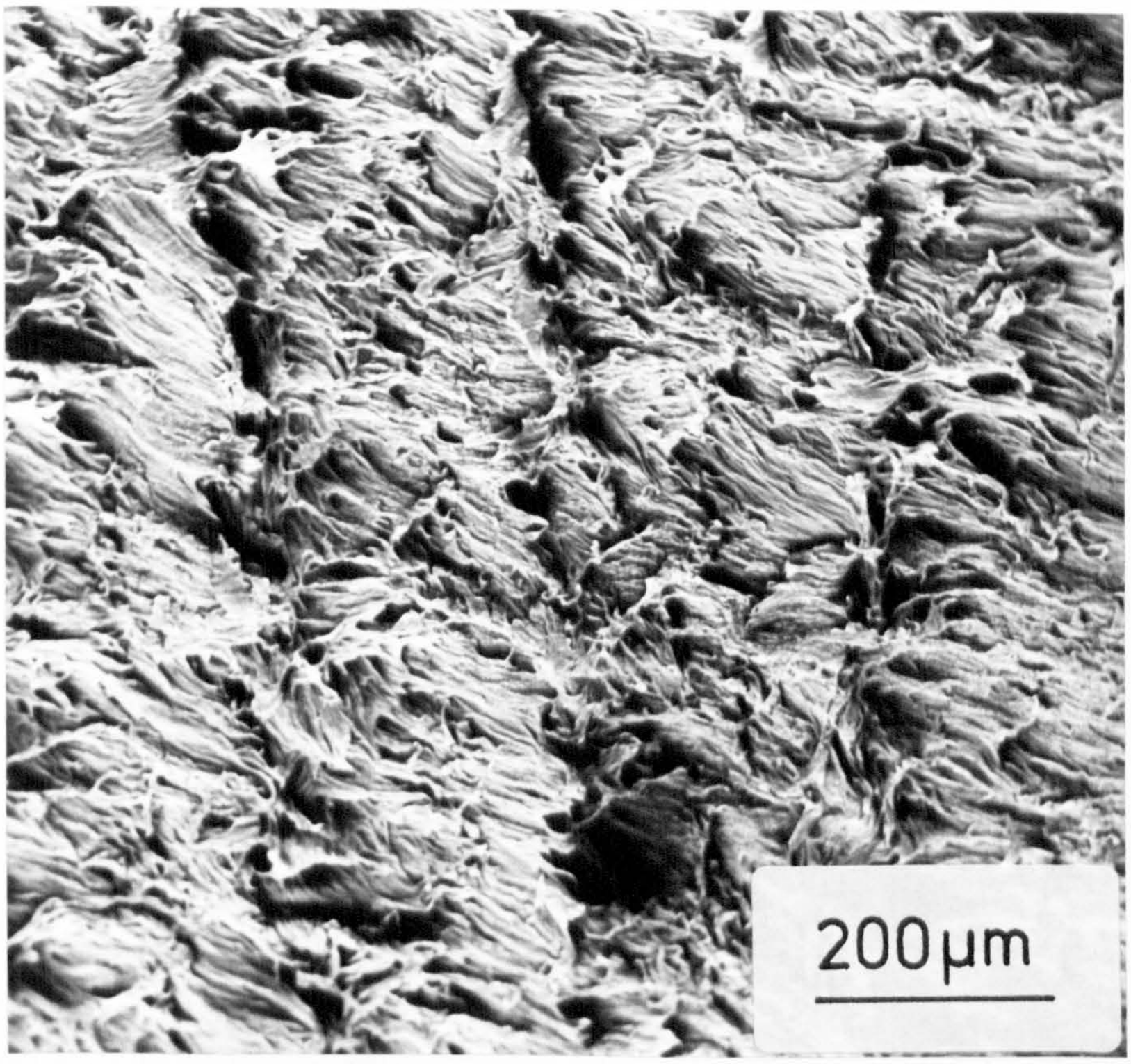

FIGURE 6.9d Scanning electron micrograph of an HDPE 1 brittle pipe fracture showing discontinuous growth bands.

CHAPTER 7

DISCUSSIONS, CONCLUSIONS AND FUTURE WORK

7.1

7.1 INTRODUCTION

The results recorded in previous chapters necessarily cover a wide range of pipe systems' performance since the objectives of the project included a comparison of pipe materials subjected to three types of internal pressure test. The data thus generated has already provided useful design information for polyethylene pipelines in the chemical process industries and it is hoped that this information gathering will continue.

The discussion presented here, will concentrate upon specific areas of behaviour which have helped to provide an understanding of the mechanical performance of PE pipelines and the processes leading to instances of premature and potentially hazardous failures.

It was only possible to evaluate the pipe systems' performances if analysis concentrated upon failures of the same general type, for example, brittle pipe section failures or circumferential failures at butt-welds between a pipe section and an injection moulded fitting. The effects of varying such parameters as frequency or internal pressure could then be readily compared.

Under fatigue an essentially square-wave loading profile was applied to the pipe specimens enabling a comparison to be made between fluctuating and the more commonly used static stress regimes. To accomplish this the previously defined parameters of τ_{SR} and $\tau_{FATIGUE}$ were utilised.

The nature of the fatigue loading profile, with a fixed rate of pressurisation and time off load, enabled frequency variations to be achieved by altering t_{max} (the time during which the internal pressure is $\geqslant 95\%$ of the set maximum value). Any physical property changes in the pipe materials due to variations in strain rate were minimised by the application of a fixed rate of pressurisation (125). The period of the fatigue cycle when the pipe systems were unloaded resulted in a constant recovery period and avoided the difficulties encountered when a sinusoidal loading profile is applied.

Such continuously varying waveforms produce different loading rates and times spent at lower stresses if frequencies are varied.

By comparing τ_{SR} with $\tau_{FATIGUE}$, at different frequencies, any weaknesses under fatigue could be readily observed. If τ_{SR} is substantially larger than $\tau_{FATIGUE}$ at any frequency, then the pipe system can be considered to exhibit fatigue weakness.

7.2 SMALL DIAMETER PIPE SYSTEMS

In Table 7.1, τ_{SR} and $\tau_{FATIGUE}$ (for the highest imposed loading frequency) for HDPE 1, HDPE 2 and MDPE 1 are tabulated and the ratio of $\tau_{FATIGUE}/\bar{\tau}_{SR}$ (where $\bar{\tau}_{SR}$ is the mean measured stress rupture life) is determined. These ratios are substantially lower for HDPE 2 pipes compared with the HDPE 1 and MDPE 1 systems. This implies that HDPE 2 exhibits a fatigue weakness and will be, thus, discussed separately.

The behaviour of the pipe systems subjected to fluctuating internal pressures can be described using two failure criteria. Firstly that rupture is the result of the accumulated damage from the time during which a stress is applied or, secondly, from the number of loading cycles imposed. (Such an approach neglects the possibility of fatigue thermal melting.) If a loading profile tending towards a square wave is applied to a pipe system then the number of cycles to cause failure can be predicted, based on cumulative damage principles, by utilising an equation similar to that quoted by Stapel (97) and stated in Chapter 2, namely

$$N_f = \left[\frac{\tau_{SR}}{t_{max}}\right]_{T,\sigma} \qquad (2.21)$$

where again τ_{SR} is the measured stress rupture life and t_{max} is essentially the time during any cycle when the load is at a maximum, both at the same stress and temperature. Thus, by substituting in equation (2.21) the measured value for τ_{SR} a calculated value for N_f can be compared to the data obtained experimentally to aid in

TABLE 7.1 - Comparison of Stress Rupture (τ_{SR}) and Fatigue Lives ($\tau_{FATIGUE}$) at the Highest Frequency for HDPE 1, HDPE 2 and MDPE 1 Pipes to Demonstrate the Presence of Fatigue Weaknesses.

MATERIAL	CONDITIONS (80°C)		$\bar{\tau}_{SR}$ (P1) (Hours)	$\tau_{FATIGUE}$ (P1) (Hours)	$\frac{\tau_{FATIGUE}\ (P1)}{\bar{\tau}_{SR}\ (P1)}$
	HOOP STRESS (MPa)	FATIGUE FREQUENCY (cpm)			
HDPE 1	4.93	6	65.6	28.1	0.43
				32.5	0.49
				35.5	0.54
				42.3	0.65
				58.8	0.90
				63.8	0.97
				43.5	0.66
					MEAN 0.66 ± 0.20
MDPE 1	3.00	6	134.4	28.9	0.22
				32.3	0.24
				79.5	0.59
				79.7	0.59
					MEAN 0.41 ± 0.21
HDPE 2	4.93	7.5	898.8	52.5	0.06
				87.7	0.10
				62.3	0.07
				86.5	0.10
				124.2	0.14
				146.9	0.16
				157.6	0.18
				55.5	0.06
				79.5	0.09
				62.3	0.07
					MEAN 0.10 ± 0.04

the identification of an appropriate failure mechanism.

Thus the use of simple parameters, such as τ_{SR}, $\tau_{FATIGUE}$, and calculated and experimental N_f values, can allow significant fatigue weaknesses and appropriate failure mechanisms to be identified.

7.2.1 Mechanical Performance of HDPE 1 and MDPE 1 Pipes

Figure 7.1 shows, for HDPE 1 and MDPE 1 pipes, the calculated value of N_f compared with the experimentally determined values. Included in the HDPE 1 data are results obtained at two different internal pressures.

For HDPE 1 pipe at the higher stress, Figures 4.20, 4.21 and 7.1 highlight the following points.

a. $\tau_{FATIGUE} \approx \tau_{SR}$ for the range of loading frequencies employed.
b. The value of N_f depended critically upon t_{max} (loading frequency). For instance, the mean value of N_f was increased by a factor of approximately 23 as the frequency increased from 0.86 to 6 cpm (0.014 to 0.1 Hz).
c. The measured values of N_f agree closely with those calculated from equation (2.21).

Thus for HDPE 1 pipes pressure tested at 80°C and at higher stresses (approaching the knee on the stress rupture curve but still resulting in brittle failures) the model of fracture based upon cumulative damage principles is most applicable. The effect of the decreasing number of cycles to failure with decreasing frequency simply reflects the increasing value of t_{max}. It is possible to infer, therefore, that the significant damage to the pipe and brittle crack propagation from the inherent defect which initiated the crack, occurred during that section of the loading cycle when pressure and stress were acting. Application of the "Paris Law" of crack growth propagation (equation 2.22) would not therefore be effective in predicting system lifetimes.

For the MDPE 1 pipes and the lower pressure tested HDPE 1 pipes the experimental and calculated values for N_f begin to diverge as shown in Figure 7.1. The deviations

or $\tau_{FATIGUE}$ and τ_{SR} which are clearly shown in Figure 4.20 also indicate that the description of behaviour using cumulative damage principles is becoming less applicable. This may be accounted for by the proposition that at lower stresses cracks propagate by a mixed mode with contributions from the actual application of stress (equation 2.22) and the time during which the stress is acting (equation 2.12). At high loading frequencies the application of the stress would induce the most damage since there would be little time for significant creep to occur during each cycle.

Since B and b (equation 2.12) and D and d (equation 2.22) are material constants and not necessarily equal, then the divergence between τ_{SR} and $\tau_{FATIGUE}$ for the HDPE 1 and MDPE 1 pipes at lower stresses and higher frequencies may be accounted for. It would be expected, however, that $\tau_{FATIGUE}$ would tend towards τ_{SR} at the lower frequencies, as indeed it does, as the cumulative damage mechanism of crack propagation exerts a predominating effect.

At the lower stresses, and for HDPE 1 pipes in particular, the testing time (τ_{TEST}) increased markedly with increasing frequency. Figures 4.63 and 4.64 indicated that peak melting temperature and the materials' crystallinity both altered during the course of a test. In addition the application of a stress increased the magnitude of this change. Therefore, since measurable and maybe significant changes in the structure of the PE materials occurred between 10 and 200 hours at 80°C the lower stress tested pipe may have been essentially different from the higher stress tested material. This may also account for the divergence between $\tau_{FATIGUE}$ and τ_{SR}.

There is no clear pattern to butt-weld failures in either of the materials examined except that MDPE 1 exhibited a preference for butt-weld failures of a circumferential nature (P/P2 Type 2). There does appear to be some frequency effect causing MDPE 1 butt-welds to have reduced $\tau_{FATIGUE}$ values with increasing frequency although this is not well defined. HDPE 1 welded pipe systems performed essentially as the straight pipe under both stress rupture and fatigue conditions.

It should be noted that both HDPE 1 and MDPE 1 pipes clearly met the manufacturers' specifications for stress rupture which were maintained under fatigue conditions with frequencies up to 7.5 cpm. The pipe to pipe butt-weld in HDPE 1 pipe systems does not appear to be a source of weakness if manufacturer's recommended conditions of temperature and pressure are used and the pipes are aligned correctly. This confirms work carried out by van Crombrugge (93) who concluded that this type of butt-weld has a weld factor of 1, i.e. that it fulfills pipe requirements.

The results obtained from MDPE 1 welded pipe systems would indicate that using conditions and equipment recommended by the manufacturers will result in a joint which is susceptible to fatigue loads of modest frequencies. Further work would be necessary to check whether or not these weaknesses are present at lower temperatures and other pressures but at this time a method of jointing 60mm OD SDR 11 MDPE 1 pipes other than mirror-plate butt-welding is recommended if such systems are to be subjected to fluctuating internal pressures.

7.2.2 Mechanical Performance of HDPE 2 Pipe Systems

Table 7.1 clearly illustrates that the behaviour of HDPE 2 pipes was very different from that observed in HDPE 1 and MDPE 1 and that for individual HDPE 2 pipe failures the values of $\tau_{FATIGUE}(P1)/\ \bar{\tau}_{SR}(P1)$ ranged from 0.06 to 0.18 and further the reduction in performance under fatigue was such that all values of $\tau_{FATIGUE}$ when compared with measured stress rupture data fell markedly on the shorter lifetime side, implying a fatigue weakness. Similar effects were not observed to the same extent for HDPE 1 and MDPE 1 pipes.

If equivalent criteria are used to describe the lifetimes under fatigue of HDPE 2 pipes as those applied to HDPE 1 and MDPE 2 pipe materials, it becomes immediately

apparent that HDPE 2 does not conform to a cumulative damage model. For instance, at 80°C and 1 MPa internal pressure (a pipe hoop stress of 4.93 MPa) the mean measured stress rupture life for HDPE 2 pipes was found to be 898.8 hours. At a frequency of 7.5 cpm (0.125 H_z) equation (2.1) predicts the number of cycles to failure to be nearly 3.24×10^6. Experimentally the mean number of cycles to failure under the same conditions were 3.24×10^5.

These PE pipes are thus exhibiting a clear fatigue weakness. Previous investigations into the response of PE pipes to fatigue or "intermittent creep loadings" found no weakness. The study by Lörtsch (92), for example, applied testing conditions of stress and temperature that would produce, under constant pressure, a ductile failure. Although not presented herein, work undertaken during the experimental programme revealed that if a pipe system, containing a known weakness under fatigue, is tested in both the ductile and brittle regions of the stress rupture curve, then only in a brittle region does the fatigue weakness become apparent. The results obtained by Lörtsch are, therefore, not surprising in that no fatigue weakness was identified. Similarly at low frequencies a fatigue weakness will not be observed since $\tau_{FATIGUE}$ tends towards τ_{SR}.

The cause of premature failure of the fatigue loaded HDPE 2 pipes can probably be attributed to either a true fatigue failure process or a tendency for a crack to start propagating very soon after the first stress application, or to some combination of these effects.

Crack propagation can often be proceeded by a short craze which can reduce the value of K, the stress intensity factor at the crack tip and in effect acts as a crack blunting or material toughening agent (90, 116). However, the action of fatigue unloading may lead to the collapse and buckling of the crazed or damaged material. On reloading the ability of this material

to resist further cracking is reduced, hence the increased rate of crack propagation under fatigue loading. Increasing the frequency of stressing and collapsing of the crazed region inevitably leads to accelerated crack growth (32, 96).

This mode of fracture is described by equation (2.22) in terms of da/dN. Under these circumstances the number of cycles to failure, N_f, should change little with reasonable alterations in t_{max}.

Evidence from an examination of fracture surfaces raises the possibility of crack growth occurring very soon after initial application of fatigue loads. The site of fracture initiation differed for HDPE 2 pipes depending upon whether the testing mode was stress rupture or fatigue. The fractures resulting from fluctuating loads initiated in the highest stressed region, near the pipe bore (see section 2.5.3), while under static pressure cracks were often found to have started near the centre of the pipe wall. Since pipes contain internal stresses residual from processing, and these exaggerate the difference between the bore and the outside wall stress (9) to further favour fracture initiation at or close to the pipe bore, then the initiation of brittle fractures from inclusions towards the centre of the pipe wall, when testing under constant pressure, supports the notion that crack growth was delayed until internal stresses were reduced by annealing. The short lifetime of the fatigue tested pipe may then simply be a result of early crack propagation.

It is interesting to note that both HDPE 2 and MDPE 2 pipes exhibited enhanced stress rupture performance compared with either HDPE 1 or MDPE 1. For example HDPE 2 demonstrated a mean measured stress rupture life nearly fourteen times that of HDPE 1 pipes under identical conditions, see Figures 3.1 to 3.4.

Manufacturers have increasingly made efforts to improve stress rupture performance since thermoplastics pipelines are at present designed with respect to this form of data in spite of the fact that under many applications fluctuating internal pressures are experienced. The results quoted above indicate that improved stress rupture performance does not necessarily lead to improved fatigue performance.

The butt-welded joint between two pipe sections in HDPE 2 did not exhibit any weaknesses under stress rupture and fatigue conditions at the temperatures and pressures imposed. In fact all fractures from fatigue tests occurred in the pipe section.

The weld factor was therefore unity under all three loading modes of short term rupture, stress rupture and fatigue with frequencies in the range up to 7.5 cpm. Butt-welding of 63mm OD SDR 11 HDPE 2 (and 1) pipe only systems is therefore considered a suitable and reliable method of jointing as long as the manufacturer's recommendations are closely followed.

7.2.3 Macro-features of Fracture Surfaces

Figures 4.31, 4.32 and 6.6 show that for all the small and large diameter PE pipes tested, the overall shape of the brittle fracture was related to the imposed loading mode. Stress rupture testing produced fracture surfaces which were nearly symmetrical about the middle of the pipe wall and similar to those previously reported (83, 126). Under fatigue the fractures tended to propagate preferentially along the pipe axis. This effect was observed in all the tested materials including those exhibiting a fatigue weakness such as HDPE 2, although the HDPE 2 fatigue fractures tended to be semi-circular rather than semi-elliptical as observed in HDPE 1 and MDPE 1 pipes. Other notable features, clearly shown in Figures 4.31 and 4.32 and summarised in Figure 7.2, included the increasing eccentricity of the crack front with increasing frequency, the apparent pinning of the crack

front on the inside wall of the pipe except for fatigued HDPE 2 and the change in fracture mode close to the outside wall of the pipe.

The preferential pinning of the crack at the pipe bore, when loaded under constant pressure, may be related to changes from plane stress to plane strain in moving from the pipe bore to the middle of the pipe wall. Such pinning did not occur to the same extent under fatigue, Figure 7.2. This preferential growth of the crack along the axial direction of the pipe occurred in the fatigue resistant HDPE 1 and MDPE 2 pipes as well as in the HDPE 2 pipes which were susceptible to fatigue loads. The effect is thus a function of the loading mode and is not related, apparently, to the material. (The larger diameter pipes exhibited crack shapes of similar proportions to the smaller diameter pipe fracture surfaces.)

This change in fracture shape with testing mode has two possible implications. Firstly, the fracture surface of a failed PE pipe could lead to an identificiation of the loading mode which caused fracture. All pipe materials tested exhibited similar responses with loading mode and frequency, Figure 4.33. Secondly, the stress intensification at the tip of a growing crack is a complex function of many variables. The influence of the crack shape, in terms of depth to length, on the stress intensification has been widely recognised (128). As the crack shape changes from semi-circular (the ratio of the crack depth to the crack length along the pipe is equal to $\frac{1}{2}$) to that characteristic of fatigue (the above ratio is less than $\frac{1}{2}$), the stress intensification increases and therefore the lifetimes of pipes having elongated fracture surfaces should be less than those with semi-circular crack shapes.

If crack shape is to influence lifetime, then the differences in shape after final rupture of the pipe must also be present as the crack grows. The appearance of stress rupture and fatigue fracture

surfaces for part ruptured pipe together with the DGB's on HDPE 2 pipe, Figure 4.32, support the contention that for significant fractions of the total wall thickness of the pipe, the crack shape was characteristic of the loading profile. It must be noted that most of the pipe lifetime is spent while the crack is still too small for any meaningful information regarding its shape to be obtained. In addition, there was no evidence to indicate that the inclusions leading to fracture in the fatigue tested pipe were any different with respect to position, size or shape from those found in stress rupture tested pipe. Thus, the initial shape of the growing fractures would appear to be similar under both loading modes. It can be inferred, then, that pipe lifetimes are not significantly influenced by the fracture surface shape.

The change in fracture mode in the final progress of the crack, from stable crack growth exhibiting only localised drawing and fibrillation to one of tearing and macroductility, can possibly be a result of the increase in hoop stress at the crack tip with increasing crack depth as shown in Figure 7.3. At some point the yield stress of the material at the testing temperature is exceeded, plane stress conditions will predominate and the remaining material in the pipe wall will deform on a macroscale.

The observation that discontinuous growth bands (DGB's) were observed on fractures of HDPE 2 and MDPE 2 pipes but were absent on HDPE 1 and MDPE 1 fracture surfaces may be related to differences in molecular weights. Laghouati et al (32) found that a high molecular weight sample ($\bar{M}w$ = 200,000) of HDPE exhibited a discontinuous propagating mechanism by the presence of several crack arrest lines, whereas low molecular weight HDPE materials with $\bar{M}w$ not exceeding 72,000 did not produce surfaces with DGB's.

One method of improving stress rupture life is by an increase in $\bar{M}w$ and since HDPE 2 has a significantly improved stress rupture performance compared with HDPE 1 the DGB's observed on HDPE 2 pipe fracture surface may well be a result of increased molecular weight. For the materials which form DGB's on fracture surfaces the mechanisms proposed by Laghouati et al (32) of large scale void formation in the plastic zone at the crack tip would appear to be the more applicable theory compared with that described by McEvily et al (116) which was also preferred by Cowley and Wylde (20).

7.2.4 Micro-features of Fracture Surfaces

(i) Mode of Fracture.

Most fractures obtained at the test temperature of 80°C would be classed as quasi-brittle (127) since they appear flat and brittle with localised ductility only on a micro-scale except that is in the last progress of the crack where gross yielding and macroductility were in evidence. The ductility varied considerably across a surface usually increasing with distance from the initiation site with the drawn fibrils exhibiting a distinct directional bias. The voids left behind also appeared to vary in size but were generally in the range 5 - 30 μm.

The so-called quasi-brittle mode of fracture has been shown (127) to occur under plane strain conditions in the interior of pipe walls at reduced stresses (below the "knee" on the stress rupture curve) and at lower temperatures.

The scale of features produced in the drawn regions (5 - 30 μm) although of the same order as expected spherulite sizes ($\approx$1 μm) they nevertheless tend to be somewhat larger. Measurements were made difficult, however, due to the masking effect of fibrillation.

In general the cracks in pipes subjected to pressures below the knee in the stress rupture curve at 80°C nucleate from defects close to but not necessarily at the inside surface of the pipe. The crack enters a period of slow stable crack growth evidenced by void formation and fibrillation due to crazing. Conditions

towards the centre of the pipe wall are predominantly plane strain which accelerates crack growth. As the crack approaches the outer surface of the pipe plane stress conditions become more important and the fibrillation is lost in gross yielding and ductility. There appears to be no substantial evidence for fast crack growth in the final stages of propagation possibly because of the elevated test temperature but also the material fracture toughness may increase to such an extent that yielding becomes the only possible rupture mode.

(ii) Character and Origin of Crack Initiating Particles.

Scanning electron microscopy enabled the sites of fracture initiation to be clearly identified and by using energy dispersive x-ray techniques such crack initiators could be elementally characterised. This sort of evidence enabled suggestions to be made as to the origin of the particulate crack initiators. Once the origin is known steps can be taken to ensure that the occurrence of such particles in the pipes is reduced by appropriate methods. This is especially important since the pipes under test could fail prematurely from internal defects when subjected to fluctuating loads (see section 7.2.4.(iii)). It is therefore essential that pipes are as free from defects as is practically possible.

Table 7.2 summarises the main types of particles observed to initiate fractures, the range of particle sizes and the materials within which they were generally observed. Possible origins and means of elimination are also tabulated.

A significant number of metallic inclusions contained iron, nickel, chromium and in some cases titanium or molybdenum. These elements are all constituents of certain grades of stainless steel (those containing Fe, Cr and Ni only are designated grade 304, those where Fe, Cr, Ni and Ti are present are usually grade 321 while Fe, Cr, Ni and Mo are constituents of 316 stainless steel). Such defects could originate from processing equipment, from accidental contamination

TABLE 7.2 - Summary of Main Types of Particulate Inclusions Observed to Initiate Fractures in Small Diameter PE Pipes.

INCLUSION TYPE - MAIN ELEMENTAL COMPONENTS	INCLUSION CHARACTER AND OTHER COMMENTS	RANGE OF INCLUSION SIZES μm				POSSIBLE ORIGIN OF INCLUSIONS	POSSIBLE MEANS OF ELIMINATION OR REDUCTION OF INCLUSIONS
		MDPE 1	MDPE 2	MDPE 1	MDPE 2		
None detected	Possibly carboniferous. In MDPE 1 inclusions are large and have an angular geometry. Found at various distances from inside surface of pipes	68 - 1030 52% of failures	40 - 303 25% of failures	42 - 536 41% of failures	206 1 out of 2 failures	1) Unplasticised or degraded polymer. 2) Plants or insects. 3) Agglomerated pigment or filler.	a) Melt filtration b) Improved homogenisation during processing.
Calcium	Agglomerates of material exhibiting a polyhedron type geometry. Found at various distances from inside surface of pipes.	76 - 338 16% of failures	303, 524 12% of failures	88 - 654 24% of failures	371 1 out of 2 failures	1) Polymer lubricant such as calcium stearate. 2) Extraneous material in feedstock, polymer sack, hopper etc.	a) Change of lubricant. b) Improved homogenisation during processing. c) Melt filtration.
Iron (Not including stainless steel particles.)	Variable size, with no well defined geometrical character. Often found close to the inside surface of the pipe.	213, 600 8% of failures	120 - 524 14% of failures	129, 129 12% of failures	None	1) Inclusions possibly abraded from the surfaces of processing equipment by the polymer. 2) Extraneous material in feedstock, polymer sack, hopper etc.	a) Melt filtration. b) Improved cleanliness during polymer handling and processing. c) Use of more abrasion resistant surfaces in processing equipment.
Stainless Steel Fe, Cr, Ni (Grade 304) Fe, Cr, Ni, Mo (Grade 316) Fe, Cr, Ni, Ti (Grade 321)	Generally smaller than other inclusions and closer to the inside surface of the pipes. No regular geometries observed.	33 - 207 16% of failures	43 - 120 18% of failures	146, 367 12% of failures	None	1) Inclusions possibly abraded from the surfaces of processing equipment by the polymer. 2) Extraneous material in feedstock, polymer sack, hopper etc.	a) Melt filtration. b) Improved cleanliness during polymer handling and processing. c) Use of more abrasion resistant surfaces in processing equipment.
Titanium	Usually found further from inside surface of pipe suggesting that particles were not abraded from surfaces of processing equipment.	83, 305 8% of failures	None	97, 131 12% of failures	None	1) Pigment in yellow MDPE 1 pipes. 2) Extraneous material in feedstock, polymer sack, hopper etc.	a) Melt filtration. b) Improved homogenisation during processing. c) Improved cleanliness during polymer handling and processing.
Silicon	Possibly glass or sand inclusions.	None	132, 303 12% of failures	129 6% of failures	371 1 out of 2 failures	1) Extraneous material in feedstock, polymer sack, hopper etc.	a) Melt filtration. b) Improved cleanliness during polymer handling and processing.
Chlorine	Possibly paper fibres the chlorine being used to help whiten the paper in the bleaching process.	>5,000	None	None	None	1) Polymer feedstock sack (normally paper) 2) Extraneous material in feedstock, hopper etc.	a) Improved cleanliness during polymer handling and processing. b) Melt filtration.

of the polymer feedstock or may have been present within the polymer granules from the outset. In general the stainless steel inclusions were found closer to the inside wall of the pipes indicating that they may result from an abrasion process occurring between the polymer and the manufacturing equipment surfaces.

Calcium rich particles are almost certainly polymer lubricants which are added to HDPE during processing to improve melt flow properties. The chemical helps in creating high internal shear which imparts good physical properties to the finished product. Other workers (126) have found agglomerates of calcium stearate in HDPE pipes and look very similar to those obtained in Figure 4.42. When analysing calcium based particles care was taken to distinguish between an actual inclusion within the pipe material and calcium carbonate particles which may have been deposited on the fracture surface, near the initiation site, by the water used for testing the pipes.

The particle initiators which failed to produce elemental traces on their x-ray spectra are considered to be carboniferous in nature. Such material may be unplasticised or degraded polymer, particles of agglomerated pigment or filler or perhaps other forms of organic matter such as plants or insects The presence of only carbon, hydrogen and perhaps oxygen would be consistent with the fact that no elemental peaks were observed. The analysis equipment was unable to detect elements with atomic numbers of sixteen or less. It is interesting to note that for HDPE pipes these carboniferous particles were in general larger than the metallic or calcium rich initiators and tended to have extremely angular shapes.

Apart from obvious precautions taken to keep the polymer feedstock free from contaminants and the processing equipment clean there would seem little else possible to eliminate significant quantities of the inclusions described above. A more abrasive resistant interior to the extrusion equipment may reduce the

presence of some metallic particles. More homogeneous mixes of molten polymer and pigments, or other additives, should also help. Assuming that particles may still be present within the polymer, however, a melt filtration system could be used on the extruder to reduce and hopefully eliminate all remaining particulate defects. Although there would be practical difficulties associated with such filtering systems the removal of a significant fraction of inclusions should result in an immediate improvement in stress rupture and fatigue performance of the finished pipes.

Since calcium rich particles have initiated a significant number of fractures in the HDPE 1 and 2 pipes a further improvement in mechanical behaviour may be observed if lubricants other than calcium stearate are utilised in the process melt.

(It should be noted that the water in which the pipes were tested contained lime, iron, potassium, copper and zinc among other substances. It was particularly important therefore, to identify inclusions specifically associated with fracture initiation, preferably embedded in the polymer, and not to analyse surface deposits originating in the test water. To satisfy this requirement two x-ray spectra were obtained for each specimen, one at the initiation site and one remote from this area, both at the same magnification. When the remote spectrum was, in effect, subtracted from the inclusion spectrum the remaining peaks were considered to be associated with elements in the crack initiating particle.)

(iii) Effect of Inclusions on Pipe Lifetimes. Equation (2.15) predicts that the size of a particle initiating fracture controls the lifetime of plastics pipes under static load, assuming that crack growth is described by an expression of the form as in equation (2.12). A correlation was therefore sought between the size of the crack initiating particle and some measure of pipe lifetime.

For HDPE 1 pipes, only a limited number of stress rupture results were obtained, so for a more complete analysis, data from fatigue tests were incorporated. This was possible since HDPE 1 was shown to behave in a manner described by cumulative damage principles, section 7.2.1. However, there was a small reduction in performance with increasing frequency as shown in Figure 4.20. To accommodate this reduction, the lifetime of a given pipe is expressed in relation to the mean lifetime of that test (conducted at a given pressure and with the same loading form and frequency) of which it was part. The data point is thus expressed as $\tau_{SR}/\ \overline{\tau}_{SR}$ or $\tau_{FATIGUE}/\ \overline{\tau}_{FATIGUE}$ where $\overline{\tau}$ is the mean lifetime, under stress rupture or fatigue, of the group of pipe samples of which τ is the lifetime of one.

Various plots were made of the "normalised" lifetime factors against the size of inclusions leading to fracture (a_o), using different measures of particle dimensions (for example, the maximum size, or the extent of the particle along and perpendicular to the pipe axis). The best fit was obtained on a log ($\tau/\overline{\tau}$) against a log (a_o) plot, where a_o is the maximum inclusion size in the plane of the fracture surface irrespective of direction. The data is presented in Figure 7.4, where the sample size of 22 gave a correlation coefficient of -0.49. The preferred log-log relationship between $\tau/\overline{\tau}$ and a_o infers that the values of τ_{SR} or $\tau_{FATIGUE}$ can best be predicted by using the fracture mechanics approach, as applied to various PE's by Gray et al (2, 79) even though the number of cycles to failure, N_f, is accurately predicted by cumulative damage principles. The negative correlation coefficient confirms the dependence of pipe lifetime on initiating particle size as described by equation (2.15). Increasing the size of the initiating particle reduced the pipe lifetime.

A value for b in equation (2.15) can be obtained from the slope of the plot in Figure 7.4. This was found to be approximately 2.36, a value which is close to figures for b obtained from similar PE materials, as measured by crack propagation studies conducted by Gray and his co-workers (2, 79). Allowing for variations in particle positions and shapes the agreement seems reasonable. In addition, for particle sizes in the range 200 - 1000 μm, the calculated values of K_c of 0.14 to 0.30 MN $m^{-3/2}$ for a hoop stress of 4.93 MPa and a semi-elliptical flaw, are within those at which measurable crack growth occurs for similar PE's (2, 79). The majority, 55%, of the particles initiating fracture in the relatively short lifetime HDPE 1 pipes were angular in nature. It may well be that these angular inclusions are of the required size and shape to enable a crack to grow almost immediately upon the application of a stress. With other types of inclusions a considerable initiation period may be necessary to enable sufficiently sharp flaws to develop and so allow a crack to propagate according to fracture mechanics principles. Other plastics pipe materials may not, however, exhibit the same responses to included defects and no straight-forward relationships could be found for the other PE materials tested.

A difference exists between work reported here and the results obtained by Gray et al (2, 79) on the fracture of PE pipe, that is with respect to the size of crack initiating particles. Gray and his co-workers predicted stress rupture lifetimes using initial defect sizes in the range 10 - 100 μm whereas Figure 4.43 shows that the measured particle sizes are considerably larger, in the range 100 - 500 μm. The difference may be due to a delay in the start of crack growth, an incubation period, or in the value of the geometrical parameter Y (see equation 2.13). Gray et al assumed the shape of the growing crack to be semi-elliptical (2, 79).

Figure 4.31 indicates that this is not always the case. Thus if Y had a smaller value, or there was a significant incubation period, then the particle size required to initiate fracture may have to be put at a higher value and then the differences may be explained.

7.2.5 Material Property Changes During Pressure Testing

Figures 4.63 and 4.64 highlight selected property changes in material structure, with testing time at 80°C, as measured by DSC. The properties examined were crystalline melting temperature T_m and DSC measured crystallinity. Any variations in mechanical performance of pipes subjected to longer testing times, (for example at higher fatigue frequencies) would then be partially explained by changes in material properties.

However, HDPE 1 pipe subjected to a pipe hoop stress of 3.8 MPa, a temperature of 80°C and a frequency of 6 cpm demonstrated a τ_{TEST} value of approximately 400 hours and a $\tau_{FATIGUE}$ value of 80 hours. The same pipe material under the same conditions of temperature but held at a static hoop stress of 3.8 MPa produced a τ_{SR} value of 320 hours. The subsequently measured T_m and crystallinity values of both pipe materials showed no statistically significant variation. In other words, the crystalline melting temperatures and crystallinities were essentially the same after similar periods at 80°C although the mechanical performances described by τ_{SR} (320 hours) and $\tau_{FATIGUE}$ (80 hours) are very different. It seems unlikely therefore that the reduction in fatigue performance of the HDPE 1 compared to stress rupture at the same conditions was due to variations in the material properties of crystallinity and melting temperature.

The general increases in T_m and crystallinity are in themselves interesting. The shift of the DSC peak to higher values of T_m with increasing time at 80^oC suggests that a more ordered and stable crystal structure is forming. T_m is related to the thickness of crystalline lamellae L_c (assuming no surface contributions) by the expression

$$T_m = T_m^o \left(1 - \frac{\text{Constant}}{L_c} \right) \qquad (7.1)$$

where $T_m = T_m^o$ when L_c is infinite or T_m^o is the equilibrium melting temperature for a crystal of infinite thickness. As the lamellae thicken so more material is drawn from amorphous areas into the ordered crystalline regions of the polymer. Hence crystallinity will also increase as well as T_m (35, 39, 40). In practice an increase in crystallinity will result in a decrease in fatigue crack propagation (94) and an increased resistance to creep deformation (4). Thus in general as crystallinity (and T_g and T_m) increases so lifetimes of thermoplastics pipe systems should be extended.

There is also an increased effect upon T_m and percent crystallinity when a pipe sample is pressurised compared with the purely aged samples. A certain amount of stress crystallisation would therefore seem to be occurring in the materials examined.

7.3 SMALL DIAMETER PIPE SYSTEMS CONTAINING INJECTION MOULDED FITTINGS

7.3.1 Mechanical Performance of HDPE 1 Pipe + Batch A 90^o Equal Tees and 90^o Bends.

In fatigue testing the imposition of intermittent internal pressure loading resulted in a trend to decrease the $\tau_{FATIGUE}$ values, with increasing frequency, of pipe systems containing the batch A HDPE injection moulded tees and bends. In all cases fracture was associated with a defect residual from processing which induced premature failure itself or indirectly caused fracture by adversely affecting the butt-welded joint between HDPE 1 pipe and a batch A fitting.

The 90^{o} equal tees exhibited two types of moulding defects which became active sites of failure under different conditions. The first was associated with the extraction of the mould core which resulted in a very ragged internal surface appearance and notch in a localised area near the intersection of the tee branch arms. This is shown clearly in Figure 5.18. The second was butt-welded to a pipe section. An internal weld line within the fitting and running parallel to the pipe axis along the spine of the tee, Figure 5.3, caused a discontinuity to develop in the butt-weld. A feature previously observed in 160mm OD SDR 11 HDPE pipe systems (20). At reduced fatigue frequencies ($\leqslant$2 cpm) this discontinuity in the butt-weld became an active failure site (T2 type 1), see Table 5.1.

Under static internal pressure the internal weld line of the tee proved to be a site of fracture (T4) when the pipe to which it was joined, HDPE 2, had a stress rupture life in excess of the tee fitting itself. This was in spite of the fact that the tee is about 50% thicker than the pipe at site T4. Thus under both fatigue and stress rupture conditions this internal weld line in the HDPE batch A 90^{o} tee proved a weakness compared with the pipe to which it is joined.

When subjected to fatigue frequencies in excess of 2 cpm (and occasionally less) the predominant mode of fracture in the batch A tees was at site T3. This mode of fracture produced a well defined correlation between $\tau_{FATIGUE}$ values and frequency, with τ_{SR} values for HDPE 1 pipe and $\tau_{FATIGUE}$ values for tees becoming increasingly divergent with a modest increase in frequency from 2 cpm to about 8 cpm at the same temperature and maximum pipe hoop stress. Clearly a well defined fatigue weakness has been demonstrated and is shown quantitatively in Table 7.3.

By comparing experimental values for the number of cycles to failure of the tees at different frequencies with those predicted from equation (2.21) some idea of the failure mechanisms at work can be obtained. Table 7.4 presents the actual and predicted N_f values for the

TABLE 7.3 - Comparison of Stress Rupture (τ_{SR}) and Fatigue Lives ($\tau_{FATIGUE}$) at Two Frequencies for HDPE 1 Pipe + Batch A 90° Equal Tees to Demonstrate the Presence of a Fatigue Weakness.

τ_{SR} (F1) (Hours)	FATIGUE FREQUENCY (cpm)	$\tau_{FATIGUE}$ (F2) (Hours)	$\tau_{FATIGUE}$ (F3) (Hours)	$\frac{\tau_{FATIGUE}\ (F3)}{\tau_{SR}\ (F1)}$	$\frac{\tau_{FATIGUE}(F3)}{\tau_{FATIGUE}(F1)}$
65.6	0.85	57.5	58.?	0.89	1.02
			64.2	0.98	1.11
			67.5	1.03	1.17
			71.1	1.08	1.24
				MEAN 0.99 ± 0.08	MEAN 1.14 ± 0.09
65.6	6.00	42.5	8.7	0.13	0.20
			7.9	0.12	0.18
			8.1	0.12	0.19
			8.7	0.13	0.20
			7.6	0.07	0.11
			2.8	0.04	0.06
			5.0	0.08	0.12
				MEAN 0.10 ± 0.04	MEAN 0.15 ± 0.06

Notes 1) All tests were conducted at 80°C and 4.93 MPa pipe hoop stress.

2) The $\tau_{FATIGUE}$ (F1) value takes account of the fact that pipe performance reduces with increasing frequency compared with τ_{SR} (F1).

TABLE 7.4 - Comparison of Mean Experimental N_f Values and Predicted N_f Values for Batch A 90° Equal Tees to Demonstrate Change in Fracture Mechanism.

FREQUENCY (cpm)	t_{max} (Secs)	τ_{SR} (Hours)	MEAN EXPERIMENTAL N_f (Cycles)	PREDICTED N_f (Cycles)	$\frac{\text{MEAN EXPERIMENTAL } N_f}{\text{PREDICTED } N_f}$
0.85	62	65.6	3797	3809	0.99
1.58	30	65.6	4733	7872	0.60
2.33	10	65.6	5871	23616	0.25
4.29	6	65.6	7342	39360	0.19
6.00	2	65.6	11762	118080	0.10
7.50	1	65.6	18157	236160	0.08

Notes 1) All tests were conducted at 4.93 MPa pipe hoop stress and at 80°C.

2) The closer N_f(experimental)/N_f(predicted) approaches unity cumulative damage principles become more applicable to the description of the failure processes.

batch A tees at 80°C and 4.93 MPa maximum pipe hoop stress for the various test frequencies. It is clear that only as the frequency drops and stress rupture conditions are approached does the cumulative damage mechanism begin to describe how fracture is occurring since predicted and experimental values are closer at these lower frequencies. In other words the time for which the stress acts during a loading cycle becomes more important than the application of the stress at reduced frequencies. The creep sensitivity of the material is apparently increasing under these conditions. As frequency is increased so a greater number of cycles are required to cause fracture, hence the mechanism cannot be cycle dependent which would produce a linear relationship of N_f against frequency parallel to the frequency axis. Once again the fracture mechanism is not well defined but crack propagation would appear to be by a mixed mode as discussed in section 7.2.1.

The batch A 90° bends also induced discontinuities to develop at butt-welds made with extruded pipe sections. These were again associated with what appeared to be internal weld lines and surface defects on the mouldings, termed mould parting lines. In all cases of B2 Type 1 fractures these discontinuities provided the sites of failure.

In fatigue conditions the moulding itself was not a source of weakness except indirectly since, as mentioned above, the butt-welds proved to be so. The effect of increasing frequency on the bend systems caused similar reductions in $\tau_{FATIGUE}$ values as those observed in tees, see Figure 5.13.

Fittings and butt-welded joints between extruded pipe and injection mouldings are, based on the evidence presented in Chapter 5, particularly susceptible to premature failure (compared with pipe stress rupture life) when subjected to fluctuating loads of modest frequency (<10 cpm). In general fatigue testing will isolate weaknesses in systems which are not apparent at all in short term rupture tests and only occasionally in stress rupture tests. In fact the T3 fracture was only observed under fatigue conditions. Since certain weak-

nesses in thermoplastics pipe systems can only be demonstrated under fluctuating internal pressures it is particularly important that more fatigue data is generated to enable engineers to design systems with reasonably predictable service lives, not solely based on stress rupture performance and so reduce the occurrences of premature failure.

The design of moulds used to fabricate bend and tee fittings must also take account of the fact that certain inherent defects remain in the moulded article after manufacture and could impair physical and mechanical properties. Thus the gating systems and conditions of processing must be selected to ensure the development of an appropriate microstructure which effectively removes sites for crack initiation and also helps to limit the rate of propagation once a crack has started to grow. Other more straightforward improvements can be made if surface defects such as notches and/or mould parting lines are eliminated. This could be achieved by careful machining and maintenance of the moulds themselves and their cores. (It is interesting to note that similar failures under fatigue conditions have been observed to start from surface notches on the inside wall of polyvinylidene fluoride (PVDF) tees.) The remarks above are related to HDPE batch A tees and bends and cannot be taken as indicative of the quality of mouldings made from other materials or designs. However, Falbe and Richter (129) have indicated that the performance of pipe fittings in general depends to a large extent on the production methods and production history of the components involved.

It should further be noted that only under fatigue conditions did some of the weaknesses in mouldings become apparent. Such results concur with the conclusions reached by Jacobi (108) that short term tests and long term tests under constant internal pressure are unsuitable to characterise completely the mechanical performance of injection moulded thermoplastics pipe fittings.

7.3.2 Mechanical Performance of HDPE 2 Pipe + Batch B 90° Equal Tees and 90° Bends

Comparison of τ_{SR} and $\tau_{FATIGUE}$ values for HDPE 2 pipe with $\tau_{FATIGUE}$ values for batch B 90° equal tees over the same range of frequencies (0.86 - 7.5 cpm) as presented in Figures 5.9 - 5.11 immediately indicates a significant fatigue weakness, reflecting similar behaviour observed in the batch A 90° equal tees. A measure of the level of reduction in lifetime when the test mode changes to fatigue from stress rupture is presented in this example. At 80°C test temperature, 3 MPa pipe hoop stress and 7.5 cpm fatigue frequency the $\tau_{FATIGUE}$ value is reduced to 14 hours compared with the manufacturer's τ_{SR} of approximately 3000 hours for brittle failure in HDPE 2 pipe, at site P1, under the same conditions of temperature and pipe hoop stress. This is a reduction of nearly 215 times and confirms under a much wider range of stresses and frequencies the previously reported aggressive nature of fatigue loading on lifetimes of thermoplastics pipeline systems (20).

A limited amount of work has also been carried out on these systems at 60°C and has resulted in a similar trend of reducing lifetimes with increasing frequency.

The site of fracture initiation of all failures in the batch B tees subjected to intermittent loads was identical with that of batch A tees at site T3. This is not surprising since as far as it was possible to ascertain the design of both types of fittings was identical and they were probably manufactured with the same moulds. The batch B tees were made of a different HDPE resin however.

Work on other polyolefin pipe systems of different designs and sizes has also revealed that under fatigue conditions tee body fractures at site T3 occur at times which are grossly reduced compared with pipe stress rupture lives. It is clear then that the T3 fracture under fatigue is not specifically related to one design, size or thermoplastic material but in fact can occur almost independently of the aforementioned variables under certain fatigue conditions. Such behaviour may well prove to be a potentially serious problem particularly in the chemical process industries where the likelihood of fatigue loadings

occurring at frequencies less than 10 cpm is quite high.

It is believed that as moulding techniques and fitting designs are improved the defects, microstructural or otherwise, will be essentially eliminated. At the present time a knowledge of the behaviour of such defects will be of particular use to the design engineer who will be able to allow for the reduced performance under certain conditions of internal pressure. Once such defects have been eliminated the results of Chapter 5 indicate that the butt-welded joint between the 90^{o} tee and the extruded pipe will then become the active site for premature failures.

The data presented in Figures 5.9 and 5.11 indicate that as the maximum internal fluctuating pressure is reduced the $\tau_{FATIGUE}$ values for the batch B tees tend to approach the material manufacturer's stress rupture curve. Tests are still being undertaken to identify the presence of a possible practical fatigue limit which would obviate the need for additional fatigue design factors at these loads. Figure 5.10 clearly demonstrates that the slopes of the log (hoop stress) against log ($\tau_{FATIGUE}$) plots are not parallel either to each other or the brittle rupture curve of the manufacturer's stress rupture data. A constant design factor related to the frequency of operation is not therefore applicable at any given maximum pressure.

It is evident from Figure 5.12 that the mode of fracture changes from a purely cycle dependent process at a pipe hoop stress of 4.93 MPa, one of the highest applied, to a mixed mechanism as the applied maximum stress is reduced. The behaviour of the batch B 90^{o} tees at the highest stress is clearly shown to be frequency independent in the range of frequencies examined and crack propagation rates should be determined solely by the Paris equation (2.22). Figure 7.5 shows clearly the difference in predicted N_f values for batch B tees at 4.93 MPa pipe hoop stress based on equation (2.21) compared with actual performance. Two extreme mechanisms are depicted here on the one diagram. Equation (7.1) would thus be inapplicable to this case. As pipe hoop stresses are reduced the effects of crack propagation during the load-on part of the fatigue

cycle become more important as the creep sensitivity of the material increases and the N_f values at the same pressures but different frequencies diverge. Cumulative damage or effects due to creep are thus affecting the crack propagation although not significantly since predicted N_f values would produce figures much higher than those actually observed. It should be noted, however, that the τ_{SR} figures used in equation (2.21) are those obtained for pipe and not for the fittings themselves.

Another interesting point is that the shapes of the Wöhler curves presented in Figure 5.11 are different at different frequencies. Two of the curves, those at frequencies of 1.57 cpm and 4.29 cpm, are sygmoidal and bear close resemblance to those obtained for uPVC and ABS pipes (97, 107, 130). At a frequency of 7.5 cpm the batch B 90° equal tees exhibit an approximately linear relationship between log (N_f) and log (σ_H). Assuming the conditions for the application of equation 2.25 are fulfilled then a value for the material constant d in the fatigue crack growth law, equation 2.22, can be calculated and is found to be 3.71. This compares favourably with many polymers (94) and metals (114) where fatigue crack growth is controlled by the stress intensity factor range (131). Such a result infers that the brittle fracture of batch B 90° equal tees under fatigue at a frequency of 7.5 cpm and subjected to a pipe hoop stress range of 4.93 MPa can be described by equation 2.22, the Paris law, whilst at lower frequencies and stresses, on the brittle fracture curve, cumulative damage principles such as equation 2.21 are more applicable.

Discussion of the performance of HDPE 2 pipe + batch B injection moulded fittings has so far been related to the most dramatic and well defined decrease in system lifetime under fatigue. Table 5.5 indicates that systems containing 90^{o} bends can also exhibit reductions in $\tau_{FATIGUE}$ of nearly seventeen times compared to measured stress rupture lifetimes (about a tenfold reduction in lifetime compared with manufacturer's stress rupture data). The site of fracture for the bend systems always lay in the mirror-plate butt-weld (B2 Type 1) and was always related to a discontinuity of the weld bead. Such defects arose from the same sources as indicated in section 7.3.1, i.e. from internal weld lines and mould parting lines.

Since tests have been conducted on more than 100 pipe to pipe mirror-plate butt-welds in HDPE under stress rupture and fatigue loading using a variety of internal pressures and frequencies and no weaknesses have been identified, this would indicate a sound welding technique and the failures observed between 90^{o} bends and extruded pipe are due to the inhomogeneities introduced into the joint by the process of butt-welding extruded pipe to injection moulded fittings.

The type of weld defect observed in the bend systems which caused premature fracture under fatigue is

also present in the butt-weld joining HDPE 2 pipe to batch B 90° equal tees. For the batch A tees this site became active at fatigue frequencies of 2 cpm or less. A similar activation could occur in the batch B tee systems once the T3 fracture site under fatigue is eliminated by improved mould design and/or microstructure.

It appears that improved mechanical performance of pipe systems containing injection moulded fittings subjected to a variety of internal pressure profiles will involve a process of progressive removal of moulding defects.

Results of tests conducted to examine the influence of a combination of stress rupture and fatigue loads on the batch B tee systems revealed that the mechanism or defect leading to fracture at site T3, under fatigue is considerably less active under static loads. The apparently beneficial effect of placing a previously fatigued sample under a static internal load may well be explained by a crack blunting or material toughening model, that is, the value of K at the crack tip may be reduced.

7.3.3 Mechanical Performance of MDPE 1 Pipe + Batch A 90° Equal Tees and 90° Bends

In a similar fashion to the behaviour observed in the HDPE systems, the performance of MDPE1pipe systems containing injection moulded fittings was substantially reduced compared with measured or manufacturer's stress rupture data. There was a particular weakness in the butt-welds joining extruded pipe to moulded fittings which became active whether the testing mode was stress rupture or fatigue. The limited number of test specimens precluded the possibility of testing under short term rupture conditions. Consistent with previous results, fatigue demonstrated that it was the most aggressive loading mode and in one case a $\tau_{FATIGUE}$ value of 0.84 hours was obtained at a pipe hoop stress of 4.93 MPa, a temperature of 80°C and a fatigue frequency of 7.5 cpm. This represented a reduction of about 160 times compared to the mean measured stress rupture life of the pipe at the same hoop stress and temperature.

The particularly poor performance of the butt-welded joints between pipe and fittings prevented identification of any weaknesses under fatigue or stress rupture within the body of the mouldings.

The method of butt-welding 60mm OD SDR 11 MDPE 1 pipes and pipe systems containing injection moulded fittings is, therefore, not recommended at the present time. It should be noted that the standard of butt-welding used to fabricate the MDPE 1 samples was deemed by the suppliers and by British Gas to be entirely satisfactory.

7.3.4 Fracture Surface Features

The T3 failure initiation site in both HDPE pipe + batch A and batch B 90° equal tees has been clearly shown by scanning electron microscopy, Figure 5.18, to occur at the area adjacent to the inside wall of the tee branch arm and be associated with damage induced by the retraction of the mould core (an effect also observed on PVDF tee fittings). Marked changes in surface morphology of both types of tee fracture surfaces are evident at different frequencies and internal pressures. Higher stresses induce a surface which exhibits a great deal more fibrillation with the long highly drawn strands bending to mask underlying structure. A result possibly of a more rapid crack growth such as that observed in the latter stages of pipe fracture. A similar highly drawn surface is observed at higher loading frequencies. The surfaces obtained from conditions of highest stress and frequency show the most drawn and ductile appearance, Figure 5.25.

The converse is also true, in that reduced internal pressures and frequencies will result in surfaces of a more brittle nature although on a microscale localised drawing is still evident. The crack growth would appear to be by a mechanism of craze formation with voids being left behind surrounded by drawn material; the diameters of the voids are similar to HDPE pipe lying in the range 5 - 30 μm (possibly spherulite size).

A change in the mode of fracture is observed just prior to the crack breaking through to the outside wall of the tee. Again there is evidence for gross yielding and macroductility which presumably occurs due to the predominance of plane stress conditions in this region. The remainder of the crack being controlled mainly by plane strain.

Marked changes in microstructure through the thickness of the moulded tee are also observed, Figure 5.19, and in some cases discontinuous growth bands normal to the crack propagation direction occur together with concentric bands which are postulated to result from polymer flow during processing and are thus probably related to the fitting microstructure and not to the fracture process.

A knowledge of the conditions which produce such surfaces can be very useful for fractographic analysis of service failures. It should again be possible to estimate the conditions of fatigue frequency and loading if these particular fractures occur and since failures of this sort can be produced in a variety of pipe materials sizes and designs of tees with very similar features to those discussed above, the information should be widely applicable to the polyolefinic pipe systems field at least.

The initiation site for Type 1 butt-weld failures were associated with butt-weld defects and appeared to grow from the notch formed between the fitting and the weld bead which showed maximum deformation on the inside wall of the system. The features of butt-welds were shown up after the crack had passed across them with heat affected zones, the weld interface and differences between extruded pipe and injection moulded fittings clearly demonstrated. On a microscale features of localised ductility and voiding due to craze formation were again apparent with the ductility varying with distance from the initiation site and position with respect to the butt-weld itself.

7.4 LARGE DIAMETER PIPE SYSTEMS

7.4.1 Mechanical Performance

Although a very limited number of pipe test specimens were examined as HDPE 1 160mm OD SDR 11, namely two straight pipes, two welded pipes, two systems containing tees and two systems containing bends, a considerable amount of useful data was nevertheless obtained.

The pipes contained massive voids as shown in Figure 6.6. These voids would have led to a major stress intensification and were apparently responsible for a considerable reduction in pipe performance under fatigue, in some cases by an order of magnitude.

Voiding can be attributed to two effects. Firstly, in the production of pipe rapid cooling from the external surfaces can introduce considerable stresses in the pipe wall which vary from compressive near the skin to tensile at the core where there is some elongation (9). This may result in voiding. Secondly, when cooled, PE materials can exhibit substantial shrinkage particularly during a change from liquid to solid phases. If the bore and outside surface of the pipe are cooled first, then the material towards the centre of the pipe wall, being at a higher temperature and hence lower modulus, cannot deform the lower temperature polymer either side to compensate for the shrinkage. Voiding can again result. It is reasonable to expect both shrinkage and internal stresses to co-operate and thus create substantial voids.

The higher crystallinity thermoplastics such as HDPE will shrink to a greater extent than the MDPE materials and should therefore contain more instances of voiding. This was, in fact, shown to be the case during the experimental programme. Finally, the control of processing conditions particularly temperatures and rates of extrusion will also have significant effect over the presence or otherwise of voids.

In systems containing injection moulded fittings failure initiation occurred either within the body of the fittings or at weld discontinuities at the joint between pipes and mouldings. Such weld defects were identical in origin and appearance to those observed in smaller diameter systems, in other words, defects produced during moulding caused weld discontinuities to develop which subsequently resulted in premature fracture.

A distinct difference between the smaller diameter and larger diameter systems containing fittings was that the T4 fracture occurred under fatigue in the 160mm OD tees whereas it could only be produced under static loads for 63mm OD tees. In fact the T4 fracture was slightly different in nature for the larger fitting in that it occurred in association with obvious flow lines on the inside wall of the tee, Figure 6.2, which were not necessarily parallel with the main pipe axis or related to internal weld lines. In one case at least three fractures of this sort had propagated some way through the fitting wall although only one had actually produced failure. All were associated with flow lines and the $\tau_{FATIGUE}$ value for the T4 fracture in 160mm OD tees was approximately 14% of the manufacturer's stress rupture life for the same SDR pipe. Clearly this is seen as a deficiency in moulding techniques which requires immediate remedy to prevent premature fracture under fatigue.

Thick walled large bore pipe is obviously more expensive and difficult to test and it is evident that problems exist with large bore pipe which are not found in the smaller diameters. The presence of voids has already been mentioned and there is no information to suggest that such defects would not reduce stress rupture lifetimes as well as $\tau_{FATIGUE}$. Care must therefore be taken during the processing of large diameter pipes to avoid such problems.

7.4.2 Fracture Surface Features

The initiation sites in all pipe fractures were associated with large voids within the pipe wall. Most were in excess of 2mm along the maximum dimension parallel to the fracture plane. These observations are consistent with those obtained by Cowley and Wylde (20). In all cases the presence of a void was associated with a greatly reduced $\tau_{FATIGUE}$ value compared with either manufacturer's or measured τ_{SR} values for the same SDR pipe.

Discontinuous growth bands similar to those identified by Cowley et al (20) were present on the surfaces but appear to be associated with the intersection of the growing crack and the inside wall of the pipe. Crack growth is again by craze formation which leaves behind fibrillated regions and voids with diameters of the same order as spherulites (5 - 30 μm). The distribution of tendril lengths indicates that where a DGB occurs the crack growth is more ductile in the lighter stress whitened regions but more brittle in the darker areas.

It should be noted, however, that the DGB's tend to disappear and do not obviously progress right across the pipe wall, an effect possibly due to the speed of crack propagation. Such effects cannot be explained by mechanisms suggested by McEvily et al (116) or Laghouati et al (32).

The previously discussed alteration in mode of fracture towards the outer surface is obvious for this size of pipe and is again characterised by gross yielding and macroductility presumably a similar mechanism to that proposed for 63mm OD HDPE 1 and 2 pipes is occurring.

The L/h parameter for 160mm pipe fractures is, within limits, the same as that obtained for 63mm OD pipes and would tend to suggest that the pipe wall thickness does not have a substantial effect upon fatigue crack growth.

Contrary to the proposal by Cowley and Wylde (20) fractures at butt-welds were associated with the notch formed between the fitting and the weld bead at a discontinuity. They were generally not initiated at a location within the bead itself.

7.5 CONCLUSIONS AND RELATED COMMENTS

7.5.1 Mechanical Performance of PE Pipe Systems

a) Performance of PE pipelines is system specific. That is, the grade of plastics compound, the diameter and wall thickness of the pipe systems, the fitting design and fabrication methods can all have a marked effect upon performance.

b) Fatigue is by far the most aggressive loading mode compared with either short term rupture or stress rupture testing. It will identify weaknesses in mouldings, pipes or butt-welded joints more consistently, thoroughly and quickly than any other standard technique for internal pressure testing of pipes. A fatigue weakness is identified by a low value of $\tau_{FATIGUE}/\ \tau_{SR}$ and in some cases $\tau_{FATIGUE}$ may be to the left of the material manufacturer's stress rupture curve.

c) Injection moulded fittings are more likely to exhibit fatigue weaknesses than pipes.

d) All brittle fractures tend to be associated with defects in pipes or fittings that are residual from processing.

e) Improved stress rupture performance in pipes does not necessarily improve mechanical behaviour under fatigue and can, in some cases, actually produce a fatigue weakness.

f) Although selected PE material properties exhibit a well defined alteration during an elevated temperature test, this does not necessarily show a marked influence on stress rupture or fatigue performance of pipe systems.

g) For the same rectilinear loading profiles, some idea of the mechanism leading to failure, whether based upon cumulative damage or fracture mechanics principles, can be obtained by comparing the number of cycles to failure obtained in practice and those predicted from

$$N_f = \frac{\tau_{SR}}{t_{max}}$$

h) The presence of voids within 160mm OD SDR 11 pipe caused a significant reduction in $t_{FATIGUE}$ values compared with pipe stress rupture lives. When failure occurred from such defects the pipe failed to meet the manufacturer's specification for t_{SR}.

i) The performance of butt-welds between two pipe sections was satisfactory under both fatigue and stress rupture for HDPE 1 and HDPE 2. MDPE 1 pipe welds generally fell short of manufacturer's stress rupture specification and did not comply in any case under fatigue loadings.

j) Butt-welding is not considered a suitable method of jointing for 60mm OD SDR 11 MDPE 1 pipe systems.

k) Under certain conditions the butt-welded joints made between pipe and injection moulded fittings proved to be sources of weakness particularly under fluctuating loads.

7.5.2 Fracture Initiation, Propagation and Failure Mechanisms

a) Figure 7.4 established that the presence of included particles reduced the useful service life of an HDPE 1 pipe. It should be stressed, however, that the data thus presented relates to one pipe material only and the same results were not repeated for other pipe grade PE's examined. (This may be related, in part, to the incubation period prior to crack growth.)

Pipe performance should thus be improved by melt filtration at the extrusion stage to reduce the size and concentration of defects.

An analysis of uPVC pipe fractures by Kirby (132) demonstrated that included particles are a major cause of premature pipe failure. In excess of 300 failures were analysed and fracture from inclusions accounted for more than 11% of the total. This

suggests that field experience with uPVC compares with the laboratory studies on PE pipes reported in earlier chapters.

b) Inclusions were traced to several sources, namely base polymer manufacture, materials handling and processing. Attention should therefore be paid to all stages of the production of a finished article if its mechanical performance is to be enhanced.

c) The flaw sizes initiating fracture in 60mm OD SDR 11 MDPE 1 pipes and in 63mm OD SDR 11 HDPE 1 and 2 pipes have been measured directly and found to lie generally within the range 80 - 300 μm. Such sizes are in excess of those predicted by other workers (2, 79) and so theories which enable estimates to be made of lifetime in PE pipes under stress rupture require modification.

d) The crack initiators in 160mm OD SDR 11 pipes were voids with dimensions in the range 2 - 3 mm.

e) Fracture initiation in fittings was always associated with moulding defects which induced failures from within the fitting body or at discontinuities in the butt-welded joint with an extruded pipe.

f) Crack growth in all instances is considered to occur from craze formation which results in fibrillated and voided regions on the fracture surfaces, the voids exhibiting diameters similar to expected spherulite sizes.

g) The process of fracture under fatigue conditions does not necessarily result in obvious fatigue striations or discontinuous growth bands.

h) Since failure in the PE pipe systems resulted from heterogeneous deformation by crazing and both frequency sensitive and frequency insensitive fractures were obtained, the hypothesis put forward by Hertzberg et al (125), that polymers exhibiting a strong FCP frequency sensitivity also exhibited a strong tendency to undergo crazing, is not substantiated at least for the materials examined.

7.6 FUTURE WORK

Several developments of the research reported in earlier chapters have been or are at present being carried out at Brunel University.

a) An assessment of the performance of tapping-tee joining systems for PE gas pipe applications. The project involved a systematic study of the dependence of impact strength of the tapping-tee joints on jointing conditions including jointing pressures, times, contaminants, aging etc. (Completed project.)

b) The influence of particulate impurities on the stress rupture and fatigue properties of PE pipe and the investigation of new melt filtration procedures for use in these applications. (Project underway.)

c) Examination of the influence of well defined misalignments in butt-welds between pipes and between pipes and fittings. This to include in-plane or lateral misalignment and axial misalignment. This would result in basic design data and specific safety factors to be applied to pipe system joints exhibiting such misalignments.

d) Fundamental investigation of the factors controlling fatigue crack propagation in semicrystalline thermoplastics used in pipeline applications. This would also include an analysis of brittle failures and an attempt at explaining crack front shapes in terms of fracture mechanics principles. Objectives of such work would be to obtain a greater understanding of the effects of specific microstructures on fatigue crack propagation and to the identification of microstructures leading to reduced FCP rates. Understanding the reasons for specific crack front shapes will also lead to a knowledge of the fundamental processes of fracture in

thermoplastics pipe systems. Recommendations should also be forthcoming as to improvements in system design, correct materials selection and jointing techniques which should help to avoid instances of premature failure.

e) A more detailed examination of the changes in pipe material properties with time when tested at elevated temperatures. This should enable variations in mechanical performances to be explained specifically by such property changes or be attributed to other effects.

f) Further generation of stress rupture and fatigue data in thermoplastics pipe systems which are joined by socket fusion or butt-fusion techniques. Materials to be investigated would include PE, PP, PB and PVDF. The effect of a variety of environments encountered by such pipe systems would also be examined at a number of different temperatures, internal pressures and frequencies.

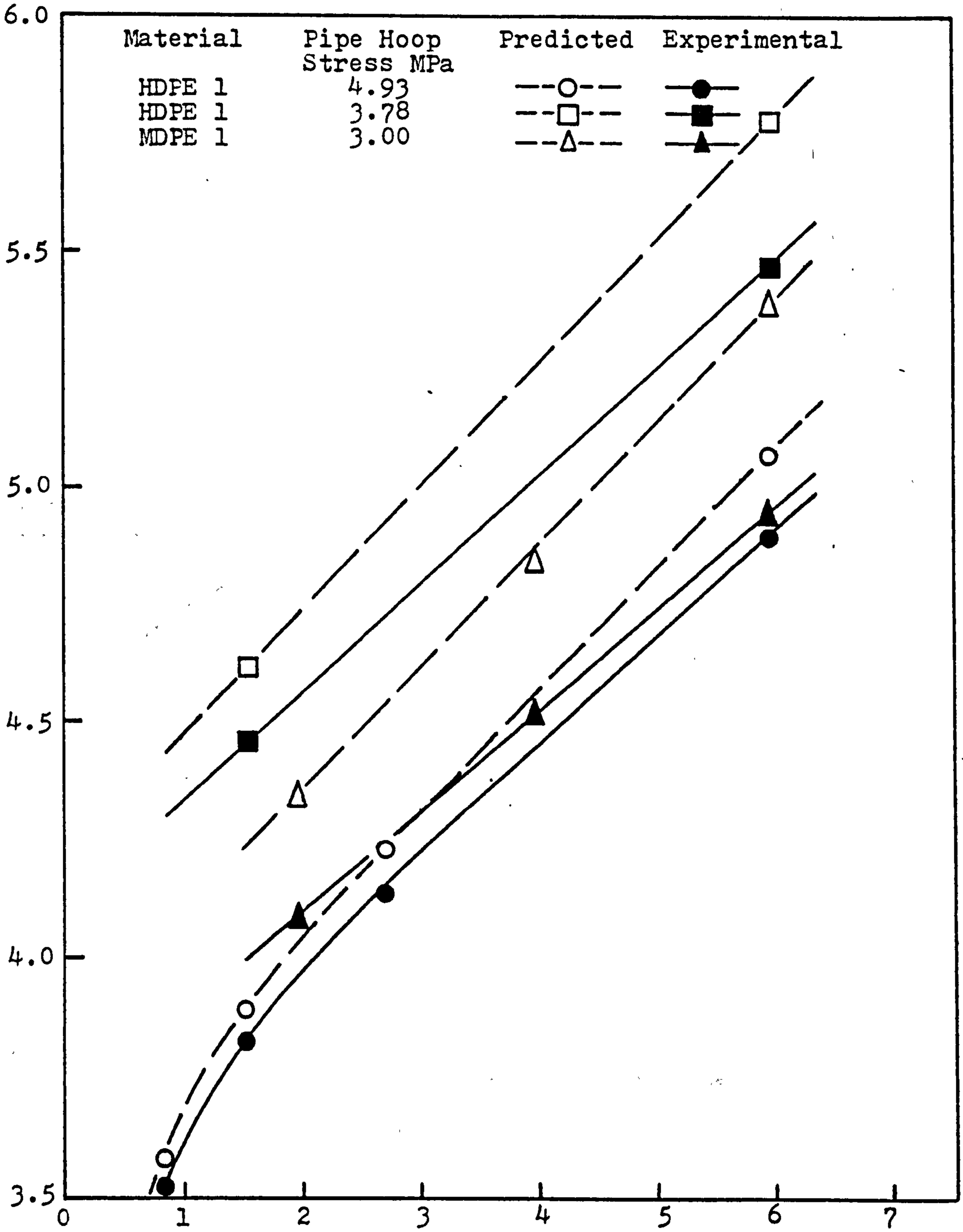

FIGURE 7.1 Comparison of predicted and experimental values of N_f as a function of frequency for HDPE 1 and MDPE 1 pipes at 80°C.

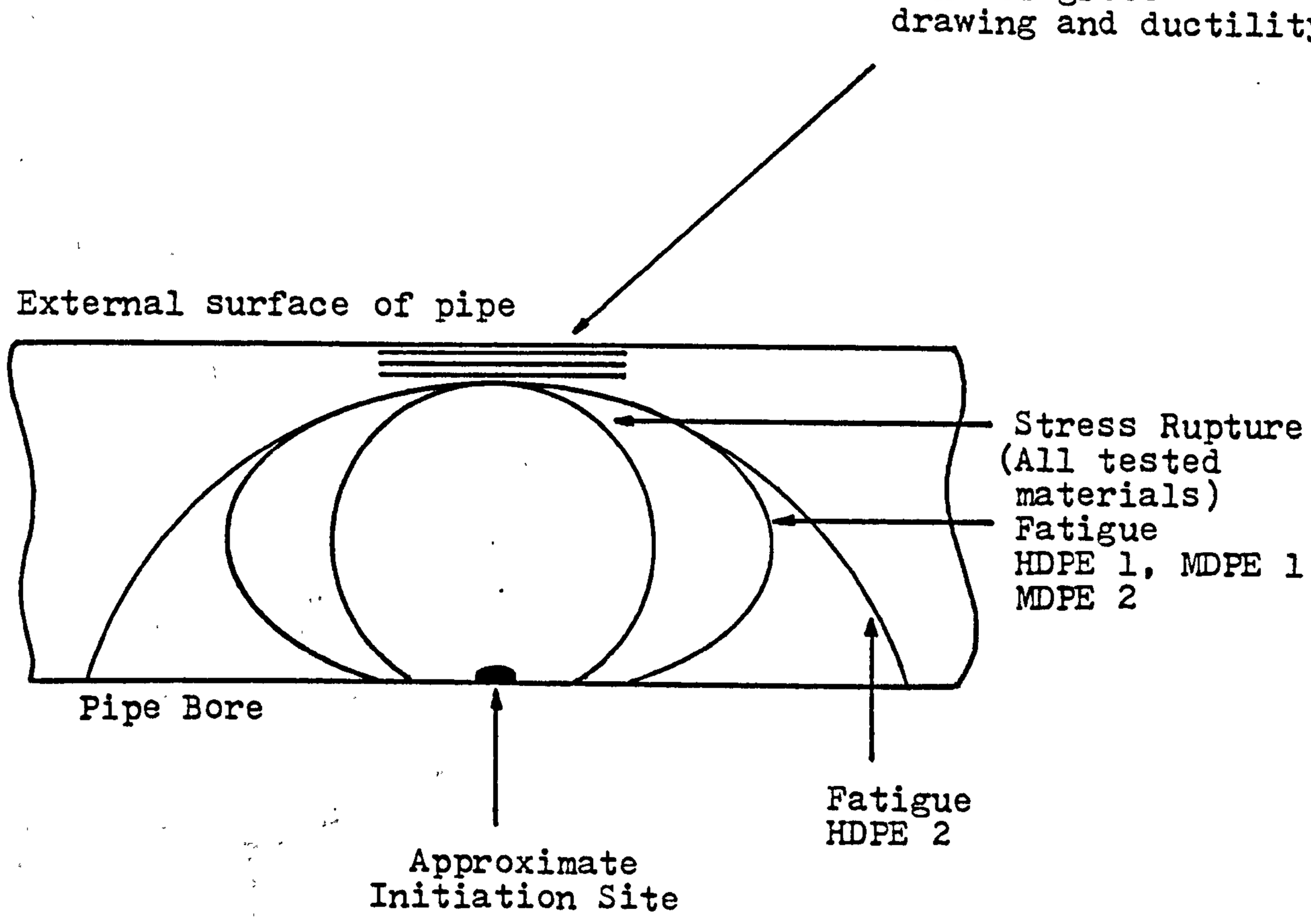

FIGURE 7.2 Schematic representations of brittle fracture surface features in PE pipe.

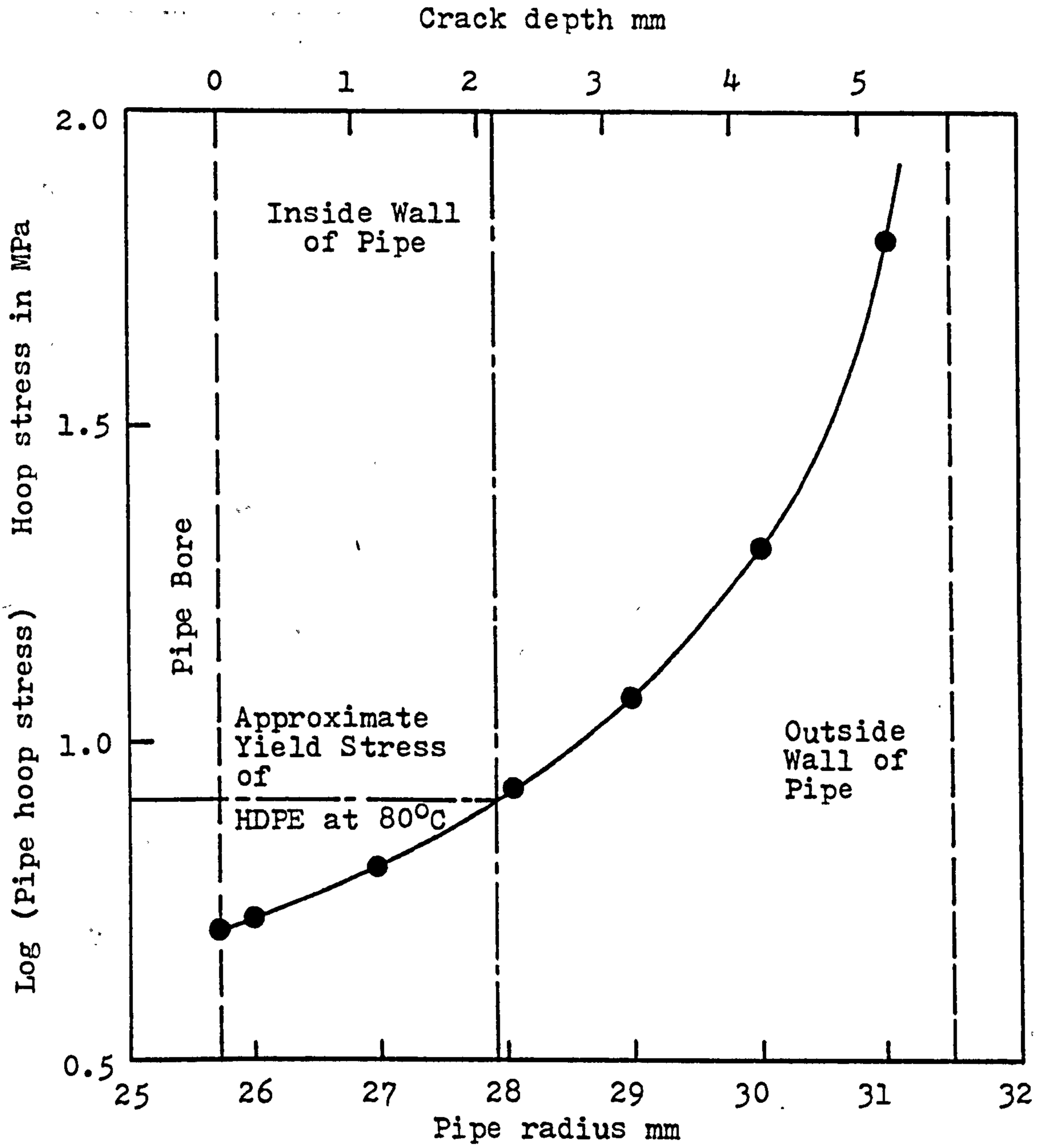

FIGURE 7.3 Variation of pipe hoop stress with increasing crack depth through the wall of an HDPE 63mm OD SDR 11 pipe subject to 1 MPa internal pressure at 80°C.

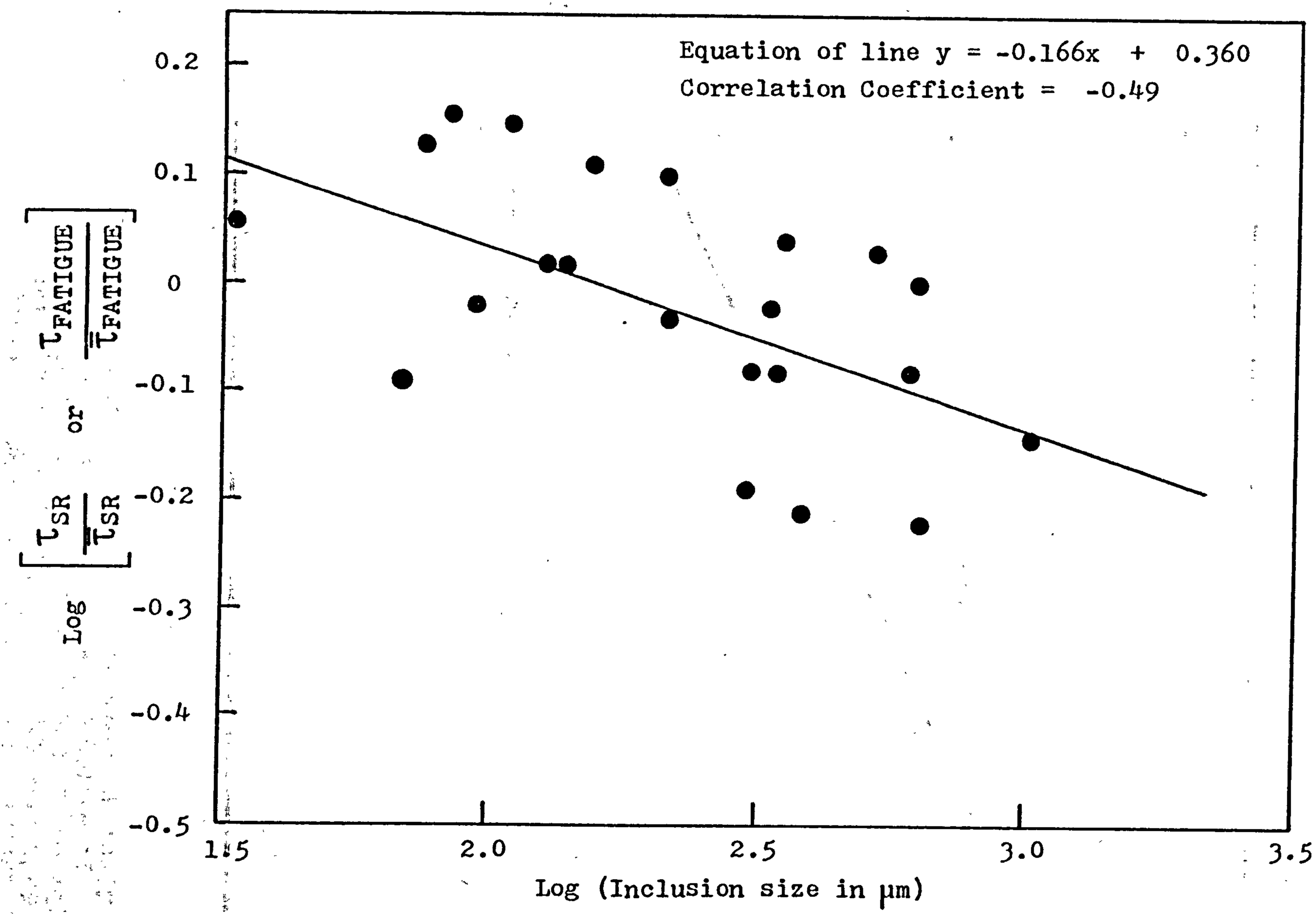

FIGURE 7.4 Variation of reduced stress rupture and fatigue lifetimes as a function of the size of crack initiating particles for HDPE 1 OD SDR 11 pipes at 80°C.

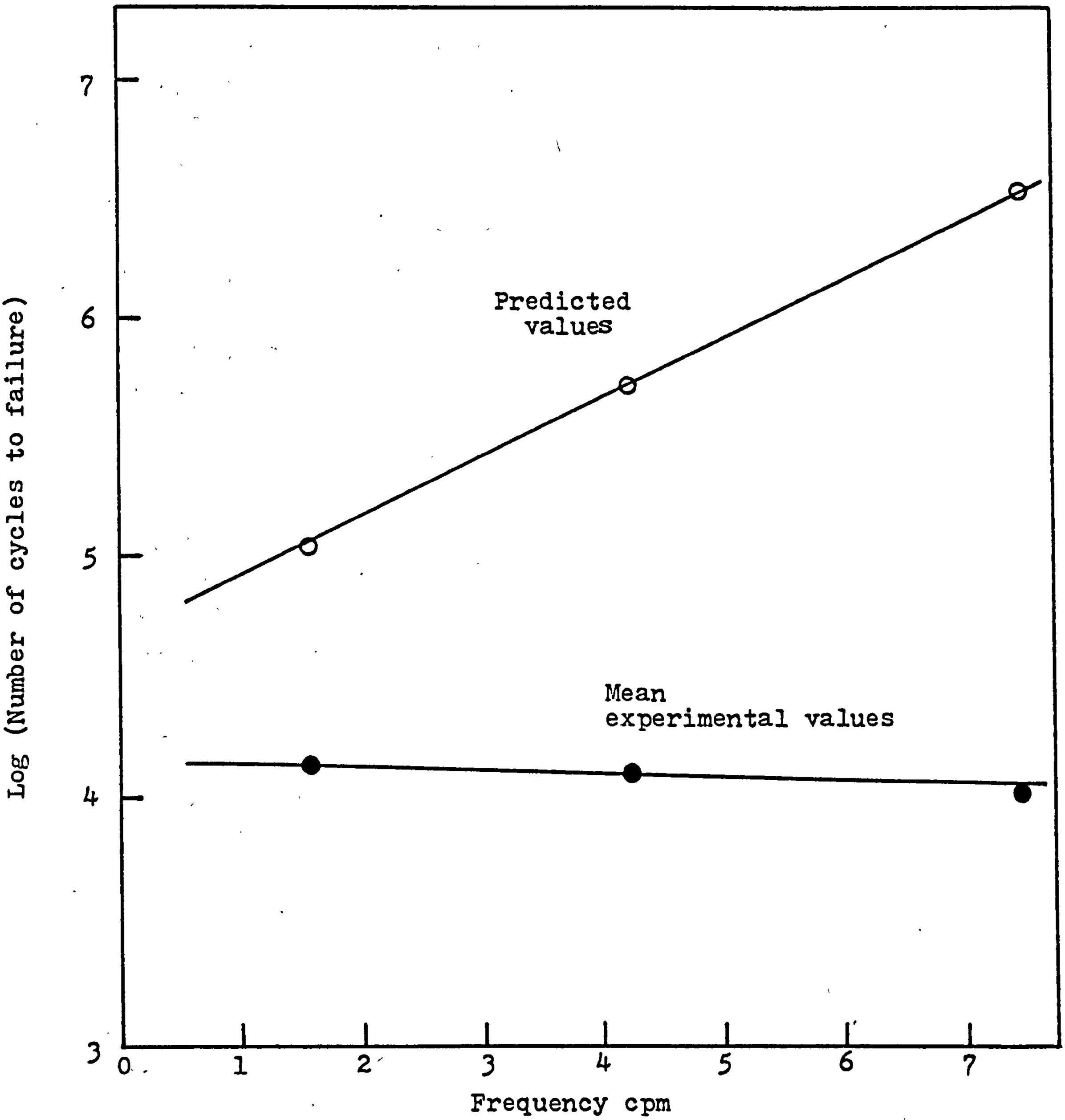

FIGURE 7.5 Comparison of predicted and experimentally determined values of N_f as a function of frequency for HDPE 2 pipe + batch B 90° equal tee systems at 80°C and 4.93 MPa pipe hoop stress. Cumulative damage principles are not applicable in this case.

REFERENCES

1. Timmer, R.C.
   Plastics in Gas Distribution
   Internal Report, E.I. Du Pont De Nemours and Company Inc.
   January 1976
2. Price, J.B., Gray, A.
   Materials Selection for HDPE Pipes
   Proc. of PRI 4th Int. Conf. Plastics Pipes
   Brighton, March 1974, Paper 20
3. Modern Plastics Encyclopaedia
   Polyethylene
   Vol 56 No.10A 1979 p 58
   McGraw-Hill
4. DeVore, R.V.
   Research on Polyolefins for Natural Gas Piping Systems
   Report for the American Gas Association
5. Cist, J.D., Smith, J.G.
   100% On-line Inspection of Plastic Pipe Using Rotating Ultrasonics
   Plastics Engineering
   Vol 34 No.6 1978 p 41
6. Hostalen GM 5010 Pipes
   Hoechst Plastics Manual
   Farbwerke Hoechst
   August 1971
7. Turner, A.
   Fabrication of Thermoplastics
   Polymers - Applied Polymer Symposium
   No.17 p 3
   Wiley-Interscience 1971
8. Powell, P.C.
   Design of Load Bearing Thermoplastics Products
   Materials in Engineering Applications
   Vol 1 1979 p 190 - 198
9. Gebler, H.
   Internal Stress Profiles in HDPE and PP Pipes
   Hoechst AG Plastics Pipes Symposium
   Frankfurt, December 1979

10. Clark, E.S.
Molecular Orientation in Injection Moulding of Acetal Homopolymers
Society of Plastics Engineers' Journal
Vol 23 No.7 1967 p 46

11. Kantz, M.R., Newman, H.D., Stigale, F.M.
The Skin-care Morphology and Structure-Property Relationships in Injection-Moulded Polypropylene
J. Appl.Polym.Sci.
Vol 16 1972 p 1249

12. Haas, T.W., Maxwell, B.
Effects of Shear Stress on the Crystallisation of Linear Polyethylene and Poly-1-Butene
Polym.Engng.Sci.
Vol 9 No.4 1969 p 225

13. Fitchmum, D.R., Newman, S., Wiggle, R.
Electroplating on Crystalline Polypropylene
I. Compression Moulding and Adhesion
J. Appl.Polym.Sci.
Vol 14 1970 p 2441

14. Fitchmun, D.R., Newman, S., Wiggle, R.
Electroplating on Crystalline Polypropylene
II. Injection Moulding and Adhesion
J. Appl.Polym.Sci.
Vol 14 1970 p 2457

15. Ogorkiewicz, R.M. (Editor)
Thermoplastics: Effects of Processing
Iliffe 1969

16. Benham, P.P., Crawford, R.J.
The Influence of Injection Moulding Conditions on the Fatigue Behaviour of an Acetal Copolymer
Proc. of PRI Conf. Designing to Avoid Mechanical Behaviour
Cranfield, January 1973

17. Gotham, K.V., Scrutton, I.N.
Effect of Molecular Orientation on the Fracture Toughness of Thermoplastics
Polymer
Vol 19 1978 p 341

18. Moore, D.R., Benham, P.P., Gotham, K.V.,
Hitch, M.J., Littlewood, M.J.
Long Term Fracture Performance of uPVC Pressure
Pipe as Influenced by Processing
Proc. of PRI 4th Int.Conf. Plastics Pipes
Brighton, March 1979, Paper 27
19. Elmco Envirotech
Europlas Monthly
Vol 47 No.4 1974 p 64
20. Cowley, W.E., Wylde, L.E.
The Behaviour of Butt-Fusion Welded Polyethylene
Pipelines Under Fatigue Loading Conditions
Chemistry and Industry
3rd June 1978 p 371
21. Bentley, S.R.
The Microstructure and Welding Properties of Thick-
Section Injection Moulded Polypropylene
M.Phil Thesis
Brunel University 1978
22. Hunter, A., Bevis, M.
Morphology of Welds in PE Pipelines Containing Injection
Moulded Components
Liverpool University Internal Report
1976
23. Barber, P., Atkinson, J.R.
Some Microstructural Changes Associated with Fusion
Welding with Particular Reference to Polyethylene and
Polybutene - 1
Proc. of PRI Conf. Designing to Avoid Mechanical Failure
January 1973
24. Lednicky, F.
Study of Polymer Supermolecular Structure by Microscopy
Int.Polym.Sci. and Tech.
Vol 5 No.12 1978 p T46
25. Sharples, A.
Chapter 4 - Crystallinity
Polymer Science: A Materials Science Handbook Vol 1
(Jenkins, A.D. - Editor)
North-Holland 1972

26. deCourcy, D.R., Atkinson, J.R.
The Use of Tensile Tests To Determine The Optimum Welding Conditions for Butt-Welding Polyethylene Pipes of Different Melt Flow Index
J.Mat.Sci
Vol 12 1977 p 1535

27. Cowley, W.E.
Design Aspects of Butt-Welded Thermoplastics Pipes.
Materials In Engineering Applications
Vol 1 1979 p 323

28. Billmeyer, F.W.
Chapter 4 - Analysis and Testing of Polymers
Textbook of Polymer Science (2nd Edition)
Wiley - Interscience 1971

29. Loginov, V.S., Kashkovskaya, E.A., Petrovskii, A.P.
Change in the Crystallinity of the Material of h.d. PE Pipes With Time.
Int. Polym. Sci. and Tech.
Vol 6 No.9 1979 p T29

30. Loginov, V.S., Kashkovskaya, E.A.
Influence of the Structure of the Surface Layer of h.d. PE Pipes on Their Crack Resistance.
Int. Polym. Sci. and Tech.
Vol 6 No.9 1979 p T83

31. Gedde, U.W., Jansson, J-F.
Determination of Thermal Oxidation of High Density Polyethylene Pipes Using Differential Scanning Calorimetry.
Polymer Testing.
Vol 1 1980 p 303

32. de Charentenay, F.X., Laghouati, F., Dewas, J.
Fatigue Crack Propagation in High Density Polyethylene.
Proc. of PRI Conf. Deformation, Yield and Fracture of Polymers.
1979 Paper 6

33. Hay, J.N.
Crystallisation Kinetics And Melting Studies.
British Polymer Journal.
Vol 11 1979 p137
34. Richardson, M.J.
Crystallinity Determination In Polymers And A Quantitative Comparison For Polyethylene.
British Polymer Journal.
Vol 1 1969 p132
35. Ghijsels, A., Waals F.M.T.A.M.
Differential Scanning Calorimetry : A Powerful Tool For The Characterisation Of Thermoplastics.
Polymer Testing.
Vol 1 1980 p149
36. Brennan, W.P.
Characterisation Of Polyethylene Films By Differential Scanning Calorimetry.
Thermal Analysis Application Study 24.
March 1978.
Perkin-Elmer Corporation.
37. Mandelkern, L., Allou, A.L., Gopalan, M.
The Enthalpy Of Fusion Of Linear Polyethylene.
J. Phys. Chem.
Vol 72 No 1 January 1968.
38. Still, R.H.
Some Problems Associated With The Application Of Thermal Methods To Polymers.
British Polymer Journal.
Vol 11 1979 p101
39. Keller, A.
The Many Faces Of Order In Solid Polymers.
Plastics And Polymers.
Vol 43 1975 p15
40. Cooney, J.L.
Effect Of Morphology On Biaxial Stress Rupture Of Polyethylene.
J. Appl. Polym. Sci.
Vol 8 1964 p1889

41. Schonefeld, C., Wintergerst, S.
Effect of Heat Treatment on Density, Internal Stress and Bursting Strength of Drinking Water Pipes of LDPE and HDPE.
Kunststoffe
Vol 61 1971 p 33

42. Barton, S.J., Cherry, B.W.
Predicting the Creep Rupture Life of Polyethylene Pipes
Proc. of PRI 4th Int. Conf. Plastics Pipes
Brighton, March 1974, Paper 21

43. Thermal and Chemical Welding of Plastics Materials
Engineering Equipment Users Association
Handbook No.35
1976

44. De Vries, A.J.
Welding of Hard Polyethylene Pipes
Eurotest Technical Bulletin
No.XEW 663

45. Menges, G., Zöhren, J.
Latest Data on Welding Thermoplastics
Plastverarbeiter
Vol 18 Part 3 1967 p 165

46. Potente, H., Reinke, M.
Welding Parameters of Polyolefin Parts
Proc. of PRI Int. Conf. Moulding of Polyolefins
London, November 1980, Paper 15

47. deCourcy, D.R.
The Microstructure and Mechanical Properties of PE Butt-Welds
Ph.D. Thesis
Leeds University 1976

48. Atkinson, J.R.
The Academic Assessment of Fusion Joint Quality
Proc. of PRI Conf. Jointing and Fabrication of Thermoplastic Pipe and Structures
Bradford
October 1980

49. Ewing, L.
Plastics in Gas Distribution
Proc. of PRI 4th Int. Conf. Plastics Pipes
Brighton, March 1979, Paper 6.

50. Ewing, L.
Insertion Replacement of Mains Using Plastic Pipe
British Gas Report ERS. E139
12th February 1975

51. Ewing, L., Richardson, W.
Polyethylene Gas Pipe Systems: An Appraisal of Joint Design and Construction Methods.
Proc. of PRI Conf. Jointing and Fabrication of Thermoplastics Pipes and Structures
Bradford, October 1980

52. Herrmann, H.
Ultrasonic Testing of Welds in HDPE and PP
Hoechst AG Plastics Pipes Symposium
Frankfurt, December, 1979

53. Potente, H., de Zeeuw, K.
Non-destructive Testing of Heated Tool Butt-Welded Pipes Using Optical Methods
Proc. of PRI 4th Int. Conf. Plastics Pipes
Brighton, March 1979, Paper 24

54. Diedrich, G., Kempe, B.
Welding Pipes and Fittings Made From Various Polyethylene Grades (HDPE)
Hoechst AG Plastics Pipes Symposium
Frankfurt, December 1979

55. Kunnecke, W.
Butt Fusion Welding of Plastics Pipes
Kunststoffe
Vol 27 No.8 1980 p 8

56. Barber, P., Atkinson, J.R.
The Use of Tensile Tests to Determine the Optimum Conditions for Butt Fusion Welding Certain Grades of Polyethylene, Polybutene-1 and Polypropylene Pipes
J.Mat.Sci.
Vol 9 1974 p 1456

57. Berry, D.B.S.
Standard Testing of Pipes and the Examination of Failures
Proc. of PRI 4th Int. Conf. Plastics Pipes Brighton, March 1974, Paper 37

58. Alf, E., Potente, H., Menges, G.
Forming of Cracks and Failure of Welded Joints Depending on Temperature, Media Influence and Strain Rate.
Proc. of PRI Conf. Designing to Avoid Mechanical Failure Cranfield, January 1973

59. ASTM D1598 - 76
Standard Method of Test for Time to Failure of Plastic Pipe Under Constant Internal Pressure

60. Jones, R.W.
National and International Standardisation Related to Plastics Pipes
Proc. of PRI 4th Int. Conf. Plastics Pipes Brighton, March 1979, Paper 35

61. Gons, J.
The Need to Revise I.S.1167 Dealing with Pressure Testing
Proc. of PRI 4th Int. Conf. Plastics Pipes Brighton, March, 1979, Paper 36

62. Design Factors for Unreinforced Thermoplastics Products With Specific Reference to Pipes
Plastics and Rubber Institute Design Booklet 1976

63. Hearn, E.J.
Mechanics of Materials
Vol 1
Chapters 9 and 10
Pergamon Press 1980

64. Williams, J.G.
Stress Analysis of Polymers (2nd Edition)
Ellis Harwood 1980

65. Sternstein, S.S., Ongchin, L.
Yield Criteria for Plastic Deformation of Glassy High Polymers in General Stress Fields
American Chemical Society Polymer Preprints
Vol 10 1969 p 117

66. British Standard 806: 1975
Ferrous Piping Systems for and in Connection With
Land Boilers
67. Design of Piping Systems
M.W.Kellogg Company (2nd Edition)
Chapman and Hall Limited
London 1956
68. ASTM D1599-69
Standard Method of Test for Short-Time Rupture
Strength of Plastic Pipe, Tubing and Fittings
69. Goldfein, S.
Estimation of Long-Time Performance of Extruded
Plastic Pipe from Short-Time Rupture Strength
Modern Plastics
May 1960 p 139
70. Sansome, L.F.
A Comparison of Short-Time Versus Long-Time Properties
of Plastic Pipe Under Hydrostatic Pressure
Society of Plastics Engineers Journal
May 1959 p 418
71. Mruk, S.A.
The Ductile Failure of Polyethylene Pipe
Society of Plastics Engineers Journal
January 1963 p 91
72. Birch, M.W., Howarth, R., Marshall, G.P.
The Use of Fracture Mechanics for the Prediction
of Failure of Thermoplastics Pipes
Proc. of PRI 4th Int. Conf. Plastics Pipes
Brighton, March 1979, Paper 25
73. Kausch, H.H.
Polymer Fracture
Polymers Properties and Applications 2
Springer-Verlag 1978
74. Gaube, E., Diedrich, G., Müller, W.
Thermoplastic Pipes
Kunststoffe
Vol 66 Part 1 1976 p 2

75. Stockmayer, P.
Inhomogenisation in Polyethylene Pipes
Stuttgarter Kunststoffe - Kolloquium 1977
Kunststoffe
Vol 67 1977 p 470
76. Horsley, R.A.

Proc. of SCI Symposium Physical Properties of Polymers
London, April 1958
77. Gladstone, S., Laidler, K.J., Eyring, H.
The Theory of Rate Processes
McGraw-Hill,
New York, 1941
78. Barton, S.J., Cherry, B.W.
Predicting the Creep Rupture Life of
Polyethylene Pipe
Polym. Engng. Sci.
Vol 19 No.8 1979 p 590
79. Gray, A., Mallinson, J.N., Price, J.B.
Fracture Behaviour of Polyethylene Pipe
Plastics and Rubber : Processing and Applications
Vol 1 No.1 1981 p 51
80. Bragaw, C.G.
The Validity of Fracture Mechanics for the
Design of Polyethylene Piping Systems
Proc. of PRI Conf. Deformation, Yield and
Fracture of Polymers,
Cambridge, April 1976
81. Kubat, J., Rigdahl, M., Seldon, R.
Internal Stresses and Activation Volumes
for the Stress Relaxation Behaviour of Polyethylene
at Low Deformations
J.Appl.Polym.Sci.
Vol 20 1976 p 2799

82. Nicklas, H., Kausch, H.H.
Molecular Structure and Mechanical Properties of Polyvinyl Chloride III. Causes of Time Dependent Strength Properties of Polyvinyl Chloride Pipes
Kunststoffe
Vol 53 Part 12 1963 p 886

83. Bragaw, C.G.
Fracture Modes in Medium Density Polyethylene Gas Piping Systems
Proc. of PRI 4th Int. Conf. Plastics Pipes
Brighton, March 1979, Paper 23

84. Hannon, M.J.
Microscopic Aspects of Brittle Failure of Polyethylene at Stress Below the Yield Stress
J.Appl.Polym.Sci.
Vol 18 1974 p 3761

85. Cann, J.M.
Plastics Pressure Pipe - Design Criteria and Performance Assessments
British Plastics
February 1967 p 44

86. Gaube, E.
Creep Rupture Strength and Stress Cracking of Low Pressure Polyethylene
Kunststoffe
Vol 49 1959 p 446

87. Richard, K., Diedrich, G.
Testing of Ziegler Polyethylene Pipes
Rubber and Plastics Age
Vol 39 1958 p 364

88. Richard, K., Gaube, E., Diedrich, G.
Long Term Behaviour of Drinking Water Pipe From Ziegler Polyethylene
Kunststoffe
December 1958 p 444

89. Kagan, D.F., Knebel'man, A.M., Kantor, L.A.
Effect of the Supramolecular Structure on the Durability of High-Density Polyethylene
Vysokomol. soyed
Vol A 14 No.5 1972 p 1207

90. Andrews, E.H.
Fatigue in Polymers
Testing of Polymers (W.Brown ed.) Vol IV
Wiley - Interscience 1969 p 237

91. Joseph, S.H.
Pressure Fatigue Testing of Plastics Pipes
Proc. of PRI 4th Int. Conf. Plastics Pipes
Brighton, March 1979, Paper 28.

92. Lörtsch, W.
Plastics Pipes Subjected to Static and Pulsating Internal Pressure
Kunststoffe
Vol 55 1965 p 460

93. Van Crombrugge, R.
Creep and Fatigue Strength of Welded Polyethylene Pipes
Plastica
Vol 26 No.5 1973 p 199

94. Hertzberg, R.W., Manson, J.A.
Fatigue in Engineering Plastics
Academic Press 1980

95. Riddell, M.N., Koo, G.P., O'Toole, J.L.
Fatigue Mechanisms of Thermoplastics
Polym.Engng.Sci.
Vol 6 1966 1 363

96. Manson, J.A., Hertzberg, R.W.
Fatigue Failure in Polymers
Crit.Rev.Macromol.Sci.
Vol 1 1973 p 433

97. Stapel, J.J.
Fatigue Properties of uPVC Related to Actual Site Conditions in Water Distribution Systems
Pipes and Pipelines International
Part 1 : February 1977 p 11
Part 2 : April 1977 p 33

98. Van Crombrugge, R.
Fatigue Properties of uPVC Pipes
RILEM Symposium on Research and Reception Tests on Synthetic Materials for Construction
Final Report
Liege 1974 p 448

99. Kirstein, C.E.
Untersuchung der Innerdruck - Schwellfestigkeit
von Rohren ans PVC Hart
Publication of the Institut für Kunststoffprufung und
Kunststoffbunder Universitat Stuttgart
1972

100. Gotham, K.V., Hitch, M.K.
Design Considerations for Fatigue in uPVC Pressure Pipes
Pipes and Pipelines International
Vol 20 1975 p 10

101. Benham, P.P., Hutchinson, S.J.
Cyclic Creep and Fracture of PVC
Plastics and Polymers
Vol 38 1970 p 259

102. McKenna, G.B., Penn, R.W.
Time-Dependent Failure in Poly(Methylmethacrylate)
and Polyethylene
Polymer
Vol 21 1980 p 213

103. Tauchert, T.R.
The Temperature Generated During Torsional Oscillations
of Polyethylene Rods
Int.J.Engng.Sci.
Vol 5 1967 p 353

104. Menges, G., Alf, E.
Creep, Self-Heating and Failure of Thermoplastics
Under Pulsating Tensile Stress
Society of Plastics Engineers 31st Annual Technical
Conference
Montreal, May 1973

105. Constable, I., Williams, J.G., Burns, D.J.
Fatigue and Cyclic Thermal Softening of Thermoplastics
J.Mech:Engng.Sci
Vol 12 No.1 1970 p 20

106. Hucks, R.T.
Designing PVC Pipe for Water Distribution System
Water Technology/Distribution Journal
AWWA 1972 p 443

107. Kirby, P.C.
Surge and Fatigue in uPVC Sewer Rising Mains
Proc. of PRI 4th Int. Conf. Plastics Pipes
Brighton, March 1979, Paper 26

108. Jacobi, H.R.
Fatigue Rupture Phenomena in Rigid PVC Pipe Fittings
Kunststoffe
Vol 55 1965 p 39

109. Oberbach, K., Heese, G.
The Effects of Loading Profile and Frequency on the
Fatigue Behaviour of Plastics
Materialprüfung
Vol 14 1972 p 173

110. Hucks, R.T.
Pressure Surges and PVC Pipe
World Construction
September 1972 p 47

111. Hucks, R.T.
Performance of PVC Pipe in Water Distribution Systems
Modern Plastics
September 1972, p 112

112. McKenna, G.B., Penn, R.W.
Time-Dependent Failure of a Polyolefin Rubber Candidate
Material for Blood Pump Applications
J.Biomedical Materials Research
Vol 14 1980 p 689

113. Paris, P.C.
The Fracture Mechanics Approach to Fatigue
Proc. of 10th Sagamore Army Mater.Res.Conf.
New York, 1964

114. Smith, R.A.
An Introduction to Fracture Mechanics for Engineers
Materials in Engineering Applications Vol 1
Part 1 December 1978 p 121, Part 2 June 1979 p 227,
Part 3 December 1979 p 316

115. White, J.R., Teh, J.W.
Fatigue of Viscoelastic Polymers 2, Fractography
Polymer
Vol 20 1979 p 764

116. McEvily, A.J. Boettner, R.C., Johnston, T.L.
On the Formation and Growth of Fatigue Cracks in Polymers
Proc. of 9th Sagamore Army Mater.Res.Conf.
New York 1963

117. Hoechst Plastics Information Sheet
Hostalen GM 5010 T2 Pipes
(See also reference 6)

118. Du Pont Bulletin HM 404
Aldyl 'A' Polyethylene Piping System
Product Description and Technical Information
November 1977

119. BP Chemicals Advance Information Sheet
Rigidex 002-40 R919 High Density Polyethylene
January 1978

120. Bell, G.R., Cook, D.C.
Microtoming: An Emerging Tool for Analysing Polymer Structures
August 1978 p 18

121. ASTM D 1238 - 79
Standard Method of Measuring Flow Rates of Thermoplastics by Extrusion Plastometer

122. ASTM D 3417 - 75
Standard Method of Test for Heats of Fusion and Crystallisation of Polymers by Thermal Analysis

123. ASTM D 638 - 77a
Standard Method of Test for Tensile Properties of Plastics

124. Englander, S.H.
The Physical and Dimensional Characterisation and Short Term Weld Reliability of Butt-Welded High Density Polyethylene Pipe
Brunel University B.Tech Dissertation
April 1980

125. Hertzberg, R.W., Manson, J.A., Skibo, M.
Frequency Sensitivity of Fatigue Processes in
Polymeric Solids.
Polym. Eng. Sci.
Vol 15 1975 p 252.

126. Engel, L., Klingele, H., Ehrenstein, G.W., Schaper, H.
An Atlas of Polymer Damage
Wolfe Publishing Limited 1981.

127. Flueler, P., Roberts, D.R., Mandel, J.F., McGarry, F.J.
Fracture Toughness Testing of HDPE Plastic Pipe
Physical Testing of Plastic - Correlation with
End-Use Performance.
ASTM STP 736 R.E. Evans (Ed.)
American Society for Testing and Materials
1981 p 15.

128. Rook, D.P., Cartwright, D.J.
Compendium of Stress Intensity Factors
H.M.S.O.

129. Falbe, J., Richter, B.
Pressure Resistant Pipe Fittings
Kunststoffe
Vol 74 1981 Part 6 p 375.

130. Moore, D.R., Gotham, K.V.
The Mechanical Properties of uPVC in Relation
to Pressure Pipes
Paper given at Brunel University as part of the course
on the "Understanding of Plastics and Designing
Thermoplastic Pipeline Systems".

131. Williams, J.G.
The Use of Fracture Mechanics in Design with Polymers
Engineering Design with Plastics: Principles
and Practice
Plasticon 81
Paper 5
September 1981
University of Warwick

132. Kirby, P.C.
Proc. Int. Conf. on Underground Plastic Pipe
A S C E
New Orleans, U.S.A.
1981